TREATMENT FOR NON SMALL CELL LUNG CANCER IN DISTINCT PATIENT POPULATIONS

EDITED BY: Junji Uchino, Torsten Goldmann and Hideharu Kimura

PUBLISHED IN: Frontiers in Oncology and Frontiers in Pharmacology

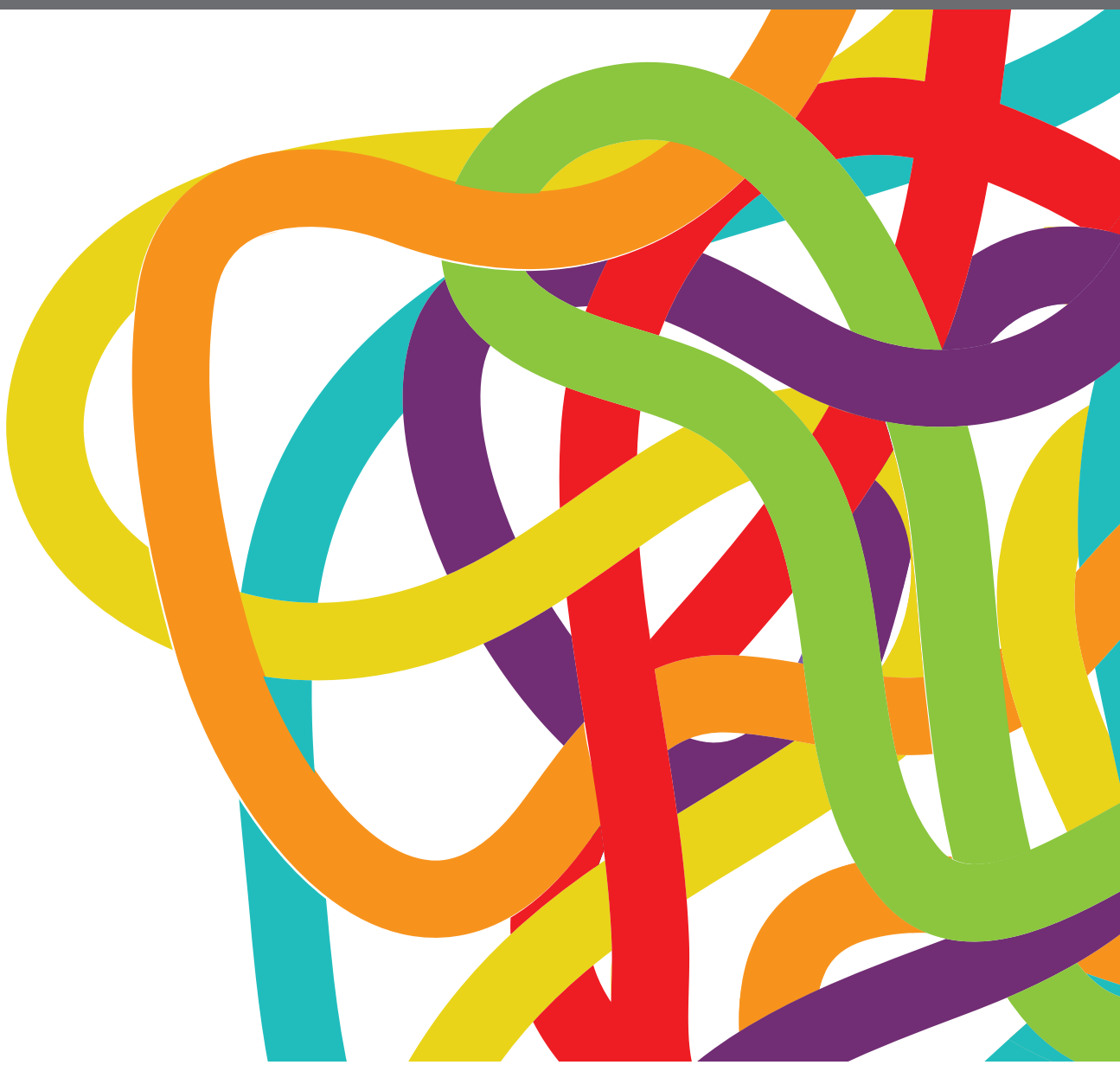

frontiers Research Topics

Frontiers eBook Copyright Statement

The copyright in the text of individual articles in this eBook is the property of their respective authors or their respective institutions or funders. The copyright in graphics and images within each article may be subject to copyright of other parties. In both cases this is subject to a license granted to Frontiers.

The compilation of articles constituting this eBook is the property of Frontiers.

Each article within this eBook, and the eBook itself, are published under the most recent version of the Creative Commons CC-BY licence. The version current at the date of publication of this eBook is CC-BY 4.0. If the CC-BY licence is updated, the licence granted by Frontiers is automatically updated to the new version.

When exercising any right under the CC-BY licence, Frontiers must be attributed as the original publisher of the article or eBook, as applicable.

Authors have the responsibility of ensuring that any graphics or other materials which are the property of others may be included in the CC-BY licence, but this should be checked before relying on the CC-BY licence to reproduce those materials. Any copyright notices relating to those materials must be complied with.

Copyright and source acknowledgement notices may not be removed and must be displayed in any copy, derivative work or partial copy which includes the elements in question.

All copyright, and all rights therein, are protected by national and international copyright laws. The above represents a summary only. For further information please read Frontiers' Conditions for Website Use and Copyright Statement, and the applicable CC-BY licence.

ISSN 1664-8714
ISBN 978-2-88974-514-2
DOI 10.3389/978-2-88974-514-2

About Frontiers

Frontiers is more than just an open-access publisher of scholarly articles: it is a pioneering approach to the world of academia, radically improving the way scholarly research is managed. The grand vision of Frontiers is a world where all people have an equal opportunity to seek, share and generate knowledge. Frontiers provides immediate and permanent online open access to all its publications, but this alone is not enough to realize our grand goals.

Frontiers Journal Series

The Frontiers Journal Series is a multi-tier and interdisciplinary set of open-access, online journals, promising a paradigm shift from the current review, selection and dissemination processes in academic publishing. All Frontiers journals are driven by researchers for researchers; therefore, they constitute a service to the scholarly community. At the same time, the Frontiers Journal Series operates on a revolutionary invention, the tiered publishing system, initially addressing specific communities of scholars, and gradually climbing up to broader public understanding, thus serving the interests of the lay society, too.

Dedication to Quality

Each Frontiers article is a landmark of the highest quality, thanks to genuinely collaborative interactions between authors and review editors, who include some of the world's best academicians. Research must be certified by peers before entering a stream of knowledge that may eventually reach the public - and shape society; therefore, Frontiers only applies the most rigorous and unbiased reviews.
Frontiers revolutionizes research publishing by freely delivering the most outstanding research, evaluated with no bias from both the academic and social point of view. By applying the most advanced information technologies, Frontiers is catapulting scholarly publishing into a new generation.

What are Frontiers Research Topics?

Frontiers Research Topics are very popular trademarks of the Frontiers Journals Series: they are collections of at least ten articles, all centered on a particular subject. With their unique mix of varied contributions from Original Research to Review Articles, Frontiers Research Topics unify the most influential researchers, the latest key findings and historical advances in a hot research area! Find out more on how to host your own Frontiers Research Topic or contribute to one as an author by contacting the Frontiers Editorial Office: frontiersin.org/about/contact

TREATMENT FOR NON SMALL CELL LUNG CANCER IN DISTINCT PATIENT POPULATIONS

Topic Editors:
Junji Uchino, Kyoto Prefectural University of Medicine, Japan
Torsten Goldmann, Research Center Borstel (LG), Germany
Hideharu Kimura, Kanazawa University, Japan

Citation: Uchino, J., Goldmann, T., Kimura, H., eds. (2022). Treatment for Non Small Cell Lung Cancer in Distinct Patient Populations. Lausanne: Frontiers Media SA. doi: 10.3389/978-2-88974-514-2

Table of Contents

07 ***Editorial: Treatment for Non-Small Cell Lung Cancer in Distinct Patient Populations***
Junji Uchino, Torsten Goldmann and Hideharu Kimura

10 ***Preoperative Folate Receptor-Positive Circulating Tumor Cell Level Is a Prognostic Factor of Long Term Outcome in Non-Small Cell Lung Cancer Patients***
Hang Li, Bin Li, Yunjian Pan, Yang Zhang, Jiaqing Xiang, Yawei Zhang, Yihua Sun, Xiang Yu, Wei He and Hong Hu

21 ***Immune-Related Adverse Events Predict the Efficacy of Immune Checkpoint Inhibitors in Lung Cancer Patients: A Meta-Analysis***
Donghui Wang, Cen Chen, Yanli Gu, Wanjun Lu, Ping Zhan, Hongbing Liu, Tangfeng Lv, Yong Song and Fang Zhang

32 ***Immune-Related Adverse Events are Associated With Clinical Benefit in Patients With Non-Small-Cell Lung Cancer Treated With Immunotherapy Plus Chemotherapy: A Retrospective Study***
Kenji Morimoto, Tadaaki Yamada, Chieko Takumi, Yuri Ogura, Takayuki Takeda, Keisuke Onoi, Yusuke Chihara, Ryusuke Taniguchi, Takahiro Yamada, Osamu Hiranuma, Yoshie Morimoto, Masahiro Iwasaku, Yoshiko Kaneko, Junji Uchino and Koichi Takayama

40 ***Transcriptome Analysis of Ivosidenib-Mediated Inhibitory Functions on Non-Small Cell Lung Cancer***
Juan Wu, Ru Chen, Huiqing Shen, Ting Yan, Yu Qian, Yaping Zhang, Zhuoya Huang, Pengzhou Kong, Min Pang and Xinri Zhang

54 ***Feasibility and Challenges for Sequential Treatments in ALK-Rearranged Non-Small-Cell Lung Cancer***
Mei Elsayed, Farastuk Bozorgmehr, Daniel Kazdal, Anna-Lena Volckmar, Holger Sültmann, Jürgen R. Fischer, Mark Kriegsmann, Albrecht Stenzinger, Michael Thomas and Petros Christopoulos

62 ***An Immune-Related lncRNA Expression Profile to Improve Prognosis Prediction for Lung Adenocarcinoma: From Bioinformatics to Clinical Word***
Boxiang Zhang, Rui Wang, Kai Li, Ziyang Peng, Dapeng Liu, Yunfeng Zhang and Liuzhi Zhou

74 ***Identification of Resectable N2 in NSCLC: A Single Center Experience and Review of the SEER Database***
Yan-qing Wang, Xu-dong Liu, Wen-liang Bai and Shan-qing Li

86 ***Identification of an Individualized Metabolism Prognostic Signature and Related Therapy Regimens in Early Stage Lung Adenocarcinoma***
Junjie Hu, Huansha Yu, Liangdong Sun, Yilv Yan, Lele Zhang, Gening Jiang and Peng Zhang

97 ***Efficacy and Resistance of Afatinib in Chinese Non-Small Cell Lung Cancer Patients With*** HER2 ***Alterations: A Multicenter Retrospective Study***
Zhengbo Song, Dongqing Lv, Shiqing Chen, Jianhui Huang, Liping Wang, Shuguang Xu, Huafei Chen, Guoqiang Wang and Quan Lin

105 ***High Expression of* ACE2 *and* TMPRSS2 *at the Resection Margin Makes Lung Cancer Survivors Susceptible to SARS-CoV-2 With Unfavorable Prognosis***
Qianqian Wang, Liangyu Li, Tianyu Qu, Jie Li, Lingxiang Wu, Kening Li, Ziyu Wang, Mengyan Zhu, Bin Huang, Wei Wu, Min Wu, Rong Ding, Zhihong Zhang, Qianghu Wang, Xinyi Xia, Pengping Li, Zhi Zhang and Renhua Guo

113 ***Beyond Conventional: The New Horizon of Targeted Therapy for the Treatment of Advanced Non Small Cell Lung Cancer***
Alfredo Tartarone, Vittoria Lapadula, Concetta Di Micco, Gemma Rossi, Carlotta Ottanelli, Andrea Marini, Roberta Giorgione, Katia Ferrari, Martina Catalano, Luca Voltolini, Enrico Mini and Giandomenico Roviello

120 ***The Efficacy and Safety of Epidermal Growth Factor Receptor Tyrosine Kinase Inhibitor Combined With Thymosin in Advanced Non-Small Cell Lung Cancer Patients Harboring Active Epidermal Growth Factor Receptor Mutations***
Yongdong Feng, Guangkuo Zhu, Song Lang, Ping Hao, Guanghui Li, Fanglin Chen, Wenlei Zhuo, Yuzhong Duan, Anmei Zhang, Zhengtang Chen and Jianguo Sun

129 ***Cost-Effectiveness of Lorlatinib as a First-Line Therapy for Untreated Advanced Anaplastic Lymphoma Kinase-Positive Non-Small Cell Lung Cancer***
SiNi Li, JianHe Li, LiuBao Peng, YaMin Li and XiaoMin Wan

138 ***A Retrospective Study on Using a Novel Single Needle Cone Puncture Approach for the Iodine-125 Seed Brachytherapy in Treating Patients With Thoracic Malignancy***
Fenge Li, Liping Wang, Yixiang Zhang, Weihong Feng, Tao Ju, Zaiping Liu, Zhenglu Wang and Xueming Du

153 ***Comparison of Clinical Efficacy of Alectinib* Versus *Crizotinib in* ALK*-Positive Non-Small Cell Lung Cancer: A Meta-Analysis***
Hao Tang, Longyu Jin, Zhang Zhang, Zhibin Jiang and Zeeshan Malik

164 ***Durable Response to the Combination of Atezolizumab With Platinum-Based Chemotherapy in an Untreated Non-Smoking Lung Adenocarcinoma Patient With* BRAF *V600E Mutation: A Case Report***
Xiaomin Niu, Yingjia Sun, David Planchard, Luting Chiu, Jian Bai, Xinghao Ai and Shun Lu

170 ***The Angiotensin-Converting Enzyme Inhibitory State Promotes the Transformation of Non-Small Cell Lung Cancer Blood Supply Pattern Toward Vasculogenic Mimicry Formation***
Kandi Xu, Huize Han, Yexin Luo, Hong Ye, Hongxia Lin and Lei Ni

183 ***Co-Occurring Potentially Actionable Oncogenic Drivers in Non-Small Cell Lung Cancer***
Yiming Zhao, Shuyuan Wang, Zhengyu Yang, Yu Dong, Yanan Wang, Lele Zhang, Hai Hu and Baohui Han

192 ***Hypofractionated Volumetric-Modulated Arc Radiotherapy for Patients With Non-Small-Cell Lung Cancer Not Suitable for Surgery or Conventional Chemoradiotherapy or SBRT***
Junyue Shen, Dan Yang, Mailin Chen, Leilei Jiang, Xin Dong, Dongming Li, Rong Yu, Huiming Yu and Anhui Shi

200 ***First-Line Chemo-Immunotherapy for Extensive-Stage Small-Cell Lung Cancer: A United States-Based Cost-Effectiveness Analysis***
Qiao Liu, Xia Luo, Lidan Yi, Xiaohui Zeng and Chongqing Tan

208 ***Therapeutic and Prognostic Implications of Immune-Related Adverse Events in Advanced Non-Small-Cell Lung Cancer***
Lea Daniello, Mariam Elshiaty, Farastuk Bozorgmehr, Jonas Kuon, Daniel Kazdal, Hannah Schindler, Rajiv Shah, Anna-Lena Volckmar, Fabienne Lusky, Leonore Diekmann, Stephan Liersch, Martin Faehling, Thomas Muley, Mark Kriegsmann, Karolina Benesova, Albrecht Stenzinger, Michael Thomas and Petros Christopoulos

222 ***Postoperative Radiotherapy for Patients With Resectable Stage III-N2 Non-Small Cell Lung Cancer: A Systematic Review and Meta-Analysis***
Tianyu Lei, Jing Li, Hao Zhong, Huibo Zhang, Yan Jin, Jie Wu, Lan Li, Bin Xu, Qibin Song and Qinyong Hu

233 ***Development and External Validation of a Nomogram for Predicting Cancer-Specific Survival of Non-Small Cell Lung Cancer Patients With Ipsilateral Pleural Dissemination***
Zhenfan Wang, Hao Li, Taorui Liu, Zewen Sun, Fan Yang and Guanchao Jiang

243 ***AI-Based Drug Discovery of TKIs Targeting L858R/T790M/C797S-Mutant EGFR in Non-small Cell Lung Cancer***
Geunho Choi, Daegeun Kim and Junehwan Oh

250 ***Hepatoid Adenocarcinoma of the Lung: A Systematic Review of the Literature From 1981 to 2020***
Zan Hou, Jiaqing Xie, Li Zhang, Gangyi Dai, Yuanhang Chen and Lang He

260 ***Efficacy of EGFR-TKI Plus Chemotherapy or Monotherapy as First-Line Treatment for Advanced EGFR-Mutant Lung Adenocarcinoma Patients With Co-Mutations***
Zhengyu Yang, Ya Chen, Yanan Wang, Shuyuan Wang, Minjuan Hu, Bo Zhang and Baohui Han

268 ***Targeted Therapy for RET Fusion Lung Cancer: Breakthrough and Unresolved Issue***
Shinkichi Takamori, Taichi Matsubara, Naoki Haratake, Gouji Toyokawa, Takatoshi Fujishita, Ryo Toyozawa, Kensaku Ito, Masafumi Yamaguchi, Kenichi Taguchi, Tatsuro Okamoto and Takashi Seto

274 ***An Indirect Comparison Between Nivolumab + Ipilimumab + Two Cycles of Chemotherapy vs. Pembrolizumab + Chemotherapy as First-Line Treatment for Metastatic Non-Small Cell Lung Cancer***
Panpan Jiang, Ziyang Mao, Qinyang Wang, Xiaohui Jia, Luying Geng, Hong Xu, Lili Jiang, Chengcheng Yang, Min Jiao and Hui Guo

283 ***Clinical Outcome of CT-Guided Stereotactic Ablative Brachytherapy for Unresectable Early Non-Small Cell Lung Cancer: A Retrospective, Multicenter Study***
Zhe Ji, Bin Huo, Shifeng Liu, Qinghua Liang, Chao Xing, Miaomiao Hu, Yanli Ma, Zhe Wang, Xinxin Zhao, Yuqing Song, Yufeng Wang, Hongmei Han, Kaixian Zhang, Ruoyu Wang, Shude Chai, Xuequan Huang, Xiaokun Hu and Junjie Wang on behalf of China North Radioactive Brachytherapy Group (CNRBG)

292 ***Comparative Study of Pulmonary Combined Large-Cell Neuroendocrine Carcinoma and Combined Small-Cell Carcinoma in Surgically Resected High-Grade Neuroendocrine Tumors of the Lung***
Yanan Wang, Fangfei Qian, Ya Chen, Zhengyu Yang, Minjuan Hu, Jun Lu, Yanwei Zhang, Wei Zhang, Lei Cheng and Baohui Han

302 ***The Prognostic Role of Blood Inflammatory Biomarkers and EGFR Mutation Status in Stage IIIA/N2 Non-Small Cell Lung Cancer Patients Treated With Trimodality Therapy***
Hui Yang, Kunlun Wang, Bingxu Li, Shenglei Li, Yan Li and Ling Yuan

frontiers in Oncology

EDITORIAL
published: 27 January 2022
doi: 10.3389/fonc.2022.838570

Editorial: Treatment for Non-Small Cell Lung Cancer in Distinct Patient Populations

Junji Uchino[1,2]*, *Torsten Goldmann*[3] *and Hideharu Kimura*[4]

[1] Department of Pulmonary Medicine, Kyoto Prefectural University of Medicine, Kyoto, Japan, [2] Bannan Central Hospital, Hamamatsu, Japan, [3] Pathology, Research Center Borstel, Airway Research Center North (ARCN), Member of the German Center for Lung Research (DZL), Borstel, Germany, [4] Department of Respiratory Medicine, Kanazawa University Graduate School of Medical Sciences, Kanazawa, Japan

Keywords: non-small cell lung cancer, tailored treatment, distinct patients, prognostic predictors, adverse event (AE)

Editorial on the Research Topic

Treatment for Non-Small Cell Lung Cancer in Distinct Patient Populations

Pharmacotherapy for lung cancer has changed considerably in recent years. In the 2000s, the discovery of driver genes triggered the discovery of accurate predictors of the therapeutic efficacy of molecular-targeted drugs. Additionally, recent studies have shown the effectiveness and safety of using angiogenesis suppressants and new cytotoxic anticancer drugs for distinct histological subdivisions. Subsequently, a number of driver genes were discovered, and molecular-targeted drugs were marketed. In this era, these drugs have been classified based on the genetic abnormalities they target. With the advent of immune checkpoint inhibitors against molecules such as programmed death protein 1 (PD-1) and programmed cell death ligand 1 (PD-L1), tumors are being classified according to their expression of PD-1 and PD-L1, increasing the complexities in the algorithms of drug selection and molecular testing. The results of many important clinical trials led to the establishment of various treatment modalities, which have resulted in the selection of better treatment strategies.

The development of biomarkers and novel pharmaceuticals has dramatically transformed the pharmacotherapy of lung cancer. Traditionally, the 5-year survival rate for advanced non-small cell lung cancer (NSCLC) was reported to be approximately 1–3% (1). In contrast, among driver gene-positive patients, the median survival was approximately 3 years, and the 5-year survival rate extended to 30% (1). Even in cases without driver gene mutations, the advent of immune checkpoint inhibitors has resulted in the 5-year survival rate increasing to more than 15% (2). However, these are the results of clinical trials, and actual clinical practice includes patients that differ from the standard patient population enrolled in clinical studies. There is little information available on the best treatment modalities for distinct patient populations, such as those who exhibit poor performance status, those who are elderly, or those with brain metastases, for whom the standard treatment regimens (e.g., platinum combination therapy or immune checkpoint inhibitors with chemotherapy) are deemed unsuitable.

Thus, in this Research Topic, we aimed to collect research tailored to these distinct patient populations and discuss novel studies that pinpoint special molecular subtypes of NSCLC. We were excited to receive 59 contributions, and 31 articles authored by more than 260 researchers from

OPEN ACCESS

Edited and reviewed by:
Olivier Feron,
Université catholique de Louvain, Belgium

Correspondence:
Junji Uchino
uchino@koto.kpu-m.ac.jp

Specialty section:
This article was submitted to Pharmacology of Anti-Cancer Drugs, a section of the journal Frontiers in Oncology

Received: *17 December 2021*
Accepted: *10 January 2022*
Published: *27 January 2022*

Citation:
Uchino J, Goldmann T and Kimura H (2022) Editorial: Treatment for Non-Small Cell Lung Cancer in Distinct Patient Populations. Front. Oncol. 12:838570. doi: 10.3389/fonc.2022.838570

various countries in the fields of cancer biology, pharmacology, and therapeutics, were finally selected for inclusion in this Research Topic. Below, we have summarized the results of these studies.

EARLY-STAGE LUNG CANCER

Wang et al. performed an analysis of driver genes using surgical specimens of combined subtypes of large-cell neuroendocrine carcinoma and SCLC respectively and reported that clinical phenotypic differences may impact the prognostic outcome in combined large-cell neuroendocrine carcinoma. Yang et al. examined the prognostic role of inflammatory biomarkers and epidermal growth factor receptor (EGFR) mutations with trimodality therapy in locally advanced lung cancer and reported that more intensive adjuvant treatment may be needed for patients with high pretreatment systemic immune-inflammation and systemic inflammation response indices, stage T2 disease, and EGFR mutations. Ji et al. reported the efficacy of computed tomography-guided stereotactic ablative brachytherapy for unresectable early-stage lung cancer and speculated that patients with stage T1 disease < 1 cm from the chest wall may have better outcomes. Lei et al. conducted a systematic review and meta-analysis of the efficacy of postoperative radiotherapy in patients with resectable stage III-N2 NSCLC and reported that it may not result in improved overall survival (OS). Hu et al. reported the usefulness of a metabolism-related gene-pair index in selecting adjuvant therapy for early-stage pulmonary adenocarcinoma. Shen et al. reported the usefulness of hypofractionated radiotherapy as an alternative therapy for patients with NSCLC not amenable to surgery or conventional chemoradiotherapy. Li et al. found that folate receptor-positive circulating tumor cell level could be a promising prognostic marker after surgery.

ADVANCED-STAGE LUNG CANCER

Jiang et al. performed an indirect comparison of nivolumab + ipilimumab + two cycles of chemotherapy and pembrolizumab + chemotherapy for advanced NSCLC using relevant databases and reported that among women who had never smoked, a better OS could be expected with pembrolizumab + chemotherapy than with nivolumab + ipilimumab+ chemotherapy. Daniello et al., Wang et al., and Morimoto et al. studied the association between immune-related adverse events and the efficacy of immunotherapy, and Morimoto et al. reported that immune-related adverse events were associated with a better therapeutic response, particularly when immunotherapy was combined with chemotherapy.

GENE MUTATION

Takamori et al. reviewed the present treatment strategies and unresolved challenges for lung cancer with RET fusion, which is a rare mutation. Li et al. examined the cost-effectiveness of lorlatinib for anaplastic lymphoma kinase (ALK)-positive lung cancer and reported that lorlatinib was unlikely to be cost-effective compared with crizotinib for patients with previously untreated advanced ALK-positive NSCLC at a willingness-to-pay threshold of $200,000/quality-adjusted life year. Yang et al. investigated the efficacy of EGFR-tyrosine kinase inhibitor (TKI) plus chemotherapy versus EGFR-TKI monotherapy in advanced EGFR-mutant lung adenocarcinoma patients with co-mutations and reported that concurrent *TP53* mutations were found to be risk factors for EGFR-TKI monotherapy, but TKI combined with chemotherapy could eliminate this heterogeneity. Zhao et al. analyzed approximately 3000 coexisting oncogenic drivers in NSCLC and found that approximately 1.5% of NSCLC patients harbored oncogenic drivers that may coexist with EGFR mutations. Choi et al. discussed the potential of artificial intelligence-based screening and drug discovery in the development of novel drugs for acquired resistance to EGFR mutations. Feng et al. examined the efficacy and safety of EGFR-TKI combined with thymosin for advanced NSCLC patients with active EGFR mutation, and they reported that the combination therapy significantly prolonged progression-free survival and OS compared with EGFR-TKI monotherapy without increasing adverse events. Song et al. reported that administration of afatinib resulted in promising outcomes for the NSCLC patients with *HER2* mutations and amplification.

OTHERS

Hou et al. performed a systematic review of locally advanced hepatoid adenocarcinoma of the lung with PIK3CA mutations and concluded that only radical surgery can significantly improve outcomes. Xu et al. discussed the tumor microenvironment and concluded that angiotensin-converting enzyme 2/angiotensin-converting enzyme inhibitors promote vasculogenic mimicry formation *via* Nodal/Notch4 activation and lead to a strong and solid structure of vasculogenic mimicry *via* inhibition of vascular endothelial-cadherin internalization. Li et al. focused on developing a single-needle cone puncture technique in Iodine-125 seeds brachytherapy for people with advanced thoracic malignancies and reported its efficacy. Wu et al. reported the usefulness of ivosidenib, an anti-leukemia drug, in lung cancer, using transcriptomic analysis.

In conclusion, as the study of gene mutations and biomarkers progresses in the future, individualization of treatment strategies will increase, and formulation of safe and effective treatment for older patients will benefit the growing aging population.

As a result, we are convinced that the content of the papers included in this Research Topic will be extremely valuable in guiding further research.

AUTHOR CONTRIBUTIONS

JU, TG, and HK wrote and reviewed this editorial. All authors contributed to the article and approved the submitted version.

REFERENCES

1. Howlader N, Hoone AM, Krapcho M, Miller D, Brest A, Yu M, et al. *SEER Cancer Statistics Review (1975–2016), Based on November 2018. SEER Data Submission*.
2. Garon EB, Hellmann MD, Rizvi NA, Carcereny E, Leighl NB, Ahn MJ, et al. Five-Year Overall Survival for Patients With Advanced Non–Small-Cell Lung Cancer Treated With Pembrolizumab: Results From the Phase I KEYNOTE-001 Study. *J Clin Oncol* (2019) 37(28):2518–27. doi: 10.1200/JCO.19.00934

Conflict of Interest: The authors declare that the research was conducted in the absence of any commercial or financial relationships that could be construed as a potential conflict of interest.

Publisher's Note: All claims expressed in this article are solely those of the authors and do not necessarily represent those of their affiliated organizations, or those of the publisher, the editors and the reviewers. Any product that may be evaluated in this article, or claim that may be made by its manufacturer, is not guaranteed or endorsed by the publisher.

Copyright © 2022 Uchino, Goldmann and Kimura. This is an open-access article distributed under the terms of the Creative Commons Attribution License (CC BY). The use, distribution or reproduction in other forums is permitted, provided the original author(s) and the copyright owner(s) are credited and that the original publication in this journal is cited, in accordance with accepted academic practice. No use, distribution or reproduction is permitted which does not comply with these terms.

frontiers in Oncology

ORIGINAL RESEARCH
published: 28 January 2021
doi: 10.3389/fonc.2020.621435

Preoperative Folate Receptor-Positive Circulating Tumor Cell Level Is a Prognostic Factor of Long Term Outcome in Non-Small Cell Lung Cancer Patients

Hang Li[1,2,3], Bin Li[1,2,3], Yunjian Pan[1,2,3], Yang Zhang[1,2,3], Jiaqing Xiang[1,2,3], Yawei Zhang[1,2,3], Yihua Sun[1,2,3], Xiang Yu[4], Wei He[4] and Hong Hu[1,2,3]**

[1] Department of Thoracic Surgery and State Key Laboratory of Genetic Engineering, Fudan University Shanghai Cancer Center, Shanghai, China, [2] Institute of Thoracic Oncology, Fudan University, Shanghai, China, [3] Department of Oncology, Shanghai Medical College, Fudan University, Shanghai, China, [4] Department of Medicine, Geno Biotech Co. Ltd., Shanghai, China

OPEN ACCESS

Edited by:
Junji Uchino,
Kyoto Prefectural University of Medicine, Japan

Reviewed by:
Noriyoshi Sawabata,
Nara Medical University, Japan
Ryosuke Hamashima,
Kyoto Prefectural University of Medicine, Japan

***Correspondence:**
Hong Hu
huhong0997@163.com
Wei He
whe@genosaber.cn

Specialty section:
This article was submitted to Thoracic Oncology, a section of the journal Frontiers in Oncology

Received: 26 October 2020
Accepted: 11 December 2020
Published: 28 January 2021

Citation:
Li H, Li B, Pan Y, Zhang Y, Xiang J, Zhang Y, Sun Y, Yu X, He W and Hu H (2021) Preoperative Folate Receptor-Positive Circulating Tumor Cell Level Is a Prognostic Factor of Long Term Outcome in Non-Small Cell Lung Cancer Patients. Front. Oncol. 10:621435. doi: 10.3389/fonc.2020.621435

Background: Surgical resection is often the preferred treatment for non-small cell lung cancer (NSCLC) patients. Predictive biomarkers after surgery can help monitoring and treating patients promptly, so as to improve the clinical outcome. In this study, we evaluated one potential candidate biomarker, the folate receptor-positive circulating tumor cell (FR^+CTC), by investigating its prognostic and predictive significance in NSCLC patients who underwent surgery.

Methods: In this prospective, observational study, we enrolled NSCLC patients who were eligible to receive surgery. Prior to operation, peripheral blood was collected from each patient for an FR^+CTC analysis. FR^+CTCs were isolated by negative enrichment using immunomagnetic beads to deplete leukocytes and then quantitatively detected by a ligand-targeted polymerase chain reaction (PCR) method. These patients were then given standard care and were actively followed up for seven years. At the end of the follow-up period, the association between the FR^+CTC level and the prognosis in these patients was evaluated.

Results: Overall, preoperative FR^+CTC level was not significantly different among NSCLC patients with adenocarcinoma or non-adenocarcinoma subtypes (P = 0.24). However, between patients with low- and high-risk pathological adenocarcinoma subtypes, the preoperative FR^+CTC level was significantly different (P = 0.028). Further, patients with lower preoperative FR^+CTC level had longer relapse-free survival (RFS) and overall survival (OS) than those with higher preoperative FR^+CTC level (RFS: not reached vs. 33.3 months, P = 0.018; OS: not reached vs. 72.0 months, P = 0.13). In a multivariate COX regression analysis, FR^+CTC level (HR = 4.10; 95% CI, 1.23–13.64; P=0.022) and pathological stage (HR = 3.16; 95% CI, 1.79–10.14; P = 0.0011) were independent

prognostic factors of RFS. Moreover, FR^+CTC level together with adenocarcinoma subtypes provided additional information on risk for disease recurrence compared with FR^+CTC or adenocarcinoma subtype alone.

Conclusion: Our study demonstrated that the preoperative FR^+CTC level was a potential predictor for the prognosis of NSCLC patients underwent surgery. Further, when preoperative FR^+CTC level is considered together with primary tumor proliferation characteristics, its prognostic value supplements that of these conventional pathological features.

Keywords: circulating tumor cell, folate receptor, non-small cell lung cancer, surgery, prognosis

INTRODUCTION

Non-small cell lung cancer (NSCLC) is a leading cause of cancer-related death worldwide (1, 2). Surgical resection is usually the preferred treatment option for NSCLC patients who are eligible. In general, for patients with stages 0-I NSCLC, five-year survival rate can be as high as 90% (3). The five-year survival rate drops to 60 and 40% for stage II and III NSCLC, respectively (3). In fact, for patients with metastasis and recurrence, the 5-year survival rate is only 15% (3). However, even for early stage NSCLC patients with R0 resection, their prognosis may vary significantly. As such, identifying patients who are at risk of developing recurrence after surgery can help better manage these patients postoperatively and improve their clinical outcomes. However, few sensitive biomarkers to predict early recurrence or metastasis postoperatively are available, limiting the options and timeliness of treating high-risk patients during their follow-up.

The prospects of circulating tumor cells (CTCs) as a "liquid biopsy" diagnostic tool are attractive given the difficulties in obtaining adequate tissue for pathological analysis in selected individuals. Over the last decade, as more sensitive and reliable methods for CTC detection were developed and adopted in practice, the clinical utilities of CTC have been established and well accepted by practitioners worldwide (4, 5). For instance, CTC has proven a significant prognostic factor in metastatic breast cancer, colorectal cancer, prostate cancer, NSCLC, and a few other cancer types (6–9). In lung cancer, the use of CTC in guiding clinical decision making is frequent and productive. A number of studies have demonstrated that CTCs can be detected at all stages of lung cancer, and in certain instances even prior to the definitive identification of the primary cancer (10, 11). In other studies, CTCs have been shown to predict treatment responses and prognosis in NSCLC (11–13).

Because it is highly expressed in a number of solid tumor types, folate receptor (FR) has been extensively studied as a drug target (14). It has also been pursued as a biomarker for *in vivo* imaging of ovarian cancer and the development of CTC detection method (15). Previous studies showed that folate receptor-positive CTCs (FR^+CTCs) have both high sensitivity (72–78%) and specificity (82–90%) for the diagnosis of lung cancer (16, 17). Further, in patients with advanced, EGFR-positive NSCLC, high level of FR^+CTC (≥ 17 FU/3 ml) prior to first-line EGFR tyrosine kinase inhibitor treatment was associated with poorer prognosis compared to lower baseline level of FR^+CTC (< 17 FU/3 ml) (18). Similarly, in small cell lung cancer patients receiving first-line chemotherapy, those having a higher baseline FR^+CTC level prior to treatment initiation had significantly shorter progression free survival (19). In a study on early stage NSCLC patients underwent surgery, Zhou et al. demonstrated that preoperative FR^+CTC level was associated with tumor invasion and, when combined with maximum tumor diameter, could satisfactorily distinguish adenocarcinoma *in situ* (AIS) from minimally invasive adenocarcinoma (MIA) and invasive pulmonary adenocarcinoma (20).

In the present study, we evaluated preoperative FR^+CTC level in peripheral blood from NSCLC patients through the ligand-targeted (LT) PCR method as described previously (10, 11). A 7-year follow-up was conducted to assess the association between preoperative FR^+CTC level and long-term survival.

MATERIALS AND METHODS

Study Subjects

This is a single-center, prospective, observational study designed to assess the long-term prognostic value of FR^+CTC level in NSCLC patients. A total of 62 patients with NSCLC who were scheduled to receive surgical resection in Fudan University Shanghai Cancer Center were enrolled from May 2012 to August 2012. All patients received FR^+CTC analysis preoperatively. Inclusion criteria were as follows: 1) the patient was between 18 and 80 years old; 2) the final pathological diagnosis confirmed NSCLC; 3) the patient's Eastern Cooperative Oncology Group score was 0–2; 4) the initial surgical treatment was R0 resection; and 5) sufficient amount of peripheral blood sample was collected from the patient for FR^+CTC analysis within 1 day before surgery. Exclusion criteria were as follows: 1) the patient had other malignant tumors in the past; 2) the patient received adjuvant chemotherapy. Patients were regularly followed up for seven years after surgery and were provided with standard care during the follow-up period. Two

Abbreviations: AIS, adenocarcinoma in situ; FR^+CTC, folate receptor-positive circulating tumor cell; LT-PCR, ligand-targeted polymerase chain reaction; MIA, minimally invasive adenocarcinoma; NSCLC, non-small cell lung cancer; OS, overall survival; PCR, polymerase chain reaction; RFS, relapse-free survival; SD, standard deviation.

patients who had other malignant tumors in the past and six patients who had received adjuvant chemotherapy were excluded. In total, 54 patients were included in the prognosis analysis. The study was approved by the ethics committee of Shanghai Cancer Center Fudan University (050432-4-1911D) and written informed consent was obtained from all patients.

FR$^+$CTC Analysis

CTCs were analyzed and quantified by the use of the CytoploRare Kit (Genosaber Biotech, Shanghai, China). Three ml of peripheral blood were withdrawn into an EDTA-containing anti-coagulant tube from each subject one day before surgery. CTCs were enriched by lysis of erythrocytes followed by immuno-magnetic depletion of leukocytes from the whole blood. Then, FR$^+$CTCs in each sample were quantified by ligand-targeted polymerase chain reaction (LT-PCR) as previously described (11, 17, 21). The primer sequences were as follows: detection probe (an oligonucleotide that is conjugated to the tumor-specific ligand folic acid), 5'–CTCAA CTGGT GTCGT GGAGT CGGCA ATTCA GTTGA GGGTT CTAA–3'; forward primer, 5'–TATGA TTATG AGGCA TGA–3'; reverse primer, 5'–GGTGT CGTGG AGTCG–3'; TaqMan probe, 5'–FAM–CAGTT GAGGG TTC–MGB–3'. The LT-PCR reaction was performed on an ABI 7500 Real-time PCR under the following conditions: denaturation at 95 °C for 2 min, annealing at 40 °C for 30 s, extension at 72 °C for 30 s, and then cooling at 8 °C for 5 min; 40 cycles of denaturation at 95 °C for 10 s, annealing at 35 °C for 30 s, and extension at 72 °C for 10 s. A self-referenced CTC unit (denoted "FU") derived from standard curve was used to indicate the abundance of FR$^+$CTCs in 3 ml peripheral blood. For examples, 8.7 FU indicates 8.7 FU in 3 ml of whole blood. A serial of standards containing oligonucleotides (10^{-14} to 10^{-9} M, corresponding to 2 to 2×10^5 CTC units/3 ml blood) are used for FR$^+$CTC quantification.

Follow-Up

Postoperative treatment and follow-up were carried out according to the NCCN Guidelines for NSCLC. Patients' demographics, tumor characteristics, surgical information, and survival outcomes were collected in the medical record system. Imaging evaluation of recurrence or metastasis was performed for all patients during their follow-up according to the Response Evaluation Criteria in Solid Tumors (RECIST V 1.1, 2009) (22). Specifically, for Stage II and III patients, contrast chest CT and ultrasound of neck and abdomen were performed every 3 months. For Stage I patients, these examinations were performed every 6 months. All patients received brain MRI every 12 months. Telephone follow-up was conducted if an in-clinic follow-up visit was not feasible. Follow-up was conducted with each patient until death or September 2019. Relapse free survival (RFS) was defined as the period between the time of surgery and cancer recurrence or metastasis. Overall survival (OS) was defined as the period between the time of surgery and death from any cause.

Statistical Analysis

Clinicopathological characteristics including age, sex, tumor size, pathological type, tumor differentiation, adenocarcinoma subtype, and TNM stages were collected. According to the degree of invasion and adenocarcinoma subtype, patients were divided into two groups (Low Risk Group: AIS, MIA, lepidic, and acinar; High Risk Group: mucinous, micropapillary, and solid) (23, 24).

Categorical data were presented as counts and percentages and compared using Fisher's exact test. FR$^+$CTC levels were presented as medians with interquartile ranges and compared using Kruskal-Wallis test or Mann-Whitney U test. The most efficient cutoff values of FR+CTC level to stratify the study population into different prognostic groups were identified using maximally selected rank statistics (R package "maxstat" https://cran.r-project.org) (25). Survival curves were estimated by Kaplan-Meier method and compared using the log-rank test. Risk factors potentially affecting the survival were assessed by Cox proportional hazard regression analysis. Potentially significant covariates ($P < 0.2$) in the univariate analysis were selected for subsequent multivariate analysis, where a backward stepwise method was applied to investigate the effect of FR$^+$CTC level on survival.

All statistical analyses were performed using R 4.0.0 (R Foundation for Statistical Computing, Vienna, Austria, https://cran.r-project.org). A P value less than 0.05 was considered to be statistically significant.

RESULTS

The study included 54 NSCLC patients who underwent surgery between May and August 2012 and were regularly followed up postoperatively for up to 7 years (**Table 1**). The average (± standard deviation, SD) age of the patients was 60.6 ± 10.2 years old. The average tumor size of these patients was 3.1 ± 2.0 cm. Pathological examinations indicated that 9.3% of the patients had pre-invasive lesion, 61.1% had adenocarcinoma, 20.4% had squamous cell carcinoma, and 9.2% had large cell carcinoma or adenosquamous carcinoma (**Table 1**). There was no significant difference in the patients' age, gender, tumor size, pathological type (AIS/MIA, adenocarcinoma, squamous cell carcinoma, large cell carcinoma, and adenosquamous carcinoma), tumor differentiation, T stage, N stage, or pathological TNM stage between two FR$^+$CTC (High v. Low, as defined in Section 3.1) groups (**Table 1**).

By the last follow-up visit, 27 (50%) patients had developed recurrence and 21 (38.9%) patients had died. The median RFS was 55.2 months and the median OS was not reached. The five-year recurrence free survival and overall survival were 49.3 and 64.2%, respectively.

Prognostic Significance of FR$^+$CTC Levels

The optimal cutoff FR+CTC level was determined using the maximally selected rank statistics (MSRS). At the cutoff of 7.9 FU/3 ml blood, the MSLS reached its local maximum at 2.5 (**Figure 1A**, indicated by the dashed line). Hence, we chose 7.9 FU/3 ml as the optimal cutoff and separated patients into the High FR$^+$CTC Group (≥ 7.9 FU/3 ml) and the Low FR$^+$CTC Group (< 7.9 FU/3 ml).

The Kaplan–Meier curves of the High FR$^+$CTC Group and the Low FR$^+$CTC Group were provided in **Figures 1B** and **1C**.

TABLE 1 | Clinicopathological Characteristics of 54 NSCLC Patients.

Characteristics	Patients n = 54, No. (%)	FR $^{+}$CTC≤7.9 FU/3 ml n = 14, No. (%)	FR $^{+}$CTC>7.9 FU/3 ml n = 40, No. (%)	*P* value
Age (years-old, mean ± SD)	60.6 ± 10.2	60.4 ± 11.2	60.7 ± 10.0	>0.999
<60	21 (38.9%)	5 (35.7%)	16 (40.0%)	
≥60	33 (61.1%)	9 (64.3%)	24 (60.0%)	
Sex				0.7725
Male	30 (55.6%)	8 (57.1%)	22 (55.0%)	
Female	24 (44.4%)	6 (42.9%)	18 (45.0%)	
Tumor size (cm, mean ± SD)	3.1 ± 2.0			0.7812
<3 cm	27 (50%)	9 (64.3%)	18 (45.0%)	
≥3 cm	27 (50%)	5 (35.7%)	22 (55.0%)	
Pathological type				NA
AIS/MIA	5 (9.3%)	1 (7.1%)	4 (10%)	
invasive adenocarcinoma	33 (61.1%)	9 (64.3%)	24 (60.0%)	
squamous cell carcinoma	11 (20.4%)	2 (14.3%)	9 (22.5%)	
large cell carcinoma	3 (5.5%)	2 (14.3%)	1 (2.5%)	
adenosquamous carcinoma	2 (3.7%)	0	2 (5%)	
Tumor differentiation[a]				0.4330
High	7 (14.6%)	3 (25.0%)	4 (11.1%)	
Middle/Middle-Low	26 (54.2%)	5 (41.7%)	21 (58.3%)	
Low	15 (31.2%)	4 (33.3%)	11 (30.6%)	
Adenocarcinoma subtyp[a]				0.2374
Leptic/Acinar	18 (%)	7 (77.8%)	11 (50.0%)	
Mucinous/micropapillary/Solid	13 (%)	2 (22.2%)	11 (50.0%)	
T stage[a]				>0.9999
Tis+T1	26 (55.3%)	7 (58.3%)	19 (54.3%)	
T2+T3	21 (44.7%)	5 (41.7%)	16 (45.7%)	
N stage[a]				0.7337
N0	31 (59.6%)	7 (58.3%)	14 (46.7%)	
N1-2	21 (40.4%)	5 (41.7%)	16 (53.3%)	
Pathological TNM stage				>0.9999
0+I	26 (48.1%)	7 (50.0%)	19 (47.5%)	
II+III	26 (48.2%)	6 (42.9%)	20 (50.0%)	
IV	2 (3.7%)	1 (7.1%)	1 (2.5%)	

[a]*Not all patients have this information.*

NA, not applicable; AIS, adenocarcinoma in situ; MIA, minimally invasive adenocarcinoma.

The median RFS was 33.3 months in the High FR^{+}CTC Group and not reached in the Low FR^{+}CTC Group, respectively (HR = 3.81; 95% CI 1.70 to 8.54, $P = 0.018$) (**Figure 1B**). The median OS was 72.0 months in the High FR^{+}CTC and not reached in the Low FR^{+}CTC Group (HR, 2.51; 95% CI, 0.98 to 6.42; $P = 0.13$) (**Figure 1C**).

FR^{+}CTC Levels and Pathological Subtypes

In a subgroup analysis, we first divided patients into an Adenocarcinoma Group and an Other Group. The former included pathological subtypes adenocarcinoma, while the latter included pathological subtypes squamous cell carcinoma, large cell carcinoma, and adenosquamous carcinoma. There was no significant difference in FR^{+}CTC level between these two subgroups ($P = 0.24$). Patients in the Adenocarcinoma Group were further grouped into a High Risk Group and a Low Risk Group based on their pathological subtypes. The High Risk Group included invasive mucinous adenocarcinoma, and invasive adenocarcinoma predominantly showing micropapillary or solid growth pattern. The Low Risk Group included AIS, MIA, and invasive adenocarcinoma predominantly showing lepidic or acinar growth pattern. **Figure 2** showed the FR^{+}CTC levels in the two risk groups. The High Risk Group had significantly higher FR^{+}CTC level than the Low Risk Group [median = 11.3 FU/3 ml, interquartile range (9.0, 18.4) vs. median = 9.0 FU/3 ml, interquartile range (7.2, 12.6), $P = 0.028$].

Cox Regression Analysis

Univariate COX proportional hazard regression analysis for RFS suggested that survival rates differed between sex, tumor size, adenocarcinoma subtype, tumor differentiation, pathological TNM stage, and FR^{+}CTC level (**Figure 3A**). These variables were further included in multivariate COX regression analysis. Adenocarcinoma subtypes favorably affected RFS in the univariable model but was not enrolled into the multivariable model due to limited number of patients. As shown in **Figure 3C**, a multivariate COX proportional hazard regression model demonstrated that high FR^{+}CTC level (HR, 4.10; 95% CI, 1.23 to 13.64; $P = 0.022$) and stage II/III disease (HR, 4.26; 95% CI, 1.79 to 10.14; $P = 0.0011$) were associated with shorter RFS.

Similar analyses were performed on these variables for the OS. In the univariate analysis, the FR^{+}CTC level was also associated with the OS (**Figure 3B**). The multivariate regression analysis revealed that gender (HR, 0.36; 95% CI, 0.13 to 0.99, $P = 0.048$) was the only independent prognostic factor for the OS (**Figure 3C**). Patients with low FR^{+}CTC level or pathological TNM stage were associated with longer OS,

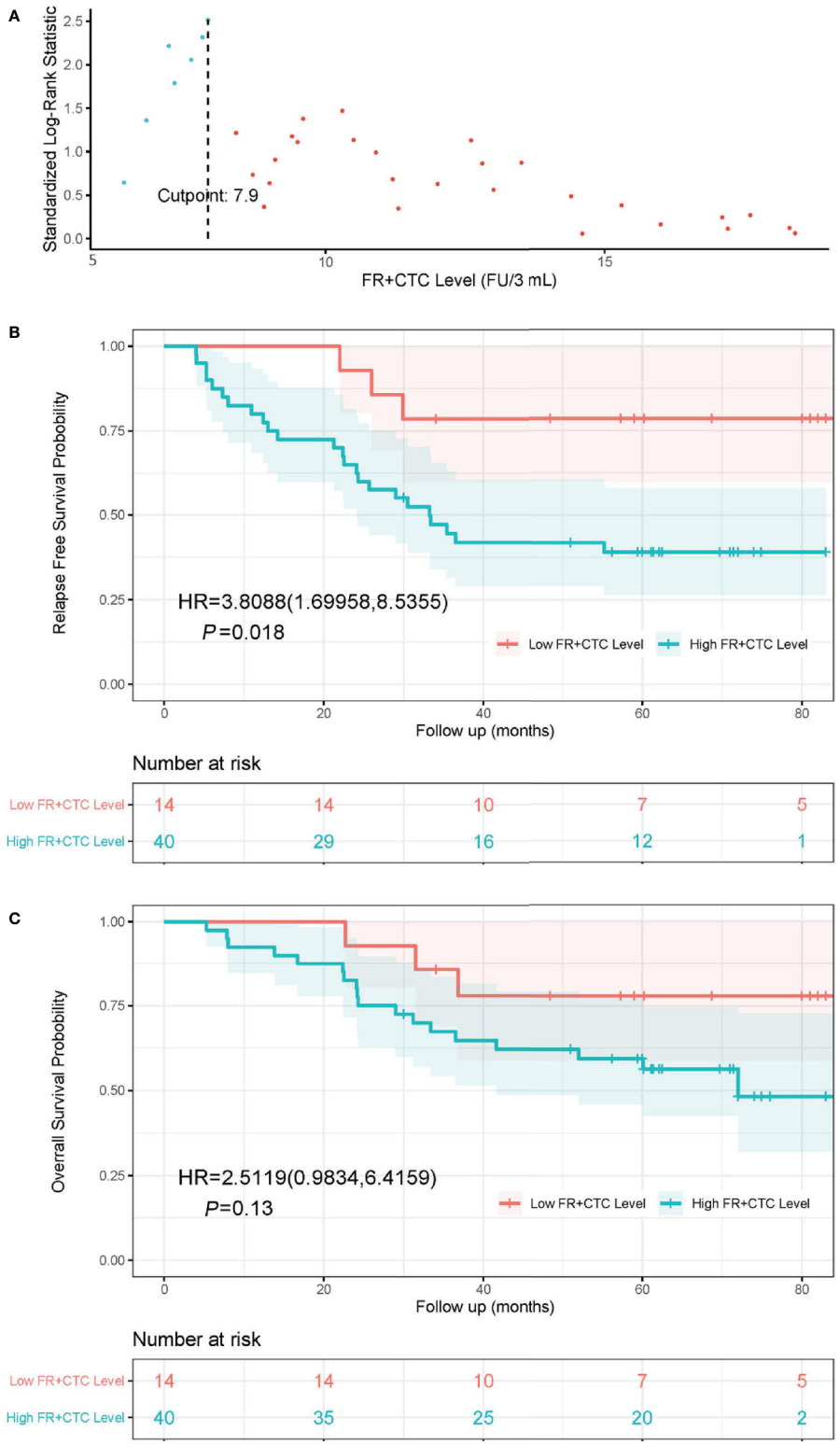

FIGURE 1 | The cutoff value of FR$^+$CTC level on prognosis and Kaplan-Meier curves of RFS and OS in NSCLC patients with different preoperative FR$^+$CTC level. **(A)** The standardized statistic of integer valued log-rank scores as a function of the hypothetical cutpoint of FR$^+$CTC level. The process obtains its maximum of 2.5 at 7.9 FU/3 ml as indicated by the dashed line. **(B)** RFS curve in patients with low (≤ 7.9 FU/3 ml) and high (> 7.9 FU/3 ml) FR$^+$CTC level. **(C)** OS curve in patients with low (≤ 7.9 FU/3 ml) and high (> 7.9 FU/3 ml) FR$^+$CTC level.

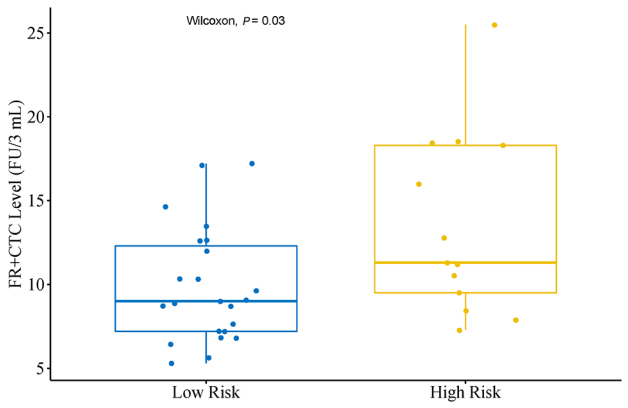

FIGURE 2 | Distribution of FR$^+$CTC level in lung adenocarcinoma patients with different subtypes. Low Risk Group (n = 23) including patients with adenocarcinoma in situ, minimally invasive adenocarcinoma and invasive adenocarcinoma predominantly showing lepidic or acinar growth pattern. High Risk Group (n = 13) including patients with invasive mucinous adenocarcinoma and invasive adenocarcinoma predominantly showing micropapillary or solid growth pattern.

although such an association did not reach statistical significance (P = 0.15 and 0.067, respectively, **Figure 3C**).

Prognostic Significance of Adenocarcinoma Subtypes

Lung adenocarcinoma patients with different pathological subtypes were grouped into a High Risk Group and a Low Risk Group as previously described. On the basis of a Kaplan-Meier analysis, the median RFS was 22.5 months in the High Risk Group and not reached in the Low Risk Group (HR, 3.53; 95% CI, 1.24 to 10.08; P = 0.0059; **Figure 4A**). The median OS was 41.6 months in the High Risk Group and not reached in the Low Risk Group (HR, 6.36; 95% CI, 1.74 to 23.23; P = 0.0016; **Figure 4B**).

Prognostic Analysis With Combination of Adenocarcinoma Subtypes and FR$^+$CTC Levels

To assess the combinational effect of adenocarcinoma subtypes (Low vs. High Risk as previously defined) and FR$^+$CTC levels on prognosis, lung adenocarcinoma patients were divided into four groups, Low Risk/Low FR$^+$CTC level (Group 1, n = 8), Low Risk/High FR$^+$CTC level (Group 2, n = 15), High Risk/Low FR$^+$CTC level (Group 3, n = 2), and High Risk/High FR$^+$CTC level (Group 4, n = 11). Group 3 was not included in the Kaplan–Meier analysis due to limited number of patients.

The 5-year RFS rates of patients in Group 1, 2, and 4 were 87.5, 58.7, and 18.2%, respectively. The median RFS in Group 4 was significantly shorter than that in Group 1 (22.5 vs. >84 months; HR = 10.75; 95% CI, 3.10 to 37.31; P = 0.0043, **Figure 5A**) and that in Group 2 (22.5 vs. 28.0 months; HR = 2.62; 95% CI, 0.92 to 7.50; P = 0.056, **Figure 5A**). Since most patients in Groups 1 and Group 2 were still alive at the end of the seven-year follow up, the OS of the three groups were not compared (**Figure 5B**).

DISCUSSION

Surgical resection is one of the most effective treatment options for NSCLC, especially for early stage tumors. Outcomes from surgery are usually satisfactory, with 5-year survival rate ranging from 73–100% for Stage 0/I and 12–65% for Stage II/III cancer (3). Nonetheless, up to 50% of patients eventually develop recurrence within two years. When recurrence occurs, the 5-year survival rate drops dramatically to approximately 15% (3). As shown in this study, of the 21 patients in whom recurrence or metastasis developed, the median time from recurrence or metastasis to death was only 1.9 months. Therefore, it is critical to identify patients who are more susceptible to recurrence and proactively manage those patients during follow up in order to improve their outcomes. Currently, however, there is a lack of biomarkers that can effectively predict recurrence or metastasis such that healthcare providers can provide prompt and adequate treatments (26).

TNM staging is one of the most commonly used predictors for lung cancer and its clinical utilities have been proven repeatedly. However, TNM staging has its limitations. For example, in TNM staging, only tumor size, the degree of tumor invasion, and the extent of lymph node metastasis are considered, while other important tumor characteristics are not included (3). Circulating biomarkers, by providing additional aspects of the tumor, can supplement traditional pathological findings and help better understand the biological nature and the clinical implications of the tumor. Serological biomarkers such as carcinoembryonic antigen (CEA) and cytokeratin 19 soluble fragment (CYFRA21-1) are tumor associated antigens (TAAs) commonly used for NSCLC, but their utilities in early stage tumors and prognosis of surgical outcome are limited (27). CTC and ctDNA, on the other hand, have recently emerged as more promising circulating tumor biomarkers due to their non-invasiveness and direct biological relevance to the tumor. Stratifying patients using these new biomarkers is not only more convenient, but also can be more effective (28). A meta-analysis by Liang, et al. suggested that both post-operative CTCs and ctDNA were promising predictive biomarkers of tumor recurrence in NSCLC patients (29). Of these two, CTCs are more likely to be detected in early stage cancers due to low abundance and quick turnover of ctDNA in systemic circulation (28).

During surgical resection, while the primary tumor and mediastinal lymph nodes have been resected and no distant metastases have been observed, it is still possible that visually undetectable micro-metastases exist, which can later develop into recurrence or metastasis (30). Circulating tumor cells are tumor cells that are shed from the primary tumor and enter the circulation (31). CTCs are thought to play an important role in disease progression and metastasis (31). The number of CTCs and the proportion of which that can escape immune surveillance, relocate, seed, and proliferate at a different

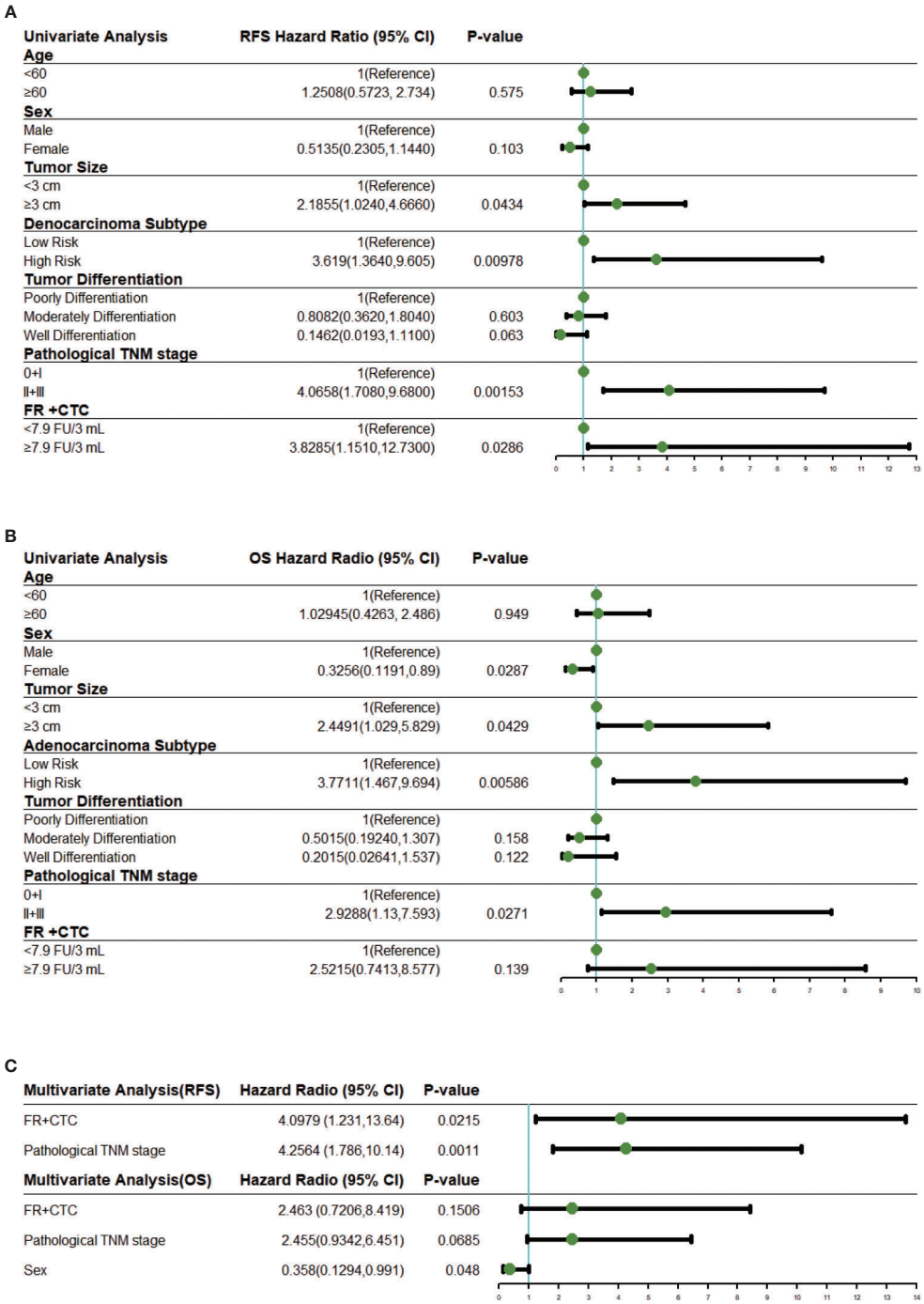

FIGURE 3 | Univariate and multivariate Cox regression analysis. **(A)** Forest plots showing the results of univariate regression analysis for RFS. **(B)** Forest plots showing the results of univariate regression analysis for OS. **(C)** Forest plots showing the results of multivariate regression analysis for RFS and OS. The x axis represents the hazard radio, and the reference line (blue) and significance were calculated using a Cox proportional hazards model. Error bars, 95% CIs. CI, confidential interval.

location of the body likely affect their ability to induce disease progression and metastasis (32, 33). For these reasons, CTC may be a potentially potent prognostic factor of disease recurrence and/or metastasis after lung cancer surgery.

The association between CTC and surgical outcome of resectable NSCLC patients has been investigated using different CTC detection technologies. In several studies, the authors suggested that postoperative CTC was an independent

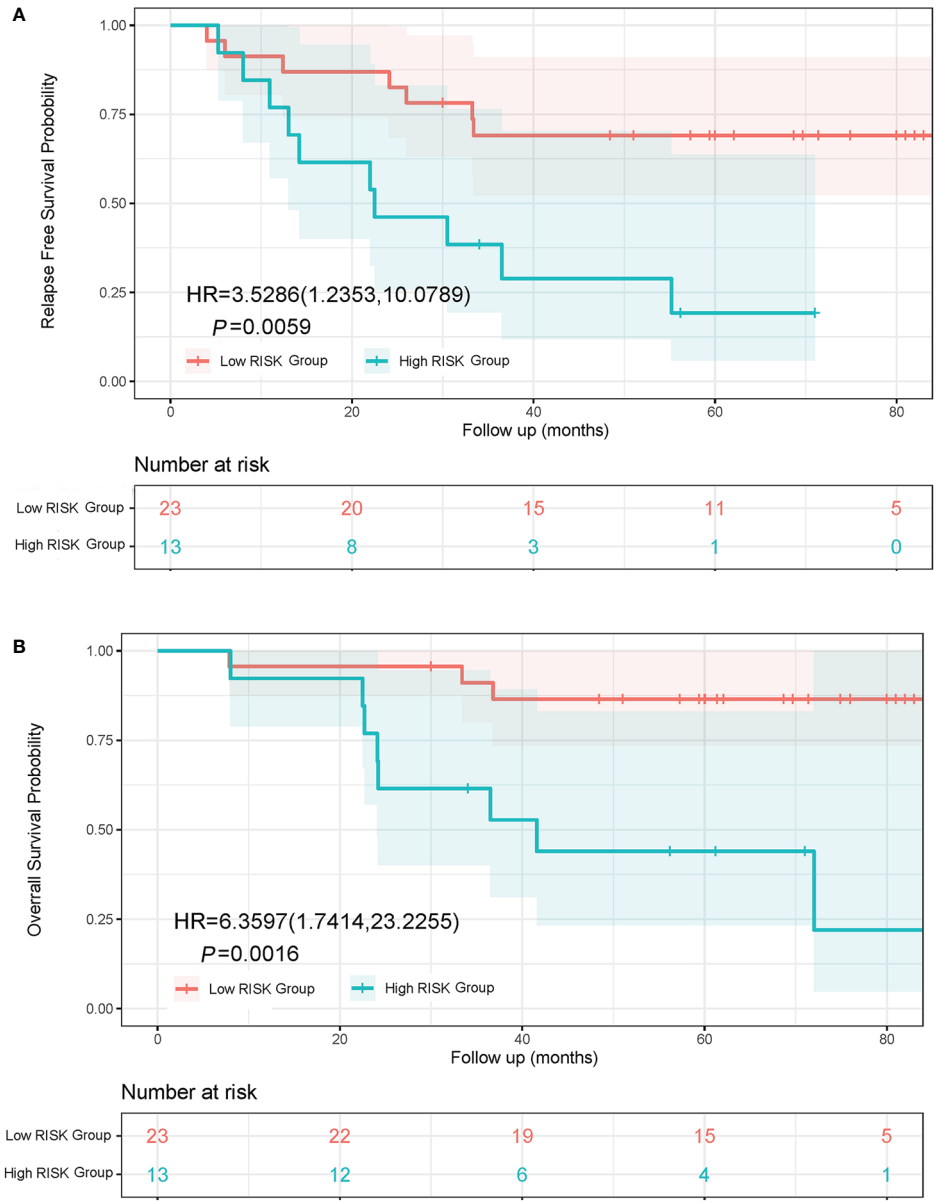

FIGURE 4 | Kaplan-Meier curves of RFS and OS in lung adenocarcinoma patients with different subtypes. **(A)** RFS curve of Low Risk Group and High Risk Group. **(B)** OS curve of Low Risk Group and High Risk Group. The Low Risk Group included adenocarcinoma in situ, minimally invasive adenocarcinoma, and invasive adenocarcinoma predominantly showing lepidic or acinar growth pattern. The High Risk Group included invasive mucinous adenocarcinoma, and invasive adenocarcinoma predominantly showing papillary or solid growth pattern.

prognostic factor of DFS, but preoperative CTC was not (13, 34–36). Murlidhar et al. studied 36 patients with resectable NSCLC (stages I–III) and found that presence of clusters in preoperative peripheral blood predicted a trend toward poorer prognosis (37). Li et al. suggested that the number of CTCs in either peripheral blood or pulmonary vein blood was an independent risk factor for tumor free survival (TFS) and OS in NSCLC patients receiving surgical resection (38). Crosbie et al. found that CTC enumeration in pulmonary vein and peripheral blood combined during the operation better identifies NSCLC patients with a higher risk of recurrence than in peripheral blood alone (12). Chem et al. demonstrated that early-disseminating pulmonary venous CTCs were responsible for disease relapse (39).

For early stage lung cancer, sampling pulmonary vein blood for CTC analysis has been considered a better strategy due to the scarcity of CTCs and the suboptimal sensitivity of existing CTC detection technologies. However, intraoperative pulmonary vein blood collection is much more complicated than peripheral blood collection. Further, peripheral blood can be conveniently and repeatedly collected during a patient's

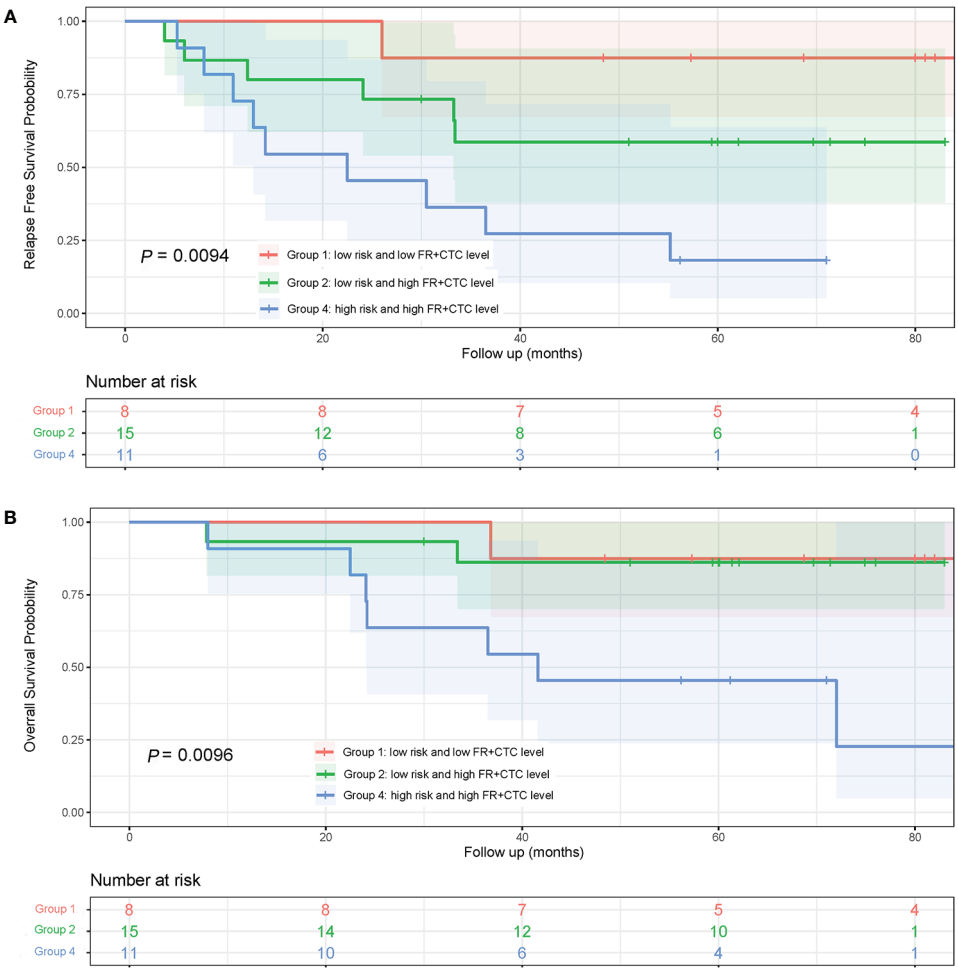

FIGURE 5 | Kaplan-Meier curves of RFS and OS in lung adenocarcinoma patients with different subtypes and FR+CTC level combination. **(A)** RFS curves of patients with different risk of adenocarcinoma subtypes and FR$^+$CTC level. **(B)** patients with different risk of adenocarcinoma subtypes and FR$^+$CTC level.

follow-up. Thus, peripheral blood would be the preferred source for CTC isolation and identification in clinical practice.

The negative enrichment and LT-PCR based FR$^+$CTC detection has proven a sensitive method for CTC analysis in peripheral blood, with sensitivity of 70–90% for different stages of NSCLC (10, 11, 17, 40). Previous studies have also demonstrated that the FR$^+$CTC is associated with tumor invasiveness and risk of recurrence for resectable NSCLC patients. In a multi-center study involving 382 patients, Zhou et al. found that the preoperative FR$^+$CTC level was significantly lower in AIS and MIA than that in invasive pulmonary adenocarcinoma, the latter is known to have worse prognosis (20). In another study assessing different surgical procedures for early stage NSCLC patients, Wei et al. demonstrated that the vein-first ligation technique led to a significantly higher decrease in FR$^+$CTC level after surgery than the artery-first ligation technique (41). Further, Wei et al. compared the long-term outcome of the two surgical procedures retrospectively and found that the former had better 5-year OS, DFS, and lung cancer specific survival (41). While these studies implicate that the FR$^+$CTC level and its change pre- and post-surgery may be prognostic of patient outcome after surgical resection, such evidence is not direct as the studies lacked long-term outcome from the patients whose FR$^+$CTC levels were measured.

To our knowledge, our study was the first one to assess the prognostic value of FR$^+$CTC in long-term surgical outcome of resectable NSCLC patients. We demonstrated that preoperative FR$^+$CTCs >7.9 FU/3 ml was an independent prognostic factor of DFS after R0 resection of NSCLC patients with a 7-year follow-up. High levels of preoperative FR$^+$CTC were also associated with a numerically shorter OS although the association was not statistically significant.

The five-year survival rates of the postoperative patients with AIS, MIA, and lepidic predominant adenocarcinoma were approximately 100, 100, and 90%, respectively, while those of other subtypes of adenocarcinoma including mucinous, micropapillary, and solid subtype were significantly lower (42). In this study, we observed a similar trend. Further, when patients

were classified into high- and low-risk groups based on these pathological subtypes, a significant higher FR^+CTC level was seen in the high-risk group (including mucinous, micropapillary, and solid). Such a finding was not surprising as the pathological subtypes reflect tumor invasiveness or proliferation characteristics and CTC level also reflects active tumor burden. Interestingly, when both FR^+CTC level and adenocarcinoma subtypes were assessed, both factors were significantly associated with long-term surgical outcome. Furthermore, patients with both high FR^+CTC level and high risk pathological subtypes had a nine-fold increase in risk of disease recurrence than those with both low FR^+CTC level and low risk pathological subtypes. These results suggest that FR^+CTC provides additional insights in recurrence risk beyond those from conventional pathological evaluation.

The present study has several limitations. First, the study was conducted in a single center and has limited sample size in part due to difficulties in patient enrollment at the initiation of the study and censoring during the 7-year follow-up. As such, the results from the study requires further validation in larger, multi-center investigations. Further, all patients received FR+CTC analysis prior to surgery but lacked longitudinal assessment of FR+CTC levels post-treatment, either during postoperative hospital stay or subsequent follow-ups. Therefore, the prognostic effect of the dynamic change in FR+CTC level cannot be assessed. Nor can the association between the degree or timing of FR+CTC change and tumor recurrence or progression be evaluated. These questions are of particular interest to thoracic surgeons as they provide direct insights on how to better manage NSCLC patients post-operation and should be addressed in future larger, multi-center studies.

In conclusion, our study demonstrated that preoperative FR^+CTC level was a potential predictor for the prognosis in NSCLC patients underwent surgery. Interestingly, while baseline FR^+CTC level was associated with primary tumor invasion or proliferation characteristics, its prognostic value appears to go beyond those well-known pathological features and thus warrants further investigation in larger, systematic studies.

DATA AVAILABILITY STATEMENT

The raw data supporting the conclusions of this article will be made available by the authors, without undue reservation.

ETHICS STATEMENT

The studies involving human participants were reviewed and approved by Shanghai Cancer Center Fudan University (050432-4-1911D). The patients/participants provided their written informed consent to participate in this study. Written informed consent was obtained from the individual(s) for the publication of any potentially identifiable images or data included in this article.

AUTHOR CONTRIBUTIONS

HL, WH, and HH made substantial contributions to the conception or design of the work. YawZ, YS, and XY collected and detected the samples. HL, BL, YanZ, YP, and JX acquired the data. HL, BL, YanZ, and WH analyzed or interpreted the data. HL, BL, XY, and HH drafted the work or revised it critically for important intellectual content. All authors contributed to the article and approved the submitted version.

FUNDING

This work was supported by the National Natural Science Foundation of China (82003285) and Shanghai Anticancer Association EYAS project (SACA-CY1A03).

ACKNOWLEDGMENTS

HH takes responsibility for the content of the manuscript, including the data and analysis.

REFERENCES

1. Siegel RL, Miller KD, Jemal A. Cancer statistics, 2020. *Ca-a Cancer J Clin* (2020) 70(1):7–30. doi: 10.3322/caac.21590
2. Chen W, Zheng R, Baade PD, Zhang S, Zeng H, Bray F, et al. Cancer Statistics in China, 2015. *Ca-a Cancer J Clin* (2016) 66(2):115–32. doi: 10.3322/caac.21338
3. Goldstraw P, Chansky K, Crowley J, Rami-Porta R, Asamura H, Eberhardt WE, et al. The IASLC Lung Cancer Staging Project: Proposals for Revision of the TNM Stage Groupings in the Forthcoming (Eighth) Edition of the TNM Classification for Lung Cancer. *J Thorac Oncol* (2016) 11(1):39–51. doi: 10.1016/j.jtho.2015.09.009
4. Divella R, Daniele A, Abbate I, Bellizzi A, Savino E, Simone G, et al. The presence of clustered circulating tumor cells (CTCs) and circulating cytokines define an aggressive phenotype in metastatic colorectal cancer. *Cancer Causes Control* (2014) 25(11):1531–41. doi: 10.1007/s10552-014-0457-4
5. Magbanua MJM, Rugo HS, Wolf DM, Hauranieh L, Roy R, Pendyala P, et al. Expanded Genomic Profiling of Circulating Tumor Cells in Metastatic Breast Cancer Patients to Assess Biomarker Status and Biology Over Time (CALGB 40502 and CALGB 40503, Alliance). *Clin Cancer Res* (2018) 24(6):1486–99. doi: 10.1158/1078-0432.Ccr-17-2312
6. Cristofanilli M, Budd GT, Ellis MJ, Stopeck A, Matera J, Miller MC, et al. Circulating tumor cells, disease progression, and survival in metastatic breast cancer. *N Engl J Med* (2004) 351(8):781–91. doi: 10.1056/NEJMoa040766
7. Cohen SJ, Punt CJA, Iannotti N, Saidman BH, Sabbath KD, Gabrail NY, et al. Relationship of circulating tumor cells to tumor response, progression-free survival, and overall survival in patients with metastatic colorectal cancer. *J Clin Oncol* (2008) 26(19):3213–21. doi: 10.1200/jco.2007.15.8923
8. Scher HI, Jia X, de Bono JS, Fleisher M, Pienta KJ, Raghavan D, et al. Circulating tumour cells as prognostic markers in progressive, castration-resistant prostate cancer: a reanalysis of IMMC38 trial data. *Lancet Oncol* (2009) 10(3):233–9. doi: 10.1016/s1470-2045(08)70340-1
9. Krebs MG, Sloane R, Priest L, Lancashire L, Hou J-M, Greystoke A, et al. Evaluation and Prognostic Significance of Circulating Tumor Cells in Patients With Non-Small-Cell Lung Cancer. *J Clin Oncol* (2011) 29(12):1556–63. doi: 10.1200/jco.2010.28.7045
10. Lou J, Ben S, Yang G, Liang X, Wang X, Ni S, et al. Quantification of Rare Circulating Tumor Cells in Non-Small Cell Lung Cancer by Ligand-Targeted PCR. *PLoS One* (2013) 8(12):e80458. doi: 10.1371/journal.pone.0080458

11. Yu Y, Chen Z, Dong J, Wei P, Hu R, Zhou C, et al. Folate Receptor-Positive Circulating Tumor Cells as a Novel Diagnostic Biomarker in Non-Small Cell Lung Cancer. *Trans Oncol* (2013) 6(6):697–702. doi: 10.1593/tlo.13535
12. Crosbie PAJ, Shah R, Krysiak P, Zhou C, Morris K, Tugwood J, et al. Circulating Tumor Cells Detected in the Tumor-Draining Pulmonary Vein Are Associated with Disease Recurrence after Surgical Resection of NSCLC. *J Thorac Oncol* (2016) 11(10):1793–7. doi: 10.1016/j.jtho.2016.06.017
13. Bayarri-Lara C, Ortega FG, Ladron de Guevara AC, Puche JL, Ruiz Zafra J, de Miguel-Perez D, et al. Circulating Tumor Cells Identify Early Recurrence in Patients with Non-Small Cell Lung Cancer Undergoing Radical Resection. *PLoS One* (2016) 11(2):e0148659. doi: 10.1371/journal.pone.0148659
14. Assaraf YG, Leamon CP, Reddy JA. The folate receptor as a rational therapeutic target for personalized cancer treatment. *Drug Resist U* (2014) 17(4-6):89–95. doi: 10.1016/j.drup.2014.10.002
15. He W, Wang H, Hartmann LC, Cheng J-X, Low PS. In vivo quantitation of rare circulating tumor cells by multiphoton intravital flow cytometry. *Proc Natl Acad Sci U S A* (2007) 104(28):11760–5. doi: 10.1073/pnas.0703875104
16. Wang L, Wu C, Qiao L, Yu W, Guo Q, Zhao M, et al. Clinical Significance of Folate Receptor-positive Circulating Tumor Cells Detected by Ligand-targeted Polymerase Chain Reaction in Lung Cancer. *J Cancer* (2017) 8 (1):104–10. doi: 10.7150/jca.16856
17. Chen X, Zhou F, Li X, Yang G, Zhang L, Ren S, et al. Folate Receptor-Positive Circulating Tumor Cell Detected by LT-PCR-Based Method as a Diagnostic Biomarker for Non-Small-Cell Lung Cancer. *J Thorac Oncol* (2015) 10 (8):1163–71. doi: 10.1097/jto.0000000000000606
18. Jiang T, Zhao J, Zhao C, Li X, Shen J, Zhou J, et al. Dynamic Monitoring and Predictive Value of Circulating Tumor Cells in EGFR-Mutated Advanced Non-Small-Cell Lung Cancer Patients Treated With First-Line EGFR Tyrosine Kinase Inhibitors. *Clin Lung Cancer* (2019) 20(2):124–+. doi: 10.1016/j.cllc.2018.11.014
19. Shen J, Zhao J, Jiang T, Li X, Zhao C, Su C, et al. Predictive and prognostic value of folate receptor-positive circulating tumor cells in small cell lung cancer patients treated with first-line chemotherapy. *Oncotarget* (2017) 8 (30):49044–52. doi: 10.18632/oncotarget.17039
20. Zhou Q, Geng Q, Wang L, Huang J, Liao M, Li Y, et al. Value of folate receptor-positive circulating tumour cells in the clinical management of indeterminate lung nodules: A non-invasive biomarker for predicting malignancy and tumour invasiveness. *Ebiomedicine* (2019) 41:236–43. doi: 10.1016/j.ebiom.2019.02.028
21. He W, Kularatne SA, Kalli KR, Prendergast FG, Amato RJ, Klee GG, et al. Quantitation of circulating tumor cells in blood samples from ovarian and prostate cancer patients using tumor-specific fluorescent ligands. *Int J Cancer* (2008) 123(8):1968–73. doi: 10.1002/ijc.23717
22. Eisenhauer EA, Therasse P, Bogaerts J, Schwartz LH, Sargent DJ, Ford RC, et al. New response evaluation criteria in solid tumours: revised RECIST guideline (version 1.1). *Eur J Cancer* (2009) 45(2):228–47. doi: 10.1016/j.ejca.2008.10.026
23. Nakamura H, Saji H, Shinmyo T, Tagaya R, Kurimoto N, Koizumi H, et al. Close association of IASLC/ATS/ERS lung adenocarcinoma subtypes with glucose-uptake in positron emission tomography. *Lung Cancer* (2015) 87 (1):28–33. doi: 10.1016/j.lungcan.2014.11.010
24. Choi SH, Jeong JY, Lee SY, Shin KM, Jeong SY, Park TI, et al. Clinical implication of minimal presence of solid or micropapillary subtype in early-stage lung adenocarcinoma. *Thorac Cancer* (2020). doi: 10.1111/1759-7714.13754
25. Hothorn T, Lausen B. On the exact distribution of maximally selected rank statistics. *Comput Stat Data Anal* (2003) 43(2):121–37. doi: 10.1016/S0167-9473(02)00225-6
26. Uhra JW, Pantel K. Controversies in clinical cancer dormancy. *Proc Natl Acad Sci U S A* (2011) 108(30):12396–400. doi: 10.1073/pnas.1106613108
27. Reinmuth N, Brandt B, Semik M, Kunze W, Achatzy R, Scheld HH, et al. Prognostic impact of Cyfra21-1 and other serum markers in completely resected non-small cell lung cancer. *Lung Cancer* (2002) 36(3):265–70. doi: 10.1016/s0169-5002(02)00009-0
28. Crosbie PAJ, Shah R, Summers Y, Dive C, Blackhall F. Prognostic and predictive biomarkers in early stage NSCLC: CTCs and serum/plasma markers. *Trans Lung Cancer Res* (2013) 2(5):382–97. doi: 10.3978/j.issn.2218-6751.2013.09.02
29. Liang H, Huang J, Wang B, Liu Z, He J, Liang W. The role of liquid biopsy in predicting post-operative recurrence of non-small cell lung cancer. *J Thorac Dis* (2018) 10:S838–S45. doi: 10.21037/jtd.2018.04.08
30. Brunsvig PF, Flatmark K, Aamdal S, Høifødt H, Le H, Jakobsen E, et al. Bone marrow micrometastases in advanced stage non-small cell lung carcinoma patients. *Lung Cancer* (2008) 61(2):170–6. doi: 10.1016/j.lungcan.2007.12.018
31. Chaffer CL, Weinberg RA. A perspective on cancer cell metastasis. *Science* (2011) 331(6024):1559–64. doi: 10.1126/science.1203543
32. Aguirre-Ghiso JA. Models, mechanisms and clinical evidence for cancer dormancy. *Nat Rev Cancer* (2007) 7(11):834–46. doi: 10.1038/nrc2256
33. Plaks V, Koopman CD, Werb Z. Circulating Tumor Cells. *Science* (2013) 341 (6151):1186–8. doi: 10.1126/science.1235226
34. De Miguelperez D, Bayarrilara CI, Ortega FG, Russo A, Rodriguez MJM, Alvarezcubero MJ, et al. Post-Surgery Circulating Tumor Cells and AXL Overexpression as New Poor Prognostic Biomarkers in Resected Lung Adenocarcinoma. *Cancers* (2019) 11(11):1750. doi: 10.3390/cancers11111750
35. Chudasama D, Barr J, Beeson J, Beddow E, McGonigle N, Rice A, et al. Detection of Circulating Tumour Cells and Survival of Patients with Non-small Cell Lung Cancer. *Anticancer Res* (2017) 37(1):169–73. doi: 10.21873/anticanres.11302
36. Sawabata N, Funaki S, Hyakutake T, Shintani Y, Fujiwara A, Okumura M. Perioperative circulating tumor cells in surgical patients with non-small cell lung cancer: does surgical manipulation dislodge cancer cells thus allowing them to pass into the peripheral blood? *Surg Today* (2016) 46(12):1402–9. doi: 10.1007/s00595-016-1318-4
37. Murlidhar V, Reddy RM, Fouladdel S, Zhao L, Ishikawa MK, Grabauskiene S, et al. Poor Prognosis Indicated by Venous Circulating Tumor Cell Clusters in Early-Stage Lung Cancers. *Cancer Res* (2017) 77(18):5194–206. doi: 10.1158/0008-5472.can-16-2072
38. Li Y, Cheng X, Chen Z, Liu Y, Liu Z, Xu S. Circulating tumor cells in peripheral and pulmonary venous blood predict poor long-term survival in resected non-small cell lung cancer patients. *Sci Rep* (2017) 7:4971. doi: 10.1038/s41598-017-05154-x
39. Chemi F, Rothwell DG, McGranahan N, Gulati S, Abbosh C, Pearce SP, et al. Pulmonary venous circulating tumor cell dissemination before tumor resection and disease relapse. *Nat Med* (2019) 25(10):1534–+. doi: 10.1038/s41591-019-0593-1
40. Xue Y, Cong W, Xie S, Shu J, Feng G, Gao H. Folate-receptor-positive circulating tumor cells as an efficacious biomarker for the diagnosis of small pulmonary nodules. *J Cancer Res Ther* (2018) 14(7):1620–6. doi: 10.4103/jcrt.JCRT_905_17
41. Wei S, Guo C, He J, Tan Q, Mei J, Yang Z, et al. Effect of Vein-First vs Artery-First Surgical Technique on Circulating Tumor Cells and Survival in Patients With Non-Small Cell Lung Cancer A Randomized Clinical Trial and Registry-Based Propensity Score Matching Analysis. *JAMA Surg* (2019) 154(7): e190972. doi: 10.1001/jamasurg.2019.0972
42. Yoshizawa A, Motoi N, Riely GJ, Sima CS, Gerald WL, Kris MG, et al. Impact of proposed IASLC/ATS/ERS classification of lung adenocarcinoma: prognostic subgroups and implications for further revision of staging based on analysis of 514 stage I cases. *Modern Pathol* (2011) 24(5):653–64. doi: 10.1038/modpathol.2010.232

Conflict of Interest: XY and WH were employed by the company Geno Biotech Co. Ltd.

The remaining authors declare that the research was conducted in the absence of any commercial or financial relationships that could be construed as a potential conflict of interest.

Copyright © 2021 Li, Li, Pan, Zhang, Xiang, Zhang, Sun, Yu, He and Hu. This is an open-access article distributed under the terms of the Creative Commons Attribution License (CC BY). The use, distribution or reproduction in other forums is permitted, provided the original author(s) and the copyright owner(s) are credited and that the original publication in this journal is cited, in accordance with accepted academic practice. No use, distribution or reproduction is permitted which does not comply with these terms.

frontiers in Oncology

SYSTEMATIC REVIEW
published: 01 March 2021
doi: 10.3389/fonc.2021.631949

Immune-Related Adverse Events Predict the Efficacy of Immune Checkpoint Inhibitors in Lung Cancer Patients: A Meta-Analysis

Donghui Wang[1], Cen Chen[2], Yanli Gu[1], Wanjun Lu[3], Ping Zhan[3], Hongbing Liu[3], Tangfeng Lv[3], Yong Song[3] and Fang Zhang[1,3*]*

[1] Department of Respiratory and Critical Care Medicine, Jinling Hospital, Nanjing Medical University, Nanjing, China, [2] Department of Respiratory and Critical Care Medicine, Jinling Hospital, The First School of Clinical Medicine, Southern Medical University, Nanjing, China, [3] Department of Respiratory and Critical Care Medicine, Jinling Hospital, Medical School of Nanjing University, Nanjing, China

OPEN ACCESS

Edited by:
Junji Uchino,
Kyoto Prefectural University of Medicine, Japan

Reviewed by:
Yunfang Yu,
Sun Yat-Sen Memorial Hospital, China
Michael Thomas Mark,
Cantonal Hospital of Graubünden, Switzerland

***Correspondence:**
Fang Zhang
zhangfanglab@163.com
Yong Song
yong.song@nju.edu.cn

Specialty section:
This article was submitted to Thoracic Oncology, a section of the journal Frontiers in Oncology

Received: 21 November 2020
Accepted: 22 January 2021
Published: 01 March 2021

Citation:
Wang D, Chen C, Gu Y, Lu W, Zhan P, Liu H, Lv T, Song Y and Zhang F (2021) Immune-Related Adverse Events Predict the Efficacy of Immune Checkpoint Inhibitors in Lung Cancer Patients: A Meta-Analysis. Front. Oncol. 11:631949. doi: 10.3389/fonc.2021.631949

Background: Immune-related adverse events (irAEs) have been reported to be associated with the efficacy of immunotherapy. Herein, we conducted a meta-analysis to demonstrate that irAEs could predict the efficacy of immune checkpoint inhibitors (ICIs) in lung cancer patients.

Methods: Literature on the correlation between irAEs and the efficacy of immunotherapy in lung cancer patients were searched to collect the data on objective response rate (ORR), overall survival (OS), or progression-free survival (PFS) of the patients. These data were incorporated into the meta-analysis.

Results: A total of 34 records encompassing 8,115 patients were examined in this study. The irAEs occurrence was significantly associated with higher ORR {risk ratio (RR): 2.43, 95% confidence interval (CI) [2.06–2.88], $p < 0.00001$} and improved OS {hazard ratio (HR): 0.51, 95% CI [0.43–0.61], $p < 0.00001$}, and PFS (HR: 0.50, 95% CI [0.44–0.57], $p < 0.00001$) in lung cancer patients undergoing ICIs. Subgroup analysis revealed that OS was significantly longer in patients who developed dermatological (OS: HR: 0.53, 95%CI [0.42–0.65], $p < 0.00001$), endocrine (OS: HR: 0.55, 95%CI [0.45–0.67], $p < 0.00001$), and gastrointestinal irAEs (OS: HR: 0.58, 95%CI [0.42–0.80], $p = 0.0009$) than in those who did not. However, hepatobiliary, pulmonary, and high-grade (≥3) irAEs were not correlated with increased OS and PFS.

Conclusion: The occurrence of irAEs in lung cancer patients, particularly dermatological, endocrine, and gastrointestinal irAEs, is a predictor of enhanced ICIs efficacy.

Keywords: immune-related adverse events (irAEs), efficacy, immune checkpoint inhibitors (ICIS), lung cancer, meta-analysis

INTRODUCTION

Immunotherapy has led to unprecedented improvements in the life expectancy of cancer patients, particularly those with lung cancer, by priming the immune system to fight against the tumor cells. ICIs target cytotoxic T-lymphocyte-associated protein 4 (CTLA-4) and programmed cell death-1 (PD-1)/programmed cell death ligand-1 (PD-L1), which are critical molecules that negatively regulate the T-cell activity and aid the tumor cells in evading immune surveillance. However, owing to the heightened immune response, the irAEs caused by ICIs are frequent and ineluctable. A meta-analysis showed that the probability of irAE incidence ranges from 54% to 76% and varies according to the types of ICIs (1). Any organ system could be involved, including the skin, endocrine glands, gastrointestinal tract, liver, pulmonary, and, less commonly, the cardiovascular and central nervous systems. Although the underlying mechanism has not been completely elucidated, increased T-cell activity, B-cell-mediated autoantibody production, and cross-reactive tumoral antigenicity have been suggested to be involved in the occurrence of irAEs (2).

The irAEs inevitably affect the treatment and prognosis of the patients. Once these events occur, clinicians adopt different management strategies according to the types and grades of irAEs. The National Comprehensive Cancer Network (NCCN), American Society of Clinical Oncology (ASCO), and European Society of Medical Oncology (ESMO) have issued guidelines for the management of irAEs and have provided comprehensive general treatment algorithms for the clinicians (3, 4). In terms of prognosis, discontinuing ICIs may affect the life expectancy of the patients. However, the clinicians have noticed that patients who developed irAEs were more likely to benefit from ICIs. Meanwhile, theoretically, both antitumor and anti-self-adverse effects could result when the immunity is enhanced. Thus, there seems to exist a correlation between the occurrence of irAEs and the efficacy of immunotherapy.

A systemic review of melanoma has been conducted, which revealed that irAEs could predict survival and response in patients treated with ICIs (5), however, comprehensive meta-analyses focusing on lung cancer have not yet been performed. Herein, our work aimed to elucidate whether the occurrence of irAEs could predict the efficacy of ICIs in patients with lung cancer. Furthermore, we performed a subgroup analysis to decipher the association of organ-specific and grade-specific irAEs with the clinical outcomes of the patients.

MATERIALS AND METHODS

Search Strategy

PubMed, Embase, and Cochrane Library databases from inception to October 15, 2020 were searched to locate eligible studies reporting the association between the efficacy of ICIs and irAEs in lung cancer patients undergoing immunotherapy. The search strategy was "[immune-related (Title/Abstract)] AND [adverse events (Title/Abstract)] AND {[lung cancer (Title)] OR [SCLC (Title)]}." The citations of relevant articles were also reviewed in case of omission. The language was restricted to English, and conference abstracts were also included.

Inclusion and Exclusion Criteria

The studies that met the following criteria were included in the review:

1. Involving patients who were diagnosed with lung cancer.
2. Involving patients who were treated with CTLA-4, PD-1, or PD-L1 inhibitors.
3. Studies reporting the association between irAEs and ICIs efficacy.
4. Studies that provided data on ORR, OS, or PFS of the patients.
5. Studies that provided the HR of OS or PFS in patients who developed irAEs versus patients without irAEs and 95% CI.
6. Studies published in the English language.

The exclusion criteria of the studies to be included in the review were as follows:

1. Studies that provided OS and PFS, but not HR, or provided HR and P-value, but not 95% CI.
2. Duplicated data or overlapping study populations (the most recent report was included).
3. The adverse events were not caused by the use of ICIs.

Data Collection and Quality Assessment

DW and CC independently extracted the data from the included studies. The following data were extracted: author, year of publication, trial design, landmark analysis, sample size, irAE type and grade, ORR of patients with and without irAEs, HRs, and 95% CIs for OS or PFS of patients with global, organ-specific, and grade-specific irAEs. Several studies provided both multivariate and univariate HRs, and we selected the former. If studies provided HRs with and without landmark analysis, we chose the former. If studies provided the HRs of global as well as organ-specific irAEs, we opted for the former. If studies provided the HRs of both grade-specific and all-grade irAEs, we selected the latter. The Newcastle-Ottawa scale (NOS) criteria were applied to assess the quality of the included studies. Discrepancies were resolved by discussions among DW, CC, and YG.

Data Analyses

Review Manager (RevMan) Version 5.4 (Nordic Cochrane Center, Copenhagen, Denmark) was used to perform the statistical analyses. The log HRs of irAEs versus non-irAEs were obtained by calculating RevMan. If the HR of non-irAEs versus irAEs was provided instead of the opposite comparison, the HR and 95% CI of irAEs versus non-irAEs were calculated by determining the reciprocal of the original HR and 95% CI (6). Heterogeneity was assessed by applying the chi-square test and I^2 statistic. A chi-square $p<0.05$ or an $I^2>50\%$ was considered to indicate significant heterogeneity (7). The random-effects model was used in case of significant heterogeneity (8); if not, the fixed-effects model was used. Publication bias was evaluated using

Begg's test and Egger's test. If there is a significant publication bias, we will further use the trim and fill method to evaluate.

RESULTS

Records Selection and Characterization of the Identified Studies

A total of 848 records were retrieved from PubMed, Embase, and Cochrane Library databases, and two were acquired from additional resources. The flowchart of the records selection is given in **Figure 1**. After removing the duplicate records and excluding the irrelevant studies, 81 records were assessed for their eligibility. Finally, 34 records encompassing 8115 patients were chosen for this meta-analysis (9–42). Among the included studies, 31 had employed a retrospective cohort design, and 12 had adopted a landmark analysis. Twenty-one studies had reported the ORR of patients with or without irAEs, 23 had provided the HR of OS and 25 had provided the HR of PFS. Seventeen studies had reported organ-specific irAEs, and four had reported grade-specific irAEs. The characteristics of the included studies were listed in **Table 1** and **Supplementary Material 1 (Table S1)**.

Association Between the Occurrence of irAEs and ORR, OS, and PFS

A total of 21 studies involving 5,256 patients had reported the ORR of patients with or without irAEs. The pooled RR for ORR was 2.43 (95% CI [2.06–2.88], $p < 0.00001$), which means that patients experiencing irAEs respond better to ICIs than those who do not (**Figure 2**). A random-effect model was utilized because of significant heterogeneity ($I^2 = 55\%$, $p = 0.001$). The occurrence of irAEs also predicted improved OS and PFS in lung cancer patients undergoing immunotherapy. The pooled HR OS was 0.51 for OS (95% CI [0.43–0.61], $p < 0.00001$) and 0.50 for PFS (95% CI [0.44–0.57], $p < 0.00001$). However, significant

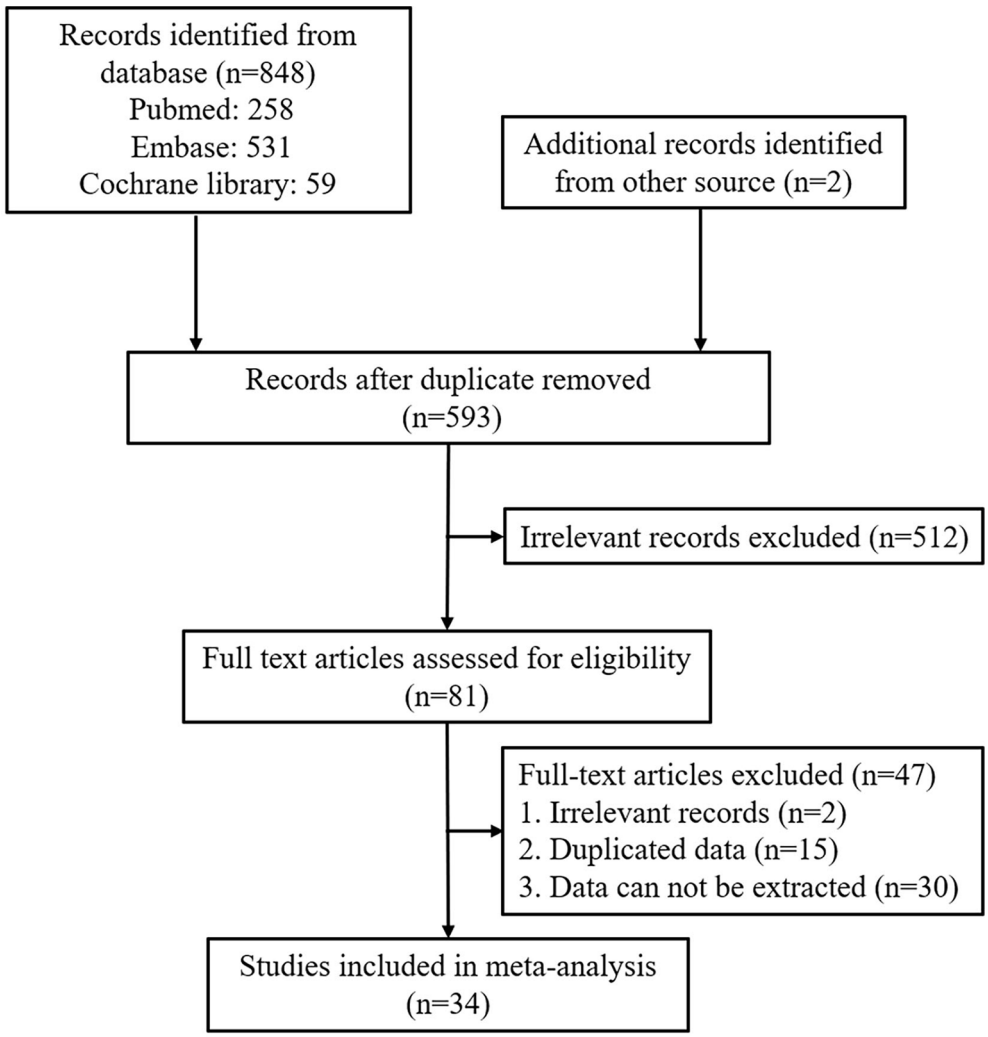

FIGURE 1 | Flowchart of the study selection process.

TABLE 1 | Main characteristics of the included studies.

Study	Design	ICIs types	Landmark analysis	irAEs types	irAEs grade	ORR (irAEs vs non-irAEs)	OS Hazard ratio (95%CI)	PFS Hazard ratio (95%CI)
Osorioet al. (9)	Retrospective	P	no	Thyroid dysfunction	1–3	NA	0.29 (0.09–0.94)	0.58 (0.27–1.21)
Teraoka et al. (10)	Prospective	N	6-week	Global	1–2	33.3%/12.5%	NA	NA
Kim et al. (11)	Retrospective	N/P	no	Thyroid dysfunction	1–2	31.6%/10.3%	0.11 (0.01–0.92)	0.38 (0.17–0.85)
Sato et al. (12)	Retrospective	N	no	Global	1–4	63.6%/7.4%	NA	0.10 (0.02–0.37)
Lisberg et al. (13)	Retrospective	P	no	Global	1–4	NA	0.75 (0.58–0.96)	0.75 (0.56–0.99)
Haratani et al. (14)	Retrospective	N	6-week	Global	1–4	52.3%/27.9%	0.285 (0.102–0.675)	0.542 (0.295–0.971)
				Skin			0.209 (0.049–0.618)	0.476 (0.232–0.912)
				Endocrine			0.504 (0.027–2.629)	0.237 (0.037–0.842)
Owen et al. (15)	Retrospective	NA	no	Global	1–5	NA	0.364 (0.203–0.649)*	NA
Grangeon et al. (16)	Retrospective	NA	no	Global	1–5	23.1%/5.7%	0.29 (0.18–0.46)	0.42 (0.32–0.57)
				Pneumonitis			1.42 (0.45–4.54)	1.19 (0.52–2.70)
				Thyroiditis			0.46 (0.25–0.86)	0.58 (0.39–0.85)
				Colitis			0.24 (0.03–1.73)	0.73 (0.35–1.50)
				Hepatitis			0.97 (0.3–3.08)	0.97 (0.45–2.08)
Ricciuti et al. (17)	Retrospective	N	no	Global	1–4	43.5%/10%	0.38 (0.26–0.56)	0.48 (0.34–0.67)
				Lung			0.46 (0.24–0.89)	0.56 (0.33–0.96)
				Gastrointestinal			0.5 (0.26–0.98)	0.52 (0.3–0.9)
				Endocrine			0.45 (0.28–0.72)	0.59 (0.4–0.89)
				Skin			0.8 (0.46–1.39)	0.57 (0.35–0.95)
				Hepatobiliary			0.94 (0.53–1.66)	0.72 (0.41–1.24)
Cortellini et al. (18)	Retrospective	NA	6-week	Global	1–4	46.5%/25.7%	0.53 (0.41–0.69)	0.57 (0.45–0.72)
				Endocrine			0.55 (0.37–0.83)	0.63 (0.45–0.89)
				Skin			0.43 (0.27–0.70)	0.46 (0.31–0.69)
				Gastrointestinal			0.61 (0.38–0.98)	0.68 (0.47–1.01)
				Hepatic			1.09 (0.48–2.45)	1.47 (0.72–2.96)
Toi et al. (19)	Retrospective	N/P	no	Global	1–4	51.5%/12.7%	0.42 (0.24–0.71)	0.45 (0.30–0.68)
Ahn et al. (20)	Retrospective	N/P	6-week	Global	1–4	41.2%/26.7%	0.484 (0.255–0.919)	0.434 (0.256–0.735)
				Skin			0.420 (0.162–1.087)	0.643 (0.350–1.180)
				Endocrine			0.255 (0.051–1.288)	0.368 (0.132–1.028)
				Pneumonitis			4.117 (1.420–11.942)	1.686 (0.618–4.597)
Berner et al. (21)	Prospective	N/P	no	Skin	NA	60%/14.6%	0.29 (0.12–0.71)	0.22 (0.09–0.49)
Fukihara et al. (22)	Retrospective	N/P	8-week	Pneumonitis	1–5	42.9%/25.4%	NA	NA
Baldini et al. (23)	Retrospective	N	no	Global	1–4	27.2%/16.5%	0.69 (0.58–0.82)*	0.69 (0.6–0.79)*
Cui et al. (24)	Retrospective	N/P/A/D	no	Pneumonitis	1–4	61.9%/29.9%	NA	NA
Naqash et al. (25)	Retrospective	N	no	Global	NA	NA	0.65 (0.52–0.8)	0.69 (0.55–0.87)
				Thyroid			0.79 (0.53–1.19)	0.98 (0.67–1.42)
				Pneumonitis			1.35 (0.89–2.02)	1.36 (0.91–2.02)
				Hepatitis			1.18 (0.63–1.97)	0.75 (0.45–1.31)
				Colitis/diarrhea			0.65 (0.35–1.21)	0.65 (0.35–1.21)
				Skin			0.67 (0.41–1.07)	0.57 (0.36–0.88)
Serrano et al. (26)	Retrospective	NA	no	Global	1–3	NA	0.53 (0.31–0.93)	0.44 (0.26–0.73)
Akamatsu et al. (27)	Retrospective	NA	no	Global	NA	48.4%/10.7%	0.45 (0.11–1.88)	0.30 (0.10–0.85)
Pawel et al. (28)	Retrospective	A	no	Global	1–4	NA	0.79 (0.60–1.05)	NA
Hosoya et al. (29)	Prospective	N	2-week	Global	1–4	60.9%/12.8%	0.92 (0.47–1.79)	0.6 (0.36–0.99)
				Rash				0.57 (0.33–0.99)
				Diarrhea				1.08 (0.46–2.5)

(Continued)

TABLE 1 | Continued

Study	Design	ICIs types	Landmark analysis	irAEs types	irAEs grade	ORR (irAEs vs non-irAEs)	OS Hazard ratio (95%CI)	PFS Hazard ratio (95%CI)
Boussageon et al. (30)	Retrospective	NA	12-week	Global	1–3	NA	NA	0.33 (0.14–0.76)
Sosa et al. (31)	Retrospective	NA	no	Global	NA	NA	0.18 (0.06–0.53)	NA
Rizzi et al. (32)	Retrospective	NA	6-week	Global	3–4	47.9%/30.0%	NA	NA
Aso et al. (33)	Retrospective	N/P	6-week	Skin	1–3	72.0%/24.0%	0.75 (0.4–1.43)	0.58 (0.33–0.99)
Riudavets et al. (34)	Retrospective	NA	2.4-month	Global	1–5	48.6%/23.2%	0.32 (0.22–0.46)	0.43 (0.28–0.64)
				Rash			0.42 (0.23–0.75)	
				Endocrine			0.59 (0.34–1)	
Kubo et al. (35)	Retrospective	NA	no	Global	NA	NA	NA	0.43 (0.24–0.76)
Lim et al. (36)	Retrospective	N	no	Global	1–4	31.6%/11.3%	0.5 (0.33–0.76)	NA
Noguchi et al. (37)	Retrospective	P	no	Global	1–4	NA	NA	0.33 (0.17–0.65)
Sugano et al. (38)	Retrospective	N/P/A	no	ILD	NA	62.5%/20.9%	NA	0.39 (0.19–0.77)
Usui et al. (40)	Retrospective	N	8-week	Skin rash	NA	22.2%/20.8%	NA	0.435 (0.105–1.196)
Ahmed et al. (39)	Retrospective	N/P	no	Thyroid	NA	NA	NA	0.38 (0.2–0.71)
Bjørnhart et al. (41)	Retrospective	N/P	no	Global	3–4	NA	0.47 (0.21–1.05)	0.71 (0.39–1.27)
Ksienski et al. (42)	Retrospective	N/P	6-week	Global	≥3	NA	2.29 (1.05–4.98)	NA

irAEs, immune-related adverse events; ORR, objective response rate; OS, overall survival; PFS, progression-free survival; CI, confidence interval; NA, not available; N, nivolumab; P, pembrolizumab; A, atezolizumab; D, durvalumab; ILD, interstitial lung disease.

**The HR and 95% CI was calculated through taking reciprocal.*

heterogeneities were observed for OS (I^2 = 69%, p < 0.00001) and PFS (I^2 = 49%, p = 0.003) (**Figures 3**, **4**).

Subgroup Analysis

Various organ systems could be affected by irAEs. Zhou et al. had found that the association between the different irAE types and patient outcomes was inconsistent by conducting a meta-analysis that covered all cancer types (43). However, this issue remains unclear in case of lung cancer. Hence, we performed subgroup analysis according to irAE types and grades exclusively in lung cancer patients. After pooling the HRs of OS according to the irAE types, the occurrence of dermatological (HR: 0.53, 95% CI [0.42–0.65], p < 0.00001), endocrine (HR: 0.55, 95% CI [0.45–0.67], p < 0.00001), and gastrointestinal (HR: 0.58, 95% CI [0.42–0.80], p = 0.0009) irAEs was found to be significantly correlated with longer OS of lung cancer patients treated with ICIs (**Figure 5**). Nevertheless, no significant association was seen between OS and the occurrence of hepatobiliary (HR: 1.06, 95% CI [0.76–1.48], p = 0.73) and pulmonary (HR: 1.28, 95% CI [0.58–2.85], p = 0.54) irAEs (**Figure 6**). The association between irAE type and the PFS of patients was identical to that of OS (**Supplementary Material 1: Figures S1, S2**). Furthermore, we conducted a subgroup analysis based on the irAE grades. It was inferred that high irAE grades (≥ 3) were not significantly associated with OS and PFS (OS: HR:0.83, 95% CI [0.49–1.43], p = 0.51; PFS: HR: 0.88, 95% CI [0.67–1.16], p = 0.37) (**Supplementary Material 1: Figure S3**). Owing to data limitations, the association between low irAE grades (≤ 2) and patient outcomes could not be analyzed. In addition, we performed subgroup analysis based on the drug types. The pooled HR of OS was 0.57 (95%CI [0.45–0.72], p < 0.00001) for nivolumab monotherapy and 0.56 (95%CI [0.24-1.31], p = 0.18) for pembrolizumab monotherapy (**Supplementary Material 1: Figure S4**).

Sensitivity Analysis and Publication Bias

Sensitivity analyses were conducted to assess the stability of our results. The results of OS and PFS remained consistent even upon deleting any included study or changing the random-effect model into the fixed-effect model (**Supplementary Material 1: Figures S5, S6**). The funnel plots assessing the publication bias of OS and PFS are presented in **Supplementary Material 1 (Figures S7, S8)**. Regarding OS analysis, Begg's test (p = 0.369) revealed no publication bias, however, Egger's test (p = 0.043) presented with the opposite result. We further adopted the trim and fill method to evaluate the publication bias. The result revealed that no study was trimmed or filled and that the pooled result of OS was unchanged, which indicated that our results were stable. Regarding PFS analysis, Begg's test (p = 0.016) and Egger's test (p < 0.001) suggested the existence of significant publication bias. The result of the trim and fill method was similar to that of OS.

DISCUSSION

Although the underlying pathophysiology has not been clearly elucidated until date, accumulating evidence suggest that the

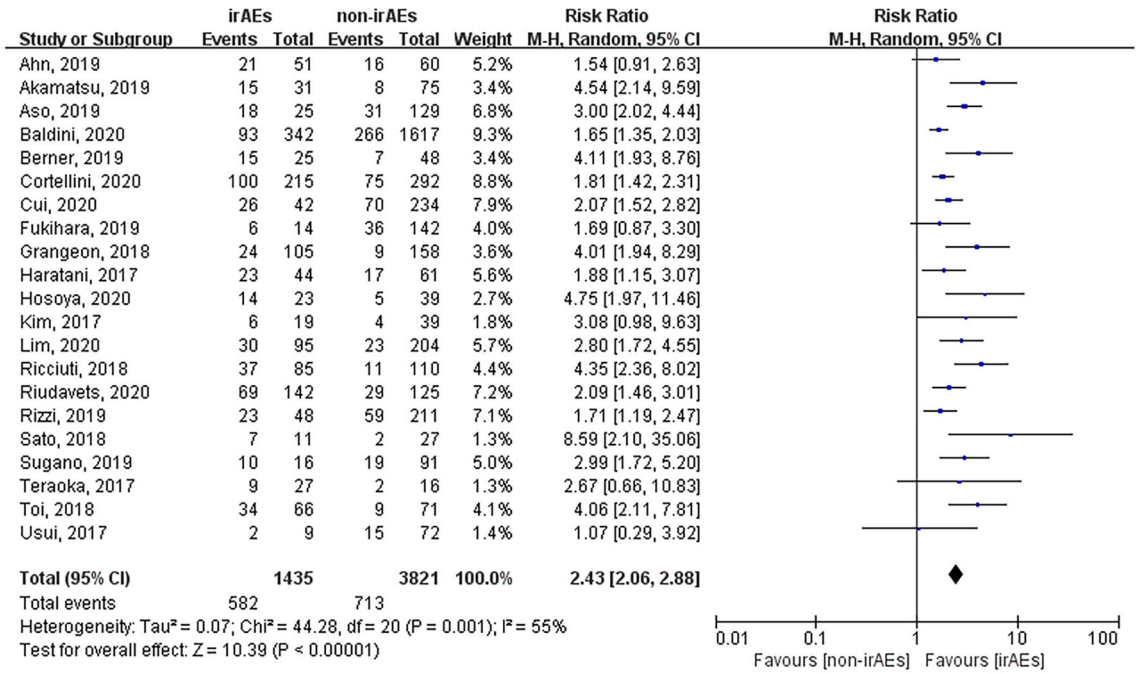

FIGURE 2 | Forest plot of the association between the occurrence of irAEs and ORR. ORR, objective response rate; irAEs, immune-related adverse events; non-irAEs, non-immune-related adverse events.

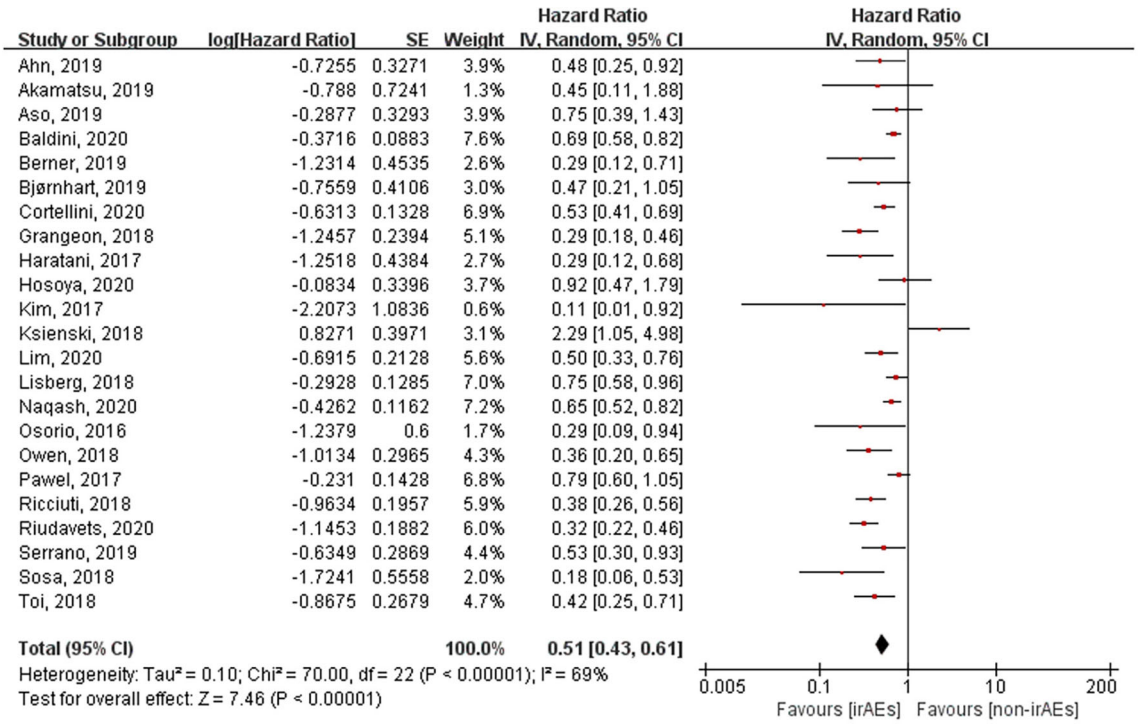

FIGURE 3 | Forest plot of the association between the occurrence of irAEs and OS. OS, overall survival; irAEs, immune-related adverse events; non-irAEs, non-immune-related adverse events.

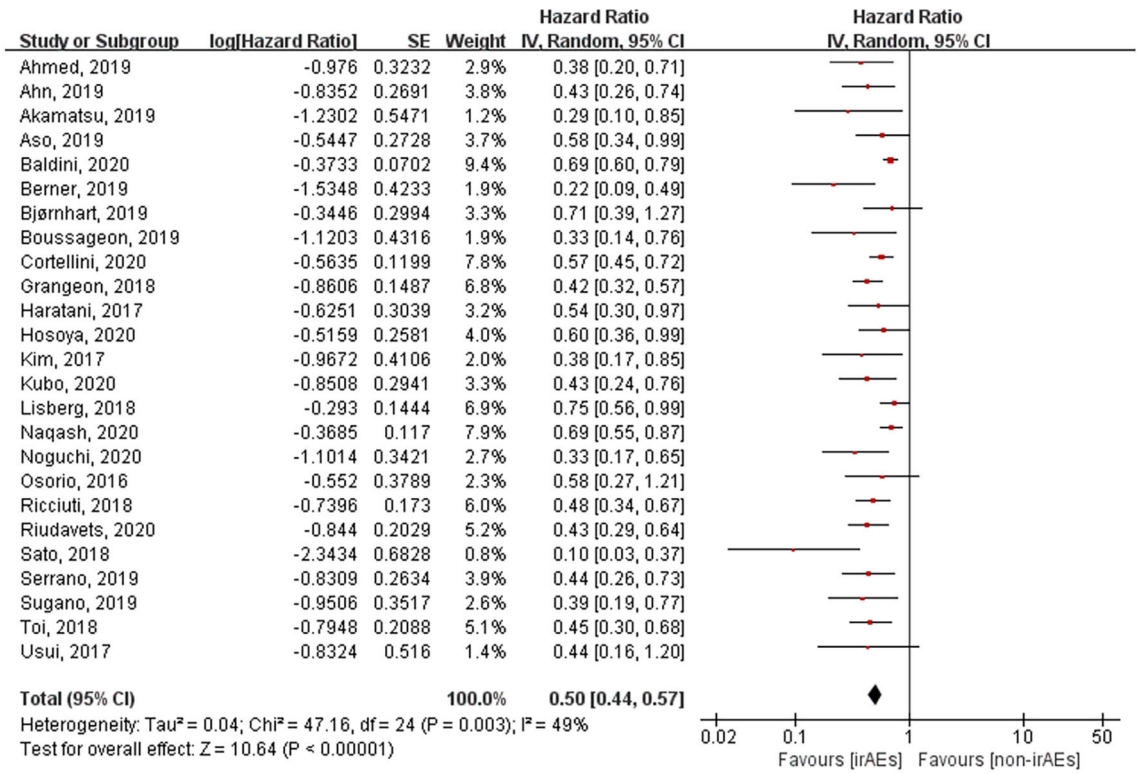

FIGURE 4 | Forest plot of the association between the occurrence of irAEs and PFS. PFS, progression-free survival; irAEs, immune-related adverse events; non-irAEs, non-immune-related adverse events.

occurrence of irAEs can predict the outcomes of patients receiving immunotherapy. In our meta-analysis focusing on lung cancer, the results demonstrated that the occurrence of irAEs was significantly associated with ORR, OS, and PFS of patients treated with ICIs. In addition, patients who experienced dermatological, endocrine, and gastrointestinal irAEs had longer OS and PFS than those who did not. Nevertheless, pulmonary and hepatobiliary irAEs and high-grade (≥3) irAEs were not correlated with OS and PFS.

Several biomarkers have been investigated to predict the efficacy of ICIs prior to the treatment. Clinical practice suggests that not all predictors are effective. PD-L1 is the commonly adopted defective biomarker in clinical practice. Its expression in tumor cells, especially when ≥50%, was found to be significantly associated with the outcomes of lung cancer patients (44). Nevertheless, patients with negative PD-L1 expression also benefit from immunotherapy (45). Another acknowledged biomarker is the tumor mutational burden (TMB), whose predictive value is comparable to that of PD-L1 (46). Both tumor tissue and blood TMB have been shown to be associated with superior survival in lung cancer patients (47–50). However, technical limitations and the absence of standardization hampered its clinical application. Our results indicate that irAEs could be predictors of clinical outcomes in lung cancer patients after the initiation of treatment. These events are routinely witnessed within a few weeks of the initial administration, which helps clinicians in the early prediction of ICI efficacy. Most irAEs related to ipilimumab develop within 8–12 weeks of initiating the medication, with skin toxicity occurring at around 2–3 weeks, gastrointestinal and hepatic toxicity at 6–7 weeks, and endocrine toxicity at 9 weeks (51). The onset time of irAEs differs between anti-CTLA-4 and anti-PD-1 inhibitors. In patients treated with nivolumab, skin irAEs occur at about 5 weeks, followed by gastrointestinal irAEs at 7 weeks, hepatic irAEs at 8 weeks, pulmonary irAEs at 9 weeks, and endocrine irAEs at 10 weeks (51).

As mentioned previously, not all irAE occurrences are related to the efficacy of immunotherapy. The overall incidence of immune-related pneumonitis (IRP) was 4% (52, 53), with grade ≥3 accounting for 16.7%–42.9% of the cases (24, 25). A meta-analysis found that IRP was the major cause of death due to irAEs (54). Immune-related hepatitis (IRH) is usually asymptomatic, with elevated serum transaminase or bilirubin levels. Most patients developing IRH tended to receive corticosteroid treatment (55). For patients with grade ≥3 irAEs, which are usually life-threatening, ICIs should be permanently discontinued and treatment with immunosuppressive drugs such as glucocorticoids should be commenced. An increased risk of mortality and treatment with corticosteroids may together counteract the efficacy of ICIs.

While Zhou et al. had conducted a meta-analysis which mainly covered melanoma and non-small cell lung cancer to investigate the association between irAEs and the efficacy of ICIs (43), there are some key differences between our work and theirs.

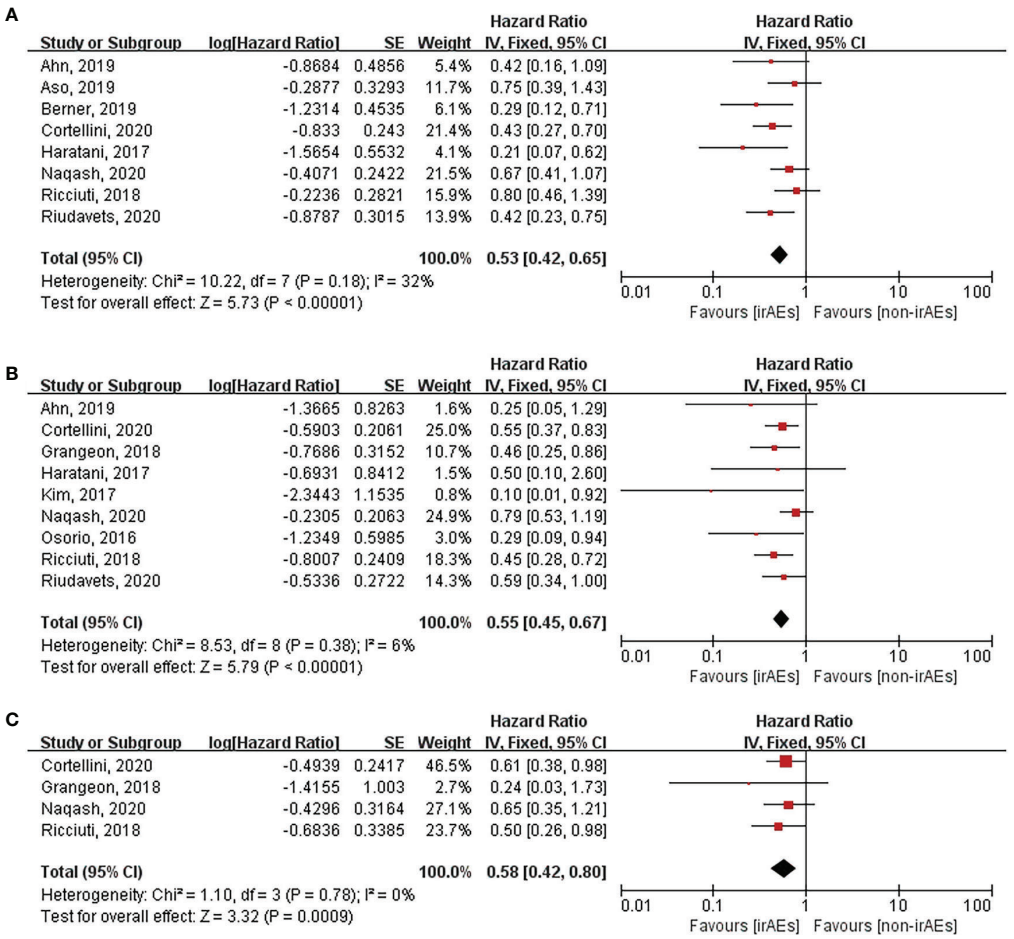

FIGURE 5 | Forest plot of the association between the occurrences of different irAEs types and OS. **(A)** dermatological irAEs; **(B)** endocrine irAEs; **(C)** gastrointestinal irAEs. OS, overall survival; irAEs, immune-related adverse events; non-irAEs, non-immune-related adverse events.

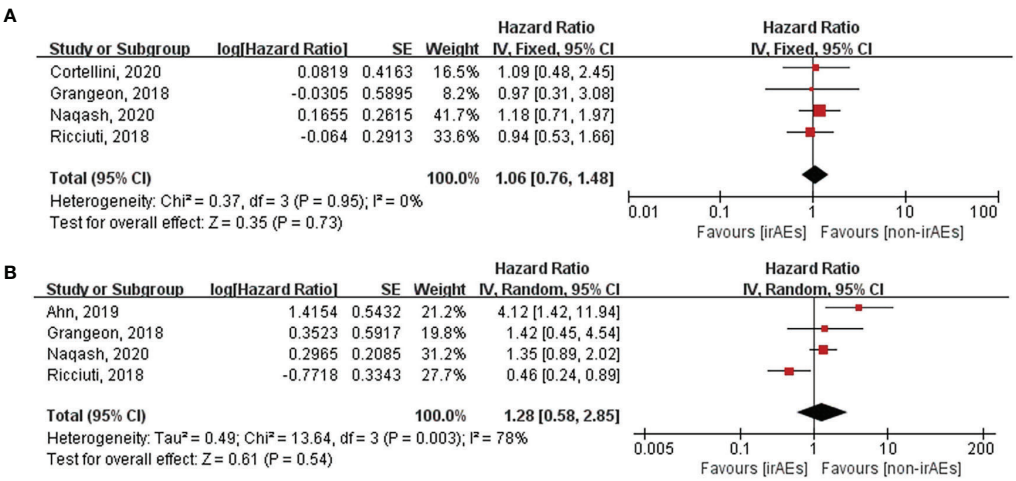

FIGURE 6 | Forest plot of the association between the occurrences of different irAEs types and OS. **(A)** hepatobiliary irAEs; **(B)** pulmonary irAEs. OS, overall survival; irAEs, immune-related adverse events; non-irAEs, non-immune-related adverse events.

First, irAE profiles tend to vary according to the cancer type (56). For example, gastrointestinal irAEs occur more frequently in melanoma than in lung cancer, while the opposite is true for pneumonia. Therefore, the results obtained for other cancers may not be applicable for lung cancer. Although the cancer types studied by us are not as extensive as those investigated by Zhou et al., our results are more representative of the actual scenario in the specific field of lung cancer. Second, we pooled the RRs of ORR, which is lacking in Zhou et al.'s work. ORR is an important indicator of the response to immunotherapy, and our results demonstrated that patients experiencing irAEs respond better to ICIs than those who do not.

However, there are some limitations in our research. First, most of the included studies were retrospective, which might affect the quality of the evidences analyzed. Second, heterogeneities were significant in the analysis of ORR, OS, and PFS. After conducting a subgroup analysis based on the types of irAEs, the heterogeneities were significantly reduced. Third, Begg's test and Egger's test suggested the existence of significant publication bias. We further adopted the trim and fill method, which indicated that our results were stable. The last, but not the least, owing to the availability of only limited data, we were unable to analyze the association between low grade irAEs and patient outcomes. Hence, more cohort studies need to be performed in the future.

In conclusion, our meta-analysis has demonstrated that the occurrence of irAEs, especially dermatological, endocrine, and gastrointestinal irAEs, could predict the enhanced efficacy of immunotherapy in lung cancer patients treated with ICIs.

DATA AVAILABILITY STATEMENT

The original contributions presented in the study are included in the article/**Supplementary Material**. Further inquiries can be directed to the corresponding authors.

AUTHOR CONTRIBUTIONS

Conceptualization, supervision: FZ and YS. Data extraction: DW and CC. Writing – original draft preparation: DW. Methodology, software: YG and WL. Writing – reviewing and editing: PZ, HL, and TL. All authors contributed to the article and approved the submitted version.

FUNDING

This work was supported by the National Natural Science Foundation of China (grant numbers 81970034 and 81570078).

SUPPLEMENTARY MATERIAL

The Supplementary Material for this article can be found online at: https://www.frontiersin.org/articles/10.3389/fonc.2021.631949/full#supplementary-material

REFERENCES

1. Xu C, Chen YP, Du XJ, Liu JQ, Huang CL, Chen L, et al. Comparative safety of immune checkpoint inhibitors in cancer: systematic review and network meta-analysis. *BMJ (Clinical Res ed)* (2018) 363:k4226. doi: 10.1136/bmj.k4226
2. Ramos-Casals M, Brahmer JR, Callahan MK, Flores-Chavez A, Keegan N, Khamashta MA, et al. Immune-related adverse events of checkpoint inhibitors. *Nat Rev Dis Primers* (2020) 6:38. doi: 10.1038/s41572-020-0160-6
3. Brahmer JR, Lacchetti C, Schneider BJ, Atkins MB, Brassil KJ, Caterino JM, et al. Management of Immune-Related Adverse Events in Patients Treated With Immune Checkpoint Inhibitor Therapy: American Society of Clinical Oncology Clinical Practice Guideline. *J Clin Oncol Off J Am Soc Clin Oncol* (2018) 36:1714–68. doi: 10.1200/JCO.2017.77.6385
4. Haanen J, Carbonnel F, Robert C, Kerr KM, Peters S, Larkin J, et al. Management of toxicities from immunotherapy: ESMO Clinical Practice Guidelines for diagnosis, treatment and follow-up. *Ann Oncol* (2017) 28: iv119–42. doi: 10.1093/annonc/mdx225
5. Ouwerkerk W, van den Berg M, van der Niet S, Limpens J, Luiten RM, et al. Biomarkers, measured during therapy, for response of melanoma patients to immune checkpoint inhibitors: a systematic review. *Melanoma Res* (2019) 29 (5):453–64. doi: 10.1097/CMR.0000000000000589
6. Tierney JF, Stewart LA, Ghersi D, Burdett S, Sydes MR. Practical methods for incorporating summary time-to-event data into meta-analysis. *Trials* (2007) 8:16. doi: 10.1186/1745-6215-8-16
7. Higgins JP, Thompson SG, Deeks JJ, Altman DG. Measuring inconsistency in meta-analyses. *BMJ (Clinical Res ed)* (2003) 327:557–60. doi: 10.1136/bmj.327.7414.557
8. DerSimonian R, Kacker R. Random-effects model for meta-analysis of clinical trials: an update. *Contemp Clin trials* (2007) 28:105–14. doi: 10.1016/j.cct.2006.04.004
9. Osorio JC, Ni A, Chaft JE, Pollina R, Kasler MK, Stephens D, et al. Antibody-mediated thyroid dysfunction during T-cell checkpoint blockade in patients with non-small-cell lung cancer. *Ann Oncol Off J Eur Soc Med Oncol* (2017) 28:583–9. doi: 10.1093/annonc/mdw640
10. Teraoka S, Fujimoto D, Morimoto T, Kawachi H, Ito M, Sato Y, et al. Early Immune-Related Adverse Events and Association with Outcome in Advanced Non–Small Cell Lung Cancer Patients Treated with Nivolumab: A Prospective Cohort Study. *J Thoracic Oncol* (2017) 12:1798–805. doi: 10.1016/j.jtho.2017.08.022
11. Kim HI, Kim M, Lee SH, Park SY, Kim YN, Kim H, et al. Development of thyroid dysfunction is associated with clinical response to PD-1 blockade treatment in patients with advanced non-small cell lung cancer. *Oncoimmunology* (2018) 7:e1375642. doi: 10.1080/2162402X.2017.1375642
12. Sato K, Akamatsu H, Murakami E, Sasaki S, Kanai K, Hayata A, et al. Correlation between immune-related adverse events and efficacy in non-small cell lung cancer treated with nivolumab. Lung cancer (Amsterdam. *Netherlands)* (2018) 115:71–4. doi: 10.1016/j.lungcan.2017.11.019
13. Lisberg A, Tucker DA, Goldman JW, Wolf B, Carroll J, Hardy A, et al. Treatment-Related Adverse Events Predict Improved Clinical Outcome in NSCLC Patients on KEYNOTE-001 at a Single Center. *Cancer Immunol Res* (2018) 6:288–94. doi: 10.1158/2326-6066.CIR-17-0063
14. Haratani K, Hayashi H, Chiba Y, Kudo K, Yonesaka K, Kato R, et al. Association of immune-related adverse events with nivolumab efficacy in non-small cell lung cancer. *JAMA Oncol* (2018) 4:374–8. doi: 10.1001/jamaoncol.2017.2925
15. Owen DH, Wei L, Bertino EM, Edd T, Villalona-Calero MA, He K, et al. Incidence, Risk Factors, and Effect on Survival of Immune-related Adverse Events in Patients With Non-Small-cell Lung Cancer. *Clin Lung Cancer* (2018) 19:e893–900. doi: 10.1016/j.cllc.2018.08.008
16. Grangeon M, Tomasini P, Chaleat S, Jeanson A, Souquet-Bressand M, Khobta N, et al. Association Between Immune-related Adverse Events and Efficacy of

Immune Checkpoint Inhibitors in Non–small-cell Lung Cancer. *Clin Lung Cancer* (2019) 20:201–7. doi: 10.1016/j.cllc.2018.10.002
17. Ricciuti B, Genova C, De Giglio A, Bassanelli M, Dal Bello MG, Metro G, et al. Impact of immune-related adverse events on survival in patients with advanced non-small cell lung cancer treated with nivolumab: long-term outcomes from a multi-institutional analysis. *J Cancer Res Clin Oncol* (2019) 145:479–85. doi: 10.1007/s00432-018-2805-3
18. Cortellini A, Friedlaender A, Banna GL, Porzio G, Bersanelli M, Cappuzzo F, et al. Immune-related Adverse Events of Pembrolizumab in a Large Real-world Cohort of Patients With NSCLC With a PD-L1 Expression ≥ 50% and Their Relationship With Clinical Outcomes. *Clin Lung Cancer* (2020) 21 (6):498–508. doi: 10.1016/j.cllc.2020.06.010
19. Toi Y, Sugawara S, Sugisaka J, Ono H, Kawashima Y, Aiba T, et al. Profiling Preexisting Antibodies in Patients Treated with Anti-PD-1 Therapy for Advanced Non-Small Cell Lung Cancer. *JAMA Oncol* (2019) 5:376–83. doi: 10.1001/jamaoncol.2018.5860
20. Ahn BC, Pyo KH, Xin CF, Jung D, Shim HS, Lee CY, et al. Comprehensive analysis of the characteristics and treatment outcomes of patients with non-small cell lung cancer treated with anti-PD-1 therapy in real-world practice. *J Cancer Res Clin Oncol* (2019) 145:1613–23. doi: 10.1007/s00432-019-02899-y
21. Berner F, Bomze D, Diem S, Ali OH, Fässler M, Ring S, et al. Association of Checkpoint Inhibitor-Induced Toxic Effects With Shared Cancer and Tissue Antigens in Non-Small Cell Lung Cancer. *JAMA Oncol* (2019) 5:1043–7. doi: 10.1001/jamaoncol.2019.0402
22. Fukihara J, Sakamoto K, Koyama J, Ito T, Iwano S, Morise M, et al. Prognostic Impact and Risk Factors of Immune-Related Pneumonitis in Patients With Non-Small-Cell Lung Cancer Who Received Programmed Death 1 Inhibitors. *Clin Lung Cancer* (2019) 20:442–450.e4. doi: 10.1016/j.cllc.2019.07.006
23. Baldini E, Lunghi A, Cortesi E, Turci D, Signorelli D, Stati V, et al. Immune-related adverse events correlate with clinical outcomes in NSCLC patients treated with nivolumab: The Italian NSCLC expanded access program. *Lung Cancer* (2020) 140:59–64. doi: 10.1016/j.lungcan.2019.12.014
24. Cui P, Huang D, Wu Z, Tao H, Zhang S, Ma J, et al. Association of immune-related pneumonitis with the efficacy of PD-1/PD-L1 inhibitors in non-small cell lung cancer. *Ther Adv Med Oncol* (2020) 12:1–10. doi: 10.1177/1758835920922033
25. Naqash AR, Ricciuti B, Owen DH, Florou V, Toi Y, Cherry C, et al. Outcomes associated with immune-related adverse events in metastatic non-small cell lung cancer treated with nivolumab: a pooled exploratory analysis from a global cohort. *Cancer Immunol Immunother CII* (2020) 69:1177–87. doi: 10.1007/s00262-020-02536-5
26. Saavedra Serrano C, Barquín García A, Corral de la Fuente E, Serrano Domingo JJ, Albarrán Artahona V, Martin Huertas R, et al. Association of immune-related adverse events (irAEs) and immunotherapy (IT) benefit in advanced non-small cell lung cancer (NSCLC). *Ann Oncol* (2019) 30:ii57–8. doi: 10.1093/annonc/mdz063.053
27. Akamatsu H, Murakami E, Oyanagi J, Shibaki R, Kaki T, Takase E, et al. Immune-Related Adverse Events by Immune Checkpoint Inhibitors Significantly Predict Durable Efficacy Even in Responders with Advanced Non-Small Cell Lung Cancer. *Oncologist* (2020) 25:e679–83. doi: 10.1634/theoncologist.2019-0299
28. Von Pawel J, Syrigos K, Mazieres J, Cortinovis D, Dziadziuszko R, Gandara DR, et al. Association between immune-related adverse events (irAEs) and atezolizumab efficacy in advanced NSCLC: Analyses from the phase III study OAK. *Ann Oncol* (2017) 28:v469. doi: 10.1093/annonc/mdx380.017
29. Hosoya K, Fujimoto D, Morimoto T, Kumagai T, Tamiya A, Taniguchi Y, et al. Association Between Early Immune-related Adverse Events and Clinical Outcomes in Patients With Non–Small Cell Lung Cancer Treated With Immune Checkpoint Inhibitors. *Clin Lung Cancer* (2020) 21:e315–28. doi: 10.1016/j.cllc.2020.01.003
30. Boussageon M, Ortiz-Cuaran S, Chabaud S, Pérol D, Avrillon V, Mastroianni B, et al. P1.01-116 Early Immune-Related Adverse Events Under PD-1/PD-L1 Inhibitors Predict Better Progression-Free Survival in NSCLC. *J Thoracic Oncol* (2019) 14:S407. doi: 10.1016/j.jtho.2019.08.831
31. Melián Sosa M, Puchades C, Mendez JA, Torres A, Rodrigo C, Gimeno G, et al. Immune-related adverse events (irAEs) and survival (OS) in metastatic non-small cell lung cancer (mNSCLC) patients (pts) treated with immunotherapy. *Ann Oncol* (2018) 29:viii501. doi: 10.1093/annonc/mdy292.014
32. Rizzi M, Rizzo M, Minatta N, Recondo G, Naveira M, Lupinacci L, et al. P1.04-82 Toxicity as a Clinical Marker for Efficacy of Immunotherapy in NSCLC: A Multicentric Experience from Argentina. *J Thoracic Oncol* (2019) 14:S474–5. doi: 10.1016/j.jtho.2019.08.985
33. Aso M, Toi Y, Sugisaka J, Aiba T, Kawana S, Saito R, et al. Association Between Skin Reaction and Clinical Benefit in Patients Treated with Anti-Programmed Cell Death 1 Monotherapy for Advanced Non-Small Cell Lung Cancer. *Oncologist* (2020) 25:e536–44. doi: 10.1634/theoncologist.2019-0550
34. Riudavets M, Mosquera J, Garcia-Campelo R, Serra J, Anguera G, Gallardo P, et al. Immune-Related Adverse Events and Corticosteroid Use for Cancer-Related Symptoms Are Associated With Efficacy in Patients With Non-small Cell Lung Cancer Receiving Anti-PD-(L)1 Blockade Agents. *Front Oncol* (2020) 10:1677. doi: 10.3389/fonc.2020.01677
35. Kubo S, Kobayashi N, Somekawa K, Hirata M, Kamimaki C, Aiko H, et al. Identification of biomarkers for non-small-cell lung cancer patients treated with an immune checkpoint inhibitor. *Anticancer Res* (2020) 40:3889–96. doi: 10.21873/anticanres.14379
36. Lim SM, Kim SW, Cho BC, Kang JH, Ahn MJ, Kim DW, et al. Real World Experience of Nivolumab in Non-Small Cell Lung Cancer in Korea. *Cancer Res Treat Off J Korean Cancer Assoc* (2020) 52(4):1112–9. doi: 10.4143/crt.2020.245
37. Noguchi S, Suminaga K, Kaki T, Kawachi H, Fukao A, Terashita S, et al. Correlation of immune-related adverse events and effects of pembrolizumab monotherapy in patients with non-small cell lung cancer. *Lung Cancer: Targets Ther* (2020) 11:53–7. doi: 10.2147/LCTT.S254146
38. Sugano T, Seike M, Saito Y, Kashiwada T, Terasaki Y, Takano N, et al. Immune checkpoint inhibitor-associated interstitial lung diseases correlate with better prognosis in patients with advanced non-small-cell lung cancer. *Thoracic Cancer* (2020) 11:1052–60. doi: 10.1111/1759-7714.13364
39. Ahmed Y, Lee J, Calvert P. EP1.01-47 Thyroid Related Adverse Events Predict Survival in NSCLC Patients Receiving Anti-PD-1/ PD-L1 Therapy. *J Thoracic Oncol* (2019) 14:S930. doi: 10.1016/j.jtho.2019.08.2020
40. Usui Y, Udagawa H, Kirita K, Umemura S, Matsumoto S, Yoh K, et al. Association between immune-related adverse events and efficacy of nivolumab in advanced non-small cell lung cancer. *Ann Oncol* (2017) 28: ix86. doi: 10.1093/annonc/mdx697.053
41. Bjørnhart B, Hansen KH, Jørgensen TL, Herrstedt J, Schytte T. Efficacy and safety of immune checkpoint inhibitors in a Danish real life non-small cell lung cancer population: a retrospective cohort study. *Acta Oncol (Stockholm Sweden)* (2019) 58:953–61. doi: 10.1080/0284186X.2019.1615636
42. Ksienski D, Wai ES, Croteau N, Fiorino L, Brooks E, Poonja Z, et al. Efficacy of Nivolumab and Pembrolizumab in Patients With Advanced Non–Small-Cell Lung Cancer Needing Treatment Interruption Because of Adverse Events: A Retrospective Multicenter Analysis. *Clin Lung Cancer* (2019) 20:e97–e106. doi: 10.1016/j.cllc.2018.09.005
43. Zhou X, Yao Z, Yang H, Liang N, Zhang X, Zhang F. Are immune-related adverse events associated with the efficacy of immune checkpoint inhibitors in patients with cancer? A systematic review and meta-analysis. *BMC Med* (2020) 18:87. doi: 10.1186/s12916-020-01549-2
44. Xu Y, Wan B, Chen X, Zhan P, Zhao Y, Zhang T, et al. The association of PD-L1 expression with the efficacy of anti-PD-1/PD-L1 immunotherapy and survival of non-small cell lung cancer patients: a meta-analysis of randomized controlled trials. *Transl Lung Cancer Res* (2019) 8:413–28. doi: 10.21037/tlcr.2019.08.09
45. Liu X, Guo CY, Tou FF, Wen XM, Kuang YK, Zhu Q, et al. Association of PD-L1 expression status with the efficacy of PD-1/PD-L1 inhibitors and overall survival in solid tumours: A systematic review and meta-analysis. *Int J Cancer* (2020) 147:116–27. doi: 10.1002/ijc.32744
46. Lu S, Stein JE, Rimm DL, Wang DW, Bell JM, Johnson DB, et al. Comparison of Biomarker Modalities for Predicting Response to PD-1/PD-L1 Checkpoint Blockade: A Systematic Review and Meta-analysis. *JAMA Oncol* (2019) 5:1195–204. doi: 10.1001/jamaoncol.2019.1549
47. Wang Z, Duan J, Cai S, Han M, Dong H, Zhao J, et al. Assessment of Blood Tumor Mutational Burden as a Potential Biomarker for Immunotherapy in Patients With Non-Small Cell Lung Cancer With Use of a Next-Generation Sequencing Cancer Gene Panel. *JAMA Oncol* (2019) 5:696–702. doi: 10.1001/jamaoncol.2018.7098

48. Hellmann MD, Callahan MK, Awad MM, Calvo E, Ascierto PA, Atmaca A, et al. Tumor Mutational Burden and Efficacy of Nivolumab Monotherapy and in Combination with Ipilimumab in Small-Cell Lung Cancer. *Cancer Cell* (2018) 33:853–861.e4. doi: 10.1016/j.ccell.2018.04.001
49. Gandara DR, Paul SM, Kowanetz M, Schleifman E, Zou W, Li Y, et al. Blood-based tumor mutational burden as a predictor of clinical benefit in non-small-cell lung cancer patients treated with atezolizumab. *Nat Med* (2018) 24:1441–8. doi: 10.1038/s41591-018-0134-3
50. Velcheti V, Kim ES, Mekhail T, Dakhil C, Stella PJ, Shen X, et al. Prospective clinical evaluation of blood-based tumor mutational burden (bTMB) as a predictive biomarker for atezolizumab (atezo) in 1L non-small cell lung cancer (NSCLC): Interim B-F1RST results. *J Clin Oncol* (2018) 36:12001–1. doi: 10.1200/JCO.2018.36.15_suppl.12001
51. Sosa A, Lopez Cadena E, Simon Olive C, Karachaliou N, Rosell R. Clinical assessment of immune-related adverse events. *Ther Adv Med Oncol* (2018) 10:1758835918764628. doi: 10.1177/1758835918764628
52. Khunger M, Rakshit S, Pasupuleti V, Hernandez AV, Mazzone P, Stevenson J, et al. Incidence of Pneumonitis With Use of Programmed Death 1 and Programmed Death-Ligand 1 Inhibitors in Non-Small Cell Lung Cancer: A Systematic Review and Meta-Analysis of Trials. *Chest* (2017) 152:271–81. doi: 10.1016/j.chest.2017.04.177
53. Nishino M, Giobbie-Hurder A, Hatabu H, Ramaiya NH, Hodi FS. Incidence of Programmed Cell Death 1 Inhibitor-Related Pneumonitis in Patients With Advanced Cancer: A Systematic Review and Meta-analysis. *JAMA Oncol* (2016) 2:1607–16. doi: 10.1001/jamaoncol.2016.2453
54. Sun X, Roudi R, Dai T, Chen S, Fan B, Li H, et al. Immune-related adverse events associated with programmed cell death protein-1 and programmed cell death ligand 1 inhibitors for non-small cell lung cancer: a PRISMA systematic review and meta-analysis. *BMC Cancer* (2019) 19:558. doi: 10.1186/s12885-019-5701-6
55. Romanski NA, Holmstroem RB, Ellebaek E, Svane IM. Characterization of risk factors and efficacy of medical management of immune-related hepatotoxicity in real-world patients with metastatic melanoma treated with immune checkpoint inhibitors. *Eur J Cancer (Oxford Engl 1990)* (2020) 130:211–8. doi: 10.1016/j.ejca.2020.02.041
56. Khoja L, Day D, Wei-Wu Chen T, Siu LL, Hansen AR. Tumour- and class-specific patterns of immune-related adverse events of immune checkpoint inhibitors: a systematic review. *Ann Oncol* (2017) 28:2377–85. doi: 10.1093/annonc/mdx286

Conflict of Interest: The authors declare that the research was conducted in the absence of any commercial or financial relationships that could be construed as a potential conflict of interest.

Copyright © 2021 Wang, Chen, Gu, Lu, Zhan, Liu, Lv, Song and Zhang. This is an open-access article distributed under the terms of the Creative Commons Attribution License (CC BY). The use, distribution or reproduction in other forums is permitted, provided the original author(s) and the copyright owner(s) are credited and that the original publication in this journal is cited, in accordance with accepted academic practice. No use, distribution or reproduction is permitted which does not comply with these terms.

frontiers in Oncology

ORIGINAL RESEARCH
published: 23 March 2021
doi: 10.3389/fonc.2021.630136

Immune-Related Adverse Events Are Associated With Clinical Benefit in Patients With Non-Small-Cell Lung Cancer Treated With Immunotherapy Plus Chemotherapy: A Retrospective Study

Kenji Morimoto[1], Tadaaki Yamada[1], Chieko Takumi[2], Yuri Ogura[3], Takayuki Takeda[3], Keisuke Onoi[4], Yusuke Chihara[4], Ryusuke Taniguchi[5], Takahiro Yamada[5], Osamu Hiranuma[6], Yoshie Morimoto[1], Masahiro Iwasaku[1], Yoshiko Kaneko[1], Junji Uchino[1] and Koichi Takayama[1]*

[1] Department of Pulmonary Medicine, Graduate School of Medical Science, Kyoto Prefectural University of Medicine, Kyoto, Japan, [2] Department of Respiratory Medicine, Japanese Red Cross Kyoto Daiichi Hospital, Kyoto, Japan, [3] Department of Respiratory Medicine, Japanese Red Cross Kyoto Daini Hospital, Kyoto, Japan, [4] Department of Respiratory Medicine, Uji-Tokushukai Medical Center, Kyoto, Japan, [5] Department of Pulmonary Medicine, Matsushita Memorial Hospital, Osaka, Japan, [6] Department of Pulmonary Medicine, Otsu City Hospital, Shiga, Japan

OPEN ACCESS

Edited by:
Meng Xu Welliver, The Ohio State University, United States
Reviewed by:
Devika Govind Das, University of Alabama at Birmingham, United States
Yasuhiro Koh, Wakayama Medical University, Japan

***Correspondence:**
Tadaaki Yamada
tayamada@koto.kpu-m.ac.jp

Specialty section:
This article was submitted to Thoracic Oncology, a section of the journal Frontiers in Oncology

Received: *16 November 2020*
Accepted: *03 March 2021*
Published: *23 March 2021*

Citation:
Morimoto K, Yamada T, Takumi C, Ogura Y, Takeda T, Onoi K, Chihara Y, Taniguchi R, Yamada T, Hiranuma O, Morimoto Y, Iwasaku M, Kaneko Y, Uchino J and Takayama K (2021) Immune-Related Adverse Events Are Associated With Clinical Benefit in Patients With Non-Small-Cell Lung Cancer Treated With Immunotherapy Plus Chemotherapy: A Retrospective Study. Front. Oncol. 11:630136. doi: 10.3389/fonc.2021.630136

Background: The immunotherapy plus chemotherapy combination is one of the most promising treatments in advanced non-small-cell lung cancer (NSCLC). Immunotherapy often causes immune-related adverse events (irAEs), which have been reported to be associated with the good clinical outcomes. However, the effects of immunotherapy plus chemotherapy remain unknown. In this study, we investigated the association between irAEs caused by immunotherapy plus chemotherapy and clinical efficacy in patients with advanced NSCLC.

Materials and Methods: We retrospectively analyzed the data of patients with advanced NSCLC, who received a combination of immunotherapy plus chemotherapy at six institutions in Japan between January 2019 and September 2019. We examined the effect of irAEs on various clinical outcomes.

Results: We included 70 patients with advanced NSCLC. Patients were divided into two groups: patients with irAEs and patients without irAEs. Patients with irAEs had significantly longer progression-free survival than those without irAEs on univariate (hazard ratio 0.53, 95% confidence interval 0.30–0.93, p = 0.026) and multivariate (hazard ratio 0.53, 95% confidence interval 0.29–0.97, p = 0.041) analyses. In addition, patients with grade 1–2 irAEs (mild irAEs) had significantly longer progression-free and overall survival than those with grade 3-5 irAEs (severe irAEs) or without irAEs on univariate (398 days versus 189 days, respectively; p = 0.0061) and multivariate (not reached versus 412 days, respectively; p = 0.021) analyses.

Conclusion: Patients with NSCLC who experienced mild irAEs showed better response to treatment with immunotherapy plus chemotherapy than those with severe irAEs or without irAEs. Further large-scale research is warranted to confirm these findings.

Keywords: combination drug therapy, immune checkpoint inhibitor, non-small-cell lung cancer, retrospective study, immune-related adverse event

INTRODUCTION

Lung cancer is the leading cause of cancer deaths (1). The appearance of immune checkpoint inhibitors (ICIs) has led to major advances in the treatment of lung cancer. Although the overall response rate to single-agent ICIs is not high in patients with lung cancer, ICIs are expected to show promising long-term efficacy compared to systemic chemotherapy (2–5). Immune-related adverse events (irAEs) are unique reactions caused by ICIs. Although the precise mechanisms remain unclear, a number of clinical studies have shown that the occurrence of irAEs correlates with therapeutic response to ICIs in patients with non-small-cell lung cancer (NSCLC) (6–9).

In recent years, immunotherapy combined with chemotherapy has become a standard treatment for advanced lung cancer. In several phase III clinical studies, the combination of immunotherapy plus chemotherapy improved the response rate and prolonged progression-free survival (PFS) as compared to platinum-doublet chemotherapy (10–13). However, to date, there is no evidence to support the association between the occurrence of irAEs and the clinical efficacy of immunotherapy combined with chemotherapy. In this study, we investigated the association between irAEs caused by immunotherapy plus chemotherapy and clinical efficacy in the real-world setting of patients with advanced NSCLC.

MATERIALS AND METHODS

Patients

We enrolled 70 patients with advanced NSCLC, who were treated with a combination of immunotherapy plus chemotherapy at six different institutions in Japan (University Hospital Kyoto Prefectural University of Medicine, Japanese Red Cross Kyoto Daiichi Hospital, Japanese Red Cross Kyoto Daini Hospital, Uji-Tokushukai Medical Center, Otsu City Hospital, and Matsushita Memorial Hospital) between January 2019 and September 2019. Patients who were alive and progression-free were censored at the last follow-up date (September 2020). The median duration of follow-up in censored cases was 14.8 months. We reviewed each patient's medical records retrospectively and collected the following data: age, sex, histological subtype, tumor–node–metastasis (TNM) stage classified using the TNM stage classification system version 8, adverse events (irAEs and other adverse drug reactions) graded using the National Cancer Institute's Common Terminology Criteria for Adverse Events version 5.0, tumor expression of programmed death-ligand 1 (PD-L1) measured using the PD-L1 IHC 22C3 pharmDx assay (Agilent Technologies, Santa Clara, CA, USA), genomic alteration (epidermal growth factor receptor and anaplastic lymphoma kinase), response rate, disease control rate assessed using the Response Evaluation Criteria in Solid Tumors (RECIST) version 1.1, Eastern Cooperative Oncology Group (ECOG) performance status (PS), smoking status, treatment regimens, PFS, and overall survival (OS). In the present study, all adverse events that were suggestive of immune-mediated events (e.g., skin rash, pneumonitis, thyroid dysfunction, nephritis, hepatitis, and hypophysitis) were defined as irAEs.

The study protocol was approved by the ethics committee of each hospital, including that of the Kyoto Prefectural University of Medicine (approval no. ERB-C-1803). The need for informed consent was waived due to the retrospective nature of the study, and the official website was used as an opt-out method; this was also approved by the ethics committee of each hospital.

Statistical Analysis

All statistical tests were two-sided, and $p < 0.05$ was considered to be statistically significant. The relationship between irAEs and other variables was examined using Fisher's exact test. Survival curves were calculated using the Kaplan–Meier method, and differences were compared using the log-rank test. On univariate and multivariate analyses, Cox proportional hazards models were used to estimate hazard ratios (HRs) and 95% confidence intervals (CIs); OS and PFS were censored at the date of last survival confirmation for patients who survived without disease progression. Landmark analyses of PFS and OS at 12 or 24 weeks were performed for patients who showed disease control or who were alive, to account for the time dependence of irAEs. Since the timing of the cutoff for landmark analyses varies between prior studies, we chose the 12-week and 24-week timepoints to evaluate the onset of various irAEs (7, 14–17). Statistical analyses were performed using EZR statistical software (version 1.40) (18).

RESULTS

Characteristics of Patients With Advanced NSCLC

We included 70 patients with a median age of 69.5 years (range: 43–85 years). The majority of patients were men (72.9%), had stage III/IV cancer (82.9%), PS 0/1 (95.7%), and adenocarcinomas (58.6%) (**Table 1**). No patients had active symptoms of autoimmune disease at the start of the combination treatment.

TABLE 1 | Characteristics of patients in with irAEs and without irAEs groups (n = 70).

Characteristics	Total (%)	With irAEs (%)	Without irAEs (%)	*p*-Value
Number	70	42	28	
Age				
Median (range)	69.5 (43-85)	69.5 (53-79)	69.5 (43-85)	
Sex				
Male	51 (72.9)	32 (76.2)	19 (67.9)	0.80
Female	19 (27.1)	10 (23.8)	9 (32.1)	
ECOG-performance status				
0/1	67 (95.7)	40 (95.2)	27 (96.4)	1.0
2	3 (4.3)	2 (4.8)	1 (3.6)	
Stage				
III/IV	58 (82.9)	35 (83.3)	23(82.1)	1.0
Recurrent	12 (17.1)	7 (16.7)	5 (17.9)	
Smoking status				
Current/Former	50 (71.4)	29 (69.0)	21 (75.0)	0.79
Never	20 (28.6)	13 (31.0)	7 (25.0)	
Histology				
Adenocarcinoma	41 (58.6)	27 (64.3)	14 (50.0)	0.27[a]
Squamous cell carcinoma	19 (27.1)	9 (21.4)	10 (35.7)	
Others	10 (14.3)	6 (14.3)	4 (14.3)	
Oncogenic driver				
EGFR mutation positive	4 (5.7)	2 (4.8)	2 (7.1)	1.0[b]
ALK rearrangement positive	0 (0)	0 (0)	0 (0)	
EGFR and ALK wild type	30 (42.9)	10 (23.8)	20 (71.4)	
Not investigated	36 (51.4)	30 (71.4)	6 (21.4)	
PD-L1 TPS				
≥50%	15 (21.4)	8 (19.1)	7 (25.0)	0.77[c]
1-49%	29 (41.4)	17 (40.4)	12 (42.9)	
<1%	16 (22.9)	9 (21.4)	7 (25.0)	
Unknown	10 (14.3)	8 (19.1)	2 (7.1)	
Sites of metastatic disease				
Brain	7 (10.0)	3 (7.1)	4 (14.3)	0.43
Liver	11 (15.7)	6 (14.2)	5 (17.9)	0.75
Regimen				
Platinum + pemetrexed + pembrolizumab	33 (47.1)	21 (50.0)	12 (42.9)	0.30[d]
Carboplatin + paclitaxel/nab-paclitaxel + pembrolizumab	28 (40.0)	14 (33.3)	14 (50.0)	
Carboplatin + pemetrexed + atezolizumab	3 (4.3)	3 (7.2)	0 (0)	
Carboplatin + paclitaxel+ bevacizumab + atezolizumab	6 (8.6)	4 (9.5)	2 (7.1)	

[a]*Squamous versus all others.*
[b]*EGFR mutation positive versus all others.*
[c]*PD-L1 TPS ≥ 50% versus all others.*
[d]*Pembrolizumab regimen versus atezolizumab regimen.*
irAE, immune-related adverse event; EGFR, Epidermal growth factor receptor; ALK, Anaplastic lymphoma kinase; PD-L1 TPS, Programmed death ligand 1 tumor proportion score.

Adverse Event Profile for Immunotherapy Plus Chemotherapy

Among the 70 included patients, 65 experienced adverse events. Among them, 42 patients were considered to have irAEs, including 12 patients who had grade 3–5 irAEs (severe irAEs); the most common irAE was rash (28.7%). The overall safety profile of the combination of immunotherapy plus chemotherapy is described in **Table 2**.

The patients were divided into two groups: patients with irAEs and patients without irAEs (**Table 1**). There were no significant differences in patient background characteristics between the two groups.

The overall response rate and disease control rate were 57.1% (95% CI: 41.0%–72.3%) and 90.4% (95% CI: 77.4%–97.3%) in patients with irAEs, and 35.7% (95% CI: 18.6%–55.9%) and 78.6% (95% CI: 59.0%–91.7%) in patients without irAEs, respectively (**Supplementary Figure 1**).

Efficacy of Immunotherapy Plus Chemotherapy

Seventy patients with NSCLC were treated with a combination of immunotherapy and chemotherapy. The median PFS was 237 days (95% CI: 189–334 days), and the median OS was not reached (95% CI: 412–not reached) (**Supplementary Figure 2**). The median PFS after the combination therapy of the patients with irAEs was significantly longer than that in the patients without irAEs (327.0 days vs. 192.5 days, p =0.023). The median OS of the patients with irAEs was better than that of the patients without irAEs (not reached vs. not reached, p = 0.29) (**Figures 1A, B**). In terms of low grade irAEs, the median PFS and OS after the combination therapy of patients with grade 1-2 irAEs (mild irAEs) were significantly longer than those of patients with severe irAEs or without irAEs (398.0 days vs. 189.0 days, p =0.0061 and not reached vs. 412 days, respectively) (**Figures 1C, D**).

TABLE 2 | Adverse events and immune-related adverse events in all patients with advanced non-small cell lung cancer.

Category	Number of patients (%)		
	Total	Grade 1-2	Grade 3-5
Any AEs	65 (92.9)	55 (78.6)	39 (55.7)
Any irAEs	42 (60.0)	31 (44.3)	12 (17.1)
Pneumonitis	10 (14.3)	6 (8.6)	4 (5.7)
Rash	20 (28.7)	18 (25.7)	2 (2.9)
Hypothyroidism/Hyperthyroidism	9 (12.9)	9 (12.9)	0 (0)
Adrenal insufficiency	3 (4.3)	2 (2.9)	1 (1.4)
Hypophysitis	1 (1.4)	0 (0)	1 (1.4)
Hepatitis	2 (2.9)	1 (1.4)	1 (1.4)
Nephritis	1 (1.4)	0 (0)	1 (1.4)
Ocular inflammatory toxicity	1 (1.4)	0 (0)	1 (1.4)
Pancreatitis	1 (1.4)	1 (1.4)	0 (0)
Colitis	1 (1.4)	0 (0)	1 (1.4)
Infusion reaction	1 (1.4)	1 (1.4)	0 (0)

AE, adverse event; irAE, immune-related adverse event.

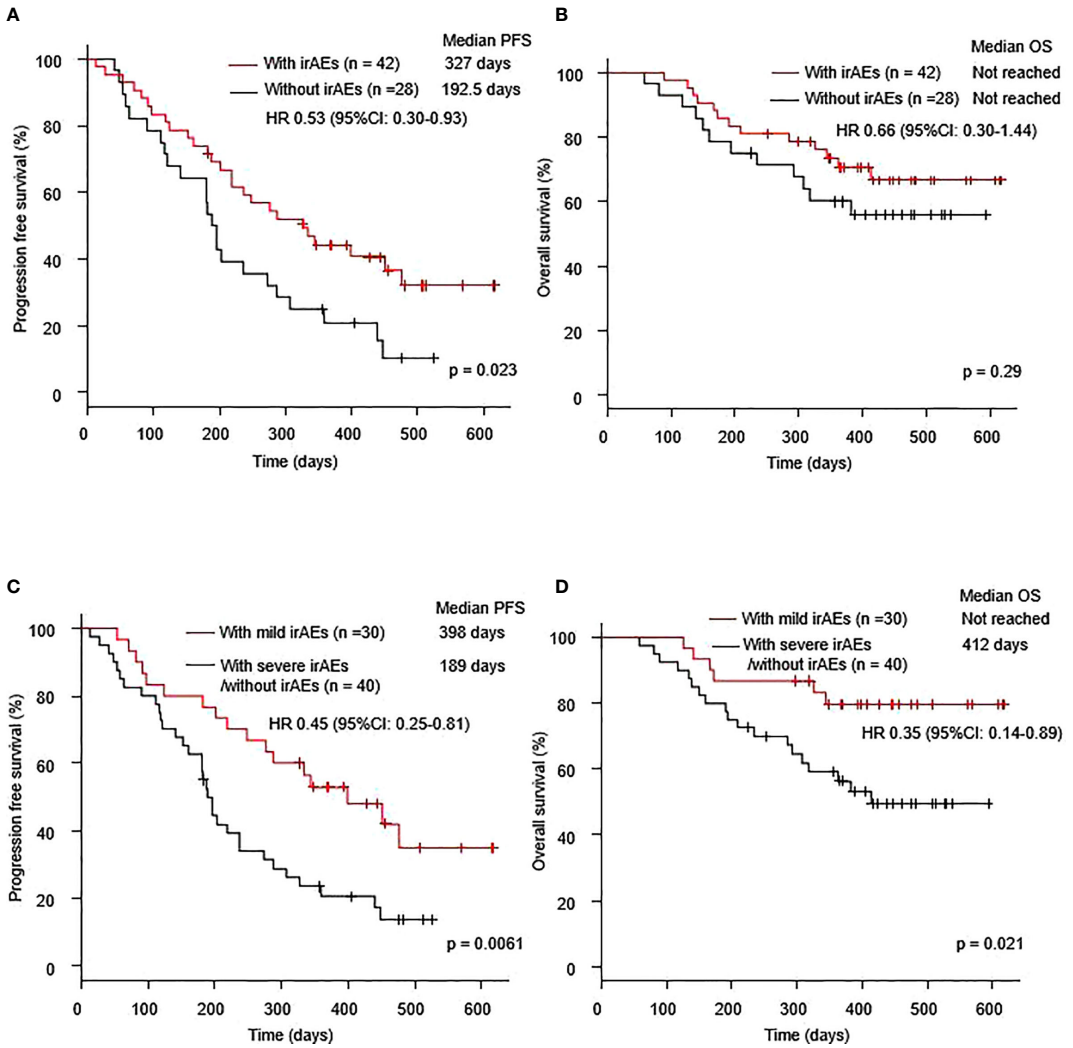

FIGURE 1 | Kaplan–Meier curves for **(A)** PFS and **(B)** OS of patients who received a combination of immunotherapy plus chemotherapy with or without irAEs. Kaplan–Meier curves for **(C)** PFS and **(D)** OS of patients who received a combination of immunotherapy plus chemotherapy with mild irAEs or with severe irAEs/without irAEs. Mild irAEs: showing in grade 1-2 irAEs, severe irAEs: showing in grade 3-5 irAEs. irAE, immune-related adverse event; OS, overall survival; PFS, progression-free survival.

Univariate analysis showed that the occurrence of irAEs was associated with prolonged PFS (HR 0.53, 95% CI: 0.30–0.93, p = 0.026) (**Table 3A**). Furthermore, multivariate analysis showed that the occurrence of irAEs was an independent predictor for prolonged PFS (HR 0.53, 95% CI: 0.29–0.97, p = 0.041) (**Table 3B**). On both univariate (HR 0.45, 95% CI: 0.25–0.81, p = 0.008) and multivariate (HR 0.41, 95% CI: 0.22–0.77, p = 0.005) analyses, the occurrence of mild irAEs was associated with prolonged PFS (**Table 3**). Furthermore, on both univariate (HR 0.35, 95% CI: 0.14–0.89, p = 0.027) and multivariate (HR 0.32, 95% CI: 0.12–0.82, p = 0.018) analyses, the occurrence of mild irAEs was associated with prolonged OS (**Table 3**).

Landmark analyses at 12 weeks (HR 0.75, 95% CI: 0.39–1.43, p = 0.38) and 24 weeks (HR 0.56, 95% CI: 0.27–1.17, p = 0.12) demonstrated a trend toward better PFS in patients with irAEs, than in those without irAEs (**Figures 2A, B**). Landmark analysis at 12 weeks also showed a trend toward better PFS in patients with mild irAEs, than in those with severe irAEs or without irAEs (HR 0.63, 95% CI: 0.32–1.25, p = 0.18). However, landmark analysis at 24 weeks revealed significantly prolonged PFS in patients with mild irAEs compared to those with severe irAEs or without irAEs (HR 0.40, 95% CI: 0.19–0.86, p = 0.018) (**Figures 2C, D**).

Landmark analysis at 12 weeks revealed no effect of mild irAEs on OS (HR 0.85, 95% CI: 0.36–2.01, p = 0.71) (**Supplementary Figure 3A**). However, landmark analysis at 24 weeks revealed a trend toward better OS in patients with mild irAEs than in those with severe irAEs or without irAEs (HR 0.34, 95% CI: 0.09–1.21, p = 0.08) (**Supplementary Figure 3B**).

DISCUSSION

In this study, the occurrence of irAEs caused by immunotherapy plus chemotherapy was associated with clinical benefit in patients with NSCLC. This is consistent with several recent retrospective studies, which showed an association between the occurrence of irAEs and the clinical efficacy of ICIs (6–9). However, to the best of our knowledge, this is the first study to identify the impact of irAEs caused by immunotherapy plus chemotherapy on clinical outcomes in patients with NSCLC. Only Japanese patients with NSCLC were included in this study.

TABLE 3A | Cox proportional hazards models for progression-free survival (PFS) and overall survival (OS) in all patients with non-small cell lung cancer excluding PD-L1 status, according to univariate (A) and multivariate (B) analyses.

Items	PFS (Univariate Analysis)		OS (Univariate Analysis)	
	HR (95% CI)	*p*-Value	HR (95% CI)	*p*-Value
Age ≥ 70	1.07 (0.62-1.88)	0.80	1.17 (0.53-2.57)	0.69
Male gender	0.69 (0.38-1.27)	0.23	1.66 (0.62-4.43)	0.31
Recurrent	0.72 (0.34-1.54)	0.40	0.38 (0.09-1.61)	0.19
ECOG-PS = 2	0.78 (0.19-3.21)	0.73	2.19 (0.52-9.30)	0.29
Smoker	0.92 (0.50-1.70)	0.79	2.13 (0.73-6.22)	0.17
PD-L1 ≥ 50%[a]	0.76 (0.37-1.55)	0.45	0.68 (0.25-1.82)	0.44
Brain metastasis	1.43 (0.61-3.36)	0.41	0.91 (0.21-3.86)	0.90
Liver metastasis	1.47 (0.71-3.04)	0.30	1.28 (0.48-3.42)	0.62
Pembrolizumab regimen[b]	0.61 (0.27-1.38)	0.23	1.06 (0.31-3.53)	0.93
Squamous Histology	1.14 (0.62-2.12)	0.67	1.27 (0.55-2.95)	0.58
With irAEs	0.53 (0.30-0.93)	0.026	0.66 (0.30-1.44)	0.29
With mild irAEs	0.45 (0.25-0.81)	0.008	0.35 (0.14-0.89)	0.027
With severe irAEs	1.37 (0.66-2.82)	0.40	2.17 (0.91-5.21)	0.08
Pneumonitis	1.05 (0.49-2.24)	0.91	1.15 (0.40-3.37)	0.79
Rash	0.74 (0.39-1.39)	0.34	0.40 (0.14-1.16)	0.09
Thyroid dysfunction	0.46 (0.17-1.29)	0.14	0.53 (0.13-2.26)	0.39
Endocrine[c]	0.38 (0.13-1.05)	0.06	0.46 (0.11-1.95)	0.29

[a]*PD-L1 TPS ≥ 50% versus all others except for unknown.*
[b]*Pembrolizumab regimen versus Atezolizumab regimen.*
[c]*Thyroid dysfunction, Adrenal insufficiency, and hypophysitis.*
Mild irAEs: showing in grade 1-2 irAEs, severe irAEs: showing in grade 3-5 irAEs.
ECOG-PS, eastern cooperative oncology group performance status; PD-L1, programmed death ligand 1; irAE, immune-related adverse event.

TABLE 3B | Cox proportional hazards models for progression-free survival (PFS) and overall survival (OS) in all patients with non-small cell lung cancer excluding PD-L1 status, according to univariate (A) and multivariate (B) analyses.

Items	PFS (Multivariate Analysis) [a]		OS (Mulitivariate Analysis) [a]	
	HR (95% CI)	*p*-Value	HR (95% CI)	*p*-Value
With irAEs	0.53 (0.29-0.97)	0.041		
With mild irAEs	0.41 (0.22-0.77)	0.005	0.32 (0.12-0.82)	0.018

[a]*Covariables included sex (male vs female), age (≥ 70 vs < 70), histology (Squamous vs others), regimen (pembrolizumab vs atezolizumab), and brain metastasis.*
Mild irAEs: showing in grade 1-2 irAEs. irAE: immune-related adverse event.

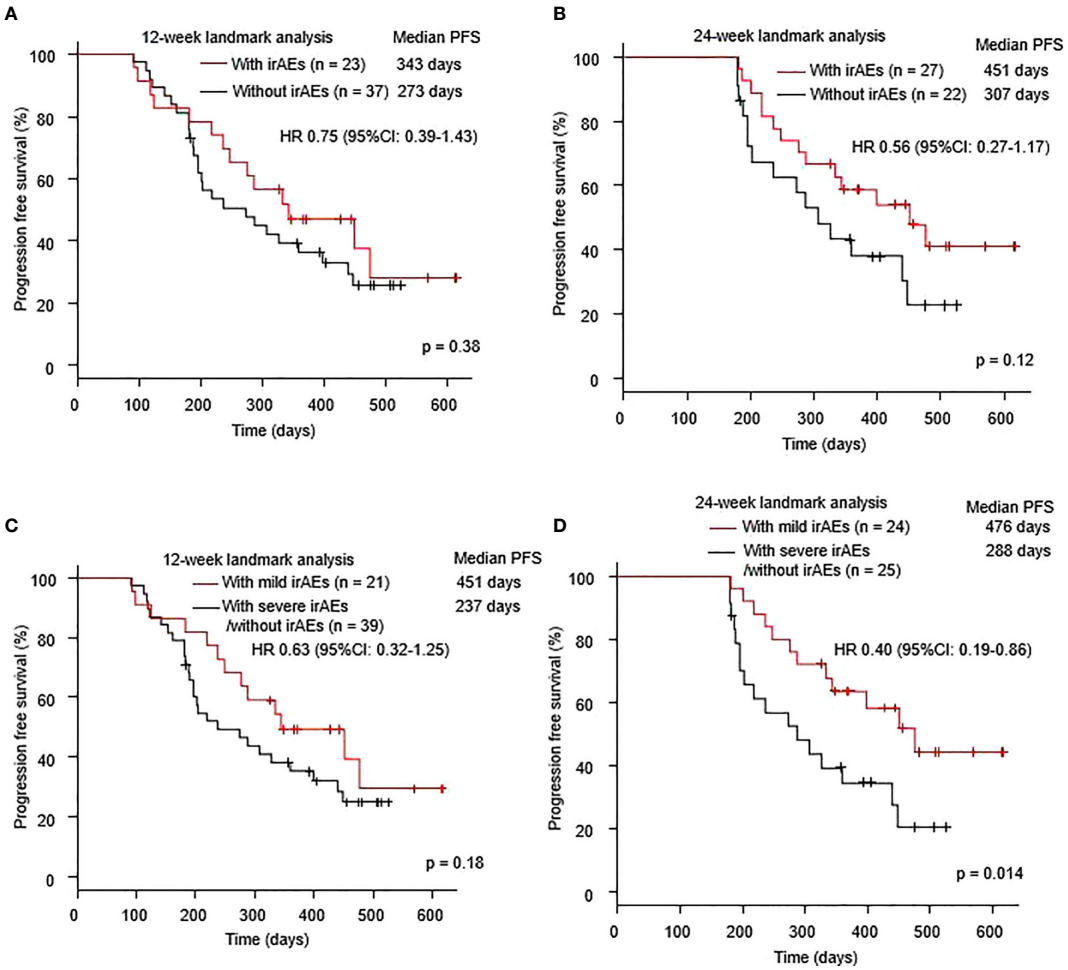

FIGURE 2 | Kaplan–Meier curves at the **(A)** 12-week and **(B)** 24-week landmark analysis for PFS in patients who received a combination of immunotherapy plus chemotherapy with or without irAEs. Kaplan–Meier curves at the **(C)** 12-week and **(D)** 24-week landmark analysis for PFS of patients who received a combination of immunotherapy plus chemotherapy with mild irAEs or with severe irAEs/without irAEs. Mild irAEs: showing in grade 1-2 irAEs, severe irAEs: showing in grade 3-5 irAEs. irAE; immune-related adverse event; PFS, progression-free survival.

Although an association has been reported between irAEs and therapeutic efficacy in ICI monotherapy regardless of race, further investigations are warranted on cohorts including other ethinicities.

Previous reports on malignant melanoma have shown an association between skin adverse events and the efficacy of programmed cell death protein 1 (PD-1) inhibitors (19). Moreover, a recent retrospective study has shown that skin reactions are associated with the clinical efficacy of anti-PD-L1 monotherapy in patients with NSCLC (20). In our retrospective study, the occurrence of skin reaction tended to be associated with clinical benefit of immunotherapy plus chemotherapy; however, the association was not significant. Interestingly, among the patients with irAEs, those with mild irAEs showed particularly good clinical outcomes, while those with severe irAEs did not show improved clinical outcomes. A recent meta-analysis reported that the occurrence of low-grade, but not high-grade irAEs is a prognostic factor for clinical outcomes in patients with solid tumors (21). Therefore, severe irAEs, which often force discontinuation of ICI treatment, may be associated with poor clinical outcomes. Moreover, severe irAEs sometimes induce serious, life-threatening events requiring strong immunosuppressive treatment and treatment discontinuation. The inflammatory tumor microenvironment may be reactivated by immunosuppressive agents, ultimately promoting tumor progression. Previous studies have also reported that ICI discontinuation owing to irAEs has a negative impact on clinical outcomes in NSCLC (22). The landmark analysis of this study showed a better trend at 24 weeks than at 12 weeks, although the difference was not significant. Although it has been reported that the various landmark points are associated with good clinical outcomes after ICI monotherapy, the results of the landmark analyses of immunotherapy plus chemotherapy may be affected by cytotoxic chemotherapy (7, 14–17). Therefore, further large-scale research is needed to identify the role of irAE grading in the clinical efficacy of immunotherapy plus

chemotherapy. Compared with clinical trials (2.8-6.6%), the occurrence of pneumonitis in our study was higher, at 14.3% (10–13). Reports suggest that the occurrence of pneumonitis may be higher in Japanese patients receiving ICI monotherapy; this suggests that the incidence of pneumonitis may be higher in Japanese patients receiving immunotherapy plus chemotherapy (23, 24).

Our study has some limitations. First, the sample size was small. This may have affected the results of landmark analyses, which failed to show statistical significance. Second, the study was retrospective, and there may have been a bias in the reporting of adverse events. Third, the combination of immunotherapy plus chemotherapy includes a multidrug regimen, and adverse events may not necessarily be irAEs. For example, pemetrexed-induced skin rashes are commonly experienced in patients with NSCLC in the real-world setting (25). However, even if all our reported irAEs were not adverse events due to ICIs, irAEs may still be associated with the clinical efficacy of immunotherapy plus chemotherapy, as they were associated with prolonged PFS.

In conclusion, our retrospective observations showed that irAEs may have a favorable therapeutic effect on the outcomes of treatment with a combination of immunotherapy plus chemotherapy in patients with advanced NSCLC. Further large-scale prospective observational studies are needed to confirm our findings.

DATA AVAILABILITY STATEMENT

The raw data supporting the conclusions of this article will be made available by the authors, without undue reservation.

ETHICS STATEMENT

The studies involving human participants were reviewed and approved by the Ethics Committees of the Kyoto Prefectural University of Medicine. Written informed consent for participation was not required for this study in accordance with the national legislation and the institutional requirements.

AUTHOR CONTRIBUTIONS

KM, TadY, and KT contributed to the conception and design. KM, CT, YO, TT, KO, YC, RT, TakY, and OH obtained the clinical data. Data were interpreted by KM, TadY, YM, MI, YK, JU, and KT. The manuscript was prepared by KM and TadY. All authors contributed to the article and approved the submitted version.

ACKNOWLEDGMENTS

We greatly thank the patients, their families, and all investigators involved in this study.

SUPPLEMENTARY MATERIAL

The Supplementary Material for this article can be found online at: https://www.frontiersin.org/articles/10.3389/fonc.2021.630136/full#supplementary-material

REFERENCES

1. Bray F, Ferlay J, Soerjomataram I, Siegel RL, Torre LA, Jemal A. Global cancer statistics 2018: GLOBOCAN estimates of incidence and mortality worldwide for 36 cancers in 185 countries. *CA Cancer J Clin* (2018) 68:394–424. doi: 10.3322/caac.21492
2. Borghaei H, Paz-Ares L, Horn L, Spigel DR, Steins M, Ready NE, et al. Nivolumab versus docetaxel in advanced nonsquamous non-small-cell lung cancer. *N Engl J Med* (2015) 373:1627–39. doi: 10.1056/NEJMoa1507643
3. Rittmeyer A, Barlesi F, Waterkamp D, Park K, Ciardiello F, von Pawel J, et al. Atezolizumab versus docetaxel in patients with previously treated non-small-cell lung cancer (OAK): a phase 3, open-label, multicentre randomised controlled trial. *Lancet* (2017) 389:255–65. doi: 10.1016/S0140-6736(16)32517-X
4. Brahmer J, Reckamp KL, Baas P, Crinò L, Eberhardt WEE, Poddubskaya E, et al. Nivolumab versus docetaxel in advanced squamous-cell non-small-cell lung cancer. *N Engl J Med* (2015) 373:123–35. doi: 10.1056/NEJMoa1504627
5. Herbst RS, Baas P, Kim DW, Felip E, Pérez-Gracia JL, Han JY, et al. Pembrolizumab versus docetaxel for previously treated, PD-L1-positive, advanced non-small-cell lung cancer (KEYNOTE-010): a randomised controlled trial. *Lancet* (2016) 387:1540–50. doi: 10.1016/S0140-6736(15)01281-7
6. Sato K, Akamatsu H, Murakami E, Sasaki S, Kanai K, Hayata A, et al. Correlation between immune-related adverse events and efficacy in non-small cell lung cancer treated with nivolumab. *Lung Cancer* (2018) 115:71–4. doi: 10.1016/j.lungcan.2017.11.019
7. Haratani K, Hayashi H, Chiba Y, Kudo K, Yonesaka K, Kato R, et al. Association of immune-related adverse events with nivolumab efficacy in non-small-cell lung cancer. *JAMA Oncol* (2018) 4:374–8. doi: 10.1001/jamaoncol.2017.2925
8. Cortellini A, Chiari R, Ricciuti B, Metro G, Perrone F, Tiseo M, et al. Correlations between the immune-related adverse events spectrum and efficacy of anti-PD1 immunotherapy in NSCLC patients. *Clin Lung Cancer* (2019) 20:237–47. doi: 10.1016/j.cllc.2019.02.006
9. Grangeon M, Tomasini P, Chaleat S, Jeanson A, Souquet-Bressand M, Khobta N, et al. Association between immune-related adverse events and efficacy of immune checkpoint inhibitors in non-small-cell lung cancer. *Clin Lung Cancer* (2019) 20:201–7. doi: 10.1016/j.cllc.2018.10.002
10. Socinski MA, Jotte RM, Cappuzzo F, Orlandi F, Stroyakovskiy D, Nogami N, et al. Atezolizumab for first-line treatment of metastatic nonsquamous NSCLC. *N Engl J Med* (2018) 378:2288–301. doi: 10.1056/NEJMoa1716948
11. Paz-Ares L, Luft A, Vicente D, Tafreshi A, Gümüş M, Mazières J, et al. Pembrolizumab plus chemotherapy for squamous non-small-cell lung cancer. *N Engl J Med* (2018) 379:2040–51. doi: 10.1056/NEJMoa1810865
12. Gandhi L, Rodríguez-Abreu D, Gadgeel S, Esteban E, Felip E, De Angelis F, et al. Pembrolizumab plus chemotherapy in metastatic non-small-cell lung cancer. *N Engl J Med* (2018) 378:2078–92. doi: 10.1056/NEJMoa1801005
13. West H, McCleod M, Hussein M, Morabito A, Rittmeyer A, Conter HJ, et al. Atezolizumab in combination with carboplatin plus nab-paclitaxel chemotherapy compared with chemotherapy alone as first-line treatment for metastatic non-squamous non-small-cell lung cancer (IMpower130): a multicentre, randomised, open-label, phase 3 trial. *Lancet Oncol* (2019) 20:924–37. doi: 10.1016/S1470-2045(19)30167-6
14. Ricciuti B, Genova C, De Giglio A, Bassanelli M, Dal Bello MG, Metro G, et al. Impact of immune-related adverse events on survival in patients with

advanced non-small cell lung cancer treated with nivolumab: long-term outcomes from a multi-institutional analysis. *J Cancer Res Clin Oncol* (2019) 145:479–85. doi: 10.1007/s00432-018-2805-3
15. Freeman-Keller M, Kim Y, Cronin H, Richards A, Gibney G, Weber JS. Nivolumab in Resected and Unresectable Metastatic Melanoma: Characteristics of Immune-Related Adverse Events and Association with Outcomes. *Clin Cancer Res* (2016) 15(22):886–94. doi: 10.1158/1078-0432.CCR-15-1136
16. Shukuya T, Mori K, Amann JM, Bertino EM, Otterson GA, Shields PG, et al. Relationship between Overall Survival and Response or Progression-Free Survival in Advanced Non-Small Cell Lung Cancer Patients Treated with Anti-PD-1/PD-L1 Antibodies. *J Thorac Oncol* (2016) 11:1927–39. doi: 10.1016/j.jtho.2016.07.017
17. Ksienski D, Wai ES, Croteau N, Fiorino L, Brooks E, Poonja Z, et al. Efficacy of Nivolumab and Pembrolizumab in Patients With Advanced Non-Small-Cell Lung Cancer Needing Treatment Interruption Because of Adverse Events: A Retrospective Multicenter Analysis. *Clin Lung Cancer* (2019) 20:e97–106. doi: 10.1016/j.cllc.2018.09.005
18. Kanda Y. Investigation of the freely available easy-to-use software 'EZR' for medical statistics. *Bone Marrow Transplant* (2013) 48:452–8. doi: 10.1038/bmt.2012.244
19. Sanlorenzo M, Vujic I, Daud A, Algazi A, Gubens M, Luna SA, et al. Pembrolizumab cutaneous adverse events and their association with disease progression. *JAMA Dermatol* (2015) 151:1206–12. doi: 10.1001/jamadermatol.2015.1916
20. Aso M, Toi Y, Sugisaka J, Aiba T, Kawana S, Saito R, et al. Association between skin reaction and clinical benefit in patients treated with anti-programmed cell death 1 monotherapy for advanced non-small cell lung cancer. *Oncologist* (2020) 25:e536–44. doi: 10.1634/theoncologist.2019-0550
21. Zhou X, Yao Z, Yang H, Liang N, Zhang X, Zhang F. Are immune-related adverse events associated with the efficacy of immune checkpoint inhibitors in patients with cancer? A systematic review and meta-analysis. *BMC Med* (2020) 18:87. doi: 10.1186/s12916-020-01549-2
22. Naqash AR, Ricciuti B, Owen DH, Florou V, Toi Y, Cherry C, et al. Outcomes associated with immune-related adverse events in metastatic non-small cell lung cancer treated with nivolumab: a pooled exploratory analysis from a global cohort. *Cancer Immunol Immunother* (2020) 69:1177–87. doi: 10.1007/s00262-020-02536-5
23. Vansteenkiste J. Nivolumab for NSCLC in Japanese patients: similar benefits, but beware of pneumonitis. *ESMO Open* (2017) 7:e000119. doi: 10.1136/esmoopen-2016-000119
24. Nishio M, Takahashi T, Yoshioka H, Nakagawa K, Fukuhara T, Yamada K, et al. KEYNOTE-025: Phase 1b study of pembrolizumab in Japanese patients with previously treated programmed death ligand 1-positive advanced non-small-cell lung cancer. *Cancer Sci* (2019) 110:1012–20. doi: 10.1111/cas.13932
25. Clark SK, Anselmo LM. Incidence of cutaneous reactions with pemetrexed: comparison of patients who received three days of oral dexamethasone twice daily to patients who did not. *J Oncol Pharm Pract* (2019) 25:1645–50. doi: 10.1177/1078155218804869

Conflict of Interest: The authors declare that the research was conducted in the absence of any commercial or financial relationships that could be construed as a potential conflict of interest.

Copyright © 2021 Morimoto, Yamada, Takumi, Ogura, Takeda, Onoi, Chihara, Taniguchi, Yamada, Hiranuma, Morimoto, Iwasaku, Kaneko, Uchino and Takayama. This is an open-access article distributed under the terms of the Creative Commons Attribution License (CC BY). The use, distribution or reproduction in other forums is permitted, provided the original author(s) and the copyright owner(s) are credited and that the original publication in this journal is cited, in accordance with accepted academic practice. No use, distribution or reproduction is permitted which does not comply with these terms.

frontiers in Oncology

ORIGINAL RESEARCH
published: 30 March 2021
doi: 10.3389/fonc.2021.626605

Transcriptome Analysis of Ivosidenib-Mediated Inhibitory Functions on Non-Small Cell Lung Cancer

Juan Wu[1†], Ru Chen[1†], Huiqing Shen[1], Ting Yan[2], Yu Qian[2], Yaping Zhang[1], Zhuoya Huang[1], Pengzhou Kong[2], Min Pang[1*] and Xinri Zhang[1*]*

[1] Department of Respiratory and Critical Care Medicine, The First Hospital, Shanxi Medical University, Taiyuan, China,
[2] Department of Pathology & Shanxi Key Laboratory of Carcinogenesis and Translational Research on Esophageal Cancer, Shanxi Medical University, Taiyuan, China

Ivosidenib is an isocitrate dehydrogenase mutant inhibitor that the US Food and Drug Administration recently approved for the treatment of leukemia. Studies suggested that ivosidenib may inhibit the progression of non-small cell lung cancer (NSCLC). In the present study, we explored RNAs and their potential regulatory mechanisms by which ivosidenib treats NSCLC cells. We used MTT assays, Transwell assays, and flow cytometry to measure the anti-tumor effects of ivosidenib in NSCLC cells. We performed whole transcriptome sequencing to determine differentially expressed mRNAs (DE-mRNAs) and non-coding RNAs (ncRNA). We used GO and KEGG pathway enrichment analyses to identify the functions and potential mechanisms. According to miRNA target interactions, we constructed a competing endogenous network. Ivosidenib inhibited the proliferation, invasion, and migration of NSCLC cells and inhibited tumor growth *in vivo*. We identified 212 DE-mRNAs, four DE-miRNAs, and 206 DE-lncRNAs in ivosidenib-treated NSCLC cells compared to untreated NSCLC cells. DE-mRNAs were significantly enriched in the cancer-associated pathways, including the TGF-β signaling pathway, the PI3K-Akt signaling pathway, the Jak-STAT signaling pathway, the MAPK signaling pathway, the Rap1 signaling pathway, and cell adhesion molecules. Based on the competing endogenous RNA hypothesis, we constructed lncRNA-miRNA-mRNA networks to elucidate the regulatory relationships between mRNA and ncRNA. We found that qRT-PCR results showed corresponding expression trends of differential genes with sequencing data. Our results provide insights into the molecular basis of ivosidenib suppression of NSCLC.

Keywords: ivosidenib, RNA-seq, bioinformatic analysis, ceRNA, non-small cell lung cancer

OPEN ACCESS

Edited by:
Junji Uchino, Kyoto Prefectural University of Medicine, Japan

Reviewed by:
Andrea Lapucci, University of Florence, Italy
Chong Teik Tan, National University of Singapore, Singapore

***Correspondence:**
Pengzhou Kong
kongpengzhou@sxmu.edu.cn
Min Pang
pangmin2009@126.com
Xinri Zhang
ykdzxr61@163.com

†These authors have contributed equally to this work

Specialty section:
This article was submitted to Pharmacology of Anti-Cancer Drugs, a section of the journal Frontiers in Oncology

Received: *06 November 2020*
Accepted: *05 March 2021*
Published: *30 March 2021*

Citation:
Wu J, Chen R, Shen H, Yan T, Qian Y, Zhang Y, Huang Z, Kong P, Pang M and Zhang X (2021) Transcriptome Analysis of Ivosidenib-Mediated Inhibitory Functions on Non-Small Cell Lung Cancer. Front. Oncol. 11:626605. doi: 10.3389/fonc.2021.626605

INTRODUCTION

Lung carcinoma carries the highest incidence and mortality among cancers (1); we divide it into small cell and non-small cell lung cancer (NSCLC). Approximately 85% of lung carcinoma is NSCLC, which includes lung adenocarcinoma (40% of NSCLC), lung squamous cell carcinoma (40% of NSCLC), large cell carcinoma (10% of NSCLC), and other less common subtypes. Despite substantial progress in cancer therapies, the 5-year survival rate of NSCLC remained about 18%, suggesting an urgent need for new agents to combat this malignancy (2).

Isocitrate dehydrogenases participate in various aspects of cellular metabolism. Isocitrate dehydrogenase 1 (IDH1) converts isocitrate to α-ketoglutarate (α-KG) by reducing NADP+ to NADPH; this is important for reduction-oxidation balance that the glutathione and thioredoxin systems establish (3). Numerous studies showed mutations in IDH1 in several malignancies, the most common mutation being IDH1 R132H (4–6). IDH1 mutations (mIDH1) lead to abnormal IDH1 function that converts α-KG into 2-hydroxyglutarate (2-HG). MIDH1 occurs in low-grade (grade I and II) glioma (5), acute myeloid leukemia (AML) (6), chondrosarcoma (7), and T cell lymphomas (8). In a large population study, a total of 298 lung carcinoma samples [179 samples by Kang et al. (9), 107 samples by Bleeker et al. (10), and 12 samples by Tan et al. (11)] showed no IDH1 mutations. Rodriguez et al. analyzed IDH1/2 mutations in 1924 NSCLC specimens (92% adenocarcinoma) using next-generation sequencing and identified IDH1/2 mutations in nine (0.5%) adenocarcinomas (12). These findings suggest that mIDH1 in NSCLC is relatively rare. A large population-based study convincingly showed elevated levels of IDH1 transcription and translation in NSCLC tissues compared with those of paired normal tissues (11, 13). Owing to its favorable specificity and sensitivity, the IDH1 level may be a diagnostic marker for NSCLC diagnosis (11). A study showed that knockdown of IDH1 by RNA interference reduced the proliferative capacity of NSCLC cells and significantly decreased *in vivo* xenograft tumor formation, suggesting that IDH1 may be a potential target in lung cancer (11).

Ivosidenib (AG-120) is a potent inhibitor of the mIDH1 that has clinical activity and safety profiles. In 2018, investigators began using ivosidenib to treat leukemia (14). Studies showed that ivosidenib exhibited rapid-equilibrium inhibition against the mIDH-R132 homodimer; research also showed that ivosidenib bound and inhibited the IDH1-WT homodimer (14). These observations suggest that ivosidenib may inhibit the progression of other cancers with high IDH1 expression. In other words, ivosidenib may be a potential therapeutic drug candidate for NSCLC treatment. Nevertheless, its effects on NSCLC, as well as the potential mechanisms, remain unclear.

Long non-coding RNAs (lncRNAs) are ncRNAs that are 200 nucleotides in length. They regulate the expression of target genes transcriptionally and post-transcriptionally, without protein-coding function. A substantial body of evidence supports the involvement of lncRNAs in carcinogenesis and cancer progression (15). MiRNAs are endogenous non-coding small RNAs (ncRNAs) with 22 nucleotides that bind to 3'-UTR of target genes' mRNA and negatively regulate their expression by inhibition of translation or degradation of mRNAs (16). Several lines of evidence suggest that miRNA mediates an extensive range of cancer processes, including cell proliferation, migration, invasion, and apoptosis (17). Fang et al. demonstrated that the overexpression of miR-20a-5p stimulated NSCLC to proliferate and invade (18). Zhang et al. suggested that miR-493-5p suppressed tumors in osteosarcoma cells; overexpression of miR-493-5p suppressed proliferation and metastasis (19). The ceRNA hypothesis states that non-coding RNAs like lncRNAs serve as microRNA (miRNA) sponges that competitively bind miRNA through miRNA response elements and inhibit miRNAs from binding to their target mRNAs and regulating their expression (16). The ceRNA network participates in carcinogenesis in various cancer types.

In the present study, we used high-throughput transcriptome sequencing on ivosidenib-treated NSCLC A549 and SK-MES-1 cells to identify differentially expressed RNAs. We performed a full-scale analysis of differentially expressed lncRNAs, miRNAs, and mRNAs using a bioinformatics approach. Finally, based on sequencing results, bioinformatics predictions, and ceRNA regulatory rules, we constructed a ceRNA network of lncRNAs, miRNAs, and mRNAs. Based on all of the above, for the first time, we elucidated the potential mechanisms of ivosidenib-mediated NSCLC cell suppression using transcriptome analysis. Our findings will help build a theoretical basis for future treatment of NSCLC using ivosidenib.

MATERIALS AND METHODS

Cell Lines and Culture Conditions

We purchased five lung cancer cell lines (A549, NCI-H1650, NCI-H1299, SK-MES-1, NCI-H226) from the Cell Bank of the Chinese Academy of Sciences (Shanghai, China). A549, NCI-H1650, and NCI-H1299 are lung adenocarcinoma cell lines, and SK-MES-1 and NCI-H226 are lung squamous cell carcinoma cell lines. We obtained human bronchial epithelial cells (BEAS-2B) and dedicated culture solutions from the Cell Bank of the Chinese Academy of Sciences (Kunming, China). We maintained lung cancer cells in RPMI-1640 supplemented with 10% fetal bovine serum (FBS) and 100 U/ml penicillin/0.1 mg/ml streptomycin at 37°C with 5% CO_2. We cultured BEAS-2B in a dedicated culture solution at 37°C with 5% CO_2. We used A549 and SK-MES-1 that had relatively higher expression of IDH1 to perform functional experiments.

Drug and Reagents

We purchased ivosidenib from MedChemExpress (Monmouth, NJ, USA). We dissolved ivosidenib powder in sterile dimethyl sulfoxide (DMSO) to prepare a 50 mM stock solution stored at −80°C. The 3-(4,5-dimethylthiazol-2-yl)-2,5-diphenyltetrazolium bromide (MTT) was from Sigma Chemical Corporation (St. Louis, MO, USA). We obtained the cell cycle detection kit from BD Biosciences (San Jose, CA, USA).

TRIzol reagent was from Invitrogen (Carlsbad, CA, USA), RT reagent Kit and SYBR Green PCR Master Mix were from Promega (Madison, WI, USA). MiRNeasy Mini Kit, miRCURY LNA RT Kit, and miRCURY LNA SYBR Green PCR Kit were from QIAGEN (Valencia, CA, USA).

RNA Extraction and RT-qPCR

We isolated total RNA from A549, NCI-H1650, NCI-H1299, SK-MES-1, NCI-H226, and BEAS-2B using TRIzol reagent and converted to cDNA according to the PrimeScript RT reagent kit manufacturer's instructions. The cDNA underwent quantitative real-time PCR to detect IDH1, following the 2–ΔΔCT method analysis. We used B2M as an internal control. The primers sequences for the genes were as follows: IDH1, forward 5'-ACTGTAACCCGTCACTACCG; reverse 5'-AGTCC TTGGTCATGAAGCCA; B2M, forward 5'-AGCAGCATCA TGGAGGTTTG; reverse 5'-AGCCCTCCTAGAGCTACCTG.

Growth Inhibition Assay

We used the MTT assay to measured proliferation. We seeded cells in the log-phase in 96-well plates cultured overnight with five repeats for each group. We treated cells with various ivosidenib concentrations incubated for 24, 48, and 72 h at 37°C with 5% CO_2. We then incubated the cells in MTT (0.25 mg/ml) for 4 h at 37°C. After medium removal, we lysed cells with DMSO. We measured absorbance 490 nm to determine the percentage of surviving cells.

Colony-Formation Assay

We seeded A549 and SK-MES-1 cells in six-well plates with 200 and 500 cells per well, respectively. After adhering overnight, we treated the cells with various concentrations of ivosidenib for 2 weeks, and replaced medium every 3 days. To visualize the results, we fixed colonies in 4% paraformaldehyde and incubated them in crystal violet solution.

Transwell Assay

Transwell migration assay occurred in chemotaxis chambers containing 24 wells. We inoculated cells into the upper chamber in 200 μl RPMI-1640 without serum that contained or did not contain ivosidenib. Bottom chambers contained RPMI-1640 medium containing 10% FBS. After 24 h of treatment, we fixed cells using 4% paraformaldehyde and stained with 0.25% crystal violet solution. The stained cells were counted using a microscope.

For the invasion assay, we added Matrigel (1:10 dilution) to the Transwell plate to form the matrix barrier. We resuspended cells in 200 μl contained 5% FBS RPMI 1640 medium that contained or did not contain ivosidenib and placed them in the upper chambers. We placed 600 μl 20% FBS RPMI 1640 medium in the lower chambers. After 48 h of treatment, we determined cell invasion using crystal violet staining. We imaged and counted stained cells as in the migration assay.

Cell Cycle Assay

We incubated cells with various concentrations of ivosidenib for 24 h. We suspended cells in 70% ethanol, incubated them at 4°C overnight, and collected them using centrifugation at 1,500 rpm for 3 min. We then added 200 μl PI/Rnase A staining solution, and incubated cells for 60 min in the dark. We measured proportions of cells in each cycle using flow cytometry.

Tumor Formation in BALB/c Nude Mice

We procured female BALB/c nude mice (5 weeks old) from the Beijing Charles River Laboratory Animal Technology Co., Ltd. (Beijing, China) to perform the xenograft experiments. We maintained all animals at 21–25°C, humidity 30–40%, and allowed them free access to food and water. To establish lung cancer xenograft model, we subcutaneously injected A549 cells (5×10^6 cells) in the logarithmic phase of growth into the mice in their left flanks. We randomly subdivided mice into two groups: the control group (PBS, n = 4) and the drug-treated group (ivosidenib, n = 4). Subsequently, each mouse in the drug-treated group received once per day by oral gavage a dose of 150 mg/kg ivosidenib for 15 days (14). We measured tumor volumes every 3 days according to the following formula: $V = (L \times W^2)/2$, where L is the longer tumor diameter and W is the smaller diameter. We sacrificed the mice 24 h after the final dose, and isolated and weighed the subcutaneous tumors. We performed animal-related procedures according to the guide for the Care and Use of Laboratory Animals, with the approval of the Shanxi Medical University (Taiyuan, China).

Whole-Transcriptome Sequencing

We performed RNA sequencing in drug-treated A549 cells (50 and 100 μM)/SK-MES-1 cells (75 and 100 μM) and their parent cell lines (A549 and SK-MES-1), Novogene Co., Ltd (Beijing, China).

Bioinformatics Analysis

We considered genes with $|\log_2 \text{FoldChange}| > 1$ and adjusted p-values <0.05 as differentially expressed genes (DEGs). We considered DE-mRNAs, DE-miRNAs, and DE-lncRNAs with the same expression trend intersecting from 100 μM ivosidenib group of A549 and SK-MES-1 as common DE-mRNAs, DE-miRNAs, and DE-lncRNAs compared to control. We drew volcano maps to generate graphical overviews of expression profile using the ggplot2 package in R software (20). We used the heatmap package in R to plot the heat map of DE-RNAs (20). To explore the possible functions of DE-mRNAs, we performed gene ontology (GO) functional enrichment using DAVID (https://david.ncifcrf.gov/) and KEGG pathway enrichment analysis using KOBAS 3.0 (http://kobas.cbi.pku.edu.cn/kobas3) (20). Briefly, GO analyses consisted of three components: biological process (BP), cellular component (CC), and molecular function (MF). We considered $p < 0.05$ Gene Ontology (GO) and Kyoto Encyclopedia of Genes and Genomes (KEGG) pathways as statistically significant. Then,

we used the STRING online database (version 11.0 https://string-db.org/) to retrieve the protein-protein interactions (PPI). We visualized PPI pairs with a combined confidence score ≥0.4 in the network using Cytoscape 3.6.1 software (21).

Construction of the LncRNA-miRNA-mRNA-Related ceRNA Regulatory Network

We screened target mRNAs of DE-miRNA using TargetScan (http://www.targetscan.org/). We predicted DE-miRNA target lncRNA using miRWalk2.0 (http://zmf.umm.uni-heidelberg.de/apps/zmf/mirwalk2/index.html). We selected miRWalk, TargetScan, and RNAhybrid to decode the relationships between the differentially expressed miRNAs and lncRNAs (22). According to the ceRNA regulatory mechanism and the changing trends of lncRNAs, miRNAs, and mRNAs, we constructed a ceRNA regulatory network using Cytoscape 3.6.1. Different shapes represent different RNA types, colors represent different regulated relationships.

Validation of Significant miRNAs and Target Genes

We validated significant DE-ncRNAs and DE-mRNAs using quantitative reverse transcription-polymerase chain reaction (qRT-PCR). We obtained the TaqMan qRT-PCR probes and primers for quantification of miRNAs from QIAGEN (Hilden, Germany) as follows: miR-148a-5p (product ID: YP00204188), miR-493-5p (product ID: YP00204166), and U6 (product ID: YP00203907). We used the 2−ΔΔCt method to calculate relative expression levels of mRNA, miRNA, and lncRNA, normalized to B2M or U6 snRNA. See **Table 1** for the display of the Gene primer list.

Statistical Analysis

We used GraphPad Prism 6.0 software for all analyses. We analyzed cell functions and qRT-PCR outputs using continuous variable two-tailed Student's t-tests. We analyzed sequencing data using bioinformatic tools. Statistical significance is presented in figures as *$p < 0.05$, **$p < 0.01$, or ***$p < 0.001$.

TABLE 1 | The primers for qRT-PCR.

Name	Sequence (5'-3')
DDIAS-Forward Primer	AGGTTCAGATGCCAGTAACTTCT
DDIAS-Reverse Primer	AGTGATTGTTAGGTGCCTGAGA
PLEKHO1-Forward Primer	AAACAGCCCGGTAACACGG
PLEKHO1-Reverse Primer	GGCATTGATCCACGATTCCTT
ZBED6-Forward Primer	GAAGGGTTTGCGAATTAAGGGG
ZBED6-Reverse Primer	GGGTCATTGGAAGCTAACAAAGC
SMAD5-Forward Primer	CCAGCAGTAAAGCGATTGTTGG
SMAD5-Reverse Primer	GGGGTAAGCCTTTTCTGTGAG
PCK2-Forward Primer	CATCCCAACTCTCGATTTTGTG
PCK2-Reverse Primer	TTCCCAGAAGTCCTTTGTGTTC
CHAC1-Forward Primer	GATTTTCGGGTACGGCTCCC
CHAC1-Reverse Primer	GAAGGTGTCTCCCTGCCAGA
PARD6G-AS1-Forward Primer	CCCACTGCCCTCCCTCCAAG
PARD6G-AS1-Reverse Primer	CGGTGTCTCCTGCTTTCTGTTCC
CTBP1-AS-Forward Primer	ACAACACAAAGCCCCGGAA
CTBP1-AS–Reverse Primer	GAAGAATGGTCTCGCCC
B2M-Forward Primer	AGCAGCATCATGGAGGTTTG
B2M-Reverse Primer	AGCCCTCCTAGAGCTACCTG

RESULTS

IDH1 mRNA Expression in NSCLC Cell Lines

The chemical structure of Ivosidenib is shown in **Figure 1A**. Ivosidenib may be a potential therapeutic drug candidate for NSCLC with high IDH1 expression. We measured IDH1 expression in five NSCLC cell lines (A549, NCI-H1299, NCI-H1650, SK-MES-1, and NCI-H226) and BEAS-2B. BEAS-2B, human normal bronchial epithelial cells, served as non-cancer reference lung cells. Expression levels of IDH1 were higher in A549 and SK-MES-1 cells than in normal BEAS-2B cells (**Figure 1B**).

Ivosidenib Inhibits Proliferation, Migration, and Invasion of A549 and SK-MES-1 Cells

To determine whether ivosidenib affects the biological behaviors of NSCLC cells, we conducted MTT assay, colony formation, and Transwell assay to measure the effects of ivosidenib on NSCLC cells. The NSCLC cell lines with high IDH1 expression were more sensitive to ivosidenib. The IC_{50} values of A549 and SK-MES-1 were 49.90 and 60.54 μM, respectively (**Figure 2**). A549 and SK-MES-1 cell viabilities were lower after treatment with ivosidenib for 24, 48, and 72 h. The suppression rates were dose-dependent but not time-dependent (**Figure 1C**). These findings suggest that 24 h of treatment was optimal, and therefore we chose this time course for subsequent experiments. As shown in (**Figure 1D**), the number of colonies inversely correlated with concentrations of ivosidenib. We performed a Transwell array in A549 and SK-MES-1 cells to evaluate the effect of ivosidenib on cell invasion and migration and found that the invasion and migration abilities of A549 and SK-MES-1 cells were significantly lower in the ivosidenib-treatment group than in the control group (**Figures 3A, B**).

Ivosidenib Induces Cell Cycle Arrest in A549 and SK-MES-1 Cells

We measured the effects of ivosidenib on the cell cycle in A549 and SK-MES-1 cells using flow cytometry. Ivosidenib treatment gave rise to concentration-dependent cell cycle arrest at the G0-G1 phase (**Figure 4**). These findings suggest that ivosidenib efficiently suppresses the proliferation of A549 and SK-MES-1 cells.

Ivosidenib Inhibits Tumor Growth in NSCLC Xenografted Mice

To study the anti-tumor effect of ivosidenib *in vivo*, we established a xenograft nude mice model using A549 cells. The detailed experimental design is shown in (**Figure 5A**). As shown in **Figures 5B, C, E, F,** compared with the vehicle group, the

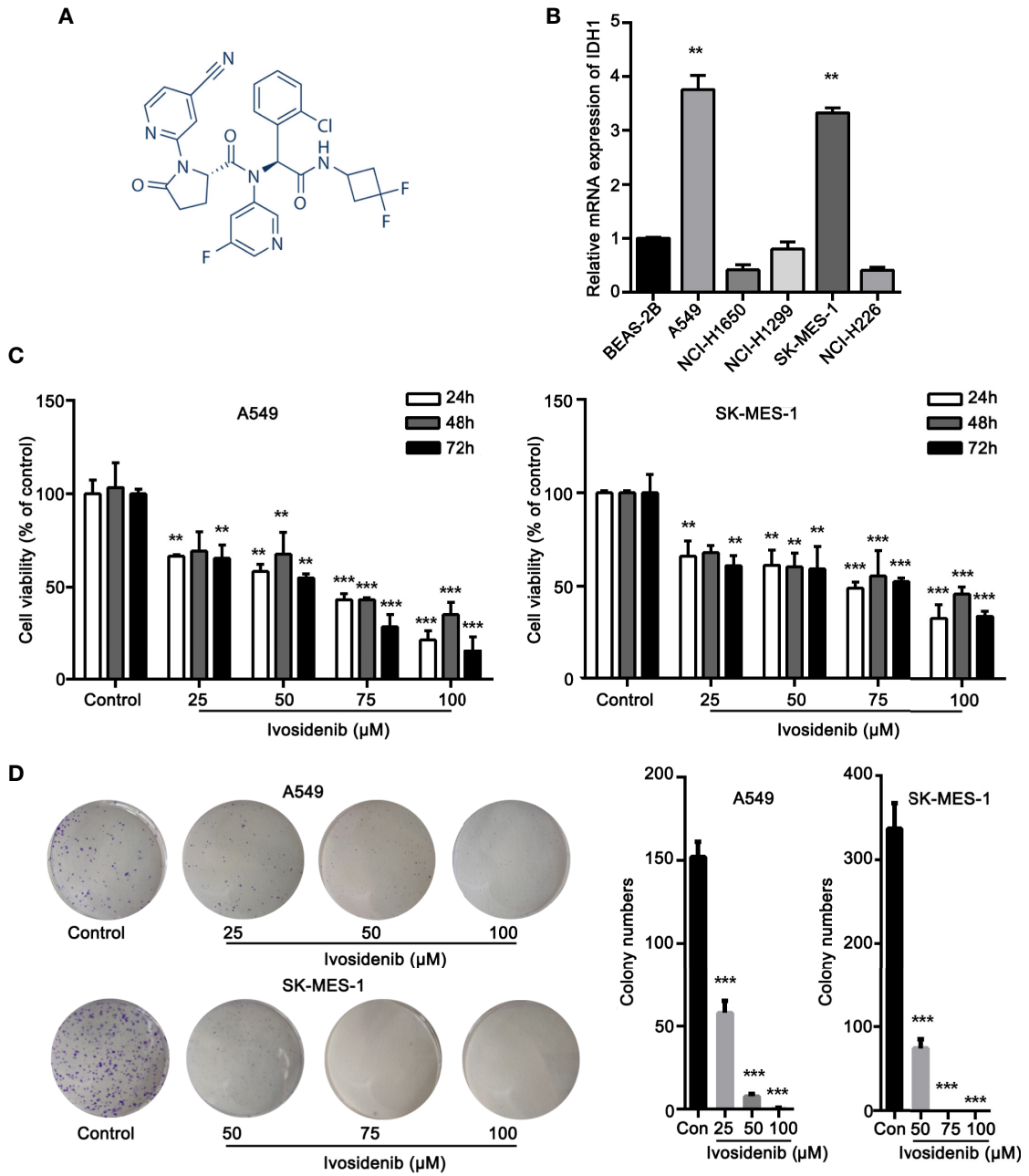

FIGURE 1 | Ivosidenib inhibits the proliferation of NSCLC cells. **(A)** Chemical structure of ivosidenib. **(B)** IDH1 expression in NSCLC and BEAS-2B cell lines. **(C)** A549 and SK-MES-1 cells were treated with various concentrations of ivosidenib for 24, 48, and 72 h, and proliferation was measured using the MTT assay. Data are expressed as mean ± SD of three separate experiments. **(D)** Colony-formation assay (representative wells are presented). $^{**}p < 0.01$, $^{***}p < 0.001$ *vs.* control.

volumes and weights of the tumors were lower in the ivosidenib groups. Ivosidenib did not significantly affect body weights (**Figure 5D**), suggesting that the drug was not toxic at the experimental dose. These results suggest that ivosidenib inhibits tumor growth of NSCLC cells *in vivo*.

Identification of Differentially Expressed mRNAs, miRNAs, and lncRNAs

To elucidate the anti-cancer mechanisms of ivosidenib, we performed RNA sequencing in drug-treated A549, SK-MES-1 cells, and their parent cell lines. Applying the cutoffs of

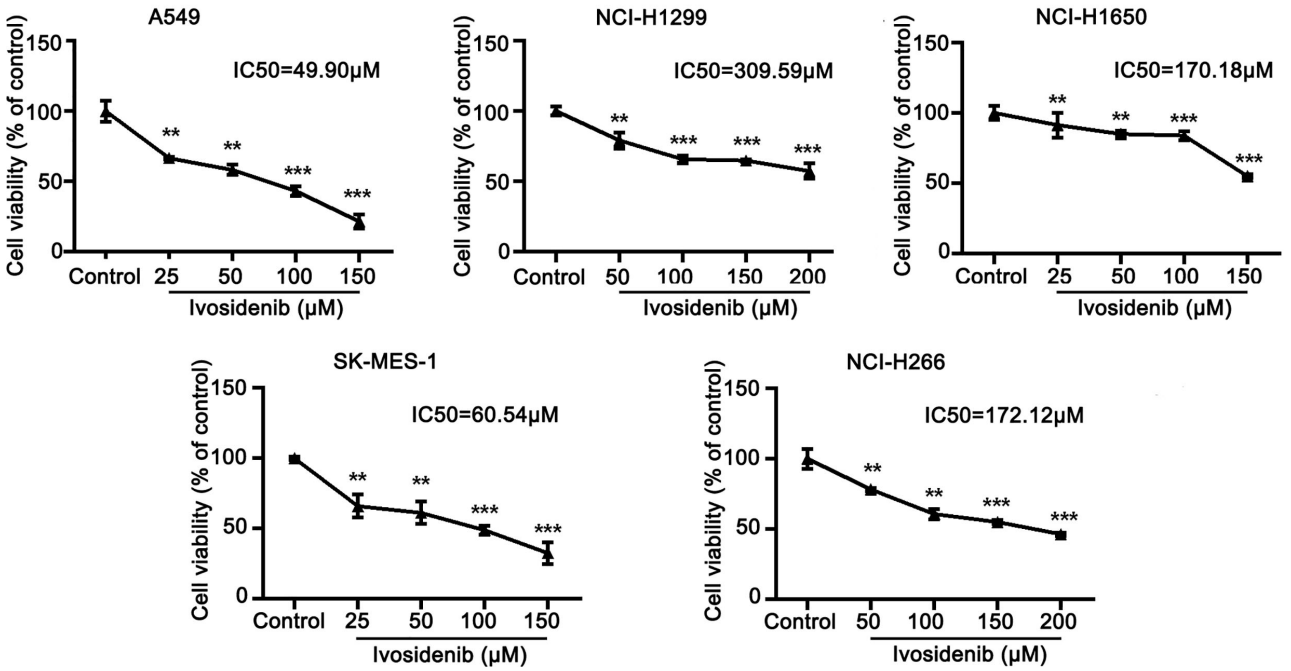

FIGURE 2 | The sensitivity of different NSCLC cell lines to ivosidenib. NSCLC cells were treated with the control (RPMI-1640 culture) and various concentrations of ivosidenib for 24 h, cell proliferation was measured using a MTT assay. The MTT assay was performed to determine cell viability and values are expressed as the mean ± SD of three separate experiments. $^{**}p < 0.01$, and $^{***}p < 0.001$ *vs.* Control.

p-value < 0.05 and |log2FoldChange| > 1, we selected DE-mRNAs. The volcano plot of mRNA revealed that a total of 1,408 and 1,477 mRNAs changed in the A549 and SK-MES-1, respectively (**Figure 6A**). Totals of 1,554 and 1,684 lncRNAs markedly changed in the A549 and SK-MES-1, respectively (**Figure 6B**). There were 18 altered miRNAs in A549 and 74 altered miRNAs in SK-MES-1 (**Figure 6C**). As shown in the Venn diagram, 212 DE-mRNAs (131 up- and 81 down-regulated), 206 DE-lncRNAs (104 up- and 102 down-regulated), and 4 DE-miRNAs (three up- and one down-regulated) appeared from two cells (**Figures 6D–F**). Heatmap analysis visually displayed expression levels of DE-mRNAs and DE-lncRNAs (**Figures 7A, B**).

Functional Enrichment Analysis of DE-mRNAs

To illuminate the biological functions of DE-mRNAs, we performed GO term enrichment analysis and KEGG pathway analysis. **Figure 8A** shows the top 20 ranked GO in terms of DE-mRNAs. DE-mRNAs ontology (GO) enrichment analysis revealed that the majority of these genes are enriched in cellular amino acid biosynthetic processes, SMAD protein signal transduction, regulation of the MAPK cascade, transforming growth factor β receptor binding, regulation of apoptosis, and others. GO enrichment analysis indicated that these cell processes were the most influential processes affected by ivosidenib.

KEGG pathway analysis helps us better understand the biological function of genes. We screened 41 pathways with significantly differential expressions (p <0.05) (**Table S1**). **Figure 8B** shows the top 20 ranked significant pathways in KEGG. DE-mRNAs were significantly enriched in metabolic and cancer-associated pathways including metabolic pathways, biosynthesis of amino acids, alanine, aspartate, and glutamate metabolism, the PI3K-Akt signaling pathway, the TGF-β signaling pathway, cell adhesion molecules (CAMs), the Jak-STAT signaling pathway, the MAPK signaling pathway, and the Rap1 signaling pathway.

To explore the connections of these DE-mRNAs, we established a protein-protein interaction (PPI) network using the STRING online database. We used Cytoscape (version 3.6.1) to visualize the PPI network (**Figure 9**). The results may provide important information regarding the activity of ivosidenib in NSCLC A549 and SK-MES-1 cells.

Validation of DE-mRNA and DE-ncRNA Expression

To determine the accuracy of transcriptome sequencing, we randomly selected 10 DE-RNAs to verify the reliability of high-throughput RNA sequencing using qRT-PCR. As shown

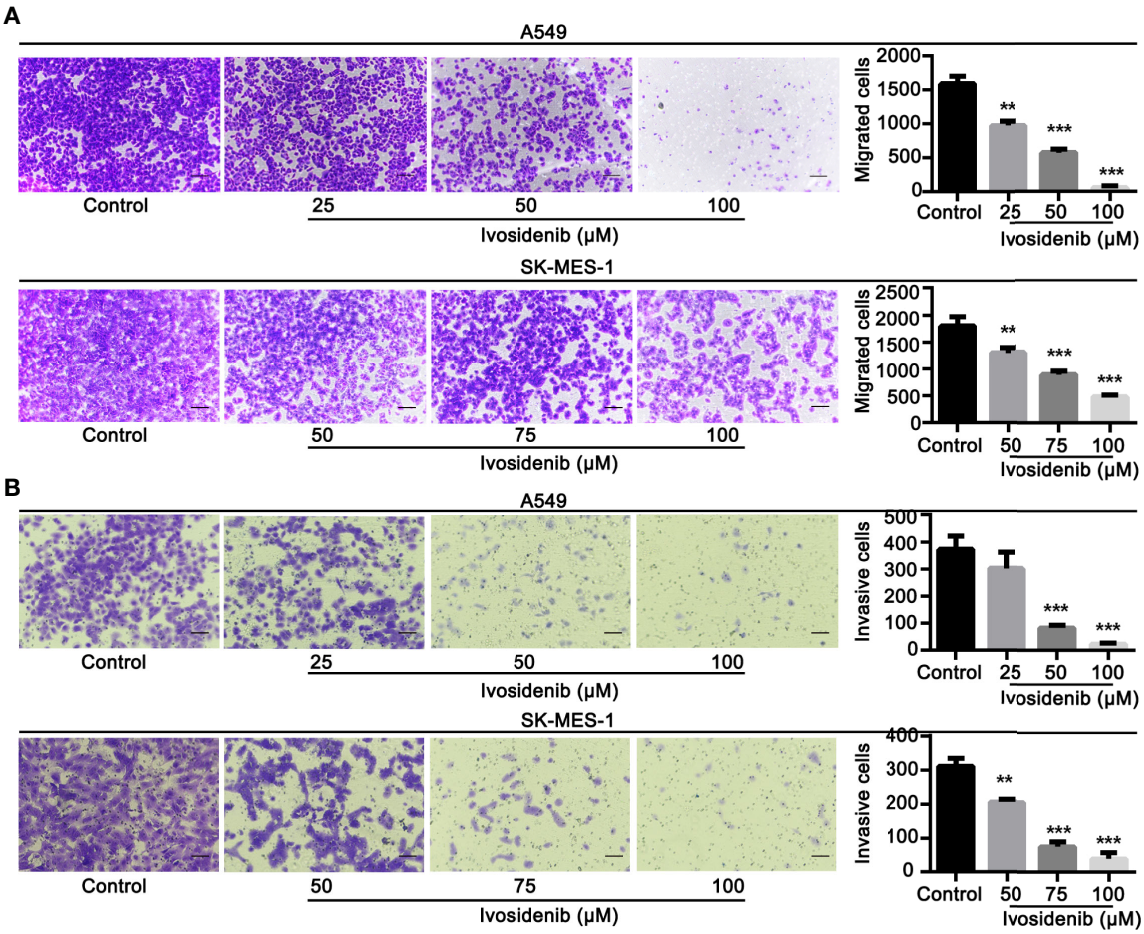

FIGURE 3 | Ivosidenib inhibits invasion and migration of NSCLC cells. **(A)** A549 were treated with 25, 50, and 100 μM of ivosidenib for 24 h to measure migration. SK-MES-1 were treated with 50, 75, and 100 μM of ivosidenib for 24 h to measure migration. **(B)** A549 were treated with 25, 50, and 100 μM of ivosidenib for 48 h to measure migration. SK-MES-1 were treated with 50, 75, and 100 μM of ivosidenib for 48 h to measure migration. The quantitative results are shown in the right panel, and data are expressed as mean ± SD of three independent experiments. ** $p < 0.01$, and *** $p < 0.001$ *vs.* control.

in **Figure 10**, the agreement between their expression trends and RNA-seq data reflects the reliability of RNA-seq data. According to the RNA-seq and qRT-PCR results, expressions levels of four mRNAs (SMAD5, PLEKHO1, ZBED6, DDIAS) and two lncRNAs (PARD6G-AS1, CTBP1-AS) were lower after ivosidenib treatment; expression levels of two mRNAs (CHAC1, PCK2) and two miRNAs (miR-148a-5p, miR-493-5p) were greater after ivosidenib treatment (**Figure 10**).

Construction of a ceRNA Regulatory Network

To further explore the roles of the altered DE-lncRNAs, DE-miRNAs, and DE-mRNAs in drug-treated NSCLC cell lines and to clarify the relationships among them, we generated a ceRNA regulatory network. First, we used Targetscan to decode the relationships between the altered miRNAs and mRNAs. The algorithm predicted three miRNAs to interact with 68 DEmRNAs (**Table S2**). Next, we used miRWalk, TargetScan, and RNAhybrid to analyze the relationships between the altered lncRNAs and miRNAs (**Table S3**). We selected the miRNAs that were negatively regulated by the lncRNAs and mRNAs to build the LncRNA-miRNA-mRNA network. We used Cytoscape (version 3.6.1) to visualize the ceRNA network. We constructed a ceRNA network including three DE-miRNAs (miR-148a-5p, miR-652-5p, and miR-493-5p), 17 target DE-mRNAs (SMAD5, PLEKHO1, PFN2, IL7R, ZNF778, MAP2K6, and others), and five target DE-lncRNAs (PARD6G-AS1, ISPD-AS1, LINC01030, AC023481.1, and AC138035.2) (**Figure 11**).

To further understand the potential function of mRNAs and to provide useful information for experiments, we identified a lncRNA-miRNA-mRNA axis based on the results of the functional analysis. From the previous steps, we identified

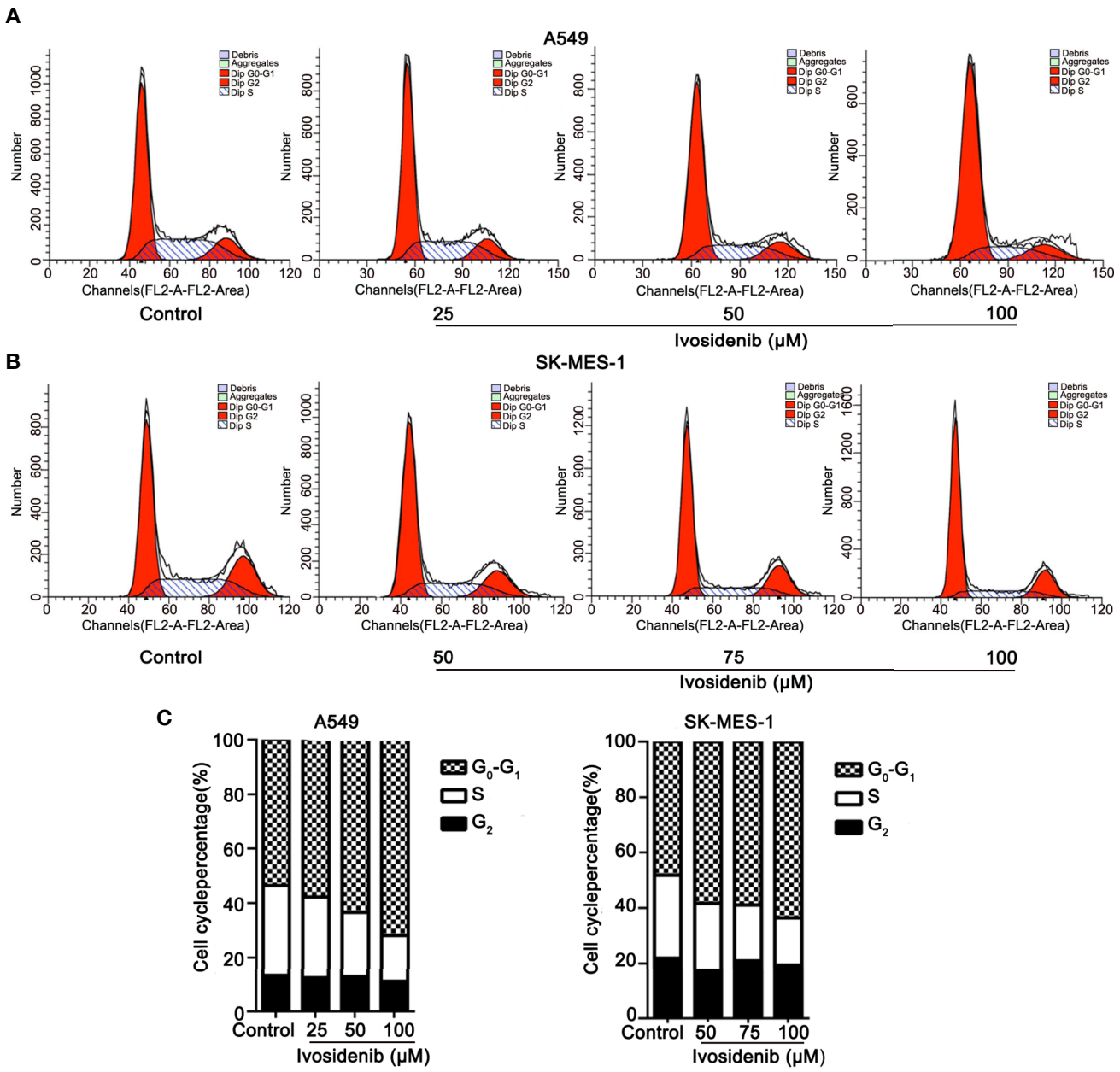

FIGURE 4 | Ivosidenib inhibits the cell cycle in NSCLC cells. **(A)** Flow cytometric analysis was used to measure cell cycle distributions of A549 cells after 24 h of culture with ivosidenib at 25, 50, and 100 μM. **(B)** Flow cytometric analysis was used to measure cell cycle distributions of SK-MES-1 cells after 24 h of culture with ivosidenib at 50, 75, and 100 μM. **(C)** The results are reported in the diagram. Data represent the means ± SD of three separate experiments.

several GO terms and KEGG pathways. Next, we reorganized the mRNAs that significantly correlated with cancer progression and linked their upstream miRNA and lncRNA, such as ISPD-AS1-has-miR-148a-5p-SMAD5, and PARD6G-AS1-has-miR-493-5p-PFN2 (**Table 2**). We believe these axes will provide more information and that are appropriate for experiments. In the future, much more lab experiments need to be conducted to further validate these findings.

DISCUSSION

The US Food and Drug Administration approved the use of ivosidenib, an inhibitor of IDH1, to treat acute myelogenous leukemia (AML) harboring IDH1 mutations in a phase I clinical trial (23). In the present study, levels of proliferation, migration, and invasion of NSCLC cells (A549, SK-MES-1) were significantly lower, and cell cycle arrested at the G0-G1 phase

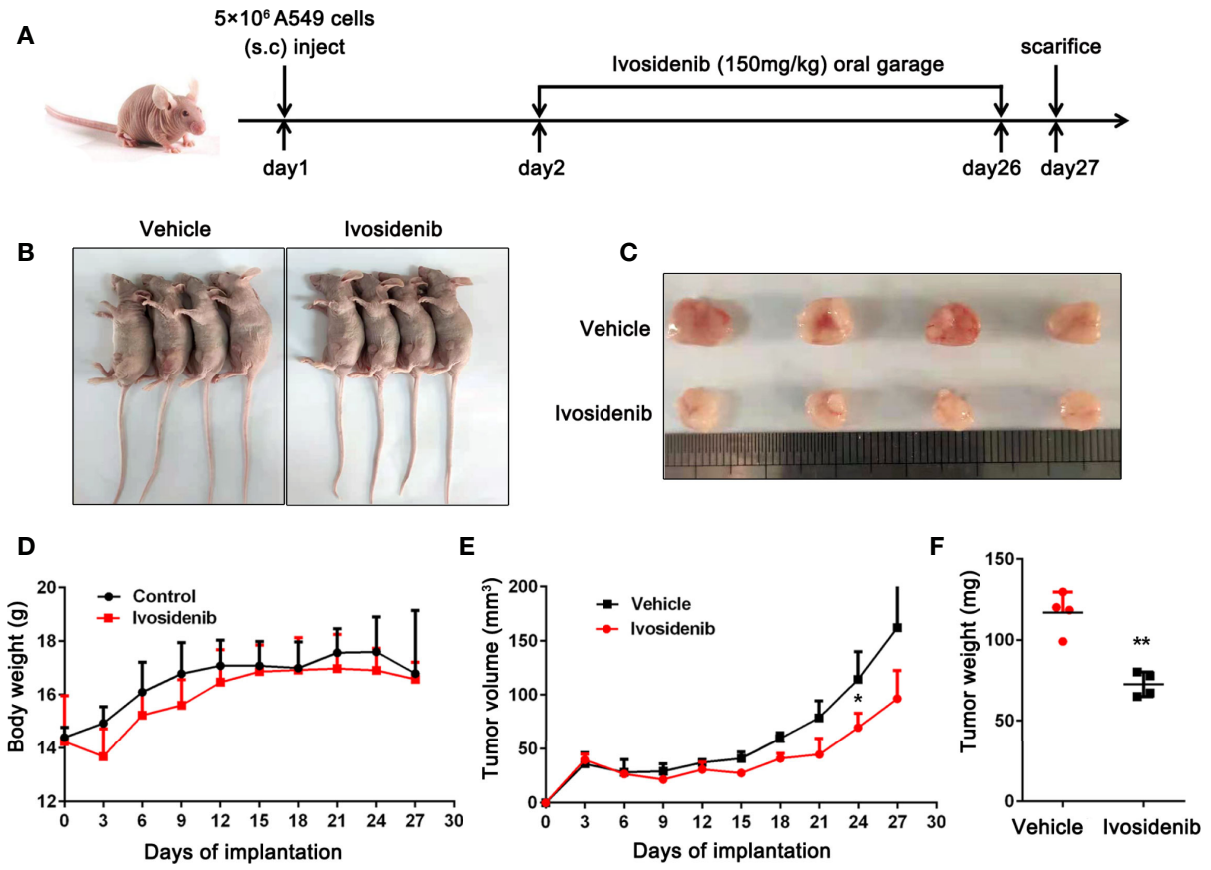

FIGURE 5 | Ivosidenib inhibits the tumor growth *in vivo*. **(A)** Diagram of the animal study protocol. **(B)** Representative images show tumor xenografts. **(C)** The image and **(E)** weight of tumor harvested. **(F)** Tumor volumes and weight were measured, and the volume of the tumor was calculated [(length × width^2)/2]. **(D)** Bodyweight calculated every 3 days after implantation. Data are expressed as the mean ± S.D. of five independent experiments. $^*p < 0.05$; $^{**}p < 0.01$ *vs.* the vehicle group.

after ivosidenib treatment. Based on this, it appears that ivosidenib acts by inhibiting cell proliferation but not by inducing cell death. The drug efficiently inhibits NSCLC progression *in vivo*. A previous study showed that knockdown of IDH1 by RNA interference reduced the proliferative capacity of NSCLC cells and significantly decreased the growth of xenograft tumors *in vivo* (11). Our results indicated that, as a mIDH1 inhibitor, ivosidenib might be appropriate for the treatment of NSCLC even without IDH1 mutation.

Using whole transcriptome resequencing, we identified 212 DE-mRNAs, 4 DE-miRNAs, and 206 DE-lncRNAs and analyzed their function and KEGG pathway, as well as the connections between mRNA, lncRNA, and miRNA. We selected the lncRNA-miRNA-mRNA axis according to the results of functional analysis. In the top 20 KEGG pathways, we identified cancer-related pathways, including the TGF-β signaling pathway (involving SMAD5), the PI3K-Akt signaling pathway (involving IL7R), the Jak-STAT signaling pathway (involving IL7R), the MAPK signaling pathway (involving genes MAP2K6), the Rap1 signaling pathway (involving MAP2K6 and PFN2), and cell adhesion molecules (involving PTPRC) (**Table 2**). Pioneering studies demonstrated that alterations of these genes might result in tumorigenesis and development; these include SMAD5 (24, 25), IL7R (26), MAP2K6 (27), and PFN2 (28, 29).

Subsequently, we evaluated the effects of ivosidenib on ncRNAs. Ivosidenib induced the up-regulation of miR-493-5p and miR-148a-5p. Other studies reported the tumor-inhibiting activity of miR-493-5p in malignant tumors (30–32). Studies showed that overexpression of miR-493-5p suppressed NSCLC growth, migration, and invasion (30). MiR-148a-5p associates with NSCLC progression (33, 34). Zhang et al. suggested that miR-148a-5p suppresses proliferation and migration and induces apoptosis in NSCLC cells *via* the PI3K/AKT signaling pathway by targeting ERBB3 and ITGA5 (34). We found that expression levels of miR-493-5p and miR-148a-5p were higher in ivosidenib-treated NSCLC cells. These findings suggest that miR-493-5p and miR-148a-5p may participate in the anti-NSCLC mechanism of ivosidenib.

Several lines of evidence suggest that lncRNAs interfere with miRNA activity as endogenous sponges. In the present study, based on the constructed lncRNA–miRNA–mRNA network, we observed that many lncRNAs contained one or more miRNA

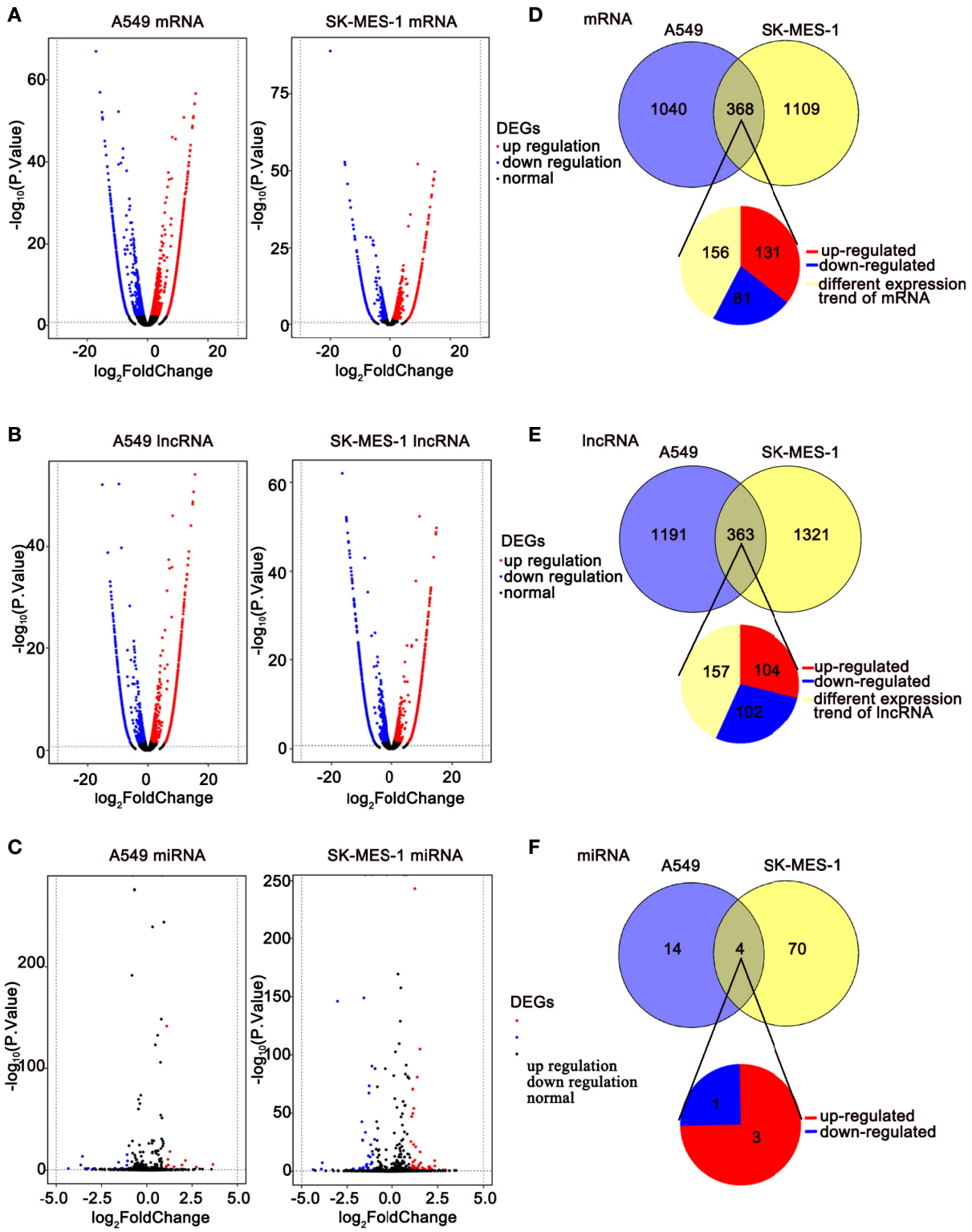

FIGURE 6 | RNA-seq revealing distinct expression patterns of miRNAs, lncRNAs, and mRNAs in control of NSCLC cells and ivosidenib-treated NSCLC cells. **(A–C)** Volcano plot of DE-mRNAs, DE-lncRNAs, and DE-miRNA expression profiles between control NSCLC cells and ivosidenib-treated NSCLC cells. **(D–F)** Venn diagram showing the overlap number of DE-mRNA, DE-lncRNA, and DE-miRNA.

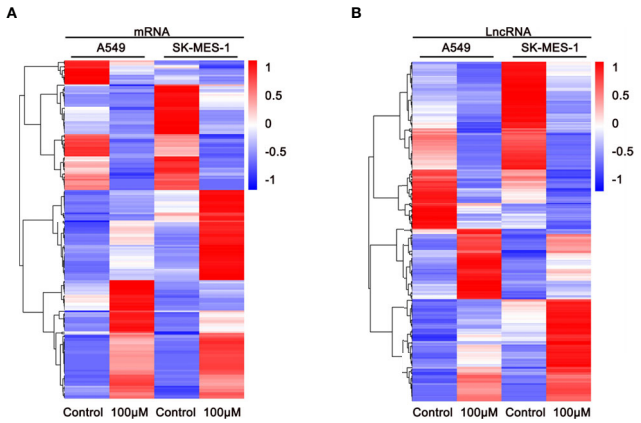

FIGURE 7 | Expression profiles of DE-mRNAs are influenced by ivosidenib. Heatmap showing expression profiles of differentially expressed mRNAs **(A)** and lncRNAs **(B)** between NSCLC cells and ivosidenib-treated NSCLC cells.

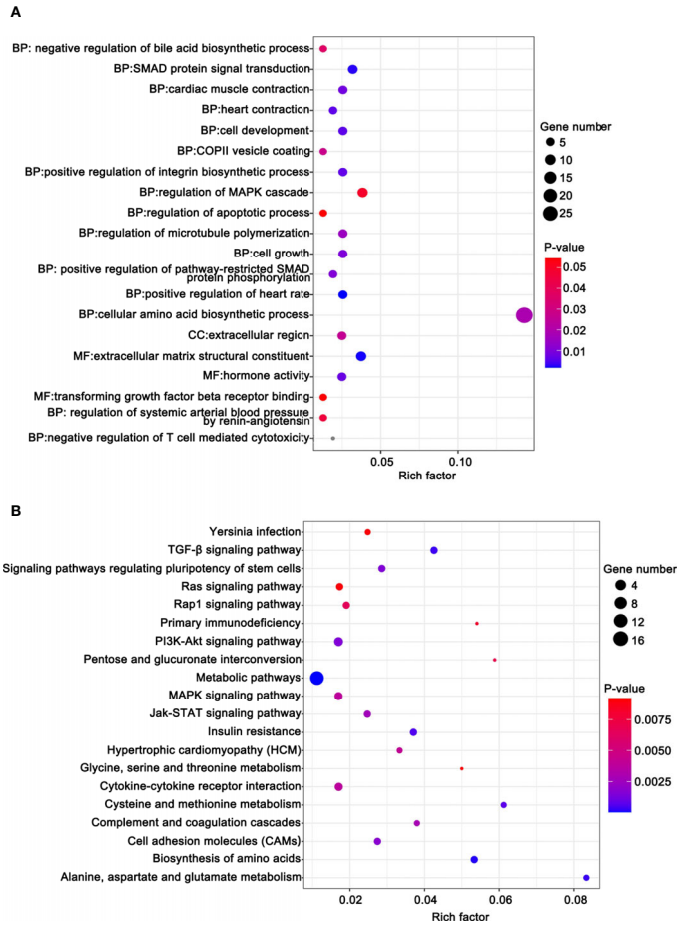

FIGURE 8 | Functional analysis for the DE-mRNAs. **(A)** Bubble diagram of the top 20 ranked GO terms of DE-mRNAs. The vertical axis indicates GO terms and the horizontal axis represents the Rich factor. The enrichment degree was stronger with a larger Rich factor. Size of the dots indicates the number of genes in the GO term. **(B)** KEGG pathway enrichment analysis of CDE-mRNAs. The vertical axis indicates the different pathways. The enrichment degree was stronger with a higher enrichment ratio. The horizontal axis indicates the Rich factor. The enrichment degree was stronger with a larger Rich factor. Size of the dots indicates the number of genes in the pathways.

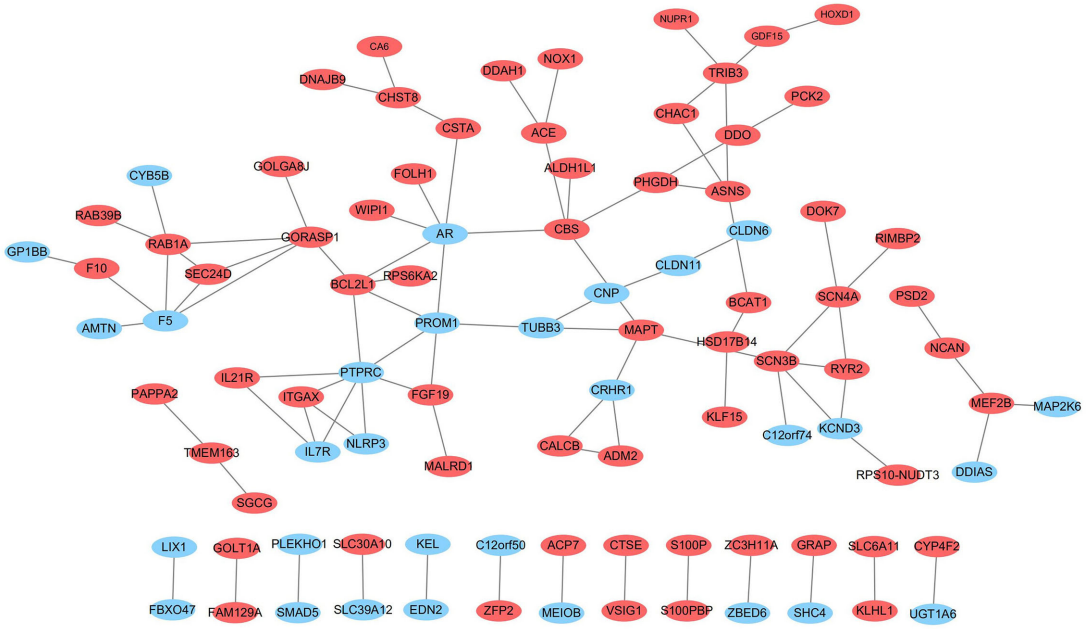

FIGURE 9 | The network of protein-protein interactions (PPI) of differentially expressed genes. Red and blue represent up- and down-regulation, respectively.

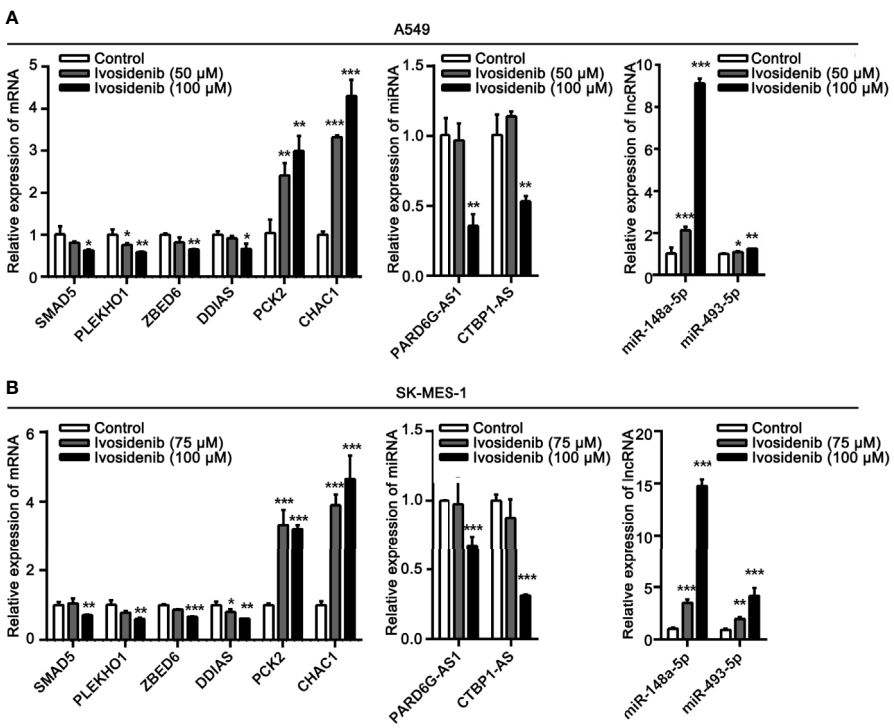

FIGURE 10 | QRT-PCR analysis of the expressions of DE-RNAs. **(A)** After treating with ivosidenib for 24 h, DE-RNAs expression was determined using RT-qPCR in A549 cells. **(B)** After treating with ivosidenib for 24 h, DE-RNAs expression was determined using RT-qPCR in SK-MES-1 cells. $^{*}p < 0.05$, $^{**}p < 0.01$, and $^{***}p < 0.001$.

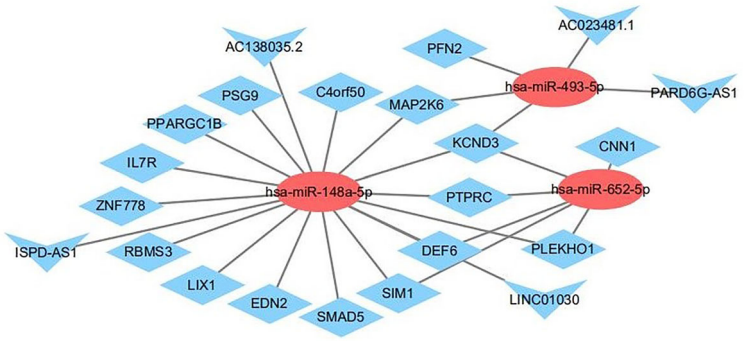

FIGURE 11 | The interaction network of lncRNA–miRNA–mRNA. Red and blue represent up- and down-regulation, respectively. Triangles represent DE-lncRNAs, circles represent DE-miRNAs, and diamonds represent DE-mRNAs.

TABLE 2 | Cancer-Related lncRNA-miRNA-mRNA Axis.

mRNA	miRNA	lncRNA	Function Term
SMAD5	hsa-miR-148a-5p	AC138035.2 ISPD-AS1 LINC01030	TGF-β signaling pathway
IL7R	hsa-miR-148a-5p	AC138035.2 ISPD-AS1 LINC01030	PI3K-Akt signaling pathway Jak-STAT signaling pathway
MAP2K6	hsa-miR-148a-5p	AC138035.2 ISPD-AS1 LINC01030	MAPK signaling pathway Rap1 signaling pathway
	hsa-miR-493-5p	PARD6G-AS1 AC023481.1	
PFN2	hsa-miR-493-5p	PARD6G-AS1 AC023481.1	Rap1 signaling pathway
PTPRC	hsa-miR-148a-5p	AC138035.2 ISPD-AS1 LINC01030	Cell adhesion molecules (CAMs)

binding sites. LncRNAs (AC138035.2, ISPD-AS1, LINC01030, PARD6G-AS1, and AC023481.1) interacted with SMAD5, IL7R, MAP2K6, and PFN2, through competitively binding with miR-493-5p or miR-148a-5p. Further study may reveal the interaction relationships of lncRNA–miRNA–mRNA in the mechanism of action of ivosidenib (**Table 2**).

In summary, ivosidenib significantly inhibited the proliferation, migration, and invasion of NSCLC cells, a result of interactions among multiple pathways and signal molecules. Interfering with a series of signal pathways, including TGF-β, PI3K-Akt, Jak-STAT, MAPK, Rap1, and cell adhesion molecules, ivosidenib influenced the malignant phenotype of NSCLC cells. Our findings helped elucidate the potential mechanism of ivosidenib, building a regulatory ceRNA in NSCLC cells, and laying the foundation for further experimental and clinical studies of ivosidenib.

DATA AVAILABILITY STATEMENT

The datasets presented in this study can be found in online repositories. The names of the repository/repositories and accession number(s) can be found below: NCBI database, and the SRA accession number is SRR13363999, SRR13364000, SRR13364001, SRR13363997, SRR13363996, SRR13363995, SRR13363994 and SRR13363998. The bioproject number is PRJNA689881.

ETHICS STATEMENT

The animal study was reviewed and approved by Shanxi Medical University.

AUTHOR CONTRIBUTIONS

JW and RC performed the experiments, collected and analyzed the data, and took part in writing the manuscript. HS, TY, YQ, YZ, and ZH performed the research and collected the data. PK, MP, and XZ initiated, designed the study, analyzed the data, and drafted the paper. All authors contributed to the article approved the submitted version.

FUNDING

This study was funded by The Special Fund Project for Guiding Local Science and Technology Development by the Central Government (No.: YDZX20191400002737).

SUPPLEMENTARY MATERIAL

The Supplementary Material for this article can be found online at: https://www.frontiersin.org/articles/10.3389/fonc.2021.626605/full#supplementary-material

REFERENCES

1. Mei D, Zhao L, Chen B, Zhang X, Wang X, Yu Z, et al. α-Conotoxin ImI-modified polymeric micelles as potential nanocarriers for targeted docetaxel delivery to α7-nAChR overexpressed non-small cell lung cancer. *Drug Delivery* (2018) 25:493–503. doi: 10.1080/10717544.2018.1436097
2. Siegel RL, Miller KD, Jemal A. Cancer statistics, 2016. *CA Cancer J Clin* (2016) 66:7–30. doi: 10.3322/caac.21332
3. Al-Khallaf H. Isocitrate dehydrogenases in physiology and cancer: biochemical and molecular insight. *Cell Biosci* (2017) 7:37. doi: 10.1186/s13578-017-0165-3
4. Hu C, Zuo Y, Liu J, Xu H, Liao W, Dang Y, et al. Licochalcone A suppresses the proliferation of sarcoma HT-1080 cells, as a selective R132C mutant IDH1 inhibitor. *Bioorg Med Chem Lett* (2020) 30:126825. doi: 10.1016/j.bmcl.2019.126825
5. Cohen AL, Holmen SL, Colman H. IDH1 and IDH2 Mutations in Gliomas. *Curr Neurol Neurosci Rep* (2013) 13:345. doi: 10.1007/s11910-013-0345-4
6. DiNardo CD, Stein EM, de Botton S, Roboz GJ, Altman JK, Mims AS, et al. Durable Remissions with Ivosidenib in IDH1-Mutated Relapsed or Refractory AML. *N Engl J Med* (2018) 378:2386–98. doi: 10.1056/NEJMoa1716984
7. Amary MF, Bacsi K, Maggiani F, Damato S, Halai D, Berisha F, et al. IDH1 and IDH2 mutations are frequent events in central chondrosarcoma and central and periosteal chondromas but not in other mesenchymal tumours. *J Pathol* (2011) 224:334–43. doi: 10.1002/path.2913
8. Bergaggio E, Piva R. Wild-Type IDH Enzymes as Actionable Targets for Cancer Therapy. *Cancers (Basel)* (2019) 11:563. doi: 10.3390/cancers11040563
9. Kang MR, Kim MS, Oh JE, Kim YR, Song SY, Seo SI, et al. Mutational analysis of IDH1 codon 132 in glioblastomas and other common cancers. *Int J Cancer* (2009) 125:353–5. doi: 10.1002/ijc.24379
10. Bleeker Fonnet E, Simona L, Sieger L, Dirk T, Theo H, Peter VW, et al. IDH1 mutations at residue p.R132 (IDH1(R132)) occur frequently in high-grade gliomas but not in other solid tumors. *Hum Mutat* (2009) 30:7–11. doi: 10.1002/humu.20937
11. Tan F, Jiang Y, Sun N, Chen Z, Lv Y, Shao K, et al. Identification of isocitrate dehydrogenase 1 as a potential diagnostic and prognostic biomarker for non-small cell lung cancer by proteomic analysis. *Mol Cell Proteomics* (2012) 11: M111.008821. doi: 10.1074/mcp.M111.008821
12. Rodriguez EF, De Marchi F, Lokhandwala PM, Belchis D, Xian R, Gocke CD, et al. IDH1 and IDH2 mutations in lung adenocarcinomas: Evidences of subclonal evolution. *Cancer Med* (2020) 9:4386–94. doi: 10.1002/cam4.3058
13. Al-Amodi H, Nabih ES, Kamel H, El Sayed MA, Dwedar I. Wild-Type Isocitrate Dehydrogenase 1 Over-Expression is Related to Cancer Stem Cells Survival in Lung Adenocarcinoma. *Cancer Invest* (2018) 36:185–9. doi: 10.1080/07357907.2018.1445262
14. Popovici-Muller J, Lemieux RM, Artin E, Saunders JO, Salituro FG, Travins J, et al. Discovery of AG-120 (Ivosidenib): A First-in-Class Mutant IDH1 Inhibitor for the Treatment of IDH1 Mutant Cancers. *ACS Med Chem Lett* (2018) 9:300–5. doi: 10.1021/acsmedchemlett.7b00421
15. Xie Y, Dang W, Zhang S, Yue W, Yang L, Zhai X, et al. The role of exosomal noncoding RNAs in cancer. *Mol Cancer* (2019) 18:37. doi: 10.1186/s12943-019-0984-4
16. Salmena L, Poliseno L, Tay Y, Kats L, Pandolfi PP. A ceRNA hypothesis: the Rosetta Stone of a hidden RNA language. *Cell* (2011) 146:353–8. doi: 10.1016/j.cell.2011.07.014
17. Ferlita A, Battaglia R, Andronico F, Caruso S, Cianci A, Purrello M, et al. Non-Coding RNAs in Endometrial Physiopathology. *Int J Mol Sci* (2018) 19:2120. doi: 10.3390/ijms19072120
18. Fang QY, Deng QF, Luo J, Zhou CC. MiRNA-20a-5p accelerates the proliferation and invasion of non-small cell lung cancer by targeting and downregulating KLF9. *Eur Rev Med Pharmacol Sci* (2020) 24:2548–456. doi: 10.26355/eurrev_202003_20522
19. Zhang Z, Luo G, Yu C, Yu G, Jiang R, Shi X. MicroRNA-493-5p inhibits proliferation and metastasis of osteosarcoma cells by targeting Kruppel-like factor 5. *J Cell Physiol* (2019) 234:13525–33. doi: 10.1002/jcp.28030
20. Wang X, Yin H, Zhang L, Zheng D, Yang Y, Zhang J, et al. The construction and analysis of the aberrant lncRNA-miRNA-mRNA network in non-small cell lung cancer. *J Thorac Dis* (2019) 11:1772–8. doi: 10.21037/jtd.2019.05.69
21. Zhang Y, Ye T, Hong Z, Gong S, Zhou X, Liu H, et al. Pharmacological and transcriptome profiling analyses of Fufang E'jiao Jiang during chemotherapy-induced myelosuppression in mice. *J Ethnopharmacol* (2019) 238:111869. doi: 10.1016/j.jep.2019.111869
22. Kong X, Hu S, Yuan Y, Du Y, Zhu Z, Song Z, et al. Analysis of lncRNA, miRNA and mRNA-associated ceRNA networks and identification of potential drug targets for drug-resistant non-small cell lung cancer. *J Cancer* (2020) 11:3357–68. doi: 10.7150/jca.40729
23. Ashworth A, Gilliland DG, Johnson CS. IDH1 inhibitor shows promising early results. *Cancer Discovery* (2015) 5:4. doi: 10.1158/2159-8290.CD-NB2014-178
24. Matsuo T, Dat le T, Komatsu M, Yoshimaru T, Daizumoto K, Sone S, et al. Early growth response 4 is involved in cell proliferation of small cell lung cancer through transcriptional activation of its downstream genes. *PloS One* (2014) 9:e113606. doi: 10.1371/journal.pone.0113606
25. Li F, Xu Y, Liu RL. SAMD5 mRNA was overexpressed in prostate cancer and can predict biochemical recurrence after radical prostatectomy. *Int Urol Nephrol* (2019) 51:443–51. doi: 10.1007/s11255-019-02096-3
26. Oliveira ML, Akkapeddi P, Ribeiro D, Melão A, Barata JT. IL-7R-mediated signaling in T-cell acute lymphoblastic leukemia: An update. *Adv Biol Regul* (2019) 71:88–96. doi: 10.1016/j.jbior.2018.09.012
27. Liu K, Zhang C, Li B, Xie W, Zhang J, Nie X, et al. Mutual Stabilization between TRIM9 Short Isoform and MKK6 Potentiates p38 Signaling to Synergistically Suppress Glioblastoma Progression. *Cell Rep* (2018) 23:838–51. doi: 10.1016/j.celrep.2018.03.096
28. Zhang Q, Pan X, You D. Overexpression of long non-coding RNA SBF2-AS1 promotes cell progression in esophageal squamous cell carcinoma (ESCC) by repressing miR-494 to up-regulate PFN2 expression. *Biol Open* (2020). doi: 10.1242/bio.048793
29. Yan J, Ma C, Gao Y. MicroRNA-30a-5p suppresses epithelial-mesenchymal transition by targeting profilin-2 in high invasive non-small cell lung cancer cell lines. *Oncol Rep* (2017) 37:3146–54. doi: 10.3892/or.2017.5566
30. Chan Z, Shangjie W, Rong S, Liu C. Long noncoding RNA NR2F1-AS1 promotes the malignancy of non-small cell lung cancer via sponging microRNA-493-5p and thereby increasing ITGB1 expression. *Aging (Albany NY)* (2020) 12:7660–7675. doi: 10.18632/aging.103564
31. Gailhouste L, Liew LC, Yasukawa K, Hatada I, Tanaka Y, Kato T, et al. MEG3-derived miR-493-5p overcomes the oncogenic feature of IGF2-miR-483 loss of imprinting in hepatic cancer cells. *Cell Death Dis* (2019) 10(8):553. doi: 10.1038/s41419-019-1788-6
32. Wang S, Wang X, Li J, Meng S, Liang Z, Xu X, et al. c-Met, CREB1 and EGFR are involved in miR-493-5p inhibition of EMT via AKT/GSK-3β/Snail signaling in prostate cancer. *Oncotarget* (2017) 8(47):82303–13. doi: 10.18632/oncotarget.19398
33. Lin Y, Lv Y, Liang R, Yuan C, Zhang J, He D, et al. Four-miRNA signature as a prognostic tool for lung adenocarcinoma. *Onco Targets Ther* (2018) 11:29–36. doi: 10.2147/OTT.S155016
34. Zhang J, Zhang Y, Shen W, Fu R, Ding Z, Zhen Y, et al. Cytological effects of honokiol treatment and its potential mechanism of action in non-small cell lung cancer. *BioMed Pharmacother* (2019) 117:109058. doi: 10.1016/j.biopha.2019.109058

Conflict of Interest: The authors declare that the research was conducted in the absence of any commercial or financial relationships that could be construed as a potential conflict of interest.

Copyright © 2021 Wu, Chen, Shen, Yan, Qian, Zhang, Huang, Kong, Pang and Zhang. This is an open-access article distributed under the terms of the Creative Commons Attribution License (CC BY). The use, distribution or reproduction in other forums is permitted, provided the original author(s) and the copyright owner(s) are credited and that the original publication in this journal is cited, in accordance with accepted academic practice. No use, distribution or reproduction is permitted which does not comply with these terms.

frontiers in Oncology

ORIGINAL RESEARCH
published: 20 April 2021
doi: 10.3389/fonc.2021.670483

Feasibility and Challenges for Sequential Treatments in ALK-Rearranged Non-Small-Cell Lung Cancer

*Mei Elsayed[1], Farastuk Bozorgmehr[1,2], Daniel Kazdal[2,3], Anna-Lena Volckmar[3], Holger Sültmann[2,4], Jürgen R. Fischer[5], Mark Kriegsmann[2,3], Albrecht Stenzinger[2,3], Michael Thomas[1,2] and Petros Christopoulos[1,2]**

[1] Department of Thoracic Oncology, Thoraxklinik and National Center for Tumor diseases (NCT) at Heidelberg University Hospital, Heidelberg, Germany, [2] Translational Lung Research Center Heidelberg, German Center for Lung Research (DZL), Heidelberg, Germany, [3] Institute of Pathology, Heidelberg University Hospital, Heidelberg, Germany, [4] Division of Cancer Genome Research, German Cancer Research Center (DKFZ), Heidelberg, Germany, [5] Department of Thoracic Oncology, Lungenklinik Löwenstein, Löwenstein, Germany

OPEN ACCESS

Edited by:
Junji Uchino,
Kyoto Prefectural University of Medicine, Japan

Reviewed by:
Marieke F. Fransen,
Academic Medical Center, Netherlands
Marco Schiavon,
University Hospital of Padua, Italy

***Correspondence:**
Petros Christopoulos
petros.christopoulos@med.uni-heidelberg.de
orcid.org/0000-0002-7966-8980

Specialty section:
This article was submitted to Thoracic Oncology, a section of the journal Frontiers in Oncology

Received: 21 February 2021
Accepted: 25 March 2021
Published: 20 April 2021

Citation:
Elsayed M, Bozorgmehr F, Kazdal D, Volckmar A-L, Sültmann H, Fischer JR, Kriegsmann M, Stenzinger A, Thomas M and Christopoulos P (2021) Feasibility and Challenges for Sequential Treatments in ALK-Rearranged Non-Small-Cell Lung Cancer. Front. Oncol. 11:670483. doi: 10.3389/fonc.2021.670483

Background: Anaplastic lymphoma kinase-rearranged non-small-cell lung cancer (ALK^+ NSCLC) is a model disease for use of targeted therapies (TKI), which are administered sequentially to maximize patient survival.

Methods: We retrospectively analyzed the flow of 145 consecutive TKI-treated ALK^+ NSCLC patients across therapy lines. Suitable patients that could not receive an available next-line therapy ("attrition") were determined separately for various treatments, based on the approval status of the respective targeted drugs when each treatment failure occurred in each patient.

Results: At the time of analysis, 70/144 (49%) evaluable patients were still alive. Attrition rates related to targeted treatments were approximately 25-30% and similar for administration of a second-generation (2G) ALK inhibitor (22%, 17/79) or any subsequent systemic therapy (27%, 27/96) after crizotinib, and for the administration of lorlatinib (27%, 6/22) or any subsequent systemic therapy (25%, 15/61) after any 2G TKI. The rate of chemotherapy implementation was 67% (62/93). Both administration of additional TKI (median overall survival [mOS] 59 *vs.* 41 months for multiple *vs.* one TKI lines, logrank p=0.002), and chemotherapy (mOS 41 vs. 16 months, logrank p<0.001) were significantly associated with longer survival. Main reason for patients foregoing any subsequent systemic treatment was rapid clinical deterioration (n=40/43 or 93%) caused by tumor progression. In 2/3 of cases (29/43), death occurred under the first failing therapy, while in 11/43 the treatment was switched, but the patient did not respond, deteriorated further, and died within 8 weeks.

Conclusions: Despite absence of regulatory obstacles and no requirement for specific acquired mutations, 25-30% of ALK^+ NSCLC patients forego subsequent systemic therapy due to rapid clinical deterioration, in several cases (approximately 1/3)

associated with an ineffective first next-line choice. These results underline the need for closer patient monitoring and broader profiling in order to support earlier and better directed use of available therapies.

Keywords: ALK-rearranged non-small-cell lung cancer, tyrosine kinase inhibitors, chemotherapy, sequential therapies, overall survival

INTRODUCTION

Anaplastic lymphoma kinase-rearranged (ALK$^+$) non-small-cell lung cancer (NSCLC) is a model disease for the implementation of targeted therapies in thoracic oncology (1). The first-generation (1G) tyrosine kinase inhibitor (TKI) crizotinib was approved by the European Medicines Agency (EMA) already in August 2011, based on superior efficacy and tolerability compared to conventional chemotherapy (2). During the last two years, it was superseded by second-generation (2G) compounds in the upfront setting, especially alectinib and brigatinib, whose even better systemic and intracranial activity was reflected in longer-lasting responses and a median overall survival (OS) exceeding 5 years in the ALEX trial (3, 4). More recently, the third-generation (3G) drug lorlatinib demonstrated even higher efficacy and is currently the standard option after failure of any next-generation ALK TKI (5, 6). Accumulating evidence from real-world retrospective analyses as well as clinical trials underlines the importance of sequential TKI administration in order to optimize patient outcome (3, 7, 8). Indeed, newer compounds are more potent ALK inhibitors and show broader activity against *ALK* resistance mutations, therefore they can salvage patients failing older TKI (9). At the same time, a current characteristic of ALK$^+$ disease is that the approval of targeted pharmaceuticals for next-line administration is "open", i.e. does not depend on the results of molecular retesting and presence of any specific resistance mutation, in contrast, for example, to the administration of osimertinib after failure of 1G/2G EGFR inhibitors, which requires detection of *EGFR* T790M (10). Nevertheless, in clinical practice a considerable number of ALK$^+$ patients will forego subsequent therapy. The aim of this study is to provide an accurate estimate for the frequency and causes of this problem.

PATIENTS AND METHODS

Study Population and Endpoints

This retrospective study included all consecutive ALK$^+$ NSCLC patients treated in the Thoraxklinik Heidelberg and Lungenklinik Löwenstein from 2011 until 2020. In order to provide a detailed and accurate picture of sequential treatments for ALK$^+$ NSCLC and their impact on patient outcome, study endpoints considered each relevant pharmaceutical class and each therapeutic context separately: i) administration of 2G ALK inhibitors after crizotinib (1G); ii) administration of lorlatinib (3G) after 2G compounds; iii) administration of any treatment after crizotinib (1G); iv) administration of any treatment after 2G compounds; v) administration of chemotherapy at any time during treatment; vi) OS after administration of multiple TKI *vs.* one single TKI line; vii) OS with TKI-only treatment *vs.* treatment with both TKI and chemotherapy. Deceased patients were considered to have been candidates for a specific class of next-line targeted therapy, when their date of death was after the time of the earliest approval within this TKI class by the European Medicines Agency (EMA), which was May 2015 for 2G ALK inhibitors (ceritinib was approved first in May 2015, followed by alectinib in February 2017 and brigatinib in November 2018), and May 2019 for lorlatinib. In addition, all patients were considered potentially eligible for chemotherapy, since the baseline ECOG performance status (PS) in our cohort ranged from 0-2, and therefore every patient could have received at least some mild cytotoxic treatment.

Data Collection and Statistical Analysis

Histologic diagnosis of NSCLC and detection of *ALK* gene fusions were performed at the Institute of Pathology Heidelberg on tissue specimens according to the criteria of the current WHO Classification (2015) for lung cancer (11). Newly diagnosed cases were screened for the presence of an ALK alteration by fluorescence *in situ* hybridization (FISH, ZytoLight SPEC ALK probe, ZytoVision GmbH, Bremerhaven, Germany) and reverse-transcription polymerase-chain reaction (RT-PCR) until 2015, or by immunohistochemistry (IHC, D5F3 clone, Roche, Mannheim, Germany) and RNA-based next-generation sequencing (NGS, ThermoFisher Lung Cancer Fusion Panel, Waltham, MA, USA) thereafter, as previously described (12). Clinical data were systematically collected from the medical records, including review of the patients' radiological images, i.e. chest/abdomen CT and brain MRI-based restaging every 6-12 weeks, by the investigators. For deceased patients, both given treatments and missed treatments were considered. For patients still under therapy, only given treatments were considered, since these patients could still receive or not receive some additional treatment in the further course. For every single patient who was eligible for some type of subsequent treatment, i.e. 2G TKI after crizotinib, lorlatinib after 2G ALK inhibitors, or chemotherapy after any TKI, but did not receive it until death, the clinical course as documented in the records was analyzed to understand why the treatment was missed. The relationship between survival and sequential administration of TKI was analyzed in the entire patient population. For chemotherapy, the survival analysis was performed in the subset of deceased patients, for which the entire disease trajectory could be analyzed, because chemotherapy is generally given after targeted therapies in ALK$^+$ NSCLC. Survival data were analyzed according to Kaplan-Meier and

compared between patient groups with the logrank test. Follow-up time was calculated using the reverse Kaplan-Meier method (13). Categorical data were compared using a chi-square test, while 95% confidence intervals (CI) of proportions were calculated with the modified Wald method (14). Statistical calculations were performed with SPSS version 24 (IBM, NY, USA) and GraphPad Prism version 9 (La Jolla, CA, USA), which was also used to make the plots.

Ethics

This study was approved by the ethics committee of the Heidelberg University (S-145/2017 and S-469/2017). Since this was a non-interventional, retrospective study, informed consent was obtained whenever possible, but its need for every participant was waived by the ethics committee.

RESULTS

Evaluable Study Patients

Overall, 145 eligible ALK$^+$ NSCLC patients that had received at least one ALK inhibitor were identified, of which 144 had complete follow-up data and were included in this study (**Figure 1**). Their clinical characteristics are given in **Table 1**. Median age was 57 years, while the majority were female (60%), never-light smokers (77%) with an ECOG performance status at initial diagnosis of 0-1. The median number of treatment lines was 2 (range 1-9), the median overall survival 51 months (CI 44-59), and the median follow-up 54 months (95% CI 46-61, **Table 1**). At the time of data cut-off, 70 patients were still alive, while 74 patients had died.

Rate of Sequential Treatments and Impact on Patient Survival

We first analyzed the percentage of ALK$^+$ NSCLC patients who received next-generation ALK inhibitors after failure of 1G or 2G TKI. The reference population for each of these calculations were all patients that could have received the respective drugs, based on approval by the EMA before the time of the patients' treatment failure ("eligible patients"), as explained in the Methods and shown in **Figure 2**. 2G TKI were offered to 78% (62/79, CI 68-86%) of eligible patients after crizotinib failure, while lorlatinib was offered to 73% (16/22, CI 52-87%) of eligible patients failing 2G ALK inhibitors (**Figure 2A**). Among patients failing crizotinib, any subsequent anticancer treatment (including chemotherapy) was given to 73% (69/96, CI 63-81%) of patients, while among patients failing 2G ALK inhibitors any subsequent anticancer treatment was given to 75% of patients (46/61, CI 63-85%, **Figure 2B**). Chemotherapy at any time during treatment was given to 67% (62/93, CI 57-75%) of patients (**Figure 2C**). Both the administration of additional TKI and additional chemotherapy were significantly associated with longer survival of TKI-treated ALK$^+$ NSCLC patients (**Figure 3**): the median OS from start of treatment for metastatic disease was 59 months (CI 43-74) for patients who received multiple TKI lines *vs.* 41 months (CI 26-55) for patients who received a single TKI line only (logrank p=0.002, **Figure 3A**); while the median OS was 41 months (CI 30-51) for patients who also received chemotherapy in addition to TKI,

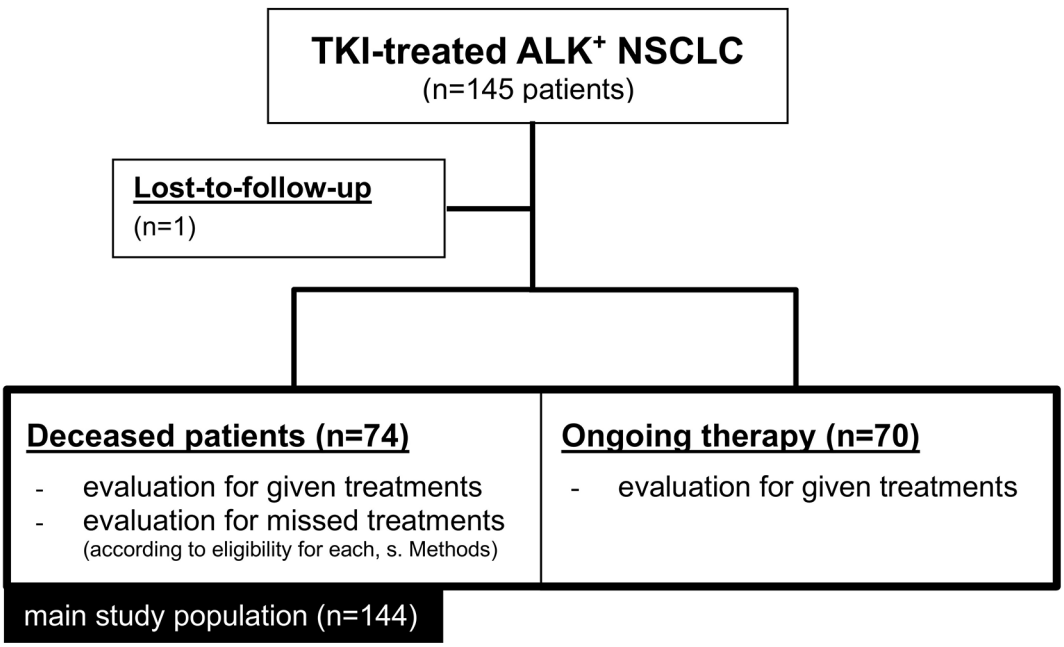

FIGURE 1 | Flowchart of study patients.

TABLE 1 | Characteristics of study patients.

		All study patients (n = 144)	Deceased patients (n = 74)
Age, median (SD; range)		57 (14; 21-85)	57 (15; 21-85)
Sex, % female (n)		60 (86)	57 (42)
ECOG, % (n)	PS 0-1	97 (140)	95 (70)
	PS 2	3 (54)	5 (4)
Never/light-smokers (< 10 pack-years), % (n)		77 (105)	78 (53)
ALK variant, % (n)	*EML-ALK* V3 (E6;A20)	41 (51)	50 (32)
	EML-ALK V1/V2	49 (60)	39 (25)
	other[1]	10 (11)	11 (7)
TP53 status at diagnosis	mutated[2]	21 (24)	25 (15)
TKI lines, median (SD; range)		1 (1.1; 1-5)	1 (1.1; 1-5)
All treatment lines, median (SD; range)		2 (1.9; 1-9)	3 (1.8; 1-9)
OS months, median (95% CI)		51 (44-59)	27 (20-33)
Follow-up months, median (95% CI)		54 (46-61)	26 (20-33)

ECOG PS, ECOG performance status; OS, overall survival; SD, standard deviation; TKI, tyrosine kinase inhibitor; 95% CI, 95% confidence interval.
[1]the ALK variant could be typed for 122 cases; other patients had E18:A20 (n=4), HIP1-ALK (n=2), KCL-ALK (n=4), KIFB-ALK (n=1).
[2]the TP53 status could be determined for 117 cases.

vs. 16 months (CI 8-23) for patients who received TKI only, but no chemotherapy (logrank p<0.001, **Figure 3B**).

Analysis of Clinical Courses for Patients Foregoing Subsequent Treatment

For all patients who missed subsequent treatment (2G ALK TKI, or 3G ALK TKI, or chemotherapy) as shown in **Figure 2**, we performed a detailed examination of their clinical courses as documented in the records in order to gain insight into the underlying circumstances. This showed that the main reason for ALK$^+$ NSCLC patients missing subsequent treatments, either TKI or chemotherapy, was rapid clinical deterioration (n=40/43 or 93%, **Figure 4**). In two-thirds of cases (29/43 or 67%), the patient died while on the first failing therapy, whereas in approximately 25% (11/43), the treatment was switched, but the patient did not respond, deteriorated further and died within 8 weeks. Other causes, such as patient decision against further anticancer therapy (n=2, both due to severe TKI side effects) and severe concomitant illness (n=1, with advanced chronic obstructive pulmonary disease and progressive respiratory failure under therapy) were rare.

DISCUSSION

Sequential administration of effective drugs is critical in order to maximize therapeutic benefit and the survival of patients with

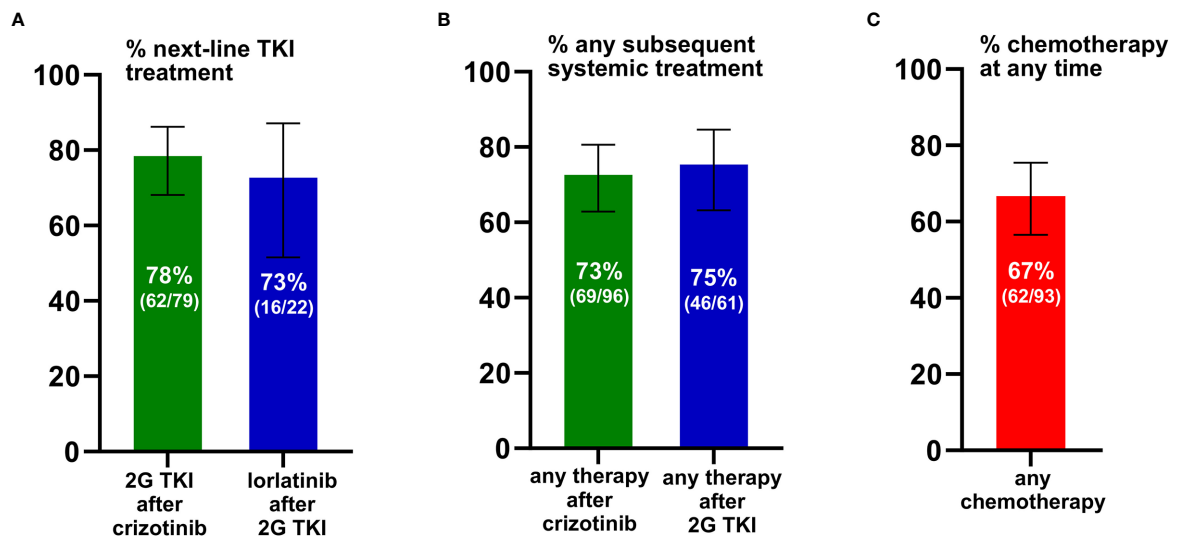

FIGURE 2 | Feasibility of sequential therapies in ALK$^+$ NSCLC. **(A)** Any second-generation (2G) ALK inhibitor was given to 78% (62/79) of eligible patients failing crizotinib, while lorlatinib (3G) was given to 73% (16/22) eligible patients failing any 2G ALK inhibitor. For each analysis, the reference population of eligible patients included all those who could have received the respective subsequent drug, based on approval by the EMA at the time of the patients' treatment failure, as explained in the *Methods*. Error bars indicate 95% confidence intervals. **(B)** Any systemic anticancer treatment (i.e. any ALK inhibitor or chemotherapy) was given to 73% (69/96) patients failing crizotinib, and to 75% (46/61) patients failing 2G ALK inhibitors. Error bars indicate 95% confidence intervals (CI). **(C)** Chemotherapy was given to 67% (62/93) of patients. Error bars indicate the 95% confidence interval.

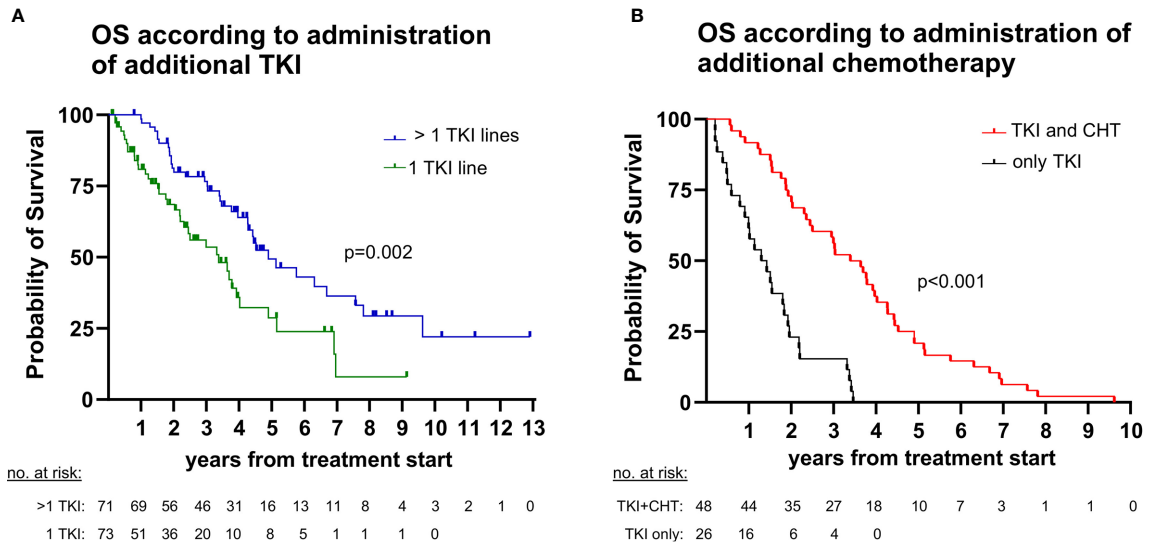

FIGURE 3 | Impact of sequential therapies on overall survival (OS) in ALK$^+$ NSCLC. **(A)** The median OS from start of treatment for metastatic disease was 59 months (95% confidence interval [CI] 43-74) for patients with > 1 tyrosine kinase inhibitor (TKI) lines *vs.* 41 months (CI 26-55) for patients with a single TKI line (logrank p=0.002). **(B)** The median OS from start of treatment for metastatic disease was 41 months (CI 30-51) for patients who also received chemotherapy (CHT) in addition to TKI *vs.* 16 months (CI 8-23) for patients who were treated with TKI only (logrank <0.001). Since chemotherapy is generally administered after TKI for ALK$^+$ NSCLC, the analysis regarding chemotherapy was performed in the subset of deceased patients (n=74, **Figure 1**), for which the entire disease trajectory could be studied.

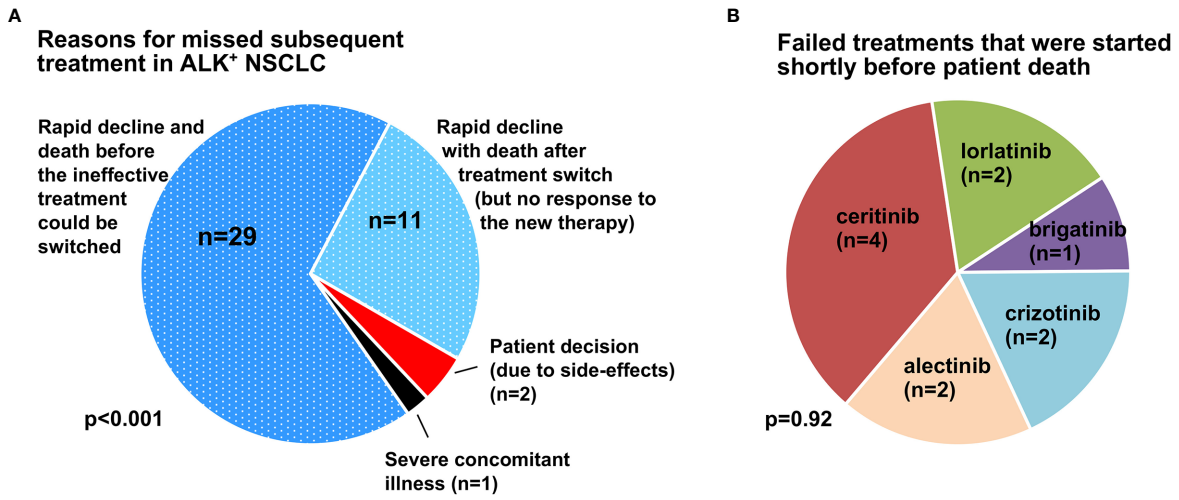

FIGURE 4 | Main causes for missed subsequent treatment in ALK $^+$ NSCLC. **(A)** The main reason for missed subsequent treatment in ALK$^+$ NSCLC patients was clinical deterioration due to rapid disease progression (n=40/43), while patient decision against further therapy (2/43, both due to treatment side-effects) and severe concomitant illness (n=1/43, one patient with advanced chronic obstructive pulmonary disease and worsening respiratory failure) were rare. In two-thirds of cases (29/43 or 67%), the patient died while on the first failing therapy, while in approximately 25% (11/43), the treatment was switched, but the patient did not respond, deteriorated further, and died within 8 weeks. The p-value was derived by chi-square testing across the various categories. **(B)** ALK TKI used in deteriorating cases as ineffective salvage therapy shortly before death (≤ 8 weeks). The p-value was derived by chi-square testing across the various categories.

metastatic lung cancer (15). In the special case of ALK$^+$ NSCLC, next-line use of ALK inhibitors is "open", i.e. not dependent on the molecular results of a tumor rebiopsy at the time of disease progression. Due to this lack of regulatory obstacles in ALK$^+$ NSCLC, main focus of previous studies has been the efficacy rather than the feasibility of therapeutic sequencing (8, 16–19). Systematic analysis of the latter is endowed with serious difficulties, mainly the rarity and generally better prognosis of

the disease compared to EGFR$^+$ and wild-type NSCLC (7), which necessitate longer study intervals in order to recruit sufficient patient numbers, the multitude of ALK-directed compounds, which are used in variable order, as well as the rapidly changing landscape of regulatory approval, which influences the availability and prioritization of various drugs.

Using a large, homogenous patient population, considering each therapeutic context separately, and taking into account the longitudinal availability of various ALK inhibitors for each patient, our study shows that the attrition of ALK$^+$ NSCLC patients between different treatments is approximately 25-30% (**Figure 2**). This holds true for the administration of 2G compounds or any treatment after crizotinib, as well as for the administration of lorlatinib or any treatment after 2G TKI. The slightly higher (33%) attrition observed for additional chemotherapy is probably due to its worse efficacy and tolerability compared to TKI, which render it less desirable early in the disease course, and also less suitable for heavily pretreated patients (2, 20, 21). Interestingly, both percentages are considerably lower than the approximately 50% loss observed between first- and second-line palliative chemotherapy in metastatic NSCLC (22–25), but comparable to the approximately 30% loss reported after first-line TKI treatment in EGFR$^+$ NSCLC patients, both in the standard arm of the phase 3 FLAURA trial [(32%, Supplementary Table S2 of the respective original publication (26)] as well as in real-world analyses from certified German lung cancer centers, including own data (27–29). To our knowledge, so far, no other detailed estimates of attrition according to each failing treatment and next-line option exist in the literature for ALK$^+$ NSCLC. Of note, the long timespan of our cohort from 2011-2020 is an important advantage, because it permits more balanced capturing of favorable and unfavorable cases. In contrast, attrition rates based on interim results of prospective clinical trials are likely to be enriched for cases with worse outcome and a higher likelihood to miss subsequent treatment, since they are necessarily focused on the patient subset with earlier treatment failure and/or death. For example, in the recently published update of the ALEX trial, the percentage of patients receiving any treatment after alectinib or crizotinib was approximately 60% (3), i.e. somewhat lower than that observed in the present study (70-75%, **Figure 2**).

This association between shorter survival and lack of subsequent therapy was evident in our patients regarding both TKI and chemotherapy (**Figure 3**). Main cause for most cases (67% or 29/43) was rapid clinical deterioration with death before any salvage therapy could be initiated (**Figure 4A**). The overall percentage of patients lost under treatment with ALK inhibitors in this "direct" way, i.e. 25-30% (**Figure 2**) x 67% (**Figure 4A**, dark blue sector) ≈ 20% defines the theoretical upper limit, i.e. approximately 80%, for implementation of any subsequent therapies in ALK$^+$ NSCLC. This limit will acquire greater importance in the near future, because it is expected to equally hinder feasibility of all next-line targeted therapies for ALK$^+$ NSCLC, for example also newly-developed fourth-generation ALK inhibitors directed against compound ALK mutations (30), or other drugs targeting other actionable resistance mechanisms, such as acquired *MET* amplifications or *KRAS* mutations (9). Therefore, this 20% direct patient loss between lines represents currently an important argument for closer patient monitoring, in order to achieve earlier detection of treatment failure, so that subsequent therapies can be selected and started while the patient can still benefit from them. Besides, in approximately 25-30% (**Figure 2**) x 25% (**Figure 4A**, light blue sector) ≈ 5-10% of cases, various next-line TKI were started, but no response occurred, further deterioration followed, and the patients died within a few weeks (**Figure 4B**). This "secondary" patient loss highlights the additional need for improved molecular profiling of acquired resistance in order to support *a priori* selection of effective drugs for subsequent treatment, since there might be no second chance. Regarding both needs, i.e. for earlier detection and for improved profiling of TKI failure, a very promising approach are longitudinal liquid biopsies (circulating tumor [ct]DNA assays). These can not only identify acquired *ALK* resistance mutations and other actionable alterations, but also monitor the tumor remission status and emergence of high-risk features, for example acquisition of *TP53* mutations (31), in a minimally-invasive manner (32, 33). Important practical advantages of blood ctDNA assays for newly symptomatic and/or clinically deteriorating patients are the easier sample collection and earlier availability of results compared to percutaneous or bronchoscopic tissue biopsies (34). For many cases without detectable alterations of individual genes, the trimmed median absolute deviation from copy number neutrality (t-MAD score) determined using low-coverage (0.5-1x) whole genome sequencing, has recently demonstrated potential clinical utility as an alternative monitoring parameter (35). Of note, monitoring of electronic patient–reported outcomes (ePROs) under chemotherapy for various solid tumors was associated with significantly longer survival in a pivotal study, and could therefore represent a cost-efficient alternative method to improve care of ALK$^+$ NSCLC patients, since quality of life can fluctuate under treatment with TKI, as well (36, 37).

With the advent of highly potent TKI, the importance of chemotherapy for ALK$^+$ NSCLC has diminished, but should not be neglected, as it confers an additional survival benefit (**Figure 3B**). In clinical practice, a particular challenge is the optimal timing of switch from TKI to chemotherapy: neither too early, in order to maximize chemotherapy-free time, nor too late, after the patient is not fit enough for cytotoxics anymore. Even though the association between administration of chemotherapy or any subsequent therapy and longer survival observed in our study could be partly indirect, i.e. due to the better clinical condition of the respective patients, this does not lessen the importance of improved monitoring and profiling in order to preserve patient fitness and facilitate therapeutic sequencing (21). In fact, among the 11 cases in our series, who received various TKI as salvage therapies, but did not respond and died soon thereafter (**Figure 4B**), some might have benefited more from an earlier decision for chemotherapy, instead. Systematic use of tissue and liquid rebiopsies at the time of disease

progression in the future could help identify patients with off-target resistance mechanisms, for which further treatment with ALK inhibitors has low chances of success, and thus indirectly support timely decisions for alternative targeted drugs or chemotherapy (1, 9, 21).

CONCLUSION

In summary, despite lack of regulatory obstacles, the attrition of ALK^+ NSCLC patients between various treatment lines is approximately 25% and represents an important limitation for survival. Main problem is rapid clinical deterioration caused by tumor progression, which could be counteracted in future studies through closer radiologic and/or ctDNA monitoring and broader molecular profiling.

DATA AVAILABILITY STATEMENT

The data supporting the results of this study will be made available by the corresponding author upon reasonable request.

ETHICS STATEMENT

The studies involving human participants were reviewed and approved by ethics committee of Heidelberg University (S-145/2017 and S-469/2017). Written informed consent for participation was not required for this study in accordance with the national legislation and the institutional rules.

AUTHOR CONTRIBUTIONS

ME: conceptualization, methodology, investigation, data curation, formal analysis, visualization, and writing - original draft. FB: investigation, data curation, validation, and writing - review & editing. DK: investigation, data curation, validation, and writing – original draft. A-LV: investigation, data curation, validation, and writing - review & editing. HS: conceptualization, validation, supervision, and writing - review & editing. JF: investigation, data curation, validation, writing - review & editing. MK: investigation, data curation, and writing - review & editing. AS: validation, supervision, project administration, and writing - review & editing. MT: conceptualization, methodology, validation, supervision, funding acquisition, and writing - review & editing. PC: conceptualization, methodology, investigation, data curation, formal analysis, visualization, supervision, project administration, writing - original draft, and writing - review & editing. All authors contributed to the article and approved the submitted version.

FUNDING

This work was supported by the German Center for Lung Research (DZL).

ACKNOWLEDGMENTS

We thank Simone Kuder and Petra Kettenring of the Clinical Trial Unit in the Thoraxklinik Heidelberg for assistance with the collection of patient data and samples.

REFERENCES

1. Lin JJ, Riely GJ, Shaw AT. Targeting ALK: Precision Medicine Takes on Drug Resistance. *Cancer Discovery* (2017) 7:137–55. doi: 10.1158/2159-8290.CD-16-1123
2. Solomon BJ, Mok T, Kim DW, Wu YL, Nakagawa K, Mekhail T, et al. First-line crizotinib versus chemotherapy in ALK-positive lung cancer. *N Engl J Med* (2014) 371:2167–77. doi: 10.1056/NEJMoa1408440
3. Mok T, Camidge DR, Gadgeel SM, Rosell R, Dziadziuszko R, Kim D-W, et al. Updated overall survival and final progression-free survival data for patients with treatment-naive advanced ALK-positive non-small-cell lung cancer in the ALEX study. *Ann Oncol* (2020) 31:1056–64. doi: 10.1016/j.annonc.2020.04.478
4. Camidge DR, Kim HR, Ahn MJ, Yang JC, Han JY, Lee JS, et al. Brigatinib versus Crizotinib in ALK-Positive Non-Small-Cell Lung Cancer. *N Engl J Med* (2018) 379:2027–39. doi: 10.1056/NEJMoa1810171
5. Solomon BJ, Besse B, Bauer TM, Felip E, Soo RA, Camidge DR, et al. Lorlatinib in patients with ALK-positive non-small-cell lung cancer: results from a global phase 2 study. *Lancet Oncol* (2018) 19:1654–67. doi: 10.1016/S1470-2045(18)30649-1
6. Shaw AT, Bauer TM, Marinis FD, Felip E, Goto Y, Liu G, et al. First-Line Lorlatinib or Crizotinib in Advanced ALK-Positive Lung Cancer. *N Engl J Med* (2020) 383:2018–29. doi: 10.1056/NEJMoa2027187
7. Christopoulos P, Budczies J, Kirchner M, Dietz S, Sultmann H, Thomas M, et al. Defining molecular risk in ALK(+) NSCLC. *Oncotarget* (2019) 10:3093–103. doi: 10.18632/oncotarget.26886
8. Duruisseaux M, Besse B, Cadranel J, Perol M, Mennecier B, Bigay-Game L, et al. Overall survival with crizotinib and next-generation ALK inhibitors in ALK-positive non-small-cell lung cancer (IFCT-1302 CLINALK): a French nationwide cohort retrospective study. *Oncotarget* (2017) 8:21903–17. doi: 10.18632/oncotarget.15746
9. Gainor JF, Dardaei L, Yoda S, Friboulet L, Leshchiner I, Katayama R, et al. Molecular Mechanisms of Resistance to First- and Second-Generation ALK Inhibitors in ALK-Rearranged Lung Cancer. *Cancer Discovery* (2016) 6:1118–33. doi: 10.1158/2159-8290.CD-16-0596
10. Planchard D, Popat S, Kerr K, Novello S, Smit EF, Faivre-Finn C, et al. Metastatic non-small cell lung cancer: ESMO Clinical Practice Guidelines for diagnosis, treatment and follow-up. *Ann Oncol* (2018) 29:iv192–237. doi: 10.1093/annonc/mdy275
11. Travis WD, Brambilla E, Nicholson AG, Yatabe Y, Austin JH, Beasley MB, et al. The 2015 World Health Organization Classification of Lung Tumors: Impact of Genetic, Clinical and Radiologic Advances Since the 2004 Classification. *J Thor Oncol* (2015) 10:1243–60. doi: 10.1097/JTO.0000000000000630
12. Volckmar AL, Leichsenring J, Kirchner M, Christopoulos P, Neumann O, Budczies J, et al. Combined targeted DNA and RNA sequencing of advanced NSCLC in routine molecular diagnostics: Analysis of the first 3,000 Heidelberg cases. *Int J Cancer* (2019) 145:649–61. doi: 10.1002/ijc.32133
13. Schemper M, Smith TL. A note on quantifying follow-up in studies of failure time. *Control Clin Trials* (1996) 17:343–6. doi: 10.1016/0197-2456(96)00075-x
14. Agresti A, Coull BA. Approximate is Better than "Exact" for Interval Estimation of Binomial Proportions. *Am Stat* (1998) 52:119–26. doi: 10.1080/00031305.1998.10480550
15. Caffo O. Treatment sequencing in oncology: balancing clinical trial and real-world evidence. *Future Oncol* (2019) 15:2887–9. doi: 10.2217/fon-2019-0415
16. Waterhouse DM, Espirito JL, Chioda MD, Baidoo B, Mardekian J, Robert NJ, et al. Retrospective Observational Study of ALK-Inhibitor Therapy

Sequencing and Outcomes in Patients with ALK-Positive Non-small Cell Lung Cancer. *Drugs Real World Outcomes* (2020) 7:261–9. doi: 10.1007/s40801-020-00207-6
17. Ito K, Hataji O, Kobayashi H, Fujiwara A, Yoshida M, D'Alessandro-Gabazza CN, et al. Sequential Therapy with Crizotinib and Alectinib in ALK-Rearranged Non-Small Cell Lung Cancer-A Multicenter Retrospective Study. *J Thorac Oncol* (2017) 12:390–6. doi: 10.1016/j.jtho.2016.07.022
18. Asao T, Fujiwara Y, Itahashi K, Kitahara S, Goto Y, Horinouchi H, et al. Sequential Use of Anaplastic Lymphoma Kinase Inhibitors in Japanese Patients With ALK-Rearranged Non-Small-Cell Lung Cancer: A Retrospective Analysis. *Clin Lung Cancer* (2017) 18:e251–8. doi: 10.1016/j.cllc.2016.11.015
19. Currà MF, Iacono D, Delmonte A, Metro G, Paglialunga L, Dubini A, et al. Sequential strategy with ALK-TKIs for ALK-positive advanced NSCLC: results of a multicenter analysis. *Ann Oncol* (2015) 26:vi75. doi: 10.1093/annonc/mdv343.08
20. Peters S, Camidge DR, Shaw AT, Gadgeel S, Ahn JS, Kim DW, et al. Alectinib versus Crizotinib in Untreated ALK-Positive Non-Small-Cell Lung Cancer. *N Engl J Med* (2017) 377:829–38. doi: 10.1056/NEJMoa1704795
21. Elsayed M, Christopoulos P. Therapeutic Sequencing in ALK+ NSCLC. *Pharmaceuticals* (2021) 14:80. doi: 10.3390/ph14020080
22. Gerber DE, Rasco DW, Le P, Yan J, Dowell JE, Xie Y. Predictors and impact of second-line chemotherapy for advanced non-small cell lung cancer in the United States: real-world considerations for maintenance therapy. *J Thorac Oncol* (2011) 6:365–71. doi: 10.1097/JTO.0b013e3181fff142
23. Sacher AG, Le LW, Lau A, Earle CC, Leighl NB. Real-world chemotherapy treatment patterns in metastatic non-small cell lung cancer: Are patients undertreated? *Cancer* (2015) 121:2562–9. doi: 10.1002/cncr.29386
24. Zietemann V, Duell T. Every-day clinical practice in patients with advanced non-small-cell lung cancer. *Lung Cancer* (2010) 68:273–7. doi: 10.1016/j.lungcan.2009.06.023
25. Zietemann V, Duell T. Prevalence and effectiveness of first-, second-, and third-line systemic therapy in a cohort of unselected patients with advanced non-small cell lung cancer. *Lung Cancer* (2011) 73:70–7. doi: 10.1016/j.lungcan.2010.10.017
26. Ramalingam SS, Vansteenkiste J, Planchard D, Cho BC, Gray JE, Ohe Y, et al. Overall Survival with Osimertinib in Untreated, EGFR-Mutated Advanced NSCLC. *N Engl J Med* (2020) 382:41–50. doi: 10.1056/NEJMoa1913662
27. Roeper J, Falk M, Tiemann M, Wesseler C, Wiest G, Sackmann S, et al. Risk of not receiving 2nd line therapy is high in EGFR mt+ pts: Real world data of certified lung cancer centers on treatment sequence in EGFR mt+ pts. *J Clin Oncol* (2018) 36:e21220–0. doi: 10.1200/JCO.2018.36.15_suppl.e21220
28. Christopoulos P, Volckmar A-L, Bozorgmehr F, Magios N, Kuon JB, Kirchner M, et al. Real-world implementation of sequential targeted therapies for EGFR-mutated NSCLC. *Ann Oncol* (2019) 30:v631–2. doi: 10.1093/annonc/mdz260.060
29. Magios N, Bozorgmehr F, Volckmar AL, Kazdal D, Kirchner M, Herth F, et al. Real-world implementation of sequential targeted therapies for EGFR-mutated lung cancer. *Ther Adv Med Oncol* (2021) 13:1–13. doi: 10.1177/1758835921996509
30. Cui JJ, Rogers E, Zhai D, Deng W, Ung J, Nguyen V, et al. AACR 2020 abstract 5226: TPX-0131: A next generation macrocyclic ALK inhibitor that overcomes ALK resistant mutations refractory to current approved ALK inhibitors. *Cancer Res* (2020) 80:5226. doi: 10.1158/1538-7445.AM2020-5226
31. Christopoulos P, Dietz S, Kirchner M, Volckmar AL, Endris V, Neumann O, et al. Detection of TP53 Mutations in Tissue or Liquid Rebiopsies at Progression Identifies ALK+ Lung Cancer Patients with Poor Survival. *Cancers (Basel)* (2019) 11(1):124. doi: 10.3390/cancers11010124
32. McCoach CE, Blakely CM, Banks KC, Levy B, Chue BM, Raymond VM, et al. Clinical Utility of Cell-Free DNA for the Detection of ALK Fusions and Genomic Mechanisms of ALK Inhibitor Resistance in Non-Small Cell Lung Cancer. *Clin Cancer Res* (2018) 24(12):2758–70. doi: 10.1158/1078-0432.CCR-17-2588
33. Dagogo-Jack I, Brannon AR, Ferris LA, Campbell CD, Lin JJ, Schultz KR, et al. Tracking the Evolution of Resistance to ALK Tyrosine Kinase Inhibitors through Longitudinal Analysis of Circulating Tumor DNA. *JCO Precis Oncol* (2018) 2:PO.17.00160. doi: 10.1200/PO.17.00160
34. Volckmar AL, Sultmann H, Riediger A, Fioretos T, Schirmacher P, Endris V, et al. A field guide for cancer diagnostics using cell-free DNA: From principles to practice and clinical applications. *Gene Chromosomes Cancer* (2018) 57:123–39. doi: 10.1002/gcc.22517
35. Dietz S, Christopoulos P, Yuan Z, Angeles AK, Gu L, Volckmar A-L, et al. Longitudinal therapy monitoring of ALK-positive lung cancer by combined copy number and targeted mutation profiling of cell-free DNA. *EBioMedicine* (2020) 62:103103. doi: 10.1016/j.ebiom.2020.103103
36. Basch E, Deal AM, Dueck AC, Scher HI, Kris MG, Hudis C, et al. Overall Survival Results of a Trial Assessing Patient-Reported Outcomes for Symptom Monitoring During Routine Cancer Treatment. *JAMA* (2017) 318:197–8. doi: 10.1001/jama.2017.7156
37. Yang S-C, Lin C-C, Lai W-W, Chang S-M, Hwang J-S, Su W-C, et al. Dynamic changes in quality of life after three first-line therapies for EGFR mutation-positive advanced non-small-cell lung cancer. *Ther Adv Med Onc* (2018) 10:1–11. doi: 10.1177/1758834018755072

Conflict of Interest: FB: research funding from BMS and travel grants from BMS and MSD. DK: advisory board and speaker's honoraria from AstraZeneca, BMS, Pfizer. HS: advisory board and speaker's honoraria from Roche. JF: advisory board honoraria from Boehringer, Roche, Celgene and AstraZeneca. AS: advisory board honoraria from BMS, AstraZeneca, ThermoFisher, Novartis, speaker's honoraria from BMS, Illumina, AstraZeneca, Novartis, ThermoFisher, MSD, Roche, and research funding from Chugai. MT: advisory board honoraria from Novartis, Lilly, BMS, MSD, Roche, Celgene, Takeda, AbbVie, Boehringer, speaker's honoraria from Lilly, MSD, Takeda, research funding from AstraZeneca, BMS, Celgene, Novartis, Roche and travel grants from BMS, MSD, Novartis, Boehringer. PC: research funding from AstraZeneca, Novartis, Roche, Takeda, and advisory board/lecture fees from AstraZeneca, Boehringer Ingelheim, Chugai, Novartis, Pfizer, Roche, Takeda.

The remaining authors declare that the research was conducted in the absence of any commercial or financial relationships that could be construed as a potential conflict of interest.

Copyright © 2021 Elsayed, Bozorgmehr, Kazdal, Volckmar, Sültmann, Fischer, Kriegsmann, Stenzinger, Thomas and Christopoulos. This is an open-access article distributed under the terms of the Creative Commons Attribution License (CC BY). The use, distribution or reproduction in other forums is permitted, provided the original author(s) and the copyright owner(s) are credited and that the original publication in this journal is cited, in accordance with accepted academic practice. No use, distribution or reproduction is permitted which does not comply with these terms.

frontiers in Oncology

ORIGINAL RESEARCH
published: 22 April 2021
doi: 10.3389/fonc.2021.671341

An Immune-Related lncRNA Expression Profile to Improve Prognosis Prediction for Lung Adenocarcinoma: From Bioinformatics to Clinical Word

Boxiang Zhang[1†], Rui Wang[1†], Kai Li[1], Ziyang Peng[1], Dapeng Liu[1], Yunfeng Zhang[1] and Liuzhi Zhou[2*]*

[1] Department of Thoracic Surgery, The First Affiliated Hospital of Xi'an Jiaotong University, Xi'an, China, [2] Department of Surgery, The Second Affiliated Hospital, Zhejiang University School of Medicine, Hangzhou, China

OPEN ACCESS

Edited by:
Junji Uchino,
Kyoto Prefectural University of Medicine, Japan

Reviewed by:
Jelena Stojsic,
University of Belgrade, Serbia
Yuxuan Song,
Tianjin Medical University General Hospital, China

***Correspondence:**
Liuzhi Zhou
zhou_liuzhi@163.com
Yunfeng Zhang
zyf119@126.com

[†]These authors have contributed equally to this work

Specialty section:
This article was submitted to Thoracic Oncology, a section of the journal Frontiers in Oncology

Received: 23 February 2021
Accepted: 29 March 2021
Published: 22 April 2021

Citation:
Zhang B, Wang R, Li K, Peng Z, Liu D, Zhang Y and Zhou L (2021) An Immune-Related lncRNA Expression Profile to Improve Prognosis Prediction for Lung Adenocarcinoma: From Bioinformatics to Clinical Word. Front. Oncol. 11:671341. doi: 10.3389/fonc.2021.671341

Background: Lung cancer is still the top-ranked cancer-related deaths all over the world. Now immunotherapy has emerged as a promising option for treating lung cancer. Recent evidence indicated that lncRNAs were also key regulators in immune system. We aimed to develop a novel prognostic signature based on the comprehensive analysis of immune-related lncRNAs to predict survival outcome of LUAD patients.

Methods: The gene expression profiles of 491 LUAD patients were downloaded from TCGA. 1047 immune-related lncRNAs were obtained through Pearson correlation analysis of immune genes and lncRNAs using statistical software R language. Univariate and multivariate Cox regression analysis were performed to determine the optimal immune-related lncRNAs prognostic signature (ITGCB-DT, ABALON, TMPO-AS1 and VIM-AS1). Finally, we validated the immune-related lncRNAs prognostic signature in The First Affiliated Hospital of Xi'an Jiaotong University cancer center cohort.

Results: A four immune-related lncRNAs prognostic signature was constructed to predict the survival outcome of LUAD patients. Statistical significance were found that the LUAD patients in high-risk group suffered shorter overall survival than those in low-risk group ($P < 0.001$). ROC curve analysis shown that the four immune-related lncRNAs prognostic signature had the best predictive effect compared with age, gender, AJCC-stage, T stage, N stage, M stage (AUC = 0.756). More importantly, clinical cohort studies proved that the signature could predict the overall survival of LUAD patients with an AUC = 0.714.

Conclusions: In summary, we demonstrated that the novel immune-related lncRNAs signature had the ability to predict the prognosis of LUAD patients, which might serve as potential prognostic biomarkers and guide the individualized treatment strategies for LUAD patients.

Keywords: lung adenocarcinoma, immune-related lncRNA, clinical assessment, prognosis, biomarkers

INTRODUCTION

According to the latest global cancer statistics released in 2020, lung cancer is still the top-ranked cancer-related deaths all over the world, with a five-year survival rate of less than 19% (1, 2). In America, there were approximately 228,820 new cases of lung cancer and 135,720 deaths in 2020 (1). There are two major types of lung cancer, including small cell lung cancer (SCLC) and non-small cell lung cancer (NSCLC). NSCLC is further divided into three main subtypes, including lung squamous cell carcinoma (LUSC), lung adenocarcinoma (LUAD) and large cell lung cancer, of which LUAD accounts for about 40% (3). Since the signs of the early stage and clinical symptoms of LUAD are often non-specific and inconspicuous, a large proportion of patients are not diagnosed until the metastatic or advanced tumor stage (4). In recent years, although immunotherapy has shown unexpected anti-tumor effects in lung adenocarcinoma (5, 6). However, only a few patients have benefited from it, and there is no exact molecular stratification of the patients. This highlights the importance of investigation on new therapeutic approaches and novel biomarkers that provide prognostic information.

Long non-coding RNAs are a type of RNA molecule that are longer than 200 nucleotides and are not translated into proteins (7, 8). Once it was considered that these long non-coding RNAs were simply cloning artifacts or transcriptional noise with limited effects and single function in pre-RNA process (9). However, recent evidence indicated that lncRNAs were also involved in various biological functions in the cytoplasm and nucleus, such as transcriptional regulation, apoptosis, cell growth, tumorigenesis and epigenetic regulation (10, 11). It was well documented that lncRNAs played a comprehensive and complex regulatory role in cancer development and progression (12, 13). Moreover, lncRNAs have shown important regulatory effects of gene expression in immune system, including but not limited to immune activation, immune escape, immune surveillance, and immune infiltration (14, 15). For instance, the HCC-derived exosomal lncRNA TUC339 affected the complicated immune microenvironmental interaction between tumor and immune cells by regulating the polarization of M1/M2 macrophages (16). Besides, lncRNA GATA3-AS1 promoted tumor development and immune escape in triple negative breast cancer by destabilizing GATA3 but stabilizing PD-L1 (17). Thus, it is essential to develop an expression profile based on immune-related lncRNAs that can predict the prognosis of LUAD patients and further guide appropriate individualized treatment strategies.

In this study, we developed a novel prognostic signature based on the comprehensive analysis of immune-related lncRNAs in 491 adenocarcinoma patients downloaded from The Cancer Genome Atlas (TCGA). Four immune-related lncRNAs were confirmed to be related to immune response using univariate and multivariate Cox regression analysis. We then verified the expression of four immune-related lncRNAs on cells and tissues and further explored the relationship between prognostic signature and other clinicopathological characteristics. Finally, we confirmed that the novel immune-related lncRNAs signature had the ability to predict the prognosis of LUAD patients, which might serve as potential prognostic biomarkers and guide the individualized treatment strategies for LUAD patients.

Abbreviations: LUAD, lung adenocarcinoma; OS, overall survival; AUC, area under the curve; TD, tumor diameter; LNM, lymph node metastasis; TCGA, The Cancer Genome Atlas; GSEA, Gene set enrichment analysis; TNM, tumor-node-metastasis; HR, hazard ratio.

MATERIALS AND METHODS

Data Acquisition and Processing

The RNA-seq data of lung adenocarcinoma and matched normal tissues were downloaded from the GDC portal (https://portal.gdc.cancer.gov/) in December 2020, and the data was normalized using "limma" package. We further classified lncRNAs and protein-coding genes according to the gene annotations in Gencode (http://gencodegenes.org/). Immune genes were obtained from Molecular Signatures Database v7.1 using Gene Set Enrichment Analysis (MSigDB, https://www.gseamsigdb.org/gsea/index.jsp). Subsequently, we obtained immune-related lncRNA through Pearson correlation analysis of immune genes and lncRNAs using statistical software R language. Finally, the corresponding clinicopathological characteristics and survival information were acquired and integrated into RNA-seq data, including age, gender, stage, and TNM.

Establishment of Prognostic Signature Using Immune-Related lncRNAs and Calculation of Risk Score

To determine the potential optimal immune-related prognostic lncRNAs, we performed univariate and multivariate Cox regression analysis on those immune-related lncRNA and survival data. Since the genes at the beginning of AC and AL belonged to conservative sequences and their functions had not been clearly clarified, we did not include them in the actual analysis. An HR value greater than one indicated an increased risk. Finally, four immune-related lncRNAs were identified and their regression correlation coefficients (β) with the lowest AIC values. We then established the optimal immune-related lncRNAs prognostic signature and calculated the risk scores of each lung adenocarcinoma patient based on the expression levels of immune-related lncRNAs and the Risk coefficients (β):Risk scores $=0.411143 \times \text{Expression}_{\text{ABALON}} - 0.259290 \times \text{Expression}_{\text{VIM-AS1}} + 0.337683 \times \text{Expression}_{\text{TMPO-AS1}} + 0.265425 \times \text{Expression}_{\text{ITGB1-DT}}$.

Cell Culture and Real-Time Quantitative PCR

To further confirm the expressions of the four immune-related lncRNAs in cells and tissues, human normal lung epithelial cell (B2B) and lung adenocarcinoma cell lines (A549, H1299, H1975) were obtained from the laboratory and cultured in DMEM medium containing 10% FBS with 1% penicillin and streptomycin in a humidified incubator. The total RNA of

various cell lines was extracted using RNA-Quick purification kit according to manufacturer's instructions (Vazyme, RN001). Total RNA were reversed into cDNA using PrimeScript™ RT reagent kit with gDNA Eraser (Takara, RR047A). Next, we performed quantitative PCR to determine the relative expression levels of the four lncRNAs (Takara, RB820A). The tissues' expressions and survival curves of the four lncRNAs were acquired from the GEPIA database (http://gepia.cancer-pku.cn/). The expression of β-actin was used as an endogenous control. All samples were analyzed using comparative $2^{-\Delta\Delta C}$ method. All primers' sequences used in PCR were shown in **Table S1**.

Predictive Analysis of Immune-Related lncRNAs Risk Score Signature

All LUAD patients were divided into high and low risk groups according to the median of risk score as threshold. We compared the survival curves of the two groups using the Kaplan–Meier method with log-rank test. ROC curve and AUC value were used to assess the accuracy of the immune-related signature. Further, univariate and multivariate Cox regression analysis were utilized to evaluate clinicopathological characteristics related to prognosis. The heat map shows the differences of the four lncRNAs in two groups. Finally, to explore the influence of single lncRNA on LUAD patients in our prognostic model, we explored the relationship of single lncRNA and clinicopathological characteristics with student's t-test.

Principal Components Analysis and Immune Infiltration

Principal Components Analysis was utilized to visualize the prognostic model. Immune Response and Immune System Process sets were acquired from MSigDB for subsequent analysis. Gene Set Enrichment Analysis were performed on the DEGs in high- and low-risk groups with P <0.05 and |log (fold change) >1|. Cibersort was conducted to evaluate the immune infiltrating cells in each sample with the Pfilter <0.05.

Validation of Immune-Related lncRNAs Prognostic Signature in The First Affiliated Hospital of Xi'an Jiaotong University Cancer Center Cohort

To further screen and verify the prognostic signature, we collected lung adenocarcinoma and adjacent tissues of 78 LUAD patients from the First Affiliated Hospital of Xi'an Jiaotong University, who underwent surgical resection from January 2011 to December 2013. All included patients were diagnosed with LUAD by histopathological examination and did not receive any radiotherapy, chemotherapy, or immunotherapy. We examined the four immune-related lncRNAs and compared them with other clinicopathological characteristics. All patients enrolled were written informed consent. The study was supported by the Ethics Committee of the Affiliated Hospital of Xi'an Jiaotong University.

Statistical Analysis

All computations were conducted using R software (version 4.0.4). Associations between risk scores and other clinicopathological features in LUAD patients were analyzed with Fisher exact test or chi-square test. Kaplan–Meier method and log-rank analysis were performed to assess survival data. Univariate and multivariate Cox regression analyses were performed to assess independent prognostic factors. P <0.05 was considered statistically significant.

RESULTS

Construction and Assessment of Immune-Related lncRNAs Signature

A total of 497 LUAD samples and 54 matched normal controls were available from TCGA database. Subsequently, we downloaded 131 lncRNAs as well as their expression profiles and screened out 331 immune genes from TCGA. Then, 1047 immune-related lncRNAs were obtained using Person correlation analysis with the standard P <0.05 and |R| >0.8. Finally, univariate and multivariate Cox regression analysis were performed to further filter out potential prognostic lncRNAs from those immune-related lncRNAs, and four immune-related lncRNAs were found to be significantly associated with the LUAD patients overall survival (**Figure 1A** and **Table 1**).

Next, we constructed a four immune-related lncRNAs prognostic signature to predict the survival outcomes of LUAD patients. We calculated the risk score of each patient using the following scheme: Risk scores = $0.411143 \times \text{Expression}_{\text{ABALON}} - 0.259290 \times \text{Expression}_{\text{VIM-AS1}} + 0.337683 \times \text{Expression}_{\text{TMPO-AS1}} + 0.265425 \times \text{Expression}_{\text{ITGB1-DT}}$. Furthermore, all LUAD patients from the TCGA data sets were divided into high and low risk groups according to the median of risk scores as threshold. We found that the LUAD patients in high risk group suffered shorter overall survival than those in low-risk group with statistical significance (**Figure 1B**). Subsequently, we sorted the risk scores of all LUAD patients and then evaluated their survival status distribution based on the four immune-related prognostic risk scores. The survival status analysis indicated that the LUAD patients had shorter overall survival and higher mortality with the risk scores increasing (**Figures 1C, D**). Next, we assessed the prediction accuracy of the prognostic signature based on the four immune-related lncRNAs through time-independent ROC curve analysis. The ROC curve analysis shown that the four immune-related lncRNAs' prognostic signature had the best predictive effect compared with age, gender, AJCC-stage, T stage, N stage, M stage (AUC = 0.756) (**Figure 1E**). These results demonstrated that our four immune-related lncRNAs' prognostic signature was capable of predicting the survival outcomes of LUAD patients.

In addition, to prove that the four immune-related lncRNAs prognostic model we constructed could be used as independent prognostic predictions for LUAD patients, we performed univariate and multivariate Cox regression analysis with the following clinicopathological characteristics: age, gender, AJCC-stage, T stage, N stage, M stage. Univariate Cox regression analysis shown that AJCC-stage (P <0.001), T stage (P <0.001), N stage (P <0.001), risk score (P <0.001) were associated with the prognostic survival in LUAD patients

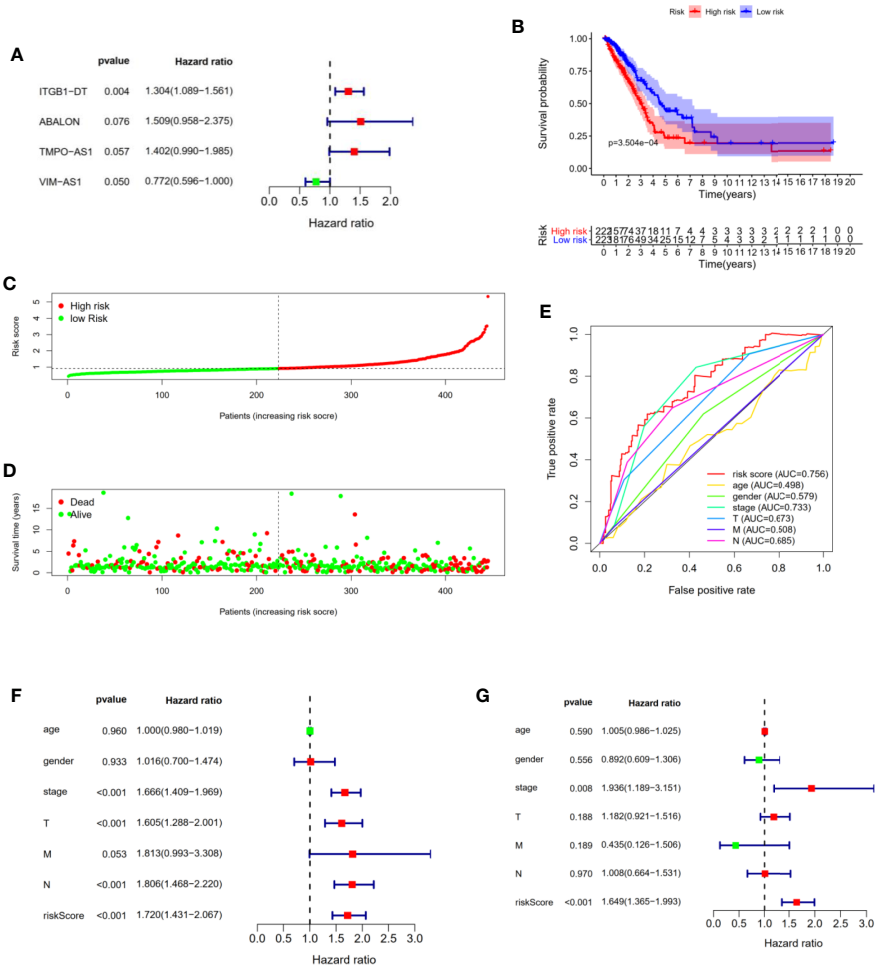

FIGURE 1 | Construction and evaluation of four immune-related lncRNAs prognostic signature for LUAD patients. **(A)** The forest plot shown the P values, Hazard Ratios of four immune-related lncRNAs from multivariate Cox regression analysis. **(B)** Kaplan–Meier analysis illustrated that high risk group had poor prognosis and shorter overall survival in LUAD patients. **(C)** Risk scores of LUAD patients were sorted with the signature. **(D)** The scatter plot of risk scores and survival status in LUAD patients. **(E)** ROC curve analysis demonstrated that risk scores (AUC = 0.756) had the highest reliability and accuracy compared with age, gender, stage, TNM. **(F, G)** Univariate and multivariate Cox regression analysis of prognostic factors combined with other clinicopathological features.

(**Figure 1F**). Multivariate Cox regression analysis indicated that AJCC-stage (P = 0.008), risk score (P <0.001) were still significantly associated with overall survival, and four immune-related lncRNAs prognostic signature could be identified as an independent prognostic factor in LUAD patients (**Figure 1G**).

TABLE 1 | The HRs, P-value, and Coef of four immune-related lncRNAs in the multivariate Cox regression analysis.

LncRNAs	HR (95% CI)	P-value	Coef
ITGB1-DT	1.3040 (1.0894–1.5608)	0.004	0.265
ABALON	1.509 (0.958–2.375)	0.076	0.411
TMPO-AS1	1.402 (0.990–1.985)	0.057	0.337
VIM-AS1	0.772 (0.596–1.000)	0.050	−0.212

HR, hazard ratio; Coef, regression coefficient; CI, confidence interval.

Evaluating Immune-Related lncRNAs Expressions in Cells and Tissues

To further identify the four immune-related lncRNAs expression profiles, we analyzed their relative expression levels in LUAD cell lines (A549, H1299, H1975) and normal lung cell (B2B) using quantitative PCR. Next, the Gepia database was used to obtain the expressions of four immune-related lncRNAs in LUAD tissues and adjacent normal tissues. Moreover, we further downloaded the survival curves of four immune-related lncRNAs from the Gepia database. As shown in **Figures 2A–C**, the ITGCB-DT, ABALON and TMPO-AS1 expressions were relatively highly expressed in LUAD cell lines (A549, H1299, H1975) compared with normal control (B2B). The same results were also found in clinical samples that ITGCB-DT, ABALON as well as TMPO-AS1 expressions were significantly up-regulated in LUAD tumor tissues compared with adjacent tissues and LUAD patients with higher expressions of

ITGCB-DT, ABALON and TMPO-AS1 tended to have shorter overall survival and worse prognosis. In contrast, VIM-AS1 was relatively lower expressed in A549, H1299 and H1975 as well as LUAD tissues, and LUAD patients with higher expression of VIM-AS1 had better prognosis and longer overall survival (**Figure 2D**). Thus, these results indicated that ITGCB-DT, ABALON, TMPO-AS1 and VIM-AS1 could serve as independent prognostic biomarkers in LUAD.

Correlations With Clinicopathological Characteristics

We also analyzed the associations between four immune-related lncRNAs and clinicopathological characteristics to explore the impact of single lncRNA in LUAD patients. The heat map shown that the four immune-related lncRNAs were obviously differentially expressed in high- and low- risk patients, of which ITGB1-DT, ABALON as well as TMPO-AS1 was up-regulated, and VIM-AS1 was down-regulated in high risk group (**Figure 3A**). In terms of single lncRNA, no statistically difference was found in the expression levels of ITGB1-DT, ABALON as well as TMPO-AS1 with AJCC-stage (**Figure 3B**), T stage (**Figure 3C**), N stage (**Figure 3D**) and M stage (**Figure 3E**). However, it could be found that there was a trend that ITGB1-DT, ABALON and TMPO-AS1 were increased with AJCC-stage and TNM stage. Besides, the expression level of VIM-AS1 was negatively associated with AJCC-stage (**Figure 3B**), T stage (**Figure 3C**), N stage (**Figure 3D**) and M stage (**Figure 3E**). These results were basically consistent with our above analysis,

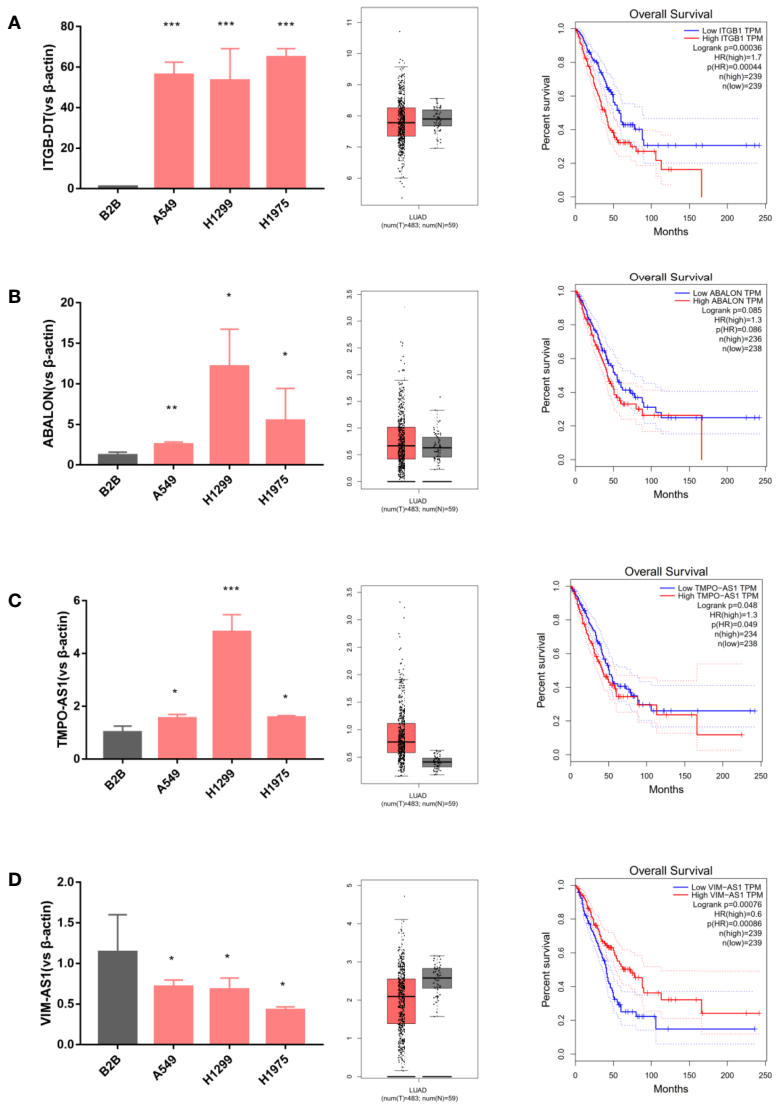

FIGURE 2 | Evaluating immune-related lncRNAs expression in cells and tissues. ITGCB-DT, ABALON and TMPO-AS1 expressions were relatively highly expressed in LUAD cell lines and LUAD tissues compared with normal controls and LUAD patients had worse prognosis with their increased expressions. The opposite of VIM-AS1. **(A)** ITGB-DT **(B)** ABALON **(C)** TMPO-AS1 **(D)** VIM-AS1. *P < 0.05; **P < 0.01; ***P < 0.001.

proving that our four-immune related lncRNAs prognostic signature was competent for predicting survival prognosis in LUAD patients.

In addition, we performed chi-square test to explore the associations of risk score and other clinicopathological characteristics in LUAD patients. As shown in **Figure 4**, there were significant differences between high- and low-risk groups in gender (P = 0.005, **Figure 4B**), AJCC stage (P = 0.007, **Figure 4C**), N stage (P = 0.026, **Figure 4E**), and M stage (P = 0.056, **Figure 4F**). These results proved that our four immune-related lncRNAs profiles could play a potential role in predicting tumor progression and survival prognosis of LUAD patients.

Functional and Pathway Enrichment Analysis of DEGs Related to Risk Score

Differentially expressed genes in high- and low- risk groups were analyzed with R software. 1029 DEGs were available using "Limma" package with the criteria P <0.05 and log (fold change) >1 (**Figure 5A**). Next, we performed Gene Ontology and KEGG analysis to further explore the DEGs' function and pathway enrichment. Obviously, in Biological Process, Cellular Component and Molecular Function, the differentially expressed genes were mainly enriched in organelle fission, chromosomal region, tubulin binding (**Figures 5B, C**). In addition, KEGG analysis shown that these risk-related DEGs were significantly enriched in alcoholism, systemic lupus erythematosus,

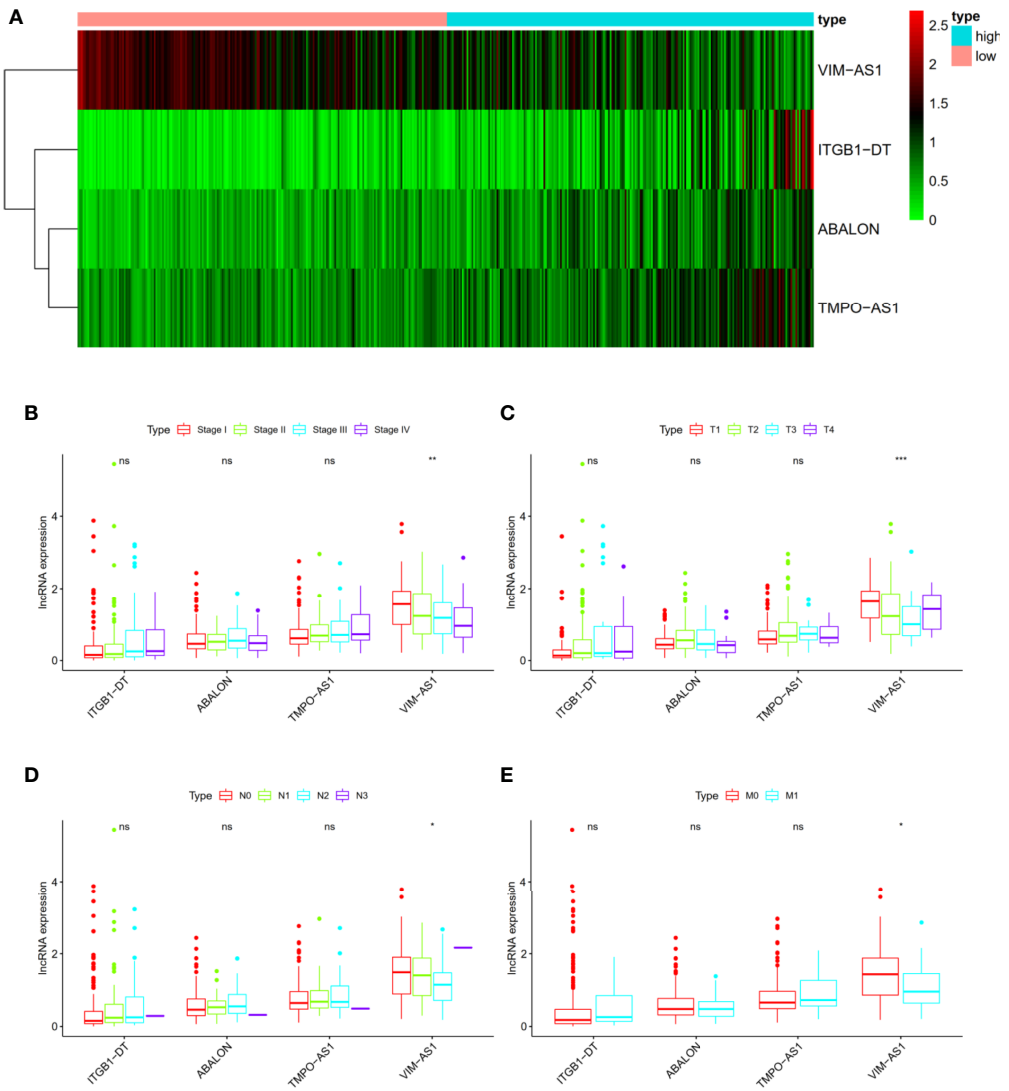

FIGURE 3 | The associations between four immune-related lncRNAs and other clinicopathological characteristics. **(A)** Heat map shown the expression levels of four immune-related lncRNAs in high- and low- risk groups. **(B–E)** The relationships of four immune-related lncRNAs and AJCC stage as well as AJCC TNM. *P < 0.05; **P < 0.01; ***P < 0.001; ns, no significance.

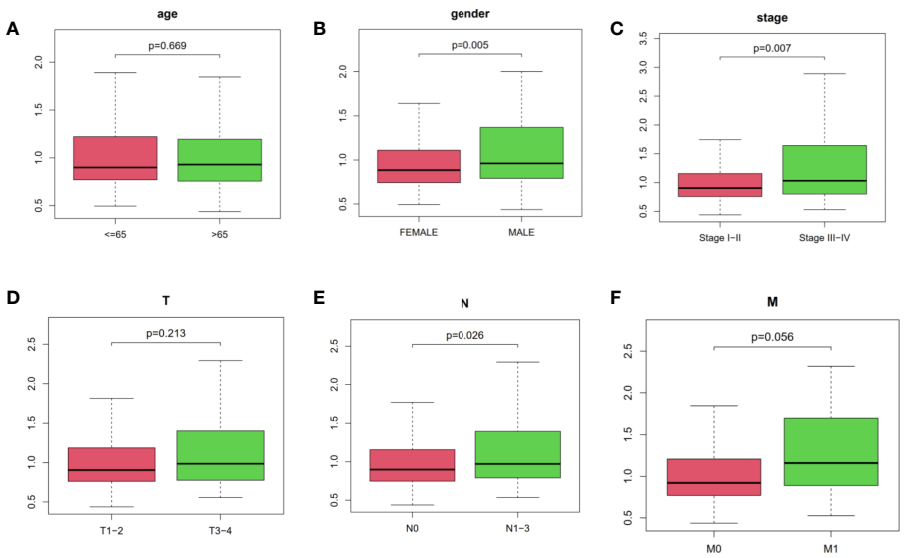

FIGURE 4 | The relationships of risk score and age, gender, AJCC stage as well as AJCC-TNM. **(A)** age, **(B)** gender, **(C)** stage, **(D–F)** AJCC-TNM, respectively. The ordinate was risk score.

neuroactive ligand–receptor interaction (**Figures 5D, E**). Moreover, we performed Gene Set Enrichment Analysis (Immunologic signatures) for the high-risk group. The top 10 differentially enriched immunologic signatures were shown in **Table S2**. We explained the risk-related DEGs in LUAD patients from a mathematical perspective, which might promote future research and treatment of LUAD.

Identification of Immune Status in High- and Low-Risk Groups

Based on principal component analysis, we further analyzed the distinct distribution of low- and high-risk groups using whole gene expression profiles, all immune-related lncRNAs and four risk genes. The results shown that the samples were not significantly separated into two sections and the immune status of LUAD patients were overlapped between high- and low- risk groups based on whole gene expression profiles and all immune-related lncRNAs sets (**Figures 6A, B**). However, significant differences were found in the immune status of high risk groups compared with low risk groups according to the four risk genes sets (**Figure 6C**).

Besides, GSEA analysis was performed and the results indicated that both immune response (**Figure 6D**) and immune system process (**Figure 6E**) were enriched in the low risk group. In addition, to further explore immune infiltration in high- and low-risk groups, we analyzed 22 immune infiltrating cells in the LUAD microenvironment based on the Cibersort algorithm. We calculated the 22 kinds of immune infiltrating cells with Pfilter <0.05 in each LUAD sample. Moreover, "Vioplot" and "limma" packages were used to visualize the immune infiltrating cells in high- and low- risk groups. As shown in **Figure 6F**, plasma cells (P = 0.002), memory CD4+ T cells (P <0.001), NK cells (P = 0.013), monocytes (P = 0.007), M1 macrophages (P = 0.006), dendritic cells (P <0.001) and mast cells (P <0.001) demonstrated significant differences, indicating that our four immune-related lncRNAs signature could distinguish immune infiltration in LUAD patients. In a word, our four immune-related lncRNAs prognostic signature was component to distinguish the immune status and predict the survival prognosis of LUAD patients.

Identification and Validation of Prognostic Signature in Clinical Cancer Cohort

To further validate the signature we constructed, we analyzed the expressions of four immune-related lncRNAs in 78 LUAD samples and 30 matched normal controls from clinical cancer cohort. As shown in **Figure 7A**, the expressions of ITGB1-DT (P <0.001), ABALON (P <0.001) as well as TMPO-AS1 (P <0.001) were significantly up-regulated in LUAD tissues compared with adjacent LUAD tissue, while VIM-AS1 (P <0.001) expressed the opposite, which were consistent with our previous analysis from TCGA database.

Additionally, to explore the relationships between risk score and other clinicopathological characteristics, we calculated the risk scores of 78 LUAD patients according to the four immune-related lncRNAs signature we established before. All 78 LUAD patients were divided into high- and low-risk subgroups with the median of risk score as threshold. Chi-square test analysis demonstrated that high risk scores were related with weight-loss (P = 0.009), tumor diameter (P <0.001), multiple lesions (P <0.001), lymph node metastasis (P = 0.011), differentiation (P <0.001) and TNM stage (P <0.001) (**Table 2**). However, there was no significant difference between risk score and other clinicopathological characteristics, such as age, smoking and vessel carcinoma embolus.

Next, to confirm the independent prognostic factors in LUAD patients, we performed univariate and multivariate Cox regression

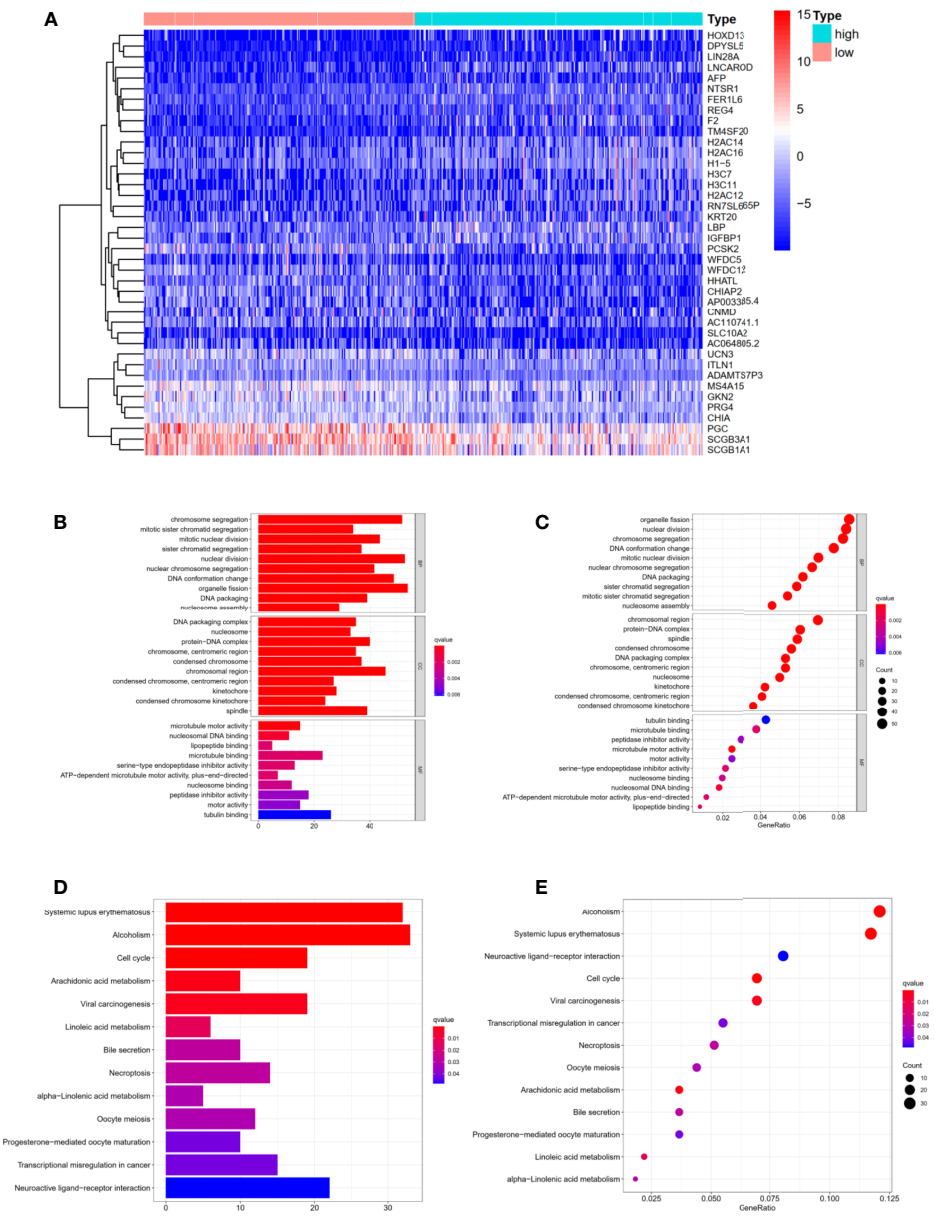

FIGURE 5 | Functional and Pathway enrichment analysis of DEGs related to risk score. **(A)** The heat map displayed DEGs in high- and low-risk groups **(B, C)** Functional enrichment analysis of DEGs using Gene Ontology. **(D, E)** Pathway enrichment analysis of DEGs using KEGG method. KEGG, Kyoto Encyclopedia of Genes and Genomes.

analysis on various clinicopathological characteristics and risk scores. Univariate Cox regression analysis demonstrated that age, tumor diameter, lymph node metastasis, TNM stage and risk scores were related to the survival prognosis of LUAD patients (**Figure 7B** and **Table 3**). Multivariate Cox regression analysis shown that age, TNM stage and risk score could serve as independent prognosis biomarkers in LUAD patients (**Figure 7C** and **Table 3**). Finally, a significant statistical difference was found in overall survival of high- and low-risk groups (P <0.001) (**Figure 7D**). And through ROC curve analysis, we demonstrated that the four immune-related lncRNAs signature has high accuracy and reliability in predicting the prognosis of LUAD patients in actual clinical application (AUC = 0.714, **Figure 7E**).

DISCUSSION

Although surgical resection had been proven to be essential for early lung adenocarcinoma and made great progress in the past thirty years, the treatment for advanced and metastatic lung

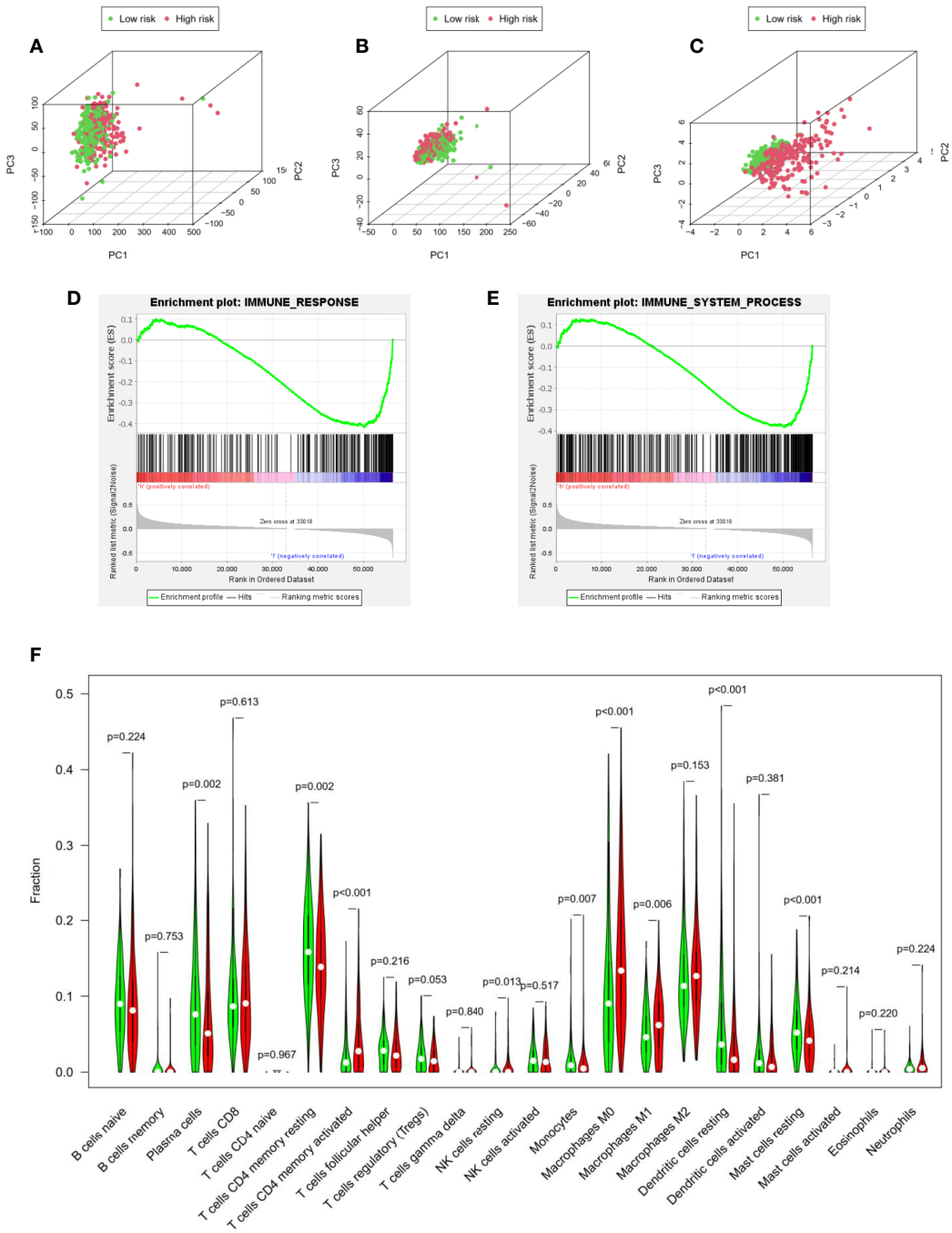

FIGURE 6 | Identification of immune status in high- and low-risk groups. **(A–C)** Principal component analysis demonstrated that significant differences were found in the immune status between two risk groups according to four immune-related lncRNAs. Whole gene expression profiles, all immune-related lncRNAs, four risk genes, respectively. GSEA analysis shown that both immune response **(D)** and immune system process **(E)** were enriched in the low risk group. **(F)** Cibersort algorithm calculated the difference of immune infiltration in high- and low-risk groups.

adenocarcinoma was still unsatisfactory (18). For some LUAD patients with similar clinical symptoms, there were significant differences in survival outcomes due to genetic heterogeneity. Therefore, in addition to traditional clinical risk indicators, exploring novel prognostic molecular classification for LUAD was crucial. With the development of bioinformatics analysis and third-generation sequencing technology, it had been confirmed that lncRNAs were involved in tumorigenesis and cancer development

TABLE 2 | Associations between risk scores and clinicopathological characteristics in clinical LUAD cohort.

Characteristics	Total	Risk Scores		*P* value
		Low (n = 39) 1.69	High (n = 39) 1.62	
Age, ys				0.172
≤65	43	25	18	
>65	35	14	21	
Gender				0.651
Female	44	17	20	
Male	34	22	19	
Smoking				0.084
Absent	54	31	23	
Present	24	8	16	
Weight-loss				0.009*
≤5%	30	21	9	
>5%	48	18	30	
Tumor diameter				<0.001*
≤5 cm	58	37	21	
>5 cm	20	2	18	
Multiple lesions				<0.001*
Absent	36	27	9	
Present	42	12	30	
Vessel carcinoma embolus				0.999
Absent	74	37	37	
Present	4	2	2	
Lymph node metastasis				0.011*
Absent	46	29	17	
Present	32	10	22	
Atelectasis				0.494
Absent	76	37	39	
Present	2	2	0	
Differentiation				<0.001*
Low	46	14	32	
High/Moderate	32	25	7	
TNM stage				<0.001*
I–II	51	34	17	
III–IV	25	4	21	

*TNM, tumor-node-metastasis; *P <0.05 was considered statistically significant; Values are mean ± standard deviation or n (%).*

(19, 20). Increased studies had shown the importance of lncRNAs in LUAD, such as carcinogenic functions (21), tumor suppressor (22) and prognosis biomarkers (23). Recently, lncRNAs were emerging as key regulators in immune system. Therefore, it was urgent to explore the immune-related lncRNAs in LUAD and its relationship with immune cell infiltration.

In this study, 1,047 immune-related lncRNAs were obtained from MSigDB using Person correlation method for further subsequent analysis. The main finding of our research was that we constructed a four immune-related lncRNAs prognostic signature and verified its stability and reliability through ROC curve and real world data. We demonstrated that our prognostic signature was significantly related with OS and could distinguish LUAD patients with good or poor prognosis based on the four lncRNAs. Our signature had been proven to be an independent prognostic factor in LUAD patients through univariate and multivariate Cox regression analysis. Different from the past immune-related lncRNA prognostic studies, we removed the conservative sequence genes at the beginning of AC or AL when constructing the model, further tested and verified our immune-related lncRNAs on cells and clinical samples. In addition, we also investigated the relationships of single lncRNA expression and clinicopathological characteristics. The results show that ABALON, ITGB-DT and TMPO-AS1 were risk-related genes, while VIM-AS1 was regarded as risk protective genes. PCA analysis indicated that our signature could clearly distinguish high- and low-risk groups compared with whole gene expression profiles or all immune-related lncRNAs. Finally, we validated the four immune-related lncRNAs prognostic model on clinical LUAD patients cohort. These findings proved that the four immune-related lncRNAs prognosis signature was related to the survival prognosis of LUAD patients, and could potentially guide clinicians in the treatment of LUAD patients.

As we know, lncRNAs participated in tumor development (including LUAD) through various mechanisms. Previous studies have indicated that up-regulation of lncRNA UCA1, TTN-AS1 and FEZF1-AS1 in LUAD were related to poor prognosis, and down-regulation of LCAL62 also promoted

TABLE 3 | Prognosis analysis of overall survival in clinical LUAD cohort.

Clinicopathologic parameters	Univariate analysis		Multivariate analysis	
	HR (95%CI)	*P*	HR (95%CI)	*P*
Age (≤65 vs >65)	3.554 (1.634–7.732)	0.001*	3.225 (1.432–7.263)	0.005*
Gender (Female vs Male)	0.901 (0.433–1.874)	0.779		
Smoking (Absent vs Present)	1.191 (0.542–2.620)	0.663		
Weight-loss (≤5% vs >5%)	1.884 (0.805–4.412)	0.145		
Tumor diameter (≤5 cm vs >5 cm)	2.889 (1.350–6.184)	0.006*	1.282 (0.490–3.355)	0.612
Multiple lesions (Absent vs Present)	1.624 (0.766–3.445)	0.206		
Vessel carcinoma embolus (Absent vs Present)	1.018 (0.242–4.287)	0.981		
Lymph node metastasis (Absent vs Present)	2.617 (1.238–5.532)	0.012*	1.002 (0.375–2.680)	0.997
Atelectasis (Absent vs Present)	1.665 (0.224–12.399)	0.619		
Differentiation (Low vs High/Moderate)	0.510 (0.231–1.124)	0.095		
TNM stage	4.454 (2.092–9.484)	<0.001*	3.266 (1.236–8.631)	0.017*
Risk score	3.227 (1.454–7.162)	0.004*	3.113 (1.252–6.952)	0.007*

*LUAD, lung adenocarcinoma; TNM, tumor-node-metastasis; HR, hazard ratio; *P <0.05 was considered statistically significant.*

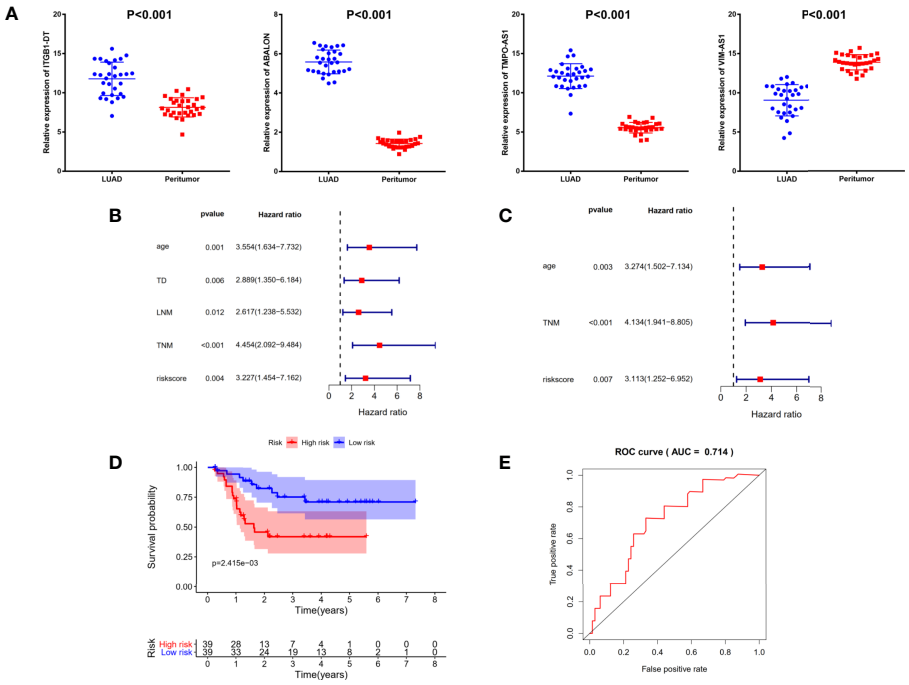

FIGURE 7 | Identification and validation of prognostic signature in clinical cancer cohort. **(A)** The expressions of ITGB1-DT (P <0.001), ABALON (P <0.001) as well as TMPO-AS1(P <0.001) were significantly up-regulated in LUAD tissues compared with adjacent LUAD tissue, while VIM-AS1 (P <0.001) expressed the opposite. **(B)** Univariate Cox regression analysis demonstrated that age, tumor diameter, lymph node metastasis, TNM stage and risk scores were related to the survival prognosis of LUAD patients **(C)** Multivariate Cox regression analysis shown that age, TNM stage and risk score could serve as independent prognosis biomarkers in LUAD patients. **(D)** Kaplan–Meier analysis confirmed four immune-related lncRNAs signature could predict the prognosis of LUAD patients in actual clinical cohort. **(E)** ROC curve analysis shown that the signature was reliable and accurate (AUC = 0.714).

tumor progression and invasion. In addition, Pan et al. indicated that lncRNA JPX regulated tumorigenesis and metastasis of lung cancer through JPX/miR-33a-5p/Twist1 axis and activating Wnt/beta-catenin signaling (24). Peng et al. show that LINC00312 induced LUAD migration and vasculogenic mimicry through directly binding to transcription factor Y-Box Binding Protein 1 (YBX1) (25). As previously reported, LncRNA HMMR-AS1 was significantly upregulated in LUAD and promoted proliferation and metastasis of lung adenocarcinoma by regulating MiR-138/sirt6 axis (26). On the other hand, Mu et al. reported that lncRNA TMPO-AS1 promoted lung adenocarcinoma progression and was negatively regulated by miR-383-5P (27). Despite great progress have achieved in the lncRNA research, the function and molecular mechanism of most lncRNA were still unclear and need further investigation.

In recent years, given that immunotherapy become the dawn of cancer treatment, it has been a hotspot to construct immune-related lncRNA signature to predict tumor prognosis. For instance, Shen et al. constructed a 11-lncRNA prognostic signature for breast cancer, which was associated with immune infiltrating cell subtypes (28). Zhou et al. reported an immune-related six-lncRNA signature to improve prognosis prediction for glioblastoma multiforme (29). In this study, we found that high expression of ITGB1-DT, ABALON as well as TMPO-AS1 and low expression of VIM-AS1 in lung adenocarcinoma were associated with poor prognosis. We successfully constructed four immune-related lncRNA prognostic signature and validated them in clinical cancer cohort for the first time.

In conclusion, we identified a four immune-related lncRNAs signature that had the ability to predict the prognosis of LUAD patients and was validated by clinical cancer cohort, which might serve as potential prognostic biomarkers and guide the individualized treatment strategies for LUAD patients.

DATA AVAILABILITY STATEMENT

The datasets presented in this study can be found in online repositories. The names of the repository/repositories and accession number(s) can be found in the article/**Supplementary Material**.

ETHICS STATEMENT

The studies involving human participants were reviewed and approved by the Ethics Committee of the Affiliated Hospital of Xi'an Jiaotong University. All patients enrolled were written

informed consent. The patients/participants provided their written informed consent to participate in this study.

AUTHOR CONTRIBUTIONS

LZ and BZ conceived and designed the study. BZ, RW, KL, and ZP conducted the study. DL contributed to the acquisition of data. BZ and RW analyzed the data. LZ, ZB and RW interpreted the data. LZ, BZ, YZ, and RW reviewed and edited the manuscript. All authors contributed to the article and approved the submitted version.

FUNDING

This work was supported by Key Research and Development Program of Shaanxi (Program No.2019SF-044 & No.2019SF-129).

SUPPLEMENTARY MATERIAL

The Supplementary Material for this article can be found online at: https://www.frontiersin.org/articles/10.3389/fonc.2021.671341/full#supplementary-material

REFERENCES

1. Siegel RL, Miller KD, Jemal A. Cancer Statistics, 2020. *CA Cancer J Clin* (2020) 70(1):7–30. doi: 10.3322/caac.21590
2. Hirsch FR, Scagliotti GV, Mulshine JL, Kwon R, Curran WJ Jr, Wu YL, et al. Lung Cancer: Current Therapies and New Targeted Treatments. *Lancet* (2017) 389(10066):299–311. doi: 10.1016/S0140-6736(16)30958-8
3. Noguchi M, Morikawa A, Kawasaki M, Matsuno Y, Yamada T, Hirohashi S, et al. Small Adenocarcinoma of the Lung. Histologic Characteristics and Prognosis. *Cancer* (1995) 75(12):2844–52.
4. Devarakonda S, Morgensztern D, Govindan R. Genomic Alterations in Lung Adenocarcinoma. *Lancet Oncol* (2015) 16(7):e342–51. doi: 10.1016/S1470-2045(15)00077-7
5. Zhang S, Bai X, Shan F. The Progress and Confusion of Anti-PD1/PD-L1 Immunotherapy for Patients With Advanced Non-Small Cell Lung Cancer. *Int Immunopharmacol* (2020) 80:106247. doi: 10.1016/j.intimp.2020.106247
6. Doroshow DB, Sanmamed MF, Hastings K, Politi K, Rimm DL, Chen L, et al. Immunotherapy in Non-Small Cell Lung Cancer: Facts and Hopes. *Clin Cancer Res* (2019) 25(15):4592–602. doi: 10.1158/1078-0432.CCR-18-1538
7. Guttman M, Rinn JL. Modular Regulatory Principles of Large Non-Coding Rnas. *Nature* (2012) 482(7385):339–46. doi: 10.1038/nature10887
8. Gutschner T, Diederichs S. The Hallmarks of Cancer: A Long Non-Coding RNA Point of View. *RNA Biol* (2012) 9(6):703–19. doi: 10.4161/rna.20481
9. Costa FF. Non-Coding Rnas: Meet Thy Masters. *Bioessays* (2010) 32(7):599–608. doi: 10.1002/bies.200900112
10. Gibb EA, Brown CJ, Lam WL. The Functional Role of Long Non-Coding RNA in Human Carcinomas. *Mol Cancer* (2011) 10:38. doi: 10.1186/1476-4598-10-38
11. Wang P, Ren Z, Sun P. Overexpression of the Long Non-Coding RNA MEG3 Impairs in Vitro Glioma Cell Proliferation. *J Cell Biochem* (2012) 113(6):1868–74. doi: 10.1002/jcb.24055
12. Bhan A, Soleimani M, Mandal SS, Long Noncoding RNA. And Cancer: A New Paradigm. *Cancer Res* (2017) 77(15):3965–81. doi: 10.1158/0008-5472.CAN-16-2634
13. Li Y, Jiang T, Zhou W, Li J, Li X, Wang Q, et al. Pan-Cancer Characterization of Immune-Related Lncrnas Identifies Potential Oncogenic Biomarkers. *Nat Commun* (2020) 11(1):1000. doi: 10.1038/s41467-020-14802-2
14. Atianand MK, Fitzgerald KA. Long Non-Coding Rnas and Control of Gene Expression in the Immune System. *Trends Mol Med* (2014) 20(11):623–31. doi: 10.1016/j.molmed.2014.09.002
15. Chen YG, Satpathy AT, Chang HY. Gene Regulation in the Immune System by Long Noncoding Rnas. *Nat Immunol* (2017) 18(9):962–72. doi: 10.1038/ni.3771
16. Li X, Lei Y, Wu M, Li N. Regulation of Macrophage Activation and Polarization by HCC-Derived Exosomal Lncrna TUC339. *Int J Mol Sci* (2018) 19(10):2958. doi: 10.3390/ijms19102958
17. Zhang M, Wang N, Song P, Fu Y, Ren Y, Li Z, et al. Lncrna GATA3-AS1 Facilitates Tumour Progression and Immune Escape in Triple-Negative Breast Cancer Through Destabilization of GATA3 But Stabilization of PD-L1. *Cell Prolif* (2020) 53(9):e12855. doi: 10.1111/cpr.12855
18. Calvayrac O, Pradines A, Pons E, Mazières J, Guibert N. Molecular Biomarkers for Lung Adenocarcinoma. *Eur Respir J* (2017) 49(4):1601734. doi: 10.1183/13993003.01734-2016
19. Chiu HS, Somvanshi S, Patel E, Chen TW, Singh VP, Zorman B, et al. Pan-Cancer Analysis of Lncrna Regulation Supports Their Targeting of Cancer Genes in Each Tumor Context. *Cell Rep* (2018) 23(1):297–312.e12. doi: 10.1016/j.celrep.2018.03.064
20. Li J, Han L, Roebuck P, Diao L, Liu L, Yuan Y, et al. TANRIC: An Interactive Open Platform to Explore the Function of Lncrnas in Cancer. *Cancer Res* (2015) 75(18):3728–37. doi: 10.1158/0008-5472.CAN-15-0273
21. Yao F, Wang Q, Wu Q. The Prognostic Value and Mechanisms of Lncrna UCA1 in Human Cancer. *Cancer Manag Res* (2019) 11:7685–96. doi: 10.2147/CMAR.S200436
22. Chen Q, Zhu C, Jin Y. The Oncogenic and Tumor Suppressive Functions of the Long Noncoding RNA MALAT1: An Emerging Controversy. *Front Genet* (2020) 11:93. doi: 10.3389/fgene.2020.00093
23. Wang J, Su Z, Lu S, Fu W, Liu Z, Jiang X, et al. Lncrna HOXA-AS2 and Its Molecular Mechanisms in Human Cancer. *Clin Chim Acta* (2018) 485:229–33. doi: 10.1016/j.cca.2018.07.004
24. Pan J, Fang S, Tian H, Zhou C, Zhao X, Tian H, et al. Lncrna JPX/Mir-33a-5p/Twist1 Axis Regulates Tumorigenesis and Metastasis of Lung Cancer by Activating Wnt/B-Catenin Signaling. *Mol Cancer* (2020) 19(1):9. doi: 10.1186/s12943-020-1133-9
25. Peng Z, Wang J, Shan B, Li B, Peng W, Dong Y, et al. The Long Noncoding RNA LINC00312 Induces Lung Adenocarcinoma Migration and Vasculogenic Mimicry Through Directly Binding YBX1. *Mol Cancer* (2018) 17(1):167. doi: 10.1186/s12943-018-0920-z
26. Cai Y, Sheng Z, Chen Y, Wang J. Lncrna HMMR-AS1 Promotes Proliferation and Metastasis of Lung Adenocarcinoma by Regulating Mir-138/Sirt6 Axis. *Aging (Albany NY)* (2019) 11(10):3041–54. doi: 10.18632/aging.101958
27. Mu X, Wu H, Liu J, Hu X, Wu H, Chen L, et al. Long Noncoding RNA TMPO-AS1 Promotes Lung Adenocarcinoma Progression and is Negatively Regulated by Mir-383-5p. *BioMed Pharmacother* (2020) 125:109989. doi: 10.1016/j.biopha.2020.109989
28. Shen Y, Peng X, Shen C. Identification and Validation of Immune-Related Lncrna Prognostic Signature for Breast Cancer. *Genomics* (2020) 112(3):2640–6. doi: 10.1016/j.ygeno.2020.02.015
29. Zhou M, Zhang Z, Zhao H, Bao S, Cheng L, Sun J. An Immune-Related Six-Lncrna Signature to Improve Prognosis Prediction of Glioblastoma Multiforme. *Mol Neurobiol* (2018) 55(5):3684–97. doi: 10.1007/s12035-017-0572-9

Conflict of Interest: The authors declare that the research was conducted in the absence of any commercial or financial relationships that could be construed as a potential conflict of interest.

Copyright © 2021 Zhang, Wang, Li, Peng, Liu, Zhang and Zhou. This is an open-access article distributed under the terms of the Creative Commons Attribution License (CC BY). The use, distribution or reproduction in other forums is permitted, provided the original author(s) and the copyright owner(s) are credited and that the original publication in this journal is cited, in accordance with accepted academic practice. No use, distribution or reproduction is permitted which does not comply with these terms.

frontiers in Oncology

ORIGINAL RESEARCH
published: 26 April 2021
doi: 10.3389/fonc.2021.647546

Identification of Resectable N2 in NSCLC: A Single Center Experience and Review of the SEER Database

*Yan-qing Wang[1], Xu-dong Liu[2], Wen-liang Bai[1] and Shan-qing Li[1]**

[1] Department of Thoracic Surgery, Peking Union Medical College Hospital, Chinese Academy of Medical Sciences & Peking Union Medical College, Beijing, China, [2] Medical Science Research Center, Peking Union Medical College Hospital, Chinese Academy of Medical Sciences & Peking Union Medical College, Beijing, China

OPEN ACCESS

Edited by:
Junji Uchino,
Kyoto Prefectural University of Medicine, Japan

Reviewed by:
Lorenzo Spaggiari,
European Institute of Oncology (IEO), Italy
Mohamed Rahouma,
Weill Cornell Medical Center, United States

***Correspondence:**
Shan-qing Li
Lishanqing_pumch@163.com

Specialty section:
This article was submitted to Thoracic Oncology, a section of the journal Frontiers in Oncology

Received: 30 December 2020
Accepted: 29 March 2021
Published: 26 April 2021

Citation:
Wang Y-q, Liu X-d, Bai W-l and Li S-q (2021) Identification of Resectable N2 in NSCLC: A Single Center Experience and Review of the SEER Database. Front. Oncol. 11:647546. doi: 10.3389/fonc.2021.647546

Background: Non-small cell lung carcinoma (NSCLC) with ipsilateral and/or subcarinal mediastinal lymphatic spread (N2) is a heterogeneous disease. The role of surgical resection in patients with N2 NSCLC remains controversial and no survival-based definition of "resectable N2" exists. The purpose of this study is to evaluate the factors that potentially affect the survival of N2 NSCLC patients who receive surgical resection and to define "resectable N2" based on the survival benefits.

Methods: Data from the open Surveillance, Epidemiology, and End Results (SEER) database from the National Cancer Institute in the United States were used to construct a nomogram. Patients who received surgery between 2010 and 2015 for N2 NSCLC were included. Independent prognostic factors for survival identified through Cox regression analysis were used to create the nomogram. The C-index, receiver operating characteristics (ROC) analyses, calibration curves, and risk stratification were used to evaluate the nomogram. The nomogram was also validated using data from 222 patients from Peking Union Medical College Hospital (PUMCH). Furthermore, lung cancer–related deaths were compared using competitive risk analysis.

Results: In total, 4267 patients were included in the SEER cohort. Male gender, old age, high T stage and grade, adenosquamous and squamous cell carcinoma, lower lobe and overlapping lesions, extended lobe or bilobectomy and pneumonectomy, no chemotherapy, radiation before and after surgery, positive number of lymph nodes, and lymph node ratio (LNR) were identified as independent risk factors for higher mortality. The nomogram was created using these parameters. The C-index was 0.665 (95% confidence interval (CI), 0.651-0.679) and 0.722 (95% CI, 0.620-0.824) in the SEER and PUMCH cohorts, respectively. The calibration curves showed satisfactory consistency between the predicted and actual survival status in both the SEER and PUMCH cohorts. Competitive risk analysis confirmed that the variables in the nomogram, except radiation, are risk factors for prognosis.

Conclusions: "Resectable N2" should be assessed by a multidisciplinary team. The novel nomogram developed in this study may help with clinical decision-making for this patient population.

Keywords: NSCLC, SEER, resectable, nomogram, prognosis

BACKGROUND

N2 refers to lung cancer metastasis in ipsilateral mediastinal lymph nodes, which accounts for approximately 20%-30% of all non-small cell lung carcinoma (NSCLC) (1, 2). Although many treatment strategies (bimodality or trimodality) exist for N2 NSCLC, the effectiveness of these therapeutic strategies remains unsatisfactory and the 5-year survival rate ranges from 23%-36% (3, 4). Patients with N2 NSCLC are a notoriously heterogeneous population with variable clinical outcomes and choosing the correct treatment strategy with or without surgery remains a challenge for clinicians.

For bulky N2, defined as mediastinal lymph nodes that have a short-axis diameter greater than 2 cm with signs of invasion in surrounding tissues on chest computed tomography (CT), positive surgical margins are highly likely, and therefore, the consensus is to refrain from surgery (5–7). However, some N2 are resectable. Resectable N2 refers to discrete lymph nodes with a short-axis diameter less than 2.5-3 cm with no extranodal extension into adjacent tissue structures (6, 8, 9). And it needs thorough pathological nodal staging completed (10). However, even for this type of N2, there is still much controversy over whether surgery is appropriate. There is no survival-based definition of what constitutes a "resectable" N2 tumor. The decision to perform or forego surgery is often made by a surgical team by examining the tumor boundaries with contrast CT.

In clinical practice, experience has shown that patients with pathology-proven N2 (pN2) who undergo surgery can have drastically different outcomes, and the 5-year overall survival rate was varied from 35%-76% (11). This might be due to N2 disease heterogeneity. Therefore, we hypothesized that the decision to perform or forego surgery should not be based only on the morphological characteristics of the lymph nodes on CT and other clinical and pathological factors that can affect prognosis should also be taken into consideration. Additionally, "resectable N2" should be defined in terms of the survival benefits of resection.

This study was conducted to identify the prognostic factors that affect survival in patients with pN2 who undergo surgery and to define "resectable N2" for NSCLC patients. We used the open Surveillance, Epidemiology, and End Results (SEER) database from the National Cancer Institute in the United States to develop a nomogram aimed at assisting multidisciplinary teams in predicting individual prognosis and improving clinical decision making for patients with N2 NSCLC. The nomogram was validated with data from the Peking Union Medical College Hospital (PUMCH).

METHODS

Training Cohort and Data

We retrieved data from the SEER database using the SEER*STAT 8.3.6 software. A custom data file was obtained from the SEER Program with permission number 15674-Nov2019. Inclusion criteria included the following: diagnosis in 2010-2015, patients underwent surgery and pN2.

Exclusion criteria were as follows: incomplete information recorded, any M1 and small cell lung cancer. (**Figure 1**)

Variables extracted from the SEER database included sex, age at diagnosis, race, marital status, primary tumor site, laterality, ICD-O-3 histology code and behavior, pathologic grade, American Joint Committee on Cancer T/M stages, pathological nodal staging, positive regional nodes, regional nodes examined, radiation sequence with surgery, chemotherapy recode, survival months, vital status recode, cause of death (COD) site recode, SEER specific death classification, and SEER other COD classification. The lymph node ratio (LNR) was obtained by dividing the number of positive regional nodes by the total number of lymph nodes examined (12). The primary outcome was overall survival (OS). The secondary outcome was NSCLC specific survival.

External Validation Cohort and Data

To validate the developed nomogram in a responsible manner, an external validation cohort treated from March 2016 to July 2019 in the Department of Thoracic Surgery at PUMCH was used. The study was approved by the PUMCH Ethical Committee (No. B260). The cohort included 222 postoperative pN2 NSCLC patients. The inclusion and exclusion criteria were the same as those for the training cohort from the SEER database. The last follow-up for the cohort was in Aug 2020 and the primary outcome was also OS.

Construction and Evaluation of Prognostic Model

We performed a univariate Cox proportional hazard regression analysis in a forward stepwise manner to identify possible independent prognostic factors. Factors found to be statistically significant in the univariate analysis were used in a multivariate analysis to estimate the hazard ratio (HR) and corresponding 95% confidence intervals (CIs) for every independent prognostic variable. The prognostic nomogram was created based on univariate Cox proportional hazard regression analysis using R packages ("survival, rms") (13).

To evaluate the nomogram, C-statistics was used to evaluate overall discrimination of the nomogram. And the AUC was used

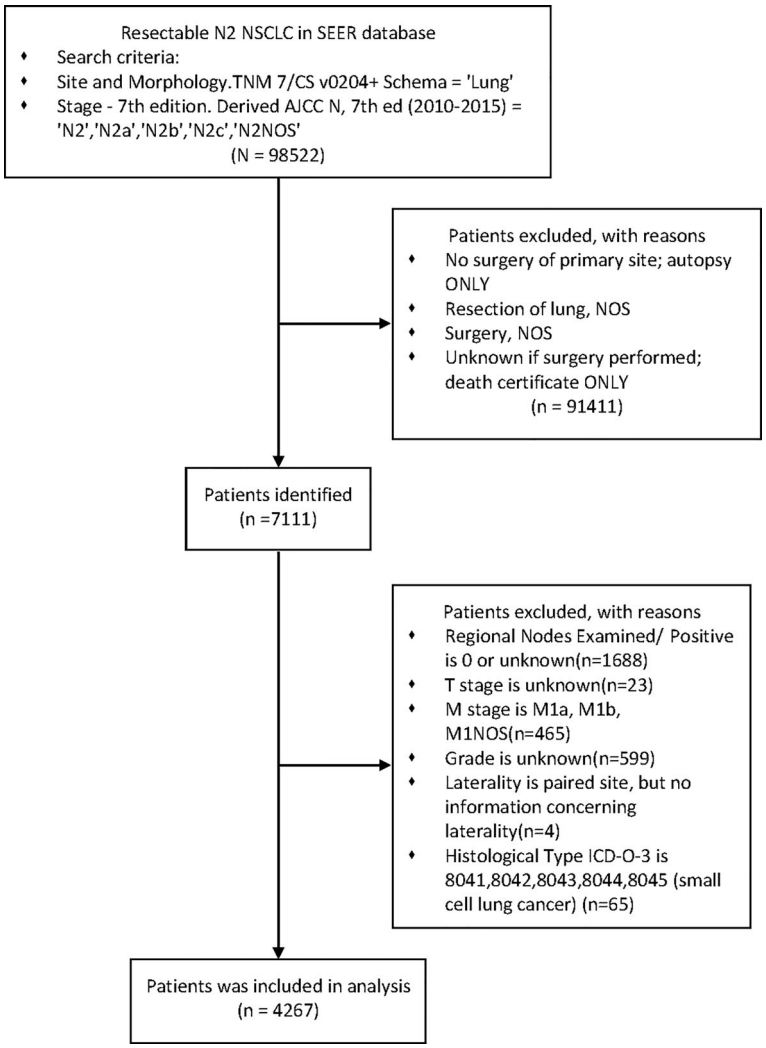

FIGURE 1 | Flow diagram of patient selection in the SEER database.

to evaluate discrimination of the nomogram at the given time (6-month, 1-year, 3-year) (14). The C-index ranged from 0.5 (no discrimination) to 1.0 (perfect discrimination). Calibration accuracy was measured with a calibration curve to determine how close the predicted probabilities were to the actual survival outcomes. The calibration curves of the nomogram for 0.5, 1, and 3-year OS were plotted with the R package ("survival, survivalROC, rms") (15, 16). for both the training and validation cohorts. All evaluation processes were performed by bootstrapping (1000 repetitions).

To further evaluate the prognostic model, the cohort was divided into two risk groups (low and high) according to the prognostic scores in the nomogram. Log-rank survival analysis was used to identify differences in survival between the low and high-risk groups. The discrimination ability of the nomogram was evaluated using the "survminer" package (17).

Competitive Risk Analysis of Cancer-Related Deaths

In addition, according to the COD code, we classified the COD into two groups: NSCLC-related death and Other-related death. We also performed competing risk analysis with the Fine & Gray model using the"cmprsk" R package to reduce the possible impact of competing risk bias, which can be significant in multivariate Cox proportional hazard regression analysis (18).

Statistics and graphing were performed using Rstudio 1.2.5003. Continuous variables were tested using two-tailed t-tests, and categorical variables were tested using chi-square tests. Mann-Whitney test was applied for nonparametric data. $P<0.20$ was considered statistically significant in univariate analysis. Otherwise, $P<0.05$ was considered statistically significant.

RESULTS

Clinicopathological Characteristics of Training and Validation Cohorts

After stepwise selection, the training cohort included 4267 cases from the SEER database and the external validation cohort included 222 cases from PUMCH. The demographics and clinicopathologic characteristics are summarized in **Table 1**.

There were no significant differences in the age at diagnosis, sex, and laterality distribution between the two cohorts. However, the histology type and grade distribution differed. Compared to the SEER cohort, the PUMCH cohort included a higher proportion of patients with adenocarcinoma (80.2% vs 65.6%), and a smaller proportion of poorly differentiated or undifferentiated tumors (19.8% vs 50.2%). The PUMCH cohort also included more patients with T1/2 stage disease. More lymph nodes were examined in the PUMCH cohort than in the SEER cohort and more metastatic lymph nodes were also found. The median LNRs were 0.20 in the PUMCH cohort and 0.25 in the SEER cohort. The patients in the PUMCH cohort also received different treatments compared to those in the SEER cohort. More patients underwent lobectomy with mediastinal lymph node dissection (LM) in the PUMCH cohort (85.1%) compared to the corresponding proportion in the SEER cohort (69.8%) and fewer underwent pneumonectomy (2.3% vs 8.9%). In the PUMCH cohort, a higher proportion of patients received chemotherapy (83.3% vs 75.2%) and a lower proportion received radiotherapy regardless of the sequence with surgery (20.3% vs 45.4%).

Risk Factors for OS

There were 1785 events (NSCLC-related deaths) in the SEER cohort and the median follow-up period was 42 months (95% CI:41-44 months) (Reverse Kaplan Meier method). According to the results of univariate Cox regression analyses, age, sex, race, histology type, grade, tumor locations, T stage, surgery, chemotherapy, radiotherapy, number of positive lymph nodes, and LNR were all significantly associated with OS. Marriage, laterality, and number of examined lymph nodes did not significantly affect OS. All 12 significant factors were entered into a multivariate Cox regression analysis, which revealed the independent prognostic factors (**Table 2**). Male sex, old age, high T stage and grade, adenosquamous and squamous cell carcinoma, lower lobe and overlapping lesions, extended lobe or bilobectomy and pneumonectomy, no chemotherapy, radiation before and after surgery, number of positive lymph nodes, and LNR were found to be associated with a higher risk of death.

Prognostic Nomogram for OS

A nomogram was constructed using the independent prognostic factors to estimate 0.5-, 1-, and 3-year OS (**Figure 2**). The value for each factor was located and a straight line was drawn upwards to the "points axis" of the nomogram to determine the number of points for the factor. The total number of points was calculated by summing the points for all factors. The value for each factor was found on the "total points axis" and a line was drawn straight downwards to the "survival axis" to estimate the probabilities of OS at 0.5, 1, and 3 years (range 0.4-0.9, 0.05-0.9, and 0.01-0.9, respectively).

Calibration and Validation of Nomogram

In the SEER cohort, the C-index was 0.665 (95%CI, 0.651-0.679) and the areas under the ROC curves (AUCs) were 0.674, 0.721, and 0.675, for 0.5, 1, and 3-year OS, respectively (**Figures 3A–C**). The calibration curves in **Figures 3D–F** show excellent consistency between the predicted and actual survival conditions in the SEER cohort, with the dots close to a 45° diagonal line (blue dotted line), thus, the nomograms were well calibrated. In the PUMCH cohort, the C-index was 0.722 (95% CI, 0.620-0.824) and the calibration curves also showed acceptable results (**Figure 4**).

All 4267 patients in the SEER cohort were divided into a high-risk group (n=2133) and a low-risk group (n=2134). High-risk patients had significantly worse OS than low-risk patients (**Figure 5A**). This result was further confirmed in the PUMCH cohort (**Figure 5B**).

Competitive Risk Analysis NSCLC-Related Deaths

To reduce the impact of competing risk bias, we performed competing risk analysis using the Fine & Gray model to further assess the risks of the independent prognostic variables. To simplify clinical decision-making, we compressed independent prognostic variables into dichotomous variables. The results confirmed that age > 65, male sex, histology with squamous cell components, poor or no differentiation, sites other than the upper and middle lobes, T3/4, surgeries other than LM (lobectomy with mediastinal lymph node dissection), no chemotherapy, positive lymph nodes > 5, and LNR > 0.345 were risk factors for poorer prognosis. However, radiotherapy may be a protective factor for better prognosis, with a borderline p-value (**Figure 6**).

DISCUSSION

In this study, we retrospectively analyzed population–based data to construct a nomogram for risk factors that affect the OS of patients with N2 NSCLC to increase our understanding of "resectable N2" and assist multidisciplinary teams in clinical decision-making. The nomogram showed good discrimination and calibration accuracy. It also increased our understanding of the heterogeneous outcomes for N2 patients who undergo surgery and the clinicopathologic characteristics that affect the OS.

N2 NSCLC is a very heterogeneous disease with different prognoses and is treated with different therapeutic strategies. Whether pN2 patients should be treated with or without surgery remains a controversial question (19). Two randomized trials evaluated the effect of surgery in this patient population, but neither showed an OS benefit from surgery (20, 21). One possible reason for the negative results of the studies could be that these trials did not sufficiently take into account the heterogeneity of N2 NSCLCs (22).

TABLE 1 | Demographics and Clinicopathologic Characteristics of Patients underwent surgery with pN2.

Demographic or Characteristic	SEER Cohort (n = 4267)		PUMCH Cohort Cohort (n = 222)		P value
	No. of Patients	%	No. of Patients	%	
Age at diagnosis					0.570
Median (IQR)	67(60-74)		61(54-68)		
Range	16-94		23-81		
Sex					
Female	2132	50.0	109	49.1	0.801
Male	2135	50.0	113	50.9	
Race					
Black	408	9.6	–		
White	3505	82.1	–		
other	354	8.3	–		
Marital status					
Married	2532	59.3	–		
Unmarried	1735	40.7	–		
Histology					**<0.001**
Adenocarcinoma	2801	65.6	178	80.2	
Squamous cell carcinoma	965	22.6	32	14.4	
Adenosquamous carcinoma	137	3.2	6	2.7	
Neuroendocrine tumors	191	4.5	4	1.8	
NSCLC NOS	86	2.1	0	0	
Others	87	2.0	2	0.9	
Histologic grade					**<0.001**
Well differentiated	289	6.8	12	6.8	
Moderately differentiated	1836	43.0	163	73.4	
Poorly/Undifferentiated	2142	50.2	44	19.8	
Laterality					0.417
Left	1906	44.7	93	41.9	
Right	2361	55.3	129	58.1	
Primary Site					**0.015**
Main bronchus	47	1.1	0	0	
Upper lobe	2398	56.2	105	47.3	
Middle lobe	221	5.2	16	7.2	
Lower lobe	1453	34.0	93	41.9	
Overlapping lesion of lung	85	2.0	3	1.3	
Lung&Bronchus, NOS	63	1.5	5	2.3	
T stage					**<0.001**
T1	1087	25.5	100	45.1	
T2	2053	48.1	108	48.6	
T3	811	19.0	8	3.6	
T4	316	7.4	6	2.7	
Type of surgery					**<0.001**
Resection of less than one lobe	458	10.7	5	2.3	
Resection of [at least one] lobe or bilobectomy	301	7.1	23	10.3	
Lobectomy with mediastinal lymph node dissection	2977	69.8	189	85.1	
Lobe or bilobectomy extended	148	3.5	0	0	
Pneumonectomy	383	8.9	5	2.3	
chemotherapy					0.005
No/Unknown	1065	24.8	37	16.7	
Yes	3202	75.2	185	83.3	
Radiation					**<0.001**
No	2328	54.6	177	79.7	
RS	2	0.0	0	0	
R+S	349	8.2	1	0.5	
S+R	1554	36.4	44	19.8	
R+S+R	34	0.8	0	0	
Lymph nodes examined, number					**<0.001**
Median (IQR)	11(6-17)		20(15-27)		
Range	1-90		2-50		
Positive lymph nodes, number					
Median (IQR)	2(1-5)		4(2-7)		**<0.001**
Range	1-61		1-34		
LNR					

(Continued)

TABLE 1 | Continued

Demographic or Characteristic	SEER Cohort (n = 4267)		PUMCH Cohort Cohort (n = 222)		P value
	No. of Patients	%	No. of Patients	%	
Median (IQR)	0.250(0.125-0.5)		0.200(0.110-0.380)		**<0.001**
NSCLC related death	1785	41.8	33	14.9	
Other related death	418	9.8	3	1.4	**<0.001**
Alive	2064	48.4	186	83.7	
Follow-up, months					0.241
Median (95%CI)	42 (41-44)		31(29-33)		
Range	0-83		5-53		

RS, Intraoperative rad with other rad before/after surgery.
R+S, Radiation prior to surgery.
S+R, Radiation after surgery.
R+S+R, Radiation before and after surgery.
LNR, Lymph node ratio.
In the p value column, the bolded values mean that they have significant difference.

TABLE 2 | Cox regression analysis of overall survival of patients underwent surgery with pN2 in SEER cohort.

Variables	Univariate HR (95% CI)	P Value	Multivariate HR (95% CI)	P value
Age at diagnosis	1.024(1.019-1.029)	**<0.001**	1.019(1.014-1.025)	**<0.001**
Sex				
Female	Ref			
Male	1.384(1.261-1.519)	**<0.001**	1.326(1.204-1.461)	**<0.001**
Race				
Black	Ref			
White	1.210(1.025-1.428)	**0.024**	1.122(0.949-1.327)	0.178
other	1.096(0.872-1.377)	0.432	1.049(0.833-1.322)	0.683
Marital status				
Married	Ref		–	
Unmarried	1.021(0.929-1.122)	0.673		
Histology			–	
Adenocarcinoma	Ref			
Squamous cell carcinoma	1.234(1.105-1.377)	**<0.001**	1.149(1.021-1.293)	**0.021**
Adenosquamous carcinoma	1.377(1.078-1.758)	**0.010**	1.363(1.063-1.745)	**0.014**
Neuroendocrine tumors	0.687(0.523-0.902)	**0.007**	0.696(0.526-0.920)	**0.011**
Nsclc NOS	1.037(0.744-1.445)	0.832	0.918(0.656-1.284)	0.616
Others	1.354(0.992-1.849)	**0.056**	1.190(0.867-1.631)	0.281
Histologic grade				
Well differentiated	Ref			
Moderately differentiated	1.237(1.000-1.529)	**0.049**	1.140(0.918-1.416)	0.236
Poorly/Undifferentiated differentiated	1.567(1.271-1.932)	**<0.001**	1.404(1.132-1.742)	**0.002**
Laterality				
Left	Ref		–	
Right	1.051(0.957-1.154)	0.299	–	
Primary Site				
341 Upper lobe	Ref			
340 Main bronchus	1.472(0.955-2.268)	**0.079**	1.167(0.737-1.848)	0.510
342 Middle lobe	0.908(0.725-1.136)	0.397	0.931(0.743-1.165)	0.528
343 Lower lobe	1.200(1.086-1.326)	**<0.001**	1.144(1.033-1.266)	**0.010**
348 Overlapping lesion of lung	1.640(1.217-2.212)	**0.001**	1.374(1.008-1.873)	**0.044**
349 Lung&Bronchus, NOS	1.200(0.833-1.747)	0.342	0.788(0.532-1.169)	0.237
T stage				
T1	Ref			
T2	1.269(1.125-1.433)	**<0.001**	1.213(1.072-1.373)	**0.002**
T3	1.796 (1.562-2.064)	**<0.001**	1.686(1.459-1.949)	**<0.001**
T4	1.542(1.275-1.866)	**<0.001**	1.489(1.217-1.823)	**<0.001**
Type of surgery				
Lobectomy with mediastinal lymph node dissection	Ref			
Resection of less than one lobe	1.301(1.124-1.507)	**<0.001**	1.153(0.984-1.351)	0.080
Resection of [at least one] lobe or bilobectomy	1.249(1.049-1.488)	**0.013**	1.172(0.982-1.398)	0.078
Lobe or bilobectomy extended	1.588(1.266-1.992)	**<0.001**	1.407(1.114-1.777)	**0.004**
Pneumonectomy	1.464(1.255-1.706)	**<0.001**	1.300(1.096-1.543)	**0.002**

(Continued)

TABLE 2 | Continued

Variables	Univariate HR (95% CI)	P Value	Multivariate HR (95% CI)	P value
chemotherapy				
No/Unknown	Ref			
Yes	0.669(0.604-0.742)	**<0.001**	0.705(0.628-0.791)	**<0.001**
Radiation				
No	Ref			
RS	8.141(1.142-58.021)	**0.036**	6.172(0.857-44.446)	0.071
R+S	0.727(0.604-0.874)	**<0.001**	0.932(0.766-1.134)	0.481
S+R	0.848(0.768-0.937)	**0.001**	0.899(0.807-1.001)	0.052
R+S+R	1.296(0.823-2.041)	**0.262**	1.865(1.175-2.960)	**0.008**
Lymph nodes examined, number	0.996(0.991-1.002)	0.173		
Positive lymph nodes, number	1.042(1.033-1.050)	**<0.001**	1.022(1.011-1.034)	**<0.001**
LNR	2.479(2.129-2.886)	**<0.001**	2.426(2.033-2.896)	**<0.001**

RS, Intraoperative rad with other rad before/after surgery.
R+S, Radiation prior to surgery.
S+R, Radiation after surgery.
R+S+R, Radiation before and after surgery.
LNR, lymph node metastatic ratio.
In the p value column, the bolded values mean that they have significant difference.

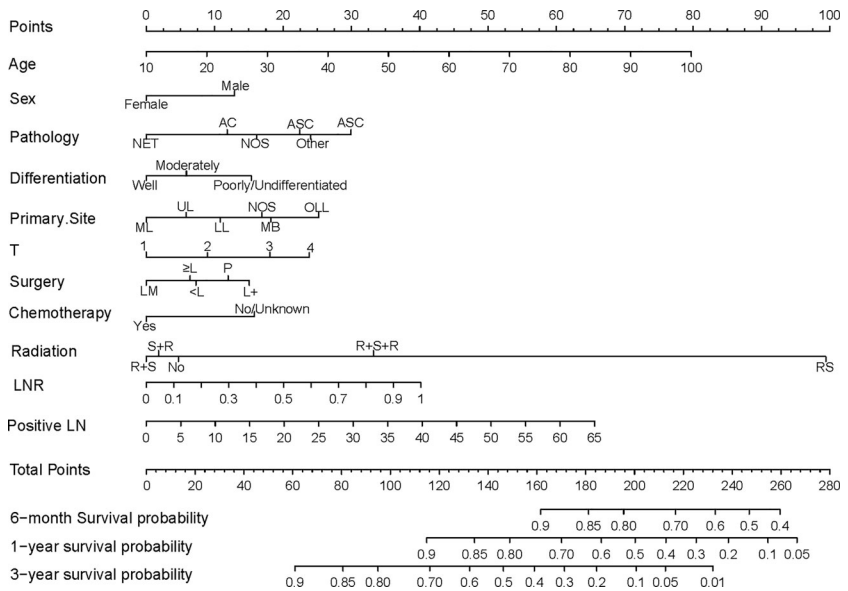

FIGURE 2 | Nomogram predicting postoperative survival of pN2 NSCLC patients who underwent surgery. The value for each factor was located and a straight line was drawn upwards to the "points axis" of the nomogram to determine the number of points for the factor. The total number of points was calculated by summing the points for all factors. The value for each factor was found on the "total points axis" and a line was drawn straight downwards to the "survival axis" to estimate the probabilities of OS at 0.5, 1, and 3 years. AC, Adenocarcinoma; NET, Neuroendocrine tumor; SCC, Squamous cell carcinoma; ASC, Adenosquamous carcinoma; NOS, Not otherwise specified; ML, Middle lobe; UL, Upper lobe; LL, Lower lobe; MB, Main bronchus; OLL, Overlapping lung lesion; LM, Lobectomy with medial lymph node dissection; ≥L, Resection of [at least one] lobe or bilobectomy; <L, Excision or resection of less than one lobe; P, Pneumonectomy; L+, Lobe or bilobectomy extended; R+S, Radiation prior to surgery; RS, Intraoperative radiation with other radiation before/after surgery; R+S, Radiation prior to surgery; S+R, Radiation after surgery; R+S+R, Radiation before and after surgery; LN, lymph node number.

Evison M (10) have proposed definition of "potentially resectable stage III NSCLC", the definition included: 1) pathologically confirmed NSCLC; 2)Thorough pathological nodal staging completed (surgical or endoscopic); 3) Thorough radiological staging including at least PET-CT and MRI brain with contrast; 4) Primary tumor resectable with high probability of clear pathological margins and complete resection; 5) Any nodal disease is discrete, easily measurable and defined, free from major mediastinal structures including the great vessels and trachea with no individual lymph node measuring >3 cm. However, this definition did not consider the patients heterogeneous clinical characteristics exist. And some clinical character may affect surgery outcome.

In this study, only pN2 patients underwent surgery were included to create the nomogram which could be a bias to assist

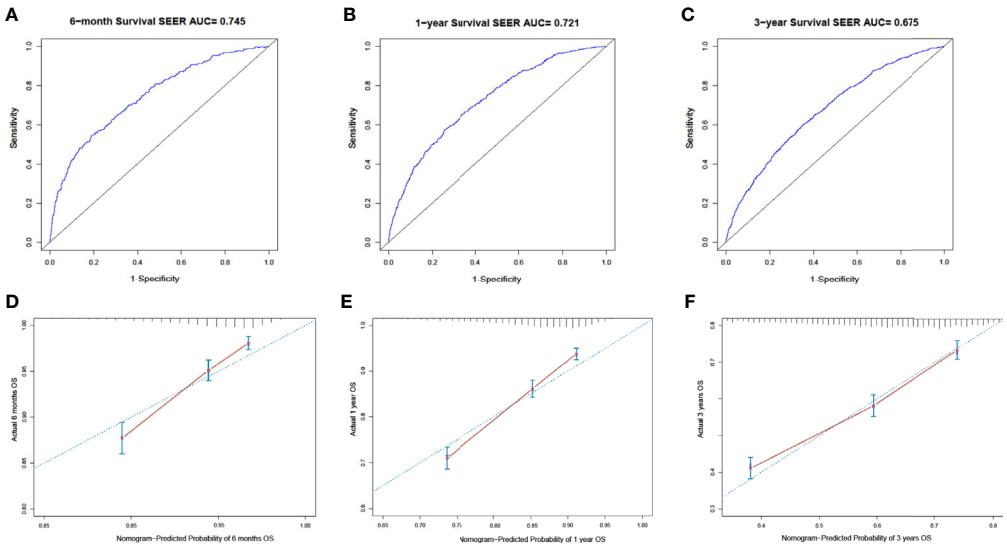

FIGURE 3 | Nomogram with ROC analyses and calibration curves for training cohort. **(A–C)** Discrimination of 6-month ($p < 0.01$) **(A)**, 1-year ($p < 0.01$) **(B)**, and 3-year ($p < 0.01$) **(C)** OS in training cohort with ROC curves. **(D–F)** Calibration curves for 6-month **(D)**, 1-year, **(E)** and 3-year **(F)** OS from model. Y-axis and x-axis indicate actual survival probability and predicated survival probability, respectively. Blue dotted line indicates prediction accordance with actuality. Error bars show 95% CI.

multidisciplinary teams in clinical decision-making before surgery. Although pN2 is not the same as cN2, there is some correlation between them. At present, the preoperative diagnosis of N2 is almost consistent with the pathological N2 according the enhanced CT and PET-CT.A meta-analysis assessed agreement between clinical N stage and pathologic N stage, the accordance between cN2 and pN2 is 67%(104/155), for these patients, before surgery the nomogram may assist multidisciplinary teams in clinical decision-making. And the study also showed the clinically overstaged patients (cN2, pN0-1) accounts for 30% (47/155), which also could be benefit from the surgery. For the clinical understaged patients (cN2, pN3), account for only 3% (4/155) (23). Actually, they have no indication for surgery, and the definitive systematic treatment is preferential. However these patients not the N2 patients and they are the real N3. So as the Matthew Evison proposed, "potentially resectable stage III NSCLC" need the thorough pathological nodal staging (10).

N2 NSCLCs are advanced and systemic diseases. Accordingly, chemotherapy including targeted therapy is beneficial for patients with N2, both pre- or postoperatively (24, 25). And the number of chemotherapy cycles was an independent prognostic factor (11). Our results confirmed that chemotherapy is a significant protective factor for N2 patients who undergo surgery. If the surgical team considers the N2 resectable, the oncologist should assess whether the patient can tolerate full doses of neoadjuvant and/or adjuvant chemotherapy. Age, age-related comorbidities, which could influence chemotherapy tolerance, should be considered by the multidisciplinary teams.

To our surprise, we found that the primary site and surgery type could affect the prognosis. Similar results were also obtained in a published meta-analysis (26). In another study, the results showed no significant difference in OS between lesions located in the upper/middle and lower lobes (27). However, we noted that the majority of patients did not undergo surgery for lung tumor. So, for patients with N2 who underwent surgery, the primary site should be considerate. Patients who receive upper/middle lobectomy have larger remaining lung volume and thus have a higher probability of completing comprehensive treatment. Additionally, if the tumor is located in the main bronchus or when the lesions are overlapped, the remaining lung volume after pneumonectomy or bilobectomy is likely to be smaller. Therefore, the risk score is higher for patients who undergo pneumonectomy or bilobectomy. For N2 patients, the surgical team should estimate whether the remaining lung volume is enough for the patient to tolerate the systematic therapy that follows surgery. Additionally, central primary tumor location is associated with significantly worse outcomes (28). Consequently, if patients are more likely to receive pneumonectomy obtained R0 resection, mediastinal staging by mediastinoscopy or endobronchial ultrasound-guided aspiration is necessary, even for mediastinal lymph nodes ≤ 2 cm with clear boundaries.

LNR was reported as a predictor of OS and a useful complement to the N stage in patients with N2 disease status (29). And we confirmed the same results. However, it is very difficult to evaluate the number of lymph node metastases through non-invasive techniques such as PET-CT before the surgery. But we can fully evaluate the number of lymph node metastasis station preoperatively, which means that if multiple stations of metastasis occurred, LNR may be higher and the prognosis worse. Therefore, patients with multi-N2 station metastasis may not benefit from the surgery because of the higher LNR although surgeons believed that each lymph node could be removed.

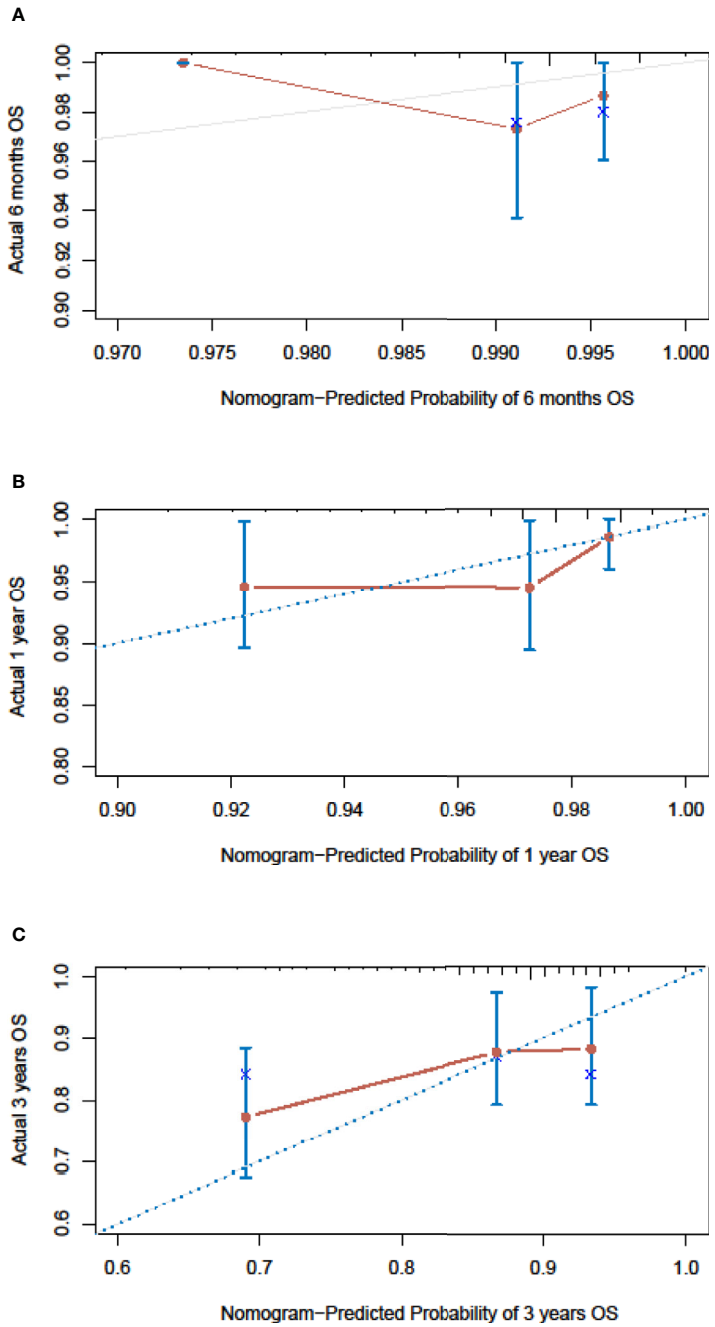

FIGURE 4 | Nomogram calibration curves for the validation cohort. The calibration curves of the model for d 6-month **(A)**, 1-year **(B)** and 3-year **(C)** of overall survival in the validation cohort.

It is undisputed that the T stage and tumor grade are significant independent predictive factors (30, 31). Besides these, we found that histology also affects prognosis. N2 patients without squamous cell components have better survival. Therefore, as many biopsies as possible should be performed if safety allows. The pathologist should also report the specific type of NSCLC and avoid the "NSCLC not otherwise specified (NOS)" designation as much as possible.

Lastly, to better identify "resectable N2" patients in the clinic, we created a nomogram to predict the individual survival rate. Variables in the nomogram were rated by a multidisciplinary team including surgeons, oncologists, pathologists, and radiologists. When applied to the external validation cohort,

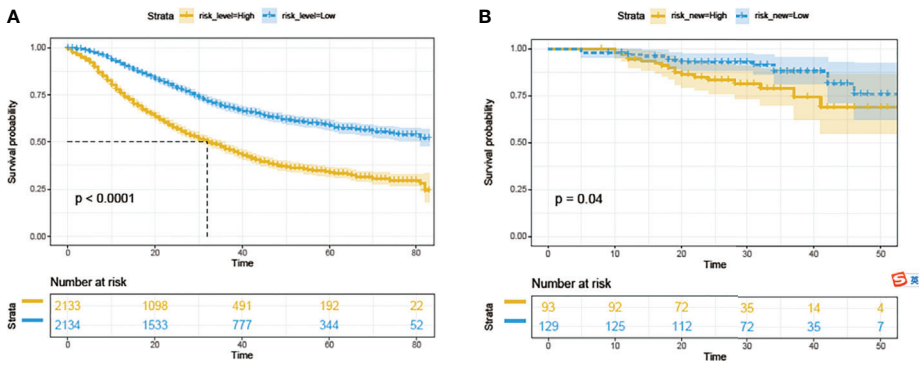

FIGURE 5 | Survival analyses with log-rank risk stratification system for the SEER cohorts **(A)** and PUMCH cohort **(B)**. Yellow and blue lines show low-risk and high-risk groups, respectively.

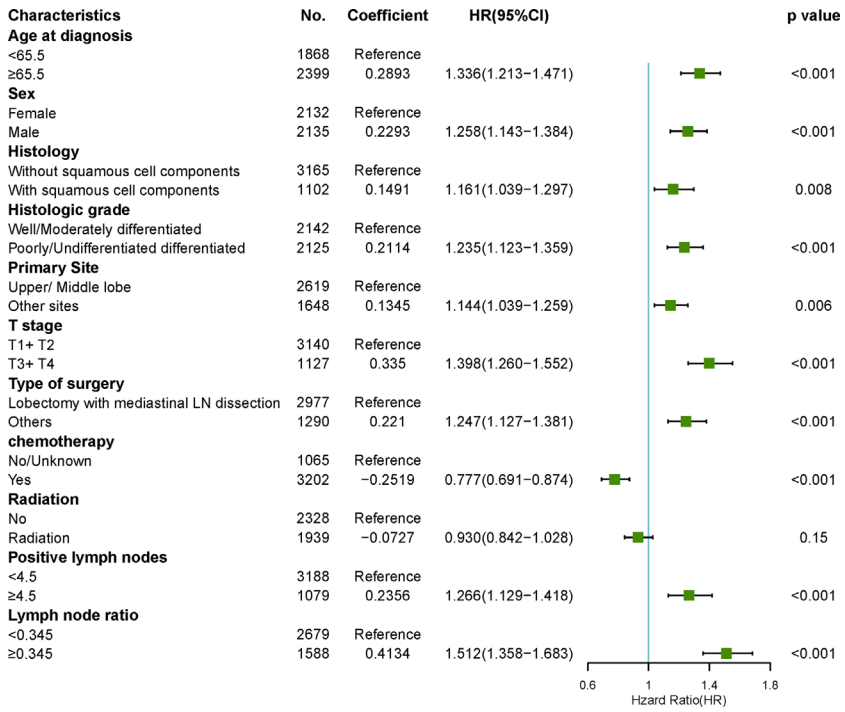

FIGURE 6 | Forest plots visualizing the hazard ratios of clinicopathological characteristics for lung cancer-specific mortality in patients with pN2 who underwent surgery using a multivariate competing risk model.

our model achieved considerable discrimination ability and calibration accuracy. Using the nomogram, we effectively stratified patients in the SEER or PUMCH cohort into two groups (high-risk and low-risk) with different OS. For high-risk patients, the effect of surgery is suboptimal, and these patients may not really have "resectable N2" although the size, shape, and borders of their lymph nodes may appear resectable to the surgeon. According to the nomogram, consideration all the risk factors that affect the OS, the appropriate selection of patients for surgery may avoid the operative risk of surgery in patients who may not benefit.

The study has some limitations. Firstly, we could not obtain all potentially relevant factors from the SEER database, such as preoperative mediastinal staging, the number of mediastinal stations of metastasis, patient comorbidities, length of progression-free survival, Eastern Cooperative Oncology Group (ECOG) performance scores, chemotherapy regimens, and molecular biomarkers. Further study is warranted to incorporate

these variables into future research. Secondly, this was a retrospective study, not a randomized experiment, and therefore cannot establish direct cause-effect relationships. Thirdly, this study only included patients with pN2 who underwent surgery, and patients with no indications for surgery as well as those unwilling to undergo surgery were not included. Thirdly, the validation cohort size was not too much. Finally, although our model exhibits acceptable performance for separating patients into two groups, more research is necessary to compare treatment strategies with and without surgery in high-risk patient groups.

CONCLUSION

N2 NSCLC is a systemic disease and its "resectability" should be assessed by a multidisciplinary team that not only takes into account the morphology of the lymph node on CT images, but also other clinical and pathological factors. This novel prognostic nomogram based on survival may be helpful for selecting patients with anatomically resectable N2 who will benefit the most from surgery.

DATA AVAILABILITY STATEMENT

The authors acknowledge that the data presented in this study must be deposited and made publicly available in an acceptable repository, prior to publication. Frontiers cannot accept a manuscript that does not adhere to our open data policies.

ETHICS STATEMENT

The studies involving human participants were reviewed and approved by the Peking Union Medical College Hospital (PUMCH) Ethical Committee (No. B260). The patients/participants provided their written informed consent to participate in this study.

AUTHOR CONTRIBUTIONS

Study concept and design: SL and YW. Data collection and assembly: WB and YW. Data analysis and interpretation: YW and XL. Manuscript preparation: YW. All authors contributed to the article and approved the submitted version.

FUNDING

This work was supported by 2019 pumch science fund for junior faculty [grant numbers pumch201912058] and National Key Research and Development Program of China (Grant 2020YFB1313700).

ACKNOWLEDGMENTS

We give special thanks for the efforts of the SEER tumor registry team.

REFERENCES

1. Warth A, Muley T, Meister M, Stenzinger A, Thomas M, Schirmacher P, et al. The novel histologic International Association for the Study of Lung Cancer/American Thoracic Society/European Respiratory Society classification system of lung adenocarcinoma is a stage-independent predictor of survival. *J Clin Oncol* (2012) 30(13):1438–46. doi: 10.1200/JCO.2011.37.2185
2. Gao F, Li N, Xu Y, Yang G. Evaluation of Postoperative Radiotherapy Effect on Survival of Resected Stage III-N2 Non-small Cell Lung Cancer Patients. *Front Oncol* (2020) 10:1135. doi: 10.3389/fonc.2020.01135
3. Asamura H, Chansky K, Crowley J, Goldstraw P, Rusch VW, Vansteenkiste JF, et al. The International Association for the Study of Lung Cancer Lung Cancer Staging Project: Proposals for the Revision of the N Descriptors in the Forthcoming 8th Edition of the TNM Classification for Lung Cancer. *J Thorac Oncol* (2015) 10(12):1675–84. doi: 10.1097/JTO.0000000000000678
4. Siegel RL, Miller KD, Jemal A. Cancer statistics, 2015. *CA Cancer J Clin* (2015) 65(1):5–29. doi: 10.3322/caac.21254
5. Cappuzzo F, Selvaggi G, Gregorc V, Mazzoni F, Betti M, Rita Migliorino M, et al. Gemcitabine and cisplatin as induction chemotherapy for patients with unresectable Stage IIIA-bulky N2 and Stage IIIB nonsmall cell lung carcinoma: an Italian Lung Cancer Project Observational Study. *Cancer* (2003) 98(1):128–34. doi: 10.1002/cncr.11460
6. De Leyn P, Dooms C, Kuzdzal J, Lardinois D, Passlick B, Rami-Porta R, et al. Revised ESTS guidelines for preoperative mediastinal lymph node staging for non-small-cell lung cancer. *Eur J Cardiothorac Surg* (2014) 45(5):787–98. doi: 10.1093/ejcts/ezu028
7. Evison M, Clive A, Castle L, Powell H, Thomas R, Buttery R, et al. Resectable Clinical N2 Non-Small Cell Lung Cancer; What Is the Optimal Treatment Strategy? An Update by the British Thoracic Society Lung Cancer Specialist Advisory Group. *J Thorac Oncol* (2017) 12(9):1434–41. doi: 10.1016/j.jtho.2017.05.023
8. Decaluwe H, De Leyn P, Vansteenkiste J, Dooms C, Van Raemdonck D, Nafteux P, et al. Surgical multimodality treatment for baseline resectable stage IIIA-N2 non-small cell lung cancer. Degree of mediastinal lymph node involvement and impact on survival. *Eur J Cardiothorac Surg* (2009) 36 (3):433–9. doi: 10.1016/j.ejcts.2009.04.013
9. Cerfolio RJ, Bryant AS. Survival of patients with unsuspected N2 (stage IIIA) nonsmall-cell lung cancer. *Ann Thorac Surg* (2008) 86(2):362–6; discussion 6-7. doi: 10.1016/j.athoracsur.2008.04.042
10. Evison M, AstraZeneca UKL. The current treatment landscape in the UK for stage III NSCLC. *Br J Cancer* (2020) 123(Suppl 1):3–9. doi: 10.1038/s41416-020-01069-z
11. Spaggiari L, Casiraghi M, Guarize J, Brambilla D, Petrella F, Maisonneuve P, et al. Outcome of Patients With pN2 "Potentially Resectable" Nonsmall Cell Lung Cancer Who Underwent Surgery After Induction Chemotherapy. *Semin Thorac Cardiovasc Surg* (2016) 28(2):593–602. doi: 10.1053/j.semtcvs.2015.12.001
12. Zhao X, Kallakury B, Chahine JJ, Hartmann D, Zhang Y, Chen Y, et al. Surgical Resection of SCLC: Prognostic Factors and the Tumor Microenvironment. *J Thorac Oncol* (2019) 14(5):914–23. doi: 10.1016/j.jtho.2019.01.019
13. Therneau T. *_A Package for Survival Analysis in R_. R package version 3.2-3.* (2020). https://CRAN.R-project.org/package=survival
14. Yang HI, Yuen MF, Chan HL, Han KH, Chen PJ, Kim DY, et al. Risk estimation for hepatocellular carcinoma in chronic hepatitis B (REACH-B): development and validation of a predictive score. *Lancet Oncol* (2011) 12 (6):568–74. doi: 10.1016/S1470-2045(11)70077-8
15. Harrell FE Jr. *rms: regression modeling strategies 2017*. Available at: https://cran.rproject.org/package=rms.

16. Heagerty PJ, Lumley T, Pepe MS. Time-dependent ROC curves for censored survival data and a diagnostic marker. *Biometrics* (2000) 56(2):337–44. doi: 10.1111/j.0006-341X.2000.00337.x
17. Kassambara A, Kosinski M, Biecek P. *survminer: Drawing Survival Curves using "ggplot2". R package version 0.4.8*. (2020). Available at: https://CRAN.R-project.org/package=survminer.
18. Austin PC, Lee DS, Fine JP. Introduction to the Analysis of Survival Data in the Presence of Competing Risks. *Circulation* (2016) 133(6):601–9. doi: 10.1161/CIRCULATIONAHA.115.017719
19. Martins RG, D'Amico TA, Loo BW, Jr., Pinder-Schenck M, Borghaei H, Chaft JE, et al. The management of patients with stage IIIA non-small cell lung cancer with N2 mediastinal node involvement. *J Natl Compr Canc Netw* (2012) 10(5):599–613. doi: 10.6004/jnccn.2012.0062
20. van Meerbeeck JP, Kramer GW, Van Schil PE, Legrand C, Smit EF, Schramel F, et al. Randomized controlled trial of resection versus radiotherapy after induction chemotherapy in stage IIIA-N2 non-small-cell lung cancer. *J Natl Cancer Inst* (2007) 99(6):442–50. doi: 10.1093/jnci/djk093
21. Albain KS, Swann RS, Rusch VW, Turrisi AT,3, Shepherd FA, Smith C, et al. Radiotherapy plus chemotherapy with or without surgical resection for stage III non-small-cell lung cancer: a phase III randomised controlled trial. *Lancet* (2009) 374(9687):379–86. doi: 10.1016/S0140-6736(09)60737-6
22. Ettinger DS, Wood DE, Aisner DL, et al. *NCCN Guidelines for Non-Small Cell Lung Cancer. Version 3.2020* (Accessed April 10, 2020). To view the most recent version, visit NCCN.org.
23. Navani N, Fisher DJ, Tierney JF, Stephens RJ, Burdett SGroup NM-aC. The Accuracy of Clinical Staging of Stage I-IIIa Non-Small Cell Lung Cancer: An Analysis Based on Individual Participant Data. *Chest* (2019) 155(3):502–9. doi: 10.1016/j.chest.2018.10.020
24. Pignon JP, Tribodet H, Scagliotti GV, Douillard JY, Shepherd FA, Stephens RJ, et al. Lung adjuvant cisplatin evaluation: a pooled analysis by the LACE Collaborative Group. *J Clin Oncol* (2008) 26(21):3552–9. doi: 10.1200/JCO.2007.13.9030
25. Scagliotti GV, Pastorino U, Vansteenkiste JF, Spaggiari L, Facciolo F, Orlowski TM, et al. Randomized phase III study of surgery alone or surgery plus preoperative cisplatin and gemcitabine in stages IB to IIIA non-small-cell lung cancer. *J Clin Oncol* (2012) 30(2):172–8. doi: 10.1200/JCO.2010.33.7089
26. Lee HW, Lee CH, Park YS. Location of stage I-III non-small cell lung cancer and survival rate: Systematic review and meta-analysis. *Thorac Cancer* (2018) 9(12):1614–22. doi: 10.1111/1759-7714.12869
27. Klikovits T, Lohinai Z, Fabian K, Gyulai M, Szilasi M, Varga J, et al. New insights into the impact of primary lung adenocarcinoma location on metastatic sites and sequence: A multicenter cohort study. *Lung Cancer* (2018) 126:139–48. doi: 10.1016/j.lungcan.2018.11.004
28. Sun W, Yang X, Liu Y, Yuan Y, Lin D. Primary Tumor Location Is a Useful Predictor for Lymph Node Metastasis and Prognosis in Lung Adenocarcinoma. *Clin Lung Cancer* (2017) 18(1):e49–55. doi: 10.1016/j.cllc.2016.06.002
29. Zhao Y, Li G, Zheng D, Jia M, Dai W, Sun Y, et al. The prognostic value of lymph node ratio and log odds of positive lymph nodes in patients with lung adenocarcinoma. *J Thorac Cardiovasc Surg* (2017) 153(3):702–9. doi: 10.1016/j.jtcvs.2016.11.053
30. Rami-Porta R, Bolejack V, Crowley J, Ball D, Kim J, Lyons G, et al. The IASLC Lung Cancer Staging Project: Proposals for the Revisions of the T Descriptors in the Forthcoming Eighth Edition of the TNM Classification for Lung Cancer. *J Thorac Oncol* (2015) 10(7):990–1003. doi: 10.1097/JTO.0000000000000559
31. Huang TW, Lin KF, Lee CH, Chang H, Lee SC, Shieh YS. The role of Thyroid Transcription Factor-1 and Tumor differentiation in Resected Lung Adenocarcinoma. *Sci Rep* (2017) 7(1):14222. doi: 10.1038/s41598-017-14651-y

Conflict of Interest: The authors declare that the research was conducted in the absence of any commercial or financial relationships that could be construed as a potential conflict of interest.

Copyright © 2021 Wang, Liu, Bai and Li. This is an open-access article distributed under the terms of the Creative Commons Attribution License (CC BY). The use, distribution or reproduction in other forums is permitted, provided the original author(s) and the copyright owner(s) are credited and that the original publication in this journal is cited, in accordance with accepted academic practice. No use, distribution or reproduction is permitted which does not comply with these terms.

frontiers in Oncology

ORIGINAL RESEARCH
published: 28 April 2021
doi: 10.3389/fonc.2021.650853

Identification of an Individualized Metabolism Prognostic Signature and Related Therapy Regimens in Early Stage Lung Adenocarcinoma

Junjie Hu[1†], Huansha Yu[2†], Liangdong Sun[1], Yilv Yan[1], Lele Zhang[3], Gening Jiang[1] and Peng Zhang[1]*

[1] Department of Thoracic Surgery, Shanghai Pulmonary Hospital, Tongji University School of Medicine, Shanghai, China, [2] Experimental Animal Center, Shanghai Pulmonary Hospital, Tongji University School of Medicine, Shanghai, China, [3] Central Laboratory of Thoracic Surgery, Shanghai Pulmonary Hospital, Tongji University School of Medicine, Shanghai, China

OPEN ACCESS

Edited by:
Junji Uchino,
Kyoto Prefectural University of Medicine, Japan

Reviewed by:
Jiajun Wang,
Fudan University, China
Azhar Ali,
National University of Singapore, Singapore

***Correspondence:**
Peng Zhang
zhangpeng1121@tongji.edu.cn

[†]These authors have contributed equally to this work

Specialty section:
This article was submitted to Thoracic Oncology, a section of the journal Frontiers in Oncology

Received: 08 January 2021
Accepted: 30 March 2021
Published: 28 April 2021

Citation:
Hu J, Yu H, Sun L, Yan Y, Zhang L, Jiang G and Zhang P (2021) Identification of an Individualized Metabolism Prognostic Signature and Related Therapy Regimens in Early Stage Lung Adenocarcinoma. Front. Oncol. 11:650853. doi: 10.3389/fonc.2021.650853

Objective: The choice of adjuvant therapy for early stage lung adenocarcinoma (LUAD) remains controversial. Identifying the metabolism characteristics leading to worse prognosis may have clinical utility in offering adjuvant therapy.

Methods: The gene expression profiles of LUAD were collected from 22 public datasets. The patients were divided into a meta-training cohort (n = 790), meta-testing cohort (n = 716), and three independent validation cohorts (n = 345, 358, and 321). A metabolism-related gene pair index (MRGPI) was trained and validated in the cohorts. Subgroup analyses regarding tumor stage and adjuvant chemotherapy (ACT) were performed. To explore potential therapeutic targets, we performed *in silico* analysis of the MRGPI.

Results: Through machine learning, MRGPI consisting of 12 metabolism-related gene pairs was constructed. MRGPI robustly stratified patients into high- *vs* low-risk groups in terms of overall survival across and within subpopulations with stage I or II disease in all cohorts. Multivariable analysis confirmed that MRGPI was an independent prognostic factor. ACT could not improve prognosis in high-risk patients with stage I disease, but could improve prognosis in the high-risk patients with stage II disease. In silico analysis indicated that B3GNT3 (overexpressed in high-risk patients) and HSD17B6 (down-expressed in high-risk patients) may make synergic reaction in immune evasion by the PD-1/PD-L1 pathway. When integrated with clinical characteristics, the composite clinical and metabolism signature showed improved prognostic accuracy.

Conclusions: MRGPI could effectively predict prognosis of the patients with early stage LUAD. The patients at high risk may get survival benefit from PD-1/PD-L1 blockade (stage I) or combined with chemotherapy (stage II).

Keywords: lung adenocarcinoma, early stage, metabolism genes, prognostic signature, adjuvant therapy

INTRODUCTION

Lung cancer is the leading cause of cancer-related death worldwide (1), and early stage lung cancer accounts for about 17% (2). Lung adenocarcinoma (LUAD) is the most common histologic subtype of lung cancer (3). Surgical resection plus lymph node dissection or sampling is the standard treatment for stage I LUAD (4). However, some patients will still suffer from disease relapse and death, and the 5-year overall survival ranges from 68 to 92% (5). According to the National Comprehensive Cancer Network (NCCN) guidelines, adjuvant systemic treatment is only considered for high-risk patients (4). The benefit of adjuvant systemic treatment for stage I LUAD remains controversial.

Biomarkers, especially gene expression, in tumor tissues are reliably related to cancer prognosis and survival (6–8). Thus, identifying the molecular features that may lead to worse prognosis may have clinical utility in offering adjuvant therapy to a subgroup of patients at high risk. The availability of large-scale public cohorts with gene expression data provides an ideal resource to identify a more individualized prognostic signature for LUAD.

Reprogramming of energy metabolism is an emerging hallmark of cancer (9) and recently has been proved to be involved in lung cancer initiation, progression, and drug resistance (10–13). Metabolic phenotypes can also be exploited to image tumors, provide prognostic information, and treat cancer (14). Therefore, understanding the metabolism characteristics by gene expression-based algorithms may be helpful for screening the patients at high risk. However, the molecular characteristics of tumor metabolism remain to be comprehensively explored regarding their prognostic potential in early stage LUAD.

In this study, we integrated multiple cohorts with gene expression profiles to develop and validate an individualized prognostic signature for early stage LUAD from metabolism-related gene pairs (MRGPs). We then explored the potential therapy regimen for the patients at high risk, which may be utilized in clinical. Further, to leverage the complementary value of molecular and clinical features, we integrated the metabolism signature with clinical factors to improve the predicted accuracy for overall survival (OS).

METHODS

Patients and Datasets

This study was approved by the Ethic Committee of Shanghai Pulmonary Hospital. We retrospectively analyzed the gene expression matrixes and corresponding clinical characteristics from 22 public datasets (**Supplementary Table S1**), including 17 microarray and two RNAseq datasets from the Gene Expression Omnibus (GEO) database (https://www.ncbi.nlm.nih.gov/geo/), one RNAseq dataset from the Cancer Genome Atlas (TCGA) database (https://portal.gdc.cancer.gov), one microarray dataset from the ArrayExpress database (https://www.ebi.ac.uk/arrayexpress/), and one RNAseq dataset from the OncoSG database (15) (https://src.gisapps.org/OncoSG/). The patients were included according to the following criteria: (1) lung adenocarcinoma, (2) stages I–II, (3) available OS information. The patients were excluded if they met any of the exclusion criteria: (1) non-adenocarcinoma or the pathologic subtypes were unknown, (2) stage III or IV or unknown, (3) lack of OS information, (4) received neoadjuvant therapy. The gene expression matrix of normal lung tissue was downloaded from the Genotype-Tissue Expression (GTEx) database (https://www.gtexportal.org/home/). The entire tumor datasets were divided into meta-training, meta-testing, and three independent validation cohorts (TCGA, GSE68465, and GSE72094) (**Supplementary Figure S1**).

Data Process

All the expression level of microarray datasets was transformed by log2. For all the datasets of RNAseq, the fragments per kilobase million (FPKM) level was used as the expression value and log2(FPKM+1) transformed. If there were duplicate genes in each dataset, the mean value was calculated by the *avereps* function from the *limma* R package.

Construction of the MRGPI

As shown in the **Figure 1**, we constructed a prognostic signature by focusing on metabolism-related genes (MRGs). From the *c2.cp.kegg.v7.0.symbols.gmt* dataset that was downloaded from the Gene Set Enrichment Analysis (GSEA) website (https://www.gsea-msigdb.org/gsea/index.jsp), 2,522 MRGs from 68 metabolism related Kyoto Encyclopedia of Genes and Genomes (KEGG) pathways were identified. Of the 2,522 MRGs, 690 MRGs were available in all datasets. The gene expression value underwent pairwise subtraction to generate a score for each metabolism-related gene pair (MRGP): MRGP score = expression value of MGP 1 − expression value of MGP 2. The score represented the log2 fold change of MGP 1 relative to MGP 2.

To screen the representative MRGPs in tumor, we identified the MRGPs that were highly variable [coefficient of variation (CV) > 0.15] in all tumor datasets and highly stable (CV < 0.15) in the normal cohort. Then the univariable Cox proportional hazards regression was used to select prognostic MRGPs in the screened MRGPs (*survival* R package). Finally, to minimize the risk of overfitting, a cox proportional hazards regression model combined with the least absolute shrinkage and selection operator (LASSO) was applied to identify the most important prognostic MRGPs (*glmnet* R package). The optimal values of the penalty parameter λ were determined by 10-fold cross-validations at 1 SE beyond the minimum partial likelihood deviance in the meta-training cohort. Based on the selected MRGPs from LASSO Cox regression model, the metabolism-related gene pair index (MRGPI) for each patient was constructed: MRGPI = MRGPI = $\Sigma_i^n\ MRGP_i\ score \times Coefficient_i$. To separate patients into low- or high-risk groups, the optimal MRGPI cutoff value was determined using the *surv_cutpoint* function of the *survminer* R package.

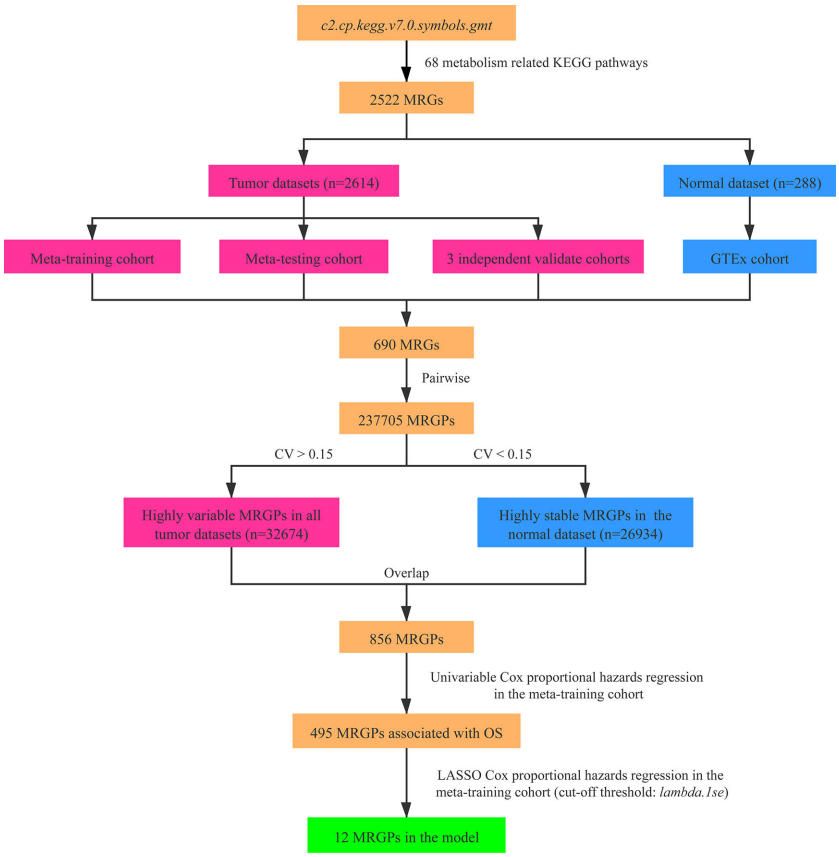

FIGURE 1 | Flowchart of the construction process of MRGPI. CV, coefficient of variation; GTEx, the Genotype-Tissue Expression; LASSO, least absolute shrinkage and selection operator; MRGs, metabolism-related genes; MRGPs, metabolism-related gene pairs; OS, overall survival.

Validation of the MRGPI

The predictive value of MRGPI for OS was evaluated in the meta-training, meta-testing and three independent validation cohorts. As described in a previous study (6), the pathologic stage was treated as continuous variable by the following converting approach: IA was coded as 1, then IB as 2, I as 1.5, I–II as 2.5, IIA as 3, IIB as 4 and II as 3.5. The univariable Cox regression model was used to evaluate the prognostic value of age, gender, smoking history, stage and MRGPI (as continuous and binary form, respectively). The multivariable Cox regression model was used to evaluate the independent prognostic value of MRGPI. Subgroup analysis was performed according to the stage.

DEGs and Gene Ontology Analysis

The gene expression differences between high and low risk were compared using the *limma* package, and genes with |log fold change| > 1 and false discovery rate adjusted P value <0.05 were considered to be significant differentially expressed genes (DEGs). To gain biological understanding of the MRGPI, we conducted an enrichment analysis of its component MRGs using the *clusterProfiler* R package. FDR-adjusted P <0.05 was used to select statistically significant gene sets.

Profiling of Infiltrating CD8 T Cells

To analyze the tumor immune microenvironment, a dataset of single cell RNAseq (scRNA-seq) with annotated cell types (16) (GSE131907) was downloaded from the GEO database. There were nine samples of stage I–II LUAD, and the cell numbers of all the samples were more than 3,200. The mean transcripts per kilobase million (TPM) value of one gene was calculated, and the log2(TPM+1) was used as the expression value of the tumor cells in each sample. Given that too less tumor cells could not reflect the characteristics of the tumor, we remove two samples whose tumor cells were less than 50, and seven samples of stage IA LUAD were included for analysis.

Construction and Validation of the MCPI

Based on the results of the multivariable Cox analysis in the all cohorts, age, stage, and MRGPI score were significantly associated with OS. Age, stage, and MRGPI score were integrated to composite a metabolism-clinical prognostic index (MCPI) by applying Cox proportional hazards regression in the meta-training cohort: MCPI score= *age* × *coefficient* + *stage* × *coefficient* + *MRGPI* × *coefficient*. The prognostic accuracy of MRGPI was estimated using the concordance index (C-index),

which range from 0 to 1.0 (*survcomp* R package). As we mentioned above, the optimal cutoff value of MCPI score was determined by the *surv_cutpoint* function in the meta-training cohort. The predictive value of MCPI for OS was evaluated in the meta-testing and three independent validation cohorts.

Statistical Analysis

All statistical analyses were conducted using R software (version 3.6.2). Pearson correlation analysis was performed to determine the correlation between two variables. The Kaplan–Meier method was used to generate survival curves, and significance of differences was compared using the log-rank test. All statistical tests were two-sided, and P values less than 0.05 were considered statistically significant.

RESULTS

Patient Characteristics of Included Cohorts

Totally, 2,614 patients with stage I–II LUAD (**Table 1**) and 288 heathy donors were included for analysis. The median age ranged from 62 to 70 in all cohorts, and the proportion of female were larger than male. Most patients (>48.2%) had smoking history, and the patients with stage I LUAD accounted for the major proportion, except GSE68465, in which most patients did not had specific stage (stages I–II). In the meta-training, meta-testing, and GSE68465 cohorts, the median follow-up time was more than 50 months, and the death events were observed in more than 35% patients. However, the median follow-up time of the TCGA and GSE72094 was shorter, and the events of death were less than those of other cohorts.

Construction of the MRGPI

After pairwise coupling of the 690 GRPs, 237,705 MRGPs were constructed, and the corresponding scores were generated. We removed 205,031 MRGPs with CV <0.15 in all datasets and 210,771 MRGPs with CV >0.15 in the normal dataset. Between the remaining 32,674 MRGPs in the tumor cohorts and 26,934 MRGPs in the normal cohort, 856 MRGPs were overlapped. The association of the 856 MRGPs with OS was assessed in the meta-training cohort, resulting in 495 prognostic MRGPs. Finally, the LASSO Cox regression model selected 12 MRGPs in the meta-training cohort (**Supplementary Figure S2A**). Based on the 12 MRGPs that consisted of 20 MRGs, the MRGPI for each patient was constructed (**Table 2**). The optimal cutoff point (−0.261) obtained from the *surv_cutpoint* function served as the cutoff to assign patients into high- and low-risk groups (**Supplementary Figure S2B**). The Kaplan–Meier curve showed the patients in the high-risk group presented with a significantly worse OS in the meta-training cohort [hazard ratio (HR): 3.584, 95% confidence interval (CI): 2.755–4.663, P < 0.001, **Supplementary Figure S2C**]. Univariable Cox analysis indicated that MRGPI (both as continuous and binary form) was a prognostic factor for OS, and multivariable Cox analysis confirmed that MRGPI (as binary form) was independently associated with OS (**Figure 3** and **Supplementary Table S2**). The C-index of the MRGPI in the meta-training cohort was 0.701 (95% CI: 0.672–0.730).

Validation of the MRGPI in Multiple Independent Cohorts

To determine whether the MRGPI was robust, the performance of the MRGPI was assessed in the meta-testing and three independent cohorts. Consistent with the outcomes of the meta-training cohort, the MRGPI significantly stratified patients into low- *vs* high-risk groups in terms of OS. The patients in the

TABLE 1 | Clinical and pathologic features of patients in meta-training, meta-testing, and independent validation cohorts.

		Meta-training	Meta-testing	TCGA	GSE68465	GSE72094
Sample size, n		790	786	345	372	321
Age in years, median (IQR)		62 (56–69)	65 (58–72)	66 (59–72)	65 (58–72)	70 (64–77)
Sex, n (%)						
	Female	429 (54.3)	423 (53.8)	194 (56.2)	188 (50.5)	174 (54.2)
	Male	361 (45.7)	363 (46.2)	151 (43.8)	184 (49.5)	147 (45.8)
Smoking history, n (%)						
	Yes	381 (48.2)	398 (50.6)	288 (83.5)	257 (69.1)	244 (76.0)
	No	216 (27.3)	190 (24.2)	49 (14.2)	41 (11.0)	27 (8.4)
	Unknown	193 (24.4)	198 (25.1)	8 (2.3)	74 (19.9)	50 (15.6)
Stage, n (%)						
Stage I		625 (79.1)	601 (76.5)	237 (68.7)	115 (30.9)	254 (79.1)
	IA	278 (35.2)	221 (28.1)	117 (33.9)	115 (30.9)	150 (46.6)
	IB	260 (32.9)	264 (33.6)	115 (33.3)	–	99 (30.8)
	IA/B	87 (11.0)	116 (14.7)	5 (1.4)	–	5 (1.6)
Stage II		155 (19.6)	185 (23.5)	108 (31.3)	95 (25.5)	67 (20.9)
	IIA	21 (2.6)	42 (5.3)	47 (13.6)	–	18 (5.6)
	IIB	72 (9.1)	98 (12.5)	59 (17.1)	95 (25.5)	49 (15.3)
	IIA/B	62 (7.8)	45 (5.7)	2 (0.6)	–	–
Stages I–II		10 (1.3)	–	–	162 (43.5)	–
Follow-up in months, median (IQR)		56 (33–78)	50 (29–72)	19 (12–30)	52 (29–76)	27 (20–34)
No of death, n (%)		279 (35.3)	285 (36.3)	98 (28.4)	175 (47.0)	77 (24.0)

IRQ, interquartile range.

TABLE 2 | Model information about MRGPI.

MRGP	MRG 1	Full name	Function	MRG 2	Full name	Function	Coefficient
1	ALDH3A2	Aldehyde Dehydrogenase 3 Family Member A2	Catalyzing the oxidation of medium and long chain aliphatic aldehydes to fatty acids	GPX3	Glutathione Peroxidase 3	Catalyzing the reduction of hydrogen peroxide, lipid peroxides and organic hydroperoxide, by glutathione	–0.0049472424
2	AOC3	Amine Oxidase Copper Containing 3	Having semicarbazide-sensitive monoamine oxidase activity	CYP4F2	Cytochrome P450 Family 4 Subfamily F Member 2	Catalyzing many reactions involved in drug metabolism and synthesis of cholesterol, steroids and other lipids	–0.0223604279
3	DCTD	Deoxycytidylate Deaminase	Catalyzing the deamination of dCMP to dUMP, the nucleotide substrate for thymidylate synthase	B3GNT3	Beta-1,3-N-Acetylglucosaminyltransferase 3	Synthesis of poly-N-acetyllactosamine	–0.1552699047
4	GMPR	Guanosine Monophosphate Reductase	Catalyzing the irreversible NADPH-dependent deamination of GMP to IMP	CA5A	Carbonic Anhydrase 5A	Catalyzing the reversible hydration of carbon dioxide	–0.0076013442
5	B3GNT3	Beta-1,3-N-Acetylglucosaminyltransferase 3	Synthesis of poly-N-acetyllactosamine	HYAL2	Hyaluronidase 2	Hydrolyzing high molecular weight hyaluronic acid to produce an intermediate-sized product	0.0115559858
6	B3GNT3	Beta-1,3-N-Acetylglucosaminyltransferase 3	Synthesis of poly-N-acetyllactosamine	IMPDH1	Inosine Monophosphate Dehydrogenase 1	Catalyzing the conversion of IMP to XMP	0.0051310730
7	B3GNT3	Beta-1,3-N-Acetylglucosaminyltransferase 3	Synthesis of poly-N-acetyllactosamine	FPGS	Folylpolyglutamate Synthase	Catalyzing conversion of folates to polyglutamate derivatives	0.0328202856
8	SORD	Sorbitol Dehydrogenase	Catalyzing the reversible NAD(+)-dependent oxidation of various sugar alcohols	HEXA	Hexosaminidase Subunit Alpha	Degradation of GM2 gangliosides, and a variety of other molecules containing terminal N-acetyl hexosamines	0.0529668933
9	RPIA	Ribose 5-Phosphate Isomerase A	Catalyzing the reversible conversion between ribose-5-phosphate and ribulose-5-phosphate	NDUFAB1	NADH : Ubiquinone Oxidoreductase Subunit AB1	Carrier of the growing fatty acid chain in fatty acid biosynthesis	–0.0795029873
10	ALPI	Alkaline Phosphatase, Intestinal	Involving in folate biosynthesis	LCAT	Lecithin-Cholesterol Acyltransferase	Central enzyme in the extracellular metabolism of plasma lipoproteins	0.0012509917
11	ADH1C	Alcohol Dehydrogenase 1C	Gamma subunit of class I alcohol dehydrogenase that catalyzes ethanol oxidation to acetaldehyde	MAN2C1	Mannosidase Alpha Class 2C Member 1	Cleaving alpha 1,2-, alpha 1,3-, and alpha 1,6-linked mannose residues from glycoproteins	–0.0454175427
12	PFKFB4	6-Phosphofructo-2-Kinase/ Fructose-2,6-Biphosphatase 4	Synthesis and degradation of fructose 2,6-bisphosphate	MAN2C1	Mannosidase Alpha Class 2C Member 1	Cleaving alpha 1,2-, alpha 1,3-, and alpha 1,6-linked mannose residues from glycoproteins	0.0756289035

dCMP, deoxycytidylic monophosphate; dUMP, deoxyuridine monophosphate; GMP, guanine monophosphate; IMP, inosine monophosphate; MRG, metabolism-related gene; MRGP, metabolism-related gene pair; NAD, nicotinamide adenine dinucleotide; NADPH, nicotinamide adenine dinucleotide phosphate; XMP, xanthosine monophosphate.

high-risk group had significantly worse OS in the meta-testing (HR: 2.011, 95% CI: 1.531–2.640, P < 0.001, **Figure 2A**), TCGA (HR: 1.657, 95% CI: 1.106–2.482, P = 0.013, **Figure 2B**), GSE68465 (HR: 1.626, 95% CI: 1.194–2.214, P = 0.002, **Figure 2C**), and GSE72094 (HR: 2.370, 95% CI: 1.514–3.714, P < 0.001, **Figure 2D**) cohorts. The MRGPI (both as continuous and binary form) was a prognostic factor for OS in all the validation cohorts in the univariate Cox analysis, and it remained as an independent prognostic factor in multivariate analysis, after adjusting for age, gender, smoking history, and tumor stage (**Figure 3** and **Supplementary Table S2**). The C-index of the meta-testing, TCGA, GSE68465, GSE72094 cohort was 0.576 (95% CI: 0.541–0.612), 0.604 (95% CI: 0.535–0.673), 0.589 (95% CI: 0.543–0.634) and 0.645 (95% CI: 0.582–709), respectively.

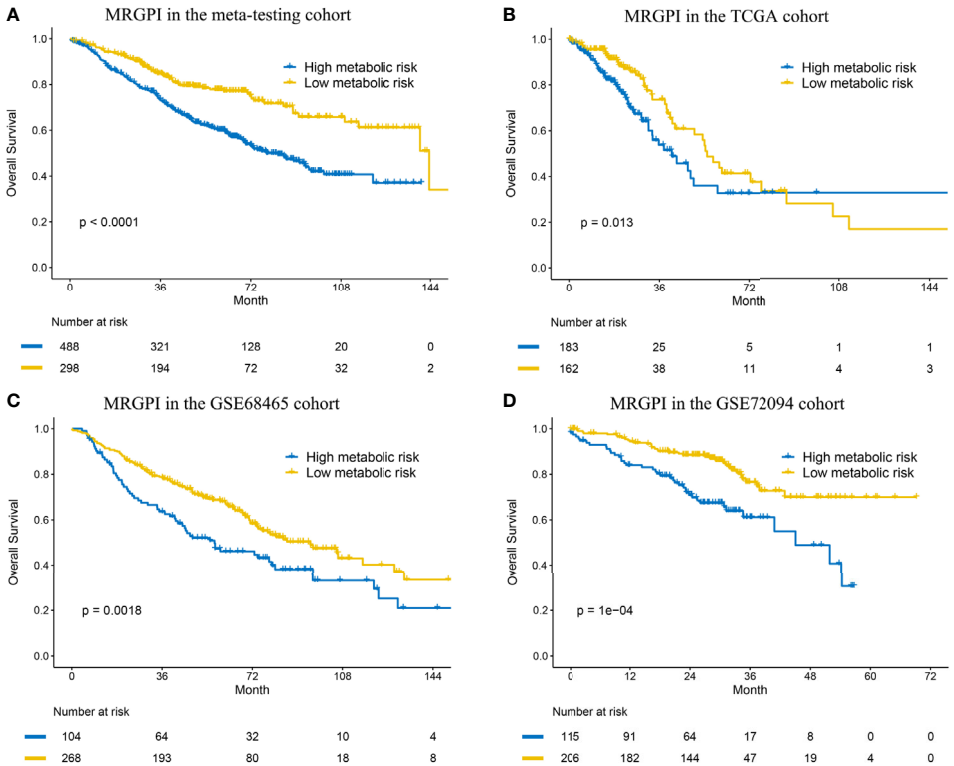

FIGURE 2 | Kaplan–Meier curves of overall survival in the meta-testing **(A)**, TCGA **(B)** and GSE68465 **(C)** and GSE72094 **(D)** cohort.

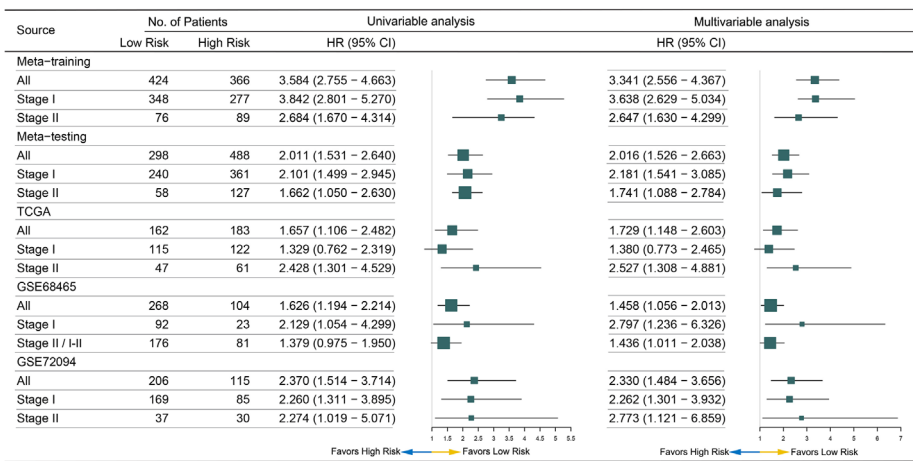

FIGURE 3 | Forest plot for the hazard ratios (HRs) of high *vs* low metabolism-related gene pair index (MRGPI) risk groups.

Subgroup Analysis of the MRGPI in Stage I Disease

In the patients with stage I disease, the MRGPI stratified patients in all cohorts into significantly different prognostic groups. The MRGPI remained highly prognostic for the meta-training (HR: 3.842, 95% CI: 2.801–5.270, P < 0.001), meta-testing (HR: 2.101, 95% CI: 1.499–2.945, P < 0.001), GSE68465 (HR: 2.129, 95% CI: 1.054–4.299, P = 0.031) and GSE72094 (HR: 2.260, 95% CI: 1.311–3.895, P = 0.003) cohort (**Supplementary Figures S2D** and **S3A–D**), and multivariable Cox analysis confirmed that MRGPI was independently associated with OS (**Figure 3** and **Supplementary Table S3**). However, the result was negative in the TCGA cohort, and the short follow-up time and less death events probably accounted for it.

Given the prognosis differences between high- and low- risk patients, we analyzed the benefit of adjuvant chemotherapy (ACT) in the two groups. Of all the validation datasets, five datasets (OncoSG, GSE42127, GSE14814, TCGA, and GSE68465) recorded the information of ACT. Compared to surgery alone, ACT did not improve OS in the low-risk group (HR: 1.817, 95% CI: 0.871–3.791, P = 0.111; **Figure 4A**). We also did not observe that patients in the high-risk group could get OS benefit from ACT (HR: 0.959, 95% CI: 0.521–1.765, P = 0.893; **Figure 4B**), which indicated that ACT may be not suitable for the patients. To improve the prognosis, other adjuvant therapy regimens should be explored.

Subgroup Analysis of the MRGPI in Stage II Disease

The MRGPI could also stratified patients in all cohorts into significantly different prognostic groups in the patients with stage II disease. The patients in the high-risk group had significantly worse OS in the meta-training (HR: 2.684, 95% CI: 1.670–4.314, P < 0.001), meta-testing (HR: 1.662, 95% CI: 1.050–2.630, P = 0.030), TCGA (HR: 2.428, 95% CI: 1.301–4.529, P < 0.001), and GSE72094 (HR: 2.274, 95% CI: 2.274, P = 0.045) cohort (**Supplementary Figures S2E** and **S4A–D**). The MRGPI remained an independent risk factor in multivariable analysis (**Figure 3** and **Supplementary Table S4**). A margin positive result (HR: 1.379, 95% CI: 0.975–1.950, P = 0.069) was observed in the GSE68465 cohort (including stages I–II, **Supplementary Figure S4C**); however, the result of multivariable analysis showed that the MRGPI was an independent risk factor (**Supplementary Table S4**).

Then, we also explored the effect of ACT in the two groups. The Kaplan–Meier curve indicated that ACT could not improve OS in the low-risk group (HR: 1.013, 95% CI: 0.561–1.829, P = 0.965; **Figure 4C**). In the high-risk group, although the result was negative (HR: 0.621, 95% CI: 0.360–1.070, P = 0.086;

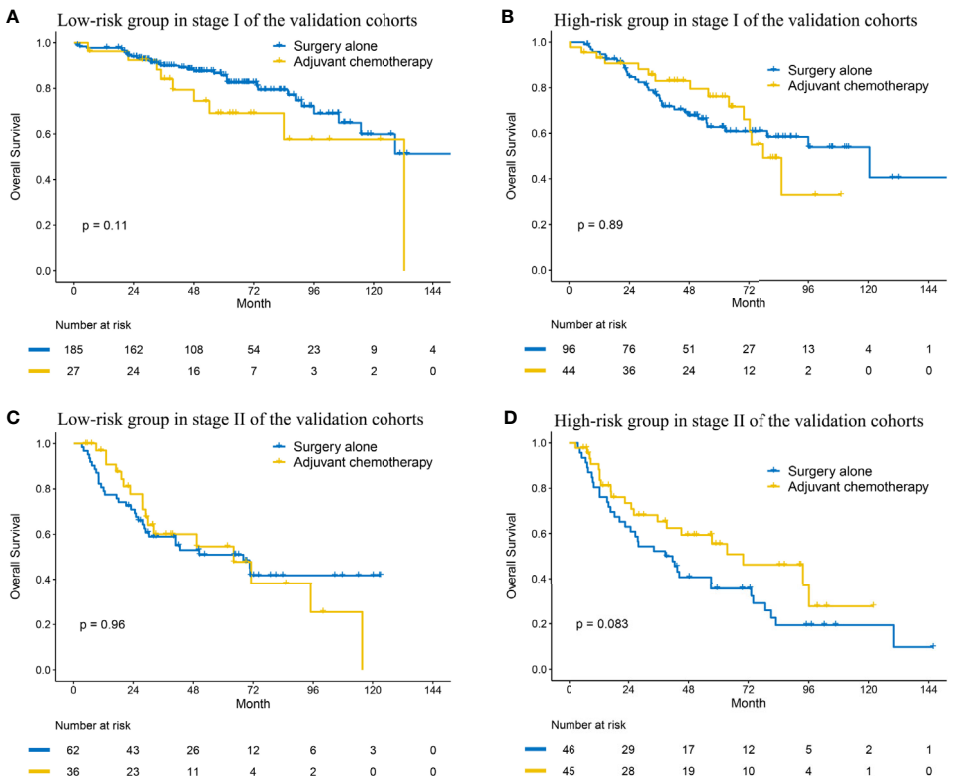

FIGURE 4 | Kaplan–Meier curves of overall survival regarding adjuvant chemotherapy in patients with stage I **(A, B)** and stage II **(C, D)** disease at low and high risk in the validation cohort.

Figure 4D), the curves had an obvious tendency to separate and the small sample size probably accounted for it.

Biological Phenotypes Associated With the MRGPI

Enrichment analysis of the 20 unique MRGs in the MRGPI identified two overrepresented biological processes (organic acid catabolic process and carboxylic acid catabolic process) in the gene ontology (**Supplementary Figure S5A**). To explore the potential survival mechanism related to the MRGPI, we analyzed the DEGs between the high and low-risk groups in the three independent validation cohorts, and we focused on the differentially expressed MRGs. Among the DEGs from the three cohorts, three MRGs (B3GNT3, ADH1B, and HSD17B6) were overlapped (**Figures 5A–C**), and their expression levels were significantly correlated with MRGPI (**Supplementary Figure S6**). The three MRGs had been reported to be associated with other cancers (17–19), but few studies reported their role in LUAD.

B3GNT3 was overexpressed in LUAD, and its expression level was positively associated with tumor stage (**Figure 5D**), which suggested that B3GNT3 played an important role in tumor carcinogenesis and prognosis. Previous study reported that N-linked glycosylation of PD-L1 that was catalyzed by B3GNT3 was required for physical contact between PD-L1 and PD-1 in triple-negative breast cancer, and then caused CD8$^+$ T cell exhausted (18). We then explored whether there was a similar mechanism in LUAD. From the scRNA-seq result, we

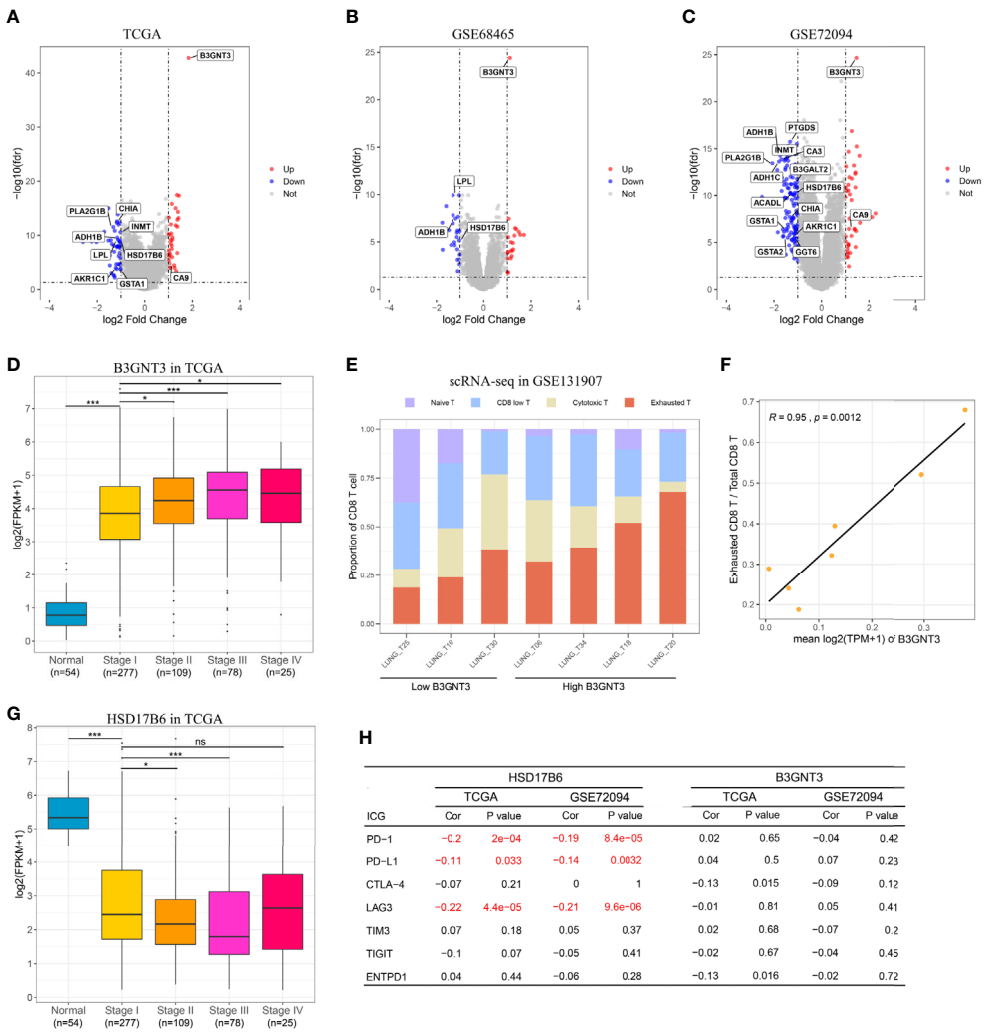

	HSD17B6				B3GNT3			
	TCGA		GSE72094		TCGA		GSE72094	
ICG	Cor	P value	Cor	P value	Cor	P value	Cor	P value
PD-1	−0.2	2e−04	−0.19	8.4e−05	0.02	0.65	−0.04	0.42
PD-L1	−0.11	0.033	−0.14	0.0032	0.04	0.5	0.07	0.23
CTLA-4	−0.07	0.21	0	1	−0.13	0.015	−0.09	0.12
LAG3	−0.22	4.4e−05	−0.21	9.6e−06	−0.01	0.81	0.05	0.41
TIM3	0.07	0.18	0.05	0.37	0.02	0.68	−0.07	0.2
TIGIT	−0.1	0.07	−0.05	0.41	−0.02	0.67	−0.04	0.45
ENTPD1	0.04	0.44	−0.06	0.28	−0.13	0.016	−0.02	0.72

FIGURE 5 | *In silico* analysis of the MRGPI. **(A–C)**: Volcano plot showing fold changes for genes differentially expressed between high- and low-risk patients in the TCGA, GSE68465, and GSE72094 cohort. **(D)** Boxplots of the expression level of B3GNT3 in the normal tissue and different tumor stages showing that upregulation of B3GNT correlated with tumor progression. **(E)** Proportion of different CD8$^+$ T cell in each patient, and the patients were divided into low and high B3GNT3 group based on the median value. **(F)** The expression level of B3GNT3 was significantly associated with the proportion of the exhausted CD8$^+$ T cell. **(G)** Boxplots of the expression level of HSD17B6 in the normal tissue and different tumor stages showing that down-regulation of HSD17B6 correlated with tumor progression. **(H)** Pearson's correlation test between B3GNT3, HSD17B6, and immune checkpoint genes. ns, not significant ($P > 0.05$), $^{**}P < 0.01$, $^{***}P < 0.001$.

noticed that the expression level of B3GNT3 in tumor cell was positively correlated with the proportion of the exhausted $CD8^+$ T cell (r = 0.95, P = 0.0012, **Figures 5E, F**). However, the expression level of B3GNT3 was not correlated with immune checkpoint genes (ICGs) in the TCGA and GSE72094 cohorts (most ICGs were not available in the GSE68465 dataset), especially PD-1 and PD-L1 (**Figure 5H**). The results demonstrated that there may be the same mechanism of B3GNT3 in LUAD.

HSD17B6 was down-expressed in LUAD, and the expression level of HSD17B6 was negatively associated with tumor stage (**Figure 5G**). HSD17B6 could convert 3 alpha-adiol to dihydrotestosterone that was closely related to the development of many tumors (20). Lv et al. (17) reported that low expression of HSD17B6 correlated with multiple ICGs expression in hepatocellular carcinoma. In this study, we observed that the expression level of HSD17B6 was negatively correlated with PD-1 (r = −0.20 and P < 0.001 in TCGA, r = −0.19 and P < 0.001 in GSE72094), PD-L1 (r = −0.11 and P = 0.033 in TCGA, r = −0.14 and P = 0.003 in GSE72094), and LAG3 (r = −0.22 and P < 0.001 in TCGA, r = -0.21 and P < 0.001 in GSE72094) (**Figure 5H**), suggesting that low HSD17B6 expression potentially played an important role in mediating immune evasion. ADH1B was also down-expressed in LUAD (**Supplementary Figure S5B**); however, its expression level was not negatively correlated with ICGs as HSD17B6 (**Supplementary Figure S5C**), which suggested that there may be other mechanisms behind it.

Together, these results indicated that B3GNT3 and HSD17B6 may make synergic reaction in immune evasion, with HSD17B6 up-regulating PD-L1 and B3GNT3 stabilizing the PD-L/PD-L1 ligation. Immune checkpoint inhibitors, especially PD-1/PD-L1 anti-body may be a therapeutic choice. Combined with the results of ACT in LUAD at different stages and risks, we thought that patients at high risk may get survival benefit from PD-1/PD-L1 blockade (stage I) or combined with chemotherapy (stage II). Although PD-1/PD-L1 anti-body as neoadjuvant therapy has been used in early stage NSCLC in clinical trials recently (21–24), there are no transcriptomic data of the tumor before treatment at present, so the regimen we proposed could not be validated in this study.

Integrated Prognostic Index by Combining the MRGPI With Clinical Factors

To further improve accuracy, we combined age, stage, and MRGPI score to fit a Cox proportional hazards regression model in the meta-training cohort and derived a MCPI: MCPI = age × 0.028 + stage × 0.312 + MRGPI × 1.726. The optimal cutoff value of the MCPI for stratifying patients was determined to be 2.007 (**Supplementary Figure S7A**). Improved estimation of OS was achieved by the binary form of MCPI compared with MRGPI (**Supplementary Figures S7B–F**), and the C-index for the meta-training, meta-testing, TCGA, GSE68465, GSE72094 cohort was 0.729 (95% CI 0.700–0.757), 0.648 (95% CI 0.613–0.682), 0.641 (95% CI 0.567–0.709), 0.665 (95% CI 0.634–0.709), and 0.666 (95% CI 0.602–0.731), respectively (**Supplementary Figure S7G**).

DISCUSSION

When diagnosed at early stages, LUAD could be effectively treated with surgical resection. However, the use of ACT for stage I LUAD in the setting of standard therapy remains controversial because several clinical trials fail to show a survival benefit among unselected patients, and the toxic effects of chemotherapy are inevitable (25). The strategy is to identify of the subset of patients at high risk for recurrence and death. A prognostic signature beyond the current staging system is desired to accurately identify the patients at high risk and to better guide adjuvant treatment (7). In this study, we developed a prognostic signature based on 12 MRGPs to predict prognosis of early stage LUAD and validated it in multiple independent cohorts across different platforms. The MRGPI was extremely robust in stratifying the patients into the low- and high-risk groups with different survival outcomes. Several models based on the expression value have already been reported to present with the ability for predicting prognosis in lung cancer (26–29). However, the models based on the absolute value of the expression level could not avoid the technical biases inherent across different platforms. The gene pairs signature proposed by Li et al. (6) is based on the relative value of gene expression level, which only refers to the pairwise comparison of the gene expression profile within a sample. Li et al. constructed a gene pair signature based on 25 immune-related gene pairs consisting of 40 immune-related genes in non-squamous lung cancer (6). Our prognostic signature was derived from MRGs in LUAD and MRGPI consisted of 12 gene pairs involving 20 MRGs. With less gene pairs, MRGPI performed comparable accuracy to Li and colleagues' model in the TCGA (C-index: 0.60 *vs* 0.62) cohort.

After identifying the patients at different risks, we explored the benefit of ACT. Not surprisingly, ACT could not bring survival benefit in stage I LUAD at low risk. However, ACT also could not improve OS in stage I LUAD at high risk, suggesting that chemotherapy may be not suitable for the patients. For stage II LUAD, ACT may improve OS in the patients at high risk, which was in accordance with the clinical practice. However, we also noticed that the patients at low risk could not get survival benefit from ACT, suggesting that ACT should also be used selectively in a subset of patients with stage II LUAD. According to the NCCN guidelines, ACT should be performed in stage IIB LUAD with R0 resection, but it is alternative in stage IIA LUAD and just required for high-risk patients (4). Besides identifying high-risk patients with stage I LUAD, MRGPI could also identify a subset of patients in stage II who may be free from ACT. However, the sample size of ACT was small in this study, and more studies were needed to validate the results.

To explore potential therapeutic targets for the patients with poor prognosis based on the MRGPI, we performed DEG analysis using the three independent datasets. Three MRGs were identified, and B3GNT3 and HSD17B6 may make synergic reaction in immune evasion by the PD-1/PD-L1 pathway. Thus, PD-1/PD-L1 blockade was an optimal therapy regimen for the patients at high risk. Compared with conventional ACT, adjuvant immunotherapy could improve

prognosis in resectable solid tumor (30, 31), and neoadjuvant therapy may get more survival benefit than adjuvant therapy (32). Recently, PD-1/PD-L1 anti-body as neoadjuvant therapy has been proved to be feasible in resectable lung cancer (21–24). Thus, the patients with stage I LUAD at high risk may be get survival benefit from PD-1/PD-L1 blockade. For the patients with stage II LUAD at high risk, both chemotherapy and PD-1/PD-L1 blockade may improve prognosis, so PD-1/PD-L1 anti-body plus chemotherapy as neoadjuvant therapy may be optimal. However, there are no transcriptomic data of the tumor before immunotherapy available at present to validate it. For the patients at low risk, surgery alone may be optimal, but the benefit of immunotherapy should also be explored in future studies.

There were some limitations in our study. First, some biases were inevitable because of the retrospective nature of this study. Second, the mutation status was not considered due to lack of information of most datasets. Since driver genes like EGFR and ALK mutation were common in LUAD, the benefit of targeted therapy in the patients at risk could not be evaluated, and adjuvant targeted therapy was proved to be better than ACT in clinical trials (33, 34). Third, as we mentioned above, the sample size of ACT was small, and more studies were needed to validate the results. Last, the therapy regimens we proposed were warranted to validate in clinical studies.

In conclusion, this study identified metabolism-related gene pair-based signature that can effectively predict survival outcomes of the patients with early stage LUAD. The patients at high risk may get survival benefit from PD-1/PD-L1 blockade (stage I) or combined with chemotherapy (stage II). Prospective studies are needed to further validate its analytical accuracy for estimating prognosis and test its clinical utility in individualized management of early stage LUAD.

DATA AVAILABILITY STATEMENT

The datasets presented in this study can be found in online repositories. The names of the repository/repositories and accession number(s) can be found in the article/**Supplementary Material**.

ETHICS STATEMENT

The studies involving human participants were reviewed and approved by Tongji University. Written informed consent for participation was not required for this study in accordance with the national legislation and the institutional requirements.

AUTHOR CONTRIBUTIONS

Conception and design: PZ. Administrative support: GJ. Provision of study materials or patients: JH, HY, and LZ. Collection and assembly of data: JH, LS, and YY. Data analysis and interpretation: JH, LS, and HY. Manuscript writing: all authors. All authors contributed to the article and approved the submitted version.

FUNDING

This work was supported by the National Key R&D Program of China (2019YFC1315803), National Natural Science Foundation of China (Grant No. 81972172), the Shanghai Municipal Health Commission (Grant No. 20174Y0111), the Shanghai Science and Technology Committee (Grant No. 19XD1423200, 18140903900, 201409001000), and Programs of Shanghai Pulmonary Hospital (No. fkcx1904).

SUPPLEMENTARY MATERIAL

The Supplementary Material for this article can be found online at: https://www.frontiersin.org/articles/10.3389/fonc.2021.650853/full#supplementary-material

REFERENCES

1. Bray F, Ferlay J, Soerjomataram I, Siegel RL, Torre LA, Jemal A. Global Cancer Statistics 2018: GLOBOCAN Estimates of Incidence and Mortality Worldwide for 36 Cancers in 185 Countries. *Ca-Cancer J Clin* (2018) 68 (6):394–424. doi: 10.3322/caac.21492
2. *Cancer Stat Facts: Lung and Bronchus Cancer*. Available at: https://seer.cancer.gov/statfacts/html/lungb.html (Accessed Sep 13, 2020).
3. Travis WD, Brambilla E, Noguchi M, Nicholson AG, Geisinger KR, Yatabe Y, et al. International Association for the Study of Lung Cancer/American Thoracic Society/European Respiratory Society International Multidisciplinary Classification of Lung Adenocarcinoma. *J Thoracic Oncol* (2011) 6(2):244–85. doi: 10.1097/JTO.0b013e318206a221
4. National Comprehensive Cancer Network. *Nccn Clinical Practice Guidelines in Oncology: non-Small Cell Lung Cancer. Version 7. 2020 - September 11, 2020*. Available at: https://www.nccn.org/professionals/physician_gls/pdf/nscl.pdf (Accessed Sep 13, 2020).
5. Goldstraw P, Chansky K, Crowley J, Rami-Porta R, Asamura H, Eberhardt WEE, et al. The IASLC Lung Cancer Staging Project: Proposals for Revision of the TNM Stage Groupings in the Forthcoming (Eighth) Edition of the TNM Classification for Lung Cancer. *J Thoracic Oncol* (2016) 11(1):39–51. doi: 10.1016/j.jtho.2015.09.009
6. Li B, Cui Y, Diehn M, Li R. Development and Validation of an Individualized Immune Prognostic Signature in Early-Stage Nonsquamous Non-Small Cell Lung Cancer. *JAMA Oncol* (2017) 3(11):1529–37. doi: 10.1001/jamaoncol.2017.1609
7. Cai WY, Dong ZN, Fu XT, Lin LY, Wang L, Ye GD, et al. Identification of a Tumor Microenvironment-Relevant Gene Set-Based Prognostic Signature and Related Therapy Targets in Gastric Cancer. *Theranostics* (2020) 10(19):8633–47. doi: 10.7150/thno.47938
8. Kandimalla R, Tomihara H, Banwait JK, Yamamura K, Singh G, Baba H, et al. A 15-Gene Immune, Stromal, and Proliferation Gene Signature That Significantly Associates With Poor Survival in Patients With Pancreatic Ductal Adenocarcinoma. *Clin Cancer Res* (2020) 26(14):3641–8. doi: 10.1158/1078-0432.Ccr-19-4044
9. Hanahan D, Weinberg RA. Hallmarks of Cancer: The Next Generation. *Cell* (2011) 144(5):646–74. doi: 10.1016/j.cell.2011.02.013

10. Hensley CT, Faubert B, Yuan Q, Lev-Cohain N, Jin E, Kim J, et al. Metabolic Heterogeneity in Human Lung Tumors. *Cell* (2016) 164(4):681–94. doi: 10.1016/j.cell.2015.12.034
11. Faubert B, Li KY, Cai L, Hensley CT, Kim J, Zacharias LG, et al. Lactate Metabolism in Human Lung Tumors. *Cell* (2017) 171(2):358. doi: 10.1016/j.cell.2017.09.019
12. Chen PH, Cai L, Huffman K, Yang CD, Kim J, Faubert B, et al. Metabolic Diversity in Human non-Small Cell Lung Cancer Cells. *Mol Cell* (2019) 76 (5):838. doi: 10.1016/j.molcel.2019.08.028
13. Kim SM, Yun MR, Hong YK, Solca F, Kim JH, Kim HJ, et al. Glycolysis Inhibition Sensitizes Non-Small Cell Lung Cancer With T790M Mutation to Irreversible Egfr Inhibitors Via Translational Suppression of Mcl-1 by AMPK Activation. *Mol Cancer Ther* (2013) 12(10):2145–56. doi: 10.1158/1535-7163.Mct-12-1188
14. Vander Heiden MG, DeBerardinis RJ. Understanding the Intersections Between Metabolism and Cancer Biology. *Cell* (2017) 168(4):657–69. doi: 10.1016/j.cell.2016.12.039
15. Chen JB, Yang HC, Teo ASM, Amer LB, Sherbaf FG, Tan CQ, et al. Genomic Landscape of Lung Adenocarcinoma in East Asians. *Nat Genet* (2020) 52 (2):177. doi: 10.1038/s41588-019-0569-6
16. Kim N, Kim HK, Lee K, Hong Y, Cho JH, Choi JW, et al. Single-Cell RNA Sequencing Demonstrates the Molecular and Cellular Reprogramming of Metastatic Lung Adenocarcinoma. *Nat Commun* (2020) 11(1):2285. doi: 10.1038/s41467-020-16164-1
17. Lv L, Zhao YJ, Wei QQ, Zhao Y, Yi QY. Downexpression of HSD17B6 Correlates With Clinical Prognosis and Tumor Immune Infiltrates in Hepatocellular Carcinoma. *Cancer Cell Int* (2020) 20:210. doi: 10.1186/s12935-020-01298-5
18. Li CW, Lim SO, Chung EM, Kim YS, Park AH, Yao J, et al. Eradication of Triple-Negative Breast Cancer Cells by Targeting Glycosylated PD-L1. *Cancer Cell* (2018) 33(2):187. doi: 10.1016/j.ccell.2018.01.009
19. Suo C, Yang YJ, Yuan ZY, Zhang TJ, Yang XR, Qing T, et al. Alcohol Intake Interacts With Functional Genetic Polymorphisms of Aldehyde Dehydrogenase (ALDH2) and Alcohol Dehydrogenase (ADH) to Increase Esophageal Squamous Cell Cancer Risk. *J Thoracic Oncol* (2019) 14(4):712–25. doi: 10.1016/j.jtho.2018.12.023
20. Chan YX, Yeap BB. Dihydrotestosterone and Cancer Risk. *Curr Opin Endocrinol* (2018) 25(3):209–17. doi: 10.1097/Med.0000000000000411
21. Forde PM, Chaft JE, Smith KN, Anagnostou V, Cottrell TR, Hellmann MD, et al. Neoadjuvant PD-1 Blockade in Resectable Lung Cancer. *N Engl J Med* (2018) 378(21):1976–86. doi: 10.1056/NEJMoa1716078
22. Gao S, Li N, Gao S, Xue Q, Ying J, Wang S, et al. Neoadjuvant PD-1 Inhibitor (Sintilimab) in NSCLC. *J Thorac Oncol* (2020) 15(5):816–26. doi: 10.1016/j.jtho.2020.01.017
23. Shu CA, Gainor JF, Awad MM, Chiuzan C, Grigg CM, Pabani A, et al. Neoadjuvant Atezolizumab and Chemotherapy in Patients With Resectable non-Small-Cell Lung Cancer: An Open-Label, Multicentre, Single-Arm, Phase 2 Trial. *Lancet Oncol* (2020) 21(6):786–95. doi: 10.1016/S1470-2045(20)30140-6
24. Provencio M, Nadal E, Insa A, Garcia-Campelo MR, Casal-Rubio J, Domine M, et al. Neoadjuvant Chemotherapy and Nivolumab in Resectable non-Small-Cell Lung Cancer (NADIM): An Open-Label, Multicentre, Single-Arm, Phase 2 Trial. *Lancet Oncol* (2020) 21(11):1413–22. doi: 10.1016/S1470-2045(20)30453-8
25. Pignon JP, Tribodet H, Scagliotti GV, Douillard JY, Shepherd FA, Stephens RJ, et al. Lung Adjuvant Cisplatin Evaluation: A Pooled Analysis by the LACE Collaborative Group. *J Clin Oncol* (2008) 26(21):3552–9. doi: 10.1200/Jco.2007.13.9030
26. Zuo SG, Wei M, Zhang HL, Chen AX, Wu JH, Wei JW, et al. A Robust Six-Gene Prognostic Signature for Prediction of Both Disease-Free and Overall Survival in non-Small Cell Lung Cancer. *J Transl Med* (2019) 17(1):152. doi: 10.1186/s12967-019-1899-y
27. Liu Y, Wu LG, Ao HJ, Zhao M, Leng X, Liu MD, et al. Prognostic Implications of Autophagy-Associated Gene Signatures in non-Small Cell Lung Cancer. *Aging-Us* (2019) 11(23):11440–62. doi: 10.18632/aging.102544
28. Li Y, Sun N, Lu ZL, Sun SG, Huang JB, Chen ZL, et al. Prognostic Alternative mRNA Splicing Signature in non-Small Cell Lung Cancer. *Cancer Lett* (2017) 393:40–51. doi: 10.1016/j.canlet.2017.02.016
29. Shukla S, Evans JR, Malik R, Feng FY, Dhanasekaran SM, Cao XH, et al. Development of a RNA-Seq Based Prognostic Signature in Lung Adenocarcinoma. *JNCI-J Natl Cancer I* (2017) 109(1):djw200. doi: 10.1093/jnci/djw200
30. Eggermont AM, Chiarion-Sileni V, Grob JJ, Dummer R, Wolchok JD, Schmidt H, et al. Adjuvant Ipilimumab Versus Placebo After Complete Resection of High-Risk Stage III Melanoma (EORTC 18071): A Randomised, Double-Blind, Phase 3 Trial. *Lancet Oncol* (2015) 16(5):522–30. doi: 10.1016/S1470-2045(15)70122-1
31. Weber J, Mandala M, Del Vecchio M, Gogas HJ, Arance AM, Cowey CL, et al. Adjuvant Nivolumab Versus Ipilimumab in Resected Stage III or IV Melanoma. *N Engl J Med* (2017) 377(19):1824–35. doi: 10.1056/NEJMoa1709030
32. Liu J, Blake SJ, Yong MCR, Harjunpaa H, Ngiow SF, Takeda K, et al. Improved Efficacy of Neoadjuvant Compared to Adjuvant Immunotherapy to Eradicate Metastatic Disease. *Cancer Discov* (2016) 6(12):1382–99. doi: 10.1158/2159-8290.Cd-16-0577
33. Zhong WZ, Wang Q, Mao WM, Xu ST, Wu L, Shen Y, et al. Gefitinib Versus Vinorelbine Plus Cisplatin as Adjuvant Treatment for Stage II-IIIA (N1-N2) EGFR-mutant NSCLC (ADJUVANT/CTONG1104): A Randomised, Open-Label, Phase 3 Study. *Lancet Oncol* (2018) 19(1):139–48. doi: 10.1016/S1470-2045(17)30729-5
34. Zhong WZ, Chen KN, Chen C, Gu CD, Wang J, Yang XN, et al. Erlotinib Versus Gemcitabine Plus Cisplatin as Neoadjuvant Treatment of Stage Iiia-N2 EGFR-Mutant non-Small-Cell Lung Cancer (Emerging-CTONG 1103): A Randomized Phase Ii Study. *J Clin Oncol* (2019) 37(25):2235. doi: 10.1200/Jco.19.00075

Conflict of Interest: The authors declare that the research was conducted in the absence of any commercial or financial relationships that could be construed as a potential conflict of interest.

Copyright © 2021 Hu, Yu, Sun, Yan, Zhang, Jiang and Zhang. This is an open-access article distributed under the terms of the Creative Commons Attribution License (CC BY). The use, distribution or reproduction in other forums is permitted, provided the original author(s) and the copyright owner(s) are credited and that the original publication in this journal is cited, in accordance with accepted academic practice. No use, distribution or reproduction is permitted which does not comply with these terms.

frontiers in Oncology

ORIGINAL RESEARCH
published: 07 May 2021
doi: 10.3389/fonc.2021.657283

Efficacy and Resistance of Afatinib in Chinese Non-Small Cell Lung Cancer Patients With *HER2* Alterations: A Multicenter Retrospective Study

Zhengbo Song[1,2†], Dongqing Lv[3†], Shiqing Chen[4†], Jianhui Huang[5], Liping Wang[6], Shuguang Xu[7], Huafei Chen[8], Guoqiang Wang[4] and Quan Lin[9*]*

[1] Department of Clinical Trial, The Cancer Hospital of the University of Chinese Academy of Sciences (Zhejiang Cancer Hospital), Hangzhou, China, [2] Institute of Basic Medicine and Cancer (IBMC), Chinese Academy of Sciences, Hangzhou, China, [3] Department of Respiratory Disease, Taizhou Hospital, Taizhou, China, [4] The Medical Department, 3D Medicines Inc, Shanghai, China, [5] Department of Medical Oncology, Lishui Center Hospital, Lishui, China, [6] Department of Medical Oncology, Baotou Cancer Hospital, Baotou, China, [7] Department of Respiratory Disease, Ningbo Medical Center, Lihuili Eastern Hospital, Ningbo, China, [8] Department of Thoracic Disease Center, Rongjun Hospital, Jiaxing, China, [9] Department of Pulmonary Medicine, The First Affiliated Hospital of Wenzhou Medical University, Wenzhou, China

OPEN ACCESS

Edited by:
Hideharu Kimura,
Kanazawa University,
Japan

Reviewed by:
Sagun Parakh,
University of Melbourne,
Australia
Valerio Gristina,
University of Palermo,
Italy

***Correspondence:**
Quan Lin
lquan007@163.com
Zhengbo Song
songzhengbo83@163.com

†These authors have contributed equally to this work

Specialty section:
This article was submitted to Thoracic Oncology, a section of the journal Frontiers in Oncology

Received: 22 January 2021
Accepted: 06 April 2021
Published: 07 May 2021

Citation:
Song Z, Lv D, Chen S, Huang J, Wang L, Xu S, Chen H, Wang G and Lin Q (2021) Efficacy and Resistance of Afatinib in Chinese Non-Small Cell Lung Cancer Patients With HER2 Alterations: A Multicenter Retrospective Study. Front. Oncol. 11:657283. doi: 10.3389/fonc.2021.657283

Background: Non-small cell lung cancer (NSCLC) patients with *HER2* mutations and amplification may benefit from HER2-targeted therapy, including afatinib. However, the data regarding the clinical activity of afatinib in Chinese patients with NSCLC harboring *HER2* alterations are limited.

Patients and methods: We retrospectively included metastatic NSCLC patients harboring *HER2* alterations who treated with afatinib. The clinical outcomes included overall response rate (ORR), progression-free survival (PFS) and overall survival (OS). The genomic profiling data after progression on afatinib were analyzed.

Results: We included 54 patients harboring *HER2* mutations and 12 patients harboring *HER2* amplification. The ORR was 24% (95% CI, 16–36%), the median PFS was 3.3 months (95% CI, 2.2–4.4), and the median OS was 13.9 months (95% CI, 11.4–16.5). Patients with *HER2* exon 20 mutations had numerically worse ORR (17% *vs* 42%), shorter PFS (2.6 *vs* 5.8 months, HR, 2.5; 95% CI, 1.2–5.5; $P = 0.015$) and OS (12.9 *vs* 33.3 months, HR, 4.4; 95% CI, 1.3–14.8; $P = 0.009$) than patients with other mutations. For HER2-amplified patients, the ORR was 33% (95% CI, 14–61%), the median PFS was 3.3 months (95% CI, 2.6–4.0), and the median OS was 13.4 months (95% CI, 0–27.6). The most frequently mutated genes in afatinib-resistant patients were *TP53* (44%) and *EGFR* (33%). Three afatinib-resistant patients harbored secondary *HER2* alterations.

Conclusions: Our results suggest that afatinib has a promising anti-tumor activity in patients with NSCLC harboring *HER2* alterations. To our knowledge, this is the largest retrospective study about the clinical activity of afatinib in NSCLC patients with *HER2* alterations.

Keywords: non-small cell lung cancer (NSCLC), *HER2*, afatinib, efficacy, resistance

INTRODUCTION

Lung cancer is one of the most common malignant tumors, causing approximate 25% of the total cancer-related deaths (1). About 85% of patients with lung cancer are histologically diagnosed as non-small cell lung cancer (NSCLC) (2). Several driver genes alterations, including *EGFR* (epidermal growth factor receptor) activating mutations, *ALK* (anaplastic lymphoma kinase) rearrangement, *ROS1* (repressor of silencing 1) fusions, *BRAF* (B-Raf proto-oncogene, serine/threonine kinase) mutations, *MET* (MET proto-oncogene, receptor tyrosine kinase) alterations, and *RET* (ret proto-oncogene) fusions, are frequently detected in the patients with NSCLC (3). Targeted therapies based on these genes have been approved by the Food and Drug Administration (FDA), changing the treatment of NSCLC (4).

Human epidermal growth factor receptor 2 (*HER2*, also known as *ERBB2*) is a cancer driver gene, and 1.7–3% of NSCLC patients harbor *HER2* mutations (5–7). Most *HER2* mutations in NSCLC are present in exon 20, such as Y772_A775dup and G778_P780dup. In addition, *HER2* gene amplification occurs in 3 to 14.3% of lung adenocarcinomas (7–9). *HER2* activating mutations and amplification may activate tyrosine kinase and downstream signaling pathways, therefore conferring sensitivity to HER2-targeted therapy, such as trastuzumab, ado-trastuzumab (T-DM1) and tyrosine kinase inhibitors (TKIs). At present, T-DM1 is the only recommended HER2-targeted inhibitor for *HER2*-mutated NSCLC patients by National Comprehensive Cancer Network (NCCN) Guidelines, with an overall response rate (ORR) of 44% (10). However, no *HER2*-targeted therapy has been approved for patients with NSCLC harboring *HER2* mutations or amplification.

Afatinib is an irreversible ERBB family inhibitor, which has been approved for *EGFR*-mutated lung cancer and become one of the most common therapy in NSCLC patients. In a phase II trial with 13 advanced NSCLC with *HER2* exon 20 mutations, the overall response rate (ORR) of afatinib as second-line treatment was 7.7% and the median progression-free survival (PFS) was 15.9 weeks (11). Several retrospective trials revealed better activity of afatinib in patients with *HER2* exon 20 mutations, with an ORR from 13 to 33% (5, 12–15). However, the interpretation of the results from all these studies were limited by the small sample sizes. In addition, the efficacy of HER2-TKI in patients with *HER* mutations besides *HER2* exon 20 mutations and *HER2* amplification has been rarely studied. Seven patients with other *HER2* mutations except exon 20 mutations were enrolled into the phase II trial of T-DM1, and two of these patients had a partial response, with a S310F (exon 8) mutation and a V659E (exon 17) mutation, respectively (10). Another research showed that three of four NSCLC patients with V659E or G660R (exon 17, located in transmembrane domain) achieved responses from afatinib treatment (16).

Herein, we conducted a multicenter, retrospective study to analyze the anti-tumor activity of afatinib in patients with NSCLC harboring *HER2* alterations including mutations and amplification. Furthermore, we tried to explore the potential secondary resistant mechanisms of afatinib by next generation sequencing (NGS). We present the following article/case in accordance with the STROBE reporting checklist.

METHODS

Patients and Study Design

This multicenter, retrospective study included patients with non-small cell lung cancer (NSCLC) harboring *HER2* alteration treated with afatinib between May 2015 and July 2019, from Zhejiang Cancer Hospital, Taizhou Hospital, Baotou Cancer Hospital, Lihuili Eastern Hospital and Rongjun Hospital. Eligible patients were 18 years or older, and had a diagnosis of stage IV NSCLC, a *HER2* alteration, measurable disease as per investigator-assessed Response Evaluation Criteria in Solid Tumors (RECIST), v1.1. Patients received afatinib at a dose of 40 mg daily until disease progression or intolerable adverse events. This retrospective study was approved by the Institutional Review Board Committee of Zhejiang Cancer Hospital. Research was conducted in accordance with the 1964 Declaration of Helsinki and its later amendments. The informed consent was waived because of the retrospective nature of this study.

Data Collection and Response Assessment

Baseline clinical information were collected from electronic medical records, including age, sex, Eastern Cooperative Oncology Group (ECOG) performance status, tumor histology, smoking status, *HER2* alteration subtype, and afatinib treatment line. These clinical data were verified independently by two oncologist physicians. Tumor size measurement according to radiologic imaging was conducted by radiologists. Best response was determined according to Response Evaluation Criteria in Solid Tumors (RECIST, v1.1). The outcomes were ORR, PFS, and overall survival (OS). ORR was defined as the proportion of patients who have a partial response (PR) or complete response (CR). PFS was defined as the time interval from initial afatinib treatment to progression or death from any cause. OS was defined as the duration from the beginning of afatinib treatment to death from any cause.

Molecular Testing

The baseline *HER2* gene alterations were tested by NGS in an accredited local laboratory (for example as shown in **Figure S1**). Genomic profiling when progression on afatinib treatment was tested in a CLIA-accredited/CAP-certified laboratory (3D Medicines Inc., Shanghai, China). The NGS panel targeted cancer-related genes was performed on the NextSeq500 platform (Illumina, CA, USA) (17). DNA extracts (30–200 ng) were sheared to 250 bp fragments using an S220 focused-ultrasonicator (Covaris). Libraries were prepared using the

KAPA Hyper Prep Kit (KAPA Biosystems) following the manufacturer's protocol. The captured libraries were loaded onto a NextSeq500 platform for 100 bp paired-end sequencing with a mean sequencing depth of 500×.

Raw data of paired samples (an FFPE sample and its normal tissue control) were mapped to the reference human genome hg19 using the Burrows–Wheeler Aligner (v0.7.12). PCR duplicate reads were removed and sequence metrics were collected using Picard (v1.130) and SAMtools (v1.1.19), respectively. Variant calling was performed only in the targeted regions. Somatic single nucleotide variants (SNVs) were detected using an in-house developed R package to execute a variant detection model based on binomial test. Local realignment was performed to detect indels. Variants were then filtered by their unique supporting read depth, strand bias, base quality as previously described. All variants were then filtered using an automated false positive filtering pipeline to ensure sensitivity and specificity at an allele frequency (AF) of ≥1%. Single-nucleotide polymorphism (SNPs) and indels were annotated by ANNOVAR against the following databases: dbSNP (v138), 1000Genome and ESP6500 (population frequency >0.015). Only missense, stopgain, frameshift and non-frameshift indel mutations were kept. Copy number variations (CNVs) and gene rearrangements were detected. The interpretation of variants were based on American College of Medical Genetics and Genomics (ACMG) standards and guidelines.

Statistical Analyses

All statistical analyses were conducted using the SPSS statistical package, version 20.0 (SPSS Inc®, Chicago, Illinois, USA) and GraphPad prism v6 (GraphPad, La Jolla, CA, USA). The PFS and OS were estimated by Kaplan–Meier curves, with *P* value determined by a log-rank test. And we calculated hazard ratio (HR) and its 95% confidence intervals (CIs) by Cox regression. Univariate and multivariate analyses were performed by Cox proportional hazard model. A two-sided $P < .05$ was considered statistically significant.

RESULTS

Baseline Characteristics

A total of 66 patients with lung cancer were included in this retrospective study. The baseline characteristics are shown in **Table 1**. The median age was 59 years (range, 30–81), and 65% (43/66) were female. Eight patients (12%) had an Eastern Cooperative Oncology Group (ECOG) performance status of 2 and the rest were ECOG 0–1. Most patients were adenocarcinoma (92%, 61/66) and non-smokers (67%, 44/66). Ten (15%) patients had brain metastases. All the patients received afatinib as a single agent. The median line of afatinib treatment was 2 (range, 1–7). Twenty-four patients (36%, 24/66) received afatinib as first-line therapy, and 42 patients (64%, 42/66) as second-line or beyond therapy (**Table 1**). The median follow-up period was 13.9 months (range: 2.1–39.5).

Fifty-four patients (82%) harbored mutations in *HER2* gene (**Figure 1**), most of which were identified in exon 20 (78%, 42/54). In addition, twelve patients carried *HER2* amplification. Among the patients with *HER2*-mutated lung cancer, the most common mutation was Y772_A775dup (33%, 18/54), followed by G778_P780dup (19%, 10/54) and G776delinsVC/LC (15%, 8/54).

Clinical Activity of Afatinib in NSCLC Patients With HER2 Alterations

The responses to afatinib were evaluated according to RECIST 1.1 (**Figure 2**), and the best response to afatinib was partial response (PR) in 16 patients (24%), stable disease (SD) in 24 patients (36%), and progressive disease (PD) in 26 patients (39%, **Table 2**). The ORR was 24% (95% CI, 16–36%), and disease control rate (DCR) was 61% (95% CI, 49–72%).

As data cutoff, 62 (94%) out of 66 patients had died or had disease progression and 40 (61%) patients had died. The median PFS was 3.3 months (95% CI, 2.2–4.4), and the median OS was 13.9 months (95% CI, 11.4–16.5) (**Table 2** and **Figure 3**). The median duration of response was 7.1 months (95%CI, 6.4–7.7 months). Furthermore, we deeply analyzed the efficacy of

TABLE 1 | Baseline characteristics.

Sex, n (%)	
Male	23 (35%)
Female	43 (65%)
Age, years	
Median (range)	59 (30–81)
ECOG performance status, n (%)	
0	12 (18%)
1	46 (70%)
2	8 (12%)
Histology, n (%)	
Adenocarcinoma	61 (92%)
Squamous carcinoma	4 (6%)
Adenosquamous carcinoma	1 (2%)
Smoking status, n (%)	
Yes	21 (32%)
No	44 (67%)
Unknown	1 (2%)
Number of metastases	
Median (range)	2 (1–7)
Previous treatments	
Chemotherapy	39 (59%)
Bevacizumab	4 (6%)
TKI	3 (5%)
Anti-PD-1/L1 inhibitors	2 (3%)
Afatinib treatment line, n (%)	
First	24 (36%)
Second or beyond	42 (64%)
HER2 alterations, n (%)	
HER2 mutations	54 (82%)
exon 20 mutations	42
other mutations	12
HER2 amplification	12 (18%)

ECOG, Eastern Cooperative Oncology Group; HER2, Human epidermal growth factor receptor 2; TKI, tyrosine kinase inhibitor.

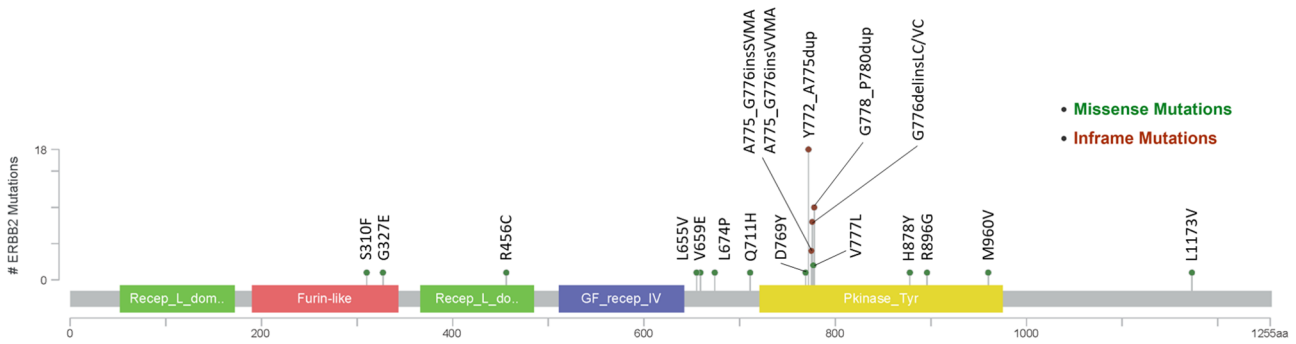

FIGURE 1 | *HER2* mutational map.

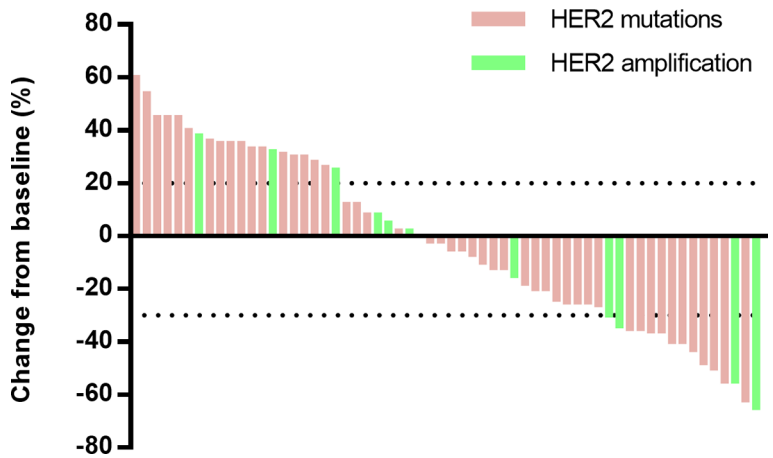

FIGURE 2 | Maximum percentage change from baseline in target lesions.

afatinib in patients with different *HER2* alterations. Among the patients with a *HER2* mutation, the ORR, mPFS and mOS were 22%, 3.4 months (95% CI, 1.4–4.7) and 14.6 months (95% CI, 11.6–17.6), similar with the whole cohort (**Table 3**). In addition, four of the patients with *HER2* amplification (33%, 4/12) achieved a PR (**Figure 2**). The mPFS and mOS of these patients were respectively 3.3 months (95% CI, 2.6–4.0) and 13.4 months (95% CI, 0–27.6), comparable to those of the patients with a *HER2* mutation (**Figures 3C, D**).

Since *HER2* exon 20 mutation is the most common mutation for *HER2* in patients with NSCLC, we further compared the outcomes of patients with exon 20 mutation and other mutations. As for *HER2* exon 20 mutations, the total ORR was 17%, and the ORRs of the patients with Y772_A775dup mutation and G778_P780dup were 33 and 10%, respectively, while the ORR was 0% in patients with other exon 20 mutations including G776delinsVC/LC, A775_G776insSVMA, A775_G776insVVMA, and V777L (**Table 3**). In patients with other *HER2* mutations, five (42%) out of 12 patients achieved a PR (L655V [exon 17], H878Y [exon 21], R896G [exon 22], M960V [exon 24] and L1173V [exon 27]). Patients with *HER2* exon 20 mutations had worse PFS (2.6 *vs* 5.8 months, HR, 2.5; 95% CI, 1.2–5.5; $P = 0.015$) and OS (12.9 *vs* 33.3 months, HR, 4.4; 95% CI, 1.3–14.8; $P = 0.009$) than patients with other *HER2* mutations (**Figure S2**).

We also performed subgroup analysis according afatinib treatment lines. The ORR was 42% in patients who received afatinib as first-line treatment compared with 14% in those who received afatinib as secondary-line or beyond treatment. Patients who received afatinib as secondary-line or beyond treatment had shorter PFS and OS compared with patients who received afatinib as first-line treatment (mPFS = 2.7 *vs* 4.7 months; OS = 11.2 *vs* 15.6 months; **Figure S3**). Multivariate analysis showed that afatinib treatment line and brain metastasis were associated with PFS ($P = 0.026$ and 0.017, respectively), and ECOG performance status was associated with OS ($P = 0.046$) (**Tables S1** and **S2**).

Potential Biomarkers for Resistance to Afatinib

To reveal potential biomarkers of resistance to afatinib, NGS was performed from blood or tissue samples of nine patients after progression on afatinib treatment. Pathogenic and likely pathogenic mutations were analyzed. We observed most patients (78%, 7/9) still harbored *HER2* alterations after afatinib treatment (**Table S3**). Among these patients, three patients harbored secondary *HER2* alterations (p.G776delinsLC [patient 3], Y772_A775dup [patient 4], and amplification [patient 6], **Table S3**). The most frequently mutated genes in afatinib-resistant patients were *TP53* (44%) and *EGFR* (33%). Besides, one patient carried a *NRAS* mutation and another patient had no *HER2* alteration nor other pathogenic mutation when progression on afatinib (**Table S3**).

TABLE 2 | Clinical activity of afatinib in NSCLC patients with *HER2* alterations.

Variable	
Best response, n (%)	
Partial response	16 (24%)
Stable disease	24 (36%)
Progressive disease	26 (39%)
Overall response rate, %	24%
Disease control rate, %	61%
Progression-free survival	
Events, n (%)	62 (94%)
Median, months (95% CI)	3.3 (2.2–4.4)
Overall survival	
Events, n (%)	40 (61%)
Median, months (95% CI)	13.9 (11.4–16.5)

CI, confidence interval.

DISCUSSION

In the present study, afatinib showed promising anti-tumor activity in patients with NSCLC harboring *HER2* alterations including *HER2* exon 20 mutations, other mutations and *HER2* amplification. To our knowledge, this is the largest retrospective study on clinical activity of afatinib in NSCLC patients with *HER2* alterations.

Most previous studies focused on *HER2* exon 20 insertions. Recent studies reported that NSCLC patients with *HER2* exon 20 insertions had an ORR of 13–19% from afatinib treatment (14, 15, 18). The sole to date prospective study (11) on afatinib in NSCLC patients with *HER2* exon 20 insertions only enrolled 13 patients, with a modest clinical outcomes (ORR = 7.7%). In the largest cohort of NSCLC patients with *HER2* exon 20 insertions, Mazières et al. (12) reported clinical activity of chemotherapy and HER2-targeted drugs. The ORR of the patients (N = 29) treated with TKIs (neratinib, afatinib, and lapatinib) was 7.4%. Among the patients (N = 11) who were treated with afatinib, the ORR was 18.2%. In the present study, most *HER2* mutations were exon 20 insertions (61%), which was similar with previous studies. We observed an ORR of 17% in these patients, which was comparable with previous retrospective studies. Of the patents with most common Y772_A775dup mutation, ORR was 33%, which suggests that these patients might have better clinical outcome from afatinib.

Moreover, we found *HER2* other mutations except exon 20 mutations were also sensitive to afatinib. Five (42%) of these patients achieved response from afatinib treatment. Among these patients who were response to afatinib, one patient with a L655V (exon 17) mutation had a PFS of 8.1 months. L655V (exon 17) is located in transmembrane domain (TMD) that is important to

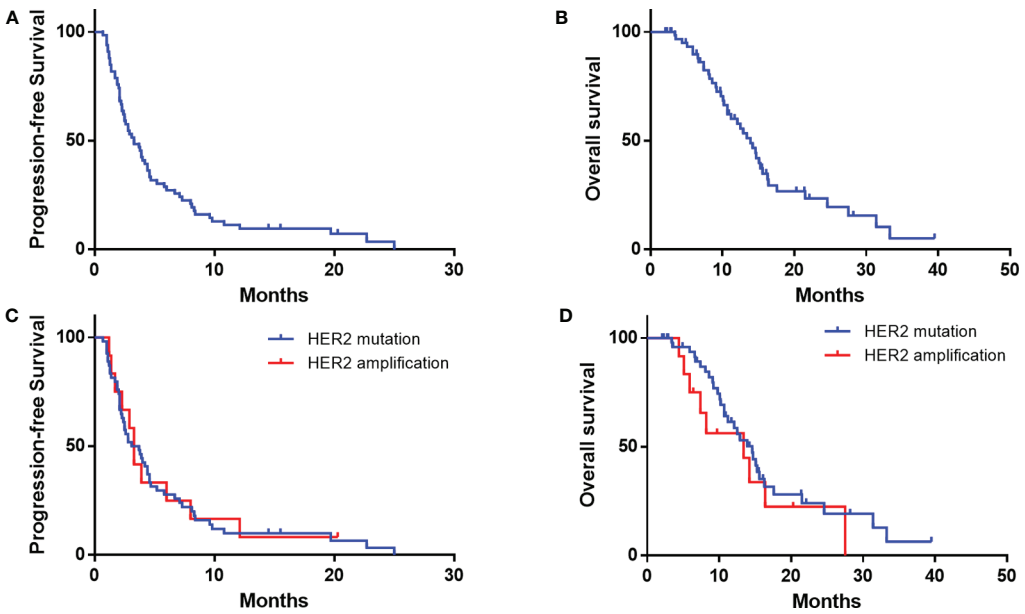

FIGURE 3 | Kaplan–Meier estimates of progression-free survival and overall survival of NSCLC Patients with *HER2* alterations. **(A, B)** progression-free survival and overall survival of the whole cohort; **(C, D)** progression-free survival and overall survival according to *HER2* mutations or amplification.

TABLE 3 | Clinical Activity of Afatinib according to *HER2* alterations.

***HER2* alterations**	**ORR, %**	**mPFS, month (95%CI)**	**mOS, month (95%CI)**
Mutations	22%	3.4 (1.4–4.7)	14.6 (11.6–17.6)
exon 20 mutations	17%	2.6 (0.9–4.1)	12.9 (8.8–17.0)
Y772_A775dup	33%		
G778_P780dup	10%		
G776delinsVC/LC	0		
775_G776insSVMA	0		
A775_G776insVVMA	0		
V777L	0		
other mutations	42%	5.8 (0–10.1)	33.3 (1.2–65.5)
Amplification	33%	3.3 (2.6–4.0)	13.4 (0–27.6)

CI, confidence interval; HER2, Human epidermal growth factor receptor 2; mOS, median overall survival; mPFS, median progression-free survival; ORR, overall response rate.

stabilize the active *HER2* homodimer (19). And L655V is close to V659/G660, which were demonstrated to be sensitive to afatinib (16). One lung squamous cell carcinoma patient with a *HER2* R896G (exon 22) mutation had a long PFS of 14.5 months, which was recently reported as a case report (20). Another patient with a M960V (exon 24) mutation received afatinib as third-line therapy, and achieved a PR and a PFS of 7.1 months. The other two patients respectively harbored H878Y (exon 21) and L1173V (exon 27), and the PFS were 22.7 and 25.0 months, respectively. These results suggest that the patients with *HER2* other mutations except exon 20 mutations could also benefit from HER2-targeted inhibitors.

So far, the standard care for NSCLC patients with *HER2* amplification is chemotherapy. Although T-DM1 is recommended by NCCN Guidelines for *HER2*-mutated NSCLC patients, no *HER2*-targerd inhibitors are approved for NSCLC patients with *HER2* mutations or amplification. In a phase II trial of dacomitinib in lung cancer patients with *HER2* alterations, none of four patients with *HER2*-amplified tumors responded (21). Recently, two studies on *HER*-mutated NSCLC patients treated with pyrotinib, a pan-HER inhibitor, showed that ORRs were 53.3 and 30%, and mPFSs were 6.4 months and 6.9 months, respectively (22, 23). An *in vitro* study and phase II trial demonstrated another pan-HER inhibitor poziotinib had potent clinical activity against *HER2* mutations (24, 25). In breast cancer, gastric Cancer, and colorectal cancer, *HER2* amplification was demonstrated to be associated with the clinical outcomes of HER2-targeted treatment (26, 27). In this study, we presented an ORR of 33% in the NSCLC patients with *HER2* amplification, and this is the first time that clinical activity of afatinib in *HER2*-amplified NSCLC patients has been reported. These results indicate HER2-targeted treatment might be one of the choices for these patients.

Primary and acquired resistance is the main reason for progression disease when patients received TKIs treatment. Currently, we know much about the mechanisms for resistance of EGFR-targeted treatment, but researches about resistance to HER2-targerted inhibitors in NSCLC patients are lacking. Chuang et al. (13) suggested PIK3CA mutation and *HER2* gene amplification may be the potential mechanisms for resistance during HER2-targeted treatment. However, the results were analyzed from four cases, which is hard to reach statistical significance. Herein, we performed NGS for nine patients when progression on afatinib treatment. Of three patients harbored secondary *HER2* alterations, two carried a *HER2* exon 20 insertion and another carried *HER2* amplification as secondary alteration. Previous studies demonstrated that secondary ALK mutations could induce resistance of ALK inhibitors (28, 29). Whether *HER2* secondary alterations resistance mechanism to afatinib need to be determined in further studies. In addition, we found *TP53* was recurrently mutated (44%) in afatinib-resistant patients. Several studies reported that *TP53* mutations were associated with inferior clinical effect of EGFR-targeted inhibitors (30–32). One patient harbored *TP53* and *RB1* co-mutations, which were associated with an increasing risk for small cell transformation and resistance to TKIs treatment (33–36).

This study still has several limitations. Firstly, we cannot completely avoid the reporting bias because of this work's retrospective nature. Secondly, due to a lack of control arm, comparison with other therapies was not feasible. Thirdly, only nine patients were performed NGS when progression, so these data cannot fully reflect the whole cohort and no statistical significance can be reached about resistance of afatinib. Despite these limitations, this study provides deep insights into clinical activity of afatinib in NSCLC with *HER2* alterations.

CONCLUSION

Our results suggest that afatinib has a potential efficacy in these patients, especially in the patients with *HER2* amplification or other pathologic mutations in exons except exon 20. Further studies, especially prospective studies, are warranted to investigate the clinical activity of afatinib and the mechanism of resistance to HER2-targeted therapy.

DATA AVAILABILITY STATEMENT

The original contributions presented in the study are included in the article. Further inquiries can be directed to the corresponding authors.

ETHICS STATEMENT

The studies involving human participants were reviewed and approved by Zhejiang Cancer Hospital. The patients/participants provided their written informed consent to participate in this study.

AUTHOR CONTRIBUTIONS

All authors listed have made a substantial, direct, and intellectual contribution to the work, and approved it for publication. ZS and QL contributed to the study design. All authors were responsible for interpretation of the results. ZS and SC contributed to statistical analysis. ZS and SC prepared the manuscript. All authors contributed to the article and approved the submitted version.

SUPPLEMENTARY MATERIAL

The Supplementary Material for this article can be found online at: https://www.frontiersin.org/articles/10.3389/fonc.2021.657283/full#supplementary-material

Supplementary Figure 1 | Next-generation sequencing result showed a *HER2* Y772_A775dup mutation. The BAM file was viewed using integrative genomics viewer.

Supplementary Figure 2 | Kaplan-Meier estimates of progression-free survival and overall survival according to according to *HER2* mutations. **(A)** progression-free survival; **(B)** overall survival.

Supplementary Figure 3 | Kaplan-Meier estimates of progression-free survival and overall survival according to lines of treatment. **(A)** progression-free survival; **(B)** overall survival.

REFERENCES

1. Siegel RL, Miller KD, Fuchs HE, Jemal A. Cancer Statistics, 2021. *CA Cancer J Clin* (2021) 71(1):7–33. doi: 10.3322/caac.21654
2. Herbst RS, Morgensztern D, Boshoff C. The Biology and Management of non-Small Cell Lung Cancer. *Nature* (2018) 553(7689):446–54. doi: 10.1038/nature25183
3. Hirsch FR, Scagliotti GV, Mulshine JL, Kwon R, Curran WJJr., Wu YL, et al. Lung Cancer: Current Therapies and New Targeted Treatments. *Lancet* (2017) 389(10066):299–311. doi: 10.1016/S0140-6736(16)30958-8
4. Thomas A, Liu SV, Subramaniam DS, Giaccone G. Refining the Treatment of NSCLC According to Histological and Molecular Subtypes. *Nat Rev Clin Oncol* (2015) 12(9):511–26. doi: 10.1038/nrclinonc.2015.90
5. Mazieres J, Peters S, Lepage B, Cortot AB, Barlesi F, Beau-Faller M, et al. Lung Cancer That Harbors an HER2 Mutation: Epidemiologic Characteristics and Therapeutic Perspectives. *J Clin Oncol* (2013) 31(16):1997–2003. doi: 10.1200/JCO.2012.45.6095
6. Song Z, Yu X, Shi Z, Zhao J, Zhang Y. HER2 Mutations in Chinese Patients With non-Small Cell Lung Cancer. *Oncotarget* (2016) 7(47):78152–8. doi: 10.18632/oncotarget.11313
7. Li BT, Ross DS, Aisner DL, Chaft JE, Hsu M, Kako SL, et al. Her2 Amplification and HER2 Mutation Are Distinct Molecular Targets in Lung Cancers. *J Thorac Oncol* (2016) 11(3):414–9. doi: 10.1016/j.jtho.2015.10.025
8. Kim EK, Kim KA, Lee CY, Shim HS. The frequency and Clinical Impact of HER2 Alterations in Lung Adenocarcinoma. *PloS One* (2017) 12(2):e0171280. doi: 10.1371/journal.pone.0171280
9. Lee J, Franovic A, Shiotsu Y, Kim ST, Kim KM, Banks KC, et al. Detection of ERBB2 (Her2) Gene Amplification Events inand Response to Anti-HER2 Agents in a Large Asian Cancer Patient Cohort. *Front Oncol* (2019) 9:212. doi: 10.3389/fonc.2019.00212
10. Li BT, Shen R, Buonocore D, Olah ZT, Ni A, Ginsberg MS, et al. Ado-Trastuzumab Emtansine for Patients With HER2-Mutant Lung Cancers: Results From a Phase Ii Basket Trial. *J Clin Oncol* (2018) 36(24):2532–7. doi: 10.1200/JCO.2018.77.9777
11. Dziadziuszko R, Smit EF, Dafni U, Wolf J, Wasag B, Biernat W, et al. Afatinib in NSCLC With HER2 Mutations: Results of the Prospective, Open-Label Phase Ii NICHE Trial of European Thoracic Oncology Platform (Etop). *J Thorac Oncol* (2019) 14(6):1086–94. doi: 10.1016/j.jtho.2019.02.017
12. Mazieres J, Barlesi F, Filleron T, Besse B, Monnet I, Beau-Faller M, et al. Lung Cancer Patients With HER2 Mutations Treated With Chemotherapy and HER2-targeted Drugs: Results From the European EUHER2 Cohort. *Ann Oncol* (2016) 27(2):281–6. doi: 10.1093/annonc/mdv573
13. Chuang JC, Stehr H, Liang Y, Das M, Huang J, Diehn M, et al. Erbb2-Mutated Metastatic non-Small Cell Lung Cancer: Response and Resistance to Targeted Therapies. *J Thorac Oncol* (2017) 12(5):833–42. doi: 10.1016/j.jtho.2017.01.023
14. Liu Z, Wu L, Cao J, Yang Z, Zhou C, Cao L, et al. Clinical Characterization of ERBB2 Exon 20 Insertions and Heterogeneity of Outcomes Responding to Afatinib in Chinese Lung Cancer Patients. *Onco Targets Ther* (2018) 11:7323–31. doi: 10.2147/OTT.S173391
15. Lai WV, Lebas L, Barnes TA, Milia J, Ni A, Gautschi O, et al. Afatinib in Patients With Metastatic or Recurrent HER2-mutant Lung Cancers: A Retrospective International Multicentre Study. *Eur J Cancer* (2019) 109:28–35. doi: 10.1016/j.ejca.2018.11.030
16. Ou SI, Schrock AB, Bocharov EV, Klempner SJ, Haddad CK, Steinecker G, et al. Her2 Transmembrane Domain (Tmd) Mutations (V659/G660) That Stabilize Homo- and Heterodimerization are Rare Oncogenic Drivers in Lung Adenocarcinoma That Respond to Afatinib. *J Thorac Oncol* (2017) 12(3):446–57. doi: 10.1016/j.jtho.2016.11.2224
17. Yang N, Li Y, Liu Z, Qin H, Du D, Cao X, et al. The Characteristics of ctDNA Reveal the High Complexity in Matching the Corresponding Tumor Tissues. *BMC Cancer* (2018) 18(1):319. doi: 10.1186/s12885-018-4199-7
18. Peters S, Curioni-Fontecedro A, Nechushtan H, Shih JY, Liao WY, Gautschi O, et al. Activity of Afatinib in Heavily Pretreated Patients With ERBB2 Mutation-Positive Advanced Nsclc: Findings From a Global Named Patient Use Program. *J Thorac Oncol* (2018) 13(12):1897–905. doi: 10.1016/j.jtho.2018.07.093
19. Bocharov EV, Lesovoy DM, Pavlov KV, Pustovalova YE, Bocharova OV, Arseniev AS. Alternative Packing of EGFR Transmembrane Domain Suggests That Protein-Lipid Interactions Underlie Signal Conduction Across Membrane. *Biochim Biophys Acta* (2016) 1858(6):1254–61. doi: 10.1016/j.bbamem.2016.02.023
20. Lin L, Ge H, Yan Z, Wang G, Wu X, Lv D. Response to Afatinib in a Patient With Non-Small Cell Lung Cancer Harboring Her2 R896G Mutation: A Case Report. *Onco Targets Ther* (2019) 12:10897–902. doi: 10.2147/OTT.S228726
21. Kris MG, Camidge DR, Giaccone G, Hida T, Li BT, O'Connell J, et al. Targeting HER2 Aberrations as Actionable Drivers in Lung Cancers: Phase II Trial of the pan-HER Tyrosine Kinase Inhibitor Dacomitinib in Patients With HER2-mutant or Amplified Tumors. *Ann Oncol* (2015) 26(7):1421–7. doi: 10.1093/annonc/mdv186
22. Wang Y, Jiang T, Qin Z, Jiang J, Wang Q, Yang S, et al. HER2 Exon 20 Insertions in non-Small-Cell Lung Cancer are Sensitive to the Irreversible pan-HER Receptor Tyrosine Kinase Inhibitor Pyrotinib. *Ann Oncol* (2019) 30(3):447–55. doi: 10.1093/annonc/mdy542
23. Zhou C, Li X, Wang Q, Gao G, Zhang Y, Chen J, et al. Pyrotinib in HER2-Mutant Advanced Lung Adenocarcinoma After Platinum-Based Chemotherapy: A Multicenter, Open-Label, Single-Arm, Phase Ii Study. *J Clin Oncol* (2020) 38(24):2753–61. doi: 10.1200/JCO.20.00297
24. Koga T, Kobayashi Y, Tomizawa K, Suda K, Kosaka T, Sesumi Y, et al. Activity of a Novel HER2 Inhibitor, Poziotinib, for HER2 Exon 20 Mutations in Lung Cancer and Mechanism of Acquired Resistance: An In Vitro Study. *Lung Cancer* (2018) 126:72–9. doi: 10.1016/j.lungcan.2018.10.019
25. Robichaux JP, Elamin YY, Vijayan RSK, Nilsson MB, Hu L, He J, et al. Pan-Cancer Landscape and Analysis of ERBB2 Mutations Identifies Poziotinib as a Clinically Active Inhibitor and Enhancer of T-DM1 Activity. *Cancer Cell* (2019) 36(4):444–57.e7. doi: 10.1016/j.ccell.2019.09.001
26. Oh DY, Bang YJ. HER2-Targeted Therapies - a Role Beyond Breast Cancer. *Nat Rev Clin Oncol* (2020) 17(1):33–48. doi: 10.1038/s41571-019-0268-3
27. Siena S, Sartore-Bianchi A, Marsoni S, Hurwitz HI, McCall SJ, Penault-Llorca F, et al. Targeting the Human Epidermal Growth Factor Receptor 2 (HER2)

Oncogene in Colorectal Cancer. *Ann Oncol* (2018) 29(5):1108–19. doi: 10.1093/annonc/mdy100
28. Gainor JF, Dardaei L, Yoda S, Friboulet L, Leshchiner I, Katayama R, et al. Molecular Mechanisms of Resistance to First- and Second-Generation Alk Inhibitors in ALK-Rearranged Lung Cancer. *Cancer Discovery* (2016) 6 (10):1118–33. doi: 10.1158/2159-8290.CD-16-0596
29. Katayama R. Drug Resistance in Anaplastic Lymphoma Kinase-Rearranged Lung Cancer. *Cancer Sci* (2018) 109(3):572–80. doi: 10.1111/cas.13504
30. Labbe C, Cabanero M, Korpanty GJ, Tomasini P, Doherty MK, Mascaux C, et al. Prognostic and Predictive Effects of TP53 Co-Mutation in Patients With EGFR-mutated non-Small Cell Lung Cancer (NSCLC). *Lung Cancer* (2017) 111:23–9. doi: 10.1016/j.lungcan.2017.06.014
31. Canale M, Petracci E, Delmonte A, Chiadini E, Dazzi C, Papi M, et al. Impact of TP53 Mutations on Outcome in EGFR-Mutated Patients Treated With First-Line Tyrosine Kinase Inhibitors. *Clin Cancer Res* (2017) 23(9):2195–202. doi: 10.1158/1078-0432.CCR-16-0966
32. Yu HA, Suzawa K, Jordan E, Zehir A, Ni A, Kim R, et al. Concurrent Alterations in EGFR-Mutant Lung Cancers Associated With Resistance to EGFR Kinase Inhibitors and Characterization of MTOR as a Mediator of Resistance. *Clin Cancer Res* (2018) 24(13):3108–18. doi: 10.1158/1078-0432.CCR-17-2961
33. George J, Lim JS, Jang SJ, Cun Y, Ozretic L, Kong G, et al. Comprehensive Genomic Profiles of Small Cell Lung Cancer. *Nature* (2015) 524(7563):47–53. doi: 10.1038/nature14664
34. Niederst MJ, Sequist LV, Poirier JT, Mermel CH, Lockerman EL, Garcia AR, et al. RB Loss in Resistant EGFR Mutant Lung Adenocarcinomas That Transform to Small-Cell Lung Cancer. *Nat Commun* (2015) 6:6377. doi: 10.1038/ncomms7377
35. Offin M, Chan JM, Tenet M, Rizvi HA, Shen R, Riely GJ, et al. Concurrent RB1 and TP53 Alterations Define a Subset of EGFR-Mutant Lung Cancers At Risk for Histologic Transformation and Inferior Clinical Outcomes. *J Thorac Oncol* (2019) 14(10):1784–93. doi: 10.1016/j.jtho.2019.06.002
36. Marcoux N, Gettinger SN, O'Kane G, Arbour KC, Neal JW, Husain H, et al. Egfr-Mutant Adenocarcinomas That Transform to Small-Cell Lung Cancer and Other Neuroendocrine Carcinomas: Clinical Outcomes. *J Clin Oncol* (2019) 37(4):278–85. doi: 10.1200/JCO.18.01585

Conflict of Interest: Authors SC and GW were employed by company 3D Medicines Inc.

The remaining authors declare that the research was conducted in the absence of any commercial or financial relationships that could be construed as a potential conflict of interest.

Copyright © 2021 Song, Lv, Chen, Huang, Wang, Xu, Chen, Wang and Lin. This is an open-access article distributed under the terms of the Creative Commons Attribution License (CC BY). The use, distribution or reproduction in other forums is permitted, provided the original author(s) and the copyright owner(s) are credited and that the original publication in this journal is cited, in accordance with accepted academic practice. No use, distribution or reproduction is permitted which does not comply with these terms.

frontiers in Oncology

ORIGINAL RESEARCH
published: 21 May 2021
doi: 10.3389/fonc.2021.644575

OPEN ACCESS

Edited by:
Meng Xu Welliver,
The Ohio State University,
United States

Reviewed by:
Paul Emile Van Schil,
Antwerp University Hospital,
Belgium
Mohsen Ibrahim,
Sapienza University of Rome,
Italy

***Correspondence:**
Xinyi Xia
xiaxynju@163.com
Pengping Li
lipengping@njmu.edu.cn
Zhi Zhang
zz5223404@163.com
Renhua Guo
rhguo@njmu.edu.cn

†These authors have contributed equally to this work and share first authorship

Specialty section:
This article was submitted to Thoracic Oncology, a section of the journal Frontiers in Oncology

Received: 21 December 2020
Accepted: 23 April 2021
Published: 21 May 2021

Citation:
Wang Q, Li L, Qu T, Li J, Wu L, Li K, Wang Z, Zhu M, Huang B, Wu W, Wu M, Ding R, Zhang Z, Wang Q, Xia X, Li P, Zhang Z and Guo R (2021) High Expression of ACE2 and TMPRSS2 at the Resection Margin Makes Lung Cancer Survivors Susceptible to SARS-CoV-2 With Unfavorable Prognosis. Front. Oncol. 11:644575. doi: 10.3389/fonc.2021.644575

High Expression of *ACE2* and *TMPRSS2* at the Resection Margin Makes Lung Cancer Survivors Susceptible to SARS-CoV-2 With Unfavorable Prognosis

Qianqian Wang[1†], Liangyu Li[2,3†], Tianyu Qu[1†], Jie Li[2,3†], Lingxiang Wu[2,3], Kening Li[2,3], Ziyu Wang[2,3], Mengyan Zhu[2,3], Bin Huang[2,3], Wei Wu[2,3], Min Wu[2,3], Rong Ding[2,3], Zhihong Zhang[4], Qianghu Wang[2,3], Xinyi Xia[5,6,7], Pengping Li[2,3*], Zhi Zhang[8*] and Renhua Guo[1*]*

[1] Department of Oncology, The First Affiliated Hospital of Nanjing Medical University, Nanjing, China, [2] Center for Global Health, School of Public Health, Nanjing Medical University, Nanjing, China, [3] Department of Bioinformatics, Nanjing Medical University, Nanjing, China, [4] Department of Pathology, The First Affiliated Hospital of Nanjing Medical University, Nanjing, China, [5] Institute of Laboratory Medicine, Jinling Hospital, Nanjing University School of Medicine, Southern Medical University, Nanjing, China, [6] Department of Laboratory Medicine & Blood Transfusion, Wuhan Huoshenshan Hospital, Wuhan, China, [7] Joint Expert Group, Wuhan Huoshenshan Hospital, Wuhan, China, [8] Department of Thoracic Surgery, Jiangsu Cancer Hospital and Jiangsu Institute of Cancer Research and Nanjing Medical University Affiliated Cancer Hospital, Nanjing, China

Background: Coronavirus disease 2019 (COVID-19) has rapidly spread worldwide. Systematic analysis of lung cancer survivors at molecular and clinical levels is warranted to understand the disease course and clinical characteristics.

Methods: A single-center, retrospective cohort study was conducted in 65 patients with COVID-19 from Wuhan Huoshenshan Hospital, of which 13 patients were diagnosed with lung cancer. The study was conducted from February 4 to April 11, 2020.

Results: During the course of treatment, lung cancer survivors infected with severe acute respiratory syndrome coronavirus 2 (SARS-COV-2) had shorter median time from symptom onset to hospitalization (P = 0.016) and longer clinical symptom remission time (P = 0.020) than non-cancer individuals. No differences were observed among indicators such as time from symptom onset to hospitalization and symptom remission time between medium-term and short-term survivors. The expression of *ACE2* (P = 0.013) and *TMPRSS2* (P <0.001) was elevated in lung cancer survivors as compared with that in non-cancer individuals.

Conclusions: *ACE2* and *TMPRSS2* levels were higher at resection margins of lung cancer survivors than those in normal tissues of non-cancerous individuals and may serve as factors responsible for the high susceptibility to COVID-19 among lung cancer survivors. Lung cancer patients diagnosed with COVID-19, including medium-term survivors, have worse outcomes than the general population.

Keywords: COVID-19, lung cancer, *ACE2*, single cell, tmprss2

INTRODUCTION

The outbreak of coronavirus disease 2019 (COVID-19) induced by severe acute respiratory syndrome coronavirus 2 (SARS-COV-2) has rapidly spread around the world (1), affecting more than 214 countries and regions. By July 28, 2020, over 17,000,000 infected cases and 670,000 deaths have been reported worldwide, and the virus continuous to rapidly spread in many countries (COVID-19 Map Johns Hopkins University and Medicine). The World Health Organization (WHO) declared COVID-19 a public health emergency of international concern and announced the current outbreak as a global pandemic.

Coronaviruses are a large family of viruses known to cause diseases ranging from common cold to more severe illnesses such as Middle East respiratory syndrome (MERS) and SARS (2, 3). In comparison with SARS and MERS, COVID-19 exhibits milder clinical impairment but shows a dramatically higher human-to-human transmission rate (4–6). SARS-CoV-2 has been reported to enter cells *via* binding to angiotensin-converting enzyme 2 (*ACE2*) and its co-factor transmembrane protease serine 2 (*TMPRSS2*), which are expressed in the lung and bronchial branches (6). Therefore, the high expression of *ACE2* and *TMPRSS2* in the lung may serve as the molecular mechanism underlying the susceptibility to SARS-CoV-2. The lung is the most frequently targeted organ in lung cancer and COVID-19 pneumonia. Recent studies have demonstrated the aberrant expression of *ACE2* in many tumors and the higher level of *ACE2* in lung adenocarcinoma (LUAD) tissues (7, 8). Lung cancer is the most common cancer and a leading cause of cancer-related death worldwide (9). Surgical resection remains the primary and preferred approach for the treatment of stages I and II non-small cell lung cancer (NSCLC) (10). The expression of *ACE2* and *TMPRSS2* in resection margin tissues, not tumors, of lung cancer survivors is more representative of the susceptibility to SARS-CoV-2.

In the present study, we compared the expression levels of *ACE2* and *TMPRSS2* at the resection margins of lung cancer patients as well as in normal tissues of non-cancer individuals to investigate the susceptibility of lung cancer patients to COVID-19. In addition, we retrospectively collected and analyzed detailed clinical data from lung cancer patients with laboratory-confirmed COVID-19 infection at the Wuhan Huoshenshan Hospital to help clinicians with the accurate treatment.

Abbreviations: COVID-19, Coronavirus disease 2019; SARS-COV-2, Severe acute respiratory syndrome coronavirus 2; MERS, Middle East respiratory syndrome; ACE2, Angiotensin-converting enzyme 2; TMPRSS2, Transmembrane protease serine 2; LUAD, Lung adenocarcinoma; NSCLC, Non-small cell lung cancer; CT, Computed tomography; TCGA, The Cancer Genome Atlas; PGK1, Phosphoglycerate kinase 1; IQR, Interquartile range; AT2, Type II alveolar cells.

MATERIALS AND METHODS

Microarray Data Analysis

The sequencing data of resection margin tissues from lung cancer patients were obtained from The Cancer Genome Atlas (TCGA) database and included 59 LUAD patients and 51 lung squamous cell carcinoma (LUSC) patients. Data on normal lung tissues from the general population were obtained from the GTEx database (https://gtexportal.org/home/) (n = 288). Phosphoglycerate kinase 1 (*PGK1*) was used for normalization between two different databases.

Single-Cell RNA-Sequencing Data Analysis

The single-cell RNA-sequencing data of resection margin tissues and normal lung tissues were obtained from existing studies (11) and subjected to analysis *via* the Seurat R package (version 3.0, https://satijalab.org/seurat/). *EPCAM* and *IDH1* were used to identify epithelial cells. The copy number score of cells was predicted using the inferCNV R package (https://github.com/broadinstitute/infercnv).

Immunohistochemistry (IHC)

After surgery, lung tissues obtained from patients with lung cancer or benign lung disease were prepared as formalin-fixed paraffin-embedded sections. Samples were cut into 4-μm-thick serial sections, deparaffinized with xylene, and rehydrated in alcohol. The samples were subsequently submerged in an antigen retrieval buffer and microwaved for antigen fixation. Sections were treated with hydrogen peroxide to block endogenous nonspecific binding activity and incubated for overnight at 4°C with diluted primary antibodies. Slides were incubated with appropriate horseradish peroxidase-conjugated secondary antibodies at 37°C for 1 h. Rabbit anti-cytokeratin 19 (CK19) antibody (Abcam, Cambridge, UK) was used as the primary antibody. Negative control slides were treated as per the same protocol except that the primary antibody was replaced with phosphate-buffered saline (PBS).

Study Population and Data Collection

We carried out a retrospective case study at the Wuhan Huoshenshan Hospital, which was specially built to treat patients infected with COVID-19. Between 4 February and 11

April, 2020, 13 patients previously diagnosed with lung cancer and with laboratory-confirmed COVID-19 were enrolled. We used propensity score matching methods to select 52 patients as a control group with appropriate controls for other factors (e.g., age, sex, and comorbidities) to investigate the impact of lung cancer on COVID-19 as an independent factor. MatchIt function of R was used to achieve it, and the covariates are gender, age, and comorbidities, such as hypertension, diabetes, with ratio = 4. Clinical data were extracted from the hospital electronic medical records, including demographic features, clinical symptoms, laboratory and chest computed tomography (CT) results, treatments, and outcomes. This study was approved by the Medical Ethical Committee of Wuhan Huoshenshan Hospital. Written informed consent was obtained from each patient.

Study Definitions

The severity of COVID-19 was evaluated as per the Seventh Revised Trial Version of the Novel Coronavirus Pneumonia Diagnosis and Treatment Guidance. (http://www.nhc.gov.cn/yzygj/s7652m/202003/a31191442e29474b98bfed5579d5af95.shtml) (8). Based on the sixth grade scale score proposed by Cao (http://www.chictr.org.cn/showproj.aspx?proj=49081) (12), time for clinical symptom remission was defined as the patient's admission status as "discharged" or "a score reduction by two points." Lung cancer patients with a survival time of more than 3 years were defined as medium-term survivors.

Statistical Analysis

For descriptive analysis, continuous variables were summarized as medians and interquartile range (IQR), and categorical variables, as counts and percentages. The Wilcoxon rank-sum test or Fisher's exact test was used to compare differences between groups, as appropriate. All statistical analyses were performed using SPSS Statistics Version 24.0 (IBM, New York, NY) and R studio (Version 1.2.1335; R Studio, Inc.). A two-sided value of P <0.05 was considered statistically significant.

RESULTS

ACE2 and *TMPRSS2* Are Overexpressed at Resection Margins of Lung Cancer Patients

Several studies have shown that coronaviruses enter cells *via* binding of the viral spike (S) proteins to cellular receptors *ACE2* and following S protein priming by host cell proteases. *TMPRSS2* as a transmembrane protease can induce the virus-plasma membrane fusion (13, 14). Hoffmann and coworkers recently demonstrated that SARS-CoV-2 uses the SARS-CoV receptor *ACE2* for entry and the serine protease *TMPRSS2* for S protein priming (15, 16). *ACE2* is broadly expressed in epithelial cells (6). We then evaluated if resection margins of lung cancer harbor more epithelial cells. We collected three resection margin tissues from lung cancer patients who underwent surgical treatment at Jiangsu Provincial Hospital in May 2020 and three other non-cancerous lung tissues. The surgical pathological stages of these three patients were all stage I, and so far, no tumor recurrence has occurred in the three patients (detailed information of control patients is listed in **Table S1**). We performed IHC to investigate the population of epithelial cells among the two groups, and found that the percentage of the stained area was much higher in the resection margin tissues than in the non-cancerous tissues (**Figures 1A, B**). We analyzed single-cell sequencing data from the existing research (11) and found that the epithelial cells at the resection margin of lung cancer were more likely to highly activate the genes related to lung cancer, such as *KRAS*, *MET*, and *EGFR* (**Figures 1C, D**). The genomic instability of these cells inferred by inferCNV (see *Materials and Methods*) in the resection margin was much higher than that in the normal tissues (**Figure 1E**), and these cells had stronger capability for invasion and infiltration (**Figure 1F**). These findings suggested that the cells at the margin of resection were more likely to be a sort of tumor-like cells.

The proportion of epithelial cells expressing *ACE2* and *TMPRSS2* was higher at the resection margin of lung cancers than in normal tissues (**Figure 1G**), suggesting that the resection margins of lung cancer tissues were still more susceptible to COVID-19 infection. We also analyzed the expression of *ACE2* in resection margin tissues of lung cancer survivors and normal lung tissues from general individuals using TCGA (n = 110) and GTEx (n = 288) databases and found that the mRNA expression of *ACE2* was higher in lung cancer patients than in general individuals (Wilcoxon's rank-sum test, $P = 0.013$) (**Figure 1H**). The expression of *TMPRSS2*, the co-factor of *ACE2*, was also significantly higher in lung cancer patients than in the general population (Wilcoxon's rank-sum test, $P < 0.001$) (**Figure 1H**), suggesting that patients with lung cancer were more likely to be susceptible to COVID-19.

To further verify our findings, we compare the median value of *ACE2* expression in different SARS-Cov-2 infected cell lines from GSE147507 (17) (**Figure 1I**). And we found the score of the signature SARS-Cov-2 infection identified by Li et al. (18) is significantly higher in *ACE2* high expressed cell lines than *ACE2* low expressed cell lines (Student's t-test, $P < 0.05$) (**Figure 1J**), indicating high *ACE2* expressed cells may be more susceptible to SARS-Cov-2, suggesting that patients with lung cancer were more likely to be susceptible to COVID-19.

Clinical Characteristics and Outcomes of Lung Cancer Patients With COVID-19 Infection

Records of 3,057 patients with confirmed COVID-19 infection were collected from the Wuhan Huoshenshan Hospital between February 4 and April 11, 2020. Thirteen patients (0.43%) who suffered from lung cancer and 52 matched patients were enrolled (see *Materials and Methods*). The demographic and clinical features of these patients are shown in **Table 1**. The median (IQR) age of lung cancer patients was 65 (63–72) years, and 10 (76.9%) of them were men. The most common comorbidities were hypertension and diabetes observed in 30.8% patients. No significant differences were found in age, sex, and main symptoms and signs between the case and control groups.

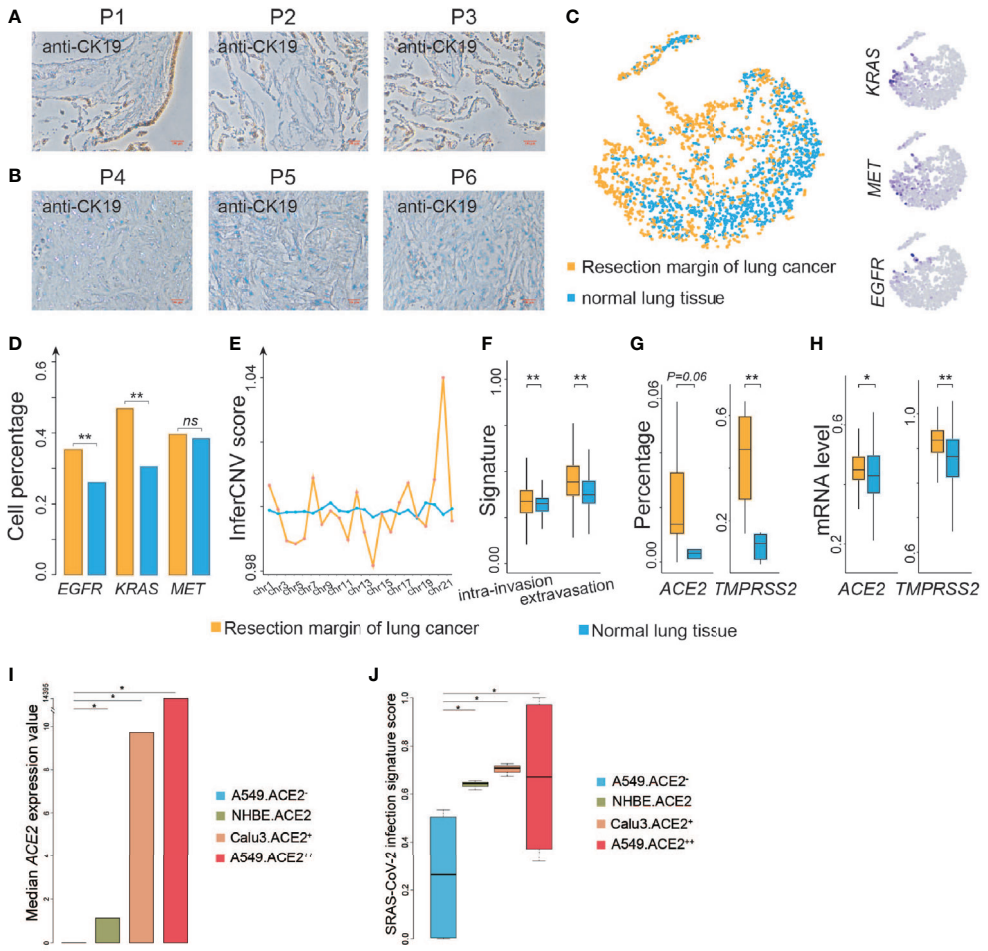

FIGURE 1 | *ACE2* and *TMPRSS2* are highly expressed at resection margins of lung cancer patients. **(A)** Immunohistochemistry images of resection margin tissues from lung cancer patients using anti-CK19 antibody. **(B)** Immunohistochemistry images of non-cancer samples using anti-CK19 antibody. **(C)** Left: t-SNE plot of epithelial cells from the resection margins of lung cancers and normal lung tissues. Right: Distribution of the indicated cell marker genes overlaid on a 2D-tSNE plot. **(D)** Comparison of the percentage of indicated genes expressed in epithelial cells between the resection margin of lung cancers and normal lung tissues. **(E)** Comparison of inferCNV scores of cells between the resection margin of lung cancers and normal tissues across indicated chromosomes. **(F)** Comparison of intra-invasion and extravasation signature scores between indicated groups. **(G)** Comparison of the percentage of *ACE2* and *TMPRSS2* expressed in cells between indicated groups. **(H)** Comparison of mRNA levels of *ACE2* and *TMPRSS2* between indicated groups. **(I)** Bar plot shows median value of *ACE2* expression in different cell lines. A549.ACE2-, none *ACE2* expressed SARS-Cov-2 infected A549 cell lines; NHBE.ACE2, low *ACE2* expressed SARS-CoV-2 infected primary human lung epithelium cell lines; Calu3.ACE2+, median *ACE2* expressed SARS-Cov-2 infected Calu3 cell lines; A549.ACE2++, high *ACE2* expressed SARS-Cov-2 infected A549 cell lines. **(J)** Boxplot shows SARS-Cov-2 infection signature score in different cell lines as shown in **(I)**. *P < 0.05 (Wilcoxon rank sum test), **P < 0.01 (Wilcoxon rank sum test), NS, not significant.

Further, the most prevalent symptom among the 65 enrolled patients was fever (n = 50, 76.9%), followed by cough (n = 41, 63.1%), fatigue (n = 30, 46.2%), and shortness of breath (n = 26, 40.0%).

One out of the thirteen patients died (7.7%) due to severe infection caused by COVID-19, while the remaining twelve patients were cured and discharged from the hospital. Five out of the thirteen lung cancer patients survived for more than three years, these five patients did not receive any anti-tumor treatment within three months before and after infection with COVID-19. The remaining eight patients were diagnosed with lung cancer less than three years, two of them did not receive any anti-tumor treatment within three months before and after infection, and six were infected with COVID-19 during anti-tumor treatment (detailed information of patients is listed in **Table S2**).

Patients with lung cancer were more likely to have dyspnea (15.4% *vs.* 1.9%; $P = 0.040$) than the other groups. Five of these patients were medium-term survivors, and none of them was diagnosed with stage IV cancer. All patients received at least one kind of antitumor treatment, including surgery ($n = 7$, 53.8%), chemotherapy ($n = 6$, 46.2%), epidermal growth factor receptor tyrosine kinase inhibitor (EGFR-TKI) therapy ($n = 2$, 15.4%), anti-angiogenesis therapy ($n = 1$, 7.7%), and radiotherapy ($n = 2$, 15.4%), while none of the medium-term survivors received

TABLE 1 | Characteristics of patients with COVID-19.

Characteristic	All patients (*n* = 65)	Lung cancer (*n* = 13)	Non-lung cancer (*n* = 52)	*P* value
Age, years	66 (56–72)	65 (63–72)	66 (56–72)	0.761
Sex				0.779
Male	48 (73.8%)	10 (76.9%)	38 (73.1%)	
Female	17 (26.2%)	3 (23.1%)	14 (26.9%)	
Comorbidities				
Any	38 (58.5%)	8 (61.5%)	30 (57.7%)	0.803
Hypertension	22 (33.8%)	4 (30.8%)	18 (34.6%)	0.795
Diabetes	17 (26.2%)	4 (30.8%)	13 (25.0%)	0.674
Chronic obstructive pulmonary disease	3 (4.6%)	1 (7.7%)	2 (3.8%)	0.557
Coronary heart disease	3 (4.6%)	1 (7.7%)	2 (3.8%)	0.557
Cerebrovascular disease	5 (7.7%)	1 (7.7%)	4 (7.7%)	1.000
Chronic liver disease	4 (6.2%)	3 (23.1%)	1 (1.9%)	0.005
Symptoms and signs				
Fever	50 (76.9%)	9 (69.2%)	41 (78.8%)	0.465
Chill	13 (20.0%)	2 (15.4%)	11 (21.2%)	0.644
Chest pain	1 (1.5%)	0 (0.0%)	1 (1.9%)	0.617
Cough	41 (63.1%)	8 (61.5%)	33 (63.4%)	0.257
Fatigue	30 (46.2%)	4 (30.8%)	26 (50.0%)	0.217
Shortness of breath	26 (40.0%)	5 (38.5%)	21 (40.4%)	0.126
Chest tightness	7 (10.8%)	3 (23.1%)	4 (7.7%)	0.112
Expectoration	10 (15.4%)	3 (23.1%)	7 (13.5%)	0.394
Dyspnea	3 (4.6%)	2 (15.4%)	1 (1.9%)	**0.040**
Diarrhea	3 (4.6%)	1 (7.7%)	2 (3.8%)	0.557
Headache	3 (4.6%)	0 (0.0%)	3 (5.8%)	0.379
Myalgia	12 (18.5%)	3 (23.1%)	9 (17.3%)	0.634
Nausea	1 (1.5%)	0 (0.0%)	1 (1.9%)	0.617
Vomiting	2 (3.1%)	0 (0.0%)	2 (3.8%)	0.476

Bold value of p-value means P < 0.05.

treatment within past 3 months. The percentage of medium-term survivors who underwent surgery was four-fold higher than that of short-term survivors (100.0% *vs*. 25.0%, $P = 0.011$). No difference was observed in comorbidities and symptoms between medium- and short-term survivors (**Table S3**).

During the course of treatment, development of severe infection was more common among lung cancer patients (Wilcoxon's rank-sum test, $P = 0.064$) (**Table 2**). The duration of symptoms before hospital admission in lung cancer patients was 10.5 (10.0–17.5) days, which was significantly shorter than that observed in other patients [30.0 (14.0–35.0); Wilcoxon's rank-sum test, $P = 0.016$] (**Table 2**). Moreover, the average time to clinical improvement in lung cancer patients was 12 (11.0–18.0) days, which was 4 days longer than that observed in non-cancer patients (5.8–14.0) (Wilcoxon's rank-sum test, $P = 0.020$) (**Table 2**). There were no differences among indicators such as time from symptoms to hospitalization and symptom remission time between medium-term and short-term survivors (**Table 3**).

DISCUSSION

In this study, we show that lung cancer patients infected with SARS-COV-2 tend to have more severe outcomes as compared to

TABLE 2 | Outcome of lung cancer patients and general population.

Characteristic	All (*n* = 65)	Lung cancer (*n* = 13)	Non-lung cancer (*n* = 52)	*P* value
Hospital stay (days)	11.0 (8.0–18.0)	13.0 (11.0–18.0)	10.0 (7.0–17.3)	0.178
Most critical type during hospitalization				0.064
Mild/Moderate	29 (44.6%)	3 (23.1%)	27 (51.9%)	
Severe/Critical	35 (53.8%)	10 (76.9%)	25 (48.1%)	
Time from symptoms to hospitalization (days)	19.0 (10.0–35.0)	10.5 (10.0–17.5)	30.0 (14.0–35.0)	**0.016**
Clinical symptoms remission time (days)	9.0 (6.0–15.0)	12.0 (11.0–18.0)	8.0 (5.8–14.0)	**0.020**
Admission to intensive care unit				0.433
Yes	4 (6.2%)	2 (15.4%)	2 (3.8%)	
No	61 (93.8%)	11 (84.6%)	50 (96.2%)	
ICU stay (days)	16.5 (13.5–21.5)	13.5 (11.3–15.8)	23.5 (19.3–27.8)	
Clinical outcomes				**0.046**
Discharge from hospital	64 (98.5%)	12 (92.3%)	52 (100.0%)	
Death	1 (1.5%)	1 (7.7%)	0 (0.0%)	
Time from diagnosis to death (days)	18.0 (18.0–18.0)	18.0 (18.0–18.0)	–	–

Bold value of p-value means P < 0.05.

TABLE 3 | Outcome of medium-term and short-term lung cancer survivor.

Characteristic	Lung cancer (*n* = 13)	Medium-term survivor (*n* = 5)	Short-term survivor (*n* = 8)	*P* value
Hospital stay (days)	13.0 (11.0–18.0)	13.0 (12.0–19.0)	13.5 (10.5–16.5)	1.000
Most critical type during hospitalization				0.841
Mild/Moderate	3 (23.1%)	1 (20.0%)	2 (25.0%)	
Severe/Critical	10 (76.9%)	4 (80.0%)	6 (75.0%)	
Time from symptoms to hospitalization (days)	10.0 (10.0–16.0)	14.0 (10.0–16.0)	10.0 (9.3–15.8)	0.552
Clinical symptoms remission time (days)	12.0 (11.0–18.0)	12.0 (11.0–19.0)	13.0 (10.5–17.3)	1.000
Admission to intensive care unit				0.221
Yes	2 (15.4%)	0 (0%)	2 (25.0%)	
No	11 (84.6%)	5 (100%)	6 (75.0%)	
ICU stay (days)	13.5 (11.3–15.8)	–	13.5 (11.3–15.8)	–
Clinical outcomes				0.429
Discharge from hospital	12 (92.3%)	5 (100%)	7 (87.5%)	
Death	1 (7.7%)	0 (0%)	1 (12.5%)	
Time from diagnosis to death (days)	18.0 (18.0–18.0)	–	18.0 (18.0–18.0)	–

the general population. The mortality was higher in the lung cancer cohort than in the control cohort and the difference was statistically significant, consistent with previous findings (19). However, the mortality (7.7%, 1/13) observed in our study was higher than that reported in the general population (2.3%) and lower than that (18.18%; 4/22) noted in a multicenter study (19, 20). Lung cancer patients seemed to be more likely to develop severe infection but without any significant difference (P = 0.064). This trend is consistent with that observed in previous studies (21–23). The median time from symptom onset to hospitalization was shorter and the clinical symptom remission time was longer in lung cancer patients infected with SARS-COV-2 than in the general population, indicating that the disease develops more rapidly in lung cancer patients. Thus, lung cancer patients represent a highly vulnerable group to the current COVID-19 outbreak.

Medium-term lung cancer survivors and short-term lung cancer patients had unexpectedly similar outcomes. Recent studies associated the increased risk of developing severe events in cancer patients to their systemic immunosuppressive state caused by antitumor treatments such as chemotherapy, radiotherapy, targeted therapy, and immunotherapy (21, 23). Our results seem to contradict those of previous studies, probably owing to the higher expression detected at the resection margin of lung cancer patients. The non-significance may not rule out the differences between medium-term and short-term lung cancer patients owing to the small sample size.

We also explored the differences in the expression of *ACE2* and *TMPRSS2* in resection margin tissues of lung cancer patients and normal lung tissues of non-cancerous patients. *ACE2* gene expression at the resection margin was higher than that in normal lung tissues, while *TMPRSS2* showed even higher expression. Given that elevated levels of *ACE2* and *TMPRSS2* may indicate higher susceptibility to SARS-CoV-2 (15), our findings show that lung cancer patients are more vulnerable to SARS-CoV-2. A recent study analyzed the expression of *ACE2* across over 30 tumors and reported *ACE2* overexpression in LUAD (7). Another study investigated the expression of *ACE2* and *TMPRSS2* genes in LUAD and LUSC and suggested higher and nearly equal *ACE2* expression in LUAD and LUSC tumor tissues than in normal tissues, respectively (8). These authors also profiled the expression of *ACE2* and *TMPRSS2* genes in each pathological stage of two lung cancer types and found consistent expression patterns in each pathological stage of lung cancer, suggesting equal susceptibility to SARS-CoV-2 among patients with different pathological stages of LUAD and LUSC (8). These two studies with consistent results imply that patients with lung cancer are more vulnerable to SARS-CoV-2 attacks. However, the expression of *ACE2* and *TMPRSS2* in resection margin tissues may be more valuable in medium-term lung cancer survivors.

The increase in the population of epithelial cells in resection margin tissues may be the possible mechanism that deems lung cancer patients highly susceptible to SARS-CoV-2. Previous studies have confirmed the high expression of *ACE2* and *TMPRSS2* in type II alveolar cells (AT2), an epithelial cell type (6, 24). Interestingly, our results show that epithelial cells were enriched in resection margin tissues and showed upregulated expression of *ACE2* and *TMPRSS2*. Despite cancer resection, the remaining tissue still retains the characteristics of cancer cells, such as genome instability and strong local infiltration and extravasation abilities. As *ACE2* and *TMPRSS2* are overexpressed in lung cancer (7, 8), their expression may be high at the resection margin of lung cancer patients. To our knowledge, this is the first study to compare the expression of *ACE2* and *TMPRSS2* in resection margin tissues of lung cancer patients and normal lung tissues from non-cancerous individuals. Our results may explain why medium-term lung cancer survivors are more susceptible to SARS-CoV-2 and highly vulnerable to the COVID-19 pandemic. These results indicate stronger personal protection not only for short-term lung cancer patients but also for medium-term survivors.

In our study, we found one out of thirteen (7.7%) median-term survival cancer patients died with the infection of SARS-COV-2, diagnosed with a series of infection symptoms, including fever, cough, shortness of breath, expectoration, dyspnea. Many studies show lung cancer patients have a higher mortality rate than the general population which is similar to our finding. For instance, Luo et al. (25) showed the COVID-19 infection associated with a high burden of severity in patients with lung cancer. 25 out of 102 (25%) patients died due to the progression of disease caused by the COVID-19 infection. Rogado et al. (26) retrospectively reviewed 1,878 medical records of all COVID-19

patients, finding that nine out of seventeen (52.3%) lung cancer patients died with COVID-19. Asymptomatic patients may influence the case fatality rate of lung cancer patients with COVID-19, nevertheless, many studies have showed lung cancer patients with COVID-19 were severer than general patients with COVID-19. Hence, we argue that our study indicates lung cancer patients with COVID-19 need to be carefully considered and shows the possible reason for lung cancer survivors are susceptible to SRAS-COV-2.

Although our study highlights the vulnerability of patients with lung cancer to the COVID-19 pandemic, it has some limitations. Since elevated levels of *ACE2* and *TMPRSS2* indicate a high susceptibility to SARS-CoV-2, and medium-term survivors did not have tumor burden, the expression of *ACE2* and *TMPRSS2* at resection margin tissue may indicate the susceptibility of lung cancer patients to SARS-CoV-2. So we detected the expression of *ACE2* and *TMPRSS2* at the resection margin of lung cancer patients to explore the molecular mechanism of lung cancer patients' high susceptibility to SARS-CoV-2. However, we failed to obtain tissue specimens from lung cancer patients with laboratory-confirmed COVID-19 infection, hence, the results could not directly reflect the relationship between the level of SARS-CoV-2 receptor expression and the outcome of lung cancer survivors. Further, not all patients had complete information on immune-related indicators; therefore, the correlation between tumor immunity and SARS-CoV-2 in lung cancer survivors should be further explored. Previous studies have shown that *ACE2* attenuated the metastasis of lung cancer and that *TMPRSS2* fusion gene may induce resistance to EGFR-TKI, a standard first-line therapy for advanced NSCLC patients harboring EGFR mutation (27, 28). Little is known about the interaction between SARS-CoV-2 and lung cancer cells and how COVID-19 affects lung cancer patients. The molecular mechanism requires further exploration. Finally, the small sample size, retrospective nature were also limitations in our study.

CONCLUSIONS

This study revealed the high expression of the SARS-CoV-2 receptors, *ACE2* and *TMPRSS2*, at resection margins of lung cancer survivors and its possible relationship with the higher susceptibility of these patients to COVID-19. Clinical data revealed that lung cancer patients, including medium-term survivors, diagnosed with COVID-19 infection may have worse outcomes and should be carefully considered.

DATA AVAILABILITY STATEMENT

The original contributions presented in the study are publicly available. This data can be found here: https://www.ebi.ac.uk/arrayexpress/experiments/E-MTAB-6149/, https://www.ebi.ac.uk/arrayexpress/experiments/E-MTAB-6653/, and https://www.tissuestabilitycellatlas.org/.

ETHICS STATEMENT

This study was approved by the Medical Ethical Committee of Wuhan Huoshenshan Hospital. Written informed consent was obtained from each patient. The patients/participants provided their written informed consent to participate in this study.

AUTHOR CONTRIBUTIONS

XX, PL, ZhiZ, and RG have full access to all of the data in the study and take responsibility for the integrity of the data and the accuracy of the data analysis. QQW, LL, TQ, and JL contributed equally. Concept and design: XX, PL, ZhiZ, and RG. Data collection: XX, QHW, TQ, and ZZ. Data analysis and interpretation: LL, JL, LW, KL, ZW, MZ, BH, WW, MW, and RD. Drafting of the manuscript: QQW, LL, TQ, and JL. All authors contributed to the article and approved the submitted version.

FUNDING

This work was supported by National Natural Science Foundation of China (NSFC 81972188, 81572893, 81972358, 81959113) and the Medical Important Talents (ZDRCA2016024).

SUPPLEMENTARY MATERIAL

The Supplementary Material for this article can be found online at: https://www.frontiersin.org/articles/10.3389/fonc.2021.644575/full#supplementary-material

Supplementary Table 1 | Characteristics of lung cancer patients with COVID-19.

Supplementary Table 2 | Characteristics of patients with donated tissues.

Supplementary Table 3 | The specific treatment and stage for each patient.

REFERENCES

1. Sohrabi C, Alsafi Z, O'Neill N, Khan M, Kerwan A, Al-Jabir A, et al. World Health Organization Declares Global Emergency: A Review of the 2019 Novel Coronavirus (COVID-19). *Int J Surg* (2020) 76:71–6. doi: 10.1016/j.ijsu.2020.02.034
2. Drosten C, Gunther S, Preiser W, van der Werf S, Brodt HR, Becker S, et al. Identification of a Novel Coronavirus in Patients With Severe Acute Respiratory Syndrome. *N Engl J Med* (2003) 348(20):1967–76.
3. Zaki AM, van Boheemen S, Bestebroer TM, Osterhaus AD, Fouchier RA. Isolation of a Novel Coronavirus From a Man With Pneumonia in Saudi Arabia. *N Engl J Med* (2012) 367(19):1814–20. doi: 10.1056/NEJMoa1211721
4. Wu JT, Leung K, Leung GM. Nowcasting and Forecasting the Potential Domestic and International Spread of the 2019-Ncov Outbreak Originating in Wuhan, China: A Modelling Study. *Lancet* (2020) 395(10225):689–97. doi: 10.1016/S0140-6736(20)30260-9

5. Rothan HA, Byrareddy SN. The Epidemiology and Pathogenesis of Coronavirus Disease (COVID-19) Outbreak. *J Autoimmun* (2020) 109:102433. doi: 10.1016/j.jaut.2020.102433
6. Lukassen S, Chua RL, Trefzer T, Kahn NC, Schneider MA, Muley T, et al. SARS-Cov-2 Receptor ACE2 and TMPRSS2 are Primarily Expressed in Bronchial Transient Secretory Cells. *EMBO J* (2020) 39(10):e105114. doi: 10.15252/embj.20105114
7. Chai P, Yu J, Ge S, Jia R. Fan X. Genetic Alteration, RNA Expression, and DNA Methylation Profiling of Coronavirus Disease 2019 (COVID-19) Receptor ACE2 in Malignancies: A Pan-Cancer Analysis. *J Hematol Oncol* (2020) 13(1):43. doi: 10.1186/s13045-020-00883-5
8. Kong Q, Xiang Z, Wu Y, Gu Y, Guo J, Geng F. Analysis of the Susceptibility of Lung Cancer Patients to SARS-Cov-2 Infection. *Mol Cancer* (2020) 19(1):80. doi: 10.1186/s12943-020-01209-2
9. Bray F, Ferlay J, Soerjomataram I, Siegel RL, Torre LA, Jemal A. Global Cancer Statistics 2018: GLOBOCAN Estimates of Incidence and Mortality Worldwide for 36 Cancers in 185 Countries. *CA Cancer J Clin* (2018) 68 (6):394–424. doi: 10.3322/caac.21492
10. Howington JA, Blum MG, Chang AC, Balekian AA, Murthy SC. Treatment of Stage I and II Non-Small Cell Lung Cancer: Diagnosis and Management of Lung Cancer, 3rd Ed: American College of Chest Physicians Evidence-Based Clinical Practice Guidelines. *Chest* (2013) 143(5 Suppl):e278S–313S. doi: 10.1378/chest.12-2359
11. Laughney AM, Hu J, Campbell NR, Bakhoum SF, Setty M, Lavallee VP, et al. Regenerative Lineages and Immune-Mediated Pruning in Lung Cancer Metastasis. *Nat Med* (2020) 26(2):259–69. doi: 10.1038/s41591-019-0750-6
12. Li L, Zhang W, Hu Y, Tong X, Zheng S, Yang J, et al. Effect of Convalescent Plasma Therapy on Time to Clinical Improvement in Patients With Severe and Life-Threatening COVID-19: A Randomized Clinical Trial. *JAMA* (2020) 324(5):460–70. doi: 10.1001/jama.2020.12607
13. Li WH, Moore MJ, Vasilieva N, Sui JH, Wong SK, Berne MA, et al. Angiotensin-Converting Enzyme 2 is a Functional Receptor for the SARS Coronavirus. *Nature* (2003) 426(6965):450–4. doi: 10.1038/nature02145
14. Matsuyama S, Nagata N, Shirato K, Kawase M, Takeda M, Taguchi F. Efficient Activation of the Severe Acute Respiratory Syndrome Coronavirus Spike Protein by the Transmembrane Protease TMPRSS2. *J Virol* (2010) 84 (24):12658–64. doi: 10.1128/JVI.01542-10
15. Hoffmann M, Kleine-Weber H, Schroeder S, Kruger N, Herrler T, Erichsen S, et al. SARS-Cov-2 Cell Entry Depends on ACE2 and TMPRSS2 and is Blocked by a Clinically Proven Protease Inhibitor. *Cell* (2020) 181(2):271–+. doi: 10.1016/j.cell.2020.02.052
16. Hirano T, Murakami M. COVID-19: A New Virus, But a Familiar Receptor and Cytokine Release Syndrome. *Immunity* (2020) 52(5):731–3. doi: 10.1016/j.immuni.2020.04.003
17. Blanco-Melo D, Nilsson-Payant BE, Liu WC, Uhl S, Hoagland D, Moller R, et al. Imbalanced Host Response to SARS-Cov-2 Drives Development of COVID-19. *Cell* (2020) 181(5):1036–45.e1039. doi: 10.1016/j.cell.2020.04.026
18. Li Y, Duche A, Sayer MR, Roosan D, Khalafalla FG, Ostrom RS, et al. SARS-Cov-2 Early Infection Signature Identified Potential Key Infection Mechanisms and Drug Targets. *BMC Genomics* (2021) 22(1):125. doi: 10.1186/s12864-021-07433-4
19. Dai MY, Liu DB, Liu M, Zhou FX, Li GL, Chen Z, et al. Patients With Cancer Appear More Vulnerable to SARS-Cov-2: A Multicenter Study During the COVID-19 Outbreak. *Cancer Discov* (2020) 10(6):783–91. doi: 10.1158/2159-8290.CD-20-0422
20. Epidemiology Working Group for Ncip Epidemic Response CCfDC, Prevention. [the Epidemiological Characteristics of an Outbreak of 2019 Novel Coronavirus Diseases (COVID-19) in China]. *Zhonghua Liu Xing Bing Xue Za Zhi* (2020) 41(2):145–51. doi: 10.3760/cma.j.issn.0254-6450.2020.02.003
21. Liang W, Guan W, Chen R, Wang W, Li J, Xu K, et al. Cancer Patients in SARS-Cov-2 Infection: A Nationwide Analysis in China. *Lancet Oncol* (2020) 21(3):335–7. doi: 10.1016/S1470-2045(20)30096-6
22. Oh WK. COVID-19 Infection in Cancer Patients: Early Observations and Unanswered Questions. *Ann Oncol* (2020) 31(7):838–9. doi: 10.1016/j.annonc.2020.03.297
23. Zhang L, Zhu F, Xie L, Wang C, Wang J, Chen R, et al. Clinical Characteristics of COVID-19-Infected Cancer Patients: A Retrospective Case Study in Three Hospitals Within Wuhan, China. *Ann Oncol* (2020). doi: 10.1016/j.annonc.2020.03.296
24. Zou X, Chen K, Zou J, Han P, Hao J, Han Z. Single-Cell RNA-Seq Data Analysis on the Receptor ACE2 Expression Reveals the Potential Risk of Different Human Organs Vulnerable to 2019-Ncov Infection. *Front Med* (2020) 14(2):185–92. doi: 10.1007/s11684-020-0754-0
25. Luo J, Rizvi H, Preeshagul IR, Egger JV, Hoyos D, Bandlamudi C, et al. COVID-19 in Patients With Lung Cancer. *Ann Oncol* (2020) 31(10):1386–96. doi: 10.1158/2159-8290.CD-20-0596
26. Rogado J, Pangua C, Serrano-Montero G, Obispo B, Marino AM, Perez-Perez M, et al. Covid-19 and Lung Cancer: A Greater Fatality Rate? *Lung Cancer* (2020) 146:19–22. doi: 10.1016/j.lungcan.2020.05.034
27. Qian Y-R, Guo Y, Wan H-Y, Fan L, Feng Y, Ni L, et al. Angiotensin-Converting Enzyme 2 Attenuates the Metastasis of Non-Small Cell Lung Cancer Through Inhibition of Epithelial-Mesenchymal Transition. *Oncol Rep* (2013) 29(6):2408–14. doi: 10.3892/or.2013.2370
28. Zhong J, Li L, Wang Z, Bai H, Gai F, Duan J, et al. Potential Resistance Mechanisms Revealed by Targeted Sequencing From Lung Adenocarcinoma Patients With Primary Resistance to Epidermal Growth Factor Receptor (EGFR) Tyrosine Kinase Inhibitors (Tkis). *J Thorac Oncol* (2017) 12 (12):1766–78. doi: 10.1016/j.jtho.2017.07.032

Conflict of Interest: The authors declare that the research was conducted in the absence of any commercial or financial relationships that could be construed as a potential conflict of interest.

Copyright © 2021 Wang, Li, Qu, Li, Wu, Li, Wang, Zhu, Huang, Wu, Wu, Ding, Zhang, Wang, Xia, Li, Zhang and Guo. This is an open-access article distributed under the terms of the Creative Commons Attribution License (CC BY). The use, distribution or reproduction in other forums is permitted, provided the original author(s) and the copyright owner(s) are credited and that the original publication in this journal is cited, in accordance with accepted academic practice. No use, distribution or reproduction is permitted which does not comply with these terms.

frontiers in Oncology

MINI REVIEW
published: 21 May 2021
doi: 10.3389/fonc.2021.632256

Beyond Conventional: The New Horizon of Targeted Therapy for the Treatment of Advanced Non Small Cell Lung Cancer

*Alfredo Tartarone[1], Vittoria Lapadula[1], Concetta Di Micco[2], Gemma Rossi[3], Carlotta Ottanelli[3], Andrea Marini[3], Roberta Giorgione[3], Katia Ferrari[4], Martina Catalano[3], Luca Voltolini[5], Enrico Mini[6] and Giandomenico Roviello[6]**

[1] Department of Onco-Hematology, Division of Medical Oncology IRCCS-CROB Referral Cancer Center of Basilicata, Rionero in Vulture, Italy, [2] Division of Medical Oncology, IRCCS Casa Sollievo della Sofferenza, San Giovanni Rotondo, Italy, [3] School of Human Health Sciences, University of Florence, Florence, Italy, [4] Respiratory Medicine, Careggi University Hospital, Florence, Italy, [5] Thoracic Surgery Unit, Careggi University Hospital, Florence, Italy, [6] Department of Health Sciences, Section of Clinical Pharmacology and Oncology, University of Florence, Florence, Italy

OPEN ACCESS

Edited by:
Francesco Petrella, European Institute of Oncology (IEO), Italy

Reviewed by:
Francesco Facchinetti, Gustave Roussy Cancer Campus, France
Haiyan Tu, Guangdong Provincial People's Hospital Lung Cancer Institute, China

***Correspondence:**
Giandomenico Roviello
giandomenicoroviello@hotmail.it

Specialty section:
This article was submitted to Thoracic Oncology, a section of the journal Frontiers in Oncology

Received: *22 November 2020*
Accepted: *20 April 2021*
Published: *21 May 2021*

Citation:
Tartarone A, Lapadula V, Di Micco C, Rossi G, Ottanelli C, Marini A, Giorgione R, Ferrari K, Catalano M, Voltolini L, Mini E and Roviello G (2021) Beyond Conventional: The New Horizon of Targeted Therapy for the Treatment of Advanced Non Small Cell Lung Cancer. Front. Oncol. 11:632256. doi: 10.3389/fonc.2021.632256

In the last few years the advent of targeted therapies against oncogenic drivers significantly improved the survival of non small cell lung cancer (NSCLC) patients with a favourable toxicity profile. Therefore, genetic testing, including at least EGFR mutations and ALK/ROS1 rearrangements, should be performed in all NSCLC patients (in particular with adenocarcinoma) who received a diagnosis of advanced disease. This review focuses on novel druggable oncogenic drivers, such as MET exon 14 mutations/MET amplification, RET fusions, BRAF V600E mutations, KRAS G12C mutations, NTRK rearrangements, and HER2 alterations.

Keywords: targeted therapies, oncogenic drivers, genetic testing, non small cell lung cancer, MET

INTRODUCTION

The recently seen improvements in NSCLC outcomes are mainly related to the advent in clinical practice of immunotherapy in non-oncogene driven cancers and of targeted therapies in tumours with druggable oncogenes. Overall targeted therapies demonstrated not only to increase survival but also patient's quality of life, due to their efficacy and favourable toxicity profile. In addition some of these drugs, such as osimertinib or alectinib, that are able to penetrate the blood-brain barrier, also showed a high effectiveness in treating or preventing brain metastases, a common clinical problem in NSCLC patients (1, 2).

The majority of oncogene-addicted NSCLC are adenocarcinomas, reason for which guidelines suggest that all patients with advanced adenocarcinoma should be tested for oncogenic drivers (3–5). In particular, testing for EGFR mutations and ALK or ROS1 rearrangements are now considered mandatory, while testing for emerging targets such as BRAF V600E mutations, MET exon 14 mutations, RET fusions, HER2 and NTRK1 are suggested. Anyhow several oncology services also routinely test for BRAF V600E mutations in view of the recent approval of BRAF/MEK inhibitors for metastatic BRAF V600E–mutated NSCLC patients.

However, even though the main guidelines recommend performing genetic testing to find out molecular disease drivers, a recent survey conducted by the International Association for the Study of Lung Cancer (IASLC) showed that 33% of respondents were unaware of the most recent guidelines for molecular testing and that less than half of the patients in their country receive molecular testing (6). As reported by the same survey, the main barriers to testing were cost, quality (inadequate tissue quality, lack of technical expertise in the laboratory, etc.), turnaround time and lack of awareness.

A multicenter Italian observational study of biomarker screening in daily clinical practice conducted from May 2017 to October 2017 in 13 institutions (N=1612 patients) reported that only 50.8% requests were related to driver mutations with target agents already available at the preplanned time, while 49.2% were associated with PD-L1, ROS1, KRAS and others (7). All participating centers considered multiplex genotyping assays such as next generation sequencing (NGS) as first approach.

The majority of driver mutations are targetable by the EGFR tyrosine kinase inhibitors (TKIs) (e.g. gefitinib, erlotinib, afatinib, and osimertinib in EGFR-mutant NSCLC; crizotinib, ceritinib, brigatinib, lorlatinib, and alectinib in ALK rearranged tumours; crizotinib in ROS1 rearranged disease). This review focuses on novel druggable oncogenic drivers such as MET Exon 14 mutations/MET amplification, RET fusions, BRAF V600E mutations, KRAS G12C mutations, NTRK rearrangements, and HER2 alterations (**Figure 1**) .

MET EXON 14 MUTATION/MET AMPLIFICATION

The mesenchymal-epithelial transition (MET) proto-oncogene located on chromosome 7 encodes a receptor tyrosine kinase with an extracellular alfa-subunit and a transmembrane beta-subunit linked by a disulfide bond. MET oncogene drives specific pathways through activation by its ligand hepatocyte growth factor (HGF) and participates in mechanisms of epithelial to mesenchymal transition. When MET exon 14 is not transcribed, there is decreased degradation of the MET receptor tyrosine kinase with a corresponding increase in signalling. It is known that MET and its ligand play a role during embryogenesis, are essential for organ protection/regeneration and also contribute to

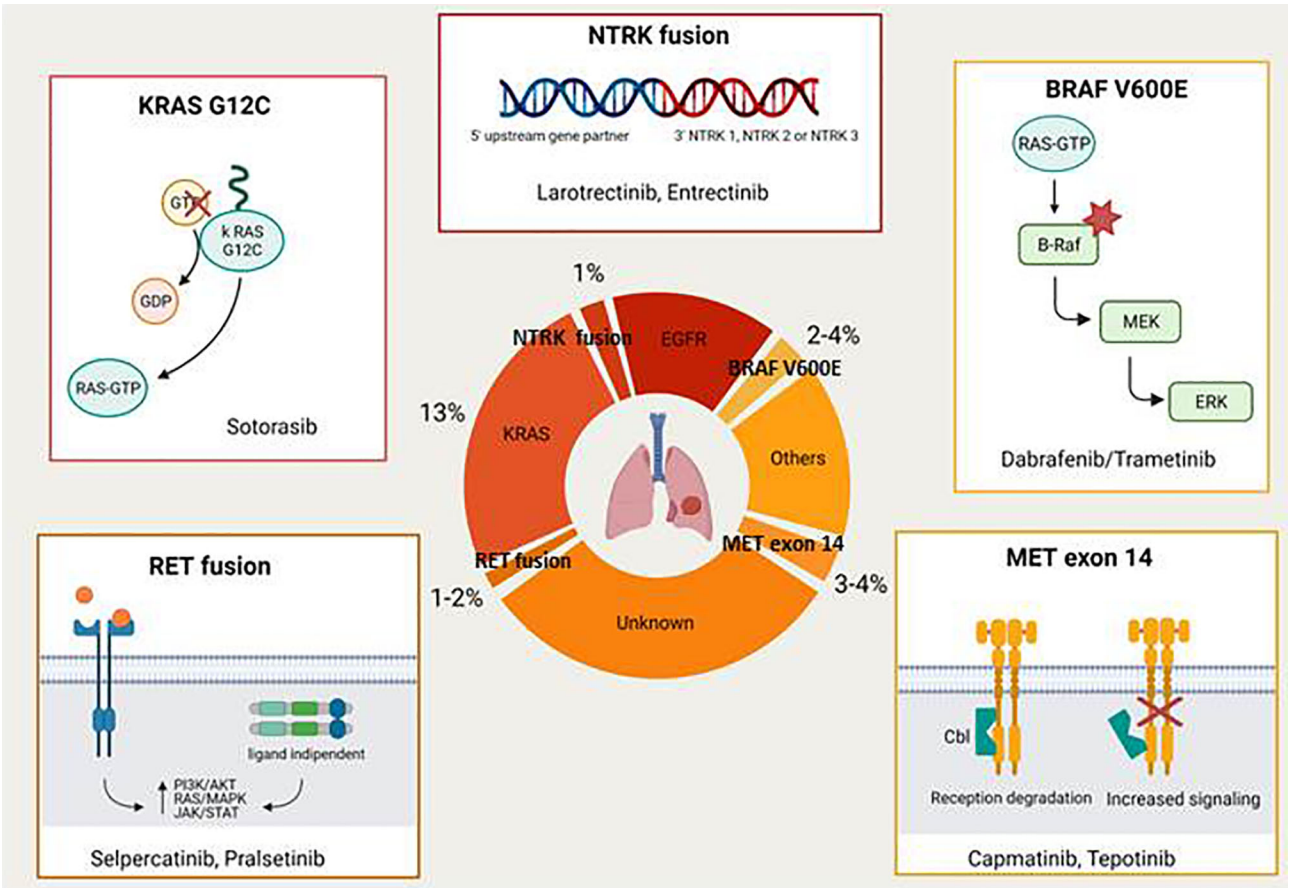

FIGURE 1 | Novel druggable oncogenic drivers in NSCLC.

the regulation of the immune system. Aberrant regulation of the MET/HGF axis with subsequent alteration of downstream signalling pathways has been associated with tumourigenesis, invasiveness and cancer progression (8, 9). MET aberrations include overexpression, gene amplification and MET exon 14 skipping mutations. MET amplification represents also the most common resistance mechanism to osimertinib, accounting for about 15% of the cases (10). This has provided the rationale for various clinical trials exploring the combination of MET and EGFR TKIs in patients with mutant EGFR and MET amplified NSCLC after progression on EGFR TKIs (11). Cases of NSCLC patients with MET exon 14 mutations or MET amplification who responded to crizotinib or other MET inhibitors were already reported in literature several years ago (12, 13).

Clinical characteristics associated with MET exon 14 mutations were reported in **Table 1A**.

Recently, two large studies published in the NEJM demonstrated the activity of the anti MET capmatinib and tepotinib in this patient population (14, 15). The GEOMETRY mono-1 study investigated the activity of capmatinib, an orally bioavailable inhibitor of the MET receptor, in MET-positive NSCLC patients. In this study patients were assigned to cohorts on the basis of MET status (MET exon 14 skipping mutation or MET amplification) and previous therapies (14). A total of 364 patients were included in the various cohorts; among patients with NSCLC with a MET exon 14 skipping mutation the overall response rate (ORR) was 41% in 69 pretreated patients and 68% in 28 patients who had not received treatment previously, while the median duration of response was 9.7 and 12.6 months, respectively. Limited efficacy was recorded only in previously treated patients with MET amplification who had a gene copy number of less than 10 (ORR in 7–12% of patients). Among patients with MET amplification and a gene copy number ≥ 10 ORR was 29% in pretreated patients and 40% in chemotherapy-naive, in any case lower RRs than those reported in patients with MET exon 14 skipping mutation.

Interestingly, capmatinib demonstrated activity also in patients with brain metastases (with responses observed in 12 out of 13 patients). About toxicity, the most frequently reported adverse events (AEs) were peripheral oedema (51%) and nausea (45%).

The VISION study evaluated the clinical activity of tepotinib, another oral MET inhibitor, in chemotherapy-naïve or pretreated patients (> 2 courses of previous therapy) with a confirmed MET exon 14 skipping mutation (cohort A) or with MET-amplified disease (cohort B); currently cohort C is enrolling patients with MET exon 14 skipping mutations for confirmatory analysis of the results reported in cohort A (15). Testing of MET exon 14 skipping mutations was performed analysing circulating free DNA (cfDNA) obtained from plasma or RNA extracted from fresh or archivial tumour tissue. Recently the authors reported the results for cohort A, which has completed recruitment. Among the 99 evaluable patients the ORR was 46% (48% in the liquid biopsy group and 50% in the tissue biopsy group), with a median duration of response of 11.1 months. The response rates were similar regardless of the number of previous therapies. About toxicity grade ≥ 3 AEs were reported in 28% of the patients, including peripheral oedema in 7% that represented the main toxic effect.

The U.S. Food and Drug Administration (FDA) granted accelerated approval to capmatinib and tepotinib, on May 2020 and February 2021 respectively, for patients with metastatic NSCLC harboring MET exon 14 skipping alterations.

The findings from the GEOMETRY and VISION study indicate not only that MET exon 14 skipping mutation represents a new therapeutic target but also the importance of routine testing for these alterations.

TABLE 1 | Clinical characteristics associated with MET exon 14 mutation/MET amplification **(A)** and RET deregulation **(B)**.

A	B
Older age (≥ 70 years)	Younger age (≤ 60 years)
Affects both smokers and non-smokers	Never-smoker status
Detectable in 3-4% of NSCLC patients	Mutually exclusive with other mutations
Can occur in any subtype of NSCLC (high frequency in pulmonary sarcomatoid carcinoma)	Observed in 1-2% of NSCLC (adenocarcinoma) patients as well as in other cancer (in particular thyroid cancer)
No gender specificity	Signet ring cells in ≥ 10% of tumor cells
	Poorly differentiated tumors
	Early lymph-node metastases
	Frequent presence of brain metastases
	Low response rate with chemotherapy

RET FUSIONS

The RET proto-oncogene encodes a transmembrane receptor tyrosine kinase with an extracellular, a transmembrane and an intracellular tyrosine kinase domain (16). RET receptor, that binds growth factors of the glial derived neurotropic factor family, when is deregulated becomes a potent oncoprotein (17). The most common identified RET aberrations are mutations, fusions and amplifications. RET germline mutations are associated with multiple endocrine neoplasia type 2A (MEN2A), MEN2B and familial medullary thyroid carcinoma.

Main clinical characteristics associated with RET deregulation are listed in **Table 1B**. Recently, were reported data regarding the use of two RET inhibitors, selpercatinib and pralsetinib, in patients with advanced RET fusion positive NSCLC (18, 19). The phase 1 to 2 LIBRETTO 001 study, conducted in RET fusion positive NSCLC patients either previously treated with platinum-based chemotherapy or chemotherapy-naïve, showed encouraging results for selpercatinib, a novel inhibitor of RET kinase (18). The authors reported an ORR of 64% in 105 pretreated patients with a median duration of response of 17.5 months; among 39 chemotherapy-naïve patients the ORR was 85% and 90% of the responses were ongoing at 6 months. Notably, 10 out of 11 patients (91%) with measurable central nervous system (CNS) metastases at enrolment obtained an objective intracranial response, including 3 complete responses.

The most common reported AEs of grade ≥ 3 were hypertension (14%), hypertransaminasemia (12%) and hyponatremia (6%); however, only 2% of patients discontinued selpercatinib due to a drug related AE.

Phase I/II ARROW study evaluated the activity of another RET inhibitor, pralsetinib (BLU-667), in RET+ solid cancers, including NSCLC (ClinicalTrials.gov Identifier: NCT03037385). In the dose-escalation phase of the study the recommended dose has been determined at 400 mg once daily. Updated analysis of this study regarding 116 NSCLC patients showed an ORR of 65% (61% in patients with prior platinum treatment, 73% in patients with no prior systemic therapy), including 6% of complete responses (19). Most treatment related AEs were grade 1 to 2 and included hypertransaminasemia, constipation, hypertension and anemia. Similarly to selpercatinib, pralsetinib demonstrated an high activity against CNS metastases. AcceleRET Lung, an ongoing phase III study, will evaluate the efficacy and safety of pralsetinib versus standard of care for first-line treatment of advanced/metastatic RET fusion-positive NSCLC (ClinicalTrials.gov Identifier: NCT04222972).

Updated National Comprehensive Cancer Network Clinical Practice Guidelines in Oncology (NCCN Guidelines®) for NSCLC indicate selpercatinib or pralsetinib as a preferred treatment option for patients with RET fusion-positive NSCLC as a first-line or subsequent therapy (20).

BRAF V600E MUTATIONS

BRAF mutations are identified in 2% to 4% of NSCLC and BRAF V600E point mutations account for 50% of these cases. BRAF mutations determine an activation of the mitogen-activated-protein-kinase (MAPK) pathway that regulates cellular growth. In addition, BRAF mutations represent an emerging mechanism of resistance to EGFR-TKIs that has been reported in 1% to 2% of cases (21).

Planchard et al. enrolled patients with advanced BRAF V600E mutant NSCLC in three cohorts (22–24). In the cohort A untreated or previously treated patients received dabrafenib (150 mg twice daily) as monotherapy, in the cohort B previously treated patients received the combination of (dabrafenib 150 mg twice daily) and trametinib (2 mg once daily), in the cohort C untreated patients were treated with dabrafenib (dabrafenib 150 mg twice daily) plus trametinib (2 mg once daily). The first two cohorts showed a higher efficacy of the combination than the one observed with dabrafenib alone (ORR 67% *vs* 33%), still bearing in mind the limits of an indirect comparison. Results of the cohort C, including untreated patients with who have received dabrafenib 150 mg twice daily and trametinib 2 mg daily, confirmed the efficacy of this combination therapy with an ORR of 64% and a median progression-free survival (PFS) of 10.9 months; the toxicity of the combination was manageable, being the most serious AEs pyrexia (11%), aspartate aminotransferase increase (8%) and ejection fraction decrease (8%). Main guidelines recommend dabrafenib plus trametinib for metastatic BRAFV600–mutated NSCLC patients (3, 20).

Vemurafenib, another BRAF inhibitor, was administered in 115 pretreated NSCLC patients (100 with BRAFV600 mutations and 15 with BRAF.nonV600 mutations) as part of the AcSè program conducted by the French National Cancer Institute (25). This study demonstrated the activity of vemurafenib in BRAFV600 mutated patients (ORR 44.9%, median PFS 5.2 and median OS 10 months, respectively), but not in patients with other BRAF mutations. The safety profile was comparable with that usually observed with dabrafenib.

KRAS G12C MUTATIONS

Carcinogenic Kirstein Rat Sarcoma viral oncogene homolog (KRAS) mutation is the most common mutation in NSCLC, accounting for approximately 30% of adenocarcinomas and 5% of squamous lung cancers. KRAS encodes small G proteins which are involved in several pathways such as proliferation, differentiation and apoptosis. KRAS mutations, that mainly occur in codon 12 (13% of NSCLC), 13 and 61, determine a loss of intrinsic GTPase activity with subsequent effects on cell proliferation signals and tumourigenesis (26). Up until now it has been very difficult to target K-RAS, probably due to its ability to activate multiple mechanisms of escape under the selective pressure of the treatment (27).

However, recent results from the phase 1 CodeBreak 100 trial (ClinicalTrials.gov Identifier: NCT03600883) with sotorasib (AMG 510), a first in class inhibitor of the KRAS G12C mutation, showed encouraging activity in heavily pre-treated advanced NSCLC and other solid tumours harbouring the KRAS G12C mutation (28). The study that included a total of 129 patients (59 with NSCLC, 42 with colorectal cancer, 28 with other tumours) showed an ORR of 32.2%, 88% of disease control (objective response or stable disease) and a median PFS of 6.3 months among patients with NSCLC. The most common reported AEs were diarrhea (any grade 29.5%, grade ≥ 3 3.9%), fatigue (any grade 23.3%, grade ≥ 3 2.3%) and nausea (any grade 20.9%, grade ≥ 3 1.6%). As reported by LoRusso and Sebolt-Leopold in their editorial on the NEJM, this trial represents the first step in "drugging the undruggable" (29).

All over the world more than 100 studies are currently ongoing to evaluate the role of novel agents administered alone or in combination in KRAS mutant NSCLC patients (30).

NTRK FUSIONS

Neurotrophic receptor tyrosine kinase (NTRK) gene fusions, that encode the tropomyosin receptor kinase (TRK) proteins, are genomic alterations that can act as an oncogenic driver, promoting cell proliferation and survival in tumour cell lines (31). NTRK fusions have been found across multiple tumour types from both adult and paediatric patients. Their frequency varies from <5% in cancer types including lung, pancreatic, colorectal, melanoma, breast cancers and other solid or haematological cancers, up to 25% in tumours including gastrointestinal stromal tumours and thyroid cancer, to >90% in rare tumours types such as infantile fibrosarcoma,

cellular or mixed congenital mesoblastic nephroma and mammary analogue secretory carcinoma (MASC). Among the various TRK inhibitors that have been investigated in the last few years larotrectinib and entrectinib are the ones with the most promising development (32–34). Larotrectinib was granted approval by U.S. Food and Drug Administration (FDA) and European Medicines Agency (EMA), in 2018 and 2019 respectively, for the treatment of patients with advanced NTRK fusion positive solid tumours based on the results of three distinct single-arm trials including also NSCLC patients (35). In particular, larotrectinib demonstrated in the first 55 enrolled patients an ORR of 75% (including 13% of complete responses) with 55% of the patients remained progression-free at 1 year. In the updated pooled efficacy analysis that included a total of 159 patients (153 evaluable for response) 121 patients (79%) had an objective response (16% complete response) with a median PFS of 28.3 months (36). Few serious AEs were observed in these trials, considering that grade 3 to 4 AEs were reported in 13% and <1% of patients respectively. The most common reported grade 3 to 4 AEs were increased alanine aminotransferase, anemia, neutropenia, fatigue and pyrexia.

Recently, also entrectinib received FDA and EMA approval for the same patient population. The decision was based on the results of three small phase 1 to 2 trials (STARTRK-1, STRTRK-2, ALKA) including 54 patients with advanced NTRK+tumours (37). In these studies the authors reported an ORR of 59.3%, including 7% complete responses, with a median duration of response of 12.9 months. In particular, in the cohort of patients with NSCLC (n=10) the ORR was 70.0%; moreover, among NSCLC patients with baseline CNS disease (n=6) 4/6 had an intracranial response (2 complete, 2 partial), 1 stable disease while 1 was not evaluable (38). Entrectinib was well tolerated with AEs of grade 1 to 2 being the most observed and a discontinuation rate of 4.4%. Entrectinib has also received FDA and EMA approval for the treatment of ROS1 positive metastatic NSCLC in view of the positive results obtained in this setting of patients in the STARTRK-1, STARTRK-2, ALKA-372-001, and STARTRK-NG trials. Finally, preliminary results showed the efficacy of selitrectinib (LOXO-195), a next generation TRK inhibitor, in TRK fusion-positive patients with resistance to prior anti-TRK kinase therapy (ClinicalTrials.gov Identifier: NCT03215511) (39).

In the era of precision medicine larotrectinib and entrectinib represent one of the few examples of the so-called agnostic therapies; in fact, they target specific genomic anomalies regardless of tumour site of origin.

HER2

The human epidermal growth factor receptor 2 (HER2) is a member of the epidermal growth factor receptor family having tyrosine kinase activity. Similarly to MET three principal HER2 alterations can be identified: HER2 amplification, HER2 overexpression and HER2 mutations. HER2 has a key role in signal transduction and oncogenesis; in particular, HER2 aberrations, including both amplification and mutations, have been considered as oncogenic drivers that contribute to 2% to 6% of lung adenocarcinoma. In addition, as well as MET amplification, also HER2 amplification represents an important mechanism for acquired resistance to EGFR TKIs (40). So far several clinical trials conducted in NSCLC patients with HER2 aberration showed a modest efficacy of small molecule TKIs (e.g. afatinib, dacomitinib), anti-HER2 antibodies administered alone (e.g. trastuzumab) or in association with chemotherapy (e.g. trastuzumab+carboplatin/paclitaxel) or antibody-drug coniugate (ADC) (e.g.T-DM1) (41). However, at the 2020 ASCO Meeting preliminary results of the phase 2 DESTINY Lung-01 trial (ClinicalTrials.gov Identifier: NCT03505710) demonstrated encouraging activity of trastuzumab deruxtecan treatment, a novel ADC, in patients (n=42) with relapsed/refractory HER2-mutant NSCLC enrolled in the cohort 2 of the study. In fact, the authors reported an ORR of 61.9% and a median PFS >1 year with a median follow-up of 8 months (42).

On May 2020, the FDA granted breakthrough therapy designation to trastuzumab deruxtecan for the treatment of patients with metastatic and pretreated NSCLC whose tumours have a HER2 mutation.

At the 2020 World Conference on Lung Cancer (WCLC) were presented preliminary results of the patients with relapsed/refractory HER2-overexpressing (IHC 3+ or 2+) NSCLC enrolled in the cohort 1 of the same study (43). Patients with HER2 overexpression achieved an ORR of 24.5% and a disease control rate (DCR) of 69.4% with a median PFS of 5.4 months. Drug-related AEs were grade ≥ 3 in 55.1% of the patients and the most common AE was neutropenia. Drug-related interstitial lung disease (ILD) was observed in 8 patients.

CONCLUSION

Over the last years NSCLC has become an example of how precision medicine can significantly improve patient outcomes. In fact in advanced NSCLC patients harboring driver mutations and treated with targeted therapies we achieved results that traditional chemotherapy never gave us.

As previously reported, novel targeted agents such as capmatinib/tepotinib, selpercatinib/pralsetinib, dabrafenib +trametinib, sotorasib, larotrectinib/entrectinib, trastuzumab-deruxtecan are already or will be soon available for special subsets of patients with metastatic NSCLC.

In addition recent data of the phase III ADAURA trial, that evaluated the efficacy of osimertinib in EGFR mutated patients in the adjuvant setting, suggest that targeted therapy will play a role also in NSCLC patients with an oncogene addicted early disease (44).

In conclusion, identifying novel molecular subsets, developing much more efficient targeted therapies as well as performing genomic testing in clinical practice, as recommended by main guidelines, represents the next challenge and the best way to achieve the goal of giving the right drug to the right patient.

AUTHOR CONTRIBUTIONS

Conceptualization, GiR and AT. Writing—original draft preparation, AT, GeR, LV, KF, CO, GiR, RG, CM, and VL. Writing—review and editing, EM. Supervision, EM. All authors contributed to the article and approved the submitted version.

REFERENCES

1. Soria JC, Ohe Y, Vansteenkiste J, Reungwetwattana T, Chewaskulyong B, Lee KH, et al. Osimertinib in Untreated Egfr-Mutated Advanced non-Small-Cell Lung Cancer. *N Engl J Med* (2018) 378:113–25. doi: 10.1056/NEJMoa1713137
2. Mok T, Camidge DR, Gadgeel SM, Rosell R, Dziadziuszko R, Kim DW, et al. Updated Overall Survival and Final Progression-Free Survival Data for Patients With Treatment-Naive Advanced ALK-positive non-Small-Cell Lung Cancer in the ALEX Study. *Ann Oncol* (2020) 31:1056–64. doi: 10.1016/j.annonc.2020.04.478
3. Planchard D, Popat S, Kerr K, Novello S, Smit EF, Faivre-Finn C, et al. Metastatic non Small Cell Lung Cancer: ESMO Clinical Practice Guidelines for Diagnosis, Treatment and Follow-Up. Updated Version 15 September 2020. *Ann Oncol* (2018) 29:iv192–237. doi: 10.1093/annonc/mdy275
4. Lindeman NI, Cagle PT, Aisner DL, Arcila ME, Beasley MB, Bernicker EH, et al. Updated Molecular Testing Guideline for the Selection of Lung Cancer Patients for Treatment With Targeted Tyrosine Kinase Inhibitors: Guideline From the College of American Pathologists, the International Association for the Study of Lung Cancer, and the Association for Molecular Pathology. *Arch Pathol Lab Med* (2018) 142:321–46. doi: 10.5858/arpa.2017-0388-CP
5. Kalemkerian GP, Narula N, Kennedy EB, Biermann WA, Donington J, Leighl NB, et al. Molecular Testing Guideline for the Selection of Patients With Lung Cancer for Treatment With Targeted Tyrosine Kinase Inhibitors: American Society of Clinical Oncology Endorsement of the College of American Pathologists/International Association for the Study of Lung Cancer/Association for Molecular Pathology Clinical Practice Guideline Update. *J Clin Oncol* (2018) 36:911–9. doi: 10.1200/JCO.2017.76.7293
6. Smeltzer MP, Wynes MW, Lantuejoul S, Soo R, Ramalingam SS, Varella-Garcia M, et al. The International Association for the Study of Lung Cancer Global Survey on Molecular Testing in Lung Cancer. *J Thorac Oncol* (2020) 15:1434–48. doi: 10.1016/j.jtho.2020.05.002
7. Vavala T, Malapelle U, Veggiani C, Ludovini V, Papotti M, Leone A, et al. Molecular Profiling of Advanced non Small Cell Lung Cancer in the Era of Immunotherapy Approach: A Multicenter Italian Observational Prospective Study of Biomarker Screening in Daily Clinical Practice. *J Clin Pathol* (2021) 0:1–7. doi: 10.1136/jclinpath-2020-207339
8. Comoglio PM, Trusolino L, Boccaccio C. Known and Novel Roles of the MET Oncogene in Cancer: A Coherent Approach to Targeted Therapy. *Nat Rev Cancer* (2018) 18:341–51. doi: 10.1038/s41568-018-0002-y
9. Petrini I. Biology of MET: A Double Life Between Normal Tissue Repair and Tumor Progression. *Ann Transl Med* (2015) 3:82. doi: 10.3978/j.issn.2305-5839.2015.03.58
10. Leonetti A, Sharma S, Minari R, Perego P, Giovannetti E, Tiseo M. Resistance Mechanisms to Osimertinib in EGFR-mutated non-Small Cell Lung Cancer. *Br J Cancer* (2019) 121:725–37. doi: 10.1038/s41416-019-0573-8
11. Sequist LV, Han JY, Ahn MJ, Cho BC, Yu H, Kim SW, et al. Osimertinib Plus Savolitinib in Patients With EGFR Mutation-Positive, MET-amplified, non-Small-Cell Lung Cancer After Progression on EGFR Tyrosine Kinase Inhibitors: Interim Results From a Multicentre, Open-Label, Phase 1b Study. *Lancet Oncol* (2020) 21:373–86. doi: 10.1016/S1470-2045(19)30785-5
12. Frampton GM, Ali SM, Rosenzweig M, Chmielecki J, Lu X, Bauer TM, et al. Activation of MET Via Diverse Exon 14 Splicing Alterations Occurs in Multiple Tumor Types and Confers Clinical Sensitivity to MET Inhibitors. *Cancer Discovery* (2015) 5:850–9. doi: 10.1158/2159-8290
13. Ou SH, Kwak EL, Siwak-Tapp C, Dy J, Bergethon K, Clark JW, et al. Activity of Crizotinib (PF02341066), a Dual Mesenchymal-Epithelial Transition (MET) and Anaplastic Lymphoma Kinase (ALK) Inhibitor, in a non-Small Cell Lung Cancer Patient With De Novo MET Amplification. *J Thorac Oncol* (2011) 6:942–6. doi: 10.1097/JTO.0b013e31821528d3
14. Wolf J, Seto T, Han JY, Reguart N, Garon EB, Groen HJM, et al. GEOMETRY Mono-1 Investigators. Capmatinib In *MET* Exon 14-Mutated Or MET-Amplified Non-Small-Cell Lung Cancer. *N Engl J Med* (2020) 383:944–57. doi: 10.1056/NEJMoa2002787
15. Paik PK, Felip E, Veillon R, Sakai H, Cortot AB, Garassino MC, et al. Tepotinib in Non-Small-Cell Lung Cancer With MET Exon 14 Skipping Mutations. *N Engl J Med* (2020) 383:931–43. doi: 10.1056/NEJMoa2004407
16. Jhiang SM. The RET Proto-Oncogene in Human Cancers. *Oncogene* (2000) 19:5590–7. doi: 10.1038/sj.onc.1203857
17. Santoro M, Melillo RM, Carlomagno F, Vecchio G, Fusco A. Minireview: RET: Normal and Abnormal Functions. *Endocrinology* (2004) 145:5448–51. doi: 10.1210/en.2004-0922
18. Drilon A, Oxnard GR, Tan DSW, Loong HHF, Johnson M, Gainor J, et al. Efficacy of Selpercatinib In RET Fusion-Positive Non-Small-Cell Lung Cancer. *N Engl J Med* (2020) 383:813–24. doi: 10.1056/NEJMoa2005653
19. Gainor GJ, Curigliano G, Kim DW, Lee DH, Besse B, Baik CS, et al. Registrational Dataset From the Phase I/II ARROW Trial of Pralsetinib (BLU-667) in Patients (Pts) With Advanced RET Fusion+ non Small Cell Lung Cancer (NSCLC). *J Clin Oncol* (2020) 38:15 Suppl, abstract 9515. doi: 10.1016/j.jtho.2020.10.142
20. *National Comprehensive Cancer Network Clinical Practice Guidelines in Oncology (Nccn Guidelines®) NSCLC Version 8.2020*. Available at: https://www.nccn.org/professionals/physician_gls/pdf/nscl.pdf (Accessed on October 1, 2020).
21. Ho CC, Liao WY, Lin CA, Shih JY, Yu CJ, Yang JC. Acquired BRAF V600e Mutation as Resistant Mechanism After Treatment With Osimertinib. *J Thorac Oncol* (2017) 12:567–72. doi: 10.1016/j.jtho.2016.11.2231
22. Planchard D, Kim TM, Mazieres J, Quoix E, Riely G, Barlesi F, et al. Dabrafenib in Patients With BRAF(V600E)-Positive Advanced non-Small-Cell Lung Cancer: A Single-Arm, Multicentre, Open-Label, Phase 2 Trial. *Lancet Oncol* (2016) 17:642–50. doi: 10.1016/S1470-2045(16)00077-2
23. Planchard D, Besse B, Groen HJM, Souquet PJ, Quoix E, Baik CS, et al. Dabrafenib Plus Trametinib in Patients With Previously Treated BRAF (V600E)-mutant Metastatic non-Small Cell Lung Cancer: An Open-Label, Multicentre Phase 2 Trial. *Lancet Oncol* (2016) 17:984–93. doi: 10.1016/S1470-2045(16)30146-2
24. Planchard D, Smit EF, Groen HJM, Mazieres J, Besse B, Helland Å, et al. Dabrafenib Plus Trametinib in Patients With Previously Untreated $BRAF^{V600E}$-mutant Metastatic non-Small-Cell Lung Cancer: An Open-Label, Phase 2 Trial. *Lancet Oncol* (2017) 18:1307–16. doi: 10.1016/S1470-2045(17)30679-4
25. Mazieres J, Cropet C, Montané L, Barlesi F, Souquet PJ, Quantin X, et al. Vemurafenib in non-Small-Cell Lung Cancer Patients With $BRAF^{V600}$ and $Braf^{nonv600}$ Mutations. *Ann Oncol* (2020) 31:289–94. doi: 10.1016/j.annonc.2019.10.022
26. Piva S, Ganzinelli M, Garassino MC, Caiola E, Farina G, Broggini M, et al. Across the Universe of K-RAS Mutations in non-Small-Cell-Lung Cancer. *Curr Pharm Des* (2014) 20:3933–43. doi: 10.2174/13816128113196660761
27. Del Re M, Rofi E, Restante G, Crucitta S, Arrigoni E, Fogli S, et al. Implications of KRAS Mutations in Acquired Resistance to Treatment in NSCLC. *Oncotarget* (2017) 9:6630–43. doi: 10.18632/oncotarget.23553
28. Hong DS, Fakih MG, Strickler JH, Desai J, Durm GA, Shapiro GI, et al. $KRAS^{G12C}$ Inhibition With Sotorasib in Advanced Solid Tumors. *N Engl J Med* (2020) 383:1207–17. doi: 10.1056/NEJMoa1917239
29. LoRusso PM, Sebolt-Leopold JS. One Step At a Time-Clinical Evidence That KRAS is Indeed Druggable. *N Engl J Med* (2020) 383:1277–8. doi: 10.1056/NEJMe2026372
30. Available at: https://clinicaltrials.gov/ct2/results?cond=Lung+Cancer&term=KRAS&cntry=&state=&city=&dist (Accessed on October 1, 2020).
31. Vaishnavi A, Le AT, Doebele RC. Trking Down an Old Oncogene in a New Era of Targeted Therapy. *Cancer Discovery* (2015) 5:25–34. doi: 10.1158/2159-8290
32. Roviello G, D'Angelo A, Sciortino M, Mini E, Nobili S, De Logu F, et al. TRK Fusion Positive Cancers: From First Clinical Data of a TRK Inhibitor to Future Directions. *Crit Rev Oncol Hematol* (2020) 152:103011. doi: 10.1016/j.critrevonc.2020.103011
33. Lavacchi D, Roviello G, D'Angelo A. Tumor-Agnostic Treatment for Cancer: When How is Better Than Where. *Clin Drug Investig* (2020) 40:519–27. doi: 10.1007/s40261-020-00915-5
34. Cocco E, Scaltriti M, Drilon A. NTRK Fusion-Positive Cancers and TRK Inhibitor Therapy. *Nat Rev Clin Oncol* (2018) 15:731–47. doi: 10.1038/s41571-018-0113-0
35. Drilon A, Laetsch TW, Kummar S, DuBois SG, Lassen UN, Demetri GD, et al. Efficacy of Larotrectinib in TRK Fusion-Positive Cancers in Adults and Children. *N Engl J Med* (2018) 378(8):731–9. doi: 10.1056/NEJMoa1714448
36. Hong DS, DuBois SG, Kummar S, Farago AF, Albert CM, Rohrberg KS, et al. Larotrectinib in Patients With TRK Fusion-Positive Solid Tumours: A Pooled

Analysis of Three Phase 1/2 Clinical Trials. *Lancet Oncol* (2020) 21:531–40. doi: 10.1016/S1470-2045(19)30856-3
37. Rolfo C, Dziadziuszko R, Doebele RC, Demetri GD, Simmons B, Huang X, et al. Updated Efficacy and Safety of Entrectinib in Patients With NTRK Fusion-Positive Tumors: Integrated Analysis of STARTRK-2, STARTRK-1 and ALKA-372-001. *Ann Oncol* (2019) 30(S5):v180, Abstract 476P. doi: 10.1093/annonc/mdx244
38. Doebele R, Paz-Ares L, Farago AF, Liu SV, Chawla SP, Tosi D, et al. Entrectinib in NTRK-fusion Positive (NTRK-FP) non Small Cell Lung Cancer (NSCLC): Integrated Analysis of Patients Enrolled in Three Trials (STARTRK-2, STARTRK-1 and ALKA-372-001). *Cancer Res* (2019) 79(S13): Abstract CT131. doi: 10.1158/1538/1538-7445.AM2019-CT131
39. Hyman D, Kummar S, Farago A, Geoerger B, Mau-Sorensen M, Taylor M, et al. Phase I and Expanded Access Experience of LOXO-195 (BAY 2731954), a Selective Next-Generation TRK Inhibitor (TRK). *Cancer Res* (2019) 79(S13): Abstract CT127. doi: 10.1158/1538-7445.Am2019-ct127
40. Takezawa K, Pirazzoli V, Arcila ME, Nebhan CA, Song X, de Stanchina E, et al. HER2 Amplification: A Potential Mechanism of Acquired Resistance to EGFR Inhibition in EGFR-mutant Lung Cancers That Lack the Second-Site EGFRT790M Mutation. *Cancer Discov* (2012) 2:922–33. doi: 10.1158/2159-8290
41. Ekman S. HER2: Defining a Neu Target in Non-Small-Cell Lung Cancer. *Ann Oncol* (2019) 30:353–5. doi: 10.1093/annonc/mdz043
42. Smit EF, Nakagawa K, Nagasaka M, Felip E, Goto Y, Li BT, et al. Trastuzumab Deruxtecan (T-Dxd, DS-8201) in Patients With HER2-mutated Metastatic non Small Lung Cancer (NSCLC): Interim Results of DESTINY-Lung01. *J Clin Oncol* (2020) 38(suppl 15):9504. doi: 10.1200/JCO.2020.38.15
43. Nakagawa K, Nagasaka M, Felip E. Trastuzumab Deruxtecan in HER2-overexpressing Metastatic non Small Cell Lung Cancer: Interim Results of DESTINY-Lung01, in: *Presented at 2020 World Conference on Lung Cancer Singapore, Virtual*, January 28-31, Abstract OA04.05.
44. Wu YL, Tsuboi M, He J, John T, Grohe C, Majem M, et al. Osimertinib in Resected EGFR-mutated non Small Cell Lung Cancer. *N Engl J Med* (2020) 383:1711–23. doi: 10.1056/NEJMoa2027071

Conflict of Interest: The authors declare that the research was conducted in the absence of any commercial or financial relationships that could be construed as a potential conflict of interest.

Copyright © 2021 Tartarone, Lapadula, Di Micco, Rossi, Ottanelli, Marini, Giorgione, Ferrari, Catalano, Voltolini, Mini and Roviello. This is an open-access article distributed under the terms of the Creative Commons Attribution License (CC BY). The use, distribution or reproduction in other forums is permitted, provided the original author(s) and the copyright owner(s) are credited and that the original publication in this journal is cited, in accordance with accepted academic practice. No use, distribution or reproduction is permitted which does not comply with these terms.

frontiers in Oncology

ORIGINAL RESEARCH
published: 28 May 2021
doi: 10.3389/fonc.2021.659065

The Efficacy and Safety of Epidermal Growth Factor Receptor Tyrosine Kinase Inhibitor Combined With Thymosin in Advanced Non-Small Cell Lung Cancer Patients Harboring Active Epidermal Growth Factor Receptor Mutations

Yongdong Feng†, Guangkuo Zhu†, Song Lang, Ping Hao, Guanghui Li, Fanglin Chen, Wenlei Zhuo, Yuzhong Duan, Anmei Zhang, Zhengtang Chen and Jianguo Sun**

Cancer Institute, Xinqiao Hospital, Army Medical University, Chongqing, China

OPEN ACCESS

Edited by:
Olivier Feron, Université catholique de Louvain, Belgium

Reviewed by:
Claudio Constantini, University of Perugia, Italy
Wenliang Li, University of Texas Health Science Center at Houston, United States

***Correspondence:**
Jianguo Sun
sunjg09@aliyun.com
Zhengtang Chen
czt05@163.com

†These authors have contributed equally to this work

Specialty section:
This article was submitted to Pharmacology of Anti-Cancer Drugs, a section of the journal Frontiers in Oncology

Received: *26 January 2021*
Accepted: *03 May 2021*
Published: *28 May 2021*

Citation:
Feng Y, Zhu G, Lang S, Hao P, Li G, Chen F, Zhuo W, Duan Y, Zhang A, Chen Z and Sun J (2021) The Efficacy and Safety of Epidermal Growth Factor Receptor Tyrosine Kinase Inhibitor Combined With Thymosin in Advanced Non-Small Cell Lung Cancer Patients Harboring Active Epidermal Growth Factor Receptor Mutations. Front. Oncol. 11:659065. doi: 10.3389/fonc.2021.659065

Objective: To explore the efficacy and safety of EGFR-TKI combined with thymosin therapy in advanced non-small cell lung cancer (NSCLC) patients harboring active EGFR mutations.

Methods: Patients confirmed as advanced NSCLC with active EGFR mutations were recruited from August 2008 to July 2018 retrospectively. Patients treated with EGFR-TKI were classified as the EGFR-TKI group. And those received EGFR-TKI and thymosin therapy were designated as the EGFR-TKI plus thymosin group. The primary endpoint was progression-free survival (PFS). The secondary endpoints included overall survival (OS), tumor response and adverse effects.

Results: The median PFS was significantly longer in EGFR-TKI plus thymosin group than that in EGFR-TKI group (14.4 months *vs*. 9.2 months; HR=0.433, 95% CI 0.322 - 0.582, $P<0.0001$). The median OS was also prolonged in EGFR-TKI plus thymosin group than that in EGFR-TKI group (29.5 months *vs*. 19.8 months; HR=0.430, 95% CI 0.319 - 0.580, $P<0.0001$). The objective response rate in EGFR-TKI plus thymosin group and EGFR-TKI group were 60.0% versus 60.8% ($P=0.918$). The disease control rate was 96.9% in EGFR-TKI plus thymosin group and 97.7% in EGFR-TKI group ($P=1.000$). There were no significant differences in adverse effects between the two groups. The number of $CD3^+$ T cells in peripheral blood decreased significantly after treatment including both $CD3^+CD4^+$T and $CD3^+CD8^+$T subsets in EGFR-TKI group, but not in EGFR-TKI plus thymosin group.

Conclusions: Combination of EGFR-TKI and thymosin can significantly prolong the PFS and OS compared with EGFR-TKI monotherapy without more adverse events, which offers a new strategy in clinic.

Keywords: NSCLC, EGFR-TKI, thymosin, active EGFR mutations, efficacy, safety

INTRODUCTION

Epidermal growth factor receptor tyrosine kinase inhibitor (EGFR-TKI) is currently recommended as a standard first-line therapy for advanced non-small cell lung cancer (NSCLC) patients harboring active EGFR mutations, which was reported to prolong progression-free survival (PFS) compared with standard platinum-based chemotherapy significantly (1–3). However, most of the NSCLC patients with an initial dramatic response to EGFR-TKI treatment developed progression disease after 8.40-13.10 months (4, 5). In order to prolong the survival time of NSCLC patients with active EGFR mutations, novel drugs including osimertinib and crizotinib were developed by targeting resistance mechanisms (6, 7). Besides, combination therapies, such as EGFR-TKI combined with angiogenesis inhibitorwas shown to improve the PFS (8), but not OS (9). EGFR-TKI combined with chemotherapy prolonged PFS and OS but increased toxicity significantly (10). At present, there is still no satisfactory combination therapy.

As reported, sensitive EGFR-TKIs caused obvious tumor microenvironmental changes including the number of immune cells and inflammatory factors in serum (11). EGFR blockade by using erlotinib reduced $CD4^+$T cell proliferation in response to soluble anti-CD3 stimulation (12). Erlotinib demonstrated an immunosuppressive activity on T-cell-mediated immune response both *in vitro* and *in vivo* (13). Therefore, the combination of immunomodulators may be a potential method to enhance the efficacy of EGFR-TKI. In clinic, thymosin such as thymosin alpha 1 and thymopentin, have been widely used as immunomodulators in kinds of cancers (14). As reported, thymosin can significantly improve patient's quality of life by enhancing T-cell function, stimulation of T cell maturation and differentiation in lung cancer (15). In addition to the effect on immunomodulatory, thymosin has been reported to exert synergistic antitumor activity without more adverse effects when combined with chemotherapy in lung cancer (16). Whether thymosin combined with EGFR-TKI can improve patients' PFS and OS needs to be illustrated.

In this study, we conducted a retrospective study to explore the efficacy and safety of EGFR-TKI plus thymosin in NSCLC patients harboring active EGFR mutations, thereby enhancing the efficacy of EGFR-TKI.

Abbreviations: AEs, adverse effects; AJCC; American Journal of Critical Care; CI, confidence interval; DCR, disease control rate; ECOG, Eastern Cooperative Oncology Group; EGFR, epidermal growth factor receptor; TKI, tyrosine kinase inhibitor; HR, hazard ratio; NSCLC, non-small cell lung cancer; ORR, objective response rate; OS, overall survival; PD, progressive disease; PFS, progression-free survival; PS, performance status; RECIST, Response Evaluation Criteria In Solid Tumors.

MATERIALS AND METHODS

Patient Population

We conducted a retrospective research during August 2008 to July 2018 in three Affiliated Hospitals of Army Medical University (Chongqing, China). Patients over the age of 18 years were histologically or cytologically confirmed as stage IV NSCLC were recruited. TNM classification (tumor, node, and metastasis) of lung cancer was made according to the American Journal of Critical Care (AJCC) 7th edition of Lung Cancer. Those patients with active EGFR mutations, including exon 19 deletion or exon 21 L858R mutation, were detected by amplification refractory mutation system or next-generation sequence. Patients received first or second-line EGFR-TKI therapy, whose Eastern Cooperative Oncology Group (ECOG) performance status (PS) score were 0-2, had one or more measurable target lesions and follow-up time >3 months were included. Exclusion criteria included incomplete medical records, EGFR-TKI treatment less than 8 weeks and thymosin therapy less than 4 weeks, loss to follow-up. This trial had been approved by the Ethics Committee, Xinqiao Hospital, Army Medical University (2018–302–01). All procedures were conducted in accordance with the Declaration of Helsinki.

Treatment

Patients treated with EGFR-TKI (erlotinib 150mg daily, gefitinib 250mg daily or icotinib 125mg three times a day) alone were classified as the EGFR-TKI group. Patients received EGFR-TKI (erlotinib 150mg daily, gefitinib 250mg daily or icotinib 125mg three times a day) and thymosin (thymosin α1 1.6mg twice a week or thymopentin 10mg daily) concurrently were designated as the EGFR-TKI plus thymosin group.

Data Collection

The data collected included the demographics, clinical characteristics, treatment, tumor response, adverse events (AEs) and T lymphocyte subsets in peripheral blood. Tumor response was assessed by two independent senior physicians in oncology according to RECIST 1.1. The initial response was assessed after 4 weeks of treatment, and tumor evaluation was repeated every 2 months. If the assessments were inconsistent, the controversial results were reassessed by the third oncologist. AEs were assessed according to the National Cancer Institute Common Toxicity Criteria version 3.0. The data of peripheral blood T lymphocyte subsets before EGFR-TKI treatment were gathered within one month before EGFR-TKI treatment. Peripheral blood T lymphocyte subsets after EGFR-TKI treatment were collected from receiving EGFR-TKI treatment to progressive disease, and data after EGFR-TKI plus thymosin

treatment were acquired from patients receiving EGFR-TKI plus thymosin treatment to progressive disease, and then taking the average of all these data. 2mL of venous blood was collected in EDTA anticoagulant tube from each patient. Peripheral blood T lymphocytes subsets were detected by flow cytometry by trained technicians in Clinical Laboratory of Xinqiao Hospital in Army Medical University. The samples were stained with antibody to human CD45, CD3, CD4, CD8 or isotype control conjugated with PerCP, FITC, APC and PE for 30 min, respectively. The indicated antibodies were obtained from Agilent Technologies (China Inc). Subsequently, stained samples were measured on a flow cytometer, NovoCyte D2040R (Agilent Technologies). The data were analyzed by NovoExpress software (Agilent Technologies).

Assessment Criteria

The primary endpoint was PFS, which was defined as the time from the initiation of EGFR-TKI treatment to the first documentation of progressive disease or death for any reason. The secondary endpoints included OS, objective response rate (ORR), disease control rate (DCR) and AEs. OS was defined as the time from the first dose of EGFR-TKI to cancer-related death or the last follow-up time.

Statistical Analysis

When comparing the baseline, brain metastasis, bone metastasis and first- or second-line EGFR-TKI treatment had significantly differences in EGFR-TKI group and EGFR-TKI plus thymosin group. Propensity score matching was applied at the ratio of 2:1 in EGFR-TKI group and EGFR-TKI plus thymosin group with these three items as covariates to avoid bias. The Chi-square test or fisher exact test was used to analyze the intergroup difference in clinical features, ORR, DCR and AEs. And the Wilcoxon rank sum test was used to analyze age difference. The Kaplan-Meier estimator was used to estimate the survival curves. The log-rank test was performed for intergroup comparison. Cox proportional hazards regression was used to calculate hazard ratios (HRs) and 95% confidence intervals (CIs) for the association of combination of EGFR-TKI and thymosin with the risk of disease progression and death. The changes of peripheral blood T lymphocyte subsets between EGFR-TKI and EGFR-TKI plus thymosin group before and after treatment were assessed by paired-samples T test. All statistical analyses were performed using R software (Version 3.6.1). The statistical significance level was set at $P < 0.05$ under a two-tailed test.

RESULTS

Patient Characteristics

From August 2008 to July 2018, a total of 908 patients were confirmed as NSCLC with active EGFR mutations. Of these patients, 495 subjects met the inclusion criteria. There were 22 patients excluded for incomplete medical records. 36 cases of the patients received EGFR-TKI therapy for less than 8 weeks. 89 patients were treated with thymosin for less than 4 weeks. And there were 16 patients lost to follow-up. Finally, 267 patients received EGFR-TKI monotherapy and 65 patients received EGFR-TKI plus thymosin treatment (**Supplementary Figure 1**).

When conducted the comparison of demographic and clinical characteristics between EGFR-TKI group and EGFR-TKI plus thymosin group, we found that brain metastasis, bone metastasis and first- or second-line EGFR-TKI treatment in two groups had significantly differences, then propensity score matching analysis was applied at a ratio of 2:1. Finally, 130 patients took EGFR-TKI monotherapy and 65 patients received EGFR-TKI plus thymosin treatment were included (**Supplementary Figure 1**). Of the 195 patients, the median age was 57.5 years old (range, 21 to 81 years old) and 120 cases were female. All of them were diagnosis as adenocarcinoma histologically. There were 144 patients received EGFR-TKI as the first line therapy and 51 patients received the second line therapy. 93 patients received gefitinib therapy, 76 patients took received erlotinib therapy and 26 patients were treated with icotinib. The baseline of EGFR-TKI group and EGFR-TKI plus thymosin group were balanced after propensity score matching (**Table 1**).

Progression-Free Survival and Overall Survival

The median PFS was 14.4 months (95% CI, 11.7-17.1) in EGFR-TKI plus thymosin group, which was significantly improved than 9.2 months (95% CI, 7.9-10.3) in EGFR-TKI group (HR=0.433, 95% CI 0.322 - 0.582, P<0.0001, **Figure 1A**). The median OS were 29.5 months (95% CI, 21.5-37.5) in EGFR-TKI plus thymosin group and 19.8 months (95% CI, 18.2-21.4) in EGFR-TKI group, respectively (HR=0.430, 95% CI 0.319 - 0.580, P<0.0001, **Figure 1B**).

A consistent benefit of EGFR-TKI plus thymosin over EGFR-TKI with respect to PFS (**Figure 2**) and OS (**Figure 3**) were shown across most subgroups that were assessed, including the subgroups based on age, EGFR mutation type (exon 19 deletion vs. exon 21 L858R mutation), the presence or absence of CNS metastases, multiple lung metastasis, pleura metastasis, bone metastasis and adrenal metastasis, treated by gefitinib or erlotinib. The advantages of PFS in EGFR-TKI plus thymosin group were not observed in males, patients whose ECOG score was 2 points, who had smoking history, suffered from liver metastasis, treated with icotinib, received the EGFR-TKI as the second line therapy and received radiotherapy (**Figure 2**). And OS in EGFR-TKI plus thymosin group had no advantage in patients who suffered from liver metastasis, treated with icotinib, received the EGFR-TKI as the second line therapy. Patients who received radiotherapy for CNS metastasis had a tendency to benefit from the combination therapy (P=0.079) (**Figure 3**).

In EGFR-TKI plus thymosin group, there were 29 patients treated with EGFR-TKI plus thymosin α1 whose median PFS were 14.7 months and 36 patients treated with EGFR-TKI plus thymopentin with the median PFS of 14.1 months (P>0.05). And there was no difference in the median OS between the two groups.

Response Rates

The objective response rate (ORR) was 60.0% in EGFR-TKI plus thymosin group and 60.8% in EGFR-TKI group (P=0.918). The

TABLE 1 | Patients' demographic and clinical characteristics in the EGFR-TKI and EGFR-TKI plus thymosin group before and after propensity score matching.

Characteristics	Before match			After match		
	EGFR-TKI n=267	EGFR-TKI plus thymosin n=65	*P*	EGFR-TKI n=130	EGFR-TKI plus thymosin n=65	*P*
Male	104	23	0.596	52	23	0.532
Median age (IQR)	57 (49-64)	58 (49-66)	0.357	57 (48-65)	58 (49-66)	0.489
ECOG PS						
0-1	260	61	0.236	127	61	0.225
2	7	4		3	4	
Smoking	65	11	0.202	34	11	0.149
EGFR mutations						
Exon 19 deletion	156	38	0.865	78	38	0.982
Exon 21 L858R mutation	112	26		53	26	
CNS metastasis	82	11	0.026	22	11	1.000
Liver metastasis	24	9	0.241	13	9	0.424
Multiple lung metastasis	136	28	0.256	69	28	0.188
Pleura metastasis	98	19	0.258	46	19	0.390
Bone metastasis	123	46	0.0004	92	46	1.000
Adrenal metastasis	17	8	0.104	8	8	0.140
EGFR-TKI						
Gefitinib	133	29	0.258	64	29	0.258
Erlotinib	96	30		46	30	
Icotinib	38	6		20	6	
Line of EGFR-TKI						
First-line	219	46	0.043	98	46	0.489
Second-line	48	19		32	19	
Radiotherapy for CNS metastasis	18	7	0.270	8	7	0.254
Radiotherapy for lung lesion	4	3	0.139	2	3	0.336
Radiotherapy for bone metastasis	10	6	0.100	6	6	0.219

EGFR, epidermal growth factor receptor; TKI, tyrosine kinase inhibitor; IQR, interquartile range; ECOG PS, eastern cooperative oncology group performance status; CNS, central nervous system.

disease control rate (DCR) was 96.9% in EGFR-TKI plus thymosin group and 97.7% in EGFR-TKI group (*P*=1.000). There were no differences in ORR and DCR between the two groups. More details about response rates were shown in **Supplementary Figure 2**.

Adverse Events

The most common adverse events were rash (40.0% in the EGFR-TKI plus thymosin group and 38.5% in the EGFR-TKI group), diarrhea (23.1% and 25.4%, respectively), dry skin (20.0% and 20.8%, respectively) and anorexia (9.2% and 10.0%, respectively). Adverse events of grade 3 or higher occurred in 2 cases in the EGFR-TKI plus thymosin group and 5 cases in the EGFR-TKI group. No fatal adverse events were found in the two groups. There were no significant differences in adverse effects between the two groups (**Table 2**). Together, the combination of EGFR-TKI and thymosin would not increase the incidences of adverse events.

Peripheral Blood T Lymphocyte Subsets

There were 23 patients detected the peripheral blood T lymphocyte subsets before and after EGFR-TKI monotherapy, and 11 patients had detected the peripheral blood T lymphocyte subsets before and after EGFR-TKI plus thymosin therapy. In the EGFR-TKI group, the number of $CD3^+T$ cells decreased after treatment (*P*<0.05, **Figure 4A**) including both the $CD3^+CD4^+T$ and $CD3^+CD8^+T$ subsets (*P*<0.05, **Figures 4B, C**). However, the ratio of $CD3^+CD4^+T$ to $CD3^+CD8^+T$ did not change

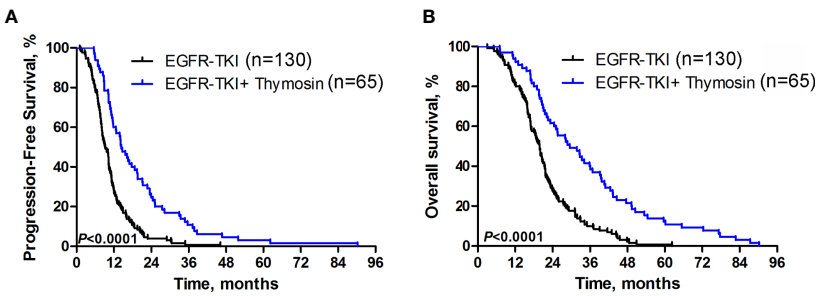

FIGURE 1 | Progression-free Survival and Overall Survival. Kaplan-Meier estimated **(A)** progression-free survival (PFS) and **(B)** overall survival (OS) in EGFR-TKI plus thymosin group and EGFR-TKI group.

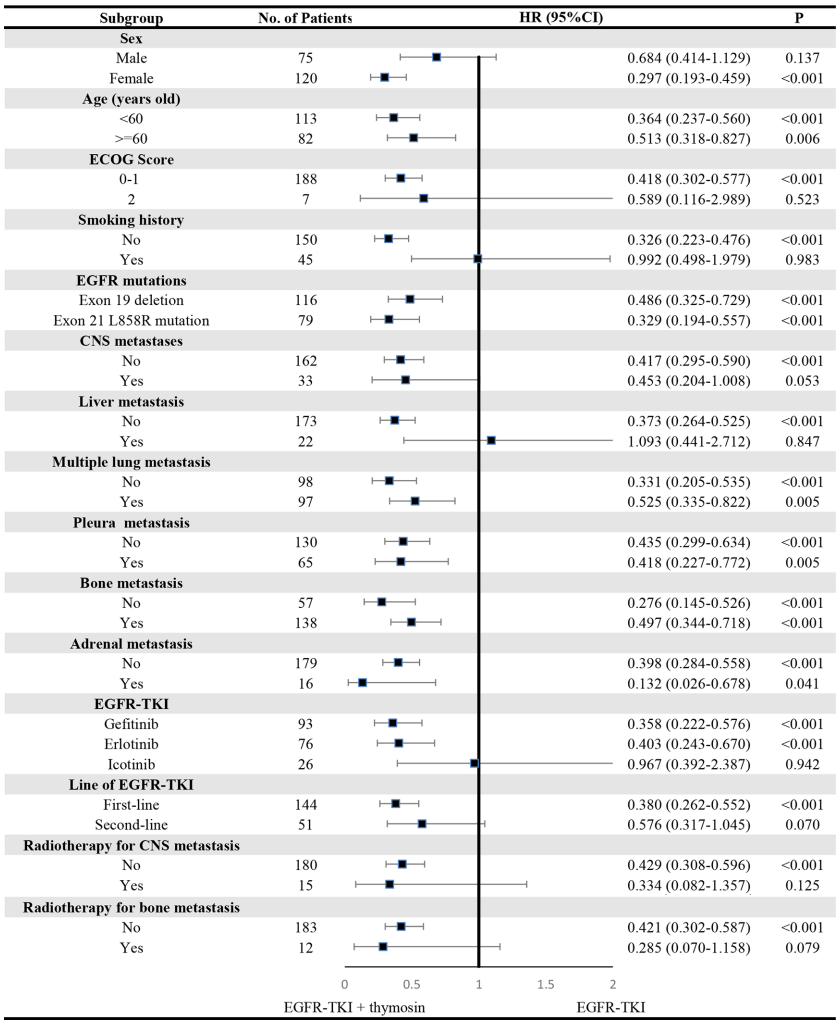

FIGURE 2 | Subgroup Analyses of Progression-free Survival. P showed the significance of the HRs. It was used to test the significance of PFS between EGFR-TKI plus thymosin group and EGFR-TKI group in a certain variable. HR, hazard ratio; CI, confidence interval; ECOG, eastern cooperative oncology group; CNS, central nervous system.

(**Figure 4D**). In the EGFR-TKI plus thymosin group, both the number of $CD3^+T$ cells and the ratio of $CD3^+CD4^+T$ to $CD3^+CD8^+T$ had no obvious changes before and after treatment (**Figure 4**). It suggested that thymosin combined with EGFR-TKI may reverse the inhibition of T cells.

DISCUSSION

In the current study, our results demonstrated that patients in EGFR-TKI plus thymosin group had significantly prolonged median PFS and OS compared with those in EGFR-TKI group. And the combination of EGFR-TKI and thymosin would not increase the incidences of adverse events. By observing the peripheral blood T lymphocyte subsets before and after treatment, we found thymosin combined with EGFR-TKI may reverse the inhibition of T cells. Therefore, combination of EGFR-TKI and thymosin may be a potential therapy to enhance the efficacy of EGFR-TKI without increasing adverse events.

To avoid the impact of inconsistent baseline, the propensity score matching analysis was applied at the ratio of 2:1 in EGFR-TKI group and EGFR-TKI plus thymosin group. The limitation of propensity score matching analysis is only to control the effect of measurable variables. New bias may appear if there is unobservable selection on variables. However, the results will be less reliable when the confounding factors exist. In this study, there were no differences in demographic and clinical characteristics between the two groups after propensity score matching.

The median PFS in EGFR-TKI plus thymosin group was 14.4 months, with a 57% lower risk of disease progression or death than that in the EGFR-TKI group. The median PFS in the EGFR-TKI group in our research is 9.2 months which is similar with

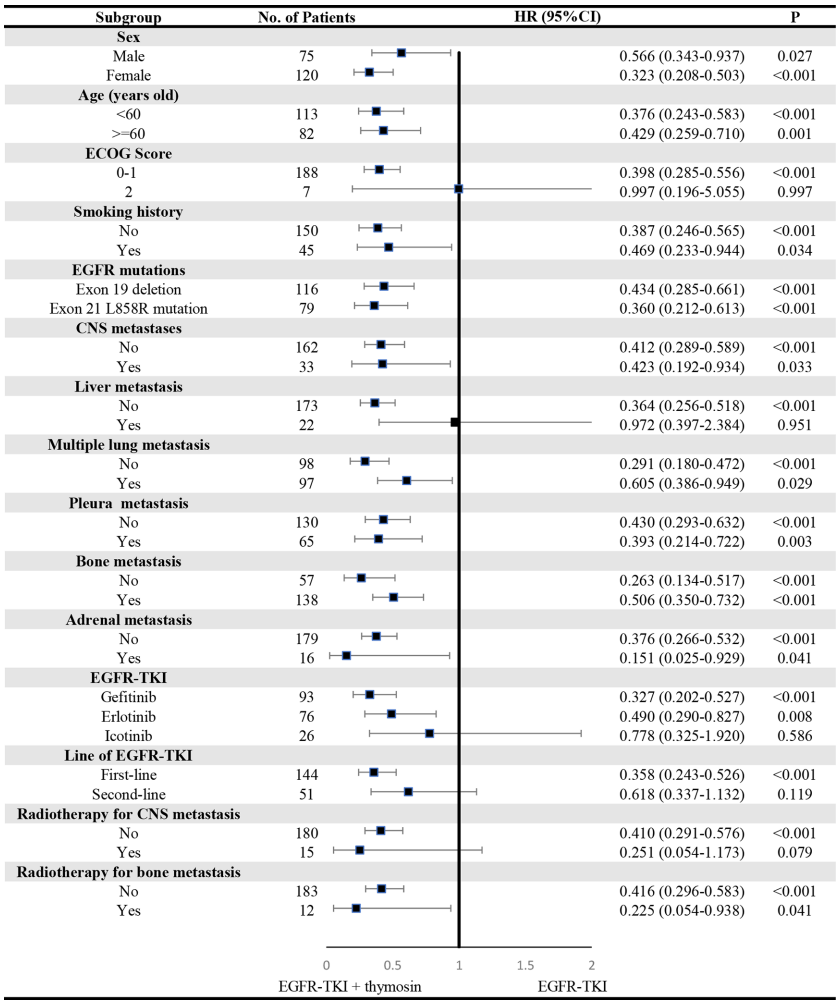

FIGURE 3 | Subgroup Analyses of Overall Survival. P showed the significance of the HRs. It was used to test the significance of OS between EGFR-TKI plus thymosin group and EGFR-TKI group in a certain variable. HR, hazard ratio; CI, confidence interval. ECOG, eastern cooperative oncology group; CNS, central nervous system.

TABLE 2 | Adverse effects in EGFR-TKI and EGFR-TKI plus thymosin group.

Adverse effect	EGFR-TKI n=130 (%)		EGFR-TKI plus Thymosin n=65 (%)		*P*
	ALL grades	Grades≥3	ALL grades	Grades≥3	
Rash	50 (38.5)	3 (2.3)	26 (40.0)	1 (1.5)	0.836
Diarrhea	33 (25.4)	2 (1.5)	15 (23.1)	1 (1.5)	0.724
Dry skin	27 (20.8)	0 (0.0)	13 (20.0)	0 (0.0)	0.900
Hand and foot syndrome	0 (0.0)	0 (0.0)	1 (1.5)	0 (0.0)	0.333
Tired	6 (4.6)	0 (0.0)	1 (1.5)	0 (0.0)	0.276
Anorexia	13 (10.0)	0 (0.0)	6 (9.2)	0 (0.0)	0.864
Nausea,vomiting	2 (1.5)	0 (0.0)	2 (3.1)	0 (0.0)	0.602
Increasing of transaminase	4 (3.1)	0 (0.0)	0 (0.0)	0 (0.0)	0.303
Mouth ulcer	6 (4.6)	0 (0.0)	0 (0.0)	0 (0.0)	0.181
Nail changes	0 (0.0)	0 (0.0)	1 (1.5)	0 (0.0)	0.333
Reduction of leukocyte	1 (0.8)	0 (0.0)	1 (1.5)	0 (0.0)	1.000
Deadlimb	0 (0.0)	0 (0.0)	1 (1.5)	0 (0.0)	0.333
Edema	0 (0.0)	0 (0.0)	1 (1.5)	0 (0.0)	0.333

EGFR, epidermal growth factor receptor; EGFR-TKI, epidermal growth factor receptor tyrosine kinase inhibitor.

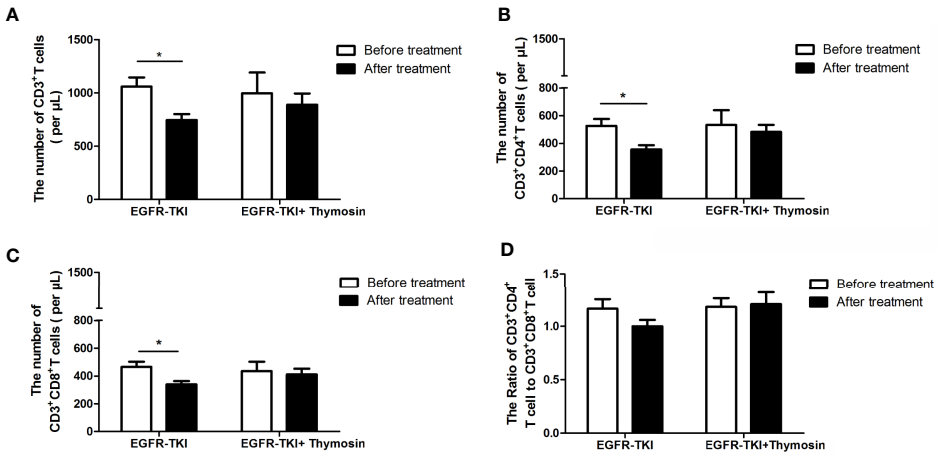

FIGURE 4 | The numbers of T cell subsets in peripheral blood in EGFR-TKI group and EGFR-TKI plus thymosin group before and after treatment. **(A)** The numbers of $CD3^+$ T cells. **(B)** The numbers of $CD3^+$ $CD4^+$T cells. **(C)** The numbers of $CD3^+$ $CD8^+$T cells. **(D)** The ratio of $CD3^+$ $CD4^+$T cells to $CD3^+$ $CD8^+$T cells. $^*P < 0.05$.

that in previous clinical trials of gefitinib with the median PFS ranges from 8.0 (5) to 10.9 (17) months, erlotinib with the median PFS 13.1 months (4) and icotinib with the median PFS 11.2 months (18). As previously reported, the median OS of EGFR-TKIs (including gefitinib, erlotinib and icotinib) ranged from 21.6 (19) to 30.5 months (2, 18), which was longer than the OS in our study. Zeng et al. (16) had summarized four trials with 269 cases to demonstrate that administration of thymosin with chemotherapy significantly increased the 1-year OS rate. Our study had also showed that combination of EGFR-TKI and thymosin could prolong the PFS and OS and would be a potential therapy to enhance the efficacy of EGFR-TKI.

In the subgroup analysis, consistent benefit of EGFR-TKI plus thymosin over EGFR-TKI with respect to PFS and OS were shown. Patients benefit from EGFR-TKI plus thymosin treatment regardless of the type of EGFR mutations. Fukuoka et al. (19) had reported that PFS was significantly longer for gefitinib versus carboplatin/paclitaxel in both the exon 19 deletions and the exon 21 L858R mutation subgroups. Combined EGFR-TKI with thymosin was more advantageous as first-line treatment compared with who received it as second-line treatment, which was consistent with the result of EGFR-TKI monotherapy (2). OS in EGFR-TKI plus thymosin group had no advantage in patients who suffered from liver metastasis. No comparison stratified by liver metastasis was retrieved in studies about EGFR-TKI combined with angiogenesis inhibitors in NEJ 026 (9) and CTONG 1509 (8). Although patients were stratified by liver metastasis and EGFR mutation, there were still no data about efficacy of EGFR mutation with liver metastasis in immunotherapy combined with angiogenesis inhibitor and chemotherapy in IMpower150 (20). In general, liver metastasis is a negative predictor for EGFR-TKIs therapy in patients with EGFR-mutant NSCLC (21) without satisfactory combination therapies. In our study, the combination of EGFR-TKI and thymosin still showed no superiority. More samples were needed to confirm whether patients who received radiotherapy for CNS metastasis benefit from the combination therapy.

In the Iressa Pan-Asia Study (IPASS) (1), the common adverse events of gefitinib are rash or acne (66.2%), diarrhea (46.2%), dry skin (23.9%), and anorexia (21.9%). Erlotinib was reported to be the most prone to skin diseases in the first-generation of EGFR-TKIs (22). And the adverse events of icotinib were observed: rash (40%), diarrhea (19%), and hepatotoxicity (8%) (23). In our study, there was no statistical comparison of safety data in EGFR-TKI plus thymosin group and EGFR-TKI group. The most common adverse events were rash (40.0% in the EGFR-TKI plus thymosin group and 38.5% in the EGFR-TKI group), diarrhea (23.1% vs 25.4%), dry skin (20.0% vs 20.8%) and anorexia (9.2% vs 10.0%). It suggested that combination of EGFR-TKI and thymosin may be a safe option.

The inhibition of peripheral blood T cell subsets by EGFR-TKI therapy may be a potential reason why combined with thymosin can prolong PFS and OS. In this study, the number of $CD3^+$T cells decreased significantly after treatment including both the $CD3^+CD4^+$T cells and $CD3^+CD8^+$T subsets decreased in the EGFR-TKI group. However, peripheral blood T cell subsets in the EGFR-TKI plus thymosin group did not change before and after treatment. It has been reported that erlotinib has the effect of immunosuppression while anti-tumor. Erlotinib could damage T-cell-mediated immune response through inhibiting T cell proliferation and activation, and inhibiting the secretion of IL-2 and IFN-γ by activated T lymphocyte cells (13). Treat with gefitinib for 4 weeks can result in a decreased percent of $CD4^+$ T cells (24).

Thymosin, as a non-specific immunomodulator, had been widely used in cancer. It can increase the release of cytokine IL-2 and the expression of IL-2 receptor (25, 26). Thymosin was reported could not only activate T cells, inducing their maturation and differentiation (27), but also enhance the

activity of natural killer and dendritic cells (28, 29). In addition, thymosin could enhance the expression of major histocompatibility complex class-I molecule and tumor associated antigens in multiple tumor cells (25, 30), thus tumor cells can be recognized by T lymphocytes easier. Several studies reported that both thymosin α1 and thymopentin could inhibit the growth of tumor cells by decreasing reactive oxygen species levels in tumor cells (31, 32). Together, thymosin plays important roles in both immunomodulatory and anti-tumor. Thus, the combination of EGFR-TKI with thymosin has synergistic effects in NSCLC.

In conclusion, our study revealed that combination of EGFR-TKI and thymosin can prolong the PFS and OS compared with EGFR-TKI monotherapy in NSCLC patients harboring active EGFR mutations without the increasing of adverse events. The combination therapy offers a new strategy for the treatment of NSCLC with active EGFR mutations.

DATA AVAILABILITY STATEMENT

The original contributions presented in the study are included in the **Supplementary Material**. Further inquiries can be directed to the corresponding authors.

ETHICS STATEMENT

The studies involving human participants were reviewed and approved by Ethics Committee, Xinqiao Hospital, Army Medical University. The patients/participants provided their written informed consent to participate in this study. Written informed consent was obtained from the individual(s) for the publication of any potentially identifiable images or data included in this article.

AUTHOR CONTRIBUTIONS

YF and GZ: Conceptualization, Methodology, Validation, Formal analysis, Investigation, Data curation, Writing - original draft, Visualization. SL, PH, GL, FC, WZ, YD, and AZ: Data curation, Methodology, Validation. ZC: Conceptualization, Resources, Data curation, Writing - review and editing, Supervision, Project administration. JS: Conceptualization, Resources, Data curation, Writing - review and editing, Supervision, Project administration, Funding acquisition. All authors contributed to the article and approved the submitted version.

FUNDING

This study was supported by the National Natural Science Foundation of China [No. 81672841, 81773245 and 81972858], the talent Foundation of Chongqing [cstccxljrc201910], the Cultivation Program for Clinical Research Talents of Army Medical University in 2018 [2018XLC1010].

ACKNOWLEDGMENTS

We would like to extend our heartfelt gratitude to patients, family members of recruited patients and clinicians for providing some follow-up information.

SUPPLEMENTARY MATERIAL

The Supplementary Material for this article can be found online at: https://www.frontiersin.org/articles/10.3389/fonc.2021.659065/full#supplementary-material

REFERENCES

1. Mok TS, Wu YL, Thongprasert S, Yang CH, Chu DT, Saijo N, et al. Gefitinib or Carboplatin-Paclitaxel in Pulmonary Adenocarcinoma. *N Engl J Med* (2009) 361:947–57. doi: 10.1056/NEJMoa0810699
2. Maemondo M, Inoue A, Kobayashi K, Sugawara S, Oizumi S, Isobe H, et al. Gefitinib or Chemotherapy for Non-Small-Cell Lung Cancer With Mutated EGFR. *N Engl J Med* (2010) 362:2380–8. doi: 10.1056/NEJMoa0909530
3. Wu YL, Zhou C, Liam CK, Wu G, Liu X, Zhong Z, et al. First-Line Erlotinib Versus Gemcitabine/Cisplatin in Patients With Advanced EGFR Mutation-Positive Non-Small-Cell Lung Cancer: Analyses From the Phase III, Randomized, Open-Label, ENSURE Study. *Ann Oncol* (2015) 26:1883–9. doi: 10.1093/annonc/mdv270
4. Zhou C, Wu YL, Chen G, Feng J, Liu XQ, Wang C, et al. Erlotinib Versus Chemotherapy as First-Line Treatment for Patients With Advanced EGFR Mutation-Positive Non-Small-Cell Lung Cancer (OPTIMAL, CTONG-0802): A Multicentre, Open-Label, Randomised, Phase 3 Study. *Lancet Oncol* (2011) 12:735–42. doi: 10.1016/S1470-2045(11)70184-X
5. Han JY, Park K, Kim SW, Lee DH, Kim HY, Kim HT, et al. First-SIGNAL: First-Line Single-Agent Iressa Versus Gemcitabine and Cisplatin Trial in Never-Smokers With Adenocarcinoma of the Lung. *J Clin Oncol* (2012) 30:1122–8. doi: 10.1200/JCO.2011.36.8456
6. Lim SM, Syn NL, Cho BC, Soo RA. Acquired Resistance to EGFR Targeted Therapy in Non-Small Cell Lung Cancer: Mechanisms and Therapeutic Strategies. *Cancer Treat Rev* (2018) 65:1–10. doi: 10.1016/j.ctrv.2018.02.006
7. Lee CK, Novello S, Rydén A, Mann H, Mok T. Patient-Reported Symptoms and Impact of Treatment With Osimertinib Versus Chemotherapy in Advanced Non-Small-Cell Lung Cancer: The Aura3 Trial. *J Clin Oncol* (2018) 36:1853–60. doi: 10.1200/JCO.2017.77.2293
8. Zhou Q, Wu Y, Cheng Y, Liu Y, Chen G, Cui J, et al. Ctong 1509: Phase III Study of Bevacizumab Withor Without Erlotinib in Untreated Chinese Patients With Advanced EGFR-Mutatednsclc. *Ann Oncol* (2019) 30 (suppl_5):v602–60. doi: 10.1093/annonc/mdz260.002
9. Saito H, Fukuhara T, Furuya N, Watanabe K, Sugawara S, Iwasawa S, et al. Erlotinib Plus Bevacizumab Versus Erlotinib Alone in Patients With EGFR-Positive Advanced Non-Squamous Non-Small-Cell Lung Cancer (NEJ026): Interim Analysis of an Open-Label, Randomised, Multicentre, Phase 3 Trial. *Lancet Oncol* (2019) 20:625–35. doi: 10.1016/S1470-2045(19)30035-X
10. Noronha V, Patil VM, Joshi A, Menon N, Chougule A, Mahajan A, et al. Gefitinib Versus Gefitinib Plus Pemetrexed and Carboplatin Chemotherapy in EGFR-Mutated Lung Cancer. *J Clin Oncol* (2020) 38:124–36. doi: 10.1200/JCO.19.01154
11. Jia Y, Li X, Jiang T, Zhao S, Zhao C, Zhang L, et al. EGFR-Targeted Therapy Alters the Tumor Microenvironment in EGFR-driven Lung Tumors:

Implications for Combination Therapies. *Int J Cancer* (2019) 145:1432–44. doi: 10.1002/ijc.32191
12. Zeboudj L, Maître M, Guyonnet L, Laurans L, Joffre J, Lemarie J, et al. Selective EGF-Receptor Inhibition in CD4+ T Cells Induces Anergy and Limits Atherosclerosis. *J Am Coll Cardiol* (2018) 71:160–72. doi: 10.1016/j.jacc.2017.10.084
13. Luo Q, Gu Y, Zheng W, Wu X, Gong F, Gu L, et al. Erlotinib Inhibits T-cell-mediated Immune Response Via Down-Regulation of the c-Raf/ERK Cascade and Akt Signaling Pathway. *Toxicol Appl Pharmacol* (2011) 251:130–6. doi: 10.1016/j.taap.2010.12.011
14. Wolf E, Milazzo S, Boehm K, Zwahlen M, Horneber M. Thymic Peptides for Treatment of Cancer Patients. *Cochrane Database Syst Rev* (2011) 2: CD003993. doi: 10.1002/14651858.CD003993.pub3
15. Attapon C, Ruangrong C. Lung Cancer Chemotherapy, New Treatment and Related Patents. *Recent Pat Anticancer Drug Discov* (2014) 9:372–81. doi: 10.2174/1574892809666140520120806
16. Zeng FL, Xiao Z, Wang CQ, Jiang Y, Shan JL, Hu SS, et al. Clinical Efficacy and Safety of Synthetic Thymic Peptides With Chemotherapy for Non-Small Cell Lung Cancer in China: A Systematic Review and Meta-Analysis of 27 Randomized Controlled Trials Following the PRISMA Guidelines. *Int Immunopharmacol* (2019) 75:105747. doi: 10.1016/j.intimp.2019.105747
17. Park K, Tan EH, O'Byrne K, Zhang L, Boyer M, Mok T, et al. Afatinib Versus Gefitinib as First-Line Treatment of Patients With EGFR Mutation-Positive Non-Small-Cell Lung Cancer (LUX-Lung 7): A Phase 2B, Open-Label, Randomised Controlled Trial. *Lancet Oncol* (2016) 17:577–89. doi: 10.1016/S1470-2045(16)30033-X
18. Shi YK, Wang L, Han BH, Li W, Yu P, Liu YP, et al. First-Line Icotinib Versus Cisplatin/Pemetrexed Plus Pemetrexed Maintenance Therapy for Patients With Advanced EGFR Mutation-Positive Lung Adenocarcinoma (CONVINCE): A Phase 3, Open-Label, Randomized Study. *Ann Oncol* (2017) 28:2443–50. doi: 10.1093/annonc/mdx359
19. Fukuoka M, Wu YL, Thongprasert S, Sunpaweravong P, Leong SS, Sriuranpong V, et al. Biomarker Analyses and Final Overall Survival Results From a Phase III, Randomized, Open-Label, First-Line Study of Gefitinib Versus Carboplatin/Paclitaxel in Clinically Selected Patients With Advanced Non-Small-Cell Lung Cancer in Asia (Ipass). *J Clin Oncol* (2011) 29:2866–74. doi: 10.1200/JCO.2010.33.4235
20. Socinski MA, Jotte RM, Cappuzzo F, Orlandi F, Stroyakovskiy D, Nogami N, et al. Atezolizumab for First-Line Treatment of Metastatic Nonsquamous Nsclc. *N Engl J Med* (2018) 378:2288–301. doi: 10.1056/NEJMoa1716948
21. Jiang T, Cheng R, Zhang G, Su C, Zhao C, Li X, et al. Characterization of Liver Metastasis and Its Effect on Targeted Therapy in EGFR-mutant Nsclc: A Multicenter Study. *Clin Lung Cancer* (2017) 18:631–9. doi: 10.1016/j.cllc.2017.04.015
22. Zhou JY, Liu SY, Wu YL. Safety of EGFR-TKIs for EGFR Mutation-Positive Non-Small Cell Lung Cancer. *Expert Opin Drug Saf* (2020) 19:589–99. doi: 10.1080/14740338.2020.1753697
23. Shi Y, Zhang L, Liu X, Zhou C, Zhang L, Zhang S, et al. Icotinib Versus Gefitinib in Previously Treated Advanced Non-Small-Cell Lung Cancer (ICOGEN): A Randomised, Double-Blind Phase 3 Non-Inferiority Trial. *Lancet Oncol* (2013) 14:953–61. doi: 10.1016/S1470-2045(13)70355-3
24. Sheng J, Fang W, Liu X, Xing S, Zhan J, Ma Y, et al. Impact of Gefitinib in Early Stage Treatment on Circulating Cytokines and Lymphocytes for Patients With Advanced Non-Small Cell Lung Cancer. *Onco Targets Ther* (2017) 10:1101–10. doi: 10.2147/OTT.S112158
25. Garaci E. Thymosin alpha1: A Historical Overview. *Ann N Y Acad Sci* (2007) 1112:14–20. doi: 10.1196/annals.1415.039
26. Sztein MB, Serrate SA. Characterization of the Immunoregulatory Properties of Thymosin Alpha 1 on Interleukin-2 Production and Interleukin-2 Receptor Expression in Normal Human Lymphocytes. *Int J Immunopharmacol* (1989) 11:789–800. doi: 10.1016/0192-0561(89)90133-1
27. Ahmed A, Wong DM, Thurman GB, Low TL, Goldstein AL, Sharkis SJ, et al. T-Lymphocyte Maturation: Cell Surface Markers and Immune Function Induced by T-lymphocyte Cell-Free Products and Thymosin Polypeptides. *Ann N Y Acad Sci* (1979) 332:81–94. doi: 10.1111/j.1749-6632.1979.tb47100.x
28. Romani L, Bistoni F, Gaziano R, Bozza S, Montagnoli C, Perruccio K, et al. Thymosin Alpha 1 Activates Dendritic Cells for Antifungal Th1 Resistance Through Toll-Like Receptor Signaling. *Blood* (2004) 103:4232–9. doi: 10.1182/blood-2003-11-4036
29. Wang Y, Cao Y, Meng Y, You Z, Liu X, Liu Z. The Novel Role of Thymopentin in Induction of Maturation of Bone Marrow Dendritic Cells (Bmdcs). *Int Immunopharmacol* (2014) 21:255–60. doi: 10.1016/j.intimp.2014.05.011
30. Giuliani C, Napolitano G, Mastino A, Di Vincenzo S, D'Agostini C, Grelli S, et al. Thymosin-Alpha1 Regulates MHC Class I Expression in FRTL-5 Cells At Transcriptional Level. *Eur J Immunol* (2000) 30:778–86. doi: 10.1002/1521-4141(200003)30:3<778::AID-IMMU778>3.0.CO;2-I
31. Qin Y, Chen FD, Zhou L, Gong XG, Han QF. Proliferative and Anti-Proliferative Effects of Thymosin Alpha1 on Cells are Associated With Manipulation of Cellular ROS Levels. *Chem Biol Interact* (2009) 180:383–8. doi: 10.1016/j.cbi.2009.05.006
32. Patruno A, Tosco P, Borretto E, Franceschelli S, Amerio P, Pesce M, et al. Thymopentin Down-Regulates Both Activity and Expression of iNOS in Blood Cells of Sézary Syndrome Patients. *Nitric Oxide* (2012) 27:143–9. doi: 10.1016/j.niox.2012.06.002

Conflict of Interest: The authors declare that the research was conducted in the absence of any commercial or financial relationships that could be construed as a potential conflict of interest.

Copyright © 2021 Feng, Zhu, Lang, Hao, Li, Chen, Zhuo, Duan, Zhang, Chen and Sun. This is an open-access article distributed under the terms of the Creative Commons Attribution License (CC BY). The use, distribution or reproduction in other forums is permitted, provided the original author(s) and the copyright owner(s) are credited and that the original publication in this journal is cited, in accordance with accepted academic practice. No use, distribution or reproduction is permitted which does not comply with these terms.

frontiers in Oncology

ORIGINAL RESEARCH
published: 28 May 2021
doi: 10.3389/fonc.2021.684073

Cost-Effectiveness of Lorlatinib as a First-Line Therapy for Untreated Advanced Anaplastic Lymphoma Kinase-Positive Non-Small Cell Lung Cancer

SiNi Li[1,2], JianHe Li[3], LiuBao Peng[3], YaMin Li[1,2†] and XiaoMin Wan[3*]*

[1] Clinical Nursing Teaching and Research Section, The Second Xiangya Hospital, Central South University, Changsha, China, [2] The Xiangya Nursing School, Central South University, Changsha, China, [3] Department of Pharmacy, The Second Xiangya Hospital, Central South University, Changsha, China

OPEN ACCESS

Edited by:
Junji Uchino,
Kyoto Prefectural University of Medicine, Japan

Reviewed by:
Maha Mohamed Saber-Ayad,
University of Sharjah,
United Arab Emirates
Ebrahim Mostafavi,
Stanford University, United States

***Correspondence:**
YaMin Li
aminny@csu.edu.cn
XiaoMin Wan
wanxiaomin@csu.edu.cn

†Present address:
YaMin Li,
Clinical Nursing Teaching and Research Section, The Second Xiangya Hospital, Central South University, Changsha, China

Specialty section:
This article was submitted to Pharmacology of Anti-Cancer Drugs, a section of the journal Frontiers in Oncology

Received: 22 March 2021
Accepted: 30 April 2021
Published: 28 May 2021

Citation:
Li S, Li J, Peng L, Li Y and Wan X (2021) Cost-Effectiveness of Lorlatinib as a First-Line Therapy for Untreated Advanced Anaplastic Lymphoma Kinase-Positive Non-Small Cell Lung Cancer. Front. Oncol. 11:684073. doi: 10.3389/fonc.2021.684073

Introduction: Recently, a phase III CROWN trial compared the efficacy of two anaplastic lymphoma kinase (ALK) inhibitors and demonstrated that lorlatinib displayed clinical improvement over crizotinib for advanced non-small cell lung cancer (NSCLC) patients. Therefore, the aim of this study was to estimate the cost-effectiveness of lorlatinib as a first-line therapy for patients with advanced ALK-positive (+) NSCLC.

Materials and Methods: A cost-effectiveness analysis was performed using a microsimulation model from the US payer perspective and a lifetime horizon (30 years) in patients with previous untreated advanced ALK+ NSCLC. Based on the CROWN trial, patient characteristics were obtained, and the transition probabilities were estimated. All direct costs were derived from official sources and published literature. The main outcomes of the model were total costs, incremental cost-effectiveness ratio (ICER), quality-adjusted life years (QALYs), and life years (LYs). One-way and probabilistic sensitivity analyses and multiple scenario analyses were conducted to test the robustness of the model outcomes.

Results: In the base case analysis, in which 1 million patients were simulated, treatment with lorlatinib or crizotinib as the first-line treatment was related to a mean cost of $909,758 and $616,230 (incremental cost: $293,528) and a mean survival of 4.81 QALYs and 4.09 QALYs (incremental QALY: 0.72) per patient, respectively. The main drivers of cost effectiveness were drug price and subsequent cost. PAS indicated that lorlatinib has 90% cost-effectiveness when compared to crizotinib when the willingness-to-pay (WTP) threshold in increased to $448,000/QALY. Scenario analysis demonstrated that lorlatinib has 100% cost-effectiveness at a WTP threshold of 200,000/QALY compared to crizotinib treatment when the price of lorlatinib is decreased to 75% ($424.5) of its original price.

Conclusions: In this study, lorlatinib was unlikely to be cost effective compared with crizotinib for patients with previously untreated advanced ALK+ NSCLC at a WTP threshold of 200,000/QALY.

Keywords: cost-effectiveness (CE), non-small cell lung cancer, ALK, lorlatinib, crizotinib

HIGHLIGHTS

1. This study reported that although lorlatinib significantly improved health outcomes, it still cannot be regarded as a cost-effective option compared with crizotinib for patients with untreated advanced ALK+ NSCLC from a US payer perspective.
2. When we adjusted the price of lorlatinib to $424.50, lorlatinib had 100% cost-effectiveness at a WTP threshold of 200,000/QALY compared with crizotinib treatment.
3. The implication of this study is not that crizotinib be used in place of lorlatinib or that lorlatinib should be withheld from patients. Rather, this study suggests that policymakers should control drug prices to within a reasonable range.

INTRODUCTION

Lung cancer, a second most common cancer in the United States (US) among both men and women, has the greatest cancer-related mortality of all cancers in the US, accounting for almost 25% of all cancer deaths (1, 2). Non-small cell lung cancer (NSCLC) accounts for approximately 85% of lung cancer cases, and of these, approximately 2–7% are anaplastic lymphoma kinase (ALK), with the majority being of the nonsquamous subtype (3–5). The American Cancer Society reported that in 2020, 228,820 new lung cancer cases were diagnosed in the US, and 135,720 lung cancer deaths occurred (1). This formidable mortality is due mainly to a combination of the high incidence of lung cancer, and survival outcomes remain poor in patients with advanced lung cancer (i.e., stage III/IV): The 5-year relative survival for patients with distant metastasis is 5.8% (6, 7).

Although treatments for late-stage lung cancer are seldom curative, new therapies are urgently needed and have shown enormous potential for lung cancer patients in clinical practice (8, 9). Tyrosine kinase inhibitors (TKIs), the first targeted therapy for NSCLC, have demonstrated clinical improvements in both progression-free survival (PFS) and response levels and are thus recommended by clinical guidelines for patients with NSCLC (10–18). ALK rearrangement, a potential mechanism for targeted therapy was soon recommended for NSCLC treatment (19). Crizotinib, a first-generation targeted TKI for advanced ALK+ NSCLC, was approved by the US Food and Drug Administration (FDA) in 2011 and has been established as the current standard of care in the US (20, 21). Subsequently, although more potent ALK inhibitors (i.e., ensartinib, alectinib and brigatinib) have been developed and showed clinical improvement superior to that of crizotinib as a first-line therapy, crizotinib is still recommended as the standard of care for ALK+ patients in some countries worldwide because of pharma-economic evaluations (22–26). Lorlatinib, a third-generation ALK inhibitor, received approval from the US FDA in 2018 for the treatment of patients with advanced ALK+ NSCLC (27). Compared with crizotinib, lorlatinib is more potent in biochemical and cellular assays and has been identified as the agent with the broadest coverage of ALK-resistant mutations (28). Moreover, lorlatinib can achieve high exposure in the central nervous system because it can cross the blood–brain barrier (28).

Recently, the CROWN trial (NCT03052608), an international randomized phase III trial comparing lorlatinib with crizotinib in patients with previously untreated advanced ALK+ NSCLC, indicated that lorlatinib was associated with a significantly longer PFS, better quality of life (QoL), and a higher intracranial response rate (28). Seventy-eight percent (95% confidence interval [CI], 70–84) and 39% (95% CI, 30–48) of patients survived with progression-free disease at 12 months after lorlatinib and crizotinib treatment, respectively, and the hazard ratio was 0.28 (95% CI, 0.19–0.41, P <0.001) for disease progression or death (28). Previous studies have demonstrated that lorlatinib not only inhibits ALK more effectively than first- or second-generation inhibitors but also more potently treats central nervous system (CNS) metastases (29–32).

With targeted therapy becoming standard practice and the availability of an increasing number of novel therapeutic agents against ALK+ NSCLC, assessing the cost-effectiveness of new therapies has become instrumental in determining the implementation of these strategies. The aim of this study was to provide an economic evaluation of lorlatinib for advanced ALK+ NSCLC patients who had previously received no systemic treatment for metastatic disease to better understand its value from the US healthcare payer perspective.

MATERIALS AND METHODS

Analytical Overview

To reflect patient heterogeneity, a microsimulation model was developed to estimate the health and cost outcomes of patients with previously untreated advanced ALK+ NSCLC from the US healthcare payer perspective using TreeAge Pro software Version 2020. The model structure and input parameters were based on the results of the CROWN trial, previously published literature and publicly available US databases. The model included four mutually exclusive health states: Progression-free (PF),

progression disease (PD), end-stage disease and death (**Figure 1**). All simulated patients entered the model in the PF health stage and could switch to PD, end-stage or death according to certain transition probabilities. Based on the CROWN trial, 2 treatment arms were included in the model, which simulated a 30-year horizon with a 28-day cycle length: First-line treatment with either oral lorlatinib (100 mg daily) or oral crizotinib (250 mg twice daily) until disease progression (See **Table S1** in the electronic **Supplementary Material** for details) (28). After disease progression, patients without CNS metastases in both the lorlatinib and crizotinib arms could receive subsequent therapy until death; otherwise, they could switch to end-stage and receive best supportive care (BSC). The main outcomes of this study were costs, quality-adjusted life years (QALYs), life years (LYs), and incremental cost-effectiveness ratios (ICERs). All cost and utility outcomes were discounted at 3% per year (33). A willingness-to-pay (WTP) threshold of $200,000/QALY was set when comparing the ICER between the two groups (34).

In the CROWN trial, a total of 296 patients were enrolled and randomly assigned to treatment with lorlatinib (n = 149) or crizotinib (n = 147). The patient characteristics are summarized in greater detail in **Supplementary Table S1**.

Clinical Data Inputs

The Kaplan–Meier (KM) survival curves used to model overall survival (OS) and PFS were obtained from the CROWN trial using GetData Graph Digitizer version 2.26 to extract the data points. The probability of death in any state for lorlatinib and crizotinib use was estimated according to the OS curves of the CROWN trial. After we extracted the data points from the OS curves, the data of pseudoindividual patients were generated using an algorithm created by Hoyle et al. (35); then, five parametric survival models (exponential, Weibull, logistic, log-logistic, and lognormal) were used to fit the pseudoindividual patient. The results of the survival model fitting showed that an exponential distribution had the lowest Akaike information criterion and was regarded as the optimum model to fit the OS curves. The 2018 US life table was also used in the model to estimate the background mortality rate (36).

The transition probability of mortality between time t − u and t for the two strategies was calculated by using formula (1) below:

$$Tp(t_u) = 1 - S(t)/S(t-u) \quad (1)$$

while $S(t) = \exp(-\lambda t)$ ($\lambda > 0$).

We used the same method to estimate the progression risk and probability of CNS metastases for lorlatinib and crizotinib based on the PFS curves from the CROWN trial. Exponential and Weibull distributions were considered the preferred models to fit the PFS curves for lorlatinib and crizotinib and were used to extrapolate progression rates.

Cost and Utility Input

In this study, we assessed the aforementioned two treatments from the US healthcare payer perspective and thus only considered the following direct costs associated with cancer therapy: Drug acquisition, laboratory tests (37), monitoring for progression-disease (CT) (37), adverse events (AEs) management, BSC with or without CNS metastases, and subsequent therapy costs (38). All the costs were obtained from relevant US sources and corrected for inflation to reflect 2020 US dollars (39) (**Table 1**). The unit costs of the drugs were derived from First Data Bank, and the treatment costs per cycle were estimated using the unit cost and dosing schedules of the drugs on the basis of the average wholesale price minus 16% (**Tables 1**, **2**) (40, 41). The AEs included in the model were those with a severity of grade 3/4 and a frequency ≥5% or a difference of more than 2% between two treatment strategies in CROWN trial. We included hypercholesterolemia, hypertriglyceridemia, edema, and hypertension in the model and obtained the costs of

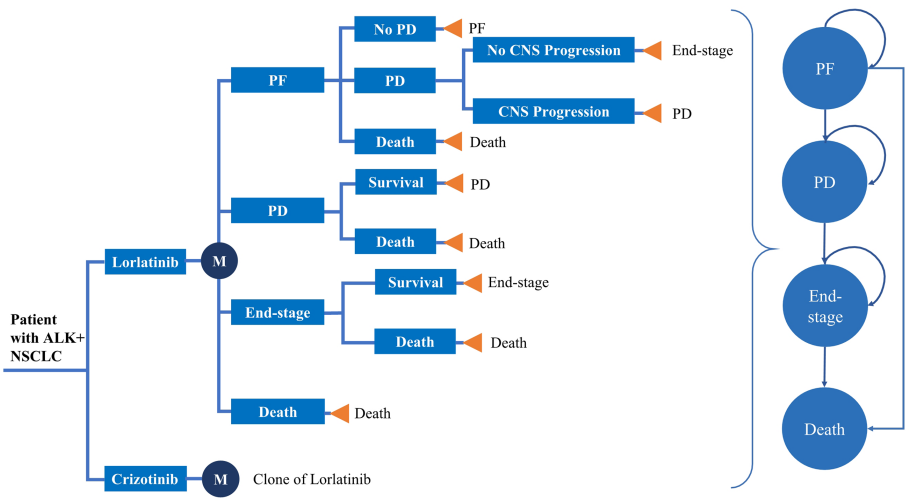

FIGURE 1 | Model structure. *ALK, anaplastic lymphoma kinase; NSCLC, Non-small cell lung cancer; PF, progression-free; PD, progressive disease.

TABLE 1 | Model parameters: baseline values, ranges, and distributions for sensitivity analysis.

Variable	Range				
	Baseline value	Minimum	Maximum	Distribution	Reference
Lorlatinib: Survival model					
OS	λ = −0.01968357 γ = −1.610781			Lognormal	Estimated (28)
PFS	λ = 0.008886453			Exponential	Estimated (28)
PFS of no CNS Progression	λ = 0.002070717			Exponential	Estimated (28)
Crizotinib: Survival model					
OS	λ = −0.110644 γ = 9.463829			Lognormal	Estimated (28)
PFS	λ = −0.01267741 γ = −2.117526			Lognormal	Estimated (28)
PFS of no CNS Progression	λ = −0.05653277 γ = −6.477169			Lognormal	Estimated (28)
Drug costs, per unit, (AWP-16%) $					
Lorlatinib, PO (100 mg)	566	453	680	Gamma	(40, 41)
Crizotinib, PO (250 mg)	257	206	308	Gamma	(40, 41)
Fenofibrate, PO (145 mg)	1.39	1.12	1.67	Gamma	(40, 41)
Lovastatin, PO (20 mg)	0.24	0.19	0.29	Gamma	(40, 41)
Support care costs, per week, $					
CNS metastases	3,538	2,830.4	4,245.6	Normal	Adjusted (42)
No CNS metastases	824.7	659.76	989.64	Normal	Adjusted (42)
Quality-of-life (utility)					
Progression free	0.81	0.79	0.84	Beta	(42)
Progression, second-line treated	0.72	0.70	0.75	Beta	(42)
Progression, best support care for CNS metastases	0.47	0.38	0.57	Beta	(42)
Lorlatinib: Incidence of AEs (%)					
Hypercholesterolemia	15	12	18	Beta	(28)
Hypertriglyceridemia	20	16	24	Beta	(28)
Edema	4	3.2	4.8	Beta	(28)
Hypertension	10	8	12	Beta	(28)
Crizotinib: Incidence of AEs (%)					
Hypercholesterolemia	0			Beta	(28)
Hypertriglyceridemia	0			Beta	(28)
Edema	1	0.8	1.2	Beta	(28)
Hypertension	0			Beta	(28)
AEs cost, $					
Hypercholesterolemia	8.12	6.496	9.744	Gamma	(40, 43, 44)
Hypertriglyceridemia	46.48	43.23	49.73	Gamma	(40, 45, 46)
Edema	2,623.65	2,098.92	3,148.38	Gamma	Adjusted (47)
Hypertension	9,410	7,528	11,292	Gamma	(48)
Discount rate	3	0	5	Uniform	
Subsequent therapy costs, $					
Lorlatinib	4,641	3,712.8	5,569.2	Gamma	Adjusted (28, 38)
Crizotinib	4,681	3,744.8	5,617.2	Gamma	Adjusted (28, 38)
CT per cycle	158	126.4	189.6	Gamma	Adjusted (37)
Laboratory	215	172	258	Gamma	Adjusted (37)

OS, Overall survival; PFS, Progression-free survival; CNS, Central nervous system; AWP, Average wholesale price; AEs, Adverse events.

AEs from previous studies (43–48). The CROWN trial reported the corresponding percentage of the population that received subsequent treatment, but it did not provide a specific protocol for subsequent treatment. Therefore, we used data from Deirdre F. Sheehan et al., whose study estimated the total cost of the following phase of care for lung cancer patients based on the Surveillance, Epidemiology, and End Results (SEER)-Medicare database to calculate the subsequent treatment cost in our study. Finally, based on the proportion of patients who received subsequent treatment in the lorlatinib group (69.1%) and the crizotinib group (24.5%) in the CROWN trial, we estimated that the subsequent costs of lorlatinib and crizotinib were $4,641 and $4,681 per cycle, respectively.

Utility values are often used to reflect a patient's preference for living in a particular health state, with zero representing the worst health and one representing the best health (37). The CROWN trial did not report QoL results or outcomes. Therefore, we used utilities of 0.81 for patients in the PF phase and 0.72 for the PD phase, obtained from a previously published cost-effectiveness analysis with patient and disease characteristics similar to those of the CROWN trial (49). Patients who experience CNS metastases will ultimately switch to end-stage and receive BSC, so we used a utility

TABLE 2 | Summary base case results.

Results	Lorlatinib	Crizotinib	ICER
Total cost of regimen, $	909,758	616,230	
Life-years	6.25	5.45	
QALYs	4.81	4.09	
Per LY			368,211
Per QALY			409,667

ICER, incremental cost-effectiveness ratio; LY, life year; QALYs, quality-adjusted life years.

of 0.47 for patients at that phase based on previous research conducted by Carlson (49) (**Table 1**).

Analysis

To determine the key drivers of the model and to evaluate the robustness of the model, univariate deterministic sensitivity analysis (DSA), including 22 variables (costs, utilities, and risk of AEs) from the fitted extrapolative model, was performed. A probability sensitivity analysis (PSA) with 1,000 iterations of 10,000 patients was conducted to test the uncertainty of the model using second-order Monte Carlo simulation. In the sensitivity analysis, all parameters were assigned at a suitable distribution and were tested at the upper or lower limits of plausible ranges (**Table 1**) (42).

We also conducted multiple scenario analyses related to patient demographics, drug price, discount rate, utility value, and time horizon to assess how our assumptions affected the model outcomes. For example, in the scenario analyses, we not only considered the heterogeneity of NSCLC patients but also varied the drug costs of lorlatinib and crizotinib to evaluate the potential implications of drug tapering.

RESULTS

Base Case Results

To deduce the effect of statistical fluctuations in the outcomes, 1 million patients were simulated for the two strategies, and the results are presented in **Table 2**. For lorlatinib, the mean cost and LYs were $909,758 and 6.25, respectively, while for crizotinib, the mean costs and LYs were $616,230 and 5.45, respectively. After adjustment for quality-adjusted life year (QALY), lorlatinib provided 4.81 QALYs, which was 0.72 QALYs more than for patients receiving crizotinib. The patients in the lorlatinib arm cost an additional $148,973, resulting in an ICER of $368,211/LYs or $409,667/QALYs compared with the crizotinib arm (**Table 2**).

Sensitivity and Scenario Analysis

The results of the one-way sensitivity analysis are presented in **Figure 2** and illustrate that the primary drivers of the model outcome were the drug prices of lorlatinib and crizotinib, the cost of subsequent treatment in the two strategies and the utility of PF. Other parameters, such as utility of PD, cost and risk of AEs, cost of BSC for CNS metastases, and sex, had moderate effects on the ICER. The PSA results in **Figure 3** show that without adjusting the drug price of lorlatinib, lorlatinib vs crizotinib had 90% cost-effectiveness only when the WTP threshold was increased to $448,000/QALY. Otherwise, it was impossible for lorlatinib to be cost-effective at the $200,000/QALY WTP threshold compared with crizotinib.

Supplementary Table S4 shows the results of six scenario analyses. Notably, in scenario 3, when we adjusted the drug cost, the ICER for lorlatinib vs crizotinib treatment changed greatly. When the drug price of lorlatinib decreased to 75% ($424.5) of its original price, lorlatinib vs crizotinib treatment had 100% cost-

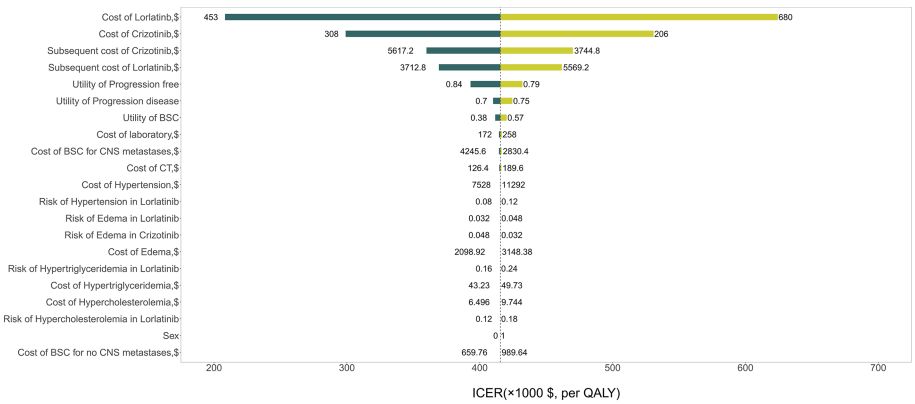

FIGURE 2 | Tornado diagram for univariable sensitivity analysis. *ICER, Incremental cost-effectiveness ratio; BSC, Best supportive care; CNS, Central nervous system; AEs, Adverse events.

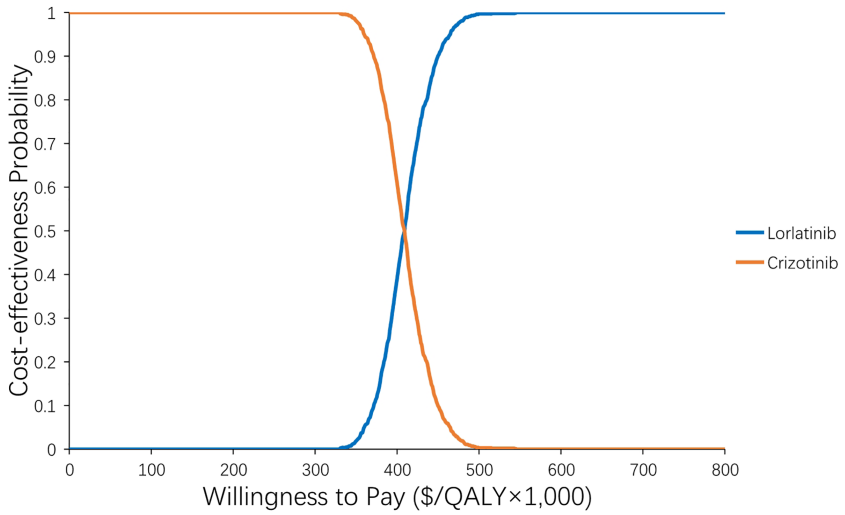

FIGURE 3 | Acceptability curve of the probability sensitivity analysis. The probability sensitivity analysis of the base case.

effectiveness at a WTP threshold of 200,000/QALY, with a lower ICER of $161,154/QALY compared with the base case analysis (**Figure 4**). When we varied the drug price of lorlatinib to 50% ($283) and 25% ($141.5) of its original cost, the ICER for lorlatinib vs crizotinib therapy decreased to −$221,179/QALY and −$518,272/QALY, respectively. The negative ICER in the above cases confirms the dominance of the lorlatinib strategy, which accumulated higher QALYs at a lower cost over the model's time horizon.

In scenario 6, the time horizon was changed to 5, 10 and 20 years to assess the impact of the OS and PFS extrapolations used in the model. Most of the costs (70%) occurred in the first 5 years of the time horizon; however, patient survival continued to increase after 5 years. Therefore, the longer the time horizon patients experienced, the greater their opportunity to accrue incremental benefit from disease progression and the lower the ICER obtained.

DISCUSSION

Over the past two decades, newly licensed anticancer drugs have been developed rapidly, which has been followed by an increase in the price of cancer drugs (50–52). Globally, the expenditure for anticancer drugs is approximately $100 billion annually, and the total expenditures for cancer have increased by a rate of 7.0% per year and are predicted to increase to $158 billion by 2025 (7, 50). The average treatment cost for a novel anticancer drug

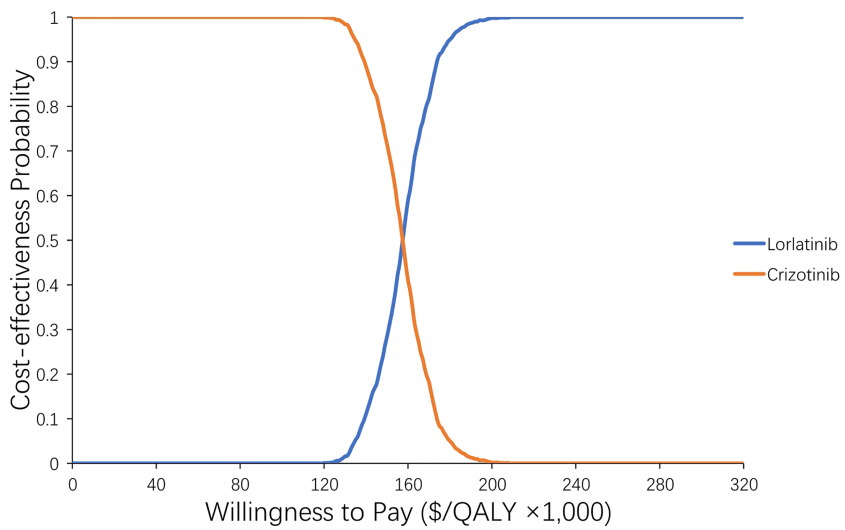

FIGURE 4 | Acceptability curve of the probability sensitivity analysis. The probability sensitivity analysis of scenario 3-2 (adjusting the price of lorlatinib to its lower limit).

often exceeds $100,000 per year in the US (52). High drug prices not only increase patients' out-of-pocket expenses, resulting in financial toxicity and low compliance, but also impose unsustainable cumulative price burdens for society (52). As a result, there is an urgent but challenging need to address extreme health care expenditures. To our knowledge, this is the first study worldwide to analyze the cost-effectiveness of a novel anticancer drug (lorlatinib) vs a standard-of-care drug (crizotinib) for the treatment of advanced ALK + NSCLC. The results revealed that compared with crizotinib, lorlatinib is unlikely to be cost effective in the current setting, although the acceptability of ICER values is subjective and depends on many other factors, such as social value and general budget (53). This lack of cost-effectiveness can be explained by the high cost of lorlatinib, since the scenario analysis and PSA results indicated that lorlatinib has 100% cost-effectiveness at a WTP threshold of 200,000/QALY vs crizotinib when the cost of lorlatinib is adjusted to the lower limit. Therefore, the implication of our study is not that lorlatinib should be withheld from patients with untreated ALK+ NSCLC; in particular, the advantages of lorlatinib treatment over crizotinib include slower progression of brain metastases for patients receiving long-term treatment (54). Rather, this study reveals the cost-effectiveness that would result from controlling the drug's price to within a reasonable range. In the US, limited drug price transparency and the lack of unified government control over drug prices result in the highest drug costs in the world (55). Fortunately, the US government has proposed reducing the high drug costs paid by US patients by linking the drug prices paid by Medicare to those paid by health systems in other advanced countries (56). Once this plan is enacted or implemented, it might lower the price of lorlatinib and lead to more favorable economic outcomes.

The sensitivity analysis also illustrated that the subsequent cost greatly impacted the model outcome. Although the CROWN trial did not provide the specific treatment sequence after first-line treatment failure, we included possible clinical practices (BSC, surgery, chemotherapy and radiation) during the continuing treatment phase and calculated the subsequent treatment cost for patients with ALK+ NSCLC based on the previous study conducted by Deirdre. Therefore, we call for more RCTs to study the therapeutic sequence of ALK+ drugs in the future to help identify the best treatment sequence and offer the best QoL for patients with ALK+ NSCLC. At that time, we can further study the cost-effectiveness of lorlatinib as a first-line treatment or at any other point in the treatment sequence.

This research has certain limitations that merit mention. First, the main limitation of all cost-effectiveness studies is that they must adopt a particular set of circumstances and cannot widely and dynamically reflect the real-world clinical scenario (57). Cost-effectiveness studies will yield different outcomes when performed in different scenarios; for example, there is a large disparity between public and private health users in the US (58), and our study was conducted on the basis of the public health system. The study results cannot be generalized from one country to another due to the wide variation in healthcare systems among different countries. Second, the CROWN trial is the only randomized phase III trial that has directly compared lorlatinib and crizotinib for patients with advanced ALK+ NSCLC, and many input parameters (OS, PFS, AEs, etc.) in our model were obtained from this trial. Therefore, the external validity of our model largely depends on that trial, and any slight biases in that trial will have impacted our model outcome to some extent. Third, this study did not compare other potential treatment options due to a lack of head-to-head trials comparing multiple agents. Therefore, we call for more direct comparison trials of multiple potential treatment options in the future, and we will update our conclusion in the future if data are available. Fourth, owing to the lack of utility information in the CROWN trial, the utility values we used in our model were obtained from published cost-effectiveness studies that had the same patient characteristics as the CROWN trial. Although this may lead to some biases, we performed a series of sensitivity analyses that included wide variation in utility values. Finally, although it is usual in cost-effectiveness analyses to conduct an additional estimation to assess the financial consequences of adopting a new intervention (59, 60), we did not consider the budget impact that adding lorlatinib would have on society. However, the results of this evaluation might be a valuable reference for policymakers and physicians since it reflects the general clinical practice in managing advanced ALK+ NSCLC.

CONCLUSION

From the US healthcare payer perspective, lorlatinib is determined not to be cost-effective when compared to crizotinib for NSCLC patients with previous untreated advanced ALK+ NSCLC at a willingness-to-pay threshold of $200,000 per QALY. However, when we decreased the drug price of lorlatinib to $424.50, the lorlatinib vs crizotinib strategy had 100% cost-effectiveness at a WTP threshold of 200,000/QALY. This implies that an appropriate drug price for lorlatinib should be taken into consideration when making policy decisions.

DATA AVAILABILITY STATEMENT

The original contributions presented in the study are included in the article/**Supplementary Material**. Further inquiries can be directed to the corresponding authors.

AUTHOR CONTRIBUTIONS

SL constructed the model, collected and analyzed the data, and drafted the manuscript. XW conceptualized the study and provided the model framework. YL contributed to the revision of the manuscript. LP and JL were the guarantors of the study and provided technical and material support. All authors contributed to the article and approved the submitted version.

FUNDING

This study was funded by the National Natural Science Foundation of China (No: 71874209) and Hunan Provincial Natural Science Foundation of China (No. 2019JJ40411).

ACKNOWLEDGMENTS

All named authors meet the International Committee of Medical Journal Editors (ICMJE) criteria for authorship for this article, take responsibility for the integrity of the work as a whole, and have given their approval for this version to be published.

SUPPLEMENTARY MATERIAL

The Supplementary Material for this article can be found online at: https://www.frontiersin.org/articles/10.3389/fonc.2021.684073/full#supplementary-material

REFERENCES

1. American Cancer Society. *Lung Cancer*. Available at: https://www.cancer.org/cancer/lung-cancer.html (Accessed December 2020).
2. Siegel RL, Miller KD, Jemal A. Cancer Statistics, 2020. *CA Cancer J Clin* (2020) 70(1):7–30. doi: 10.3322/caac.21590
3. Tembuyser L, Tack V, Zwaenepoel K, Pauwels P, Miller K, Bubendorf L, et al. The Relevance of External Quality Assessment for Molecular Testing for ALK Positive non-Small Cell Lung Cancer: Results From Two Pilot Rounds Show Room for Optimization. *PloS One* (2014) 9(11):e112159. doi: 10.1371/journal.pone.0112159
4. Chia PL, Mitchell P, Dobrovic A, John T. Prevalence and Natural History of ALK Positive non-Small-Cell Lung Cancer and the Clinical Impact of Targeted Therapy With ALK Inhibitors. *Clin Epidemiol* (2014) 6:423–32. doi: 10.2147/CLEP.S69718
5. Claxton L, O'Connor J, Woolacott N, Wright K, Hodgson R. Ceritinib for Untreated Anaplastic Lymphoma Kinase-Positive Advanced non-Small-Cell Lung Cancer: An Evidence Review Group Evaluation of a NICE Single Technology Appraisal. *Pharmacoeconomics* (2019) 37(5):645–54. doi: 10.1007/s40273-018-0720-8
6. National Cancer Institute. *SEER Cancer Statistics Factsheets: Lung and Bronchus Cancer* (2020). Available at: https://seer.cancer.gov/statfacts/html/lungb.html (Accessed December 2020).
7. Criss SD, Mooradian MJ, Sheehan DF, Zubiri L, Lumish MA, Gainor JF, et al. Cost-Effectiveness and Budgetary Consequence Analysis of Durvalumab Consolidation Therapy vs No Consolidation Therapy After Chemoradiotherapy in Stage III Non-Small Cell Lung Cancer in the Context of the US Health Care System. *JAMA Oncol* (2019) 5(3):358–65. doi: 10.1001/jamaoncol.2018.5449
8. Gridelli C, de Marinis F, Cappuzzo F, Di Maio M, Hirsch FR, Mok T, et al. Treatment of Advanced non-Small-Cell Lung Cancer With Epidermal Growth Factor Receptor (EGFR) Mutation or ALK Gene Rearrangement: Results of an International Expert Panel Meeting of the Italian Association of Thoracic Oncology. *Clin Lung Cancer* (2014) 15(3):173–81. doi: 10.1016/j.cllc.2013.12.002
9. Reck M, Paz-Ares L. Immunologic Checkpoint Blockade in Lung Cancer. *Semin Oncol* (2015) 42(3):402–17. doi: 10.1053/j.seminoncol.2015.02.013
10. Wu YL, Zhou C, Hu CP, Feng J, Lu S, Huang Y, et al. Afatinib Versus Cisplatin Plus Gemcitabine for First-Line Treatment of Asian Patients With Advanced Non-Small-Cell Lung Cancer Harbouring EGFR Mutations (LUX-Lung 6): An Open-Label, Randomised Phase 3 Trial. *Lancet Oncol* (2014) 15(2):213–22. doi: 10.1016/S1470-2045(13)70604-1
11. Rosell R, Carcereny E, Gervais R, Vergnenegre A, Massuti B, Felip E, et al. Erlotinib Versus Standard Chemotherapy as First-Line Treatment for European Patients With Advanced EGFR Mutation-Positive Non-Small-Cell Lung Cancer (EURTAC): A Multicentre, Open-Label, Randomised Phase 3 Trial. *Lancet Oncol* (2012) 13(3):239–46. doi: 10.1016/S1470-2045(11)70393-X
12. Zhou C, Wu YL, Chen G, Feng J, Liu XQ, Wang C, et al. Erlotinib Versus Chemotherapy as First-Line Treatment for Patients With Advanced EGFR Mutation-Positive Non-Small-Cell Lung Cancer (OPTIMAL, CTONG-0802): A Multicentre, Open-Label, Randomised, Phase 3 Study. *Lancet Oncol* (2011) 12(8):735–42. doi: 10.1016/S1470-2045(11)70184-X
13. Mok TS, Wu YL, Thongprasert S, Yang CH, Chu DT, Saijo N, et al. Gefitinib or Carboplatin-Paclitaxel in Pulmonary Adenocarcinoma. *N Engl J Med* (2009) 361(10):947–57. doi: 10.1056/NEJMoa0810699
14. Gatzemeier U, Pluzanska A, Szczesna A, Kaukel E, Roubec J, De Rosa F, et al. Phase III Study of Erlotinib in Combination With Cisplatin and Gemcitabine in Advanced non-Small-Cell Lung Cancer: The Tarceva Lung Cancer Investigation Trial. *J Clin Oncol* (2007) 25(12):1545–52. doi: 10.1200/JCO.2005.05.1474
15. Herbst RS, Prager D, Hermann R, Fehrenbacher L, Johnson BE, Sandler A, et al. TRIBUTE: A Phase III Trial of Erlotinib Hydrochloride (OSI-774) Combined With Carboplatin and Paclitaxel Chemotherapy in Advanced non-Small-Cell Lung Cancer. *J Clin Oncol* (2005) 23(25):5892–9. doi: 10.1200/JCO.2005.02.840
16. Kris MG, Natale RB, Herbst RS, Lynch TJJr., Prager D, Belani CP, et al. Efficacy of Gefitinib, an Inhibitor of the Epidermal Growth Factor Receptor Tyrosine Kinase, in Symptomatic Patients With non-Small Cell Lung Cancer: A Randomized Trial. *Jama* (2003) 290(16):2149–58. doi: 10.1001/jama.290.16.2149
17. Fukuoka M, Yano S, Giaccone G, Tamura T, Nakagawa K, Douillard JY, et al. Multi-Institutional Randomized Phase II Trial of Gefitinib for Previously Treated Patients With Advanced non-Small-Cell Lung Cancer (the IDEAL 1 Trial) [Corrected]. *J Clin Oncol* (2003) 21(12):2237–46. doi: 10.1200/JCO.2003.10.038
18. Ettinger DS, Wood DE, Aisner DL, Akerley W, Bauman J, Chirieac LR, et al. Non-Small Cell Lung Cancer, Version 5.2017, NCCN Clinical Practice Guidelines in Oncology. *J Natl Compr Canc Netw* (2017) 15(4):504–35. doi: 10.6004/jnccn.2017.0050
19. Rekhtman N, Leighl NB, Somerfield MR. Molecular Testing for Selection of Patients With Lung Cancer for Epidermal Growth Factor Receptor and Anaplastic Lymphoma Kinase Tyrosine Kinase Inhibitors: American Society of Clinical Oncology Endorsement of the College of American Pathologists/International Association for the Study of Lung Cancer/Association for Molecular Pathology Guideline. *J Oncol Pract* (2015) 11(2):135–6. doi: 10.1200/JOP.2014.002303
20. Pinto JA, Raez LE, Domingo G. Clinical Consequences of Resistance to ALK Inhibitors in non-Small Cell Lung Cancer. *Expert Rev Respir Med* (2020) 14(4):385–90. doi: 10.1080/17476348.2020.1721285
21. Vuong HG, Nguyen TQ, Nguyen HC, Nguyen PT, Ho ATN, Hassell L. Efficacy and Safety of Crizotinib in the Treatment of Advanced non-Small-Cell Lung Cancer With ROS1 Rearrangement or MET Alteration: A Systematic Review and Meta-Analysis. *Target Oncol* (2020) 15(5):589–98. doi: 10.1007/s11523-020-00745-7
22. Camidge DR, Kim HR, Ahn MJ, Yang JC, Han JY, Lee JS, et al. Brigatinib Versus Crizotinib in ALK-Positive Non-Small-Cell Lung Cancer. *N Engl J Med* (2018) 379(21):2027–39. doi: 10.1056/NEJMoa1810171
23. Peters S, Camidge DR, Shaw AT, Gadgeel S, Ahn JS, Kim DW, et al. Alectinib Versus Crizotinib in Untreated ALK-Positive Non-Small-Cell Lung Cancer. *N Engl J Med* (2017) 377(9):829–38. doi: 10.1056/NEJMoa1704795
24. Camidge DR, Dziadziuszko R, Peters S, Mok T, Noe J, Nowicka M, et al. Updated Efficacy and Safety Data and Impact of the EML4-ALK Fusion Variant on the Efficacy of Alectinib in Untreated ALK-Positive Advanced non-Small Cell Lung Cancer in the Global Phase III Alex Study. *J Thorac Oncol* (2019) 14(7):1233–43. doi: 10.1016/j.jtho.2019.03.007

25. Gristina V, La Mantia M, Iacono F, Galvano A, Russo A, Bazan V. The Emerging Therapeutic Landscape of ALK Inhibitors in Non-Small Cell Lung Cancer. *Pharm (Basel)* (2020) 13(12):474. doi: 10.3390/ph13120474
26. Singhi EK, Horn L. Background and Rationale of the eXalt3 Trial Investigating X-396 in the Treatment of ALK+ Non-Small-Cell Lung Cancer. *Future Oncol* (2018) 14(18):1781–7. doi: 10.2217/fon-2017-0619
27. Peled N, Gillis R, Kilickap S, Froesch P, Orlov S, Filippova E, et al. Glass: Global Lorlatinib for ALK(+) and ROS1(+) Retrospective Study: Real World Data of 123 NSCLC Patients. *Lung Cancer* (2020) 148:48–54. doi: 10.1016/j.lungcan.2020.07.022
28. Shaw AT, Bauer TM, de Marinis F, Felip E, Goto Y, Liu G, et al. First-Line Lorlatinib or Crizotinib in Advanced ALK-Positive Lung Cancer. *N Engl J Med* (2020) 383(21):2018–29. doi: 10.1056/NEJMoa2027187
29. Horn L, Whisenant JG, Wakelee H, Reckamp KL, Qiao H, Leal TA, et al. Monitoring Therapeutic Response and Resistance: Analysis of Circulating Tumor DNA in Patients With ALK+ Lung Cancer. *J Thorac Oncol* (2019) 14(11):1901–11. doi: 10.1016/j.jtho.2019.08.003
30. Shaw AT, Felip E, Bauer TM, Besse B, Navarro A, Postel-Vinay S, et al. Lorlatinib in Non-Small-Cell Lung Cancer With ALK or ROS1 Rearrangement: An International, Multicentre, Open-Label, Single-Arm First-in-Man Phase 1 Trial. *Lancet Oncol* (2017) 18(12):1590–9. doi: 10.1016/S1470-2045(17)30680-0
31. Gainor JF, Dardaei L, Yoda S, Friboulet L, Leshchiner I, Katayama R, et al. Molecular Mechanisms of Resistance to First- and Second-Generation ALK Inhibitors in ALK-Rearranged Lung Cancer. *Cancer Discov* (2016) 6(10):1118–33. doi: 10.1158/2159-8290.CD-16-0596
32. Zou HY, Friboulet L, Kodack DP, Engstrom LD, Li Q, West M, et al. PF-06463922, an ALK/ROS1 Inhibitor, Overcomes Resistance to First and Second Generation ALK Inhibitors in Preclinical Models. *Cancer Cell* (2015) 28(1):70–81. doi: 10.1016/j.ccell.2015.05.010
33. Sanders GD, Neumann PJ, Basu A, Brock DW, Feeny D, Krahn M, et al. Recommendations for Conduct, Methodological Practices, and Reporting of Cost-effectiveness Analyses: Second Panel on Cost-Effectiveness in Health and Medicine. *JAMA* (2016) 316(10):1093–103. doi: 10.1001/jama.2016.12195
34. Neumann PJ, Cohen JT, Weinstein MC. Updating Cost-Effectiveness–the Curious Resilience of the $50,000-per-QALY Threshold. *N Engl J Med* (2014) 371(9):796–7. doi: 10.1056/NEJMp1405158
35. Hoyle MW, Henley W. Improved Curve Fits to Summary Survival Data: Application to Economic Evaluation of Health Technologies. *BMC Med Res Methodol* (2011) 11:139. doi: 10.1186/1471-2288-11-139
36. Arias E, Xu J. United States Life Tables, 2018. *Natl Vital Stat Rep* (2020) 69(12):1–45.
37. She L, Hu H, Liao M, Xia X, Shi Y, Yao L, et al. Cost-Effectiveness Analysis of Pembrolizumab Versus Chemotherapy as First-Line Treatment in Locally Advanced or Metastatic non-Small Cell Lung Cancer With PD-L1 Tumor Proportion Score 1% or Greater. *Lung Cancer* (2019) 138:88–94. doi: 10.1016/j.lungcan.2019.10.017
38. Sheehan DF, Criss SD, Chen Y, Eckel A, Palazzo L, Tramontano AC, et al. Lung Cancer Costs by Treatment Strategy and Phase of Care Among Patients Enrolled in Medicare. *Cancer Med* (2019) 8(1):94–103. doi: 10.1002/cam4.1896
39. US Department of Labor. *Calculators*. Available at: http://www.bls.gov/data/#calculators (Accessed December 27, 2020).
40. First DataBank Inc. *Analy$Ource Online: The Online Resource for Drug Pricing and Deal Information* (2020). Available at: https://www.analysource.com.
41. Curtiss FR, Lettrich P, Fairman KA. What is the Price Benchmark to Replace Average Wholesale Price (AWP)? *J Managed Care Pharm JMCP* (2010) 16(7):492–501. doi: 10.18553/jmcp.2010.16.7.492
42. Caldwell D. Decision Modelling for Health Economic Evaluation. A Briggs, M Sculpher, K Claxton. *Int J Epidemiol* (2007) 36(2):476–7. doi: 10.1093/ije/dym062%JInternationalJournalofEpidemiology
43. Benner JS, Smith TW, Klingman D, Tierce JC, Mullins CD, Pethick N, et al. Cost-Effectiveness of Rosuvastatin Compared With Other Statins From a Managed Care Perspective. *Value Health J Int Soc Pharmacoecon Outcomes Res* (2005) 8(6):618–28. doi: 10.1111/j.1524-4733.2005.00055.x
44. Duong H, Bajaj T. *Lovastatin*. Treasure Island (FL: StatPearls (2020).
45. Yuan G, Al-Shali KZ, Hegele RA. Hypertriglyceridemia: its Etiology, Effects and Treatment. *CMAJ* (2007) 176(8):1113–20. doi: 10.1503/cmaj.060963
46. Sidhu G, Tripp J. *Fenofibrate*. Treasure Island (FL: StatPearls (2020).
47. Wong W, Yim YM, Kim A, Cloutier M, Gauthier-Loiselle M, Gagnon-Sanschagrin P, et al. Assessment of Costs Associated With Adverse Events in Patients With Cancer. *PloS One* (2018) 13(4):e0196007. doi: 10.1371/journal.pone.0196007
48. Lin S, Luo S, Zhong L, Lai S, Zeng D, Rao X, et al. Cost-Effectiveness of Atezolizumab Plus Chemotherapy for Advanced Non-Small-Cell Lung Cancer. *Int J Clin Pharm* (2020) 42(4):1175–83. doi: 10.1007/s11096-020-01076-3
49. Carlson JJ, Suh K, Orfanos P, Wong W. Cost Effectiveness of Alectinib vs. Crizotinib in First-Line Anaplastic Lymphoma Kinase-Positive Advanced non-Small-Cell Lung Cancer. *Pharmacoeconomics* (2018) 36(4):495–504. doi: 10.1007/s40273-018-0625-6
50. Aguiar PNJr., Haaland B, Park W, San Tan P, Del Giglio A, de Lima Lopes G Jr. Cost-Effectiveness of Osimertinib in the First-Line Treatment of Patients With EGFR-Mutated Advanced Non-Small Cell Lung Cancer. *JAMA Oncol* (2018) 4(8):1080–4. doi: 10.1001/jamaoncol.2018.1395
51. Savage P, Mahmoud S. Development and Economic Trends in Cancer Therapeutic Drugs: A 5-Year Update 2010-2014. *Br J Cancer* (2015) 112(6):1037–41. doi: 10.1038/bjc.2015.56
52. Mailankody S, Prasad V. Five Years of Cancer Drug Approvals: Innovation, Efficacy, and Costs. *JAMA Oncol* (2015) 1(4):539–40. doi: 10.1001/jamaoncol.2015.0373
53. Djalalov S, Beca J, Hoch JS, Krahn M, Tsao MS, Cutz JC, et al. Cost Effectiveness of EML4-ALK Fusion Testing and First-Line Crizotinib Treatment for Patients With Advanced ALK-Positive non-Small-Cell Lung Cancer. *J Clin Oncol* (2014) 32(10):1012–9. doi: 10.1200/JCO.2013.53.1186
54. Lorlatinib Outperforms Crizotinib in NSCLC. *Cancer Discov* (2020). doi: 10.1158/2159-8290.CD-NB2020-110
55. Prasad V, De Jesus K, Mailankody S. The High Price of Anticancer Drugs: Origins, Implications, Barriers, Solutions. *Nat Rev Clin Oncol* (2017) 14(6):381–90. doi: 10.1038/nrclinonc.2017.31
56. Dyer O. US Drug Prices Should be Tied to Foreign Prices to Tackle "Global Freeloading," Says Trump. *BMJ (Clinical Res ed)* (2018) 363:k4542. doi: 10.1136/bmj.k4542
57. Earle CC, Coyle D, Evans WK. Cost-Effectiveness Analysis in Oncology. *Ann Oncol* (1998) 9(5):475–82. doi: 10.1023/a:1008292128615
58. Yorio JT, Xie Y, Yan J, Gerber DE. Lung Cancer Diagnostic and Treatment Intervals in the United States: A Health Care Disparity? *J Thorac Oncol* (2009) 4(11):1322–30. doi: 10.1097/JTO.0b013e3181bbb130
59. Sullivan SD, Mauskopf JA, Augustovski F, Jaime Caro J, Lee KM, Minchin M, et al. Budget Impact Analysis-Principles of Good Practice: Report of the ISPOR 2012 Budget Impact Analysis Good Practice II Task Force. *Value Health J Int Soc Pharmacoecon Outcomes Res* (2014) 17(1):5–14. doi: 10.1016/j.jval.2013.08.2291
60. Wu B, Lu S. The Effect of PD-L1 Categories-Directed Pembrolizumab Plus Chemotherapy for Newly Diagnosed Metastatic Non-Small-Cell Lung Cancer: A Cost-Effectiveness Analysis. *Transl Lung Cancer Res* (2020) 9(5):1770–84. doi: 10.21037/tlcr-19-605

Conflict of Interest: The authors declare that the research was conducted in the absence of any commercial or financial relationships that could be construed as a potential conflict of interest.

Copyright © 2021 Li, Li, Peng, Li and Wan. This is an open-access article distributed under the terms of the Creative Commons Attribution License (CC BY). The use, distribution or reproduction in other forums is permitted, provided the original author(s) and the copyright owner(s) are credited and that the original publication in this journal is cited, in accordance with accepted academic practice. No use, distribution or reproduction is permitted which does not comply with these terms.

frontiers in Oncology

ORIGINAL RESEARCH
published: 31 May 2021
doi: 10.3389/fonc.2021.640131

A Retrospective Study on Using a Novel Single Needle Cone Puncture Approach for the Iodine-125 Seed Brachytherapy in Treating Patients With Thoracic Malignancy

*Fenge Li[1,2], Liping Wang[3], Yixiang Zhang[4], Weihong Feng[1], Tao Ju[1], Zaiping Liu[5], Zhenglu Wang[6] and Xueming Du[1]**

[1] Department of Oncology, Tianjin Beichen Hospital, Tianjin, China, [2] Department of Melanoma Oncology, University of Texas M.D. Anderson Cancer Center, Houston, TX, United States, [3] Department of Oncology, Weifang People's Hospital, Weifang, China, [4] Pulmonary Medicine, Weifang People's Hospital, Weifang, China, [5] Department of Pathology and Laboratory Medicine, IWK Women's and Children's Health Center, Halifax, NS, Canada, [6] Pathology Department, Tianjin First Central Hospital, Tianjin, China

OPEN ACCESS

Edited by:
Junji Uchino,
Kyoto Prefectural University of Medicine, Japan

Reviewed by:
Lei Zheng,
Peking University Hospital of Stomatology, China
Zhe Ji,
Peking University Third Hospital, China

***Correspondence:**
Xueming Du
dudaming73@163.com

Specialty section:
This article was submitted to Thoracic Oncology, a section of the journal Frontiers in Oncology

Received: 10 December 2020
Accepted: 06 May 2021
Published: 31 May 2021

Citation:
Li F, Wang L, Zhang Y, Feng W, Ju T, Liu Z, Wang Z and Du X (2021) A Retrospective Study on Using a Novel Single Needle Cone Puncture Approach for the Iodine-125 Seed Brachytherapy in Treating Patients With Thoracic Malignancy. Front. Oncol. 11:640131. doi: 10.3389/fonc.2021.640131

Background: Patients with progressive thoracic malignancy characterized by large irregular tumors with necrosis and life-threatening symptoms lack effective treatments. We set out to develop a single needle cone puncture method for the Iodine-125 seed (SNCP-^{125}I) brachytherapy, and aim to report the initial results.

Methods: 294 patients with advanced thoracic malignancy were treated with local SNCP-^{125}I brachytherapy between March 2009 and July 2020, followed by thorough evaluation of clinical outcome, overall survival (OS), progression-free survival (PFS) and procedure-related complications after treatment.

Results: The overall response rate (ORR) among the treated patients was 81.0% (238/294). Life-threatening symptoms due to tumor oppression, hemoptysis and large irregular tumor with necrosis were successfully alleviated after the SNCP-^{125}I treatment with a remission rate at 91% to 94%. The median OS and PFS were 13.6 months and 5.8 months, respectively. Procedure-related side effects including pneumothorax (32/294), blood-stained sputum (8/294), subcutaneous emphysema (10/294), puncture site bleeding (16/294) and chest pain (6/294) were observed. Patients who were able to follow with chemotherapy or immunotherapy experienced extended OS and PFS, as compared with patients who opted to receive hospice care (16.5 months Vs. 11.2 months). Further pathological and immunological analysis showed that SNCP-^{125}I induced tumor lymphocytes infiltration and long-term tumor necrosis.

Conclusion: SNCP-^{125}I brachytherapy effectively eliminates life-threatening symptoms due to local tumor oppression, hemoptysis and large irregular and necrotic tumors in patients with unresectable chest malignancy and significantly induces local tumor

regression. SNCP-^{125}I brachytherapy combines with chemotherapy significantly prolong OS and PFS compare with SNCP-^{125}I brachytherapy alone.

Keywords: radioactive iodine-125 brachytherapy, single needle cone puncture, thoracic malignancy, life-threatening symptom, survival

INTRODUCTION

Successful treatment of local incurable thoracic malignancy, including lung squamous cell carcinoma, metastatic esophageal cancer, and unresectable malignant thymoma, has been hampered by the lack of clinically effective regimens. This represents a particular obstacle for patients who experience rapid tumor progression as a result of large irregular and necrotic tumors, hemoptysis and lethal symptoms, but are not susceptible to local interventiondue to limited access to the site of tumors. As such, despite systemic therapeutic treatment, coupled with advanced imaging technology, local lesions still reoccur and develop. Further, tumor pathology is closely associated with disease progression and therapy responses (1–3). Patients with squamous cell carcinoma exhibit unfavorable outcomes when treated with chemotherapy, immunotherapy, and molecularly targeted therapy, especially for central lung cancer and mediastinal tumors that are frequently surrounded by large blood vessels and trachea. This elevates the potential risk for performing local puncture operations. It should be further noted that the tumors often progress aggressively, thereby constricting adjacent trachea, blood vessels, heart and esophagus and leading to lethal dyspnea, hemoptysis, dysphagia and superior vena cava syndrome, which primarily accounts for the mortality in cancer patients (4–7). Even though there is a low risk resulting from puncture operations for large tumors, the irregular necrosis, ribs, blood vessels and trachea often compromise the obstacle of the conventional interventional treatment. However, there is no effective approach to overcome these clinical challenges for patients with advanced malignancy, and the outcome after conventional treatment remains poor for those with squamous cell carcinomas of lung cancer, invasive thymic carcinoma, and chest metastatic tumors (8–10). Therefore, instead of hospice care, effective clinical strategies for these patients is urgently needed.

Computerized tomography (CT)-guided local radioactive Idione-125 (^{125}I) seed brachytherapy has been widely used for various types of advanced cancers, including lung cancer, uveal melanoma, breast cancer, malignant gliomas and retroperitoneal malignant tumors (11–17). Treatment planning systems (TPS) are employed in CT-guided local radioactive ^{125}I seed brachytherapy to ensure that the tumor site receives the maximum therapeutic dose while sparing surrounding tumor tissue, which represents one of the most effective approaches for maximum clinical benefit to the patient (18, 19). Conventional multiple-needle ^{125}I brachytherapy method is only suitable for patients who can make required postures and have multiple parallel sites accessible for the puncture operation. However, this is not practical for patients with lung hilar and mediastinal tumors, because multiple needle puncture poses a great risk of damaging large blood vessels, and patients can quickly develop respiratory failure. In addition, additional criteria must be satisfied before the treatment. Foremost, the tumor lesion is located adjacent to the main bronchus, blood vessels, esophagus and heart. Secondly, the patient experiences the typical symptoms including dyspnea, hemoptysis, dysphagia, arrhythmia and superior vena cava syndrome as a result of local tumor oppression. Thirdly, the tumor is larger than 7 cm in size with irregular necrosis (20). Additional technical difficulties also prevents utilization and effectiveness of the multiple-needle brachytherapy, including lack of multiple puncture sites, uneven distribution of radioactive doses for large tumors, inability to maintain a posture for the operation, and extra poor performance status of these patients. Unfortunately, these patients are ultimately only able to choose hospice care with unfavorable survival outcomes.

To tackle this challenge, herein we report a single needle cone puncture method for the ^{125}I seed brachytherapy, with which we implement a radioactive dose covering over 90% of the tumor volume using a single needle through one puncture site on the skin. We show greatly reduced risk associated with the operation and satisfied recovery rate upon treatment, especially in patients with lung hilar and mediastinum tumors. Utilizing this novel intervention method, we successfully and effectively treated thoracic malignancy patients with large irregular tumors and severe symptoms due to local tumor oppression and hemoptysis (ORR=81.0%). Detailed pathological and immunological analysis uncovers that ^{125}I seed brachytherapy causes tumor necrosis within 15 to 20 days, associated with increased infiltration of tumor lymphocytes. Taken together, these results provide informative and critical insights into a new treatment strategy which helps to prolong survival for patients with advanced thoracic malignancy.

MATERIALS AND METHODS

Patients Information and Characteristics

Two hundred and ninety-four patients with unresectable thoracic cancer showing severe symptoms resulting from tumor oppression received local radioactive ^{125}I seed brachytherapy from March 2009 until July 2020 at Tianjin Beichen Hospital (Tianjin, China) were investigated in this study. This study conformed to the ethical guidelines of the 1975 Declaration of Helsinki and was approved by the Tianjin Anti-Cancer Association and ethics committee of Tianjin Beichen Hospital. All cases were selected according to the following inclusion criteria: 1) diagnosis with stage III/IV thoracic cancer with unresectable tumor; 2) confirmed malignancy with biopsy; 3) recurrence after conventional

treatment including surgery, chemotherapy, immunotherapy and systematic radiotherapy, with no active treatment options available; 4) at least one type of the symptoms including dyspnea, hemoptysis, dysphagia, and super vena cava syndrome due to local tumor oppression, or tumor larger than 7 cm causing cachexia; 5) no history of chronic lung disease including pneumonia and Chronic Obstructive Pulmonary Disease (COPD); 6) no liver and kidney dysfunction, severe heart disease, impaired hematopoietic function or systemic infection. Patients were excluded if they did not meet the criteria above. Patient clinical characteristics are shown in **Table 1**. Of the 294 patients, there were 290 with squamous cell carcinoma and 4 with malignant thymic carcinoma (**Table 1** and **Supplemental Figure 1**). Of the 294 patients received ^{125}I seeds, 117 patients received chemotherapy, two patients received immunotherapy 3 to 6 months after treatment, and 175 patients did not receive any other therapeutic treatments during follow-up. All patients' data were collected from the hospital medical records which were described precisely, and those with incomplete information were excluded. Informed consents of all patients were obtained for the study.

Local Single Needle Cone Puncture-^{125}I seed (SNCP-^{125}I) Brachytherapy Procedure

To achieve an accurate and dosimetric distribution of ^{125}I-seed implantation, treatment-planning system was applied for the ^{125}I treatment (TPS; standard version; Beijing ASTRO Technology Development Co., Ltd.) based on the American Association of Physicists in Medicine TG43 brachytherapy formalism (21–25). Dose, seed distribution, and depth of needles of each patient were determined preoperatively *via* TPS (**Table 2** and **Supplemental Figure 2**). Dosimetric evaluation parameters were: 1) D90, dose covering 90% tumor volume; 2) V90, tumor volume covered by 90% dose; 3) V100, tumor volume covered by 100% dose; and 4) V150, tumor volume covered by 150% dose. V90 ≥90% was considered as adequate dosage and distribution. Under general anesthesia, patients lay down in appropriate operational positions and an intraoperative stereotactic CT was performed. Thereafter, puncture paths were selected according to the preoperative planning under the CT scanning with a slice thickness of 5mm and seed brachytherapy of each needle channel was completed using 18G needle (15–20 cm\18G-needle, Zhuhai Hejia Inc., China). Enhanced CT scan was generally applied during operation due to the complicated structure of mediastinum and lung hilar. Seeds distribution and dose was verified through TPS after operation, and there is no significant difference between TPS predicted and implanted dose (**Table 2**). ^{125}I seeds used in this study was 4.50 ± 0.3 mm long, sealed and covered with an envelope of nickel titanium alloy (Atomic High-Tech Co., Ltd., Beijing). It is with an outer diameter of 0.80 ± 0.03mm, half-life of 59.6 days and an activity of 0.8 mCi. Summary of implanted ^{125}I seed parameters was shown in **Table 3**.

Particularly, we developed the Single Needle Cone Puncture method for the ^{125}I seed implantation (SNCP-^{125}I). We first selected one puncture site on the skin, withdrew the needle upon completion of ^{125}I seed implantation in the first needle channel until the needle tip was 1 to 2 cm from the tumor, then adjusted puncture direction avoiding blood vessels and performed the second puncture with the needle still inside the thoracic cavity. Similarly, the third or fourth puncture path was conducted inside the thoracic cavity according to the tumor shape, size and TPS plan, the needle direction was adjusted inside the thoracic cavity. Three needle channels form a three-dimensional cone shape covering over 90% of tumor volume. The end of each needle channel was close to be parallel with a minimum distance of 1.5cm between each two adjacent needle tracks to ensure the distribution of radioactive seeds covering most of the tumor area. Further, tumor with a diameter of 3 to 4 cm usually can be covered with one three-needle channel formed cone structure. It can be completed with several separate cones or superimposed

TABLE 1 | Clinical and demographic characteristics of patients at baseline.

Characteristics	Patients (n=294)
Gender (Male-Female)	223-71
Age (year, mean ± SD)	65.8 ± 9.6
Weight (kg, mean ± SD)	65.6 ± 9.1
Height (cm, mean ± SD)	169.2 ± 7.5
Smoking history, n (%)	225 (76.5)
Pleural effusion, n (%)	36(12.2)
Tumor size (cm, mean ± SD)	6.7± 2.2
Cancer type	
Lung cancer, n (%)	287 (97.6)
Malignant thymoma, n (%)	5 (1.7)
Esophageal cancer, n (%)	2 (0.7)
Disease stage	
IIIA	64 (21.8)
IIIB	118 (40.1)
IV	112 (38.1)
Tumor Pathology	
Squamous cell carcinoma, n (%)	290 (98.6)
Malignant thymic carcinoma, n (%)	4 (1.4)
Previous treatments:	
Surgery, n (%)	9 (3.1)
Systematic Radiotherapy, n (%)	8 (2.7)
Chemotherapy, n (%)	205 (69.7)
Immunotherapy, n (%)	2 (0.7)
Lymphocyte (%,mean ± SD)	21.7± 8.6
ECOG Performance Score (PS)	
2	11 (3.7)
3	194 (66.0)
4	89 (30.3)

SD, standard deviation.

TABLE 2 | Comparisons of seed parameters between TPS prediction and implanted dose.

Parameter	TPS prediction (n=294)	Implanted (n=294)	*p* value
D90 (cGy)	10490 ± 87.98	10570 ± 88.34	0.496
V90 (%)	95.67 ± 0.13	95.64 ± 0.13	0.906
V100 (%)	91.25 ± 0.10	91.19 ± 0.10	0.635
V150 (%)	75.42 ± 0.27	75.31 ± 0.26	0.777

TPS, Treatment Planning System; D90, Dose covering 90% tumor volume; V90, tumor volume covered by 90% dose; V100, tumor volume covered by 100% dose; V150, tumor volume covered by 150% dose. Data shown as mean ± SEM. Student t test was used for comparisons between groups.

TABLE 3 | Overall I^{125} seeds implantation parameters.

Parameter	Mean ± SD (n=294)	Range
Total radiotherapy dose (cGy)	11027.2 ± 1502.9	8000-14000
Individual seed activity (mCi)	0.8	0.8
Total seeds activity (mCi)	44.4± 16.6	10.4-151.2
Number of seeds implanted	55.2± 20.9	13-189
Total puncture channels	5.0 ± 1.6	3-10
Number of cones formed	3.0 ± 1.6	1-8
Implanted seeds parameters		
D90 (cGy)	10573.0 ± 1514.7	7978.7-13084.4
V90 (%)	95.6 ± 2.2	85.3-98.0
V100 (%)	91.2 ± 1.6	82.1-93.0
V150 (%)	75.3 ± 4.5	67.2-83.0

D90, dose covering 90% tumor volume; V90, tumor volume covered by 90% dose; V100, tumor volume covered by 100% dose; V150, tumor volume covered by 150% dose.

cones when tumors are larger than 4cm according to the shape of tumors. The ultimate goal is to make sure the radioactive sources as evenly distributed in the tumor as possible under the premise of patient safety. It is worth to note that, we always try to keep a minimal distance of 1.5 to 1.7 cm of the seeds and normal tissues/organs to limit radiation dose outside the tumor and avoid radioactive complications.

Tumor Measurement and Observation of Therapeutic-Related Side Affects

CT scans were performed to measure tumor size pre- and 3 to 6 months post treatment. Tumor response evaluations were conducted according to the Response Evaluation Criteria in Solid Tumors (RECIST version 1.1) guidelines. Tumor size was measured by the sum of biggest diameter of all target lesions. Objective responses were defined as follows: CR, complete response; PR, partial response, described as a 30% decrease in the biggest diameters of all targeted tumors; PD, progressive disease, defined as new tumor appearance or a minimum 20% increase in the biggest diameters of all targeted tumors; and SD, stable disease, determined as tumor change between PR and PD. Procedure related side effects were recorded during treatment and follow-up according to Common Terminology Criteria for Adverse Events (CTCAE) version 4.0 (26). Disease-related symptoms before treatment were not disclosed unless they worsened after ^{125}I brachytherapy.

Hematoxylin and Eosin (H&E) Staining and Immunohistochemical Analysis

Tumor core biopsy tissues pre- and post- treatment were fixed with 10% neutral formalin, dehydrated, embedded and serially sectioned (4 μm thick) for H&E staining using an automatic linear slide stainer (BOND-MAX) to assess pathological changes after treatment. Pathological diagnosis was made by two independent blinded pathologists. All sections were immunohistochemically (IHC) stained with p40 (Cat. No.:ZM-0472, clone# BC28) and P63 (Cat. No.: ZM-0406, clone# 4A4 + UMAB4) *via* automatic IHC stainer (BOND-MAX). Second antibodies are provided by Leica Biosystems Co., Ltd. p40, p63, CD8+, and Ki67-positive cells were stained for brown nucleus. To count CD8+ and Ki67 positive cells, the richest positive cell areas were identified at low magnification (×10) were selected, images were took at a magnification of ×20, and then CD8+ and Ki67 positive cells were evaluated quantitatively by two independent observers who analyzed five fields from these areas under a high-power (×40) field using an Olympus confocal microscope (Center Valley, PA, USA).

Follow-Up Assessment

All patients were followed from the date of the treatment of SNCP-^{125}I brachytherapy up to September 2020 or up to the time of death. Treatment-related adverse events were recorded during the treatment and follow-up.

Statistical Analysis

All statistical analyses were performed using the GraphPad Prism 5 (GraphPad Software Inc., La Jolla, CA). Survival curves and rates were calculated using the Log-rank (Mantel-Cox) Test or Gehan-Breslow-Wilcoxon Test, and survival was measured from the date of the treatment of local radioactive Iodine-125 seed brachytherapy up to September 2020 or the time of death. A student t test was used to analyze the statistical significance between groups. Spearman test was used to analysis correlations between groups. A p value less than or equal to 0.05 was the threshold used to determine statistical significance.

RESULTS

Clinical Outcomes of SNCP-^{125}I Brachytherapy-Treated Patients With Incurable Thoracic Malignancy

We investigated 294 patients with advanced thoracic malignancy who were diagnosed as squamous cell carcinoma and progressed on multiple types of conventional treatments (**Figure 1A**). Particularly, 238 of the patients experienced dyspnea, 54 dysphagia, 18 super vena cava syndrome due to local tumor oppressions and 176 hemoptysis. A high proportion of patients developed two or more types of the above symptoms (**Supplemental Figures 3**, **4**). Following SNCP-^{125}I treatment, the symptoms were successfully alleviated in 91 to 94% patients (**Figures 1B, C**). Of note, all the patients showed limited anatomical puncture site that restricted to traditional multiple parallel needle-^{125}I seed brachytherapy. Following the SNCP-^{125}I treatment, which we implement a radioactive dose covering over 90% of the tumor volume using a single needle through one puncture site on the skin, the overall response rate (ORR, including PR and CR) in 3 months was 81.0% (238/294) with significantly regressed tumors and improved performance status (**Figures 1D, E** and **Table 4**). Patients with large irregular and necrotic tumors also show clinical improvements (**Figure 1D**). Of the 294 patients, 117 patients underwent chemotherapy, 2 patients followed with immunotherapy and 175 patients opted to receive hospice cares 3 to 6 months post SNCP-^{125}I treatment (**Table 4**). The 1-, 2-, 3- and 5- year overall survivals of these patients were 60.2%, 18.5%, 7.7% and 2.7%, respectively. The median OS and PFS were 13.6 months and 5.8 months (**Figures 1F, G**). Procedure-related side effects of pneumothorax (32/294), blood-stained sputum (8/294), subcutaneous emphysema (10/294),

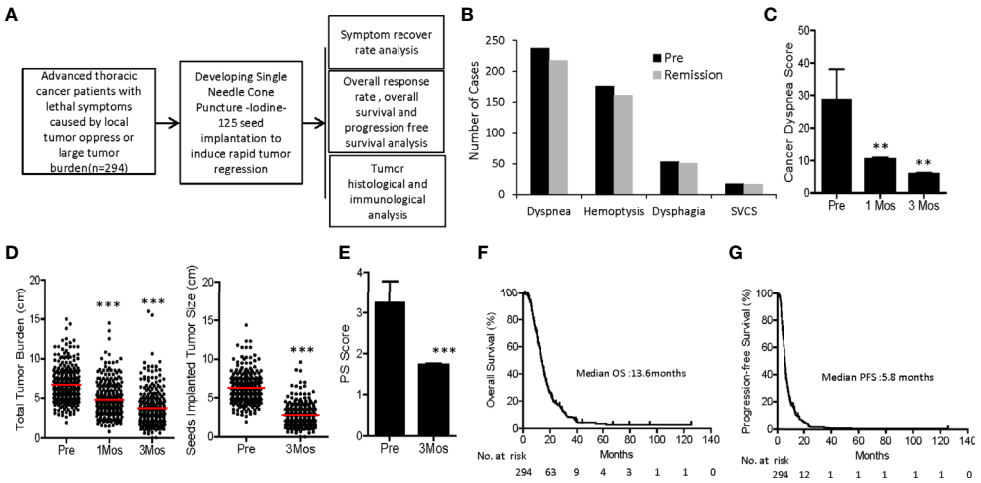

FIGURE 1 | Flow chart and clinical outcomes of SNCP-^{125}I brachytherapy-treated patients with incurable thoracic malignancy. **(A)** An overall workflow of the present study. **(B)** Hemoptysis and life-threatening symptoms including dysponea, dysphagia and superior vena cava syndrome due to local tumor oppressions were greatly alleviated in 2 weeks to 1 month. **(C)** Cancer dysponea score was significantly decreased 1- and 3-month after treatment. Cancer dysponea score was calculated according to the widely used Cancer Dyspnoea Scale reported by Tanaka et al. (27). **(D)** Overall tumor burden and change of tumor size after treatment in 294 patients 1 month and 3 months post SNCP-^{125}I brachytherapy. 26 patients showed partial response (PR), 1 patient with complement response (CR) and 3 patients with stable disease (SD). **(E)** Performance status of all 294 patients was greatly improved following SNCP-^{125}I brachytherapy. **(F, G)**. Overall survival (OS) and progression-free survival (PFS) curves of 294 patients. The median OS and PFS were 13.6 months and 5.8 months, respectively. Survival curves were analyzed using the Log-rank (Mantel-Cox) Test. SVCS, superior vena cava syndrome. *p < 0.05; **p < 0.01; ***p < 0.001.

puncture site bleeding (16/294) and chest pain (6/294) were observed (**Table 4**). These results suggest that, as a further local treatment opportunity, SNCP-^{125}I brachytherapy can effectively and safely treat incurable thoracic malignancy, particularly for patients with inaccessible puncture sites, complications from tumor oppression and tumor bleeding.

Importantly, further survival analysis showed that patients who were able to follow with chemotherapy or immunotherapy experienced extended overall and progression free survival, as compared with patients who opted to receive hospice care (16.5 months Vs. 11.2 months, $p<0.0001$; 6.8 months Vs. 5.2 Months, $p<0.001$, respectively, **Figure 2**). Basic clinical characteristic factor comparisons of these two groups showed no significantly difference (**Table 5**). We also show greatly reduced risk associated with the operation and satisfied recovery rate upon treatment, especially in patients with lung hilar and mediastinum tumors. To further explain how the SNCP-^{125}I approach provides an optimal clinical benefit for patients, we show the detailed treatment process for representative patients below by different clinical symptom categories.

TABLE 4 | Clinical outcomes and therapeutic-related side effects of SNCP-^{125}I brachytherapy treated patients.

Parameter	Patients (n=294)
Clinical response at 2-6Mos follow-up	
Complete response, n (%)	2(0.7)
Partial response, n (%)	236 (80.3)
Stable disease, n (%)	45 (15.3)
Progressive disease, n (%)	11(3.7)
Procedure-related side affects	
Pneumothorax, n (%)	32(10.9)
Blood-stained sputum, n (%)	8 (2.7)
Subcutaneous emphysema, n (%)	10 (3.4) 1 (3.3)
Puncture site bleeding, n (%)	16 (5.4)
Chest pain, n (%)	6(2.0)
Following treatment (3-6 months after I^{125} initiation)	
Chemotherapy, n (%)	117 (39.8)
Immunotherapy, n (%)	2 (0.7)
Hospice supportive only, n (%)	175(60.2)

SNCP-^{125}I Brachytherapy Induces Rapid Tumor Regression of Large Recurring Solid Tumor After Conventional Treatment Failure

It is common that patients develop large lung squamous cell carcinoma and metastasis esophageal squamous cell carcinoma, and some even grow tumors on the skin surface with rupture and infection. These patients are often accompanied by serious systematic symptoms due to large tumor consumption including anemia, hypoalbuminemia, high fever and pain, with a poor performance status of Performance Score (PS) >3. Few traditional treatment strategies are currently available for these patients except hospice care. Particularly, Patient 53 was diagnosed as advanced mediastinal lung squamous cell carcinoma which compressed the heart and esophagus and caused arrhythmia and dysphagia (**Figure 3A**). Patient 11 progressed on chemotherapy and radiotherapy, developed lung squamous cell carcinoma in the left lung with no druggable targets as revealed by DNA sequencing, and exhibited a poor performance status (PS=4) (**Figure 3A**). Patient 282 was diagnosed as esophageal cancer with a large and ruptured

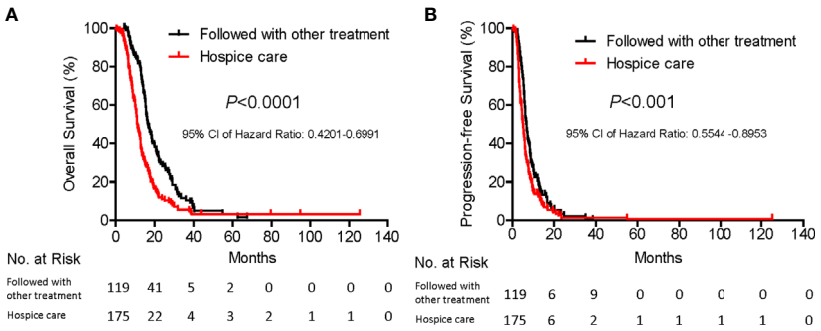

FIGURE 2 | Subgroup survival analysis of patients with and without curative treatment after SNCP-^{125}I brachytherapy. Among 294 patients, 119 were followed with chemotherapy and immunotherapy and 175 patients with hospice care. Patients who were followed with other types of treatment showed significantly prolonged overall survival (**A**, 16.5 months Vs. 11.2 months, $p<0.0001$) and progression-free survival (**B**, 6.8 months Vs. 5.2 Months, $p<0.001$).

TABLE 5 | Clinical and demographic characteristic comparisons of two groups' patient at baseline.

Characteristics	Patients followed with hospice care (n=175)	Patients followed with other treatment (n=119)	*P* Value
Gender (male-female)	133-42	90-29	1.000
Age (year, mean ± SD)	66.86 ± 9.56	64.33 ± 9.39	0.043
Weight (kg, mean ± SD)	64.75 ± 9.11	66.76 ± 8.92	0.051
Height (cm, mean ± SD)	168.70 ± 7.63	170.00 ± 7.29	0.149
Smoking history (yes-no)	137-38	89-30	0.485
Pleural effusion (yes-no)	21-154	14-105	1.000
Tumor size (cm, mean ± SD)	6.44 ± 1.78	6.07 ± 1.90	0.090
Cancer type			0.963
Lung cancer, n	171	116	
Malignant thymoma, n	3	2	
Esophageal cancer, n	1	1	
Disease stage			0.341
IIIA	33	31	
IIIB	73	45	
IV	69	43	
Previous treatments:			0.173
Surgery, n	6	3	
Systematic Radiotherapy, n	6	2	
Chemotherapy, n	146	59	
Immunotherapy, n	0	2	
Lymphocyte (%, mean ± SD)	21.03 ± 7.78	21.02 ± 7.84	0.865
ECOG Performance Score (PS)			0.146
2	5	6	
3	110	84	
4	60	29	

SD, standard deviation.

metastatic neck tumor, and experienced severe subclavian vein oppression, edema in the right upper limb, persisting fever, anemia and low platelets levels (**Figure 3B**). We successfully administered local SNCP-^{125}I treatment for these and other 84 similar patients, and found that the tumors regressed in 3 weeks (Pt.53), 4 weeks (Pt.11) and 2 months (Pt.282) respectively (**Figures 3A, B**, data not shown). The symptoms due to tumor oppression were subsequently alleviated, and the performance status greatly improved (**Figure 1E**).

Severe Dyspnea Due to Thoracic Tumor Oppression was Completely Remedied by SNCP-^{125}I Brachytherapy

Patients with squamous cell carcinoma of the lung often develop dyspnea (~60%) and acute respiratory failure, when the tumor is located adjacent to trachea, especially to the large main bronchus (28) Among the 294 patients in the present study, 238 developed dyspnea, and showed a significantly correlation with the degree of tracheal stenosis (**Figures 1B** and **4A**) (27, 29). The patients usually die in a short time if the airway cannot be recovered rapidly. However, they are unlikely to undergo conventional radiotherapy and chemotherapy as an optimal treatment strategy due to insensitivity to targeted drugs. Furthermore, the tumors are adjacent to trachea and no multiple puncture sites are readily accessible for conventional ^{125}I seed brachytherapy. Consequently, rapid control and elimination of local tumor lesions represents an effective means to completely relieve the respiratory distress and severe hypoxia. As shown in **Figures 3C, D**, as representative individuals, Patients 1, 7, 35 and 95 with progressive squamous cell carcinoma of the lung all experienced dyspnea due to airway obstruction, and continued to exhibit dyspnea, orthopnea, tracheal inhalation wheeze, and declined blood oxygen saturation. Remarkably, the symptoms due to airway obstruction gradually improved in two weeks after SNCP-^{125}I treatment and disappeared 1month after. The tumor significantly regressed and the main airway became significantly reconstructed in 1 to 3 months with a greatly improved cancer dyspnea score (**Figures 1C** and **4B**) (27, 29). It is worth to note that it was changeling for the patients to lie

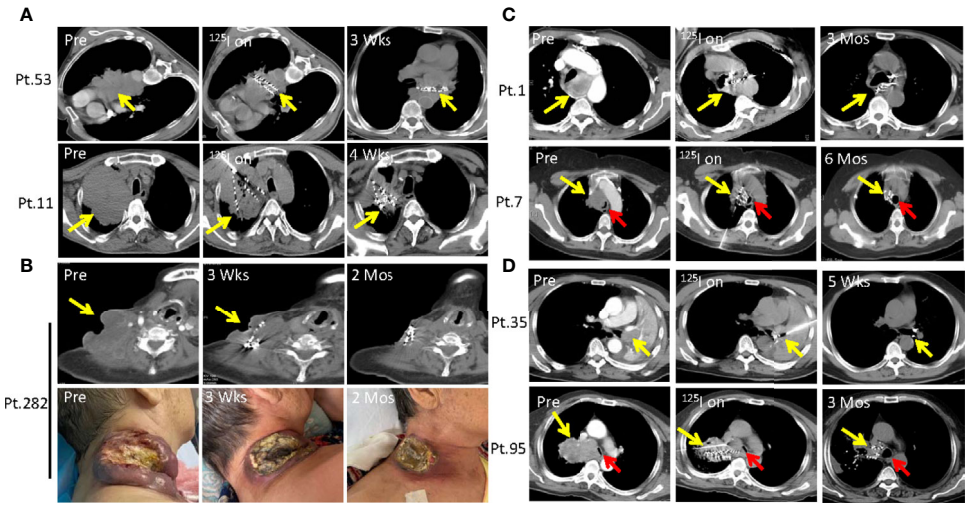

FIGURE 3 | SNCP-^{125}I brachytherapy induces rapid regression of large solid tumor that recurred after conventional treatment. **(A)** Patient 53 was diagnosed with large advanced mediastinal lung squamous cell carcinoma that constricted the heart and the esophagus and caused arrhythmia and dysphagia. Patient 11 progressed on chemotherapy and radiotherapy, developed a large lung squamous cell carcinoma in the left lung with no druggable targets as detected by DNA sequencing, and eventually showed a poor performance status. Tumors of Patient 11 and 53 rapidly regressed 3 and 4 weeks after SNCP-^{125}I brachytherapy, respectively**. (B)** Patient 282 was diagnosed as esophageal cancer with a large metastatic and rupturing tumor in the neck. Following SNCP-^{125}I brachytherapy, the tumor regressed in 3 weeks. **(C, D).** Patients 1, 7, 35 and 95 with progressive lung squamous cell carcinoma all experienced acute dyspnea because of airway obstruction. Tumors significantly regressed and the main airway was completely reconstructed in 5 weeks to 6 months. Yellow arrow-tumor, Red arrow-airway.

down and maintain a posture for more than 5 min due to breathing difficulties, thus limiting the operation time and requiring quick determination of the puncture site and completion of the seeds implantation within 5 to 10 min. Bleeding and severe pneumothorax during the operation will aggravate the breathing difficulty for the patients, and sufficient preparation for secondary complication and clinical emergency is needed before the operation.

SNCP-125I Brachytherapy Successfully Alleviated Fatal Hemoptysis in Advanced Lung Cancer Patients

Hemoptysis due to lung tumors is one of the most common causes for patient death, with a mortality rate of about 59% and 80% in those with hemoptysis >1,000 ml per 24 h (30, 31). This normally happens in patients with squamous cell carcinoma developing in the central lung after ineffective standard treatment. In the present study, we utilized the SNCP-^{125}I treatment to reduce local tumor burden and control bleeding in 176 lung cancer patients with hemoptysis. For example, Patient 284 with squamous cell carcinoma in the hilar region of the right lung progressed on chemotherapy and developed hemoptysis, dyspnea and atelectasis, with the tumor blocking the main trachea. Following the SNCP-^{125}I treatment, the bleeding stopped as shown under tracheoscopy examination (**Figure 5A**). Similarly, Patients 12, 15, 264 and 271 with squamous cell carcinoma of the lung also developed hemoptysis and progressed on typical treatments and hemostatic drugs.

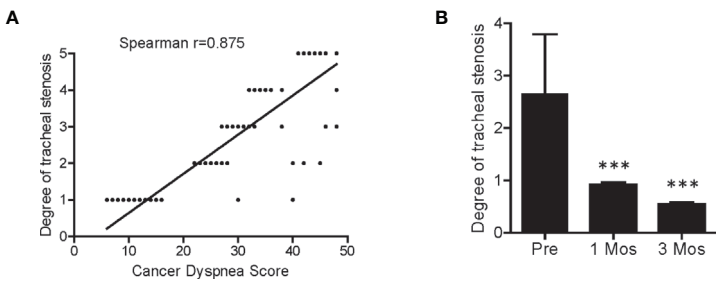

FIGURE 4 | Correlation between cancer dyspnea score and degree of tracheal stenosis. **(A)** Patient cancer dyspnea score was significantly correlated with the degree of tracheal stenosis. **(B)** The degree of tracheal stenosis in patients was significantly decreased 1- and 3-month after SNCP-^{125}I brachytherapy. Spearman correlation test was used for the analysis. ***$p < 0.001$.

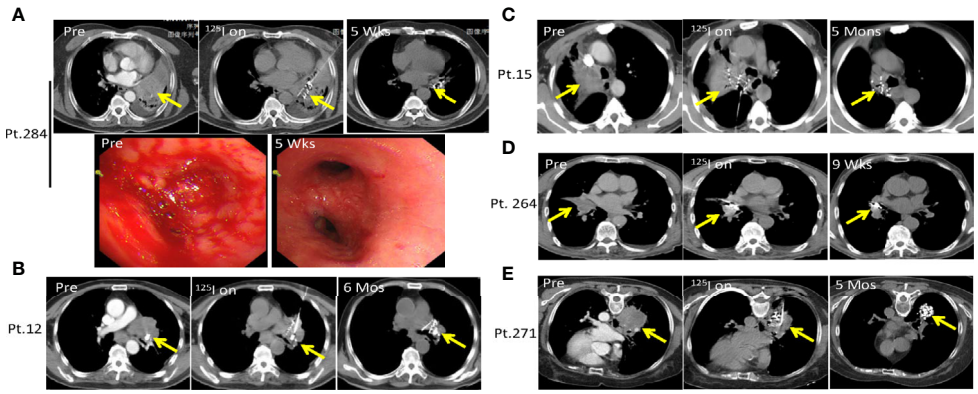

FIGURE 5 | SNCP-^{125}I brachytherapy successfully alleviates life-treatening hemoptysis in advanced lung cancer. **(A).** Patient 284 with squamous cell carcinoma in the hilar region of the right lung progressed on chemotherapy and developed hemoptysis, with the tumor also blocking the main trachea accompanied by dyspnea and atelectasis. Following SNCP-^{125}I brachytherapy, bleeding was successfully stopped as shown under the tracheoscopy examination 5 weeks later. **(B–E)** Patients 12, 15, 264 and 271 with lung squamous cell carcinoma developed hemoptysis and progressed after unsatisfied treatment of hemostatic drugs. The tumors greatly regressed through SNCP-^{125}I brachytherapy treatment in 6 months, 3months, 9 weeks and 5 months, respectively. Yellow arrow-tumor.

We also effectively stopped bleeding using local SNCP-^{125}I treatment which primarily reduced local tumor load and restored the trachea (**Figures 5B–E**).

Dysphagia, Arrhythmia, and Superior Vena Cava Syndrome Caused by Mediastinal and Lung Tumors Oppressions Is Recovered by SNCP-^{125}I Brachytherapy

Malignant aggressive thymoma is a rare epithelial tumor that often occurs in the anterior superior mediastinum. Thymoma is categorized into four stages according to the Masaoka staging system: stage I, grossly and microscopically encapsulated; stage II, the thymoma invades beyond the capsule and into the nearby fatty tissue or to the pleura; stage III, macroscopic invasion of neighboring organs; stage IV, pleural, pericardial, hematogenous, or lymphatic dissemination (32–34). Stage I and II patients generally undergo surgery, while stage III and IV patients, also called malignant aggressive thymoma, usually fail after surgical resection and require combined radiotherapy and chemotherapy. However, in some cases, aggressive thymoma quickly compresses the heart, esophagus and superior vena cava, which causes life-threatening symptoms including dysphagia, arrhythmia and super vena cava syndrome. Local SNCP-^{125}I treatment is invasive and can effectively treat such tumors. Patient 75 was 84 years old with malignant aggressive thymoma progressing on surgery and radiotherapy and refused chemotherapy. The tumor

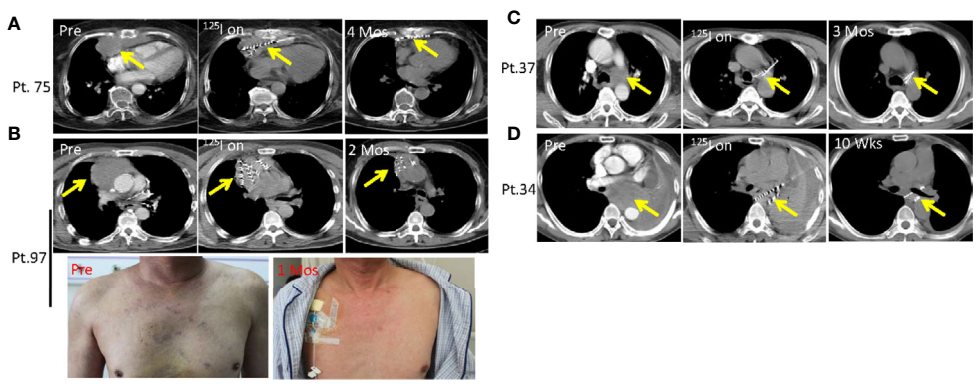

FIGURE 6 | Dysphagia, arrhythmia and superior vena cava syndrome due to compression of mediastinal and lung tumors is alleviated by SNCP-^{125}I brachytherapy. **(A)** Patient 75 was an 84 years old patient with malignant aggressive thymoma and progressed on surgery and radiotherapy. The tumor significantly regressed after SNCP-^{125}I brachytherapy treatment in 4 months. **(B)** Patient 97 was diagnosed as malignant aggressive thymoma, experienced compression of the superior vena cava causing superficial venous dilation of the chest wall. Following SNCP-^{125}I brachytherapy, the tumor significantly regressed in 2 months and superior vena cava syndrome was alleviated in 1 month. **(C)** Patient 37 with a lung tumor repressing the laryngeal nerve, invading both pulmonary artery and trachea. The tumor shrunk in 3 months *via* SNCP-^{125}I brachytherapy. **(D)** Patient 34 was diagnosed as mediastinal lung cancer with the tumor compressing the esophagus and causing dysphagia. The dysphagia symptom disappeared through SNCP-^{125}I treatment within a month followed by tumor regression. Yellow arrow-tumor.

oppressed the heart and caused arrhythmia which was recovered after SNCP-^{125}I treatment (**Figure 6A**). Patient 97 was also diagnosed as malignant aggressive thymoma who was insensitive to radiotherapy and chemotherapy, experienced compression of the superior vena cava causing swollen head, face, and upper limbs and superficial venous dilation of the chest wall (**Figure 6B**). Following SNCP-^{125}I brachytherapy, the tumor significantly regressed and superior vena cava syndrome was completely alleviated (**Figure 6B**).

Dysphagia as a result of tumor compression is another difficult-to-cure symptom. The lung tumor in Patient 37 compressed the laryngeal nerve and caused dysphagia, and experienced choking after eating. The tumor in this patient also invaded both pulmonary artery and trachea causing dyspnea (**Figure 6C**). Patient 34 was diagnosed as mediastinal lung cancer with the tumor compressing the esophagus and causing dysphagia (**Figure 6D**). Dysphagia was completely remedied in these two patients within a month after SNCP-^{125}I treatment, and this was followed by tumor regression (**Figures 6C, D**). Herein, we successfully treated 54 patients who developed severe dysphagia. Taken together, the findings demonstrated that, instead of supportive care, SNCP-^{125}I brachytherapy is an effective approach to reduce tumor burden when treating the life-threatening symptoms due to thoracic tumor compression.

SNCP-^{125}I Brachytherapy Is an Effective Approach in Treatment of Thoracic Malignancies With Limited Anatomic Puncture Site

As described above, SNCP-^{125}I was effective in treating incurable thoracic malignancies. We herein highlight multiple rationales underlying the design of the SNCP-^{125}I method. Foremost, tumors located in the mediastinum or hilus of the lung are normally blocked by blood vessels and trachea and thus become inaccessible to puncture. Particularly, only one accessible CT scan layer can be the puncture site with an available insertion gap of about 0.5 to 1 cm, for which typical multiple-needle puncture-^{125}I brachytherapy is difficult to administer. Representative CT images of Patients 1, 12, 37, 42 and 95 were showing in **Figures 7A–E**. Secondly, patients with poor performance status require the operation to be promptly carried out, but conventional multiple needles puncture-^{125}I brachytherapy usually takes over 1 h, longer than what the patients can withstand. In addition, patients cannot maintain a proper posture required for the operation because of dyspnea

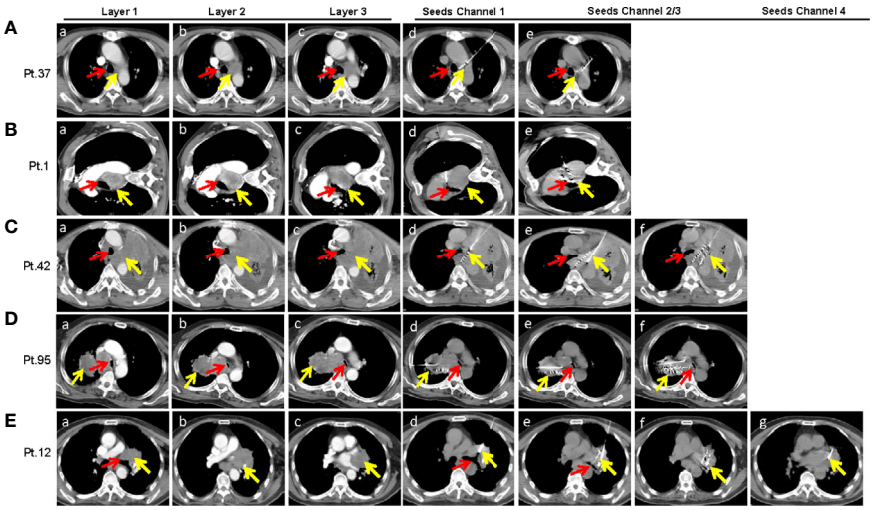

FIGURE 7 | SNCP-^{125}I brachytherapy is a unique approach in treating thoracic malignancies with limited numbers of accessible anatomic puncture site as shown in several representative cases. **(A)** A lung tumor in Patient 37 was surrounded by the main trachea, aortic arch and left pulmonary artery (a–c). To avoid damage to large blood vessels, only one CT layer could be the gap for needle insertion, which was less than 1 cm (c). The puncture had to pass through the whole left lung (10 cm from the tumor) that only allowed a single needle insertion (c). The first puncture was done under the aortic arch (d), and the second and third puncture through the right pulmonary artery by adjusting the needle in the aortic window without exiting the vascular space (e). **(B)** A lung tumor in patient 1 in the aortic window compressed the main trachea. The patient was only able to lie on the left side due to breathing difficulty, and this greatly limited the operation time (a–c). The first puncture was done through the intercostal space and the aortic window (d), and the second and third punctures by adjusting the direction of the needle from the edge of the diaphragm (e). **(C)** An irregular left lilar tumor in Patient 42 invaded the mediastinum, oppressed the left main trachea and the esophagus (a–c). The needle was inserted into the posterior mediastinum through the left anterior chest wall and the left hilum (d). Withdrawing the needle until 1cm from the edge of the tumor and changing puncture direction for the second punctures (e, f). **(D)** A right hilar tumor in Patient 95 invaded the mediastinum, oppressed the main trachea which was narrowed by nearly 80% (a–c). Only one needle could be inserted into the side chest wall with a total puncture path of about 20 cm to reach the distal side of the tumor because the tumor in the mediastinum that compressed the trachea was blocked by the superior vena cava and aorta (c). Both the first and second punctures reached the dorsal side of the tumor which formed a conical distribution with the third puncture (d–f). Particularly, the operation was required to be completed in 5 to 10mins due to breathing difficulty. **(E)** A left hilar tumor in Patient 12 invaded the hilar, heart and trachea (a–c). Four punctures were superimposed due to the large size of the tumor. The four punctures were done through the intercostal space (d–g). Scans of each patient were enhanced continuous CT scan with a thickness at 5mm. Yellow arrow-tumor, Red arrow-Airway.

due to tumor oppression. Given these practical challenges, SNCP-^{125}I becomes a feasible and effective approach which works though only one puncture site and can be completed in 5 to 10 min. Furthermore, for patients who were treated with bronchial stent but re-developed tracheal stenosis, SNCP-^{125}I brachytherapy still restored the tracheal stenosis (**Supplemental Figure 5**). An example CT scan showing how two punctures were carried out using a single needle is shown in **Figure 8A**. Patient 37 is shown as an example to explain how the three-dimensional cone shape formed using a single needle. As illustrated in **Figure 8B**, three seed paths covered 90% of the tumor volume by forming a three-dimensional (3D) tapered path as verified through TPS plan (**Figure 8C**). Afterward, we selected one puncture site, implanted seeds into three channels by withdrawing, adjusted the direction of the needle and performed the other two punctures inside the tumor, and a 3D tapered path then formed as shown by the 3D reconstructed seeds (**Figure 8D**). As described in the method, It is important to make sure the distal ends of each channel as parallel as practical to ensure an evenly distribution of radioactive sources in the tumor. Three more representative cases of Patient 11, 256 and 284 treated with SNCP-^{125}I were shown in **Figure 8E**. It was worth to note that the numbers of total puncture channels and formation of the cones were associated with the size of treated tumor (**Supplemental Figures 6A, B**). Taken together, SNCP-^{125}I brachytherapy is an effective method for incurable thoracic cancer patients with mediastinum or lung hilum invasion and inaccessible anatomical puncture site.

SNCP-^{125}I Brachytherapy Causes Rapid and Long-Term Tumor Cell Necrosis and Induces Tumor Lymphocyte Infiltration

^{125}I brachytherapy induces rapid tumor regression (**Figure 1D**) (11–17), but the pathological feature of irradiated tumor cells remains poorly defined. We thus assessed pathological alterations in tumor tissues from eight patients before and after SNCP-^{125}I brachytherapy. We found that the majority of tumor cells underwent necrosis in 15 to 20 days after treatment (**Figure 9A**). After 2 or 3 months, no or little live cells were observed in the treated tumor site, which is usually difficult to confirm *via* CT scans (**Figure 9B**). Surprisingly, after 9 months, the remaining tumor cells became fibrotic (**Figure 9C**), although CT scans still show a high density shadow in the treated tumor area in most cases. All pathological alterations were further confirmed by staining with tumor specific markers p40 and p63 for squamous cell carcinoma that treated tumor fails to identify any residual cancer cells 2 to 3 months after treatment (**Figures 9A–C**). In parallel, immunohistochemistry (IHC) staining with tumor cell proliferation marker Ki67 in Patients 291,292 and 284 pre- and 1 month post- SNCP-^{125}I brachytherapy showed that tumor

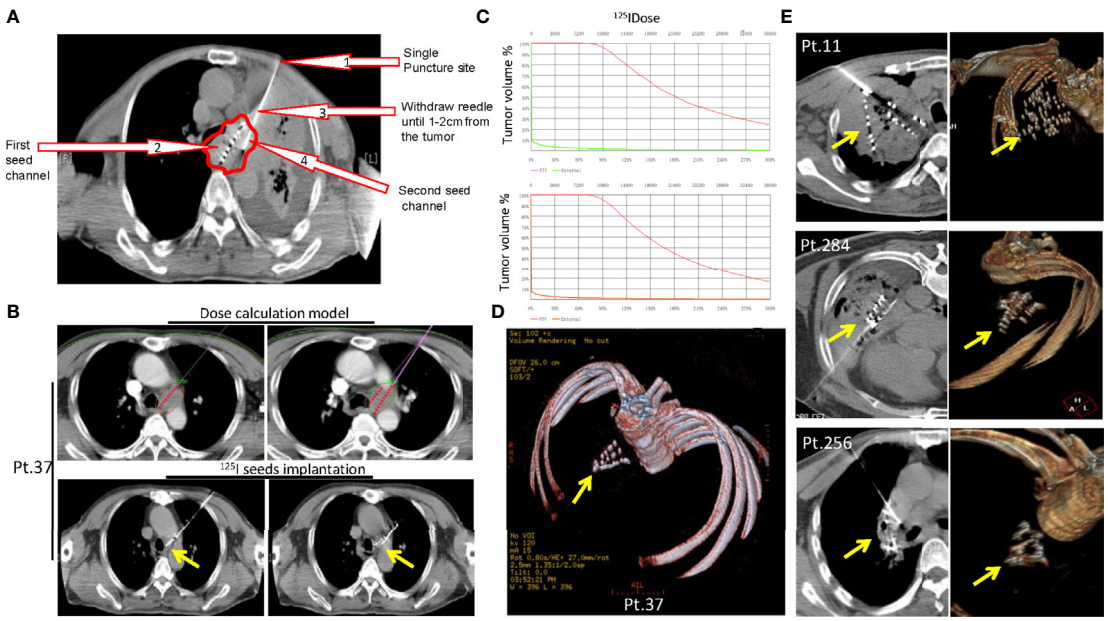

FIGURE 8 | Three-dimensional cone shape was formed using a single needle. **(A)** An example CT scan showing how to operate two punctures using a single needle. SNCP-^{125}I was achieved by selecting one puncture site on the skin (Arrow 1), withdrawing the needle upon completion of ^{125}I seed implantation in the first needle channel (Arrow 2) until the needle tip was 1-2cm from the tumor (Arrow 3), then adjusting puncture direction and performing the second puncture (Arrow 4) with the needle still inside the thoracic cavity. Red circle-tumor. **(B)** Representative CT scans of pre-treatment radioactive dose calculation in Patient 37 through treatment planning system (TPS), and post-treatment implanted seeds paths as shown in CT scans. **(C)** Three seed paths were able to cover 90% of the tumor volume by forming a three-dimensional (3D) tapered path pre-calculated through TPS plan. **(D)** 3D reconstruction of the implanted seeds in Patient 37 showed formation of a cone shape. **(E)** Three other representative 3D reconstructed implanted seeds in Patient 11, 284 and 256 undergoing SNCP-^{125}I brachytherapy. Yellow arrow-tumor.

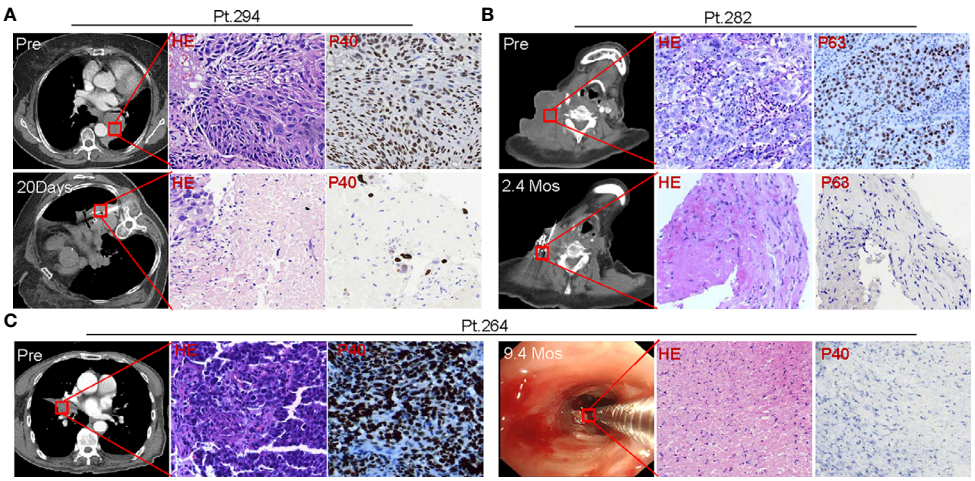

FIGURE 9 | Tumor pathologic alterations following SNCP-^{125}I brachytherapy. **(A)** Pre-treatment needle biopsy of the lung mass in Patient 294 showed a moderately differentiated squamous cell carcinoma, and immunostain for p40, a specific marker for squamous cell carcinoma, showed strong and diffuse nuclear expression in squamous cell carcinoma. 20 days post ^{125}I seed brachytherapy, a needle biopsy within one 1cm of the seed implantation site showed scant clusters of residual cancer cells surrounded by amorphous necrotic tissue, ghost tumor cells and inflammatory cells. Residual cancer cells exhibited cytological atypia, in line with a radiation treatment effect, including enlarged hyperchromatic nuclei, multiple nuclei, cytoplasmic vacuoles. p40 staining highlights the residual cancer cells. **(B)** Pre-treatment resection biopsy of a massive metastatic cervical lymph node in Patient 282 showed poorly differentiated squamous cell carcinoma, and p63 immunostain showed strong and diffuse nuclear expression in squamous cell carcinoma cells. 2.4 months post ^{125}I seed implant, a needle biopsy within one 1cm of the seed implantation site, showed spindle fibroblasts, amorphous collagen tissue, and scattered inflammatory cells. There were no visible residual cancer cells on H&E stain slides. p63 staining identified no residual cancer cells. **(C)** Pre-treatment bronchoscopic biopsy of the lung mass in Patient 264 showed poorly differentiated basaloid squamous cell carcinoma, and strong and diffuse nuclear stain pattern showed p40 expression in squamous cell carcinoma. At 9.4 months post ^{125}I seed implant, a bronchoscopic biopsy at the previous biopsy site showed fibrotic tissue, great infiltration of inflammatory cells, and necrotic surface indicative of ulcer. There were no visible residual cancer cells or normal epithelial cells lining the bronchus surface on H&E stain slides. p40 staining identified no residual cancer cells. All images were taken in a 40X magnification. HE, hematoxylin and eosin staining. 8 patients were tested and 3 patients were shown here as representative cases.

proliferation was significantly suppressed after SNCP-^{125}I brachytherapy (p=0.012, **Figures 10A, B** and **Supplemental Figure 7A**). This result suggests that ^{125}I brachytherapy induces tumor necrosis and fibrosis to eliminate tumor cells in a long-term manner, in line with the rapid tumor regression as observed through CT images (**Figure 1D**).

In vitro studies have revealed that systematic radiotherapy increases T-cell infiltration (35, 36). We therefore asked whether SNCP-^{125}I brachytherapy plays a role in tumor microenvironment alteration in the patients. We found that tumor infiltrated CD8+T cells were significantly increased 4 weeks after SNCP-^{125}I brachytherapy, while CD4+T cell tumor infiltration showed no change (p=0.043, **Figures 10C, D** and **Supplemental Figure 7B**). These results provide an additional mechanistic rationale for combining ^{125}I brachytherapy with immunotherapy that modulates tumor infiltrated CD8+T cell in the clinic. However, only a small population of patients was evaluated, and increasing numbers of patients are needed to confirm this result. In addition, the dynamics of CD8+T cells infiltration remains another key question that needs to addressed.

DISCUSSION

^{125}I brachytherapy is known to be safe and effective in advanced cancer patients (11–17), and the multiple-needle parallel puncture method is the most common and widely used treatment regimen for ^{125}I brachytherapy (11–17, 37). It requires multiple accessible puncture sites without obstruction, and is suitable for tumors with relatively regular shapes. The treatment can be carried out with technical ease, and radioactive ^{125}I seeds can be readily distributed evenly through multiple paralleled needles with an equal distance in between. However, critical challenges remain as it may cause severe lung injury with bleeding and pneumothorax, especially for lung hilar and mediastinal tumors (38–40). Furthermore, this approach is not applicable to larger tumors with severe irregular ulcers (**Figure 3B**), and the overall survival benefit of this treatment needs to be further determined in future controlled studies involving large populations of patients.

Herein, we present the clinical and pathological outcomes of 294 patients treated with SNCP-^{125}I brachytherapy that we developed for incurable thoracic cancers. All the patients were stage III/IV thoracic malignancies, with 289 developing lung hilar and mediastinal invasion, 240 experiencing vascular and tracheal invasion, and 283 showing a performance score of 3 or 4 indicative of a high death risk. To design effective treatment strategies urgently needed to for these patients, we developed SNCP-^{125}I brachytherapy which represents a highly localized treatment option and rapidly reduces local tumor burden (ORR of 81.0%), thereby significantly improving quality of life and

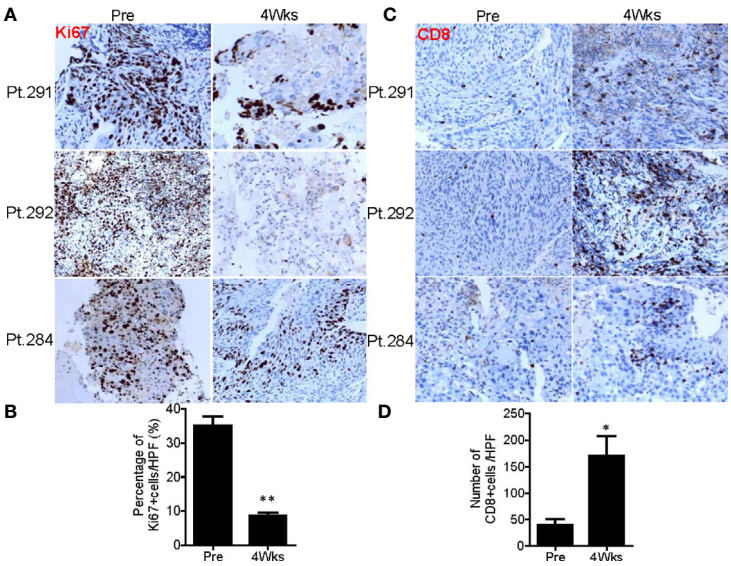

FIGURE 10 | SNCP-^{125}I brachytherapy enhances tumor lymphocyte infiltration. **(A)** Immunohistochemistry (IHC) staining against a tumor cell proliferation maker Ki67 in Patients 284, 291 and 292 at pre and 4 weeks post SNCP-^{125}I brachytherapy. **(B)** Quantification data showed tumor proliferation was significantly inhibited after SNCP-^{125}I brachytherapy (p=0.013, n=4). **(C)** IHC staining against tumor infiltrated CD8+T cell in Patient 284, 291 and 292 at pre and 4 weeks post SNCP-^{125}I brachytherapy. **(D)** Quantification data showed a significant increase in tumor infiltrated CD8+T cells after treatment (p=0.043, n=4). A student t test was used to analyze the statistical significance before and after treatment. All images were taken in a ×20 magnification and zoomed out. Data were collected under a high-power (×40) field. HPF, High power field. *, p<0.05; **, p<0.01.

extending treatment window for the patients (**Figure 1E** and **Table 4**). In this retrospective clinical study, we report that SNCP-^{125}I brachytherapy produced a median overall survival of 13.6 months. Moreover, we found that SNCP-^{125}I brachytherapy combines with chemotherapy is more efficacious than SNCP-^{125}I brachytherapy alone. Importantly, we show our procedures are safe, easy to deploy, and improved quality of life for this group of patients. SNCP-^{125}I brachytherapy thus represents an effective and unique treatment strategy that offers a major clinical benefit for patients with incurable mediastinal and lung hilum malignancies accompanied with life-threatening symptoms.

This SNCP-^{125}I method is promising and advantageous for the following reasons: 1) multiple puncture routes can be completed with only one puncture site and one needle, and this is carried out by withdrawing and adjusting the needle direction inside the thoracic cavity; 2) it is effective treating incurable mediastinal and lung hilum tumors and large tumors with irregular ulcers; 3) it enables rapid control of life-threatening symptoms as a result of local tumor oppressions including dyspnea, hemoptysis, dysphagia and super vena cava syndrome; 4) it leads to minimal collateral tissue damage and operation-related complications (**Table 4**); 5) The procedure can be completed promptly within 5 to 10 min for patients who developed severe dyspnea; and 6) it can restore tracheal stenosis even after ineffective bronchial stent treatment (**Supplemental Figure 5**). In addition, there are several alternative approaches can be used to control the life-threatening symptoms of these patients: 1) tracheal stent placement can be used to relieve dyspnea. However, the tumor burden is not resolved, as the tumor progresses, the airway will restenosis, and the stent can also cause expectoration difficulty by continuously stimulation of the endotracheal lining. Therefore, patient's life of quality and overall survival will not be much improved; 2) interventional vascular embolization technology can be used to control hemoptysis. Blood supply of lung tumors is usually supported by both pulmonary artery and vein. Therefore, interventional embolization is not effective as the tumor changes following treatment that will likely cause hemoptysis occurs again; 3) esophageal stent implantation is usually used to treat dysphagia. Dysphagia of these patients usually caused by mediastinal tumor compression, however, esophageal stent implantation does not treat solid tumors, but temporarily solves the eating difficult. Re-stenosis usually occurs in a short time as tumor grows, and the stent implantation will bring a lot of pain to the patients. By comparing with these approaches, the SNCP-^{125}I brachytherapy treatment solves the problem of tumor compression by shrinking solid tumors in a relatively long time; thus, the curative effect, overall survival and patient quality of life are much better improved.

It is worth to note that multiple technical details must be paid attention to for SNCP-^{125}I brachytherapy to succeed: 1) the puncture paths need to be design to avoid thick blood vessels and trachea, as otherwise blood vessel injury causes hemoptysis, and trachea injury causes cough and pneumothorax during and after the operation; 2) the distance between the puncture sites on the skin and the tumor should be as short as possible, which will greatly minimize the possibility of tissue injury and puncture deviation; 3) keep the needle and the predicted puncture paths

relatively static following the breath floating of patients to avoid puncture deviation; 4) for new operators, can insert the needle in stages and correct in real time the direction of the needle to avoid blood vessels and trachea as found appropriate. For example, for a predicted puncture channel of 10 cm, insert the needle for 3cm to 4cm first, stop and check if the puncture direction is correct, adjust needle direction as necessary and insert another 3cm to 4cm until 10cm. It is also important to note that for lung cancer patients, the lung tissue is elastic and eligible for sufficient safe angles for needle adjustment once the tip of the needs nearly reaches to the tumor; 5) the end of each needle channel is designed to be close to be parallel with a minimum distance of 1.5cm between each two adjacent needle tracks to ensure the distribution of radioactive seeds covering most of the tumor area; and 6) the aortic window is a narrow path (normally 1 cm wide) surrounded by the aortic arch and pulmonary artery which can be used as an important path to insert into the mediastinum to avoid blood vessels.

Moreover, we assessed the impact of SNCP-^{125}I brachytherapy on tumor pathological and tumor immune microenvironment, and found long-term tumor cell necrosis and fibrosis, and increase tumor CD8+T cell infiltration after the treatment. These results further provide a mechanistic rationale for further exploring combination strategies manipulating tumor-infiltrated T cells. In conclusion, SNCP-^{125}I brachytherapy is a unique, feasible and effective minimally invasive therapy for patients with incurable thoracic malignancies, especially for those who develop life-threatening symptoms due to tumor oppression and exhibit limited numbers of accessible anatomical puncture sites for the conventional multiple-needle^{125}I brachytherapy.

DATA AVAILABILITY STATEMENT

The raw data supporting the conclusions of this article will be made available by the authors, without undue reservation.

ETHICS STATEMENT

The studies involving human participants were reviewed and approved by Tianjin Beichen Hospital Ethics Committee. The patients/participants provided their written informed consent to participate in this study.

AUTHOR CONTRIBUTIONS

FL and XD designed the study. FL wrote and prepared the manuscript with assistance and feedback of XD. FL, LW, and YZ conducted statistical plan and analyzed the data. TJ and WF collected the data. XD performed the imaging, treatments, and biopsies. ZW provided reagents or performed the histological experiments. ZL determined pathological diagnosis. XD read and measured the patient CT scans. XD provided project oversight. All authors contributed to the article and approved the submitted version.

FUNDING

This work was supported by Tianjin Beichen Hospital (Grant number: Beichen District Health System Technology Project, SHGY-2020006).

SUPPLEMENTARY MATERIAL

The Supplementary Material for this article can be found online at: https://www.frontiersin.org/articles/10.3389/fonc.2021.640131/full#supplementary-material

Supplementary Figure 1 | Representative tumor pathology of patients determined by Hematoxylin and Eosin (H&E) staining. 290 of 294 patients were diagnosed as squamous cell carcinoma, and 4 as malignant thymic carcinoma. Images of other patients were not reported. All images were taken in a 40X magnification.

Supplementary Figure 2 | Pre-treatment puncture design of SNCP-^{125}I brachytherapy for 30 representative patients *via* treatment planning system (TPS). Puncture paths were designed following several criteria: 1) avoid thick blood vessels and trachea as practical as possible; 2) the distance between the puncture site on the skin and the tumor should be as short as possible, so as to decrease the risk of tissue injury and puncture deviation; 3) try to keep the end of each needle channel parallel with a minimum distance of 1.5cm between each two adjacent needle tracks to ensure that the distribution of radioactive seeds covers most of the tumor area; 4) the aortic window is a narrow path (normally 1cm wide) surrounded by the aortic arch and pulmonary artery that can be used as a path to insert into the mediastinum to avoid blood vessels. Magenta line-predicted puncture needle path, Red dots-^{125}I seeds.

Supplementary Figure 3 | Summary of life-threatening symptoms in 294 patients including the cases of one, two and three types of the symptoms.

Supplementary Figure 4 | Representative CT scans of patients with two types of life-threatening symptoms. **(A).** Patient 174 with lung squamous cell carcinoma developed both dyspnea and super vena cava syndrome. CT images showed that the right trachea (yellow arrow) and super vena cava (red arrow) were severely compressed by the tumor, and this was alleviated 3 months after SNCP-^{125}I brachytherapy. **(B).** Patient 211 with lung squamous cell carcinoma experienced both hemoptysis and dysphagia. CT scans showed that esophagus was compressed and the right lung hilum was invaded by the tumor, and this was alleviated in 3 months and until 12 months.

Supplementary Figure 5 | An example of tracheal stenosis relapse after tracheal stent implantation in a lung cancer patient. **(A).** Relapse tracheal stenosis in Patient 250 was successfully controlled by SNCP-^{125}I brachytherapy in 3 months and tracheal reconstruction lasted until 12 months (yellow arrow). Thrombosis was found in the vena cava stent (red arrow), which was not curable with collateral circulation established. **(B).** 3D reconstruction of tracheal stent (white arrow) and vena cava stent (red arrow), and tracheal stent (white arrow) was seen under bronchoscopy 12 months after treatment.

Supplementary Figure 6 | The tumor size in treated patients is significantly correlated with the number of puncture channels **(A)** and the number of 3D cones formed **(B)**. Spearman correlation test was used for the analysis.

Supplementary Figure 7 | Raw microscopy images on tumor core biopsy tissues staining with Ki67 **(A)** and CD8 **(B)** for **Figure 10**. All images were taken in a ×20 magnification.

REFERENCES

1. Couvreur K, Naert E, Jaeghere ED, Philippe T, Amin M, Pieter DV, et al. Neo-Adjuvant Treatment of Adenocarcinoma and Squamous Cell Carcinoma of the Cervix Results in Significantly Different Pathological Complete Response Rates. *BMC Cancer* (2018) 18:1101. doi: 10.1186/s12885-018-5007-0
2. Zhang C, Ma T. Poorer Prognosis of Ovarian Squamous Cell Carcinoma Than Serous Carcinoma: A Propensity Score Matching Analysis Based on the SEER Database. *J Ovarian Res* (2020) 13:75. doi: 10.1186/s13048-020-00675-y
3. Theelen WSME, Krijgsman O, Monkhorst K, Kuilman T, Peters DDGC, Cornelissen S, et al. Presence of a 34-Gene Signature is a Favorable Prognostic Marker in Squamous non-Small Cell Lung Carcinoma. *J Transl Med* (2020) 18:271. doi: 10.1186/s12967-020-02436-3
4. Derman BA, Mileham KF, Bonomi PD, Batus M, Fidler MJ. Treatment of Advanced Squamous Cell Carcinoma of the Lung: A Review. *Transl Lung Cancer Res* (2015) 4:524–32. doi: 10.3978/j.issn.2218-6751.2015.06.07
5. Pirker R, Pereira JR, Szczesna A, Pawel JV, Krzakowski M, Ramlau R, et al. Cetuximab Plus Chemotherapy in Patients with Advanced non-Small-Cell Lung Cancer (FLEX): An Open-Label Randomised Phase III Trial. *Lancet* (2009) 373:1525–31. doi: 10.1016/S0140-6736(09)60569-9
6. Garon EB, Gandhi L, Rizvi N, Hui R, Balmanoukian AS, Patnaik A, et al. Antitumor Activity of Pembrolizumab (Pembro; MK-3475) and Correlation with Programmed Death Ligand (PD-L1) Expression in a Pooled Analysis of Patients (Pts) with Advanced non-Small Cell Lung Carcinoma (NSCLC). *Ann Oncol* (2014) 25:1–41. doi: 10.1093/annonc/mdu438.51
7. Socinski MA, Bondarenko I, Karaseva NA, Makhson AM, Vynnychenko I, Okamoto I, et al. Weekly Nab-Paclitaxel in Combination With Carboplatin Versus Solvent-Based Paclitaxel Plus Carboplatin as First-Line Therapy in Patients with Advanced non-Small-Cell Lung Cancer: Final Results of a Phase III Trial. *J Clin Oncol* (2012) 30:2055–62. doi: 10.1200/JCO.2011.39.5848
8. Vergnenègre A, Hominal S, Tchalla AE, Bérard H, IMonnet I, Fraboulet G, et al. Assessment of Palliative Care for Advanced non-Small-Cell Lung Cancer in France: A Prospective Observational Multicenter Study (GFPC 0804 Study). *Lung Cancer* (2013) 82:353–7. doi: 10.1016/j.lungcan.2013.07.014
9. Duggan KT, Duffus SH, D'Agostino RBJr, Petty WJ, Streer NP, Stephenson RC. The Impact of Hospice Services in the Care of Patients with Advanced Stage Nonsmall Cell Lung Cancer. *J Palliat Med* (2017) 20:29–34. doi: 10.1089/jpm.2016.0064
10. Duggan KJ, Wiltshire J, Strutt R, Boxer MM, Berthelsen A, Descallar J, et al. Alliative Care and Psychosocial Care in Metastatic non-Small Cell Lung Cancer: Factors Affecting Utilisation of Services and Impact on Patient Survival. *Support Care Cancer* (2019) 27:911–9. doi: 10.1007/s00520-018-4379-7
11. Xiang ZW, Li GH, Liu ZY, Huang JH, Zhong ZH, Sun L, et al. 125I Brachytherapy in Locally Advanced Nonsmall Cell Lung Cancer After Progression of Concurrent Radiochemotherapy. *Med (Baltimore)* (2015) 94: e2249. doi: 10.1097/MD.0000000000002249
12. Jaradat I, Zewar A, AlNawaiseh I, AlRawashdeh K, Khurma S, Mehyar M, et al. Characteristics, Management, and Outcome of Patients With Uveal Melanoma Treated by Iodine-125 Radioactive Plaque Therapy in a Single Tertiary Cancer Center in Jordan. *Saudi J Ophthalmol* (2018) 32:130–3. doi: 10.1016/j.sjopt.2017.12.002
13. Yu YH, Wei CY, Qin QH, Mo QG, Huang Z, Lian B. Efficacy of iodine-125 Seed Implantation in Locoregionally Recurrent and Unresectable Breast Cancer: A Retrospective Study. *Pathol Oncol Res* (2019) 25:327–32. doi: 10.1007/s12253-017-0361-9
14. Wang CX, Liu SF, Peng LJ, Zhang K, Li W, Zhang H, et al. Permanent iodine-125 Brachytherapy for Patients with Progressive or Recurrent High-Grade Gliomas. *BMC Cancer* (2020) 20:591. doi: 10.1186/s12885-020-07246-w
15. Larson DA, Suplica JM, Chang SM, Lamborn KR, McDermott MW, Sneed PK, et al. Permanent Iodine 125 Brachytherapy in Patients with Progressive or Recurrent Glioblastoma Multiforme. *Neuro Oncol* (2004) 6:119–26. doi: 10.1215/S1152851703000425
16. Ruge MI, Kickingereder P, Grau S, Dorn F, Galldiks N, Treuer H, et al. Stereotactic iodine-125 Brachytherapy for the Treatment of WHO Grades II and III Gliomas Located in the Central Sulcus Region. *Neuro Oncol* (2013) 15:1721–31. doi: 10.1093/neuonc/not126
17. Li QC, Tian Y, Yang DY, Liang Y, Cheng XB, Gai BD. Permanent iodine-125 Seed Implantation for the Treatment of Nonresectable Retroperitoneal Malignant Tumors. *Technol Cancer Res Treat* (2019) 18:1533033819825845. doi: 10.1177/1533033819825845
18. Huang W, Lu J, Chen KM, Wu ZY, Wang QB, Liu JJ, et al. Preliminary Application of 3D-Printed Coplanar Template for iodine-125 Seed Implantation Therapy in Patients with Advanced Pancreatic Cancer. *World J Gastroenterol* (2018) 24:5280–7. doi: 10.3748/wjg.v24.i46.5280
19. Hu YY, Qi EP, Liu FY, Lu YH, Tan SL, Sun Y, et al. The Application of a Three-Dimensional Visualized Seed Planning and Navigation System in 125 I Seed Implantation for Pancreatic Cancer. *Onco Targets Ther* (2018) 11:619–27. doi: 10.2147/OTT.S141245
20. Zhang FJ, Wang JJ, Guo JH, Li YL, Huang XQ, Guan ZY, et al. Chinese Expert Consensus Workshop Report: Guideline for Permanent iodine-125 Seed Implantation of Primary and Metastatic Lung Tumors. *Thorac Cancer* (2019) 10:388–94. doi: 10.1111/1759-7714.12912
21. Chaudhari S, Deshpande S, Anand V, De S, Saxena S, Dash A, et al. Dosimetry and Treatment Planning of Occu-Prosta I-125 Seeds for Intraocular Lesions. *J Med Phys* (2008) 33:14–8. doi: 10.4103/0971-6203.39419
22. Zoberi JE, Garcia-Ramirez J, Hedrick S, Rodriguez V, Bertelsman CG, Mackey S, et al. MRI-Based Treatment Planning and Dose Delivery Verification for Intraocular Melanoma Brachytherapy. *Brachytherapy* (2018) 17:31–9. doi: 10.1016/j.brachy.2017.07.011
23. Chen GH, Han MY. Comparison of Pre-Implant Treatment Planning and Post-Implant Dosimetry in I-125 Spinal Metastases Brachytherapy. *Oncol Lett* (2020) 19:309–16. doi: 10.3892/ol.2019.11106
24. Huang MW, Liu SM, Zheng L, Shi Y, Zhang J, Li YS, et al. A Digital Model Individual Template and CT-guided 125I Seed Implants for Malignant Tumors of the Head and Neck. *J Radiat Res* (2012) 53:973–7. doi: 10.1093/jrr/rrs046
25. Yang YW, Shao KN, Zhang J, Chen M, Chen YY, Shan GP. Automatic Planning for Nasopharyngeal Carcinoma Based on Progressive Optimization in RayStation Treatment Planning System. *Technol Cancer Res Treat* (2020) 19:1533033820915710. doi: 10.1177/1533033820915710
26. U.S. Department of Health and Human Services NIH, National Cancer Institute. *Common Terminology Criteria for Adverse Events (Ctcae) Version 4.0* (2009). Available at: http://evs.nci.nih.gov/ftp1/CTCAE/CTCAE_4.03_2010-06-14_QuickReference_5x7.
27. Tanaka K, Akechi T, Okuyama T, Nishiwaki Y, Uchitomi Y. Development and Validation of the Cancer Dyspnoea Scale: A Multidimensional, Brief, Self-Rating Scale. *Br J Cancer* (2000) 82:800–5. doi: 10.1054/bjoc.1999.1002
28. Beckles MA, Spiro SG, Colice GL, Rudd RM. Initial Evaluation of the Patient with Lung Cancer: Symptoms, Signs, Laboratory Tests, and Paraneoplastic Syndromes. *Chest* (2003) 123:97S–104S. doi: 10.1378/chest.123.1_suppl.97S
29. Freitag L, Ernst A, Unger M, Kovitz K, Marquette CH. A Proposed Classification System of Central Airway Stenosis. *Eur Respir J* (2007) 30:7–12. doi: 10.1183/09031936.00132804
30. Corey R, Hla KM. Major and Massive Hemoptysis: Reassessment of Conservative Management. *Am J Med Sci* (1987) 294:301–9. doi: 10.1097/00000441-198711000-00003
31. Gershman E, Guthrie R, Swiatek K, Shojaee S. Management of Hemoptysis in Patients with Lung Cancer. *Ann Transl Med* (2019) 7:358. doi: 10.21037/atm.2019.04.91
32. Koga K, Matsuno Y, Noguchi M, Mukai K, Asamura H, Goya T, et al. A Review of 79 Thymomas: Modification of Staging System and Reappraisal of Conventional Division Into Invasive and non-Invasive Thymoma. *Pathol Int* (1994) 44:359–67. doi: 10.1111/j.1440-1827.1994.tb02936.x
33. Thomas CR, Wright CD, Loehrer PJ. Thymoma: State of the Art. *J Clin Oncol* (1999) 17:2280–9. doi: 10.1200/JCO.1999.17.7.2280
34. Detterbeck FC, Parsons AM. Thymic Tumors. *Ann Thorac Surg* (2004) 77:1860–9. doi: 10.1016/j.athoracsur.2003.10.001
35. Chen HY, Xu L, Li LF, Liu XX, Gao JX, Bai YR. Inhibiting the CD8 + T Cell Infiltration in the Tumor Microenvironment After Radiotherapy is an Important Mechanism of Radioresistance. *Sci Rep* (2018) 8:11934. doi: 10.1038/s41598-018-30417-6
36. Zeng H, Zhang WJ, Gong Y, Xie CH. Radiotherapy Activates Autophagy to Increase CD8 + T Cell Infiltration by Modulating Major Histocompatibility Complex Class-I Expression in non-Small Cell Lung Cancer. *J Int Med Res* (2019) 47:3818–30. doi: 10.1177/0300060519855595
37. Zhao J, Zhi Z, Zhang HT, Zhao JX, Di Y, Xu K, et al. Efficacy and Safety of CT-guided 125 I Brachytherapy in Elderly Patients with non-Small Cell Lung Cancer. *Oncol Lett* (2020) 20:183–92. doi: 10.3892/ol.2020.11550

38. Ji Z, Jiang YL, Guo FX, Peng R, Sun H, Fan JH, et al. Radiation-Related Adverse Effects of CT-guided Implantation of 125 I Seeds for Thoracic Recurrent and/or Metastatic Malignancy. *Sci Rep* (2019) 9:14803. doi: 10.1038/s41598-019-51458-5
39. Kelly P, Balter PA, Rebueno N, Sharp HJ, Liao ZX, Komaki R, et al. Stereotactic Body Radiation Therapy for Patients With Lung Cancer Previously Treated with Thoracic Radiation. *Int J Radiat Oncol Biol Phys* (2010) 78:1387–93. doi: 10.1016/j.ijrobp.2009.09.070
40. Trovo M, Minatel E, Durofil E, Polesel J, Avanzo M, Baresic T, et al. Stereotactic Body Radiation Therapy for Re-Irradiation of Persistent or Recurrent non-Small Cell Lung Cancer. *Int J Radiat Oncol Biol Phys* (2014) 88:1114–9. doi: 10.1016/j.ijrobp.2014.01.012

Conflict of Interest: The authors declare that the research was conducted in the absence of any commercial or financial relationships that could be construed as a potential conflict of interest.

Copyright © 2021 Li, Wang, Zhang, Feng, Ju, Liu, Wang and Du. This is an open-access article distributed under the terms of the Creative Commons Attribution License (CC BY). The use, distribution or reproduction in other forums is permitted, provided the original author(s) and the copyright owner(s) are credited and that the original publication in this journal is cited, in accordance with accepted academic practice. No use, distribution or reproduction is permitted which does not comply with these terms.

frontiers in Oncology

ORIGINAL RESEARCH
published: 02 June 2021
doi: 10.3389/fonc.2021.646526

Comparison of Clinical Efficacy of Alectinib *Versus* Crizotinib in *ALK*-Positive Non-Small Cell Lung Cancer: A Meta-Analysis

Hao Tang[1], *Longyu Jin*[1], *Zhang Zhang*[2], *Zhibin Jiang*[1] *and Zeeshan Malik*[1]*

[1] Department of Cardio-Thoracic Surgery, The Third Xiangya Hospital, Central South University, Changsha, China,
[2] Department of Cardio-Thoracic Surgery, Changsha Central Hospital, Changsha, China

Objective: To systematically evaluate the efficacy and safety of alectinib versus crizotinib in the treatment of anaplastic lymphoma kinase (*ALK*) positive non-small-cell lung cancer.

Methods: Studies about the efficacy of alectinib versus crizotinib in the treatment of *ALK*-positive non-small cell lung cancer were searched in PubMed, Scopus, Embase and the Cocharane Library from inception to February 15, 2020. Two reviewers independently screened these studies, extracted the data, assessed the risk of bias in the included studies by using the Cochrane risk assessment tool, and then used review manager 5.3 software for meta-analysis.

Results: Three studies comprising a total of 697 patients with *ALK*-positive non-small cell lung cancer were included, 380 in the alectinib group and 317 in the crizotinib group. The dose of alectinib (300 mg) in J-ALEX were lower than the approved dose (600 mg), however the crizotinib group in all three studies received the recommended dose (250 mg). Performance bias was high in all three studies whereas, and the attrition bias was high in two studies (Toyoaki Hida 2017 and Solange peters 2017). The results of meta-analysis showed that: the overall response rate [OR = 2.07, 95% CI (1.41, 3.06), P = 0.0002], the progression free survival [HR = 0.34, 95% CI (0.21, 0.55), P <0.0001], the partial response [OR = 1.71, 95% CI (1.19, 2.46), P = 0.003], P = 0.001], in alectinib group were higher than that of crizotinib group. Though the total number of events in complete response and the disease control rate were more in alectinib group than that of crizotinib group, the meta-analysis results shows no significant differences between two drugs in the disease control rate [OR = 2.24, 95% CI (0.56, 8.88), P = 0.25], the complete response [OR = 1.82, 95% CI (0.75, 4.45), P = 0.19]. In addition, the number of events in the stable disease [OR = 0.45, 95% CI (0.28, O.74), P = 0.001], and the adverse events [OR = 0.50, 95% CI (0.23, 0.81), P = <0.0001] in alectinib group were lower than that of crizotinib group.

Conclusion: Alectinib in terms of overall response rate, progression-free survival and partial response is superior to crizotinib in the treatment of *ALK*-positive non-small cell lung cancer and is well tolerated. Compared with crizotinib, alectinib is more effective than

OPEN ACCESS

Edited by:
Junji Uchino,
Kyoto Prefectural University of Medicine, Japan

Reviewed by:
Felice Crocetto,
Federico II University Hospital, Italy
Jun-Ling Li,
Chinese Academy of Medical Sciences and Peking Union Medical College, China

***Correspondence:**
Zeeshan Malik
dr-zeeshan10@csu.edu.cn

Specialty section:
This article was submitted to Thoracic Oncology, a section of the journal Frontiers in Oncology

Received: *27 December 2020*
Accepted: *11 May 2021*
Published: *02 June 2021*

Citation:
Tang H, Jin L, Zhang Z, Jiang Z and Malik Z (2021) Comparison of Clinical Efficacy of Alectinib Versus Crizotinib in ALK-Positive Non-Small Cell Lung Cancer: A Meta-Analysis. Front. Oncol. 11:646526. doi: 10.3389/fonc.2021.646526

crizotinib and has a lower incidence of total adverse reactions. Meta-analysis results confirm the strong base for alectinib as a first-line treatment for *ALK*-positive NSCLC.

Keywords: alectinib, crizotinib, *ALK* inhibitors, non-small cell lung cancer, efficacy and safety

INTRODUCTION

Lung cancer is the second most commonly occurring cancer worldwide accounting for 11.4% of the total new cancer cases. It was estimated that the number of new lung cancer cases in the world exceed 2.2 million in 2020, second only to breast cancer. In many countries, lung cancer is currently the leading cause of cancer deaths, and accounting for approximately 20% of all cancer death rate. Lung cancer deaths in China is comparatively high compared to most countries (1). It is foreseen that lung cancer deaths in China may increase by roughly 40% between 2015 and 2030 (2). By 2017, the incidence of lung cancer in China had risen to 800,000 cases, while the mortality had reached 700,000. This shows that China's primary bronchial lung cancer morbidity and mortality have an alarming growth rate, non-small cell lung cancer (NSCLC) is the most common form of lung cancer, accounting for approximately 85% of all lung cancer cases (3, 4). For early stage (I, II) NSCLC, surgery is the best treatment. But NSCLC is usually advanced at the time of diagnosis, and systemic treatment is its mainstay of treatment (5, 6). As it is well known that, many patients with advanced NSCLC benefit from chemotherapy to a certain level. Platinum-based chemotherapy is the standard treatment for patients with advanced NSCLC (7). However, chemotherapy and radiotherapy often has more side effects. Moreover, the 5-year survival rate of NSCLC is still below 27% (8). Hence, due to aforementioned reasons, we need more and better treatment strategies for advanced NSCLC.

In recent years, a meta-analysis result showed that crizotinib is more effective than chemotherapy in treating anaplastic lymphoma kinase (*ALK*) positive advanced NSCLC (9). Crizotinib is ALK's first small molecule inhibitor and was approved in the US in 2011 for the treatment of patients with *ALK*-positive advanced NSCLC (10). However crizotinib resistance occurs, often within 12 months of the start of treatment ultimately resulting in disease progression (11). Due to crizotinib resistance the second generation alectinib was developed and get approval by US drug and food administration (FDA) in 2015 (12). The three recently conducted studies (11–13) exhibited that the alectinib is more effective than crizotinib.

In 2007, researchers found a fusion gene of echinoderm microtubule-associated protein-like protein 4 (*EML4*) and *ALK* in NSCLC tissue specimens (14, 15). The activated *ALK* fusion protein leads to abnormal ALK signaling through several molecular signaling pathways, including PI3K/AKT/mTOR, JAK/STAT, and RAS/MEK/ERK, and finally leads to cancer. According to statistics, about 3–7% of patients with NSCLC have *ALK* gene rearrangement, and it is more common in young patients with adenocarcinoma and patients who have never or have a slight history of smoking (16).

In more than 13 years of discovery of NSCLC containing *ALK* gene mutations, scientists are devoted to the development of ALK inhibitors. Currently, five ALK inhibitors have been approved by the FDA for *ALK*-positive advanced NSCLC including crizotinib, alectinib, ceritinib, brigatinib and lorlatinib.

Alectinib once was used as second line treatment of crizotinib-resistant patients, but now it is recommended as the first-line therapy in *ALK*-positive NSCLC. Crizotinib affirmed by FDA in 2011 is still the first-line treatment standard in numerous locales of the world due to the adequacy illustrated within the randomized stage III clinical trial when compared with platinum-based chemotherapy, in terms of both by overall response rate (ORR) and progression-free survival (PFS) (17, 18). Despite of better results of crizotinib compared with platinum based chemotherapy, resistance to crizotinib finally occurs more often within 12 months of beginning of treatment (19, 20).

Next-generation, alectinib, a highly selective central nervous system (CNS)-active ALK inhibitor, was developed to confer resistance to crizotinib (21, 22). Alectinib was approved by FDA in 2015. To assess its clinical efficacy, alectinib versus crizotinib comparative ALEX trial was conducted, in which alectinib shows superiority over crizotinib in terms of ORR, PFS and toxicity profile (13, 23, 24). To further evaluate the efficacy of alectinib another comparative study J-ALEX was conducted, which continued to show superiority of alectinib over crizotinib, PFS (34.1 vs 10.2 months; HR 0.80), median OS not reached alectinib vs 43.7 months crizotinib, and toxicity profile (adverse events grade ≥3 (36.9% *vs* 60.6% crizotinib) (12, 25). Another, recently conducted comparative study of alectinib versus crizotinib (ALESIA), shows better results in favor of alectinib ORR (91% *vs* 48%), PFS (not reached *vs* 11.1 months), and grades 3–5 adverse events (29% *vs* 48%) (11).

Due to the significant efficacy shown in the phase I clinical trial, ceritinib was approved by FDA in 2014 for the treatment of patients with *ALK*-positive metastatic NSCLC that progressed or could not be tolerated after crizotinib treatment. Ceritinib showed superiority to standard of care platinum-pemetrexed chemotherapy in the phase III ASCEND-4 trial (ORR, 72.5% *vs* 26.7%; PFS, 16.6 *vs* 8.1 months). This agent also demonstrates essential intracranial and extra cranial activity. Unluckily, the toxicity profile of ceritinib can limit its clinical utility. Within the significant randomized trial, the predominance of measurements alterations or interruptions was 80% within the ceritinib arm compared with 45% within the chemotherapy arm, separately (26, 27). In ASCEND-5 trial ceritinib appears longer PFS (5.4 vs 1.6 months; HR 0·49; p <0·0001), 43% in ceritinib shows serious adverse events (AEs) while 32% in chemotherapy (28). However, in single-arm trial comparative study of alectinib versus ceritinib, median OS with alectinib was prolonged 24.3 *vs* 15.6 with

ceritinib; HR: 0.65; 95% CI: 0.48–0.88 (29). It was also confirmed by the recently published cross-study indirect comparison, which demonstrated 22% lower hazard ratio compared to ceritinib; HR: 0.78 (30).

On April 28, 2017, Brigatinib got approval by the US FDA for use in patients with *ALK*-positive metastatic NSCLC who are intolerant to crizotinib or whose disease has progressed after treatment. In recently conducted phase 3 ALTA-1L trial comparing brigatinib versus crizotinib, 275 patients were randomized; brigatinib (n = 137), crizotinib (n = 138), 26% patients in brigatinib while 27% patients in crizotinib group earlier received chemotherapy for advanced disease, 29% (brigatinib)/30% (crizotinib) had baseline brain metastases, at the data cutoff median follow-up was brigatinib/crizotinib: 11.0/9.25 months; BIRC-assessed PFS (HR 0.49, 95% CI 0.33, 0.74, p = 0.0007), brigatinib PFS (not reached *vs* 9.8 months), investigator-assessed PFS (HR 0.45 (95% CI 0.30, 0.68), p = 0.0001), most common treatment related adverse events (AEs) with brigatinib were elevated creatine phosphokinase (CPK) (16.2%), elevated lipase (13.2%), hypertension (9.6%); crizotinib: increased ALT (9.5%), AST (5.8%), and lipase (5.1%). Any grade ILD/pneumonitis: brigatinib, 3.7%; crizotinib, 2.2%. Discontinuations due to AEs (brigatinib/crizotinib): 11.8%/8.8% (31). There is another ongoing study comparing efficacy of brigatinib versus alectinib with an expected duration of five years to obtain the final results of the trial (NCT03596866).

Third generation ALK inhibitor Lorlatinib approved by US FDA in 2018. The efficacy of lorlatinib was then confirmed in a global phase II trial in patients with *ALK*- or *ROS1*-positive advanced NSCLC (32). Based on *ALK* and *ROS1* status as well as on pretreatment, patients were enrolled into six different expansion cohorts, 100 mg dose was prescribed once a day, patients (n = 276) had been listed in one of the following groups, ALK treatment naive (n = 30; EXP1), 59 who were *ALK* positive and received previous crizotinib without (n = 27; EXP2) or with (n=32; EXP3A), previously received one non-crizotinib ALK inhibitor with or without chemotherapy (n = 28, EXP3B), 112 who were *ALK* positive with two (n = 66; EXP4) or three (n = 46; EXP5) previous ALK inhibitors with or without chemotherapy, 47 who were ROS1 positive with any previous treatment (EXP6). Among *ALK*-positive patients, the OR was 90% for treatment-naive patients (EXP1) and 47% for those with at least one previous ALK TKI (n = 198; EXP2-5), Intracranial responses were seen in 2/3 (67%) treatment-naïve patients and 51/81 (63%) patients pretreated with at least one ALK TKI, in patients with only crizotinib pretreatment (EXP2-3A) responses were 69.5% (41/51), 9/28 (32.1%) patients with one previous non-crizotinib ALK TKI (EXP3B), and 43/111 (38.7%) patients with two or more previous ALK TKIs (EXP4-5). Intracranial responses were seen in 20/23 (87%) patients in EXP2-3A; 5/9 (55.6%) patients in EXP3B; and 26/49 (53.1%) patients in EXP4-5. Treatment-related adverse events were hypercholesterolemia (81% of patients; 15% grades 3–4), hypertriglyceridemia (60%; 16% grades 3–4), edema (43%; 2% grades 3–4) and peripheral neuropathy (30%; 2% grades 3–4). Weight gain was common with 10–20% increase in 31% of patients. Serious treatment-related adverse events were seen in 7% of patients. Lorlatinib is currently also compared with crizotinib in previously untreated patients within a randomized trial (NCT03052608) (33). Due to its late approval, there are no clinical studies comparing alectinib and other ALK TKIs.

Alectinib is first-line ALK TKI due to its PFS advantage, brain metastasis cumulative incidence reduction and favorable toxicity profile, for *ALK*-positive stage III or IV NSCLC, the current NCCN guidelines preferred the alectinib as first-line drug therapy (34). At present, there is no meta-analysis of the efficacy comparison between Alectinib and Crizotinib, we combined three studies to evaluate the systemic efficacy and safety of Alectinib versus Crizotinib to provide the further reliable basis for Alectinib as the most recommended first-line medication for *ALK*-positive stage III or IV NSCLC.

MATERIALS AND METHODS

Inclusion Criteria

Type of Study

Randomized controlled trial (RCT), Clinical Controlled Trial (CCT), retrospective analysis.

Research Objective

ALK-positive patients with advanced (stage IIIB or stage IV) NSCLC. ECOG or WHO score is 0–2 points.

Intervention

The experimental group was treated with Alectinib. The control group was treated with Crizotinib.

Outcome Indicators

Overall response rate (ORR), progression-free survival (PFS), disease control rate (DCR), complete response (CR), partial response (PR), stable disease (SD), adverse events (AEs).

Exclusion Criteria

① One-arm study, ② Meeting report, ③ News, ④ Republished research, ⑤ studies not reporting outcome of our interest. ⑥ Studies where data is difficult to extract.

Literature Retrieval Strategy

Computer search of four databases: PubMed, Scopus, Embase and the Cocharane Library. We search for relevant clinical studies on the efficacy of Alectinib compared with Crizotinib in treating *ALK*-positive advanced NSCLC. The last search was performed on February 15, 2020. The aforementioned online data basses were systematically searched with one or combination of the following terms: "Lung Neoplasms", "Carcinoma, Non-Small-Cell Lung", "*ALK*-positive", "Alectinib", and "Crizotinib." Mesh terms and free terms were used for each search and there were no restrictions based on language. The search strategies and results were recorded and uploaded as **Supplementary Material**. In addition, the reference

lists of included studies were also manually searched to hunt potentially eligible articles.

Literature Screening and Data Extraction

The two researchers independently screened the literature, extracted the materials needed for this study, and exchanged the results with each other. If the opinions of the two were not consistent, they asked for the intervention of a third party. According to the third party's opinion, the three parties discuss together to solve the problem, and try to supplement the lack of information through other methods, such as contacting the author directly to obtain it. During literature screening, duplicate documents were deleted first, and then the titles and abstracts were quickly assessed. After excluding documents that were not significantly related to the study, the full-text of the remaining documents were thoroughly assessed, and finally it was determined whether to include in the study.

The contents of the data extraction mainly include: ① the basic characteristics of the included research, including the article title, the time of publication, and the first author; ② the basic characteristics of the research object, such as the number of samples in each group, whether they smoke, and ethnicity; ③ specific intervention measures, such as which ALK inhibitor to use and its usage and dosage, etc. ④ Specific elements of bias risk assessment; ⑤ outcome indicators.

Literature Quality Evaluation

Two researchers used the Cochrane risk bias assessment tool to independently generate random distributions of the literature, allocate concealment, blind to researchers and subjects, blind to outcome indicators, completeness of outcome data, selective reporting studies. The results and other sources of bias are evaluated for the risk of bias. If the opinion of the two parties was not consistent, a third party's opinion was sought and discussed and resolved.

Statistical Analysis

Meta-analysis was performed using RevMan 5.3 software. The two categorical variables use odd ratio as the effect indicator, and the time survival variable uses HR as the effect indicator. Each effect amount gives its point estimate and 95% CI. Heterogeneity among the included studies was judged by P and I^2 values. If there is no significant statistical heterogeneity between the results of each study ($I^2 \leq 50\%$, $P \geq 0.1$), a meta-analysis is performed using a fixed-effects model; if statistical heterogeneity exists between the results of each study ($I^2 > 50\%$, $P < 0.1$), then further analyze the source of heterogeneity, after excluding the effects of obvious clinical heterogeneity, use a random effects model for meta-analysis, the test level of the meta-analysis was set to $p = 0.05$.

RESULTS

Study Selection

After layer-by-layer screening according to the inclusion and exclusion criteria mentioned in **Table 1**, a total of 834 articles were retrieved from four databases: PubMed, Scopus, Embase and the Cocharane Library. Three articles (11–13) were finally included. The three articles were all in English. A total of 697 patients with *ALK*-positive advanced NSCLC were included, 380 in the Alectinib group and 317 in the Crizotinib group. The literature screening process and results are shown in **Figure 1**.

Basic Characteristics of Included Studies and Evaluation of Literature Quality

The basic characteristics of the included studies are shown in **Tables 2** and **3**. The bias risk assessment tables included in the study are shown in **Tables 4** and **5**. The bias risk map for the included studies is shown in **Figure 2**. A summary of the risks of bias included in the study is shown in **Figure 3**.

TABLE 1 | Study Eligibility Criteria.

Level 1 Screening Questions (Title and Abstract)

● Covidence screening based on exclusion criteria

1) Exclude if any study does not look at ALK-positive NSCLC.

2) Exclude if the comparison of alectinib versus crizotinib includes other ALK inhibitors or other treatment options such as compare with chemotherapy, radiotherapy, immunotherapy, etc. in ALK-positive NSCLC patients.

3) Exclude if any study is not assessing the effectiveness of comparison of Alectinib versus Crizotinib in terms of Progression-free survival (PFS), Overall response rate (ORR), Complete response (CR), Disease control rate (DCR), Partial response (PR). Stable disease (SD), Adverse events (AEs).

4) Exclude if the study is not a primary study.

5) Exclude if the study is not in English.

6) Exclude if the study is not a comparative study.

Level 2 Screening Questions (Full Text)

● Covidence screening based on exclusion criteria.

1) Exclude the study if it consists of the following combined drug therapy:

a. Alectinib versus Crizotinib combined with other ALK inhibitors.
b. Alectinib versus Crizotinib combined with chemotherapy.
c. Alectinib versus Crizotinib combined with Immunotherapy.
d. Alectinib versus Crizotinib combined with radiotherapy.

2) Exclude if the study does not compare Alectinib versus Crizotinib in ALK-positive NSCLC.

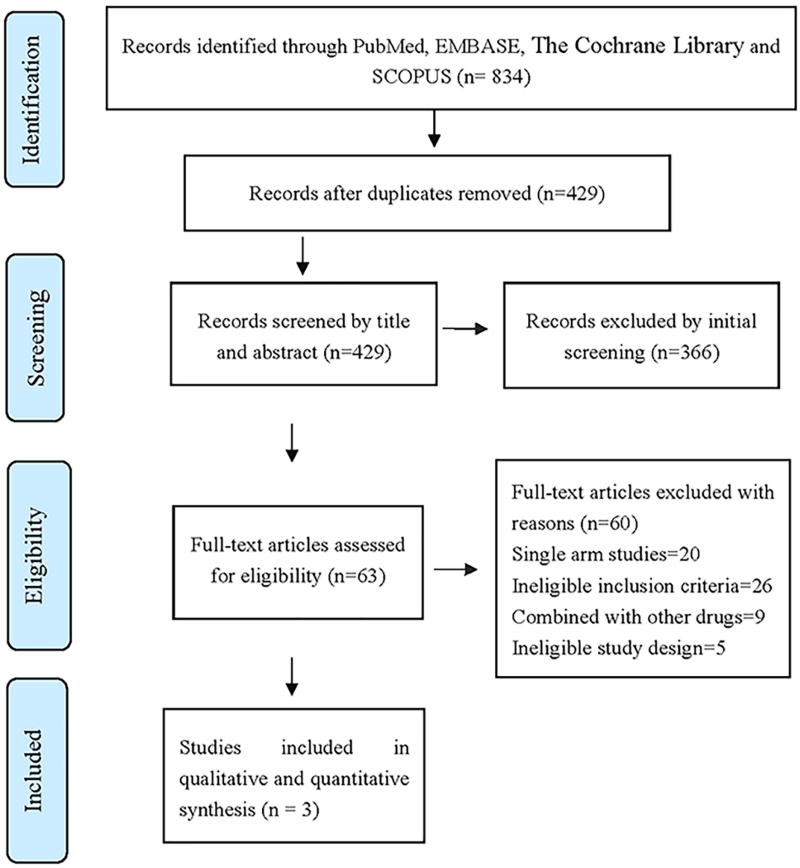

FIGURE 1 | The database retrieved by 834 articles and the number of documents detected are as follows: PubMed (n = 158), Embase (n = 360), Scopus (n = 270), The Cochrane Library (n = 46).

TABLE 2 | Basic characteristics of included studies.

Type of Studies (RCT)	Number of samples		Age (Years)		Sex	
	Experimental Group	Control Group	Experimental Group	Control Group	Male	Female
Toyoaki Hida 2017 (12)	103	104	60 (median)	59.5 (median)	82	125
Solange Peters 2017 (13)	152	151	58 (median)	54 (median)	132	171
Caicun Zhou 2019 (11)	125	62	51 (median)	49 (median)	98	89

TABLE 3 | Basic characteristics of included studies.

Included Studies	Patients had received systemic treatment before enrollment?	Intervention measures Experimental group	Control group
Toyoaki Hida 2017 (12)	Uncertain	Alectinib 300 mg, Bid	Crizotinib 250 mg, Bid
Solange Peters 2017 (13)	NO	Alectinib 600 mg, Bid	Crizotinib 250 mg, Bid
Caicun Zhou 2019 (11)	NO	Alectinib 600 mg, Bid	Crizotinib 250 mg, Bid

TABLE 4 | Risk of bias in included studies.

Included Studies	Random sequence Generation	Allocation Concealment	Blinding of participants and personal
Toyoaki Hida 2017 (12)	Low Risk	Low Risk	High Risk
Solange Peters 2017 (13)	Low Risk	Low Risk	High Risk
Caicun Zhou 2019 (11)	Low Risk	Low Risk	High Risk

TABLE 5 | Risk of bias in included studies.

Included Study	Blinding of outcome Assessment	Incomplete outcome Data	Selective Reporting	Other Bias
Toyoaki Hida 2017 (12)	Low Risk	High Risk	Low Risk	Low Risk
Solange Peters 2017 (13)	Low Risk	High Risk	Low Risk	Low Risk
Caicun Zhou 2019 (11)	Low Risk	Low Risk	Low Risk	Low Risk

Meta-Analysis Results

Overall Response Rate (ORR)

Three studies reported total response rates, There were 380 patients in alectinib and 317 patients in the crizotinib, The study indicates very low statistical heterogeneity (P = 0.38, I^2 = 0%), Due to low heterogeneity among the studies, the fixed effect model was used for Meta-analysis. Meta-analysis results shown in **Figure 4** suggest that Overall response rate of the alectinib was higher than that of crizotinib, and the difference was statistically significant. [0R = 2.07, 95%CI (1.41, 3.06), P = 0.0002].

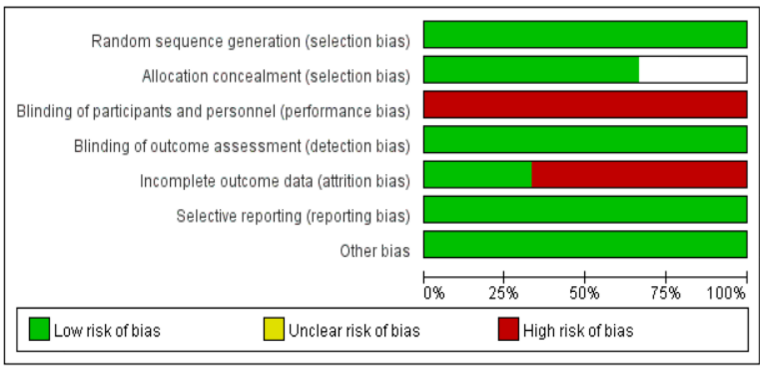

FIGURE 2 | Risk of bias assessment tool for included studies.

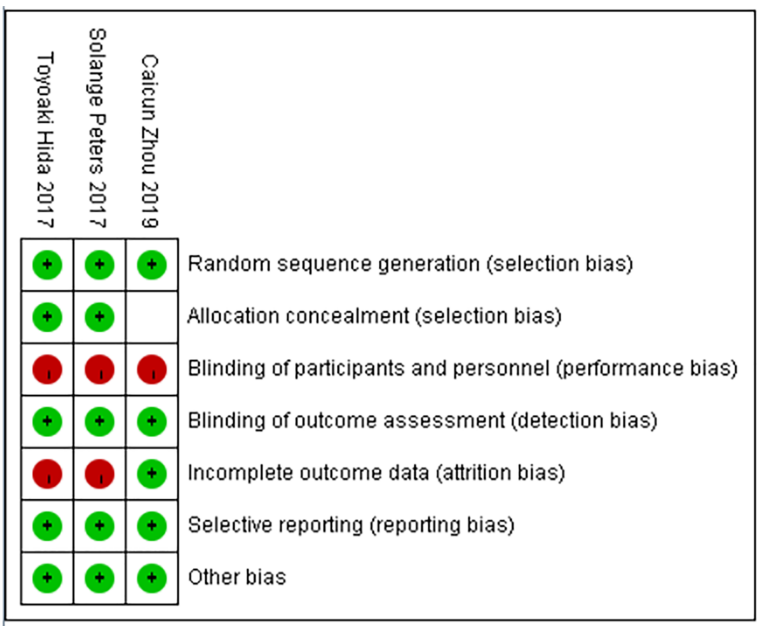

FIGURE 3 | Summary of risk of bias in included studies.

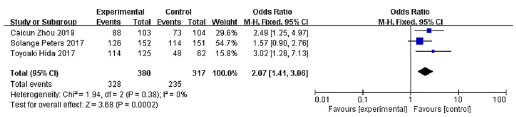

FIGURE 4 | Meta-analysis of alectinib group and crizotinib group overall response rate.

Progression-Free Survival (PFS)

Three studies all reported progression-free survival, There were 380 patients in the alectinib and 317 patients in the crizotinib, with moderate statistical heterogeneity between the studies (P = 0.06, I^2 = 64%), but there was an obvious clinical heterogeneity, and a random effect model was used for meta-analysis. Meta-analysis results shown in **Figure 5** suggest that the progression-free survival of the alectinib was higher than that of crizotinib, and the difference was statistically significant [HR = 0.34, 95%CI (0.21, 0.55), P <0.0001].

Disease Control Rate (DCR)

Three studies reported disease control rates. There were 380 patients in the alectinib group and 317 patients in the crizotinib group. There was slight statistical heterogeneity between the studies (P = 0.02, I^2 = 76%), but there was no obvious clinical heterogeneity, and a random effect model was used for meta-meta-analysis. Meta-analysis results shown in **Figure 6** suggest that the difference was not statistically significant, indicating no difference in DCR between the two drugs [OR = 2.24, 95% CI (0.56, 8.88), P = 0.25].

Complete Response (CR)

Three studies reported complete response rates, 380 patients in the alectinib group and 317 in the crizotinib group, with no significant statistical heterogeneity between the studies (P = 0.42, I^2 = 0%), Meta-analysis was performed using a fixed effects model. Meta-analysis results shown in **Figure 7** suggest that the difference was not statistically significant, indicating no difference in CR between the two drugs [OR = 1.82, 95% CI (0.75, 4.45), P = 0.19].

Partial Response (PR)

Three studies reported partial response rates, 380 patients in the alectinib group and 317 patients in the crizotinib group, with slight statistical heterogeneity between the studies (P = 0.33, I^2 = 10%), but no obvious clinical heterogeneity, a fixed effect model was used for meta-analysis. Meta-analysis results shown in **Figure 8** suggest that the partial response rate of alectinib group was higher than that of crizotinib group, and the difference was statistically significant [OR = 1.71, 95% CI (1.19, 2.46), P = 0.003].

Stable Disease (SD)

Three studies reported disease stability rates, 380 patients in the alectinib group and 317 in the crizotinib group, with slight statistical heterogeneity between the studies (P = 0.49, I^2 = 0%), but no obvious clinical heterogeneity, a fixed effect model was used for meta-analysis. Meta-analysis results shown in **Figure 9** suggest that the disease stability rate of the alectinib group was lower than that of the crizotinib group, and the difference was statistically significant [OR = 0.45, 95% CI (0.28, O.74), P = 0.001].

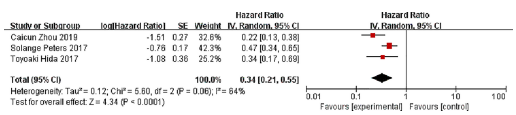

FIGURE 5 | Meta-analysis of alectinib group and crizotinib group progression-free survival.

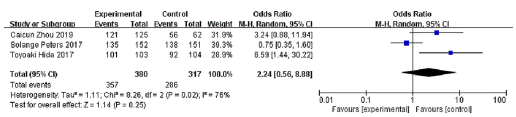

FIGURE 6 | Meta-analysis of disease control rate between the alectinib group the crizotinib group.

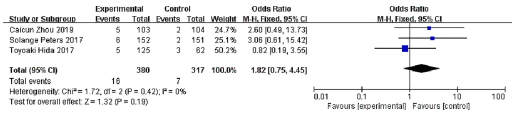

FIGURE 7 | Meta-analysis of complete response rate between alectinib group and crizotinib group.

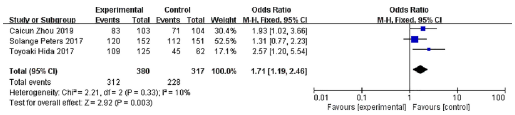

FIGURE 8 | Meta-analysis of partial response rate between alectinib group and crizotinib group.

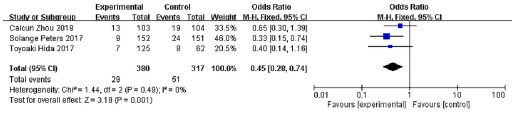

FIGURE 9 | Meta-analysis of disease stability rate between the alectinib group and crizotinib group.

Adverse Events (AEs)

Three studies have reported common adverse reactions in alectinib and Crizotinib, we focuses on the Grades 3 to 5 adverse events and we done a meta-analysis on grades 3 to 5 adverse events on alectinib and crizotinib, there were 380 patients in the alectinib group and 126 patients showed grades 3 to 5 adverse events while in Crizotinib group there were 317 patients and 160 patients showed grades 3 to 5 adverse events, with slight statistical heterogeneity between the studies (P = 0.12, I^2 = 53%), but no obvious clinical heterogeneity the fixed effect model was used. Meta-analysis results shown in **Figure 10** suggest that the adverse events of alectinib group were lower than that of Crizotinib group, and the difference was statistically significant [OR = 0.50, 95% CI (0.23, 0.81), P = <0.0001].

DISCUSSION

Normally ALK inhibitors binds to the proteins pair of *EML4-ALK* fusion gene, ultimately break the signaling pathways (MAPK/STAT3/P13K/AKT) binds to fusion protein, resulting in decreased cellular proliferation. ALK inhibitors emerged as a key targeted gene therapy for the *ALK*-positive advance NSCLC in recent years. Crizotinib was the first ALK inhibitor approved for the treatment of *ALK*-positive NSCLC. In the foremost study on the clinical activity and safety of crizotinib soon after its development. In phase 1 study (35), 149 patients were enrolled, for the response-evaluable population 143 of whom were included; OR were seen in 87 (60.8%), including three complete responses and 84 partial responses. First documented objective response median time was 7.9 weeks (range 2.1–39.6) and median duration response was 49.1 weeks (95% CI 39.3–75.4); median PFS was 9.7 months (95% CI 7.7–12.8); estimated overall survival at 6 and 12 months was 87.9% (95% CI 81.3–92.3) and 74.8% (66.4–81.5). Overall 144 (97%) faced treatment-related adverse events, more of them were grade 1 or 2, most common AEs were visual effects, nausea, diarrhea, constipation, vomiting, and peripheral edema. Grade 3 or 4 AEs were neutropenia (n = 9), lymphopenia (n = 6), hypophosphatemia (n = 6), raised alanine aminotransferase (n = 6), results interpreted that Crizotinib is well tolerated with durable, rapid responses in patients with *ALK*-positive NSCLC.

PROFILE 1007, was conducted to evaluate crizotinib efficacy and safety in comparison with chemotherapy, 347 patients were included who had gotten one earlier platinum-based regimen. The primary end point was progression-free survival (PFS), results demonstrated that, median PFS in crizotinib was 7.7 *vs* 3.0 months in chemotherapy, HR 0.49; P <0.001, The response rate with crizotinib were 65% vs 20% with chemotherapy. Visual disorder, gastrointestinal side effects, and elevated liver aminotransferase levels were common adverse events related with crizotinib, while fatigue, alopecia, and dyspnea were common AEs with chemotherapy (36). The updated (PROFILE 1014) study which included 343 patients who had no any prior systemic treatment, primary end point was progression-free survival, PFS with crizotinib was 10.9 vs 7.0 months; HR 0.45; P <0.001; ORR 74% *vs* 45%; P <0.001. One-year survival probability was 84% *vs* 79%. Most common AEs, diarrhea, vision disorders, nausea, and edema were seen in patients receiving crizotinib, while adverse events associated with chemotherapy were nausea, vomiting, fatigue and decreased appetite (17). Though, patients getting crizotinib, regularly experience disease progression often within 12 months of starting treatment, partly due to secondary resistance mutations happening, additionally, due to poor blood–brain-barrier penetration of crizotinib (19, 20). Progression to the CNS is a common problem in patients with *ALK*-positive NSCLC treated with crizotinib. Thus, alternate ALK inhibitors, which have a dual function of high CNS efficacy and a wider range of overall survival against secondary *ALK* mutations were required.

Next generation, Alectinib is a highly selective oral ALK inhibitor, to evaluate its activity and safety, AF-001JP study, recruited ALK inhibitors naive patients, stage IIIB/IV, phase I part of the study approved dose of 300 mg twice per day in Japan. 46 patients in phase II part of the study received recommended dose, 43 achieved objective response (OR) 93.5% (95% CI, 82 to 99) of whom; two CRs (4·3%) and 41 PRs (89.1%). Grade 3 AEs were recorded as 26% and serious AEs were 11% (37). To further assess alectinib safety profile over a long administration period, 3 year follow-up (AF-001JP) study demonstrated that 18 of 46 patients had disease progression (39%); 3-year PFS 62%; (95% CI, 45 to 75); 3-year OS rate was 78% (13 events). At baseline 14 patients had brain metastasis, six patients in this study remained without CNS and systemic progression. Common treatment-related AE (all grades) was increased blood bilirubin (36.2%) (38). To assess its efficacy and safety in patients who have failed to prior crizotinib treatment, global phase 2 study (NP28673) included 138 patients from 16 countries, median age was 52 years, 80% had earlier chemotherapy, and at baseline 60% had CNS metastasis, median follow-up was 30 weeks, IRC assessed response in 122 with measurable disease at baseline exhibited OR of 49.2% (95% CI 40.0–58.4; all PRs); DCR 79.5%. In 96 patients with prior crizotinib or chemo; OR was 43.8%; DCR 78.1%. For 34 patients with measurable CNS disease at baseline, OR was 55.9% (including five CRs). Grades 3–5 AEs were observed in 27.5% (commonly, pulmonary embolism and dyspnea), dose interruptions 19.6%, reductions 8.7%, and withdrawals 8.0% (39). Another part of phase II (NP28761) study in US./Canadian population included 87 patients, median age was 54 y; 74% of the patients had prior chemotherapy; baseline CNS metastasis 55%; median follow-up 21 weeks. IRC-assessed response (69 with measurable disease at baseline) exhibited OR of 47.8% (95% CI 35.6–60.2); DCR 79.7%.

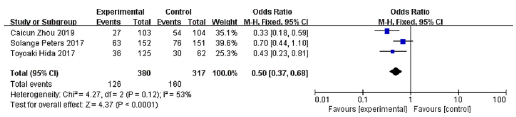

FIGURE 10 | Meta-analysis of grades 3 to 5 adverse events between the alectinib group and crizotinib group.

In 16 patients with baseline CNS disease; OR was 68.8% (95% CI 41.3–89.0) including two CRs; DCR 100%. In 48 patients (with or without baseline CNS disease); DCR was 87.5% including nine CRs. Grades 3–5 AEs were observed in 31% (commonly; increased blood CPK, increased ALT, and increased AST). One patient had grade 5 hemorrhage. Dose interruptions were seen in (29%), reductions (14%), and withdrawals (2%) (40). Pooled overall survival and safety data from the pivotal phase II studies (NP28673 and NP28761). Pooled data of 225 patients exhibited that, 53.3% patients died at the final data cut-off time, 39.1% were alive and 7.6% withdrawn. Alectinib exhibit median overall survival (OS) 29.1 months (95% CI: 21.3–39.0) in the pooled analysis (NP28673 29.2 months [95% CI: 21.5–44.4]; NP28761 27.9 months [95% CI: 17.2–NE]). Mean dose intensity was 94.2%. Grade ≥3 adverse events occurred in 44.0%, common AEs included constipation (39.1%), fatigue (35.1%), peripheral edema (28.4%), myalgia (26.2%) and nausea (24.0%). Despite the longer treatment duration (median 48.6 weeks) alectinib demonstrated a tolerable safety profile consistent with previous studies. Dose reductions were seen in 14.7%, dose interruptions 37.3%, withdrawal 6.2% (41).

Depending upon the long term survival and safety in phase II trial and to evaluate its efficacy and safety in comparison with crizotinib on previously untreated patients, the first head-to-head comparative study on alectinib and crizotinib was conducted. In J-ALEX (phase 3) trial in Japanese patients, 207 patients were enrolled, alectinib (n = 103) and crizotinib (n = 104). Grade 3 or 4 AEs were lower with alectinib 26% *vs* 52% with crizotinib; Dose interruptions were also lower with alectinib 29% *vs* 74%; withdrawal with alectinib 9% *vs* 20% with crizotinib (12). In final PFS results of J-ALEX, median follow-up with alectinib was 42.4 *vs* 42.2 months with crizotinib, IRF-assessed PFS with alectinib shows HR 0.37, 95% CI: 0.26–0.52; median PFS 34.1 *vs* 10.2 months with crizotinib. Second interim OS analysis could not be concluded HR 0.80; P = 0.3860; median OS not estimable with alectinib *vs* 43.7 months crizotinib. Grade ≥3 AEs with alectinib were lower than crizotinib (36.9% *vs* 60.6%). OS follow-up continues (25). Another combined study for J-ALEX trial in western people included 303 patients (alectinib 152 *vs* 151 in crizotinib). During a median follow-up of (18.6 alectinib *vs* 17.6 months crizotinib) an event of disease progression or death ratio with alectinib were 41% versus 68% crizotinib. Investigator-assessed PFS (12 months events free) with alectinib 68.4% (95% CI 61.0 to 75.9) versus 48.7% (95% CI 40.4 to 56.9) in crizotinib; HR 0.47; P <0.001; median PFS not reached. Events of CNS progression with alectinib 12% *vs* 45% with crizotinib; HR 0.16; P <0.001. Overall response rate (ORR) with alectinib 82.9% (95% CI 76.0 to 88.5) *vs* 75.5 (95% CI 67.8 to 82.1) with crizotinib. Grades 3 to 5 AEs with alectinib were 41% *vs* 50% with crizotinib (13). In ALESIA (phase 3) study in Asian patients 187 patients were randomly enrolled (alectinib 125 *vs* 62 in crizotinib). Median follow-up with alectinib was 16.2 and 15.0 months in crizotinib. Investigator-assessed PFS in alectinib was significantly prolonged HR 0.22; P <0.0001; median PFS not estimable *vs* 11.1. IRC-PFS with alectinib was also prolonged HR 0.37; P <0.0001. OR with alectinib was 91% *vs* 48% with crizotinib, with a longer duration of response with alectinib versus crizotinib HR 0.22; P <0.0001. Objective response (OR) in baseline measurable or non-measurable CNS lesions were improved with alectinib 73% *vs* 22% with crizotinib. Grades 3 to 5 AEs with alectinib were lower despite of longer duration than crizotinib (29% *vs* 48%); serious AEs with alectinib were 15% *vs* 26% with crizotinib (11).

All the comparative studies showed significant results in favor of alectinib in terms of its efficacy and safety. Some experimental researches may also support the conclusion. Alectinib, as a highly selective ALK inhibitor, was specifically designed to overcome crizotinib resistance. In pre-clinical models, Alectinib overcome several gate-keeper mutations that impart resistance to Crizotinib like *ALK* L1196M mutation (42). The G1202R substitution that confers resistance to Alectinib is found in only approximately 2% of crizotinib-resistant patients (22). Unlike crizotinib, as evidence shown in *in vitro* studies, Alectinib is not a substrate of P-Glycoprotein (P-gp), which can promote the efflux of the blood–brain barrier (43). This could explain its higher ratio in cerebrospinal fluid (CSF) and significantly prolonged CNS PFS in clinical trials. This meta-analysis included three studies which are published in top international journals. The meta-analysis results showed that, Alectinib's ORR, PFS, and PR are superior to crizotinib, and the side effects of Grades 3–5 are lower than crizotinib. Meta-analysis results provided an important basis for alectinib as the first-line drug for *ALK*-positive advanced NSCLC. For further enhancement in terms of overall survival and long term benefits whether the combination of alectinib and chemotherapy or the combination of alectinib and PD-L1 inhibitor can further improve the survival of patients.

In this meta-analysis only three studies are included but to confirm and analyze the sources of heterogeneity more clinical studies are needed. The advantages of this study are; first, the quality of the included literature is high and the results are highly reliable, secondly this is the first meta-analysis on the clinical efficacy and safety of alectinib versus crizotinib, which included the articles of high quality and are published in top ranked international journals. In this study, three articles are included (11–13), all international RCT studies; one article was published in the *Lancet Oncology* (12), one in *The New England Journal of Medicine* (13) and one in *Lancet Respiratory Medicine Journal* (11). In addition, this meta-analysis has certain limitations; ① There are few randomized controlled trials, comparing the efficacy and safety of alectinib versus crizotinib. ② Due to the high quality literature required for meta-analysis, there is lack of high quality published literature. To further elucidate the efficacy and safety of alectinib versus crizotinib, more randomized control trials on comparative studies of these two drugs are required.

CONCLUSION

(1) For *ALK*-positive advanced NSCLC, alectinib is more effective than crizotinib.

(2) Compared with crizotinib, alectinib has a lower incidence of total adverse reactions.

DATA AVAILABILITY STATEMENT

The original contributions presented in the study are included in the article/**Supplementary Material**. Further inquiries can be directed to the corresponding author.

AUTHOR CONTRIBUTIONS

Study designing: ZM, HT, and LJ. Data search: ZM and HT. Data extraction: ZM and LJ. Data analysis and interpretation: ZM and ZZ. Manuscript drafting: HT and ZM. Manuscript critical intellectual content revision: ZM and ZJ. All authors contributed to the article and approved the submitted version.

FUNDING

This work was supported by Hunan Province Science and Health Union Foundation (Nos. 2018JJ6135, 2018JJ6053).

ACKNOWLEDGMENTS

Authors are thankful to Xiangya School of Medicine, Central South University, and Xiangya Third Hospital for providing world-class facilities for this study. We are also thankful to Dr. Feng Wei, Dr. Saeed Ali Nagri, Dr. Shahnila Javed, and Dr. Muhammad Jahangir for language grammar and valuable comments.

SUPPLEMENTARY MATERIAL

The Supplementary Material for this article can be found online at: https://www.frontiersin.org/articles/10.3389/fonc.2021.646526/full#supplementary-material

REFERENCES

1. Ferlay J, Ervik M, Lam F, Colombet M, Mery L, Piñeros M, et al. Global Cancer Observatory: Cancer Today.(2018). Available at: https://gco.iarc.fr/today/online-analysis-table (Accessed June 20, 2020).
2. Martín-Sánchez JC, Lunet N, González-Marrón A, Lidón-Moyano C, Matilla-Santander N, Clèries R, et al. Projections in Breast and Lung Cancer Mortality Among Women: A Bayesian Analysis of 52 Countries Worldwide. *Cancer Res* (2018) 78(15):4436–42. doi: 10.1158/0008-5472.Can-18-0187
3. Lynch TJ, Bell DW, Sordella R, Gurubhagavatula S, Okimoto RA, Brannigan BW, et al. Activating Mutations in the Epidermal Growth Factor Receptor Underlying Responsiveness of Non-Small-Cell Lung Cancer to Gefitinib. *N Engl J Med* (2004) 350(21):2129–39. doi: 10.1056/NEJMoa040938
4. Katayama R, Lovly CM, Shaw AT. Therapeutic Targeting of Anaplastic Lymphoma Kinase in Lung Cancer: A Paradigm for Precision Cancer Medicine. *Clin Cancer Res* (2015) 21:2227–35. doi: 10.1158/1078-0432.CCR-14-2791
5. Horn L, Pao W. Eml4-Alk: Honing in on a New Target in Non-Small-Cell Lung Cancer. *J Clin Oncol* (2009) 27(26):4232–5. doi: 10.1200/JCO.2009.23.6661
6. Shaw AT, Yeap BY, Mino-Kenudson M, Digumarthy SR, Costa DB, Heist RS, et al. Clinical Features and Outcome of Patients With Non-Small-Cell Lung Cancer Who Harbor EML4-ALK. *J Clin Oncol* (2009) 27(26):4247–53. doi: 10.1200/JCO.2009.22.6993
7. Rodig SJ, Mino-Kenudson M, Dacic S, Yeap BY, Shaw A, Barletta JA, et al. Unique Clinicopathologic Features Characterize Alk-Rearranged Lung Adenocarcinoma in the Western Population. *Clin Cancer Res* (2009) 15:5216–23. doi: 10.1158/1078-0432.CCR-09-0802
8. Howlader N, Noone AM, Krapcho M, Miller D, Brest A, Yu M, et al. SEER Cancer Statistics Review, 1975-2017. (2021). Available at: https://seer.cancer.gov/archive/csr/1975_2017/results_merged/sect_15_lung_bronchus.pdf.
9. Sun J-M, Lira M, Pandya K, Choi Y-L, Ahn JS, Mao M, et al. Clinical Characteristics Associated With ALK Rearrangements in Never-Smokers With Pulmonary Adenocarcinoma. *Lung Cancer* (2014) 83:259–64. doi: 10.1016/j.lungcan.2013.11.009
10. Ventana ALK. (D5f3) CDx Assay Labeling Information. (2016). Available at: https://www.accessdata.fda.gov/cdrh_docs/pdf14/P140025c.pdf.
11. Zhou C, Kim SW, Reungwetwattana T, Zhou J, Zhang Y, He J, et al. Alectinib Versus Crizotinib in Untreated Asian Patients With Anaplastic Lymphoma Kinase-Positive Non-Small-Cell Lung Cancer (ALESIA): A Randomised Phase 3 Study. *Lancet Respir Med* (2019) 7(5):437–46. doi: 10.1016/S2213-2600(19)30053-0
12. Hida T, Nokihara H, Kondo M, Kim YH, Azuma K, Seto T, et al. Alectinib Versus Crizotinib in Patients With ALK-Positive Non-Small-Cell Lung Cancer (J-ALEX): An Open-Label, Randomised Phase 3 Trial. *Lancet* (2017) 390:29–39. doi: 10.1016/S0140-6736(17)30565-2
13. Peters S, Camidge DR, Shaw AT, Gadgeel S, Ahn JS, Kim DW, et al. Alectinib Versus Crizotinib in Untreated ALK-Positive Non–Small-Cell Lung Cancer. *New Engl J Med* (2017) 377:829–38. doi: 10.1056/NEJMoa1704795
14. Peled N, Palmer G, Hirsch FR, Wynes MW, Ilouze M, Varella-Garcia M, et al. Next-Generation Sequencing Identifies and Immunohistochemistry Confirms a Novel Crizotinib-Sensitive ALK Rearrangement in a Patient With Metastatic Non-Small-Cell Lung Cancer. *J Thoracic Oncol* (2012) 7(9):e14–6. doi: 10.1097/JTO.0b013e3182614ab5
15. Arcila ME, Yu HA, Drilon AE, Riely GJ, Zehir A, Sadowska J, et al. Comprehensive Assessment of Targetable Alterations in Lung Adenocarcinoma Samples With Limited Material Using MSK-IMPACT, a Clinical, Hybrid Capture-Based, Next-Generation Sequencing (NGS) Assay. *J Clin Oncol* (2015) 33:e22160–e. doi: 10.1200/jco.2015.33.15_suppl.e22160
16. Vysis ALK Break Apart Fish Probe Kit Labeling Information. Available at: https://www.accessdata.fda.gov/cdrh_docs/pdf11/P110012c.pdf.
17. Solomon BJ, Mok T, Kim DW, Wu YL, Nakagawa K, Mekhail T, et al. First-Line Crizotinib Versus Chemotherapy in ALK-Positive Lung Cancer. *N Engl J Med* (2014) 371(23):2167–77. doi: 10.1056/NEJMoa1408440
18. Solomon BJ, Kim DW, Wu YL, Nakagawa K, Mekhail T, Felip E, et al. Final Overall Survival Analysis From a Study Comparing First-Line Crizotinib Versus Chemotherapy in Alk-Mutation-Positive Non–Small-Cell Lung Cancer. *J Clin Oncol* (2018) 36:2251–8. doi: 10.1200/JCO.2017.77.4794
19. Katayama R, Shaw AT, Khan TM, Mino-Kenudson M, Solomon BJ, Halmos B, et al. Mechanisms of Acquired Crizotinib Resistance in ALK-Rearranged Lung Cancers. *Sci Trans Med* (2012) 4:120ra17–ra17. doi: 10.1126/scitranslmed.3003316
20. Doebele RC, Pilling AB, Aisner DL, Kutateladze TG, Le AT, Weickhardt AJ, et al. Mechanisms of Resistance to Crizotinib in Patients With ALK Gene Rearranged Non–Small Cell Lung Cancer. *Clin Cancer Res* (2012) 18:1472–82. doi: 10.1158/1078-0432.CCR-11-2906
21. Kodama T, Tsukaguchi T, Yoshida M, Kondoh O, Sakamoto H. Selective ALK Inhibitor Alectinib With Potent Antitumor Activity in Models of Crizotinib Resistance. *Cancer Lett* (2014) 351:215–21. doi: 10.1016/j.canlet.2014.05.020
22. Gainor JF, Dardaei L, Yoda S, Friboulet L, Leshchiner I, Katayama R, et al. Molecular Mechanisms of Resistance to First- and Second-Generation ALK Inhibitors in ALK -Rearranged Lung Cancer. *Cancer Discovery* (2016) 6(10):1118–33. doi: 10.1158/2159-8290.CD-16-0596

23. Camidge DR, Dziadziuszko R, Peters S, Mok T, Noe J, Nowicka M, et al. Updated Efficacy and Safety Data and Impact of the EML4-ALK Fusion Variant on the Efficacy of Alectinib in Untreated Alk-Positive Advanced Non–Small Cell Lung Cancer in the Global Phase III Alex Study. *J Thoracic Oncol* (2019) 14:1233–43. doi: 10.1016/j.jtho.2019.03.007
24. Gadgeel S, Peter S, Mok T. Alectinib Versus Crizotinib in Treatment-Naive Anaplastic Lymphoma Kinase-Positive (ALK+) Non-Small-Cell Lung Cancer: CNS Efficacy Results From the ALEX Study. *Ann Oncol* (2018) 29 (11):2214–22. doi: 10.1093/annonc/mdy405
25. Nakagawa K, Hida T, Nokihara H, Morise M, Azuma K, Kim YH, et al. Final Progression-Free Survival Results From the J-ALEX Study of Alectinib Versus Crizotinib in ALK-Positive Non-Small-Cell Lung Cancer. *Lung Cancer (Amsterdam Netherlands)* (2020) 139:195–9. doi: 10.1016/j.lungcan.2019.11.025
26. Soria J-C, Tan DSW, Chiari R, Wu Y-L, Paz-Ares L, Wolf J, et al. First-Line Ceritinib Versus Platinum-Based Chemotherapy in Advanced ALK -Rearranged Non-Small-Cell Lung Cancer (ASCEND-4): A Randomised, Open-Label, Phase 3 Study. *Lancet* (2017) 389:917–29. doi: 10.1016/S0140-6736(17)30123-X
27. Cho BC, Obermannová R, Bearz A, Kim D, Orlov S, Borra G, et al. Oa 05.07 Efficacy and Updated Safety of Ceritinib (450 Mg or 600 Mg) With Low-Fat Meal vs 750 Mg Fasted in ALK+ Metastatic NSCLC. *J Thoracic Oncol* (2017) 12:S1757. doi: 10.1016/j.jtho.2017.09.352
28. Shaw AT, Kim TM, Crinò L, Gridelli C, Kiura K, Liu G, et al. Ceritinib Versus Chemotherapy in Patients With ALK-Rearranged Non-Small-Cell Lung Cancer Previously Given Chemotherapy and Crizotinib (ASCEND-5): A Randomised, Controlled, Open-Label, Phase 3 Trial. *Lancet Oncol* (2017) 18:874–86. doi: 10.1016/S1470-2045(17)30339-X
29. Davies J, Martinec M, Delmar P, Coudert M, Bordogna W, Golding S, et al. Comparative Effectiveness From a Single-Arm Trial and Real-World Data: Alectinib Versus Ceritinib. *J Comp Effectiveness Res* (2018) 7:855–65. doi: 10.2217/cer-2018-0032
30. Chan CPK, Li J, Knoll S, Tang W, Bocharova I, Signorovitch J. Comparative Efficacy of First-Line Ceritinib and Alectinib in Advanced ALK+ NSCLC: A Cross-Study Indirect Comparison. *Ann Oncol* (2018) 29:ix163. doi: 10.1093/annonc/mdy425.040
31. Califano R, Camidge D, Kim HR, Ahn MJ, Yang J, Han JY, et al. Brigatinib Versus Crizotinib in Patients With ALK Inhibitor–Naive Advanced ALK+ NSCLC: Results From the Phase 3 ALTA-1L Trial. *Lung Cancer* (2020) 139: S59–60. doi: 10.1016/s0169-5002(20)30164-1
32. Solomon BJ, Besse B, Bauer TM, Felip E, Soo RA, Camidge DR, et al. Lorlatinib in Patients With ALK-Positive Non-Small-Cell Lung Cancer: Results From a Global Phase 2 Study. *Lancet Oncol* (2018) 19(12):1654–67. doi: 10.1016/S1470-2045(18)30649-1
33. Pirker R, Filipits M. From Crizotinib to Lorlatinib: Continuous Improvement in Precision Treatment of ALK-Positive Non-Small Cell Lung Cancer. *ESMO Open* (2019) 4(5):e000548. doi: 10.1136/esmoopen-2019-000548
34. Ettinger DS, Aisner DL, Wood DE, Akerley W, Bauman J, Chang JY, et al. NCCN Guidelines Insights: Non–Small Cell Lung Cancer, Version 5.2018. *J Natl Compr Cancer Network* (2018) 16(7):807–21. doi: 10.6004/jnccn.2018.0062
35. Camidge DR, Bang YJ, Kwak EL, Iafrate AJ, Varella-Garcia M, Fox SB, et al. Activity and Safety of Crizotinib in Patients With ALK-Positive Non-Small-Cell Lung Cancer: Updated Results From a Phase 1 Study. *Lancet Oncol* (2012) 13:1011–9. doi: 10.1016/S1470-2045(12)70344-3
36. Shaw AT, Kim DW, Nakagawa K, Seto T, Crinó L, Ahn MJ, et al. Crizotinib Versus Chemotherapy in Advanced ALK-Positive Lung Cancer. *New Engl J Med* (2013) 368:2385–94. doi: 10.1056/NEJMoa1214886
37. Seto T, Kiura K, Nishio M, Nakagawa K, Maemondo M, Inoue A, et al. CH5424802 (RO5424802) for Patients With ALK-Rearranged Advanced Non-Small-Cell Lung Cancer (AF-001JP Study): A Single-Arm, Open-Label, Phase 1-2 Study. *Lancet Oncol* (2013) 14(7):590–8. doi: 10.1016/S1470-2045(13)70142-6
38. Tamura T, Kiura K, Seto T, Nakagawa K, Maemondo M, Inoue A, et al. Three-Year Follow-Up of an Alectinib Phase I/II Study in ALK-Positive Non–Small-Cell Lung Cancer: AF-001JP. *J Clin Oncol* (2017) 35:1515–21. doi: 10.1200/JCO.2016.70.5749
39. Ou S-HI, Ahn JS, De Petris L, Govindan R, Yang JC-H, Hughes BGM, et al. Efficacy and Safety of the ALK Inhibitor Alectinib in ALK + Non-Small-Cell Lung Cancer (NSCLC) Patients Who Have Failed Prior Crizotinib: An Open-Label, Single-Arm, Global Phase 2 Study (NP28673). *J Clin Oncol* (2015) 33 (15_suppl):8008. doi: 10.1200/jco.2015.33.15_suppl.8008
40. Leena Gandhi AS, Gadgeel SM, Riely G, Cetnar J. A Phase II, Open-Label, Multicenter Study of the ALK Inhibitor Alectinib in an ALK+ Non-Small-Cell Lung Cancer (NSCLC) U.S./Canadian Population Who had Progressed on Crizotinib (NP28761). *J Clin Oncol* (2015) 33(7):254–70. doi: 10.1200/jco.2015.33.15_suppl.8019
41. Yang JCH, Ou SHI, De Petris L, Gadgeel S, Gandhi L, Kim DW, et al. Pooled Systemic Efficacy and Safety Data From the Pivotal Phase II Studies (NP28673 and NP28761) of Alectinib in ALK-Positive Non-Small Cell Lung Cancer. *J Thoracic Oncol* (2017) 12(10):1552–60. doi: 10.1016/j.jtho.2017.06.070
42. Sakamoto H, Tsukaguchi T, Hiroshima S, Kodama T, Kobayashi T, Fukami TA, et al. CH5424802, a Selective Alk Inhibitor Capable of Blocking the Resistant Gatekeeper Mutant. *Cancer Cell* (2011) 19(5):679–90. doi: 10.1016/j.ccr.2011.04.004
43. Katayama R, Sakashita T, Yanagitani N, Ninomiya H, Horiike A, Friboulet L, et al. P-Glycoprotein Mediates Ceritinib Resistance in Anaplastic Lymphoma Kinase-Rearranged Non-Small Cell Lung Cancer. *EBioMedicine* (2016) 3:54–66. doi: 10.1016/j.ebiom.2015.12.009

Conflict of Interest Statement: The authors declare that the research was conducted in the absence of any commercial or financial relationships that could be construed as a potential conflict of interest.

Copyright © 2021 Tang, Jin, Zhang, Jiang and Malik. This is an open-access article distributed under the terms of the Creative Commons Attribution License (CC BY). The use, distribution or reproduction in other forums is permitted, provided the original author(s) and the copyright owner(s) are credited and that the original publication in this journal is cited, in accordance with accepted academic practice. No use, distribution or reproduction is permitted which does not comply with these terms.

frontiers in Oncology

CASE REPORT
published: 10 June 2021
doi: 10.3389/fonc.2021.634920

Durable Response to the Combination of Atezolizumab With Platinum-Based Chemotherapy in an Untreated Non-Smoking Lung Adenocarcinoma Patient With *BRAF* V600E Mutation: A Case Report

Xiaomin Niu[1], Yingjia Sun[1], David Planchard[2], Luting Chiu[3], Jian Bai[3], Xinghao Ai[1] and Shun Lu[1]**

[1] Department of Shanghai Lung Cancer Center, Shanghai Chest Hospital, Shanghai Jiao Tong University, Shanghai, China, [2] Gustave Roussy, Department of Medical Oncology, Thoracic Unit, Villejuif, France, [3] Berry Oncology Corporation, Beijing, China

OPEN ACCESS

Edited by:
Junji Uchino,
Kyoto Prefectural University of Medicine, Japan

Reviewed by:
Chunxia Su,
Shanghai Pulmonary Hospital, China
Ruiguang Zhang,
Huazhong University of Science and Technology, China
Takehito Shukuya,
Juntendo University, Japan

***Correspondence:**
Xinghao Ai
axh73@qq.com
Shun Lu
shunlu@sjtu.edu.cn

Specialty section:
This article was submitted to Pharmacology of Anti-Cancer Drugs, a section of the journal Frontiers in Oncology

Received: 04 December 2020
Accepted: 19 May 2021
Published: 10 June 2021

Citation:
Niu X, Sun Y, Planchard D, Chiu L, Bai J, Ai X and Lu S (2021) Durable Response to the Combination of Atezolizumab With Platinum-Based Chemotherapy in an Untreated Non-Smoking Lung Adenocarcinoma Patient With BRAF V600E Mutation: A Case Report. Front. Oncol. 11:634920. doi: 10.3389/fonc.2021.634920

Background: Immune checkpoint inhibitor (ICPi) has become a major treatment in advanced non-small cell lung cancer (NSCLC) and demonstrated a clinical benefit for NSCLC patients with high programmed death ligand-1 (PD-L1) expression without *EGFR/ALK/ROS1* drivers; however, the benefit in *BRAF* V600E NSCLC is so far unknown. Here, we report a case of prolonged tumor response to the combination of immunotherapy with chemotherapy in a non-smoking *BRAF* V600E NSCLC patient.

Materials and Methods: We verify a co-expression of *BRAF* V600E mutation and PD-L1 high expression more than 50% on formalin-fixed paraffin-embedded tumor sample of a newly diagnosed lung adenocarcinoma patient by immunohistochemistry and *BRAF* V600E/*EGFR*/*ALK*/*ROS1* Mutations Detection Kit. The tissue and liquid biopsies were further subjected to next-generation sequencing (NGS) for identification of mutations with progression on immunotherapy and BRAF inhibitor (BRAFi). The patient had provided written informed consent and authorized the publication of clinical case.

Results: We demonstrate the case of 62-year-old female non-smoker with high PD-L1 expression and *BRAF* V600E mutated NSCLC. The progression-free survival (PFS) of first-line combination of atezolizumab with platinum-based chemotherapy and sequential second-line treatment with BRAFi Vemurafenib are 20 and 5.5 months, respectively.

Conclusion: This case shows a durable response to ICPi in *BRAF* V600E non-smoking lung adenocarcinoma with PFS of 20 months under first-line atezolizumab plus

chemotherapy treatment. The case supports the idea that the combination immunotherapy may be an attractive option for *BRAF* V600E mutated non-smoking NSCLC with high PD-L1 expression.

Keywords: non-small cell lung cancer, proto-oncogene protein B-raf, programmed death ligand-1, BRAF inhibitor, immunotherapy

INTRODUCTION

Approximately 2% of non-small cell lung cancer (NSCLC) harbors a *BRAF* mutation, and *BRAF* V600E mutation accounts for 50–70% of *BRAF* mutated lung adenocarcinomas. Recently, the European Medicines Agency (EMA) and the Food and Drug Administration (FDA) approved the combination of dabrafenib with trametinib as an effective treatment for *BRAF* V600E mutated patients. Another study reported an objective response rate (ORR) of 44.9% and a median progression-free survival (PFS) of 5.2 months in 100 *BRAF* V600 mutated NSCLC patients treated with Vemurafenib (1).

However, the question of the therapeutic options beyond BRAF inhibitor (BRAFi) remains a critical issue. Recently, FDA approved immune checkpoint inhibitor (ICPi) atezolizumab for *BRAF* V600 unresectable or metastatic melanoma based on the result of IMspire150 trial (NCT02908672) (2). NSCLC patients who had high programmed death ligand-1 (PD-L1) expression without *EGFR/ALK/ROS1* drivers and had benefited from ICPi have been reported, while, the benefit in *BRAF* V600E NSCLC is still unclear. IMMUNOTARGET registry study is to investigate the activity of ICPi across NSCLC harboring oncogenic alterations in 24 centers from 10 countries, the result showing that ORR was 24% and median PFS was 3.1 months for 43 *BRAF* NSCLC patients, with the data of 4.1 months for smokers and 1.9 months for never smokers,1.8 months for V600E and 4.1 months for other *BRAF* mutations; however there were only around 5% patients in the first line setting (3). The *BRAF* V600E non-smoking NSCLC patients left unsolved the question of the place of immunotherapy, especially in first line setting. In this study, we report a TKI naïve non-smoker female with a lung adenocarcinoma driven by *BRAF* V600E mutation concomitant with high PD-L1 expression treated with atezolizumab in combination with chemotherapy followed by BRAFi Vemurafenib, which could open a new perspective of treatment for non-smoking *BRAF* mutated lung cancer.

MATERIALS AND METHODS

The tissue biopsy at diagnosis was detected by BRAF V600E/EGFR/ALK/ROS1 Mutations Detection Kit (AmoyDx®). PD-L1 expression was confirmed by immunohistochemical (IHC) assay using E1L3N (Cell Signaling Technology, Danvers, MA). The cell-free DNA (cfDNA) at diagnosis and the tumor DNA and cfDNA at progression on immunotherapy and BRAFi were analyzed by next-generation sequencing (NGS) including 457 genes (BerryOncology Inc.). Objective tumor response was measured by computed tomography (CT) using RECIST v1.1criteria. The patient provided written informed consent authorizing publication of clinical case.

CASE PRESENTATION

A 62-year-old female non-smoker experienced a month-lasting fatigue, and PET/CT demonstrated an enlarged lung nodule on right lower lobe, bilateral supraclavicular and mediastinal lymphadenectases and multiple bony metastases confirming stage IV-T1bN3M1c (**Figure 1A**). Endobronchial ultrasound-guided transbronchial biopsy on subcarinal lymph node on 2018/03/28 revealed poorly differentiated lung adenocarcinoma with co-expressing tumors of *BRAF* V600E and PD-L1 ≥50% (**Figure 1B**). The concomitant liquid biopsy using NGS confirmed *BRAF* V600E mutation (**Supplementary Table 1**).

The patient enrolled in the trial IMpower132 (NCT02657434) and randomly assigned into the combination group was given atezolizumab/cisplatin/pemetrexed every three weeks during four-induction cycle period before atezolizumab/pemetrexed maintenance. The first cycle of atezolizumab (1,200 mg)/cisplatin/pemetrexed in the induction period was commenced on 2018/04/18. The patient experienced pyrexia (40°C) and grade III gastrointestinal toxicity, leading to a 25% dose reduction of chemotherapy from the second cycle, but without dose interruption or reduction of atezolizumab per protocol. A partial response (PR) of 57.3% including 60% of primary lung and 56.0% of metastatic lymph nodes was observed on first CT-scan evaluation after two cycles of atezolizumab in combination with cisplatin/pemetrexed treatment (**Figure 2**), and a continued PR was achieved for the following 14 cycles of atezolizumab/pemetrexed maintenance. Patient received atezolizumab maintenance from the 19th cycle on 2019/05/09 considering grade II AST and ALT elevation. Unfortunately, disease progressed with the new pericardial effusion on 2019/12/17 after eighth cycles of atezolizumab maintenance, with a total of 20-months PFS of first-line treatment (**Figure 2**). The patient was treated with second-line treatment of BRAFi Vemurafenib (960 mg bid po) on 2019/12/20 and disease showed stable disease (SD) after two cycles. Unfortunately, the disease continued to progress with the new left supraclavicular lymphadenectasis but still with the controllable primary lung after 5.5 months. NGS showed the blood-based tumor mutation burden (bTMB) was decreased from 9.63/Mb at diagnosis to 3.50/Mb at post-ICPi-progression and bounced off to 10.51/Mb at post-BRAFi-progression (**Figure 3A** and **Supplementary Table 1**). The variant allele fraction (VAF) of mutation clusters in liquid

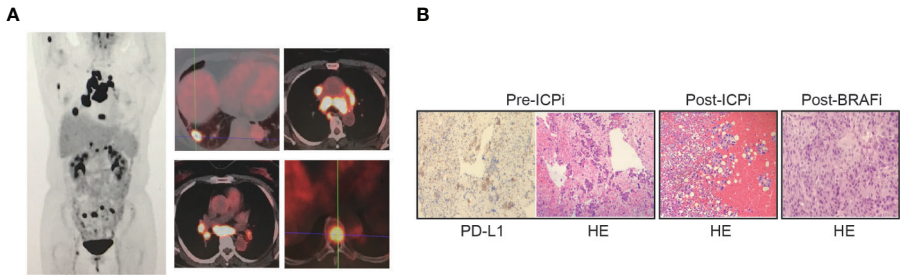

FIGURE 1 | PET/CT imaging and histological finding. **(A)** PET/CT imaging on 2018/03/19 revealed an enlarged nodule measuring 2.0 × 1.6 cm on right lower lobe (RLL) with SUVmax 8.4, bilateral supraclavicular lymph nodes (0.5 cm and 0.6 cm on the right and left sides respectively) with SUVmax 2.8, enlarged mediastinal lymphadenectases including station 2R, 4R, 4L, 3A, 3P, 5, 6, 7, and right hilar lymphadenectasis with SUVmax 26.4 of the largest diameter of 4.2 cm, multiple bony metastases including right humerus, right scapula, T5 and T8 vertebral body, multiple sacrum, right acetabulum, right sciatic bone with a SUVmax 7.8. **(B)** Histological examination on the metastatic subcarinal lymphadenectasis tissue of pre-ICPi (first-biopsy), pericardial effusion of post-ICPi/pre-BRAFi (second-biopsy), and left supraclavicular lymphadenectasis of post-BRAFi (third biopsy) (hematoxylin and eosin stain, magnification ×100) and programmed death ligand-1 (PD-L1) expression in pre-ICPi (immunohistochemical stain, magnification ×100; E1L3N, Cell Signaling Technology, Danvers, MA); poorly differentiated lung adenocarcinoma positive for CK, TTF1, and NapsinA, negative for CD56 and P40 by immunohistochemistry stain in pre-ICPi (03/28/2018), post-ICPi/pre-BRAFi (12/20/2019), and post-BRAFi (06/04/2020). ICPi, immune check-point inhibitor; BRAFi, BRAF inhibitor.

biopsy was dropped at post-ICPi-progression compared with pre-ICPi; conversely, it drastically increased (excluding cluster 4) and new mutations occurred at post-BRAFi-progression compared with pre-/post-ICPi (**Figure 3B**).

DISCUSSION

Nowadays the therapeutic strategies of *BRAF*-mutated NSCLC are often introduced from melanoma treatment regimes. Due to the insufficiency of the study on *BRAF*-mutated subgroup in immunotherapy trials in NSCLC, which therapeutic strategy, immunotherapy, or targeted therapy was used as first-line remains an issue. Patients with *BRAF* V600E melanoma had longer PFS than those with *BRAF* V600K melanoma in targeted-therapy, and conversely the shorter PFS in the immunotherapy, providing the differences in gene expression and mutational load between V600E and V600K *BRAF*-mutant melanomas with the differences in response to BRAFi−/+ MEKi inhibitors and immunotherapy (4). Immuno-target therapy might work better for *BRAF*-mutant NSCLC smokers and seldom beneficial to non-smokers and light smokers (3). Indeed, never-smoking status with a targetable driver is usually accompanied with low TMB and low PD-L1 expression, which might partially explain the low efficacy of ICPi (5). While a retrospective study reported that all eight Asian lung cancer patients with *BRAF* V600E and PD-L1

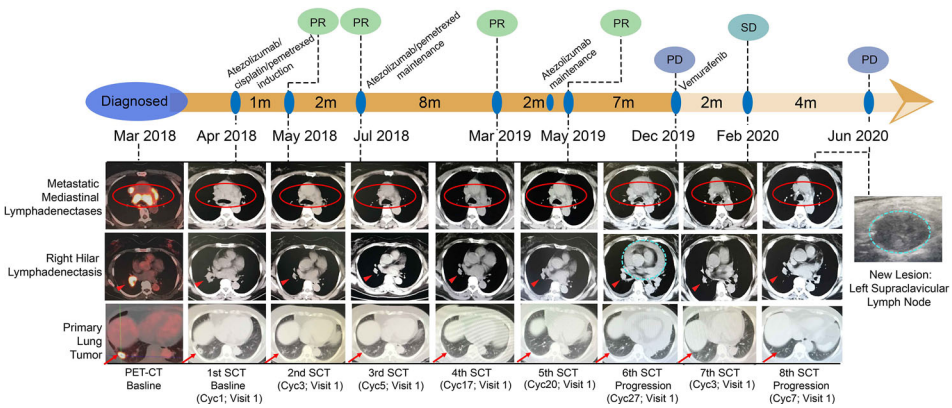

FIGURE 2 | Course of the disease, treatment history, and response evaluation. 1st surveillance CT (SCT): baseline, atezolizumab/cisplatin/pemetrexed induction (Cyc1, 2018/04/11); 2nd SCT: post-induction two cycles (Cyc3, 2018/05/28), PR; 3rd SCT: post-induction four cycles, atezolizumab/pemetrexed maintenance (Cyc5, 2018/07/12), PR; 4th SCT: post-atezolizumab/pemetrexed maintenance 12 cycles (Cyc17, 2019/03/25), PR; 5th SCT: post-atezolizumab maintenance one cycle (Cyc20, 2019/05/27), PR. NOTE: Atezolizumab maintenance on C19V1. Tumor assessment every 9 weeks (three cycles) after the completion of the week 48 tumor assessment per protocol (Cyc20, 2019/05/27); 6th SCT: post-atezolizumab maintenance eight cycles (Cyc27, 2019/12/17), PD; 7th SCT: post-Vemurafenib two cycles (Cyc3, 2020/02/03), SD; 8th SCT: post-Vemurafenib six cycles (Cyc7, 2020/06/04), PD. Red circles: metastatic mediastinal lymphadenectases; Red short arrows: right hilar lymphadenectasis; Red long arrows: primary lung tumor; Blue dotted cycle: new lesion; lesion 1: pericardial effusion (progression on ICPi); lesion 2: left supraclavicular lymph node (progression on BRAFi). PR, partial response; SD, stable disease; PD, progressive disease; ICPi, immune check-point inhibitor; BRAFi, BRAF inhibitor.

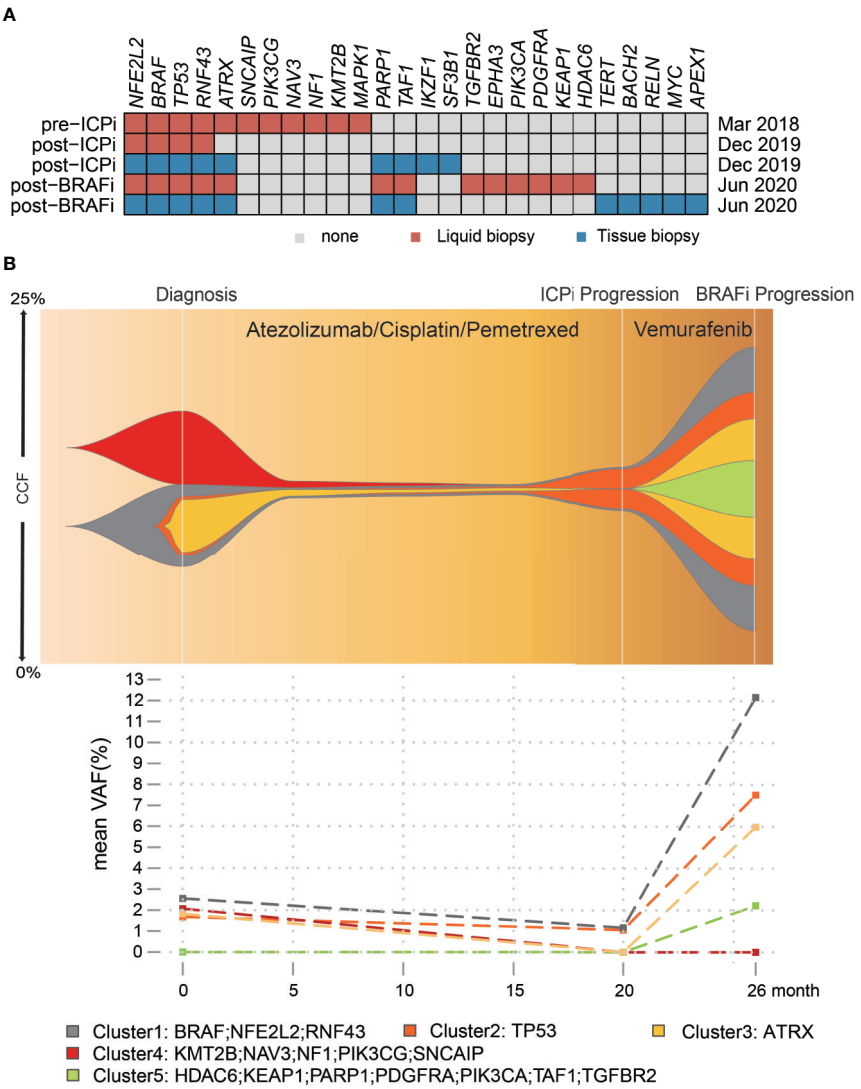

FIGURE 3 | Somatic mutation profiles of pre-ICPi, post-ICPi/pre-BRAFi, and post-BRAFi. **(A)** The heatmap shows an overview of mutations in pre-ICPi, post-ICPi/pre-BRAFi, and post-BRAFi within liquid biopsy, pericardial effusion biopsy, and left supraclavicular lymph node. **(B)** Clonal evolution in liquid biopsy dynamic monitoring (Upper) and mean variant allele frequency (VAF) change (Lower) during immunotherapy and BRAF inhibitor Vemurafenib treatment. Variants from cfDNA using Bayesian cluster with PyClone. CCF, cancer cell fraction; ICPi, immune check-point inhibitor; BRAFi, BRAF inhibitor.

≥50% had co-expressing tumors, six were non-smokers (6), which is unlikely the same as that in Caucasian population. Co-expressing tumors account for 42% in NSCLC west Asian population (6) that is much higher compared to 28% in NSCLC with around 70% Caucasian population (7), which may partially explain the difference of immunotherapy efficacy in *BRAF* non-smoking NSCLCL. In ICPi/chemotherapy NSCLC clinical cohorts (8–13), combination groups demonstrated longer median PFS or OS than chemotherapy alone groups. Especially, the trials KEYNOTE-189, IMpower150, and IMpower130 which investigated the patients with previously untreated metastatic non-squamous NSCLC also displayed that the combination treatment was superior to single-chemotherapy. Furthermore, the magnitude of PFS and OS benefit with ICPi/chemotherapy combination correlated well with PD-L1 and was observed in these cohorts (8–13). The similarities of these cohorts and our case are that patients were EGFR/ALK negative, and some of them presented high PD-L1 expression. Here we reported the first-line combination of atezolizumab with chemotherapy improved PFS to 20 months in a non-smoking *BRAF* V600E-mutated NSCLS patient. The comparison of the result of the IMMUNOTARGET registry study showed median PFS was 1.8 months with ICPi treatment for V600E in the later line which is much shorter than that in the first line.

Interestingly, in our case, bTMB dropped at progression on immunotherapy, implying immunotherapy resistance occurred as the result of the loss of neoantigen (14). At progression, *BRAF* V600E mutation was both identified in pericardial effusion (new

lesion) and plasma. A *PARP1* mutation occurred in pericardial effusion lesion at progression on the combination of immunotherapy and chemotherapy, though no direct evidence has pointed out the relationship between *PARP1* mutation and immunotherapy resistance yet. However, new finding shows that PARP inhibition can synergy with ICPi (15). PARP inhibition regulates the DNA damage response pathway and accumulates DNA injuries, which may lead to the accumulation of neoantigens for ICPi (16). In addition, the research of PARP-inhibitor-mediated upregulation of PD-L1 has been reported (17).

There was a median PFS of 5.2 months in 100 *BRAF* V600-mutated NCSLC patients treated with Vemurafenib found by J. Mazieres et al. (1) and our case with around 5.5 months. BRAFi therapy yields high ORR, while therapeutic duration is limited by diverse mechanisms of acquired resistance. Our result showed a rapid increase of VAF of all mutation clusters (excluding cluster 4) during BRAFi treatment to progression, and reactivation of the MAPK/Erk pathway is a major contributor to BRAFi treatment failure. A *PDGFR*α G853D mutation was found after BRAFi treatment in liquid biopsy; PDGFR is upstream of RAS in the MAPK pathway and strong autophosphorylation was observed in PDGFRα G853D mutation (18). Deregulation of the PI3K pathway which was found out by the presence of *PI3KCA*, *AKT1*, *PTEN*, or *PPP2R1A* mutations can cause resistance to BRAFi. Our case showed *PI3KCA* mutations after BRAFi progression. Furthermore, the genomic alterations in *PIK3CA* have been depicted in resistance to BRAFi in *BRAF* V600E melanoma and NSCLC (19).

CONCLUSION

This case shows the durable response to the combination of atezolizumab with chemotherapy and the prolonged PFS of 20 months in an untreated patient with non-smoking *BRAF* V600E-mutated lung adenocarcinoma, supporting the idea that combination immunotherapy may be an attractive option for *BRAF* V600E non-smoking NSCLC with high PD-L1 expression patients. This case highlights the need for further research to explore the efficacy of immuno-target therapy and ICPi in correlation with different molecular parameters in *BRAF* mutant NSCLC.

DATA AVAILABILITY STATEMENT

The datasets presented in this study can be found in online repositories. The names of the repository/repositories and accession number(s) can be found in the article/**Supplementary Material**.

ETHICS STATEMENT

The studies involving human participants were reviewed and approved by Shanghai Chest Hospital. The patients/participants provided their written informed consent to participate in this study. Written informed consent was obtained from the individual for the publication of any potentially identifiable images or data included in this article.

AUTHOR CONTRIBUTIONS

Design and supervision of this study: XN, SL, and XA. Data collection and analysis: XN, YS, LC, and JB. Manuscript writing: XN, DP, and LC. Final approval: XN, YS, DP, LC, JB, XA, and SL. All authors contributed to the article and approved the submitted version.

FUNDING

This work was supported by grants from the National Natural Science Foundation of China (No. 81972187), Projects of the Committee of Shanghai Science and Technology (Nos. 19ZR1449800, 20Y11913700, 19411950500, 18DZ1910702), National Key Research and Development Program of China (No. 2016YFC1303300), Clinical Research Project of Shanghai Municipal Public Health Bureau (No. 201840122), Advanced Appropriate Technology Promotion Project of Shanghai Municipal Public Health Bureau (No. 2019SY048), Doctoral Innovation Fund of Shanghai Jiao Tong University School of Medicine (No. BXJ201952), and Interdisciplinary Program of Shanghai Jiao Tong University (No. YG2017MS80),Project of Shanghai Talent Development Fund (No. 2019074).

ACKNOWLEDGMENTS

The authors would like to acknowledge the patient for her willingness to publish her clinical case.

SUPPLEMENTARY MATERIAL

The Supplementary Material for this article can be found online at: https://www.frontiersin.org/articles/10.3389/fonc.2021.634920/full#supplementary-material

REFERENCES

1. Mazieres J, Cropet C, Montané L, Barlesi F, Souquet PJ, Quantin X, et al. Vemurafenib in non-Small-Cell Lung Cancer Patients With BRAF(V600) and BRAF(nonV600) Mutations. *Ann Oncol* (2020) 31(2):289–94. doi: 10.1016/j.annonc.2019.10.022
2. Gutzmer R, Stroyakovskiy D, Gogas H, Robert C, Lewis K, Protsenko S, et al. Atezolizumab, Vemurafenib, and Cobimetinib as First-Line Treatment for Unresectable Advanced BRAFV600 Mutation-Positive Melanoma (Imspire150): Primary Analysis of the Randomised, Double-Blind, Placebo-Controlled, Phase 3 Trial. *Lancet* (2020) 395(10240):1835–44. doi: 10.1016/S0140-6736(20)30934-X
3. Mazieres J, Drilon A, Lusque A, Mhanna L, Cortot AB, Mezquita L, et al. Immune Checkpoint Inhibitors for Patients With Advanced Lung Cancer and Oncogenic Driver Alterations: Results From the IMMUNOTARGET Registry. *Ann Oncol* (2019) 30(8):1321–8. doi: 10.1093/annonc/mdz167

4. Pires da Silva I, Wang KYX, Wilmott JS, Holst J, Carlino MS, Park JJ, et al. Distinct Molecular Profiles and Immunotherapy Treatment Outcomes of V600E and V600K. *BRAF-Mutant Melanoma Clin Cancer Res* (2019) 25 (4):1272. doi: 10.1158/1078-0432.CCR-18-1680
5. Rangachari D, VanderLaan PA, Shea M, Le X, Huberman MS, Kobayashi SS, et al. Correlation Between Classic Driver Oncogene Mutations in EGFR, ALK, or ROS1 and 22C3-PD-L1 >/=50% Expression in Lung Adenocarcinoma. *J Thorac Oncol* (2017) 12(5):878–83. doi: 10.1016/j.jtho.2016.12.026
6. Dudnik E, Peled N, Nechushtan H, Wollner M, Onn A, Agbarya A, et al. Braf Mutant Lung Cancer: Programmed Death Ligand 1 Expression, Tumor Mutational Burden, Microsatellite Instability Status, and Response to Immune Check-Point Inhibitors. *J Thorac Oncol* (2018) 13(8):1128–37. doi: 10.1016/j.jtho.2018.04.024
7. Herbst RS, Baas P, Kim DW, Felip E, Pérez-Gracia JL, Han JY, et al. Pembrolizumab Versus Docetaxel for Previously Treated, PD-L1-positive, Advanced non-Small-Cell Lung Cancer (Keynote-010): A Randomised Controlled Trial. *Lancet* (2016) 387(10027):1540–50. doi: 10.1016/S0140-6736(15)01281-7
8. Langer CJ, Gadgeel SM, Borghaei H, Papadimitrakopoulou VA, Patnaik A, Powell SF, et al. Carboplatin and Pemetrexed With or Without Pembrolizumab for Advanced, Non-Squamous non-Small-Cell Lung Cancer: A Randomised, Phase 2 Cohort of the Open-Label Keynote-021 Study. *Lancet Oncol* (2016) 17:1497–508. doi: 10.1016/S1470-2045(16)30498-3
9. Paz-Ares L, Luft A, Vicente D, Tafreshi A, Gümüş M, Mazières J, et al. Pembrolizumab Plus Chemotherapy for Squamous non–Small-Cell Lung Cancer. *NEJM* (2018) 379:2040–51. doi: 10.1056/NEJMoa1810865
10. Gandhi L, Rodríguez-Abreu D, Gadgeel S, Esteban E, Felip E, De Angelis F, et al. Pembrolizumab Plus Chemotherapy in Metastatic non–Small-Cell Lung Cancer. *NEJM* (2018) 378:2078–92. doi: 10.1056/NEJMoa1801005
11. West H, McCleod M, Hussein M, Morabito A, Rittmeyer A, Conter HJ, et al. Atezolizumab in Combination With Carboplatin Plus Nab-Paclitaxel Chemotherapy Compared With Chemotherapy Alone as First-Line Treatment for Metastatic non-Squamous non-Small-Cell Lung Cancer (Impower130): A Multicentre, Randomised, Open-Label, Phase 3 Trial. *Lancet Oncol* (2019) 20:924–37. doi: 10.1016/S1470-2045(19)30167-6
12. Greillier L, Tomasini P, Barlesi F. The Clinical Utility of Tumor Mutational Burden in Non-Small Cell Lung Cancer. *Transl Lung Cancer Res* (2018) 7:639–46. doi: 10.21037/tlcr.2018.10.08
13. Socinski MA, Jotte RM, Cappuzzo F, Orlandi F, Stroyakovskiy D, Nogami N, et al. Atezolizumab for First-Line Treatment of Metastatic Nonsquamous Nsclc. *NEJM* (2018) 378:2288–301. doi: 10.1056/NEJMoa1716948
14. Anagnostou V, Smith KN, Forde PM, Niknafs N, Bhattacharya R, White J, et al. Evolution of Neoantigen Landscape During Immune Checkpoint Blockade in Non-Small Cell Lung Cancer. *Cancer Discovery* (2017) 7 (3):264–76. doi: 10.1158/2159-8290.CD-16-0828
15. Mouw KW, Goldberg MS, Konstantinopoulos PA, D'Andrea AD. Dna Damage and Repair Biomarkers of Immunotherapy Response. *Cancer Discovery* (2017) 7(7):675–93. doi: 10.1158/2159-8290.CD-17-0226
16. Vikas P, Borcherding N, Chennamadhavuni A, Garje R. Therapeutic Potential of Combining Parp Inhibitor and Immunotherapy in Solid Tumors. *Front Oncol* (2020) 10:570. doi: 10.3389/fonc.2020.00570
17. Ding L, Chen X, Xu X, Qian Y, Liang G, Yao F, et al. Parp1 Suppresses the Transcription of PD-L1 by Poly(ADP-Ribosyl)ating Stat3. *Cancer Immunol Res* (2019) 7(1):136–49. doi: 10.1158/2326-6066.CIR-18-0071
18. Dai J, Kong Y, Si L, Chi Z, Cui C, Sheng X, et al. Large-Scale Analysis of PDGFRA Mutations in Melanomas and Evaluation of Their Sensitivity to Tyrosine Kinase Inhibitors Imatinib and Crenolanib. *Clin Cancer Res* (2013) 19(24):6935–42. doi: 10.1158/1078-0432.CCR-13-1266
19. Ortiz-Cuaran S, Mezquita L, Swalduz A, Aldea M, Mazieres J, Leonce C, et al. Circulating Tumor Dna Genomics Reveals Potential Mechanisms of Resistance to BRAF-targeted Therapies in BRAF-mutant Metastatic non-Small Cell Lung Cancer Patients. *Clin Cancer Res* (2020) 2020: clincanres.1037.2020. doi: 10.1158/1078-0432.CCR-20-1037

Conflict of Interest: LC and JB were employed by the company Berry Oncology Corporation.

The remaining authors declare that the research was conducted in the absence of any commercial or financial relationships that could be construed as a potential conflict of interest.

Copyright © 2021 Niu, Sun, Planchard, Chiu, Bai, Ai and Lu. This is an open-access article distributed under the terms of the Creative Commons Attribution License (CC BY). The use, distribution or reproduction in other forums is permitted, provided the original author(s) and the copyright owner(s) are credited and that the original publication in this journal is cited, in accordance with accepted academic practice. No use, distribution or reproduction is permitted which does not comply with these terms.

frontiers in Oncology

ORIGINAL RESEARCH
published: 16 June 2021
doi: 10.3389/fonc.2021.663671

The Angiotensin-Converting Enzyme Inhibitory State Promotes the Transformation of Non-Small Cell Lung Cancer Blood Supply Pattern Toward Vasculogenic Mimicry Formation

Kandi Xu[1,2†], Huize Han[3†], Yexin Luo[4†], Hong Ye[5†], Hongxia Lin[1,2] and Lei Ni[1,2]*

[1] Department of Respiration and Critical Care Diseases, Ruijin Hospital, School of Medicine, Shanghai Jiao Tong University, Shanghai, China, [2] Institute of Respiratory Diseases, School of Medicine, Shanghai Jiao Tong University, Shanghai, China, [3] Respiratory and Critical Care Center, Shanghai East Hospital, Tongji University, Shanghai, China, [4] First Clinical Medical College, Anhui Medical University, Anhui, China, [5] School of Foreign Studies, Anhui University, Anhui, China

OPEN ACCESS

Edited by:
Hideharu Kimura,
Kanazawa University, Japan

Reviewed by:
Veronica Aran,
Instituto Estadual do Cérebro Paulo Niemeyer (IECPN), Brazil
Keyue Ding,
Queen's University, Canada

***Correspondence:**
Lei Ni
nilei625@139.com

[†]These authors have contributed equally to this work and share first authorship

Specialty section:
This article was submitted to Thoracic Oncology, a section of the journal Frontiers in Oncology

Received: 03 February 2021
Accepted: 27 May 2021
Published: 16 June 2021

Citation:
Xu K, Han H, Luo Y, Ye H, Lin H and Ni L (2021) The Angiotensin-Converting Enzyme Inhibitory State Promotes the Transformation of Non-Small Cell Lung Cancer Blood Supply Pattern Toward Vasculogenic Mimicry Formation. Front. Oncol. 11:663671. doi: 10.3389/fonc.2021.663671

Tumor microenvironment plays an important role in tumor proliferation, metastasis, and angiogenesis. Local RAS is a key factor to tumor proliferation and metastasis in NSCLC microenvironment, but its role on angiogenesis and VM formation remains unclear. Although overwhelming majority of previous studies suggested that VM is well established in aggressive tumor and facilitates tumor growth and metastasis, we put forward different views from another angle. We proved that status of tumor blood supply patterns, including VM channels and endothelial vessels, can dynamically exchange with each other along with local RAS fluctuations in microenvironment. Quantitatively, ACE2/ACEI promotes VM formation *via* Nodal/Notch4 activation; while structurally, ACE2/ACEI leads to a strong and solid structure of VM *via* inhibition of VE-cadherin internalization. These changes induced by ACE2/ACEI relate to relatively low metastasis rate and comforting prognoses of NSCLC patients.

Keywords: renin-angiotensin system, angiotensin-converting enzyme 2, vasculogenic mimicry, VE-cadherin, nodal, Notch4, non-small cell lung cancer

INTRODUCTION

Lung cancer (LC), the most common cancer worldwide, due to its highly invasive and metastatic potential, is also the predominant cause of cancer-related death, of which non-small cell lung cancer (NSCLC) accounts for approximately 80% (1, 2). Tumor microenvironment plays an important role in tumor proliferation and metastasis. Hypoxia and angiogenesis, two of the most significant tumor environmental factors, are related to increased distant metastasis and poor survival in various tumor types (3, 4).

Due to tumor heterogeneity, an intricate tumor angiogenic pattern, considered to contain, among other things, vasculogenesis, sprouting angiogenesis, vessel co-option, vascular

intussusception, vasculogenic mimicry, is becoming increasingly appealing currently (5). The existence of vasculogenic mimicry (VM), a novel blood perfusion way different from blood vessels, is found to be well established in aggressive tumor especially within an oxygen deficient environment, such as neuroblastoma, melanoma, and NSCLC (6–8). Cancer stem cells (CSCs), a subgroup of malignant tumor cells which express both endothelial and tumor markers, enable themselves to mimic vascular endothelial cells to participate in the formation of VM due to its plasticity. Comprised of cancer-derived endothelial-like cells in malignancies, VM has recently been recognized as a resistance mechanism of anti-angiogenesis inhibitor as it facilitates tumor growth and metastasis in anoxic environment. As biomarkers of VM, VE-cadherin and EphA2 co-express at cell junction of VM, and the interaction of which mediates VM like a switch. Moreover, classic signal pathway (PI3K/AKT and MAPK) and HIF-1α can motivate cancer cell growth, invasion, angiogenesis, and the generation of VM as well in NSCLC (9–11). There is another notion which doubts VM might be a degenerative trace of tumor vessels (12), but the structure and attribute of VM with different generation modes have not been compared.

The systemic renin–angiotensin system (RAS) controls the cardiovascular system, and the local RAS is a key factor to tumor proliferation and metastasis in tumor microenvironment. The expression of angiotensin II (Ang II), part of RAS, is increased locally in microenvironment and related to tumor growth, angiogenesis, and prognosis (13). However, the biological effect of Ang II on tumor can be reversed by angiotensin-converting enzyme inhibitors (ACEIs), angiotensin II type 1 receptor blockers (ARBs), or angiotensin-converting enzyme 2 (ACE2). Previously, we proved that the level of ACE2 in NSCLC tissues is reduced. Functionally, ACE2 can suppress tumor proliferation, invasion, angiogenesis, and metastasis by downregulating the expression of Ang II and vascular endothelial growth factor a (VEGFa) (14–16). Nevertheless, the role of ACE2 in VM and the underlying mechanisms are not clear.

In the present study, we explored the alternate pattern of angiogenesis in ACE2-overexpression model. We confirmed the overexpression of ACE2 promotes solid VM formation which is induced by Nodal/Notch4 and VE-cadherin in NSCLC.

MATERIALS AND METHODS

Patient Samples and Tissue Microarray

All clinical investigations were approved by Ruijin Hospital Ethics Committee and conducted according to the Declaration of Helsinki. Eighty three NSCLC patients with detailed clinical and pathological information received surgery and follow-up (5 years after surgery) in Ruijin Hospital from 2013 to 2016. Patients who died within 1 month after surgery and who were lost during the follow-up were not enrolled in present study. In order to reduce the risk of bias due to confounding factors, we restricted sample by including only certain patients that have similar values of potential confounding variables (age, gender, race, BMI, comorbidity, *etc.*), and in the following univariate analysis, the reported association would not be confounded by other factors. All pathological patterns of removed tumor tissues used for TMA construction were double confirmed by the Pathology Department of Ruijin Hospital and Shanghai Outdo Biotech Co, Ltd (China). Two 1-mm cores were punctured in each tissue sample to create TMA, and the score of each sample was calculated as the mean score of two cores.

Cell Culture

Human non-small cell lung cancer cell line A549 (Shanghai Institute of Cells, China) and NCI-H1650 (Cell Bank of the Type Culture Collection of the Chinese Academy of Sciences, China) were grown in Dulbecco's modified Eagle's medium supplemented with 10% fetal bovine serum (all from Gibco BRL, USA), 1% penicillin/streptomycin and 1% Glutamax at 37°C with 5% CO_2.

Plasmid Construction

Human ACE2 cDNA (5′ CGATCTTAATTAAATGCAG ATGGCGGACGC-3′, 5′-TCAGTGGCGCGCCCTATTTG GAAAGTTTGCTTATAACTCTG-3′) was synthesized and cloned by polymerase chain reaction (PCR), then ligated into plenti6.3-MCS-IRES-EGFP (Yingrun Biotechnologies Inc., China, **Figure 3A**) between Pac1 and Asc1 restriction sites to construct the overexpression vector pLenti6.3-ACE2 in 293T cells.

The pLenti6.3-ACE2 plasmid was confirmed by PCR and sequencing.

Overexpression of ACE2 in A549 Cells

Lenti-ACE2-EGFP and Lenti-EGFP, harvested from the supernatants, were added into A549 cells with polybrene (8 μg/ml) and incubated for 24 h to obtain ACE2 overexpressing A549 cells (A549-ACE2-OE cells) and ACE2 negative control cells (A549-NC cells), (MOI = 20) respectively.

Transfection efficiency, fluorescence of reporter gene EGFP in both cell lines, were observed using a fluorescence microscope. Western blot was carried out to examine the ACE2 protein expression level in A549-ACE2-OE cells and A549-ACE2-NC cells.

Overexpression Plasmid and Transient Transfection in NCI-H1650

ACE2 overexpression plasmid (pENTER-ACE2) and a control vector were designed and constructed by Vigene Biosciences Inc. (Jinan, China). NCI-H1650 cells, 6 × 105, were transfected with 1.5 μg pENTER-ACE2 using Lipo6000™ transfection reagent (C0526, Beyotime, Shanghai, China) according to the manufacturer's instructions. Protein samples were extracted 72 h after transfection.

Western Blot

Equal amounts of protein samples were extracted from cells and separated by sodium dodecyl sulfate polyacrylamide gel electrophoresis, transferred onto a polyvinylidene fluoride membrane (Millipore, USA), blocked with 5% fat-free milk, then incubated with antibodies against ACE2 (1:3,000,

ab108252, Abcam, US), VE-cadherin (1:1,000, ab33168, Abcam), EphA2 (1:1,000, 6997s, CST, USA), AKT (1:1,000, 4691, CST), p-AKT (1:2,000, 4060, CST), p38 (1:2,000, ab7952, Abcam), p-p38 (1:1,000, 4511, CST), Nodal (1:2,000, ab55676, Abcam), Notch4 (1:2,000, ab184742, Abcam), and Actin (1:2,000, ab8226, Abcam) overnight at 4°C, and the corresponding secondary antibodies (1:5,000, Thermo Fisher, USA) for 1 h at room temperature (RT). The blots were examined by an enhanced chemiluminescence detection kit (Millipore). Actin was used as a loading control, and all experiments were repeated three times independently. Expression quantification of proteins was performed using ImageJ software (National Institutes of Health, USA).

Real-Time Quantitative Reverse Transcription-Based Polymerase Chain Reaction

Total RNA was extracted using the TRIzol reagent and subjected to reverse transcription and qPT-PCR according to the manufacturer's instructions (all from Takara, Japan). Relative expression level of ACE2, VE-cadherin, and EphA2 was assessed by the comparative quantification in triplicate. ACTB was an internal control.

The primer sequences used for qRT-PCR are listed in **Table 1**.

Three-Dimensional Culture

Wells of 24-well plate coated with a mixture of Matrix and Type I Collagen (both from BD Biosciences, the Netherlands, 1:1, 250 μl per well) were laid for 1 h at 37°C. 60×10^4 A549-ACE2-OE cells, or A549-NC cells with or without Captopril (concentration: 1, 5, and 10 nM/L, HY-B0368, MedChemExpress, New Jersey, USA) were seeded onto each well. Images were captured using a Leica DMi8 microscope, and net structure was analyzed by ImageJ.

Immunohistochemistry and Scoring System

Protein expression was detected by IHC in fixed, embedded paraffin sections of allograft tissues and TMAs. The sections were dewaxed, rehydrated, treated with antigen retrieval, hatched with primary antibodies of ACE2 (1:200), VE-cadherin (1:200), EphA2 (1:100), and CD34 (1:200, ab81289, Abcam) overnight at 4°C, individually exposed to secondary antibody (SA1020, BOSTER, USA) 1 h at RT, and colored with DAB peroxidase substrate. After counterstaining with hematoxylin, sections were recorded with a Leica-SP8.

For TMAs, a semi-quantitative scoring manner was utilized in a high-power field (HPF: 40× magnification) of each core visually by two pathologists blinded to patient information and the aim of this study. Staining intensity of cells was graded as follows: 0 = undetectable, 1 = weak, 2 = moderate, 3 = high. Percentage of stained cells was graded as follows: 0: 0–1%; 1: 2–25%; 2: 26–50%; 3: 51–75%; 4: 76–100%. The overall scoring points were calculated as the product of score of staining intensity of cells and percentage of stained cells.

For allograft tissues, Image-Pro Plus 6.0 soft was run to obtain the mean optical density of four HPFs in each section.

TABLE 1 | The primer sequences of genes used in qRT-PCR.

Genes	Primer sequences (5′–3′)	Products
ACTB	F: GGCACTCTTCCAGCCTTCC R: GAGCCGCCGATCCACAC	255 bp
ACE2	F: TGGCTACAGAGGATCAGGAGT R: GAACTTGGGTTGGGCGCTATT	2418 bp
VE-cadherin	F: CATCGGTTGTTCAATGCGTC R: GGTACATGACAGAGGCGTGG	118 bp
EphA2	F: CCGTATGGCAAAGGGTGG R: TCGGCATAGTAGAGGTTGAAAGT	236 bp

Periodic Acid-Schiff Stain

A PAS staining kit (395B, Sigma, USA) was applied after CD34 IHC (CD34/PAS double staining) or alone to take count of endothelial micro vessel (MV) and tumor-derived VM of TMAs or four HPFs in each tissue section. Briefly, the sections were exposed to 1% sodium periodate (10 min) and Schiff's buffer (10 min) at 37°C in turn.

MV is considered to be lined by $CD34^+/PAS^-$ endothelial cells, while VM is regarded as closely arranged by $CD34^-/PAS^+$ tumor cells whose nuclei are large and hyperchromatic within blood cells or free cancer cells.

Immunofluorescent Staining

Cells, 4×10^4, were plated on glass slides and cultured overnight. Then cells were fixed with 4% paraformaldehyde (15 min) and permeabilized with 0.5% Triton-100 for 10 min. Four percent BSA was used to block non-specific protein–protein interactions (1 h). The cells were treated with antibody against human HIF1-a (ab92498, Abcam) overnight followed by anti-rabbit Alexa Fluor 488 (ab150077, Abcam) and Alexa Fluor 594 (R37117, Thermo Fisher) secondary antibodies. After counterstaining with DAPI, cells were recorded, and the mean optical density was researched by Image J.

Animal Experiments

C57BL/6 mice of 5–6 weeks were purchased from Bethesda (USA) and randomly divided into three groups (A549-NC; A549-ACE2-OE; A549 + ACEI). The corresponding cells (5×10^6) were injected (s.c.) into the mice flanks, and a common ACEI drug Captopril (0.3 mg/kg) was used (i.g.). Tumor length and width were measured by a caliper every 4 days, and the volume was calculated (tumor volume = (length * width^2)/2). Twenty days later or when the tumor volumes reached 1,000 mm^3, the mice were euthanized and tumors were isolated. The removed tumors were weighed and underwent subsequent tests. Laparotomies were performed to clear the distant metastasis of vital organs. All animal operations were carried out in accordance with institution guidelines of Ruijin Hospital.

Statistical Analysis

All data analyses were performed with SPSS 23.0 (IBM, USA) and GraphPad Prism 6.0 (GraphPad Software Inc., USA). If not mentioned, the data are shown as mean ± SD. The groupings of patients are all based on the median of variable data sets, respectively. Differences between groups were analyzed by two-tailed Student's t-test (for quantitative data) and Chi-square test (for categorical data). OS of patients was calculated by Kaplan–Meier survival analysis, and differences were analyzed by log-

rank (Mantel–Cox) test. Pearson's test was used for correlation analysis. P ≤0.05 was considered statistically significant.

RESULTS

High ACE2 Expression Was Linked to Increased VM and Better Prognosis in NSCLC

To accurately study the association between ACE2 status and disease progression in NSCLC, 83 patients who had accepted radical excisions were dichotomized into either ACE2 low (≤1) or high (>1) expression group with a cut-off value, the median ACE2 score of excised tumors. Whereafter we did a comparative analysis of clinicopathological data of the two groups (**Table 2**). Patients with low ACE2 expression were mostly female (62.5 *vs* 37.2%, P = 0.021) or smokers (75.0 *vs* 53.5%, P = 0.042), concealed more advanced vascularization (39.38 ± 39.33 *vs* 23.03 ± 27.43, P = 0.032), and owned a reduced 5-year survival (47.5 *vs* 71.4%, P = 0.027); by comparison, more patients among the ACE2 high expression group retained VM generation (44.2 *vs* 20.0%, P = 0.019), VE-cadherin (VE-cadherin score > 0, 53.5 *vs* 30.0%, P = 0.030), EphA2 (EphA2 score ≥ 8, 72.1 *vs* 50.0%, P = 0.039) high expression, escaped recurrence or metastasis 5 years after surgery (46.5 *vs* 25.0%, P = 0.042). In TMA, VM frequently occurred in NSCLC tissues with ACE2 high level in the form of regular and integrated small pipes or large blood lakes (**Figure 1A**), and the majority of $ACE2^+$/VE-cadherin$^+$/$EphA2^+$ cells were assembled into them; howbeit immature and discontinuous $CD34^+$ (regarded as an endothelial marker) MVs were easily caught in ACE2 low expressing tissues. Univariate survival analysis also affirmed that compared with patients in ACE2 high expressing group, patients with ACE2 low expressing status had a poorer 5-year survival (P = 0.044, **Figure 1B**).

TABLE 2 | The relativity between ACE2 expression and clinicopathological characteristics in NSCLC patients.

Factors		ACE2 low expression patients (n = 40, %)	ACE2 high expression patients (n = 43, %)	P value
Sex	Male	15 (37.5)	27 (62.8)	0.021
	Female	25 (62.5)	16 (37.2)	
Age (years)	<65	25 (62.5)	26 (60.5)	0.849
	≥65	15 (37.5)	17 (39.5)	
Smoking	No	10 (25.0)	20 (46.5)	0.042
	Yes	30 (75.0)	23 (53.5)	
Primary tumor size (diameter)	≤3	25 (62.5)	25 (58.1)	0.685
	>3	15 (37.5)	18 (41.9)	
Clinical stage	I	20 (50.0)	20 (46.5)	0.936
	II	4 (10.0)	5 (11.6)	
	III	16 (40.0)	18 (41.9)	
Lymph node status	N0	21 (52.5)	24 (55.8)	0.696
	N1	3 (7.5)	5 (11.6)	
	N2	16 (40.0)	14 (32.6)	
CEA	Negative	22 (57.9)	27 (64.3)	0.558
	Positive	16 (42.1)	15 (35.7)	
CYFRA21-1	Negative	26 (66.7)	30 (73.2)	0.526
	Positive	13 (33.3)	11 (26.8)	
NSE	Negative	31 (79.5)	37 (86.0)	0.430
	Positive	8 (20.5)	6 (14.0)	
5-year prognosis	Survival	19 (47.5)	30 (71.4)	0.027
	Death	21 (52.5)	12 (28.6)	
5-year recurrence or metastasis	Negative	10 (25.0)	20 (46.5)	0.042
	Positive	30 (75.0)	23 (53.5)	
MV		39.38 ± 39.33	23.03 ± 27.43	0.032
VM	Negative	32 (80.0)	24 (55.8)	0.019
	Positive	8 (20.0)	19 (44.2)	
VE-cadherin	Negative	28 (70.0)	20 (46.5)	0.030
	Positive	12 (30.0)	23 (53.5)	
EphA2	Low expression	20 (50.0)	12 (27.9)	0.039
	High expression	20 (50.0)	31 (72.1)	

ACE2-Induced Better Outcome in NSCLC Patients Might Be Attributed to Less Vessels and More VM Formation

To make further efforts on the relation of the transformed pattern of blood supply triggered by ACE2 with prognosis, patients were further divided into two groups according to the presence of VM and the number of MV (cut-off value: 10), respectively. Noticeably, in ACE2 low expressing group, positive VM presence was related to shorter periods of NSCLC patients than negative VM presence (P = 0.021, **Figures 2A, B**); but with respect to patients with ACE2 high level, there was no significant difference in survival between two groups (P = 0.179, **Figures 2C, D**). On the other hand, patients with shortage of MV possessed better prognoses than those with abundance of MV in ACE2 high level group (P = 0.009, **Figures 2G, H**), but this kind of advantage no longer existed in ACE2 low level group (P = 0.315, **Figures 2E, F**). In summary, the alternate pattern of angiogenesis promoted by ACE2 plays a decisive role in NSCLC prognosis.

Human ACE2 Was Stably Overexpressed in A549-ACE2-OE Cells

To intensively assess the effect of ACE2 on VM formation of NSCLC, an ACE2 overexpressing A549 cell model was established. pLenti6.3-ACE2 expression vector was successfully constructed using pLenti6.3-MCS/V5 DEST (**Figure 3A**) and was detected by PCR and sequencing. The PCR product post restriction enzyme digestion shared the same number of bases (2,418 bp) with ACE2 gene (**Figure 3B**). A549 cells were transfected with pLenti6.3-ACE2 expression vector (A549-ACE2-OE) or empty vector as a negative control (A549-NC), then fluorescence of EGFP in both cell lines was observed to determine the transfection efficiency and photographically recorded (**Figure 3C**). Next, the persistent overexpression of ACE2 by lentivirus was demonstrated by RT-PCR and Western blot analysis 72 h later (**Figures 3D, E**), and there was a more than three-fold increase of ACE2 protein expression in A549-ACE2-OE cells shown in **Figure 3F**, compared with negative control. All these data above suggested an ACE2 overexpressing A549 cell line was successfully constructed.

We also transiently transfected NCI-H1650 with pENTER-ACE2 and determined the transfection efficiency by western blotting (**Supplement 1A, B**).

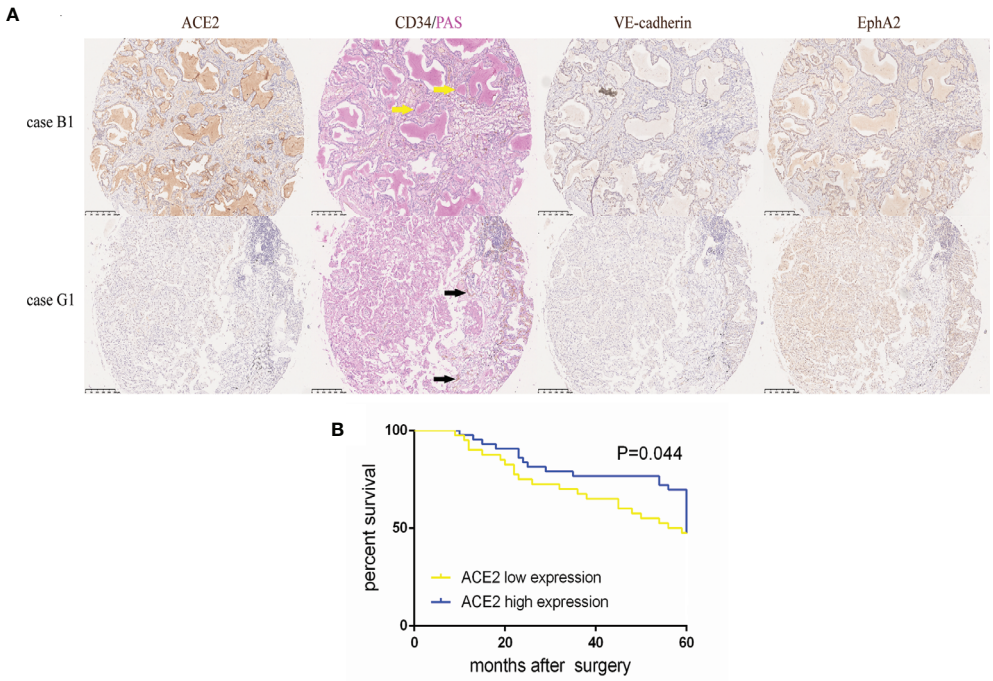

FIGURE 1 | High ACE2 expression was linked to increased VM and better prognosis in NSCLC. **(A)** Typical image of ACE2, VE-cadherin, EphA2 protein expression and CD34/PAS double staining in TMA tissues. Case B1 had massive $CD34^{-}/PAS^{+}$ VM (yellow arrows) lined by ACE2, VE-cadherin and EphA2 high expressing tumor cells. Case G1 had abundant $CD34^{+}/PAS^{-}$ MVs (black arrows) with ACE2, VE-cadherin and EphA2 low expressing tumor cells. **(B)** Kaplan-Meier analysis of OS in NSCLC patients with ACE2 low or high expression. P = 0.044.

Tube Formation Ability of A549 Cells Was Improved With ACE inhibitory State

Surprisingly, we found a significant difference of morphologies between A549-ACE2-OE cells and paired cells following a 72-h culture in conventional 2D culture plates: different percentages of sheet-like or thread-like cell types were shown in A549-ACE2-OE cells and parental cells (**Figure 4A**). A549-ACE2-OE cells, growing in a more dispersed state, provided many more elongated spouting cells than pebble-like cells, compared with A549-NC cells (**P < 0.01, **Figure 4B**), which means the overexpression of ACE2 might harbor a trans-differentiation of endothelial features in A549 cells. Next, the capability of tube formation of both above cell lines was examined by 3D Matrix gel culture and images were digitally captured 72 h later (**Figure 4C**). Notably, more nodes (**P < 0.01), branches (*P < 0.05), and meshes (*P < 0.05) were produced in tubes formed by A549-ACE2-OE cells, with an increased mean mesh size (*P < 0.05), while more isolated segments were found in negative control (*P < 0.05, **Figures 4D, E**). Thus, A549-ACE2-OE cells were competent to shape larger, more massive and more substantial tubes, yet tubes carried out by A549-NC cells were few, scattered, and fragile.

We went a step further to the pharmacological action of ACEI on VM formation *in vitro*. Hereby a series of ACEI dilution was added into A549 cell culture system, and an adequate concentration (10 nM/L, **P < 0.01) was found. ACEI has an analogous effect on VM formation to ACE2 overexpression in a dose-dependent manner in conventional 2D culture and 3D culture.

VM Formation Was Increased and Vasculature Was Lessened Due to Inhibition of RAS *In Vivo*

To better prove changes of angiogenesis pattern resulting from local RAS in tumor microenvironment, mice were injected with A549-ACE2-OE cells or A549-NC cells, administered with ACEI. Tumor growth was abated in A549-ACE2-OE group and ACEI group (*P < 0.05, *P < 0.05, **Figure 5A**), respectively, compared with that in A549-NC group. Xenografts were also lightened (**P < 0.01, *P < 0.05, **Figure 5B**). All mice (3/3) from the A549-NC group had distant multiple organ metastasis, whereas in A549-ACE2-OE group and ACEI group there was one (1/3) and zero (0/3). Consequently, tumor loads were alleviated by both ACE2 overexpression and ACEI treatment.

Furthermore, consecutive sections of allograft tumor tissues, stained with PAS, CD34, VE-cadherin, or EphA2 (**Figure 5C**), were scanned to count the number of MV ($CD34^{+}/PAS^{-}$) and VM ($CD34^{+}/PAS^{-}$). We validated allayed micro vessels (***P < 0.001, **P < 0.01, **Figure 5D**) and multiplied VM (***P < 0.001, ***P < 0.001, **Figure 5E**) should be ascribed to ACE2 augmentation and ACE inhibition.

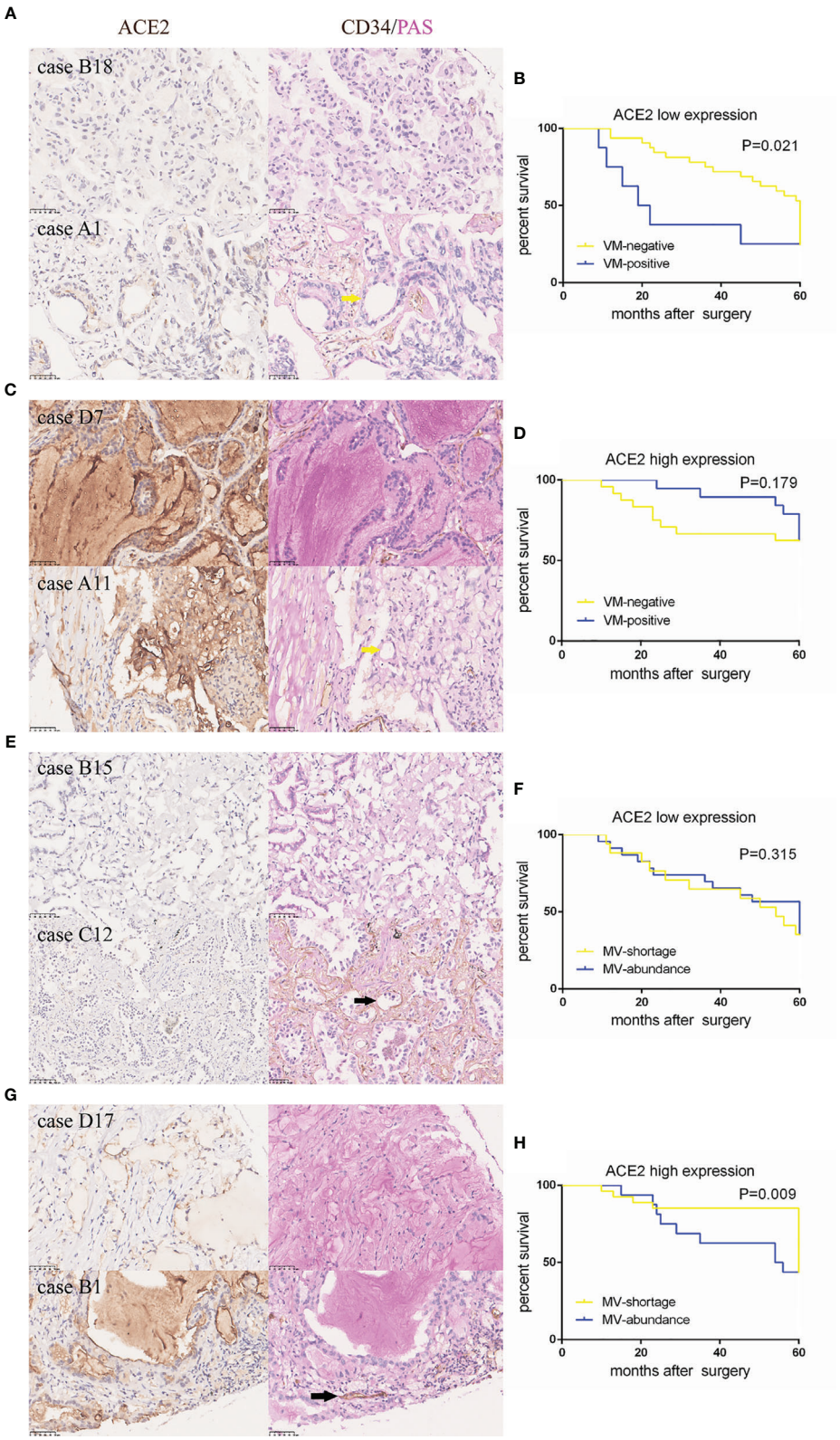

FIGURE 2 | ACE2-induced better outcome in NSCLC patients might be attributed to less vessels and more VM formation. **(A, C, E, G)** Typical tissue images of each group stained with ACE2 or CD34/PAS. Yellow arrows: $CD34^{-}/PAS^{+}$ VMs; black arrows: $CD34^{+}/PAS^{-}$ MV. **(B, D, F, H)** Kaplan–Meier analysis of OS in each group.

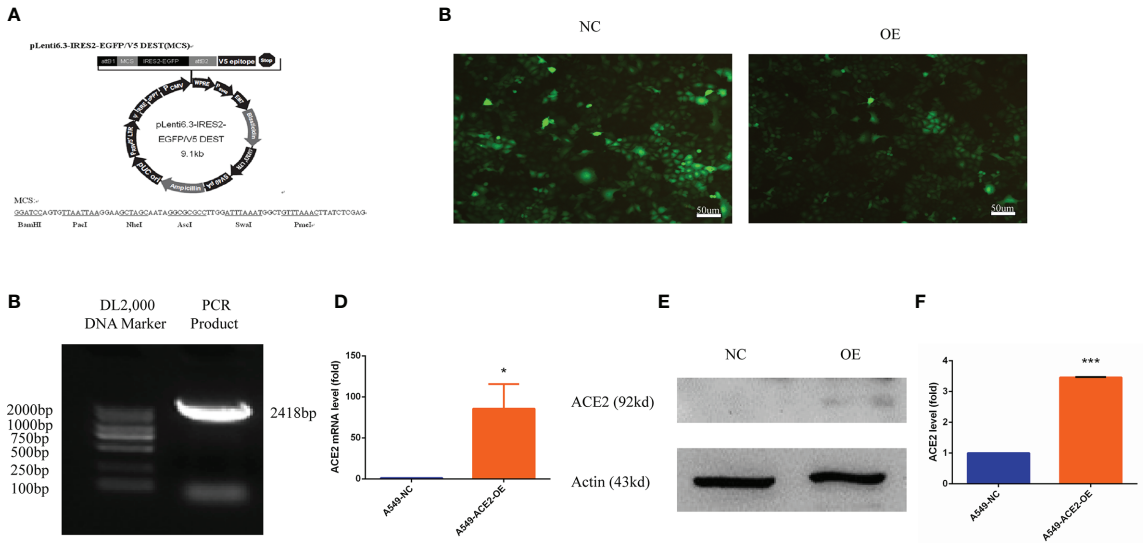

FIGURE 3 | Human ACE2 was stably overexpressed in A549-ACE2-OE cells. **(A)** Schematic representation of pLenti6.3-MCS/V5 DEST. **(B)** pLenti6.3-ACE2 expression vector was detected by PCR. **(C)** Fluorescence of EGFP in A549-ACE2-OE cells (left) and parental cells (right) was determined by fluorescence microscopy. **(D)** RT-PCR experiment of ACE2 mRNA level in A549-ACE2-OE cells and control cells, Mean ± SD, n = 3, *$p < 0.05$. **(E)** Western blot analysis of ACE2 expression level in A549-ACE2-OE cells and parental cells. **(F)** Quantification of ACE2 expression level in A549-ACE2-OE cells and parental cells. Mean ± SD, n = 3, ***$p < 0.001$.

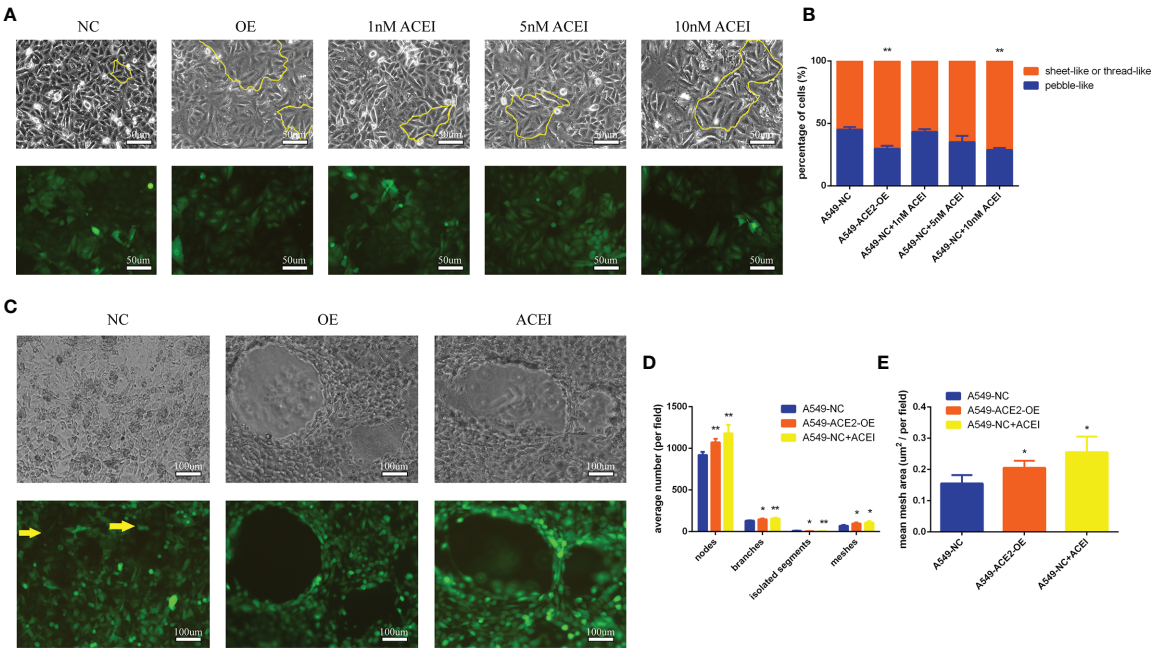

FIGURE 4 | Tube formation ability of A549 cells was improved with ACE inhibitory state. **(A)** Morphologies of a panel of A549-ACE2-OE cells, A549-NC cells, and A549-NC cells treated with ACEI (1, 5, and 10 nM/L) were shown as sheet-like and thread-like cell types in 2D culture, which were outlined partly with yellow lines. Representative images were shown above. Upper: white light; lower: fluorescence. **(B)** Quantification of sheet-like or thread-like cells and pebble-like cells in three groups, representatively, Mean ± SD, n = 3, **$p < 0.01$. **(C)** Images of both above cell lines grown in 3D Matrix gel. A 10 nM/L ACEI dilution was performed. Representative images were shown above. Yellow arrows point out the free cancer cells escaping from tube wall and isolated segments. Upper: white light; lower: fluorescence. **(D, E)** Images of 3D culture were applied to determine average number of nodes, branches, isolated segments, meshes and mean mesh area in those groups, per field, Mean ± SD, n = 3, **$p < 0.01$, *$p < 0.05$. ns, no significance.

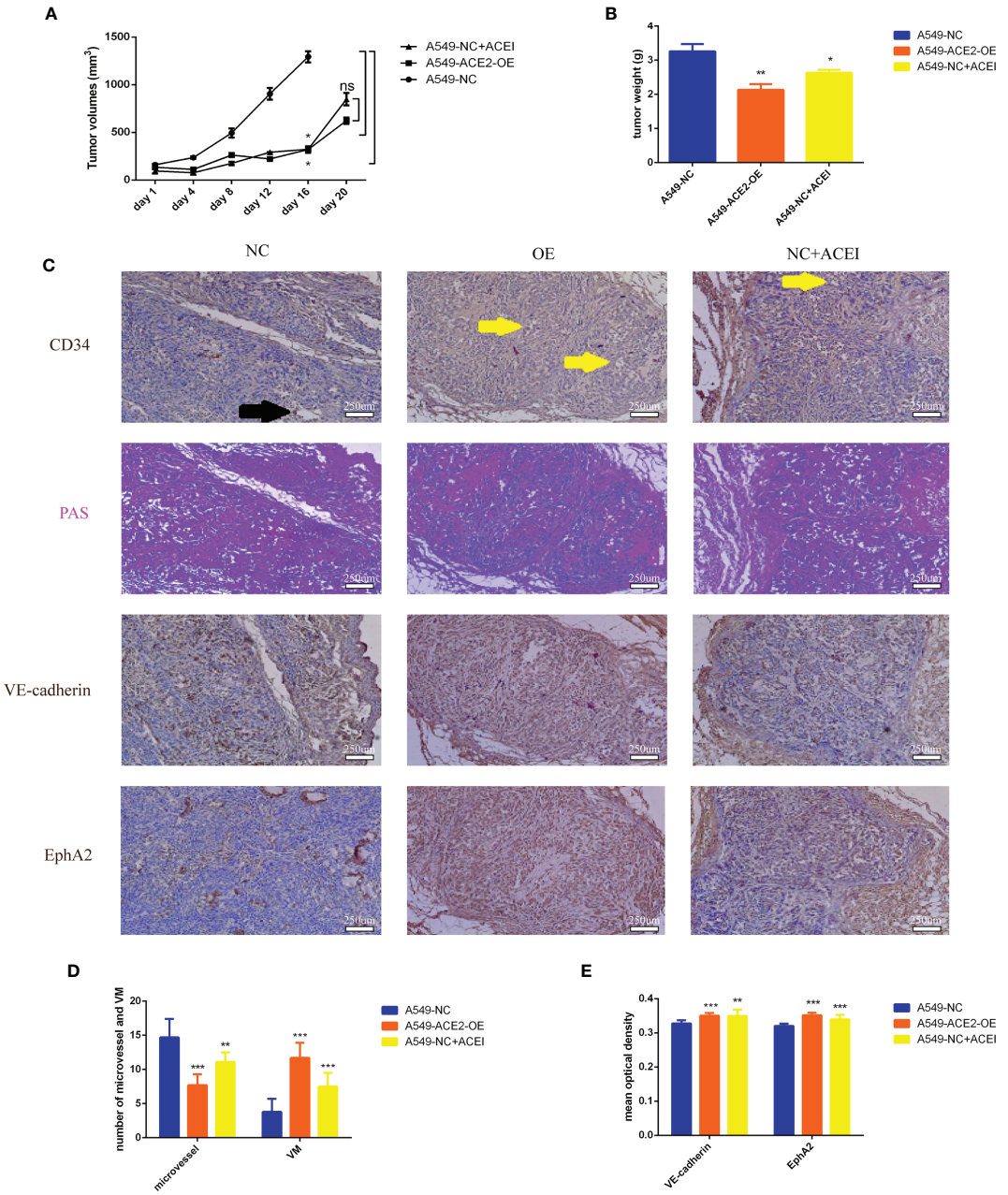

FIGURE 5 | VM formation was increased, and vasculature was lessened due to inhibition of RAS *in vivo*. **(A)** Growth curve of allograft tumors of A549-ACE2-OE cells, A549-NC cells with or without ACEI treatment, Mean ± SD, n = 3, *p < 0.05. ns, no significance. **(B)** Weight of resected tumors, Mean ± SD, n = 3, **p < 0.01, *p < 0.05. **(C)** Continuous sections of allograft tumor tissues stained with PAS, CD34, VE-cadherin, or EphA2 immunohistochemical stain. Black arrow points out a typical MV ($CD34^+/PAS^-$); yellow arrows point out typical VM ($CD34^-/PAS^+$). **(D)** Quantification of MV and VM in different groups, Mean ± SD, n = 3, per field, ***p < 0.001, **p < 0.01. **(E)** Quantification of VE-cadherin and EphA2 mean optical density in three groups, Mean ± SD, n = 3, ***p < 0.001, **p < 0.01.

VE-Cadherin and EphA2 Expression Was Upregulated in A549 Cells and NSCLC Tissues With Impaired Local RAS Status

The accepted crucial VM molecular markers VE-cadherin and EphA2 expression were detected in our ACE2 overexpressing A549 cell model after 3D Matrigel culture. We announced that, by contrast, the elevated ACE2 expression led to approximately 10 times enhancement of VE-cadherin mRNA expression by RT-PCR experiment (***P < 0.001, **Figure 6A**), accompanied by marked upregulation of EphA2 mRNA (***P < 0.001, **Figure 6B**). Accordingly, there were similar trends in VE-cadherin (***P < 0.001, **Figures 6C, D**) and EphA2 (***P <

0.001, **Figures 6C, E**) protein expression level confirmed by Western blot analysis. Similar results were obtained upon transient transfection of NCI-H1650 (**Supplement 2A**).

VE-cadherin (***P < 0.001, **P < 0.01) and EphA2 (***P < 0.001, ***P < 0.001) expression was also heightened in ACE2 high expressing and ACEI disposed allograft tumor tissues (**Figures 5C, E**). In ACE2 high expressing patient cohort, we found that VM number positively corelated with both VE-cadherin (r = 0.7094, P < 0.0001, **Figure 6F**) and EphA2 (r = 0.3848, P = 0.0108, **Figure 6G**) expression at their protein level. Tissues with VE-cadherin$^+$/VM$^+$ in TMA were reviewed, then 2/7 of patients in ACE2 low expressing group and 8/18 of patients in ACE2 high expressing group were found to be expressing VE-cadherin on membrane of tumor cells (**Figure 6H**).

These results proved that VE-cadherin and EphA2 are worthy of molecular markers in ACE2-triggered VM.

PI3K/AKT, p38MAPK, HIF1-a Were Inactivated and Nodal/Notch4 Pathway Was Activated in A549-ACE2-OE Cell Model

Apart from adhesion factors, the changes of vascularity-related classic signal pathways, hypoxia and embryonic/stem cell signaling caused by ACE2 overexpression were unraveled in turn.

Both AKT and p-AKT expression levels were abated relatively (***P < 0.001, ***P < 0.001, **Figures 7A, B**), and what is more, AKT activation by phosphorylation was restrained in A549-ACE2-OE cells compared with paired cells (***P < 0.001, **Figure 7C**). Consistent results were discovered in p38 and p-p38 (**P < 0.01, ***P < 0.001, **Figures 7A, D**, ***P < 0.001, **Figure 7E**).

As for HIF1-a, immunofluorescence affirmed that overexpressing ACE2 remarkably reduced total HIF1-a expression (*P < 0.05) and nuclear HIF1-a accumulation (*P < 0.05) compared with control (**Figures 7F, G**).

Contrarily, compared with that in negative control, Nodal (***P < 0.001) and Notch4 (**P < 0.01) expression levels were correspondingly increased in A549-ACE2-OE cell model (**Figures 7H, I**). Similar results were obtained upon transient transfection of NCI-H1650 (**Supplement 3A, B**).

DISCUSSION

The status of tumor blood supply patterns, including VM channels, mosaic blood vessels, and endothelial vessels, can dynamically exchange with each other along with fluctuations in microenvironment (11). The dynamic balance of local RAS system in tumor is proved to be of great concern to tumor homeostasis. Bound to angiotensin type 1 receptor (AT1), Ang II, with elevated expression in tumor microenvironment, is able to facilitate tumor progression and angiogenesis and results in poor prognosis (13). As part of the negative feedback mechanism in RAS, ACE2 converts Ang II to Ang-(1-7), a peptide with vasodilator and anti-proliferative properties. Besides, ACEI, stopping the transition of Ang I to Ang II catalyzed by ACE, still has a controversial impact on incidence and mortality of cancer (17–19). Previously, description of local RAS regulation among NSCLC blood supply patterns was confined to endothelial vessels, but VM was rarely involved.

VM closely relates to tumor progression, metastasis, and poor survival rate and is generally considered to be a mark emblem of serious neoplastic conditions (5). In the current study, ACE2 protein had a heterogeneous expression in NSCLC tissues, and high ACE2 expression might be protective and might be linked to a better prognosis in NSCLC. During ACE suppression (including ACE2 high status and ACEI-treated condition), NSCLC patients or animal model gained better outcomes, and in addition, this benefit might be achieved by means of both reduced MV and increased VM formation, which seems to contradict general knowledge. Earlier reports hinted VM could also be a consequent of vessel normalization, which usually occurs after anti-VEGF (bevacizumab) and capecitabine therapy (12, 20, 21). Regular and integrated VM in ACE2 high level group should be stronger than immature and discontinuous MV in the low group in barrier function. Therefore, naive vessels might be replaced by solid VM in ACE2 high status to ensure low permeability and guarantee the chemotherapy drugs will arrive at intratumoral designated location.

Apart from vessel normalization, whether there is an ACE2-induced spontaneous VM formation needs to be made clear. An ACE2-OE cell line was used alone to exclude interference from endothelial cells, then quantitative and structural differences were shown. Due to more isolated segments in A549-NC cell production, cancer cells outlining the tubes (**Figure 4G**, yellow arrows) were more readily released into matrix gel, which could reveal the origin of circulating tumor cells on the mechanism and the potential function of VM of prognostic prediction in NSCLC. ACE2 overexpressing endowed NSCLC cells with endothelial phenotype and VM building capacity, but ACE2-induced VM was not as fragile as the general one, which might profit from tight intercellular connections (22).

We elaborated ACE2/ACEI-related VM also had characteristic VE-cadherin and EphA2 expression. Endothelial cells' barrier function is mediated in part by homotypic binding of transmembrane adherent junction proteins such as VE-cadherin. Post-translational VE-cadherin modifications trigger VE-cadherin internalization and increase vascular permeability, which can modulate tumor cell extravasation (23–25). VE-cadherin seemed more likely to appear on membranes of tumor cells instead of nuclei at the ACE2/ACEI-related VM border, which explained solid frame and low probability of metastasis.

Both ACE2/ACEI-related VM and angiogenesis function on tubular fluid-conduction and share vascularity-related classic signal pathways as well as hypoxia cell signaling. Since ACE2/ACEI regulated MV and VM differently, candidate pathways were checked and Nodal/Notch4 was found to be activated in ACE2/ACEI-related VM. Nodal/Notch belongs to the superfamily of the transforming growth factor β (TGF-β) (11). The crosstalk of Notch and Nodal participates in embryonic stem cell maintenance and VM formation in melanoma, breast cancer

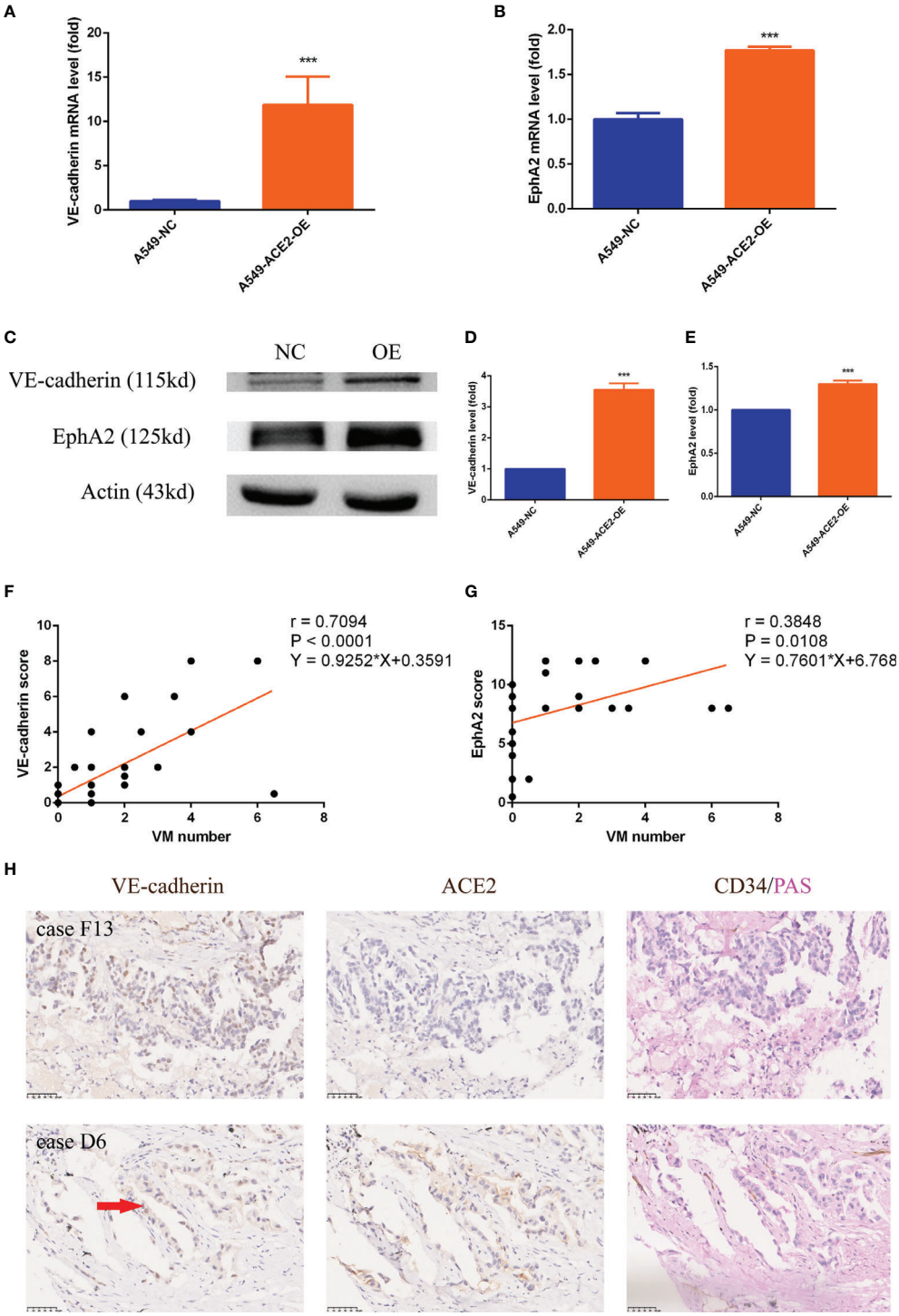

FIGURE 6 | VE-cadherin and EphA2 expression was upregulated in A549 cells and NSCLC tissues with impaired local RAS status. **(A, B)** RT-PCR experiment of VE-cadherin and EphA2 mRNA level in A549-ACE2-OE cells and control cells, Mean ± SD, n = 3, ***p < 0.001. **(C–E)** Western blot analysis and quantification of VE-cadherin and EphA2 expression level in A549-ACE2-OE cells and control cells, Mean ± SD, n = 3, ***p < 0.001. **(F, G)** Linear regressions of VM number and VE-cadherin (P < 0.0001) or EphA2 (P = 0.0108) score in TMA. **(H)** Typical tissue images of both groups stained with VE-cadherin, ACE2 or CD34/PAS. Case F13 with ACE2 low status was provided with rambling VM covered by tumor cells which only expressed VE-cadherin in nuclei; case D6 with ACE2 high status had ordered VM lined by tumor cells expressing VE-cadherin in both nuclei and cytomembranes. Red arrow: VE-cadherin membrane expression.

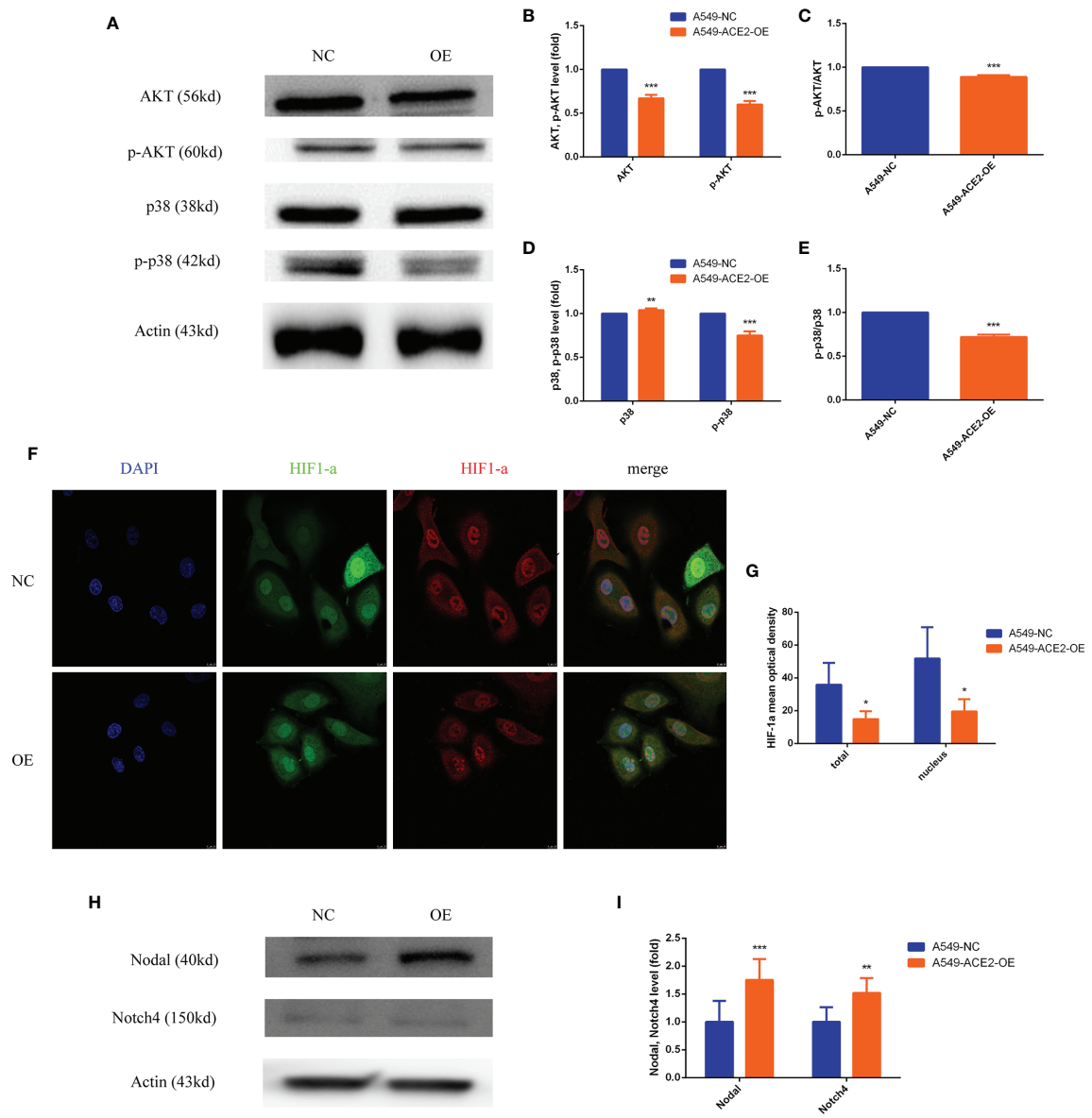

FIGURE 7 | PI3K/AKT, p38MAPK, and HIF1-a were inactivated, and Nodal/Notch4 pathway was activated in A549-ACE2-OE cell model. **(A–E)** Western blot analysis and quantification of AKT, p-AKT, p38, and p-p38 expression level in A549-ACE2-OE cells and negative control, Mean ± SD, n = 3, ***p < 0.001, **p < 0.01. **(F, G)** Immunoflurescence assay and quantification of HIF1-a mean optical density in A549-ACE2-OE cells and negative control, Mean ± SD, n = 4, *p < 0.05. **(H, I)** Western blot analysis and quantification of Nodal and Notch4 expression level in A549-ACE2-OE cells and negative control, Mean ± SD, n = 3, ***p < 0.001, **p < 0.01.

cells (26). However, Nodal is not typically expressed in normal adult tissues including mature vascular endothelial cells. Activated Nodal/Notch4 may mediate enhanced plasticity and VM formation of ACE2/ACEI-treated NSCLC cells.

More attractive, high ACE2 level might prevent females and smokers from NSCLC. Our sample size had limitation, and no multivariable analysis was performed. Patients with high grade clinical stage had no surgical indications and were excluded from this study, which might lead to the irrelevance of ACE2 level and clinical stage. In this research, insufficient cell lines or animals were applied. Because of incomplete medical history, ACEI impact on local RAS and VM was not explored. These defects will be improved in future studies.

Here, we try to portray a macro picture of dynamic change between vascularization and VM formation within aberrant local RAS. In NSCLC, the generation of VM was promoted by ACE2/ACEI, but the generation of MV was inhibited; ACE2/ACEI led to a strong and solid structure of VM; in ACE2 high level group,

patients with VM had better prognoses. VM function is determined by structure, and it seems, not only quantity, but also structure and quality are part of the measure of VM function. High ACE2 level might indicate a relatively comforting prognosis, which suggests an up-to-date direction of NSCLC treatment; but patients with low ACE2 status need to be closely monitored after surgery.

High ACE2 expression improves VM formation quantitatively and structurally, which is conducive to prognosis of NSCLC patients.

DATA AVAILABILITY STATEMENT

The original contributions presented in the study are included in the article/**Supplementary Material**. Further inquiries can be directed to the corresponding author.

ETHICS STATEMENT

The studies involving human participants were reviewed and approved by Ethics Committee of Shanghai Jiao Tong University School of Medicine Affiliated Ruijin Hospital. The patients/participants provided their written informed consent to participate in this study. The animal study was reviewed and approved by Ethics Committee of Shanghai Jiao Tong University School of Medicine Affiliated Ruijin Hospital.

AUTHOR CONTRIBUTIONS

KX and LN designed this study. KX, HH, and HL performed the experiments. YL performed the data analysis. HY and KX wrote this manuscript. All authors agree to be accountable for the content of the work. All authors contributed to the article and approved the submitted version.

FUNDING

Our study is supported by the Shanghai Key Discipline for Respiratory Diseases (2017ZZ02014) and the Science and Technology Commission of Shanghai Municipality (15ZR1426200).

ACKNOWLEDGMENTS

We thank Shanghai Ruisai Biotechnology Co., Ltd for the support of experiment platform and Si Leiyang of Shanghai Tute Technology Co., Ltd for image processing.

SUPPLEMENTARY MATERIAL

The Supplementary Material for this article can be found online at: https://www.frontiersin.org/articles/10.3389/fonc.2021.663671/full#supplementary-material

REFERENCES

1. Siegel RL, Miller KD, Jemal A. Cancer Statistics, 2018. *CA Cancer J Clin* (2018) 68(1):7–30. doi: 10.3322/caac.21442
2. Chen W, Zheng R, Baade PD, Zhang S, Zeng H, Bray F, et al. Cancer Statistics in China, 2015. *CA Cancer J Clin* (2016) 66(2):115–32. doi: 10.3322/caac.21338
3. Rankin EB, Giaccia AJ. Hypoxic Control of Metastasis. *Science (New York NY)* (2016) 352(6282):175–80. doi: 10.1126/science.aaf4405
4. Joyce JA. Therapeutic Targeting of the Tumor Microenvironment. *Cancer Cell* (2005) 7(6):513–20. doi: 10.1016/j.ccr.2005.05.024
5. Luo Q, Wang J, Zhao W, Peng Z, Liu X, Li B, et al. Vasculogenic Mimicry in Carcinogenesis and Clinical Applications. *J Hematol Oncol* (2020) 13(1):19. doi: 10.1186/s13045-020-00858-6
6. Villasante A, Sakaguchi K, Kim J, Cheung NK, Nakayama M, Parsa H, et al. Vascularized Tissue-Engineered Model for Studying Drug Resistance in Neuroblastoma. *Theranostics* (2017) 7(17):4099–117. doi: 10.7150/thno.20730
7. Maniotis AJ, Folberg R, Hess A, Seftor EA, Gardner LM, Pe'er J, et al. Vascular Channel Formation by Human Melanoma Cells In Vivo and In Vitro: Vasculogenic Mimicry. *Am J Pathol* (1999) 155(3):739–52. doi: 10.1016/s0002-9440(10)65173-5
8. Wu S, Yu L, Wang D, Zhou L, Cheng Z, Chai D, et al. Aberrant Expression of CD133 in Non-Small Cell Lung Cancer and its Relationship to Vasculogenic Mimicry. *BMC Cancer* (2012) 12:535. doi: 10.1186/1471-2407-12-535
9. Sun B, Zhang D, Zhang S, Zhang W, Guo H, Zhao X. Hypoxia Influences Vasculogenic Mimicry Channel Formation and Tumor Invasion-Related Protein Expression in Melanoma. *Cancer Lett* (2007) 249(2):188–97. doi: 10.1016/j.canlet.2006.08.016
10. Chiba R, Akiya M, Hashimura M, Oguri Y, Inukai M, Hara A, et al. ALK Signaling Cascade Confers Multiple Advantages to Glioblastoma Cells Through Neovascularization and Cell Proliferation. *PLoS One* (2017) 12(8): e0183516. doi: 10.1371/journal.pone.0183516
11. Delgado-Bellido D, Serrano-Saenz S, Fernández-Cortés M, Oliver FJ. Vasculogenic Mimicry Signaling Revisited: Focus on Non-Vascular VE-Cadherin. *Mol Cancer* (2017) 16(1):65. doi: 10.1186/s12943-017-0631-x
12. Plate KH, Scholz A, Dumont DJ. Tumor Angiogenesis and Anti-Angiogenic Therapy in Malignant Gliomas Revisited. *Acta Neuropathol* (2012) 124 (6):763–75. doi: 10.1007/s00401-012-1066-5
13. Arrieta O, Pineda-Olvera B, Guevara-Salazar P, Hernández-Pedro N, Morales-Espinosa D, Cerón-Lizarraga TL, et al. Expression of AT1 and AT2 Angiotensin Receptors in Astrocytomas is Associated With Poor Prognosis. *Br J Cancer* (2008) 99(1):160–6. doi: 10.1038/sj.bjc.6604431
14. Qian YR, Guo Y, Wan HY, Fan L, Feng Y, Ni L, et al. Angiotensin-Converting Enzyme 2 Attenuates the Metastasis of Non-Small Cell Lung Cancer Through Inhibition of Epithelial-Mesenchymal Transition. *Oncol Rep* (2013) 29 (6):2408–14. doi: 10.3892/or.2013.2370
15. Feng Y, Ni L, Wan H, Fan L, Fei X, Ma Q, et al. Overexpression of ACE2 Produces Antitumor Effects Via Inhibition of Angiogenesis and Tumor Cell Invasion In Vivo and In Vitro. *Oncol Rep* (2011) 26(5):1157–64. doi: 10.3892/or.2011.1394
16. Feng Y, Wan H, Liu J, Zhang R, Ma Q, Han B, et al. The Angiotensin-Converting Enzyme 2 in Tumor Growth and Tumor-Associated Angiogenesis in Non-Small Cell Lung Cancer. *Oncol Rep* (2010) 23(4):941–8. doi: 10.3892/or_00000718
17. Makar GA, Holmes JH, Yang YX. Angiotensin-Converting Enzyme Inhibitor Therapy and Colorectal Cancer Risk. *J Natl Cancer Inst* (2014) 106(2):djt374. doi: 10.1093/jnci/djt374
18. Opelz G, Döhler B. Treatment of Kidney Transplant Recipients With ACEi/ARB and Risk of Respiratory Tract Cancer: A Collaborative Transplant Study Report. *Am J Transplant* (2011) 11(11):2483–9. doi: 10.1111/j.1600-6143.2011.03681.x
19. Attoub S, Gaben AM, Al-Salam S, Al Sultan MA, John A, Nicholls MG, et al. Captopril as a Potential Inhibitor of Lung Tumor Growth and Metastasis. *Ann N Y Acad Sci* (2008) 1138:65–72. doi: 10.1196/annals.1414.011

20. Chae SS, Kamoun WS, Farrar CT, Kirkpatrick ND, Niemeyer E, de Graaf AM, et al. Angiopoietin-2 Interferes With Anti-VEGFR2-Induced Vessel Normalization and Survival Benefit in Mice Bearing Gliomas. *Clin Cancer Res* (2010) 16(14):3618–27. doi: 10.1158/1078-0432.ccr-09-3073
21. Zhang Y, Sun M, Huang G, Yin L, Lai Q, Yang Y, et al. Maintenance of Antiangiogenic and Antitumor Effects by Orally Active Low-Dose Capecitabine for Long-Term Cancer Therapy. *Proc Natl Acad Sci U S A* (2017) 114(26):E5226–e35. doi: 10.1073/pnas.1705066114
22. Quaresmini D, Guida M. Neoangiogenesis in Melanoma: An Issue in Biology and Systemic Treatment. *Front Immunol* (2020) 11:584903. doi: 10.3389/fimmu.2020.584903
23. Delgado-Bellido D, Fernández-Cortés M, Rodríguez MI, Serrano-Sáenz S, Carracedo A, Garcia-Diaz A, et al. VE-Cadherin Promotes Vasculogenic Mimicry by Modulating Kaiso-Dependent Gene Expression. *Cell Death Differ* (2019) 26(2):348–61. doi: 10.1038/s41418-018-0125-4
24. Dejana E, Tournier-Lasserve E, Weinstein BM. The Control of Vascular Integrity by Endothelial Cell Junctions: Molecular Basis and Pathological Implications. *Dev Cell* (2009) 16(2):209–21. doi: 10.1016/j.devcel.2009.01.004
25. Giannotta M, Trani M, Dejana E. VE-Cadherin and Endothelial Adherens Junctions: Active Guardians of Vascular Integrity. *Dev Cell* (2013) 26(5):441–54. doi: 10.1016/j.devcel.2013.08.020
26. Hardy KM, Kirschmann DA, Seftor EA, Margaryan NV, Postovit LM, Strizzi L, et al. Regulation of the Embryonic Morphogen Nodal by Notch4 Facilitates Manifestation of the Aggressive Melanoma Phenotype. *Cancer Res* (2010) 70 (24):10340–50. doi: 10.1158/0008-5472.can-10-0705

Conflict of Interest: The authors declare that the research was conducted in the absence of any commercial or financial relationships that could be construed as a potential conflict of interest.

Copyright © 2021 Xu, Han, Luo, Ye, Lin and Ni. This is an open-access article distributed under the terms of the Creative Commons Attribution License (CC BY). The use, distribution or reproduction in other forums is permitted, provided the original author(s) and the copyright owner(s) are credited and that the original publication in this journal is cited, in accordance with accepted academic practice. No use, distribution or reproduction is permitted which does not comply with these terms.

frontiers in Oncology

ORIGINAL RESEARCH
published: 16 June 2021
doi: 10.3389/fonc.2021.665484

Co-Occurring Potentially Actionable Oncogenic Drivers in Non-Small Cell Lung Cancer

Yiming Zhao[1,2†], Shuyuan Wang[2†], Zhengyu Yang[2†], Yu Dong[2], Yanan Wang[2], Lele Zhang[2], Hai Hu[1] and Baohui Han[2*]*

[1] Department of Medical Oncology, Sun Yat-sen Memorial Hospital, Sun Yat-sen University, Guangzhou, China, [2] Department of Pulmonary Medicine, Shanghai Chest Hospital, Shanghai Jiao Tong University, Shanghai, China

OPEN ACCESS

Edited by:
Hideharu Kimura,
Kanazawa University, Japan

Reviewed by:
Jiajia Zhang,
Johns Hopkins University,
United States
Alessandro Morabito,
Istituto Nazionale Tumori
Fondazione G. Pascale (IRCCS), Italy

***Correspondence:**
Baohui Han
18930858216@163.com
Hai Hu
huhai@mail.sysu.edu.cn

[†]These authors have contributed equally to this work

Specialty section:
This article was submitted to Thoracic Oncology, a section of the journal Frontiers in Oncology

Received: 08 February 2021
Accepted: 16 April 2021
Published: 16 June 2021

Citation:
Zhao Y, Wang S, Yang Z, Dong Y, Wang Y, Zhang L, Hu H and Han B (2021) Co-Occurring Potentially Actionable Oncogenic Drivers in Non-Small Cell Lung Cancer. Front. Oncol. 11:665484. doi: 10.3389/fonc.2021.665484

Background: Several oncogenic drivers in non-small cell lung cancer (NSCLC) are considered actionable with available or promising targeted therapies. Although targetable drivers rarely overlap with each other, there were a minority of patients harboring co-occurring actionable oncogenic targets, whose clinical characteristics and prognosis are not yet clear.

Methods: A total of 3,077 patients with NSCLC who underwent molecular analysis by NGS were included, and their demographic and clinical data were retrospectively collected.

Results: Our study found that the frequency of NSCLC patients harboring co-occurring potentially actionable alterations was approximately 1.5% (46/3077); after excluding patients with *EGFR*-undetermined mutations, the incidence was 1.3% (40/3077); 80% (37/46) harbored both *EGFR* mutations and other potentially actionable drivers such as *MET* amplification (21.6%; 8/37) and alterations in *ERBB2* including mutations (27%; 10/37) and amplification (21.6%; 8/37); other combinations of potentially actionable drivers including alterations in *ERBB2*, *KRAS*, *MET*, *ALK*, and *RET* were also identified. Additionally, *de novo MET/ERBB2* amplification in patients harboring *EGFR*-mutant NSCLC treated with first-generation *EGFR* tyrosine kinase inhibitors (TKIs) was associated with shorter PFS ($p < 0.05$). The efficacy of TKIs in NSCLC patients harboring other co-occurring potentially actionable drivers varied across different molecular subtypes.

Conclusions: Approximately 1.5% of NSCLCs harbored co-occurring potentially actionable oncogenic drivers, commonly involving *EGFR* mutations. Co-occurring actionable targets may impact the efficacy of TKIs; therefore, future clinical trials in these patients should be anticipated to tailor the combination or sequential treatment strategies.

Keywords: non-small cell lung cancer, actionable oncogenic drivers, *EGFR*, tyrosine kinase inhibitors, next-generation sequencing

INTRODUCTION

The heterogeneity of non-small cell lung cancer (NSCLC) is mainly determined by different oncogenic drivers (1). Although dozens of oncogenic drivers are considered to be involved in the development of lung cancer, there are only several actionable targets with widely available targeted therapies, such as *EGFR* mutations, *ALK* rearrangements, *ROS1* rearrangements, *BRAF* V600E mutation, *NTRK* rearrangements, and *RET* rearrangements (2–4). The targeted therapies for *MET* alterations (exon 14 splicing site mutations also known as skipping mutations or amplification), *ERBB2* alterations (mutations or amplification), and *KRAS* G12C mutation also demonstrated promising efficacies in clinical trials, paving a way for precision medicine of NSCLC (4–8).

More and more targeted drugs were put into the first-line setting, greatly influencing the treatment strategies; however, even with the same type of actionable drivers, the efficacy of targeted therapies varies from patient to patient (9). Several studies have proved that both progression-free survival (PFS) and overall survival (OS) of *EGFR* mutant or *ALK* rearranged NSCLCs with *TP53* mutations receiving *EGFR* or *ALK* TKIs, respectively, were significantly lower than those of patients without *TP53* mutations (10–12). Later, increasing evidence has demonstrated that other concomitant alterations such as *RB1* mutations or *PIK3CA* amplification also accelerated the resistance to *EGFR* TKIs (13, 14). In addition to these common co-existing mutations without available targeted drugs, co-occurring targetable oncogenic drivers can also be found in a small number of NSCLCs (15–18); however, there is still little evidence to make precision treatment plans for these patients, whose demographic and clinical characteristics remained largely unknown.

Based on a large population who underwent next-generation sequencing (NGS) in Shanghai Chest Hospital, our study revealed the characteristics and prognosis of NSCLC patients with co-occurring potentially actionable oncogenic drivers, trying to optimize the treatment strategies.

PATIENTS AND METHODS

Patients

Between March 2018 and June 2019, patients with NSCLC analyzed for possible actionable targets by NGS in Shanghai Chest Hospital were enrolled. All patients were diagnosed as adenocarcinoma, squamous cell carcinoma, and other NSCLCs according to World Health Organization criteria assessed by experienced pathologists. The baseline clinical and demographic characteristics including age, gender, pathology, and stage were retrospectively collected. Our study has been approved by the institutional review board of Shanghai Chest Hospital. Written consent forms were obtained from patients before all invasive procedures and initiation of tyrosine kinase inhibitors (TKIs).

Next-Generation Sequencing

NGS is routinely carried out for patients with advanced NSCLCs, especially adenocarcinomas, in our center unless they refuse to do so. Patients with early stage NSCLCs can also choose to receive NGS in case of recurrence. A total of 3,077 formalin-fixed, paraffin-embedded (FFPE) tumor samples acquired from resected lung or small biopsies from NSCLCs were prepared according to standard procedure. Samples with more than 5% tumor content were sent for NGS. Tissue DNA was extracted by QIAamp DNA FFPE Tissue Kit (Qiagen, Hilden, Germany) and then evaluated with the Qubit 3.0 dsDNA assay (Life Technologies, CA, USA). DNA was fragmented by the Covaris M220 Focused-Ultrasonicator (Covaris, Woburn, MA), followed by end repair, phosphorylation, and adaptor ligation. Fragments of 200–400 bp in length were selected using Agencourt AMPure beads (Beckman Coulter, Fullerton, CA, USA), followed by hybridization with capture probes baits, hybrid selection with magnetic beads, and PCR amplification. After evaluating the quality and size of the fragments by a high-sensitivity DNA assay, the samples were sequenced on a Nextseq500 sequencer (Illumina, Inc., San Diego, CA, USA) with paired-end reads. A panel of 68 cancer-related genes described previously (19, 20) were used to detect the genetic alterations of our patients, and the details of our panel are also listed in **Supplemental Table 1**. The mean depth of was >1,000×. The sequencing data in the FASTQ format were mapped to the human genome (hg19) using BWA aligner 0.7.10. Local alignment optimization, variant calling, and annotation were assessed using GATK 3.2, MuTect, and VarScan, respectively. DNA translocation analysis was performed using both Tophat2 and Factera 1.4.3. Gene-level copy number variation was assessed using a *t* test statistic after normalizing read depths at each region by total read number and region size, and correcting GC bias using a locally estimated scatterplot smoothing (LOESS) model.

Defining MET/ERBB2 Amplification According to NGS

Although no consensus exists on the cut-off gene copy number (GCN) for *MET* amplification detected by NGS; however, GCN ≥4 as a cut-off for *MET* amplification by FISH was frequently used in several clinical trials (21, 22). Moreover, a recent study from our hospital using the same sequencing technique showed that *MET*-amplified patients with GCN >4 after crizotinib treatment tended to have longer PFS compared with GCN ≤4 (23). Therefore, the GCN for *MET* amplification in our study was greater than 4.

Similarly, there is still no recommended cut-off for *ERBB2* amplification in NSCLC. However, *ERBB2* amplification using *in situ* hybridization (ISH) in breast cancer according to 2018 ASCO/CAP clinical practice guideline was defined as *ERBB2* GCN ≥6 (24). As a result, an *ERBB2* GCN ≥6 was considered amplified in this study.

Treatment and Follow-Up

EGFR-sensitizing mutations included L858R, L861Q, G719X, and S768I mutations as well as exon 19 deletions; *EGFR*-undetermined mutations refer to other mutations without well-documented clinical significance. Some of NSCLC patients harboring *EGFR*-sensitizing mutations in our study were treated with first-generation *EGFR* TKIs including gefitinib (Iressa, AstraZeneca Pharmaceuticals) (25), erlotinib (Tarceva, Roche) (26), and icotinib (Conmana, Betta) (27) at doses of 250

mg once daily, 150 mg once daily, and 125 mg three times daily, respectively, afatinib (28) (Gilotrif, Boehringer-Ingelheim), and osimertinib (29) (Tagrisso, AstraZeneca Pharmaceuticals) at doses of 40 mg once daily and 80 mg once daily, respectively. *ALK*-rearranged patients were treated with crizotinib (Xalkori, Pfizer) (30) at 250 mg twice daily or alectinib (Alecensa, Roche) (31) at 600 mg twice daily. For some patients with high-level *MET* amplification, crizotinib at 250 mg twice daily was tried. Savolitinib (Hutchison Whampoa) at 600 or 400 mg once daily was given in a clinical trial (NCT02897479) to patients with *MET* exon 14 skipping mutations. Clinical evaluation was performed every 4–6 weeks according to the Response Evaluation Criteria in Solid Tumors (RECIST1.1). Progression-free survival (PFS) was defined from the initiation of TKIs to radiographic or clinical progression or the last follow-up time (January 31, 2020).

Statistical Analysis

The baseline characteristics between *EGFR*-mutant patients and patients with co-occurring actionable drivers receiving *EGFR* TKIs were compared with Chi-square test or two-sample t test as appropriate. Survival curves were generated for comparing PFS and OS by Kaplan–Meier methods and further compared by the log-rank test. A P value of <0.05 was considered statistically significant. All the analyses were performed using the Statistical Package for Social Science (SPSS, Chicago, IL, USA) version 22.0 for Windows.

RESULTS

Baseline Characteristics of All Patients

A total of 3,077 NSCLC patients were analyzed for oncogenic alterations by NGS, among whom, 81% (2481/3077), 11% (333/3077), and 8% (263/3077) were diagnosed as adenocarcinoma, squamous cell carcinoma, and other subtypes, respectively. The detailed characteristics were shown in **Table 1**. Of the patients, 69% (2120/3077) harbored at least one potentially actionable oncogenic drivers, namely *EGFR* mutations, *ALK* rearrangements, *ROS1* rearrangements, *BRAF* V600E mutation, *MET* amplification, *MET* exon 14 skipping mutations, *RET* rearrangements, *NTRK* rearrangements, *ERBB2* alterations (mutations and amplification), and *KRAS* G12C mutation. Among patients with at least one potentially actionable target, 75% (1587/2120) harbored *EGFR* mutations including exon 21 L858R mutation (47%; 750/1587), exon 19 deletions (40%; 634/1587), and other uncommon mutations (13%; 203/1587). The details of all potentially actionable oncogenic targets were listed in **Figure 1A**.

Baseline Characteristics of Patients Harboring Co-Occurring Potentially Actionable Targets

Of the patients, 1.5% (46/3077) had co-occurring potentially targetable oncogenic drivers. The characteristics of these patients were shown in **Table 2**. These patients are commonly seen in females (70 *vs* 30%), non-smokers (76 *vs* 24%), and adenocarcinomas (89 *vs* 11%). 80% (37/46) had *EGFR* mutations and other concomitant potentially actionable drivers, while 20% (9/46) did not harbor *EGFR* mutations. After excluding patients with *EGFR*-undetermined mutations, the remaining patients harboring co-occurring potentially actionable oncogenic drivers accounted for 1.3% (40/3077) of all NSCLCs (**Figure 1B**).

TABLE 1 | Demographic and clinico-pathological characteristics of all patients who underwent NGS.

Variables	
Total number of patients	3077
Age median (range)	62 (22–88)
Gender N (%)	
Male	1561 (51)
Female	1516 (49)
Smoking N (%)	
Yes	1490 (48)
No	1587 (52)
Pathology N (%)	
ADC	2481 (81)
SQCC	333 (11)
Others	263 (8)
Stage	
IA-IIIA	1915 (62)
IIIB-IV	1162 (38)
Potentially targetable drivers	
Yes	2120 (69)
No	957 (31)

ADC, adenocarcinoma; SQCC, squamous cell carcinoma.

A total of 37 (80%; 37/46) patients harbored both *EGFR*-sensitizing (84%; 31/37) or -undetermined (16%; 6/37) mutations and other oncogenic drivers. The concomitant potentially targetable drivers included *de novo MET* amplification (21.6%; 8/37), *de novo ERBB2* amplification (21.6%; 8/37), *ERBB2* mutations (27.0%; 10/37), *KRAS* G12C mutation (8.1%; 3/37), *ALK* rearrangements (5.4%; 2/37), *MET* exon 14 skipping mutations (8.1%; 3/37), *NTRK* rearrangements (5.4%; 2/37), and *RET* rearrangements (2.7%; 1/37). All the molecular subtypes of these patients were shown in **Figure 1B**.

Among the patients harboring co-occurring potentially actionable targets without *EGFR* mutations, 44.4% (4/9) had both *ERBB2* amplification and *ERBB2* mutations; 11.1% (1/9) had *KRAS* G12C mutation and concurrent *MET* amplification; 11.1% (1/9) had *MET* amplification and a concurrent *MET* exon 14 splicing mutation; 22.2% (2/9) harbored both *ALK* rearrangements and *ERBB2* mutations, and one patient (11.1%; 1/9) had *RET* rearrangement and an *ERBB2* mutation (**Figure 1C**).

The Impact of Co-Occurring Potentially Actionable Oncogenic Drivers on Targeted Therapies

A total of 23 patients with co-occurring patterns were treated with different kinds of TKIs, whose treatment types, response, and progression events were shown in a swimmer plot (**Supplemental Figure 1**). A total of 17 *EGFR*-mutant patients with other potentially actionable oncogenic drivers were treated with first-generation *EGFR* TKIs. The demographic and clinical characteristics of these

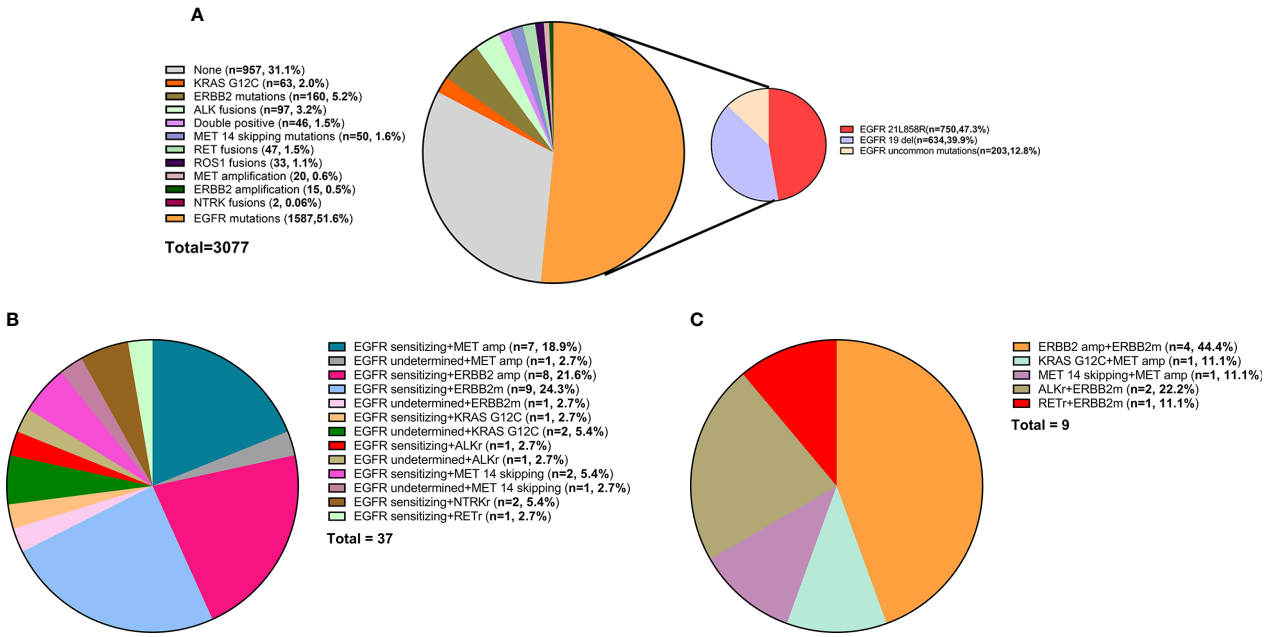

FIGURE 1 | **(A)** The frequency of different oncogenic drivers in all patients. **(B)** Composition of *EGFR*-mutant NSCLC patients harboring other potentially actionable oncogenic drivers. **(C)** Composition of NSCLC patients harboring co-occurring potentially actionable drivers without *EGFR* mutations. Composition of patients with lung adenocarcinoma from MKSCC harboring co-occurring potentially actionable oncogenic drivers. double-positive, with two potentially actionable oncogenic drivers; triple-positive, with three potentially actionable oncogenic drivers; del, deletions; *EGFR* sensitizing, sensitizing *EGFR* mutations, *EGFR* undetermined, undetermined *EGFR* mutations; amp, amplification; *ERBB2*m, *ERBB2* mutation; *MET* 14 skipping, *MET* exon 14 skipping mutation; *ALK*r, *ALK* rearrangement; *NTRK*r, *NTRK* rearrangement; *RETr*, *RET* rearrangement.

TABLE 2 | The demographic and clinico-pathological characteristics of patients harboring co-occurring potentially actionable targets.

Characteristics	
Total number of patients	46
Median age (range)	62 (35–81)
Gender N, (%)	
Male	14 (30)
Female	32 (70)
Smoking N, (%)	
Non-smoker	35 (76)
Smoker	11 (24)
Pathology N, (%)	
ADC	41 (89)
Non-ADC	5 (11)
Stage	
I–IIIA	19 (41)
IIIB–IV	27 (59)

ADC, adenocarcinoma.

patients were listed in **Table 3** and **Supplemental Table 2**. Of patients, 29% (5/17) and 29% (5/17) harbored concurrent *de novo MET* amplifications and *ERBB2* amplifications, respectively. From March 2018 to June 2019, a total of 205 patients with *EGFR* mutations alone who underwent NGS analysis were treated with first-generation *EGFR* TKIs and had full medical records to evaluate the efficacy, whose baseline characteristics including TP53 mutation status were not significantly different from those of *EGFR*-mutant patients harboring other concurrent oncogenic drivers except that there were more females in the double-positive cohort (**Supplemental Table 3**).

As shown in **Figure 2A**, *EGFR*-mutant patients with other concurrent potentially actionable drivers demonstrated significantly lower PFS compared to patients with *EGFR* mutations alone (5.4 *vs* 10.5 months; HR = 1.94, 95% CI: 1.16–3.25, p = 0.0042). Further analysis of molecular subtypes found that both *de novo MET* amplification (2.8 *vs* 10.5 months; HR = 6.03, 95% CI: 2.43–15.00; p < 0.0001) and *de novo ERBB2* amplification (4.2 *vs* 10.5 months; HR = 2.5, 95% CI, 1.03–6.09; p = 0.0005) significantly reduced PFS of *EGFR* TKIs. However, *EGFR*-mutant patients harboring other potentially targetable drivers except *MET*/*ERBB2* amplification showed no significant difference in PFS compared with patients harboring *EGFR* mutations alone (11.0 *vs* 10.5 months; HR = 1.13, 95% CI: 0.48–2.69; p = 0.76) (**Figure 2B**), although the PFS of these patients still fluctuated greatly across different molecular subtypes (**Supplemental Table 2**).

A total of six patients with co-occurring potentially targetable oncogenic drivers were treated with other TKIs. One *EGFR*-mutant patient carrying concurrent *de novo ERBB2* amplification was treated with afatinib, reaching a PFS of 4.6 months, while PFS of one *EGFR*-mutant patient with concurrent *de novo MET* amplification receiving osimertinib was 14.2 months. One *EGFR*-mutant patient with concomitant high-level *MET* amplification

TABLE 3 | The characteristics of *EGFR* mutant patients harboring other potentially actionable drivers treated with first-generation *EGFR* TKIs.

Characteristics	
Total number of patients	17
Median age (range)	60 (35–72)
Gender N, (%)	
Male	3 (18)
Female	14 (82)
Smoking N, (%)	
Non-smoker	14 (82)
Smoker	3 (18)
Pathology N, (%)	
ADC	15 (88)
Non-ADC	2 (12)
EGFR mutation type N, (%)	
21L858R	12 (71)
19del	4 (23)
18G719A	1 (6)
Concomitant alterations N, (%)	
MET amplification	5 (29)
ERBB2 amplification	5 (29)
ERBB2 mutations	3 (18)
MET exon 14 splicing mutation	1 (6)
RET rearrangement	1 (6)
NTRK rearrangement	1 (6)
KRAS G12C mutation	1 (6)

ADC, adenocarcinoma.

(copy number = 8.8) received crizotinib, yet with a PFS of only 2.5 months. One *ALK*-rearranged patient with a concurrent *ERBB2* mutation was treated with alectinib, achieving partial response. One *MET*-amplified patient with a concomitant *MET* exon 14 skipping mutation was treated with crizotinib, having satisfying response with PFS of 14.4 (**Table 4**).

DISCUSSION

Our study found that the incidence of NSCLC patients harboring co-occurring potentially actionable alterations was approximately 1.5% (46/3077), likely to be found in females, non-smokers, and adenocarcinomas. Among these patients, 80% (37/46) harbored *EGFR*-sensitizing (84%; 31/37) or -undetermined (16%; 6/37) mutations and other concurrent potentially targetable oncogenic drivers such as *de novo MET* amplification (21.6%; 8/37) and alterations in *ERBB2* including mutations (27.0%; 10/37) and amplification (21.6%; 8/37). Other concurrent potentially actionable targets in *EGFR*-mutant patients treated with first-generation *EGFR* TKIs were associated with shorter PFS (5.4 *vs* 10.5 months; HR = 1.94, 95% CI: 1.16–3.25, p = 0.0042), suggesting that co-occurring potentially targetable oncogenic drivers may impact the efficacy of *EGFR* TKIs. Further analysis showed that it

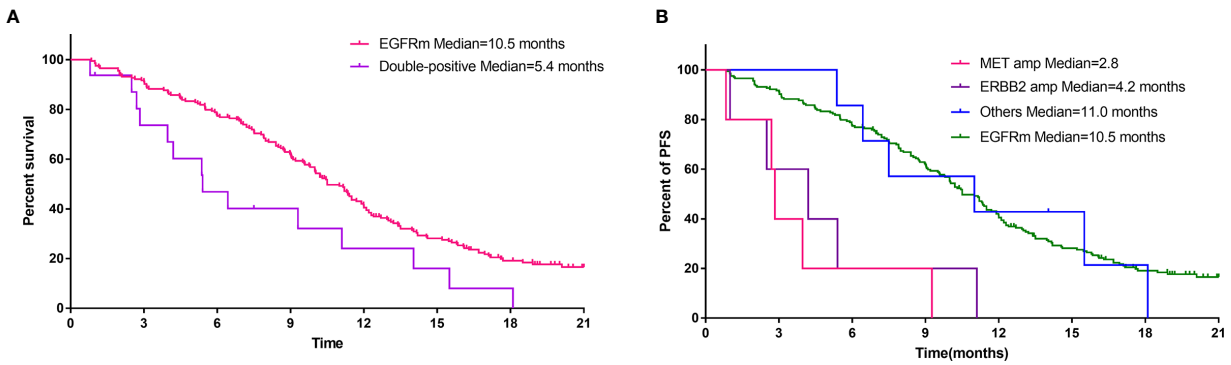

FIGURE 2 | **(A)** Comparison of PFS of first-generation *EGFR* TKIs for patients with EGFR mutations alone and patients harboring both *EGFR* mutations and other potentially actionable oncogenic drivers. **(B)** PFS of first-generation *EGFR* TKIs for *EGFR*-mutant patients with concurrent *MET* amplification, *ERBB2* amplification, and other oncogenic drivers.

TABLE 4 | Characteristics of patients harboring other co-occurring actionable drivers receiving targeted therapies.

No.	Sex	Age, y	Pathology	Smoking	Therapies	Alterations	Stage	Response	PFS
1	female	42	PSC	never	Afatinib	*EGFR* exon 18 G719A + *ERBB2* amp	IV	SD	4.6
2	male	68	SQCC	current	Crizotinib	*EGFR* exon 19 del + *MET* amp (CN=8.8)	IV	SD	2.5
3	male	66	ADC	former	gefitinib+ chemo	*EGFR* exon 11 P411S + *KRAS* exon 2 G12C	IV	PR	13
4	female	41	ADC	never	Alectinib	*EML4*-ALK(E13:A20) +*ERBB2* 27A1216V	IV	PR	11.2*
5	male	70	ADC	former	Crizotinib	*MET* exon 14 skipping mutation + *MET* amp	IV	PR	14.4
6	female	61	ADC	never	Osimertinib	*EGFR* exon 21 L858R + *MET* amp	IV	PR	14.2*

**The diseases have not progressed in these patients at the time of last follow-up.*
PSC, pulmonary sarcomatoid carcinoma; SQCC, squamous cell carcinoma; ADC adenocarcinoma; amp, amplification.

was *de novo MET*/*ERBB2* amplification that played major roles in the primary resistance to first-generation *EGFR* TKIs, while the third-generation *EGFR* TKI, osimertinib, may bring better benefits to these patients. In addition, the efficacy of TKIs in NSCLC patients harboring other co-occurring potentially actionable targets varied across different molecular subtypes with overall encouraging responses.

With the advent and rapid development of NGS, the genomic alterations of lung cancer have been fully investigated, helping to move forward to the era of precision medicine. There are three generations of TKIs for *EGFR* mutations, one of the most common oncogenic drivers in NSCLC. The first-generation *EGFR* TKIs including gefitinib, erlotinib, and icotinib were usually used as the first-line treatments in China due to their wide availability and affordable prices. Our study found that the PFS of the first-generation TKIs in *EGFR*-mutant patients was 10.5 months, similar to the results from previous clinical trials (25–27). Owing to the greatly heterogeneous responses to *EGFR* TKIs across individuals harboring *EGFR* mutations, many research studies were carried out to study the factors that may affect the efficacy, among which, concurrent genomic alterations were mostly investigated. For example, a retrospective study from Korea included patients who underwent molecular analysis by NGS before treatment with first-/second-generation *EGFR* TKIs (cohort 1) or third-generation *EGFR* TKIs after failure in the previous TKIs (cohort 2). Their results showed that *TP53* mutations were independently associated with worse outcomes in cohort 1, while in cohort 2, *TP53*, *RB1*, and *PTEN* mutations as well as *MDM2* amplifications all resulted in shorter PFS (11), suggesting that concurrent genomic alterations accelerated the resistance to *EGFR* TKIs. Additionally, co-occurring *TP53* mutations were reported to be associated with worse outcomes of *EGFR* TKIs in several studies (10, 11, 13, 32). However, these concomitant genetic alterations in previous studies were mostly considered untargetable without available drugs. There are only a few oncogenic drivers in NSCLC having commercially available or promising targeted therapies, including alterations in *EGFR*, *ALK*,*ROS1*, *BRAF*, *MET*, *RET*, *ERBB2*, *NTRK*, and *KRAS*. Although these drivers were considered mutually exclusive previously (33), increasing evidence demonstrated that a minority of NSCLCs harbored co-occurring potentially actionable alterations (17, 34–36), whose overall characteristics remained largely unknown due to the small sample size of previous reports. Our findings showed that the incidence of NSCLC patients harboring co-occurring potentially actionable alterations was approximately 1.5% (46/3077), and they were commonly found in females, non-smokers, and adenocarcinomas.

Similar results were also shown in western populations, although the frequency of oncogenic drivers, especially *EGFR* mutations, in western patients with NSCLC was reported to be lower than that of eastern population (1, 37, 38). The patients with co-occurring potentially actionable targets accounted for 3.6% (31/860) of all lung adenocarcinoma according to the data presented by MSKCC (38). Among these patients, 84% (26/31) harbored *EGFR*-sensitizing (81%; 21/26) or -undetermined (19%; 5/26) mutations with other concurrent potentially actionable drivers including *ERBB2* amplification (50%; 13/26), *MET* amplification (27%; 7/26), *KRAS* G12C mutation (11.5%; 3/26), and *ERBB2* mutations (11.5%; 3/26), similar to the eastern population. There are five (16%; 5/31) patients harboring other types of co-occurring potentially actionable targets. However, the GCNs for *MET*/*ERBB2* amplification were not known in this database.

Among NSCLC patients with co-occurring potentially oncogenic drivers, 80% (37/46) harbored *EGFR* mutations and other concurrent potentially targetable drivers, commonly involving *de novo MET* amplifications (21.6%; 8/37) and alterations in *ERBB2* including mutations (27.0%; 10/37) and amplification (21.6%; 8/37). It was found that concurrent actionable drivers, especially *MET*/*ERBB2* amplification, contributed to the primary resistance to *EGFR* TKIs. *MET* amplification often occurred in *EGFR*-mutant NSCLC after failure of previous TKIs as an acquired resistance mechanism by activating *ERBB3* signaling (39, 40). From a cytological prospective, a small proportion of *EGFR*-mutant cells already harbored *MET* amplifications before initiation of TKIs, finally resulting in drug resistance (41). A previous study showed that approximately 3.2% (5/154) of *EGFR*-mutant patients harbored concurrent *MET* amplifications before treatment with *EGFR* TKIs, and the PFS for these patients was significantly shorter than that of the patients with *EGFR* mutations alone (17), but the sample size was too small to reach a concrete conclusion. In our study, five *EGFR*-mutant patients with concurrent *de novo MET* amplifications treated with first-generation *EGFR* TKIs demonstrated worse PFS compared to the patients with *EGFR* mutations alone, further supporting the conclusion that *de novo MET* amplification contributed to the primary resistance of first-generation *EGFR* TKIs. Additionally, one *EGFR*-mutant patient with high-level *MET* amplification received crizotinib with stable disease lasting for only 2.5 months, suggesting that these patients may respond poorly to only one targeted drug. A phase Ib/II clinical trial demonstrated promising efficacy of capmatinib plus gefitinib after failure of *EGFR* TKIs in patients having *EGFR*-mutant and *MET*-amplified NSCLC with acceptable toxicities (21). Therefore, the combination regimen can also be tried in *EGFR*-mutant patients with *de novo MET* amplifications in clinical practice to overcome primary resistance. Additionally, one *EGFR*-mutant patient with both *de novo MET* amplification was treated with osimertinib, achieving prolonged partial response, suggesting the third-generation *EGFR* TKI, osimertinib, might overcome the primary resistance from *de novo MET* amplification.

Similar to concurrent *de novo MET* amplification, *de novo ERBB2* amplification was also associated with shorter PFS. Approximately 13% of patients with *EGFR*-mutant NSCLC will acquire *ERBB2* amplification after failure of first-generation *EGFR* TKIs. However, the role of *de novo ERBB2* amplification in *EGFR*-mutant NSCLC has not been fully revealed. A previous study showed that 4% (8/200) of all *EGFR*-mutant NSCLC harbored concurrent *ERBB2* amplifications before treatment with TKIs, leading to a shorter PFS compared to patients with *EGFR* mutations alone (14). In our study, it was found patients having both *EGFR*-mutant and *ERBB2* amplified NSCLC treated with first-generation EGFR TKIs reached a median PFS of 4.2 months, which was significantly shorter than that of patients

with EGFR mutations alone (4.2 *vs* 10.5 months; HR = 2.5, 95% CI, 1.03–6.09; p = 0.0005). A recent phase II basket trial demonstrated a 51% response rate in 49 patients with *ERBB2*-amplified or mutant NSCLC treated with ado-trastuzumab emtansine (T-DM1), an anti-*ERBB2*/*HER2* antibody-drug conjugate (ADC), suggesting that ADCs are effective in patients with *ERBB2*-aberrant NSCLC. Therefore, the future clinical trials of *EGFR* TKIs plus ADCs can be launched in *EGFR*-mutant patients with concurrent *ERBB2* amplification.

Additionally, there were *EGFR*-mutant patients harboring other concurrent potentially actionable drivers such as *KRAS* mutations. Sotorasib, a *KRAS* inhibitor, in a recent clinical trial showed encouraging efficacy in patients with heavily pretreated advanced solid tumors harboring *KRAS* G12C mutation, paving a way for targeted therapy in *KRAS*-mutant patients. There are several gene fusions in NSCLC with corresponding targeted drugs including *ALK*, *ROS1*, *RET*, and *NTRK* (42). Although these fusions rarely overlap with other oncogenic drivers (43, 44), our study found that they can co-exist with other actionable targets such as *EGFR* mutations and *ERBB2* mutations. Moreover, there were four patients harboring both *ERBB2* mutations and *ERBB2* amplifications, although a previous study showed that *ERBB2* mutations were not associated with *ERBB2* amplification (45).

There were some drawbacks of our study. Firstly, this was a retrospective study with a relatively small sample size, which cannot avoid selection bias and reflect the entire population with co-occurring potentially actionable oncogenic drivers. Secondly, *MET* and *ERBB2* amplifications were not further confirmed by fluorescence *in situ* hybridization (FISH), although NGS was frequently applied in both clinical trials and routine practice to detect amplifications (6, 8, 21),. Furthermore, several studies showed high concordance between NGS and FISH or immunohistochemistry in detecting amplification (46–48). Additionally, the efficacy of ADCs in *ERBB2*-amplified NSCLC varied across different clinical trials (5, 6, 49); however, a recent study has revealed that the overall response rate by RECIST of T-DM1 in *ERBB2*-amplified NSCLC was 50% (5/10) (6), suggesting *ERBB2* amplification was also a promising target. Moreover, the efficacy of *EGFR* TKIs in some of the *EGFR*-undetermined mutations considered potentially actionable in our study still needed to be explored. Finally, there is a potential risk of confounders by patient clinical characteristics in the survival analysis, especially in the subgroup analysis.

CONCLUSIONS

In conclusion, our study showed approximately 1.5% (46/3077) of all NSCLCs harbored co-occurring potentially actionable oncogenic drivers, commonly involving *EGFR* mutations; after excluding patients with *EGFR*-undetermined mutations, the incidence was 1.3% (40/3077). These patients are likely to be found in females, non-smokers, and adenocarcinomas. In *EGFR*-mutant patients, *de novo MET*/*ERBB2* amplification was associated with shorter PFS, and the combination of *EGFR* and *MET*/*ERBB2* inhibitions or third-generation *EGFR* TKIs can be tried in future to achieve better response. The efficacy of TKIs in NSCLC patients harboring other co-occurring potentially actionable drivers varied across different molecular subtypes. Many molecular subtypes of co-occurring actionable oncogenic drivers were found in our study, suggesting the complexity of oncogene-addicted NSCLC. In order to tailor the combination or sequential treatment strategies, future clinical trials for these patients should be anticipated.

DATA AVAILABILITY STATEMENT

The original contributions presented in the study are included in the article/**Supplementary Material**. Further inquiries can be directed to the corresponding authors.

ETHICS STATEMENT

Ethical approval was not provided for this study on human participants because this was a retrospective study. The patients/participants provided their written informed consent to participate in this study. Written informed consent was obtained from the individual(s) and minor(s)' legal guardian/next of kin for the publication of any potentially identifiable images or data included in this article.

AUTHOR CONTRIBUTIONS

YZ, SW, and ZY have substantial contributions to the conception or design of the work, the collection and analysis of data, the writing and editing of the article. BH and HH contributed to interpretation of data and revision of the manuscript. The rest of the authors have given substantial contributions to the work by providing editing and writing assistance. All authors contributed to the article and approved the submitted version.

FUNDING

This study was supported in part by grants from the State Key Program of National Natural Science of China (8173077) and Shanghai Rising-Star Program (2YF1428100).

SUPPLEMENTARY MATERIAL

The Supplementary Material for this article can be found online at: https://www.frontiersin.org/articles/10.3389/fonc.2021.665484/full#supplementary-material

Supplementary Figure 1 | A swimmer plot for patients with co-occurring patterns treated with different kinds of TKIs. *EGFR*m, *EGFR* mutations alone; double-positive, with two potentially actionable oncogenic drivers; amp, amplification.

REFERENCES

1. Zhang XC, Wang J, Shao GG, Wang Q, Qu X, Wang B, et al. Comprehensive Genomic and Immunological Characterization of Chinese Non-Small Cell Lung Cancer Patients. *Nat Commun* (2019) 10(1):1772. doi: 10.1038/s41467-019-09762-1
2. Hirsch FR, Scagliotti GV, Mulshine JL, Kwon R, Curran WJ Jr, Wu YL, et al. Lung Cancer: Current Therapies and New Targeted Treatments. *Lancet* (2017) 389(10066):299–311. doi: 10.1016/s0140-6736(16)30958-8
3. Drilon A, Laetsch TW, Kummar S, DuBois SG, Lassen UN, Demetri GD, et al. Efficacy of Larotrectinib in TRK Fusion-Positive Cancers in Adults and Children. *N Engl J Med* (2018) 378(8):731–9. doi: 10.1056/NEJMoa1714448
4. Hu Z, Li M, Chen Z, Zhan C, Lin Z, Wang Q. Advances in Clinical Trials of Targeted Therapy and Immunotherapy of Lung Cancer in 2018. *Transl Lung Cancer Res* (2019) 8(6):1091–106. doi: 10.21037/tlcr.2019.10.17
5. Peters S, Stahel R, Bubendorf L, Bonomi P, Villegas A, Kowalski DM, et al. Trastuzumab Emtansine (T-DM1) in Patients With Previously Treated HER2-Overexpressing Metastatic Non-Small Cell Lung Cancer: Efficacy, Safety, and Biomarkers. *Clin Cancer Res* (2019) 25(1):64–72. doi: 10.1158/1078-0432.Ccr-18-1590
6. Li BT, Michelini F, Misale S, Cocco E, Baldino L, Cai Y, et al. Her2-Mediated Internalization of Cytotoxic Agents in ERBB2 Amplified or Mutant Lung Cancers. *Cancer Discov* (2020) 10(5):674–87. doi: 10.1158/2159-8290.Cd-20-0215
7. Hong DS, Fakih MG, Strickler JH, Desai J, Durm GA, Shapiro GI, et al. Kras (G12c) Inhibition With Sotorasib in Advanced Solid Tumors. *N Engl J Med* (2020) 383(13):1207–17. doi: 10.1056/NEJMoa1917239
8. Guo R, Luo J, Chang J, Rekhtman N, Arcila M, Drilon A. MET-Dependent Solid Tumours - Molecular Diagnosis and Targeted Therapy. *Nat Rev Clin Oncol* (2020) 17(9):569–87. doi: 10.1038/s41571-020-0377-z
9. Hong S, Gao F, Fu S, Wang Y, Fang W, Huang Y, et al. Concomitant Genetic Alterations With Response to Treatment and Epidermal Growth Factor Receptor Tyrosine Kinase Inhibitors in Patients With EGFR-Mutant Advanced Non-Small Cell Lung Cancer. *JAMA Oncol* (2018) 4(5):739–42. doi: 10.1001/jamaoncol.2018.0049
10. Hou H, Qin K, Liang Y, Zhang C, Liu D, Jiang H, et al. Concurrent TP53 Mutations Predict Poor Outcomes of EGFR-TKI Treatments in Chinese Patients With Advanced NSCLC. *Cancer Manag Res* (2019) 11:5665–75. doi: 10.2147/cmar.S201513
11. Kim Y, Lee B, Shim JH, Lee SH, Park WY, Choi YL, et al. Concurrent Genetic Alterations Predict the Progression to Target Therapy in EGFR-Mutated Advanced NSCLC. *J Thorac Oncol* (2019) 14(2):193–202. doi: 10.1016/j.jtho.2018.10.150
12. Kron A, Alidousty C, Scheffler M, Merkelbach-Bruse S, Seidel D, Riedel R, et al. Impact of TP53 Mutation Status on Systemic Treatment Outcome in ALK-Rearranged Non-Small-Cell Lung Cancer. *Ann Oncol* (2018) 29 (10):2068–75. doi: 10.1093/annonc/mdy333
13. VanderLaan PA, Rangachari D, Mockus SM, Spotlow V, Reddi HV, Malcolm J, et al. Mutations in TP53, Pik3ca, PTEN and Other Genes in EGFR Mutated Lung Cancers: Correlation With Clinical Outcomes. *Lung Cancer* (2017) 106:17–21. doi: 10.1016/j.lungcan.2017.01.011
14. Yu HA, Suzawa K, Jordan E, Zehir A, Ni A, Kim R, et al. Concurrent Alterations in EGFR-Mutant Lung Cancers Associated With Resistance to EGFR Kinase Inhibitors and Characterization of MTOR as a Mediator of Resistance. *Clin Cancer Res* (2018) 24(13):3108–18. doi: 10.1158/1078-0432.Ccr-17-2961
15. Baldi L, Mengoli MC, Bisagni A, Banzi MC, Boni C, Rossi G. Concomitant EGFR Mutation and ALK Rearrangement in Lung Adenocarcinoma Is More Frequent Than Expected: Report of a Case and Review of the Literature With Demonstration of Genes Alteration Into the Same Tumor Cells. *Lung Cancer* (2014) 86(2):291–5. doi: 10.1016/j.lungcan.2014.09.011
16. Chen RL, Zhao J, Zhang XC, Lou NN, Chen HJ, Yang X, et al. Crizotinib in Advanced Non-Small-Cell Lung Cancer With Concomitant ALK Rearrangement and c-Met Overexpression. *BMC Cancer* (2018) 18(1):1171. doi: 10.1186/s12885-018-5078-y
17. Lai GGY, Lim TH, Lim J, Liew PJR, Kwang XL, Nahar R, et al. Clonal MET Amplification as a Determinant of Tyrosine Kinase Inhibitor Resistance in Epidermal Growth Factor Receptor-Mutant Non-Small-Cell Lung Cancer. *J Clin Oncol* (2019) 37(11):876–84. doi: 10.1200/jco.18.00177
18. Zhu YC, Liao XH, Wang WX, Xu CW, Zhuang W, Wei JG, et al. Dual Drive Coexistence of EML4-ALK and TPM3-ROS1 Fusion in Advanced Lung Adenocarcinoma. *Thorac Cancer* (2018) 9(2):324–7. doi: 10.1111/1759-7714.12578
19. Xiong L, Li R, Sun J, Lou Y, Zhang W, Bai H, et al. Erlotinib as Neoadjuvant Therapy in Stage IIIa (N2) EGFR Mutation-Positive Non-Small Cell Lung Cancer: A Prospective, Single-Arm, Phase II Study. *Oncol* (2019) 24(2):157–e64. doi: 10.1634/theoncologist.2018-0120
20. Zhao Y, Dong Y, Zhao R, Zhang B, Wang S, Zhang L, et al. Expression Profiling of Driver Genes in Female Never-Smokers With Non-Adenocarcinoma Non-Small-Cell Lung Cancer in China. *Clin Lung Cancer* (2020) 21(5):e355–62. doi: 10.1016/j.cllc.2020.02.005
21. Wu YL, Zhang L, Kim DW, Liu X, Lee DH, Yang JC, et al. Phase Ib/II Study of Capmatinib (Inc280) Plus Gefitinib After Failure of Epidermal Growth Factor Receptor (EGFR) Inhibitor Therapy in Patients With EGFR-Mutated, Met Factor-Dysregulated Non-Small-Cell Lung Cancer. *J Clin Oncol* (2018) 36 (31):3101–9. doi: 10.1200/jco.2018.77.7326
22. Angevin E, Spitaleri G, Rodon J, Dotti K, Isambert N, Salvagni S, et al. A First-in-Human Phase I Study of SAR125844, a Selective MET Tyrosine Kinase Inhibitor, in Patients With Advanced Solid Tumours With MET Amplification. *Eur J Cancer* (2017) 87:131–9. doi: 10.1016/j.ejca.2017.10.016
23. Li J, Wang Y, Zhang B, Xu J, Cao S, Zhong H. Characteristics and Response to Crizotinib in Lung Cancer Patients With MET Amplification Detected by Next-Generation Sequencing. *Lung Cancer* (2020) 149:17–22. doi: 10.1016/j.lungcan.2020.08.021
24. Wolff AC, Hammond MEH, Allison KH, Harvey BE, Mangu PB, Bartlett JMS, et al. Human Epidermal Growth Factor Receptor 2 Testing in Breast Cancer: American Society of Clinical Oncology/College of American Pathologists Clinical Practice Guideline Focused Update. *J Clin Oncol* (2018) 36 (20):2105–22. doi: 10.1200/jco.2018.77.8738
25. Mok TS, Wu YL, Thongprasert S, Yang CH, Chu DT, Saijo N, et al. Gefitinib or Carboplatin-Paclitaxel in Pulmonary Adenocarcinoma. *N Engl J Med* (2009) 361(10):947–57. doi: 10.1056/NEJMoa0810699
26. Zhou C, Wu YL, Chen G, Feng J, Liu XQ, Wang C, et al. Erlotinib Versus Chemotherapy as First-Line Treatment for Patients With Advanced EGFR Mutation-Positive Nn-Small-Cell Lung Cancer (OPTIMAL, CTONG-0802): A Multicentre, Open-Label, Randomised, Phase 3 Study. *Lancet Oncol* (2011) 12(8):735–42. doi: 10.1016/s1470-2045(11)70184-x
27. Shi YK, Wang L, Han BH, Li W, Yu P, Liu YP, et al. First-Line Icotinib Versus Cisplatin/Pemetrexed Plus Pemetrexed Maintenance Therapy for Patients With Advanced EGFR Mutation-Positive Lung Adenocarcinoma (CONVINCE): A Phase 3, Open-Label, Randomized Study. *Ann Oncol* (2017) 28(10):2443–50. doi: 10.1093/annonc/mdx359
28. Park K, Tan EH, O'Byrne K, Zhang L, Boyer M, Mok T, et al. Afatinib Versus Gefitinib as First-Line Treatment of Patients With EGFR Mutation-Positive Non-Small-Cell Lung Cancer (LUX-Lung 7): A Phase 2B, Open-Label, Randomised Controlled Trial. *Lancet Oncol* (2016) 17(5):577–89. doi: 10.1016/s1470-2045(16)30033-x
29. Soria JC, Ohe Y, Vansteenkiste J, Reungwetwattana T, Chewaskulyong B, Lee KH, et al. Osimertinib in Untreated EGFR-Mutated Advanced Non-Small-Cell Lung Cancer. *N Engl J Med* (2018) 378(2):113–25. doi: 10.1056/NEJMoa1713137
30. Shaw AT, Kim DW, Nakagawa K, Seto T, Crinó L, Ahn MJ, et al. Crizotinib Versus Chemotherapy in Advanced ALK-Positive Lung Cancer. *N Engl J Med* (2013) 368(25):2385–94. doi: 10.1056/NEJMoa1214886
31. Peters S, Camidge DR, Shaw AT, Gadgeel S, Ahn JS, Kim DW, et al. Alectinib Versus Crizotinib in Untreated Alk-Positive Non-Small-Cell Lung Cancer. *N Engl J Med* (2017) 377(9):829–38. doi: 10.1056/NEJMoa1704795
32. Chen H, Liu M, Dai Z, Li S, Luo Y, Wang Y, et al. Concomitant Genetic Alterations Are Associated With Response to EGFR Targeted Therapy in Patients With Lung Adenocarcinoma. *Transl Lung Cancer Res* (2020) 9 (4):1225–34. doi: 10.21037/tlcr-20-679
33. Gainor JF, Varghese AM, Ou SH, Kabraji S, Awad MM, Katayama R, et al. ALK Rearrangements Are Mutually Exclusive With Mutations in EGFR or KRAS: An Analysis of 1,683 Patients With Non-Small Cell Lung Cancer. *Clin Cancer Res* (2013) 19(15):4273–81. doi: 10.1158/1078-0432.Ccr-13-0318
34. Chen M, Xu Y, Zhao J, Zhong W, Zhang L, Bi Y, et al. Concurrent Driver Gene Mutations as Negative Predictive Factors in Epidermal Growth Factor Receptor-Positive Non-Small Cell Lung Cancer. *EBioMedicine* (2019) 42:304–10. doi: 10.1016/j.ebiom.2019.03.023

35. Tiseo M, Gelsomino F, Boggiani D, Bortesi B, Bartolotti M, Bozzetti C, et al. EGFR and EML4-ALK Gene Mutations in NSCLC: A Case Report of Erlotinib-Resistant Patient With Both Concomitant Mutations. *Lung Cancer* (2011) 71(2):241–3. doi: 10.1016/j.lungcan.2010.11.014
36. Cai W, Lin D, Wu C, Li X, Zhao C, Zheng L, et al. Intratumoral Heterogeneity of ALK-Rearranged and ALK/EGFR Coaltered Lung Adenocarcinoma. *J Clin Oncol* (2015) 33(32):3701–9. doi: 10.1200/jco.2014.58.8293
37. Wen S, Dai L, Wang L, Wang W, Wu D, Wang K, et al. Genomic Signature of Driver Genes Identified by Target Next-Generation Sequencing in Chinese Non-Small Cell Lung Cancer. *Oncol* (2019) 24(11):e1070–81. doi: 10.1634/theoncologist.2018-0572
38. Jordan EJ, Kim HR, Arcila ME, Barron D, Chakravarty D, Gao J, et al. Prospective Comprehensive Molecular Characterization of Lung Adenocarcinomas for Efficient Patient Matching to Approved and Emerging Therapies. *Cancer Discov* (2017) 7(6):596–609. doi: 10.1158/2159-8290.Cd-16-1337
39. Yu HA, Arcila ME, Rekhtman N, Sima CS, Zakowski MF, Pao W, et al. Analysis of Tumor Specimens At the Time of Acquired Resistance to EGFR-TKI Therapy in 155 Patients With EGFR-Mutant Lung Cancers. *Clin Cancer Res* (2013) 19(8):2240–7. doi: 10.1158/1078-0432.Ccr-12-2246
40. Engelman JA, Zejnullahu K, Mitsudomi T, Song Y, Hyland C, Park JO, et al. MET Amplification Leads to Gefitinib Resistance in Lung Cancer by Activating ERBB3 Signaling. *Science (New York NY)* (2007) 316(5827): 1039–43. doi: 10.1126/science.1141478
41. Turke AB, Zejnullahu K, Wu YL, Song Y, Dias-Santagata D, Lifshits E, et al. Preexistence and Clonal Selection of MET Amplification in EGFR Mutant NSCLC. *Cancer Cell* (2010) 17(1):77–88. doi: 10.1016/j.ccr.2009.11.022
42. Gainor JF, Shaw AT. Novel Targets in Non-Small Cell Lung Cancer: ROS1 and RET Fusions. *Oncol* (2013) 18(7):865–75. doi: 10.1634/theoncologist.2013-0095
43. Lin JJ, Ritterhouse LL, Ali SM, Bailey M, Schrock AB, Gainor JF, et al. Ros1 Fusions Rarely Overlap With Other Oncogenic Drivers in Non-Small Cell Lung Cancer. *J Thorac Oncol* (2017) 12(5):872–7. doi: 10.1016/j.jtho.2017.01.004
44. Entrectinib OK'd for Cancers With NTRK Fusions, NSCLC. *Cancer Discov* (2019) 9(10):Of2. doi: 10.1158/2159-8290.Cd-nb2019-101
45. Li BT, Ross DS, Aisner DL, Chaft JE, Hsu M, Kako SL, et al. Her2 Amplification and HER2 Mutation Are Distinct Molecular Targets in Lung Cancers. *J Thorac Oncol* (2016) 11(3):414–9. doi: 10.1016/j.jtho.2015.10.025
46. Cenaj O, Ligon AH, Hornick JL, Sholl LM. Detection of ERBB2 Amplification by Next-Generation Sequencing Predicts Her2 Expression in Colorectal Carcinoma. *Am J Clin Pathol* (2019) 152(1):97–108. doi: 10.1093/ajcp/aqz031
47. Hoda RS, Bowman AS, Zehir A, Razavi P, Brogi E, Ladanyi M, et al. Next-Generation Assessment of Human Epidermal Growth Factor Receptor 2 Gene (ERBB2) Amplification Status in Invasive Breast Carcinoma: A Focus on Group 4 by Use of the 2018 American Society of Clinical Oncology/College of American Pathologists HER2 Testing Guideline. *Histopathology* (2020) 78 (4):498–507. doi: 10.1111/his.14241
48. Robinson CL, Harrison BT, Ligon AH, Dong F, Maffeis V, Matulonis U, et al. Detection of ERBB2 Amplification in Uterine Serous Carcinoma by Next-Generation Sequencing: An Approach Highly Concordant With Standard Assays. *Mod Pathol* (2020) 34(3):603–12. doi: 10.1038/s41379-020-00695-5
49. Kris MG, Camidge DR, Giaccone G, Hida T, Li BT, O'Connell J, et al. Targeting HER2 Aberrations as Actionable Drivers in Lung Cancers: Phase II Trial of the Pan-HER Tyrosine Kinase Inhibitor Dacomitinib in Patients With HER2-Mutant or Amplified Tumors. *Ann Oncol* (2015) 26(7):1421–7. doi: 10.1093/annonc/mdv186

Conflict of Interest: The authors declare that the research was conducted in the absence of any commercial or financial relationships that could be construed as a potential conflict of interest.

Copyright © 2021 Zhao, Wang, Yang, Dong, Wang, Zhang, Hu and Han. This is an open-access article distributed under the terms of the Creative Commons Attribution License (CC BY). The use, distribution or reproduction in other forums is permitted, provided the original author(s) and the copyright owner(s) are credited and that the original publication in this journal is cited, in accordance with accepted academic practice. No use, distribution or reproduction is permitted which does not comply with these terms.

frontiers in Oncology

ORIGINAL RESEARCH
published: 16 June 2021
doi: 10.3389/fonc.2021.644852

Hypofractionated Volumetric-Modulated Arc Radiotherapy for Patients With Non-Small-Cell Lung Cancer Not Suitable for Surgery or Conventional Chemoradiotherapy or SBRT

Junyue Shen[1†], Dan Yang[1†], Mailin Chen[2†], Leilei Jiang[1], Xin Dong[1], Dongming Li[1], Rong Yu[1], Huiming Yu[1] and Anhui Shi[1]*

[1] Department of Radiation Oncology, Key Laboratory of Carcinogenesis and Translational Research (Ministry of Education/Beijing), Peking University Cancer Hospital & Institute, Beijing, China, [2] Departments of Radiology, Key Laboratory of Carcinogenesis and Translational Research, Ministry of Education, Peking University Cancer Hospital and Institute, Beijing, China

OPEN ACCESS

Edited by:
Junji Uchino,
Kyoto Prefectural University of Medicine, Japan

Reviewed by:
Jun Liang,
Chinese Academy of Medical Sciences and Peking Union Medical College, China
Arnold Manfred Herskovic,
Rush University, United States

***Correspondence:**
Anhui Shi
anhuidoctor@163.com

[†]These authors have contributed equally to this work and share first authorship

Specialty section:
This article was submitted to Thoracic Oncology, a section of the journal Frontiers in Oncology

Received: 22 December 2020
Accepted: 20 May 2021
Published: 16 June 2021

Citation:
Shen J, Yang D, Chen M, Jiang L, Dong X, Li D, Yu R, Yu H and Shi A (2021) Hypofractionated Volumetric-Modulated Arc Radiotherapy for Patients With Non-Small-Cell Lung Cancer Not Suitable for Surgery or Conventional Chemoradiotherapy or SBRT. Front. Oncol. 11:644852. doi: 10.3389/fonc.2021.644852

Background: Hypofractionated radiotherapy (HypoRT) has been used to pursue an alternative treatment regimen for patients with non-small-cell lung cancer (NSCLC) who are not eligible for stereotactic ablative radiotherapy (SABR), surgery or concurrent chemoradiotherapy (CCRT) and has shown good local control and safety. We analyzed the feasibility of using volumetric-modulated arc radiotherapy (VMAT) with the simultaneous integrated boost (SIB) technique to achieve high local control with few treatment-related toxicities.

Patients and Methods: A total of 55 patients with stage I-IV NSCLC who were not candidates for SABR, surgery or CCRT were included in the present study. All patients received a prescribed dose of 60 to 66 Gy in 15 fractions. Local progression-free survival (LPFS), PFS, overall survival (OS), and toxicities were retrospectively analyzed.

Results: Thirty-three patients (60.0%) had stage IV or recurrent disease in this study. The median follow-up time was 8 months (interquartile range: 5.0-16.3 months). The 1-year and 2-year OS rates were 84.3% and 69.9%, and the 1-year and 2-year LPFS rates were 91.0% and 63.0%. The median OS (mOS) and median LPFS (mLPFS) were not reached, and median PFS (mPFS) was 15 months. Twenty-eight (51.9%) patients had disease progression at the time of analysis. Of these, 7 (13.0%), 7 (13.0%) and 21 (38.9%) had local recurrence, locoregional failure and distant metastasis, respectively. All cases of local recurrence were found within the SIB region. Four patients had grade 2-3 pneumonitis, and 8 patients had grade 2-3 esophagitis. Patients with grade 2-3 esophagitis had significantly higher maximum dose and dose to 5 cm^3 volume to esophagus than those with grade 0-1 esophagitis. No grade 4 or higher toxicity was observed.

Conclusion: The 60 to 66 Gy in 15 fractions RT regimen provides favorable local control and survival with well-tolerated toxicities. Hypofractionated VMAT+SIB is an alternative treatment option for patients with NSCLC who cannot tolerate standard definitive therapy.

Keywords: radiation therapy, hypofractionation, NSCLC, tumor control, toxicities

INTRODUCTION

Radiation therapy has been commonly used in the treatment of patients with non-small-cell lung cancer (NSCLC). Stereotactic body radiation treatment (SBRT), known as stereotactic ablative radiotherapy (SABR), is being increasingly accepted as a definitive treatment strategy for patients who are not candidates for surgery or refuse surgical resection. Concurrent chemoradiotherapy (CCRT) is the standard treatment option for inoperable, locally advanced NSCLC.

However, some patients with early-stage, inoperable NSCLC are not candidates for SBRT due to the size or location of the lesion (1). In addition, for patients with a poor performance status (PS), CCRT is not always tolerable because the risk of adverse effects outweighs potential treatment benefits. For such patients, RT alone with standard fractionation (60-63 Gy in 30-33 fractions) has been used as front-line therapy, although with a poorer overall survival (OS) and local control. In recent years, increasing attention has been focused on hypofractionated radiotherapy (HypoRT), taking into account its shorter treatment time. With regard to early-stage NSCLC, HypoRT with a treatment dose of 60 Gy in 3-Gy fractions and 48-60 Gy in 4-Gy fractions has indicated potent 2-year local control (2–5). However, for patients with locally advanced NSCLC, or with a poor PS and metastasis, the 45 Gy in 3-Gy fractions HypoRT regimen has only been indicated to provide comparable local control to the standard RT regimen (6, 7). Thus, alternative radiation regimens were explored. More recently, a phase I dose-escalation trial demonstrated that doses up to 60 Gy in 4-Gy fractions were well tolerated in NSCLC patients with a poor PS (8). A previous study reported a favorable outcome with the 60 Gy in 4-Gy fractions regimen compared to the 60-66 Gy (9) in 3-Gy fractions regimen (10, 11). Although HypoRT at a dose of 60 Gy in 4-Gy fractions still showed no difference in OS or progression-free survival (PFS) compared to conventional RT (60 Gy/30 fractions) in a recent interim analysis of a phase III trial, it consumed half of the time and caused less toxicity (12).

HypoRT has been used at our institution for patients with stage I-III NSCLC who are not candidates for surgery, CCRT or SBRT, either due to a comorbidity or tumor size and location. In addition, stage IV patients with a low burden of metastases and a good PS are eligible for this strategy. We used the simultaneous integrated boost (SIB) technique to achieve a gross tumor volume (GTV) dose of over 60 Gy and a planning target volume (PTV) dose of over 45 Gy in 15 fractions. We report our experience with hypofractionated volumetric-modulated arc radiotherapy (VMAT) + SIB, including local control and toxicities.

PATIENTS AND METHODS

Patients Characteristics

This retrospective study was approved by the institutional review board. A total of 55 patients who visited our hospital between December 2017 and November 2020 were included in this retrospective study. The inclusion criteria were as follows: 1) patients with pathologically confirmed NSCLC; 2) patients with stage I-III NSCLC who were not candidates for surgery, SBRT or CCRT; and 3) patients with stage IV NSCLC who had a low burden of metastases and a good PS.

Target Volume and Organ at Risk Delineation

All patients were immobilized in the supine position, and contrast enhanced computed tomography (CT) scans were performed with 3 mm thick slices. The GTV was contoured unless the internal gross target volume (IGTV) was contoured to encompass the tumor throughout the respiratory cycle if a four-dimensional simulation was undertaken. The clinical target volume (CTV), including the primary tumor and metastatic lymph nodes, with a margin of 0.6 to 0.8 cm for microscopic extension of the primary tumor and 0.5 cm for regional lymph nodes (with adaption to the anatomy), was expanded with an additional 5-mm margin to create the PTV. OARs, such as the trachea, great vessels, spinal cord, esophagus, heart and lung, were outlined on each image.

Planning Techniques and Objectives

In all patients, radiation therapy was delivered using the VMAT+SIB technique. The GTV/IGTV was prescribed at a dose of 60-66 Gy, and the PTV was prescribed at a dose of 45-60 Gy. All the treatment plans were designed to deliver prescription doses in 15 fractions using the Eclipse treatment planning system with a 6-MV photon beam from a Varian linear accelerator (True Beam or Edge). All plans aimed to achieve a minimum dose larger than 95%. Given the lack of established dose constraints for OARs using this regimen, we defined the primary objectives as follows based on our experience: trachea: Dmax ≤ 54 Gy; heart: Dmax ≤ 54 Gy; great vessels: Dmax ≤ 60 Gy; esophagus: Dmax ≤ 54 Gy; spinal cord: Dmax ≤ 37.5 Gy; ribs: Dmax ≤ 60 Gy; lungs: V20 ≤ 30%; and mean lung dose ≤ 15 Gy.

Follow-Up Protocol

Patients were examined once per week during the RT course. Patients routinely underwent chest and abdominal contrast-enhanced CT, cranial magnetic resonance imaging (MRI) and superficial lymph node ultrasound 4-6 weeks after the RT course, every 3 months thereafter for the first 2 years, and every 6 months

for the next 3 years. During the follow-up, treatment-related toxicities were evaluated with the Common Terminology Criteria for Adverse Events, version 5.0.

Locoregional failure was defined as a recurrent or progressed lesion within the ipsilateral lung, hilum or mediastinum after RT, while local failure was determined if occurring within the PTV. Failure was further defined as within-SIB-field after a side-by-side comparison of the diagnostic image with the radiation treatment plan if the center of the failure was encompassed by the SIB field. Patients were advised to undergo positron emission tomography (PET) and tissue biopsy if locoregional recurrence was suspected; however, cross-sectional imaging alone was also eligible to determine failure in some patients.

Statistical Analysis

All statistical analyses were performed using IBM SPSS Statistics software, version 23.0.0 (Chicago, IL). OS, PFS, and local PFS (LPFS) were evaluated using the Kaplan-Meier method, and the log-rank test was used to assess the equality of the survivor function across groups. The time-to-event was defined from the start of the RT course to the occurrence of the event. The dosimetric differences between groups were analyzed using student T-test. Differences were considered statistically significant at $P \leq 0.05$.

RESULTS

Patient, Tumor and Treatment Characteristics

Detailed patient, tumor and treatment characteristics are presented in **Table 1**. A total of 55 patients were included in this study, with one patient experiencing myocardial infarction during the RT course. Given his past medical history of coronary heart disease, the myocardial infarction was not considered a treatment-related toxicity, and such patient was not included in the toxicity and survival analyses. Most of the patients had metastatic or recurrent disease (60.0%). Patients with early-stage NSCLC were either inoperable or refused surgical resection and were not candidates for SABR. Patients with locally advanced NSCLC were inoperable and could not tolerate CCRT. Twenty (36.4%) patients had central disease. A central lesion was defined according to International Association for the Study of Lung Cancer (IASLC) guidelines as a GTV located within 2 cm of the bronchial tree, great vessels, heart or spinal cord. All patients completed the RT course and received the prescribed dose. All patients received the prescribed dose, with 8 (14.5%), 21 (38.2%), 1 (1.8%), 5 (9.1%), 20 (36.4%) patients receiving the 60 Gy/45 Gy/15 fractions, 60 Gy/54 Gy/15 fractions, 66 Gy/45 Gy/15 fractions, 66 Gy/54 Gy/15 fractions, and 66 Gy/60 Gy/15 fractions RT regimens, respectively. The majority of the patients (42, 76.4%) received chemo-agent therapy before HypoRT; however, only 16 patients had an interval to the start of RT from the end of the last cycle of chemo-agent therapy of less than 1 month, and 8 of whom received targeted therapy. Thirteen patients received concurrent targeted therapy during the RT course, of theses, 10, 1, 1, and 1 of whom received EGFR-tyrosine kinase inhibitors (TKIs), anlotinib, crizotinib and alectinib, respectively. Post-RT chemo-agent therapy was undertaken in 30 (54.5%) patients, with 12 initiating treatment for disease progression. No patients received immunotherapy before or during the RT course. Eight patients received immunotherapy after RT, with 5 initiating treatment for disease progression and 3 for maintenance therapy.

Survival and Patterns of Failure

A total of 54 patients were included in the survival analysis. The median follow-up time from the start of RT was 8 months (interquartile range: 5.0-16.3 months). The mOS was not reached, and the 1-year and 2-year OS rates were 84.3% and 69.9% (**Figure 1A**). Cancer progression was the most common cause of death in this study. The cause of death was pulmonary embolism in one patient and disseminated intravascular coagulation in another patient.

The mPFS was 15 months, with 12-month, 18-month and 24-month PFS rates of 52.1%, 32.8% and 26.2%, respectively (**Figure 1B**). The median LPFS was not reached, with 1-year and 2-year LPFS rates of 91.0% and 63.0% (**Figure 1C**). **Figure 1** shows the Kaplan-Meier curves for OS, PFS and LPFS for all patients.

Twenty-eight (51.9%) patients had disease progression at the time of analysis. Of these, 7 (13.0%), 7 (13.0%) and 21 (38.9%) had local recurrence, locoregional failure and distant metastasis, respectively. All local recurrences were found within the SIB region, and representative examples are illustrated in **Figure 2**.

The dose to the GTV/IGTV and PTV had no significant influences on OS, PFS and LPFS. No significant differences in survival or failure patterns were found among the RT regimens.

Toxicity

The treatment-related toxicities observed in this study are presented in **Table 2**. Three patients had grade 2 pneumonitis. One patient had fever and persistent cough along with radiologic changes on the thoracic CT imaging 60 days after the end of RT course, and the other two had shortness of breath and cough 127 and 149 days after RT and then found radiologic changes on CT imaging. All patients received glucocorticoid therapy and recovered within 2 months. One patient had grade 3 pneumonitis 76 days after RT and recovered within 3 months after hospitalization. Five patients had grade 2 esophagitis, and 3 patient had grade 3 esophagitis. No grade 4 or higher toxicity was observed. No significant dosimetric difference was found between patients with grade 0-1 pneumonitis and grade 2-3 pneumonitis. Patients experiencing grade 2 and 3 esophagitis had significantly higher maximum dose (47.43 Gy ± 17.03 Gy vs. 30.46 Gy ± 15.69 Gy, $p = 0.007$) and D5cc (30.76 Gy ± 15.13 Gy vs. 15.76 Gy ± 11.04 Gy, $p = 0.003$) to esophagus than those experiencing grade 0 and 1 esophagitis. The mean esophageal dose in patients with grade 2 and 3 esophagitis appeared to be greater than those who had grade 0 and grade 1 esophagitis ($p = 0.079$) (**Table 3**). The sizes of the PTV and GTV/IGTV were not related to pneumonitis or esophagitis. Late treatment-related toxicities were not analyzed in all patients given the short follow-up time. Three and 1 patients observed grade 1 and 2 dysphagia, and 6 patients had grade 1 pulmonary fibrosis.

TABLE 1 | Patient, dosimetry and treatment characteristics.

Characteristic	Patients (n = 55)
Age (yr)	
Median	65.7
Range	32-88
Gender	
Female	24 (43.6)
Male	31 (56.4)
Smoking history (pack-year)	
<30	32 (58.2)
≥30	23 (41.8)
ECOG PS	
0-1	46 (83.6)
2-4	9 (16.4)
Histologic type	
Squamous cell carcinoma	18 (32.7)
Adenocarcinoma	24 (43.6)
Others	13 (23.7)
Gene mutation	
EGFR	14 (25.5)
ALK	2 (3.6)
ROS	1 (1.8)
None detected	11 (20.0)
Unknown	27 (29.1)
PD-L1 expression	
<1%	5 (9.1)
1%-49%	4 (7.3)
≥50%	2 (3.6)
Unknown	44 (80.0%)
AJCC 8th stage	
I	4 (7.3)
II	5 (9.1)
III	13 (23.6)
IV	29 (52.7)
Recurrent	4 (7.3)
Location	
Central	20 (36.4)
Peripheral	35 (63.6)
Target Volume	
Primary	34 (61.8)
Primary and Lymph nodes	21 (38.2)
PTV volume (cm^3)	
Median	149.4
Range	20.3 - 988.4
GTV/IGTV volume (cm^3)	
Median	45.6
Range	2.3 – 438.2
RT regimen (GTV/PTV/fractions)	
60 Gy/54 Gy/15 fractions	21(38.2)
66 Gy/60 Gy/15 fractions	20 (36.4)
Others	14 (25.4)
Chemo-agent therapy[a]	
Induction	16 (29.1)
Concurrent	13 (23.6)
Post-RT	30 (54.5)

Data presented as n (%) or mean ± standard deviation.
[a]including chemotherapy, targeted therapy and immunotherapy.
AJCC, American Joint Committee on Cancer; ECOG PS, Eastern Cooperative Oncology Group performance status; PTV, planning tumor volume; GTV, gross tumor volume; IGTV, interval gross tumor volume; RT, radiotherapy.

DISCUSSION

HypoRT has been investigated in an increasing number of studies in recent years due to its short treatment time. The potential advantages or the shorter treatment time may be threefold: 1) the short RT time may minimize the negative influence of rapid tumor cell proliferation (6); 2) the shorter treatment time can be easier to tolerate for patients with a poor PS; and 3) hypofractionated regimens may be particularly suitable for patients with weak financial repayment ability given their lower treatment costs (although the third advantage will only be considered if HypoRT has acceptable outcomes and treatment-related toxicities).

HypoRT was initially used for patients with NSCLC with a poor PS (13). Nguyen et al. (6) compared a hypofractionated regimen of 45 Gy in 15 fractions to the standard RT regimen of 60-66 Gy over 6 weeks in patients with stage II-III NSCLC. They demonstrated that HypoRT had comparable OS and locoregional control to standard RT despite the significantly poor PS found in HypoRT patients. Moreover, no significant differences in either acute or late toxicity with regard to pulmonary and esophageal toxicities were found between the two groups. A phase I dose-escalation trial (8) indicated that HypoRT consisting of 60 Gy in 15 fractions is generally well tolerated in patients with stage II to IV NSCLC and a poor PS. Furthermore, an interim analysis of a phase III randomized study evaluating survival outcomes in a comparison of standard RT versus HypoRT indicated that the 60 Gy in 15 fractions RT regimen had equivalent OS and PFS outcomes to the conventional RT regimen in patients with stage II-III NSCLC and a poor PS. They also found that fewer grade 3-5 toxicities were observed in the HypoRT arm (12).

More recently, the use of the HypoRT regimen has not been limited to patients with a poor PS (14, 15). Pollom et al. (9) explored HypoRT in patients with stage II-IV NSCLC who were not eligible for surgery, CCRT or SBRT. Most of the patients received 60 Gy in 15 fractions in this study. The mOS was 15.1 months, with a 1-year OS rate of 63% and a 1-year PFS rate of 22.5%. The cumulative incidence of in-field failure at 12 months was 16.1%. Their local control results compared favorably to the outcomes with 60-66 Gy in 3-Gy fractions (10, 11). Swanick et al. (16, 17) investigated HypoRT using the IMRT+SIB technique in a similar group of patients to those examined in the Pollom study. All patients received IGTV doses of 52.5 to 60 Gy and PTV doses of 45 to 52.5 Gy, and most patients received a RT regimen consisting of 52.5 Gy to the IGTV and 45 Gy to the PTV. The mOS was 9.0 months, with 3-, 6-, and 12-month OS rates of 86%, 66%, and 34%, respectively, and 3-month, 6-month, and 12-month LPFS rates of 92%, 78%, and 60%, respectively. Furthermore, they found that 17 (24%) patients had local failure, and all but 1 failure occurred within the high-dose region. These results led to the more frequent use of HypoRT in patients who were not candidates for surgery, CCRT or SBRT in our institutions. The VMAT+SIB technique has been used in our institution in recent years for patients with NSCLC. Since both the 45 Gy in 15 fractions and 60 Gy in 15 fractions RT regimens showed comparable OS, local control, and toxicities to the standard RT regimen and local recurrence was found mostly in the SIB region, we have been using the VMAT+SIB technique to prescribe a high dose to the GTV and a relatively low dose to the PTV to provide satisfactory local control and few toxicities.

All patients received prescribed doses of 60-66 Gy to the IGTV/GTV and 45-60 Gy to the PTV in this study, and

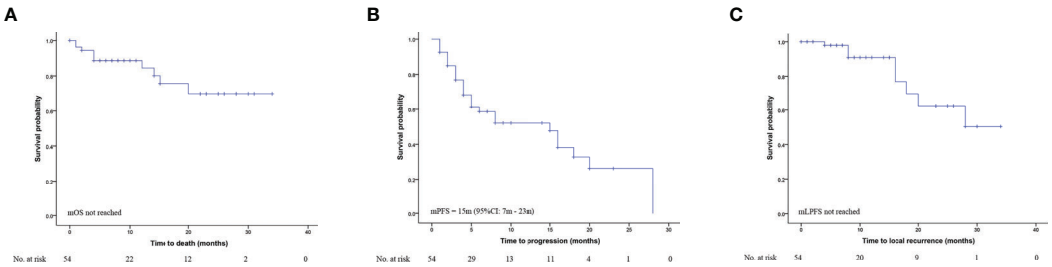

FIGURE 1 | Overall survival **(A)**, Progression free survival **(B)** and Local progression free survival **(C)** for all patients.

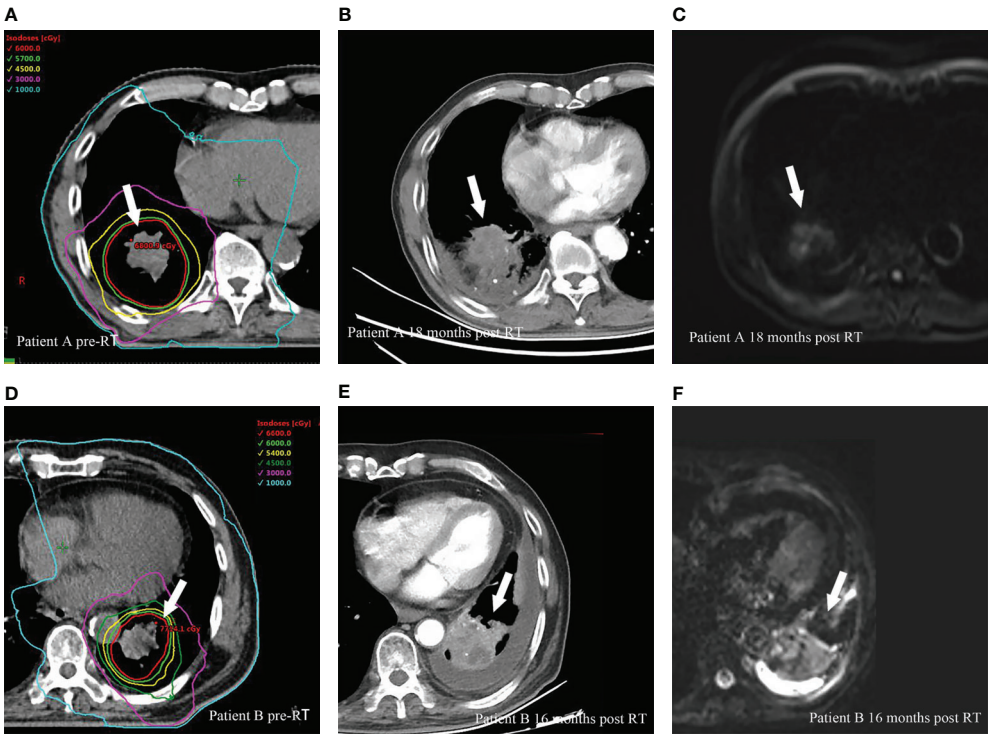

FIGURE 2 | Representative cases of local recurrences within SIB region for two patients after HypoRT treatment. Planning computed tomography fused with isodose levels before RT courses for patient A **(A)**, diagnostic computed tomography **(B)** and magnetic resonance diffusion weighted imaging **(C)** showed a local recurrence (arrows) 18 months after RT. **(D–F)** presented the planning imaging, the local recurrence in diagnostic computed tomography and magnetic resonance diffusion weighted imaging 16 months after RT for patient B.

the majority of patients in our study received either 66 Gy to the IGTV/GTV and 60 Gy to the PTV (n = 20, 36.4%) or 60 Gy to the IGTV/GTV and 54 Gy to the PTV (n = 21, 38.2%). The 1-year OS rate (84.3% vs. 63%), PFS rate (52.1% vs. 22.5%) and LPFS rate (91% vs. 83.9%) were better than those in Pollom group study. Although more patients in our study had stage III and stage IV disease, our patients had younger age, better performance status and smaller PTV volume. In addition, 10 patients received concurrent EGFR-TKIs in our study. Given the recent published results in RECEL study (18), concurrent EGFR-TKIs may result in better prognosis. We obtained a higher LPFS rate at 12 months than Swanick study (91% vs. 60%). Although we prescribed a higher dose to the GTV and PTV than did Swanick (most patients received 52.5 Gy to the IGTV and 45 Gy to the PTV), we hypothesize that this difference is likely attributed to the much smaller size of the PTV observed in our study (149.4 cm3 vs. 421.2 cm3). These findings indicated that better performance status and reasonable tumor burden could be important selection criteria when using this RT regimen. Moreover, we found no significant difference on OS, PFS and LPFS between patients received dose over 60 Gy to GTV/IGTV and those received dose ≤ 60 Gy to GTV/IGTV. Our finding is in

TABLE 2 | Toxicity.

Toxicities	CTCAE, version 5.0				2-3
	0	1	2	3	
Acute toxicities (n=54)					
fatigue	32 (59.3)	14 (25.9)	7 (13.0)	1 (1.9)	8 (14.8)
cough	34 (63.0)	17 (31.5)	3 (5.6)	0	1 (1.9)
pneumonitis	37 (68.5%)	13 (24.1)	3 (5.6)	1 (1.9)	4 (7.4)
esophagitis	44 (81.5)	2 (3.7)	5 (9.3)	3 (5.6)	8 (14.8)
nausea and emesis	38 (70.4)	7 (13.0)	8 (14.8)	1 (1.9)	9 (16.7)
Late toxicities (n=50)					
dysphagia	46 (92.0%)	3 (6.0%)	1 (2.0%)	0	1 (2.0%)
pulmonary fibrosis	42 (84.0%)	8 (16.0%)	0	0	0

Data presented as n (%).
CTCAE, Common Terminology Criteria for Adverse Events.

TABLE 3 | Dose statistics stratified by toxicities grade.

	Grade 2-3	Grade 0-1	P value
Pneumonitis	n = 4	n = 51	
Mean lung dose	7.44 ± 1.96	8.04 ± 3.65	0.748
V5	32.9 ± 13.8	32.2 ± 14.6	0.926
V15	18.8 ± 8.0	16.8 ± 9.0	0.662
V18	13.6 ± 4.2	14.5 ± 7.9	0.809
V20	12.2 ± 4.1	13.2 ± 7.2	0.786
Esophagitis	n = 8	n = 46	
Mean esophagus dose	15.05 ± 9.59	8.02 ± 5.46	0.079
Maximum dose	47.43 ± 17.03	30.46 ± 15.69	0.007
D5cc	30.76 ± 15.13	15.76 ± 11.04	0.003

Data presented as average ± standard deviation.
V5, volume of target receiving at least 5 Gy given as a percent of total lung; V15, volume of target receiving at least 15 Gy given as a percent of total lung; V18, volume of target receiving at least 18 Gy given as a percent of total lung; V20, volume of target receiving at least 20 Gy given as a percent of total lung; D5cc, dose to 5 cm^3 volume.

line with previous studies where have reported inconsistent results between improved tumor control and a prescribed dose over 60 Gy to the tumor volume under conventional RT regimens (19, 20). Despite the lack of prospective dose-escalation studies investigating HypoRT, our results implicate that tumor control is not improved by irradiating tumors at doses over 60 Gy in a 4-Gy per fraction regimen; however, further studies need to be performed to answer this question.

We found only 1 case of grade 3 pneumonitis and 3 cases of grade 3 esophagitis and no cases of grade 4 or 5 toxicities in this study. In accordance with previous studies (8, 9, 21), we found that patients with grade 2-3 esophagitis had significantly higher maximum dose and D5ccto esophagus than those experiencing grade 0-1 esophagitis. However, we found no significant dosimetric differences in pulmonary profiles, e.g., V18 of the lungs. Late toxicities in the lungs and esophagus were assessed in 50 patients who were followed up for more than 3 months, only 3 and 1 patients observed grade 1 and 2 dysphagia, and 6 patients had grade 1 pulmonary fibrosis. Of note, 10 (20%) of these patients were followed up for only 4 or 5 months.

Several limitations to the present study should be acknowledged. First, this was a retrospective study with a relatively short follow-up time. Although short-term outcomes and acute toxicities were assessed, long-term survival and late toxicities could be more interesting given the radiobiological nature of HypoRT. Second, the present study was conducted on a small sample size with multiple confounding factors that may have influenced the outcomes, including clinical stage, tumor volume and chemotherapy options. Third, local failure was determined primarily from CT imaging. MRI, histologic confirmation and PET-CT were not always undertaken except when considered necessary.

In summary, the 60 to 66 Gy in 15 fractions RT regimen provides favorable local control and survival with well-tolerated toxicities. Hypofractionated VMAT+SIB is an alternative treatment option for patients with NSCLC who cannot tolerate SABR, surgery or CCRT.

DATA AVAILABILITY STATEMENT

The raw data supporting the conclusions of this article will be made available by the authors, without undue reservation.

ETHICS STATEMENT

The studies involving human participants were reviewed and approved by Key Laboratory of Carcinogenesis and Translational Research (Ministry of Education/Beijing), Peking University Cancer Hospital & Institute. The patients/participants provided

their written informed consent to participate in this study. Written informed consent was obtained from the individual(s) for the publication of any potentially identifiable images or data included in this article.

AUTHOR CONTRIBUTIONS

JS, DY, and MC finished the majority of data entry and data analysis, and composed the manuscript. These three authors have contributed equally to this work and share first authorship. LJ and XD reviewed the database prior to the data analysis. DL, RY, and HY provided part of the cases and profession advises of the treatment of NSCLC. AS provided most of the cases and gave advises to data analysis and outcomes interpretation. All authors contributed to the article and approved the submitted version.

FUNDING

This study was funded by the Beijing Health and Health Science Technology Achievements and Appropriate Technology Promotion Project (No. BHTPP202026).

This study was funded by Chinese Society of Clinical Oncology (CSCO) – Linghang cancer research (No. Y-2019AZMS-0519).

ACKNOWLEDGMENTS

This present study was supported in part by a grant from Beijing Health and Health Science Technology Achievements and Appropriate Technology Promotion Project (No. BHTPP202026) and a grant from Chinese Society of Clinical Oncology (CSCO) – Linghang cancer research (No. Y-2019AZMS-0519). We thank the American Journal Experts (AJE) for the writing assistance.

REFERENCES

1. Timmerman R, McGarry R, Yiannoutsos C, Papiez L, Tudor K, DeLuca J, et al. Excessive Toxicity When Treating Central Tumors in a Phase II Study of Stereotactic Body Radiation Therapy for Medically Inoperable Early-Stage Lung Cancer. *J Clin Oncol* (2006) 24(30):4833–9. doi: 10.1200/JCO.2006.07.5937
2. Cheung P, Faria S, Ahmed S, Chabot P, Greenland J, Kurien E, et al. Phase II Study of Accelerated Hypofractionated Three-Dimensional Conformal Radiotherapy for Stage T1-3 N0 M0 Non-Small Cell Lung Cancer: NCIC Ctg Br.25. *J Natl Cancer Inst* (2014) 106(8):dju164. doi: 10.1093/jnci/dju164
3. Soliman H, Cheung P, Yeung L, Poon I, Balogh J, Barbera L, et al. Accelerated Hypofractionated Radiotherapy for Early-Stage Non-Small-Cell Lung Cancer: Long-Term Results. *Int J Radiat Oncol Biol Phys* (2011) 79(2):459–65. doi: 10.1016/j.ijrobp.2009.11.003
4. Bogart JA, Hodgson L, Seagren SL, Blackstock AW, Wang X, Lenox R, et al. Phase I Study of Accelerated Conformal Radiotherapy for Stage I Non-Small-Cell Lung Cancer in Patients With Pulmonary Dysfunction: CALGB 39904. *J Clin Oncol* (2010) 28(2):202–6. doi: 10.1200/JCO.2009.25.0753
5. Yung T, Giuliani ME, Le LW, Sun A, Cho BC, Bezjak A, et al. Outcomes of Accelerated Hypofractionated Radiotherapy in Stage I Non-Small-Cell Lung Cancer. *Curr Oncol* (2012) 19(4):e264–9. doi: 10.3747/co.19.976
6. Nguyen LN, Komaki R, Allen P, Schea RA, Milas L. Effectiveness of Accelerated Radiotherapy for Patients With Inoperable Non-Small Cell Lung Cancer (NSCLC) and Borderline Prognostic Factors Without Distant Metastasis: A Retrospective Review. *Int J Radiat Oncol Biol Phys* (1999) 44 (5):1053–6. doi: 10.1016/s0360-3016(99)00130-3
7. Amini A, Lin SH, Wei C, Allen P, Cox JD, Komaki R. Accelerated Hypofractionated Radiation Therapy Compared to Conventionally Fractionated Radiation Therapy for the Treatment of Inoperable Non-Small Cell Lung Cancer. *Radiat Oncol (London Engl)* (2012) 7:33. doi: 10.1186/1748-717X-7-33
8. Westover KD, Loo BW Jr., Gerber DE, Iyengar P, Choy H, Diehn M, et al. Precision Hypofractionated Radiation Therapy in Poor Performing Patients With Non-Small Cell Lung Cancer: Phase 1 Dose Escalation Trial. *Int J Radiat Oncol Biol Phys* (2015) 93(1):72–81. doi: 10.1016/j.ijrobp.2015.05.004
9. Pollom EL, Qian Y, Durkee BY, von Eyben R, Maxim PG, Shultz DB, et al. Hypofractionated Intensity-Modulated Radiotherapy for Patients With Non-Small-Cell Lung Cancer. *Clin Lung Cancer* (2016) 17(6):588–94. doi: 10.1016/j.cllc.2016.05.024
10. Osti MF, Agolli L, Valeriani M, Falco T, Bracci S, De Sanctis V, et al. Image Guided Hypofractionated 3-Dimensional Radiation Therapy in Patients With Inoperable Advanced Stage Non-Small Cell Lung Cancer. *Int J Radiat Oncol Biol Phys* (2013) 85(3):e157–63. doi: 10.1016/j.ijrobp.2012.10.012
11. Harris JP, Chang-Halpenny CN, Maxim PG, Quon A, Graves EE, Diehn M, et al. Outcomes of Modestly Hypofractionated Radiation for Lung Tumors: Pre- and Mid-Treatment Positron Emission Tomography-Computed Tomography Metrics as Prognostic Factors. *Clin Lung Cancer* (2015) 16 (6):475–85. doi: 10.1016/j.cllc.2015.01.007
12. Iyengar P, Westover K, Patel M, Shivnani A, Saunders M, Li Y, et al. A Phase III Randomized Study of Image Guided Conventional (60 Gy/30 Fx) Versus Accelerated, Hypofractionated (60 Gy/15 Fx) Radiation for Poor Performance Status Stage II and III NSCLC Patients—An Interim Analysis. *Int J Radiat Oncol Biol Phys* (2016) 96:E451. doi: 10.1016/j.ijrobp.2016.06.1763
13. Eze C, Taugner J, Roengvoraphoj O, Schmidt-Hegemann NS, Kasmann L, Wijaya C, et al. Initial Report on Feasibility of PET/CT-Based Image-Guided Moderate Hypofractionated Thoracic Irradiation in Node-Positive Non-Small Cell Lung Cancer Patients With Poor Prognostic Factors and Strongly Diminished Lung Function: A Retrospective Analysis. *Radiat Oncol (London Engl)* (2019) 14(1):163. doi: 10.1186/s13014-019-1304-2
14. Koukourakis MI, Patlakas G, Froudarakis ME, Kyrgias G, Skarlatos J, Abatzoglou I, et al. Hypofractionated Accelerated Radiochemotherapy With Cytoprotection (Chemo-HypoARC) for Inoperable Non-Small Cell Lung Carcinoma. *Anticancer Res* (2007) 27(5B):3625–31.
15. Tsoutsou PG, Froudarakis ME, Bouros D, Koukourakis MI. Hypofractionated/Accelerated Radiotherapy With Cytoprotection (HypoARC) Combined With Vinorelbine and Liposomal Doxorubicin for Locally Advanced Non-Small Cell Lung Cancer (NSCLC). *Anticancer Res* (2008) 28(2B):1349–54.
16. Swanick CW, Lin SH, Sutton J, Naik NS, Allen PK, Levy LB, et al. Use of Simultaneous Radiation Boost Achieves High Control Rates in Patients With Non-Small-Cell Lung Cancer Who Are Not Candidates for Surgery or Conventional Chemoradiation. *Clin Lung Cancer* (2015) 16(2):156–63. doi: 10.1016/j.cllc.2014.10.005
17. Swanick CW, Allen PK, Tao R, Olanrewaju AM, Sutton JR, Lin SH, et al. Incidence and Predictors of Chest Wall Toxicity After High-Dose Radiation Therapy in 15 Fractions. *Pract Radiat Oncol* (2017) 7(1):63–71. doi: 10.1016/j.prro.2016.05.009
18. Xing L, Wu G, Wang L, Li J, Wang J, Yuan Z, et al. Erlotinib Versus Etoposide/Cisplatin With Radiation Therapy in Unresectable Stage III Epidermal Growth Factor Receptor Mutation-Positive Non-Small Cell Lung Cancer: A Multicenter, Randomized, Open-Label, Phase 2 Trial. *Int J Radiat Oncol Biol Phys* (2021) 109(5):1349–58. doi: 10.1016/j.ijrobp.2020.11.026
19. Brower JV, Amini A, Chen S, Hullett CR, Kimple RJ, Wojcieszynski AP, et al. Improved Survival With Dose-Escalated Radiotherapy in Stage III Non-Small-Cell Lung Cancer: Analysis of the National Cancer Database. *Ann Oncol* (2016) 27(10):1887–94. doi: 10.1093/annonc/mdw276
20. Werner-Wasik M, Swann RS, Bradley J, Graham M, Emami B, Purdy J, et al. Increasing Tumor Volume is Predictive of Poor Overall and Progression-Free Survival: Secondary Analysis of the Radiation Therapy Oncology Group 93-11 Phase I-II Radiation Dose-Escalation Study in Patients With Inoperable non-Small-Cell Lung Cancer. *Int J Radiat Oncol Biol Phys* (2008) 70(2):385–90. doi: 10.1016/j.ijrobp.2007.06.034
21. Wu AJ, Williams E, Modh A, Foster A, Yorke E, Rimner A, et al. Dosimetric Predictors of Esophageal Toxicity After Stereotactic Body

Radiotherapy for Central Lung Tumors. *Radiother Oncol J Eur Soc Ther Radiol Oncol* (2014) 112(2):267–71. doi: 10.1016/j.radonc.2014.07.001

Conflict of Interest: The authors declare that the research was conducted in the absence of any commercial or financial relationships that could be construed as a potential conflict of interest.

Copyright © 2021 Shen, Yang, Chen, Jiang, Dong, Li, Yu, Yu and Shi. This is an open-access article distributed under the terms of the Creative Commons Attribution License (CC BY). The use, distribution or reproduction in other forums is permitted, provided the original author(s) and the copyright owner(s) are credited and that the original publication in this journal is cited, in accordance with accepted academic practice. No use, distribution or reproduction is permitted which does not comply with these terms.

frontiers in Oncology

ORIGINAL RESEARCH
published: 29 June 2021
doi: 10.3389/fonc.2021.699781

First-Line Chemo-Immunotherapy for Extensive-Stage Small-Cell Lung Cancer: A United States-Based Cost-Effectiveness Analysis

Qiao Liu[1], Xia Luo[1], Lidan Yi[1], Xiaohui Zeng[2] and Chongqing Tan[1]**

[1] Department of Pharmacy, The Second Xiangya Hospital of Central South University, Changsha, China, [2] Department of Nuclear Medicine/PET Image Center, The Second Xiangya Hospital of Central South University, Changsha, China

OPEN ACCESS

Edited by:
Junji Uchino,
Kyoto Prefectural University of Medicine, Japan

Reviewed by:
Pengfei Zhang,
Sichuan University, China
Jiuwei Cui,
The First Hospital of Jilin University, China
Maobai Liu,
Fujian Medical University Union Hospital, China

***Correspondence:**
Xiaohui Zeng
zengxiaohui2008@csu.edu.cn
Chongqing Tan
tanchongqing@csu.edu.cn

Specialty section:
This article was submitted to Thoracic Oncology, a section of the journal Frontiers in Oncology

Received: 24 April 2021
Accepted: 10 June 2021
Published: 29 June 2021

Citation:
Liu Q, Luo X, Yi L, Zeng X and Tan C (2021) First-Line Chemo-Immunotherapy for Extensive-Stage Small-Cell Lung Cancer: A United States-Based Cost-Effectiveness Analysis. Front. Oncol. 11:699781. doi: 10.3389/fonc.2021.699781

Objective: This study aimed to assess the cost-effectiveness of two recently approved first-line chemo-immunotherapies [atezolizumab combined with etoposide and platinum (AEP) and durvalumab combined with etoposide and platinum (DEP)] for patients with extensive-stage small-cell lung cancer (ES-SCLC) in the United States.

Material and Methods: A Markov model was built to compare the cost and effectiveness of AEP, DEP, and etoposide plus platinum (EP) over a 10-year time horizon. Clinical efficacy and safety data were extracted from the IMpower 133 and CASPIAN trials. Health state utilities were obtained from published literature. Costs were collected from an US payer perspective. Deterministic and probabilistic sensitivity analyses were used to explore the uncertainty bound to model parameters.

Results: For the model cohort of adult patients with treatment-naive ES-SCLC, AEP was associated with marginal improved quality adjusted life years (QALYs) by 0.016 and reduced costs by $5,737 compared with DEP. When comparing the two chemo-immunotherapies with EP chemotherapy, AEP and DEP increased the QALYs by 0.162 QALYs and 0.146, respectively. However, both chemo-immunotherapies were associated with substantially health costs than EP, resulting in ICERs of $382,469 per QALY and $464,593 per QALY, respectively.

Conclusion: In this cost-effectiveness study, first-line AEP represented a dominant treatment strategy compared with DEP. Despite neither first-line AEP nor first-line DEP was cost-effective compared with EP chemotherapy, AEP was able to provide a more efficient balance between incremental cost and QALY than DEP. When new combination therapies with remarkable effect become pivotal in the first-line treatment, the price reduction of these drugs may be essential to achieving cost-effectiveness.

Keywords: cost-effectiveness, extensive-stage small-cell lung cancer, atezolizumab, durvalumab, etoposide-platinum

INTRODUCTION

Small cell lung cancer (SCLC) contributes to approximately 14% of all lung malignancies (1, 2), and up to two thirds of patients diagnosed with SCLC are classified as having extensive-stage small-cell lung cancer (ES-SCLC) (3). Over the past few decades, etoposide plus platinum (EP) remained the mainstay of standard-of-care first-line treatment for ES-SCLC, with few alternatives (4–6). Although ES-SCLC is highly sensitive to first-line chemotherapy, almost all cases experience a recurrence within 6 months, resulting in a dismal prognosis with a 5-year survival rate lower than 5% (7, 8). To improve patients' prognosis and outcomes, immune checkpoint inhibitors (ICIs) in combination with EP chemotherapy has emerged as a new first-line treatment option for ES-SCLC.

Atezolizumab was the first ICI approved by the US Food and Drug Administration (FDA) in March 2019 to combine with EP chemotherapy as a first-line option for treating ES-SCLC (9). The study underpinning this approval was a randomized phase III IMpower 133 trial (ClinicalTrials.gov number:NCT02763579) showing that the combination therapy of atezolizumab and EP chemotherapy significantly improved overall survival (OS) and progression-free survival (PFS) in patients with ES-SCLC compared with the standard-of-care EP chemotherapy (10). Driven by this promising result, there is a growing interest in exploring novel chemo-immunotherapy. At the end of 2019, the randomized phase III trial, CASPIAN (ClinicalTrials.gov number: NCT03043872), demonstrated that adding durvalumab to the first-line EP chemotherapy significantly improve patients' survival compared with EP chemotherapy (11). Based on these data, durvalumab in combination with EP became the second chemo-immunotherapy approved for the first-line treatment for ES-SCLC (12).

The introduction of chemo-immunotherapy in the first-line setting of ES-SCLC is of great clinical importance and significance, given that a potentially huge population may benefit from the two innovative combination therapies. A total of 235,760 new cases of lung cancers were projected to occur in the United States in 2021 (13), forming a potential beneficiary population of nearly 22,000 ES-SCLC patients. Although the approval of the two chemo-immunotherapies represented a major step forward in providing more successful strategies for the first-line treatment of ES-SCLC, their prohibitive cost cannot be ignored, given the growing demand of providing value-based healthcare in the US (14). Thus, cost-effectiveness studies to assess the clinical benefits and potential financial consequences of an innovative combination therapy are necessary to determine the appropriateness of its widespread use.

Previous US-based studies demonstrated that adding atezolizumab or durvalumab to the first-line EP chemotherapy were associated with higher costs and greater benefits and concluded that the combinations were not a cost-effective choice for ES-SCLC as compared with chemotherapy alone (15, 16). Despite this, these two combination therapies are recommended as the first-line treatment for ES-SCLC over EP chemotherapy alone in the current treatment guidelines (17). However, whether these two approved chemo-immunotherapies are similarly cost-effective, or one is superior to another, remains unclear due to lack of relevant evidence. To answer this question, we conducted this study to compare the cost-effectiveness of atezolizumab combined with etoposide and platinum (AEP) and durvalumab combined with etoposide and platinum (DEP) among ES-SCLC patients from an US payer perspective

MATERIALS AND METHODS

This economic evaluation used existing patient data from two published phase III clinical trials (the IMpower 133 trial and the CASPIAN trial) and did not involve human subject research. Therefore, it was deemed exempt from the institutional review board approval. Our study followed the Consolidated Health Economic Evaluation Reporting Standards (CHEERS) reporting guideline.

Using TreeAge Pro 2020 software (TreeAge Software LLC), we constructed a Markov model to compare the long-term health and cost outcomes of patients with ES-SCLC. Three first-line treatment options were evaluated in our model, including two chemo-immunotherapies (AEP and DEP), and the traditional EP chemotherapy. Adding an EP chemotherapy group into the model is because EP chemotherapy is still recommended as a first-line option for ES-SCLC based on the latest national comprehensive cancer network (NCCN) guidelines (17).

Patients and Treatment

Model patients in the AEP group and the DEP group mirrored the cohorts of participants that were enrolled in the IMpower 133 and CASPIAN trial, respectively (10, 12). We assumed the model patient cohort in the EP group was a combination of two chemotherapy groups in the IMpower 133 and CASPIAN trials. First-line treatment schedule and dosage followed those detailed by the abovementioned two clinical trials. **Supplementary Table 1** in the Supplement provides detail information on each first-line treatment.

After progression, subsequent therapy options for ES-SCLC patients are generally limited, and the current standard-of-care is chemotherapy with topotecan. Considering that other subsequent therapy types are far less used than the topotecan chemotherapy and the specific drugs for subsequent therapies were not detailed in these two clinical trials, we modeled patients as receiving only topotecan as the subsequent therapy. In the IMpower 133 and CASPIAN trials, almost half of patients who exhibited evidence of disease progression were reported to receive a subsequent therapy (51.7% in the AEP group; 42.0% in the DEP group, and a pooled estimated of 51.6% in the EP group) (10, 12). Subsequent topotecan treatment schedule and dosage were given based on the representative clinical trial (18).

Model Construction

We constructed a Markov model consisting of three health states in this cost-effectiveness analysis: PFS, progressed survival (PS), and death (**Figure 1**). All ES-SCLC patients entered the model in PFS state and could receive three first-line treatments randomly. In the PS state, patients were considered for topotecan if there was a

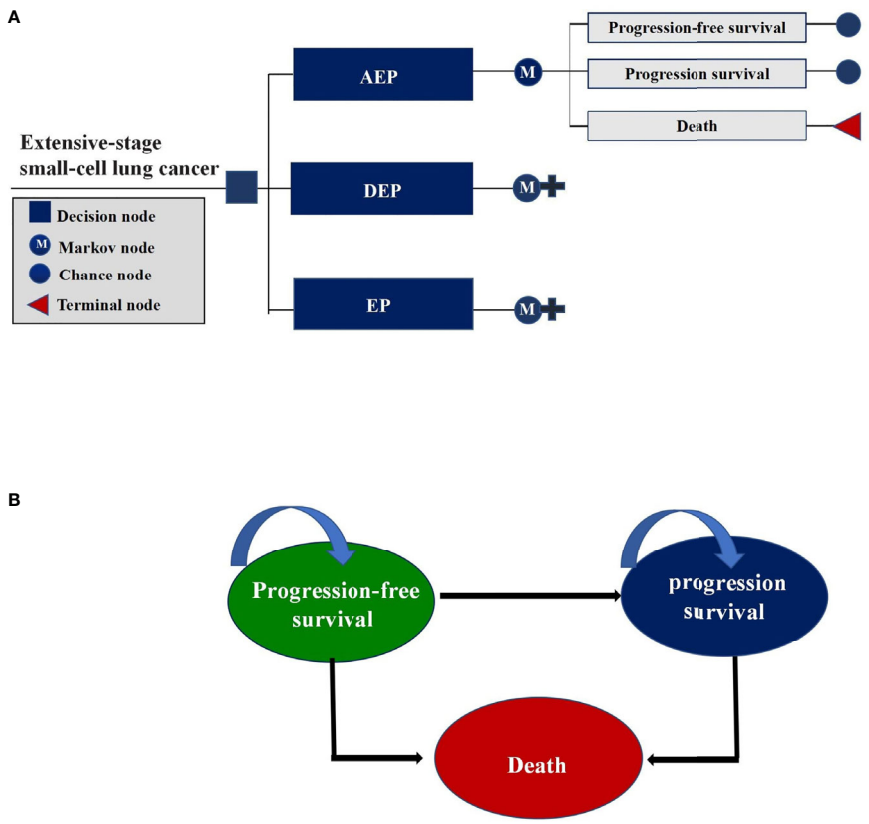

FIGURE 1 | Markov Model. **(A)** Schematics of the decision tree showing 3 treatment strategies compared in our model for patients with extensive-stage small-cell lung cancer; **(B)** Markov state transition model diagram showing 3 health states that represented the process of disease progression. M indicates Markov model.

continued benefit; otherwise, supportive treatment was considered (17). To better accommodate the current clinical practice, patients were assumed to receive palliative care before death.

In view of the clinical treatment plan and the expected overall survival time of ES-SCLC, a 3-week Markov cycle and a 10-year time horizon were chosen for our model to project the cumulative costs and effectiveness in quality adjusted life years (QALYs) for each treatment strategy. Cost-effectiveness was assessed by the incremental cost-effectiveness ratios (ICERs) between treatment strategies under comparison, which reflected the incremental cost for each QALYs gained. In this analysis, ICERs were compared with a willingness-to-pay (WTP) of $100,000 per QALY gained (19), and both costs and effectiveness were discounted at an annual rate of 3%. The Markov model was constructed using TreeAge Pro software (version 2021, https://www.treeage.com/), and parametric survival modeling was performed using R software (version 4.0.4, http://www.r-project.org).

Transition Probabilities

Transition probabilities were estimated from the IMpower 133 and CASPIAN trials (10, 12). For AEP group, the OS and PFS data over first 2 years were extracted from the Kaplan-Meier (KM) curves using GetData Graph Digitizer software package (version 2.26; http://getdata-graph-digitizer.com/index.php), and best fit with log-logistic survival distribution according to the Akaike's information criterion (AIC) and Bayesian information criterion (BIC) (**Supplementary Table 2** and **Figure 1**). For DEP group, the log-logistic survival distribution was adjusted using the HRs of OS and PFS for DEP versus AEP generated by network meta-analysis, and the survival rates for DEP were calculated according to the following formula: $S_{DEP} = (S_{AEP})^{HR}$. For EP chemotherapy, using the method proposed by Hoyle et al. (20), we recreated two sets of individual patient-level OS and PFS data based on the IMpower 133 trial and the CASPIAN trial, respectively. Then we integrated the two sets of PFS and OS data into the PFS and OS data of EP group in our model. Weibull distribution was used to fit these integrated PFS and OS data (**Supplementary Table 2** and **Figure 1**). The final distribution parameters used to calculate the transition probabilities were outlined in **Table 1**.

PFS projections beyond the 2-year follow-up period were based on the survival distributions selected for the estimated PFS data for first 2 years. OS projections beyond the 2-year follow-up period were based on Surveillance, Epidemiology, and End Results data from 2000 to 2017 for patients with ES-SCLC which allowed the overall survival of ES-SCLC to closely reflect clinical practice (**Supplementary Table 3**) (26).

TABLE 1 | Model Parameters and Assumptions.

Parameters	Baseline value	Ranges	Distribution	Ref
Survival				
Log-logistic survival model for AEP[a]				
OS	θ=0.003072, κ=2.297440	–	–	(10)
PFS	θ=0.008895, κ=2.852489	–	–	(10)
HR for AEP *vs* DEP[b]				
OS	1.04	0.83–1.25	Lognormal	(10, 12)
PFS	1.01	0.81–1.21	Lognormal	(10, 12)
Weibull survival model for EP[c]				
OS	λ=0.016073, γ=1.593409	–	–	(10, 12)
PFS	λ=0.042826, γ=1.712046	–	–	(10, 12)
Costs				
Atezolizumab price/mg	7.83	5.87–9.78	Gamma	(21)
Durvalumab price/mg	7.60	5.70–9.50	Gamma	(21)
Etoposide price/mg	1.51	1.13–1.89	Gamma	(21)
Carboplatin price/mg	0.06	0.04–0.07	Gamma	(21)
Topotecan price/mg	12.75	9.56–15.94	Gamma	(21)
Advent event (1st-line atezolizumab plus chemotherapy)	4959.82	3719.87–6199.78	Gamma	(22)
Advent event (1st-line durvalumab plus chemotherapy)	4743.05	3557.29–5928.81	Gamma	(22)
Advent event (1st-line chemotherapy)	6100.94	4508.96–7514.93	Gamma	(22)
Advent event (2nd-line topotecan)	14487.33	10865.50–18109.16	Gamma	(22)
Administration intravenous, first hour	142.55	106.91–178.19	Gamma	(23)
Administration intravenous, additional hour	30.68	23.01–38.35	Gamma	(23)
Monthly physician visit	148.33	111.25–185.41	Gamma	(23)
Three-monthly imaging	122.71	92.03–153.39	Gamma	(23)
Monthly supportive care	637.00	477.75–796.25	Gamma	(24)
Death associated costs	9433.00	7074.75–11791.25	Gamma	(24)
Utilities				
PFS	0.673	0.538–0.808	Beta	(15, 16)
PS	0.473	0.378–0.568	Beta	(15, 16)
Disutility for EP	0.112	0.090–0.134	Beta	(25)
Disutility for AEP	0.090	0.072–0.108	Beta	(25)
Disutility for DEP	0.094	0.075–0.113	Beta	(25)
Others				
Proportion of subsequent therapy in the atezolizumab plus chemotherapy group	0.517	0.414–0.620	Beta	(10)
Proportion of subsequent therapy in the durvalumab plus chemotherapy group	0.420	0.336–0.504	Beta	(12)
Proportion of subsequent therapy in the chemotherapy group	0.516	0.413–0.619	Beta	(10, 12)
Body surface area (meters^2)	1.80	1.35–2.25	Gamma	(16)
Creatinine clearance rate(ml/min)	70.00	52.50–87.50	Gamma	(16)

[a]*Theta (θ) and kappa (γ) represented two parameters of log-logistic distribution.*
[b]*The OS HR and PFS HR for AEP vs DEP were generated using network meta-analysis.*
[c]*Lambda (λ) and gamma (γ) represented two parameters of Weibull distribution.*
AEP, atezolizumab combined with etoposide and platinum; DEP, durvalumab combined with etoposide and platinum; EP, etoposide plus platinum; OS, overall survival; PFS, progression-free survival; PS, progressed survival.

Costs and Utilities

Direct medical costs collected from the US payer perspective included drug acquisition and administration costs for the first-line and subsequent therapy, adverse event (AE) management costs, routine follow-up costs, supportive care costs, and death-associated costs.

Drug prices were taken from the October 2020 Centers for Medicare & Medicaid Services (CMS) Average Sales Price Drug Pricing Files (21). For the sake of simplification, the cost of platinum was modeled as the cost of carboplatin in three treatment groups, to take into account the clinical preference for carboplatin over cisplatin. In calculating the drug costs per cycle, the model patient cohort was modeled as a baseline patient with a body surface area of 1.8 m^2 and a creatinine clearance rate of 70 ml/min (16). Drug administration costs were searched from the CMS Physician Fee Schedule Look-Up Tool (23). For calculating drug administration costs, the durations of EP chemotherapy, and chemo-immunotherapy infusion were modeled as 3 and 4 hour per cycle, respectively. Furthermore, the durations of ICIs were adjusted based on the median treatment cycles to take into account patients' discontinuations that were not just because of disease progression, but also because of AEs, physician decision, and other reasons (10, 12).

Costs for managing grade III/IV AEs with an incidence of ≥3% were included in the model. The AE management cost for each first-line treatment was estimated by summing the product of the unit cost and the incidence corresponding to each AE. The cost estimation of each AE was sourced from the Healthcare Cost and Utilization Project using diagnosis Code selection for ICD-10 (22). In the model, we assumed that all AEs occur in the first cycle, and the incidence of each AE was quoted from the IMpower 133 and CASPIAN trials (**Supplementary Table 4**). We assumed routine follow-up including a monthly physician visit and a three-monthly

imaging examination. Supportive care costs and death-associated costs were derived from published literature (24).

Neither the IMpower 133 trial nor the CASPIAN trial collected information for the quality of life for patients with ES-SCLC. According to the previously published economic evaluation, the PFS and PS health states in our model were assigned the utilities of 0.673 and 0.473, respectively (15, 16). In addition, the utility decrements caused by common grade III/IV AEs associated with treatment were considered in our model (**Supplementary Table 4**) (25).

Statistical Analysis

To address uncertainty bound to the model parameters, a series of sensitivity analysis were performed. In deterministic sensitivity analyses, model parameters were varied individually to confirm the influence degree of each parameter on the model results. Health state utilities and proportions of subsequent therapy were tested at the upper and lower of their respective 95% CIs. Other parameters were tested within a range of ±25% of baseline values. In probabilistic sensitivity analyses, model parameters were varied simultaneously to verify the robustness of our model. 10,000 Monte Carlo simulations were carried out by randomly sampling model parameters to general 10,000 cost and effectiveness estimates for each treatment strategy. **Table 1** detailed the baseline values, ranges, and distributions of model parameters in the sensitivity analysis.

In addition, we incorporated a scenario analysis in our model, in which the duration of first-line ICIs increased from the median treatment cycles to the treatment cycles of receiving ICIs until disease progression, to explore whether the duration of ICIS had a substantial impact on our results.

RESULTS

Base Case Results

The model patient cohort was adult patients with treatment-naive histologically or cytologically documented ES-SCLC. Within a 10-year time horizon, use of AEP was associated with a marginal improvement in QALYs and reduced health care costs of $5,737 compared with use of DEP (**Table 2**). Therefore, AEP was the dominant treatment strategy compared with DEP. The comparisons between the two chemo-immunotherapies and EP chemotherapy demonstrated that adding atezolizumab and durvalumab to the first-line EP chemotherapy gained additional 0.162 and 0.146 QALYs, respectively, which were equivalent to 2 months of perfect health. Due to the improvement in QALYs, AEP, and DEP were associated with substantially greater health care costs than EP chemotherapy, resulting in ICERs of $382,469/QALY and $464,593/QALY, respectively.

Sensitivity Analysis

In deterministic sensitivity analyses, when comparing the two chemo-immunotherapies, except the price of durvalumab and atezolizumab, as well as the OS HR of DEP versus AEP, other model parameters failed to change the preferred strategy from AEP to DEP (**Figure 2**). When comparing the two chemo-immunotherapies with EP chemotherapy, first-line AEP and DEP were not cost-effective within the variable range of any tested parameters (**Supplementary Figures 2**, **3**). However, both ICERs were extremely sensitive to the price of the ICIs. A 77% reduction in the price of atezolizumab would allow the ICER for AEP *vs* EP below the WTP threshold of $100,000 per QALY, while a 80% reduction in the price of durvalumab would make the ICER for DEP *vs* EP lower than the WTP threshold of $100,000 per QALY gained.

In probabilistic sensitivity analyses, the comparison of two chemo-immunotherapies suggested that first-line AEP could achieve cost-effectiveness in 100% simulations. When comparing the two chemo-immunotherapies with EP chemotherapy, the probabilities of first-line AEP and DEP being cost-effective were 6.6% and 4.1% at the WTP threshold of $100,000/QALY, respectively (**Supplementary Figure 4**).

The result of our scenario analysis suggested that with the increase of treatment cycles of ICIs, the health costs associated with first-line AEP and DEP increase sharply, but our conclusion had not changed substantially. For example, when we assumed that patients received first-line ICIs until disease progression, the health costs of the fist-line AEP and DEP were $115,595 and $131,987, respectively. However, AEP still dominated DEP, and the ICERs for AEP and DEP were $542,305/QALY and $715,247/QALY, respectively.

DISCUSSION

Using a Markov model, we estimated the 10-year time horizon costs and effectiveness associated with first-line AEP and DEP by pooling the clinical efficacy and safety data from two large, randomized, phase III clinical trials and collecting costs mainly from the Medicare in 2020. Results of this cost-effectiveness study

TABLE 2 | Base case results.

Outcomes	EP	AEP	DEP	Incremental		
				DEP *vs* AEP	AEP *vs* EP	DEP *vs* EP
Cost, $US	24,582	86,655	92,391	5,737	62,073	67,810
QALY	0.578	0.740	0.724	−0.016	0.162	0.146
ICER, $/QALY				Dominated[a]	382,469	464,593

[a]*DEP showed lower effectiveness and higher cost, as compared with the AEP.*

EP, etoposide plus platinum; AEP, atezolizumab combined with etoposide and platinum; DEP, durvalumab combined with etoposide and platinum; QALY, quality adjusted life year; ICER, incremental cost-effectiveness ratio.

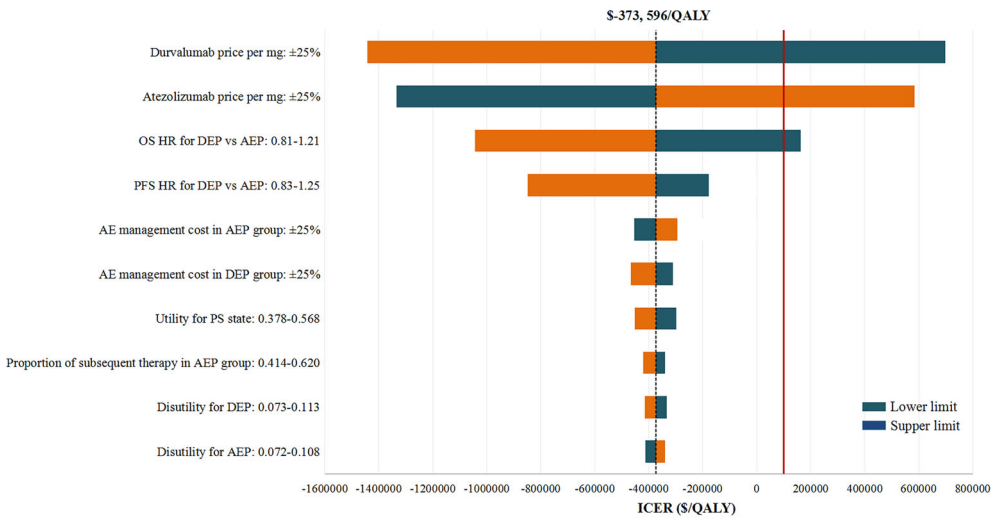

FIGURE 2 | Deterministic Sensitivity Analysis. The red solid line represents the willingness-to-pay threshold of $100,000 used this analysis. The black dotted line represents the incremental cost-effectiveness ratio (ICER) between alternatives under comparison. The top 10 most influential parameters of the ICERs are displayed. AEP indicated atezolizumab combined with etoposide and platinum; DEP, durvalumab combined with etoposide and platinum; QALY, quality adjusted life year; ICER, incremental cost-effectiveness ratio; AE, adverse event; PFS, progression-free survival; PS, progressed survival.

conducted in United States for patients with ES-SCLC demonstrated that first-line AEP was the dominant treatment strategy compared with DEP, which achieved higher effectiveness at lower health care cost. Furthermore, the current economic evaluation found that the first-line AEP and DEP are not cost-effective compared with EP chemotherapy that was in agreement with previous cost-effectiveness studies (15, 16), but AEP was found to provide a more-efficient balance between the increment cost and QALYs than was DEP.

Sensitivity analyses focusing on uncertainty bound to model parameters confirmed the robustness of our model. The most influential parameters to the model were the price of atezolizumab and durvalumab. We found that the price increase of atezolizumab by more than 10% and the price decrease of durvalumab by more than 9% would allow DEP dominate AEP economically. While the price reduction of atezolizumab by more than 77% and durvalumab by more than 80% would allow the ICERs for AEP *vs* EP and DEP *vs* EP lower than the WTP threshold of $100,000/QALY. After drug prices, the HRs of DEP *vs* AEP had significant effects on the model results, underscoring the necessity of robust head-to-head clinical data. Because changing other parameters had no substantial impact on our results, price decreases for atezolizumab and durvalumab were considered to be the most practical measures for first-line AEP and DEP to achieve cost-effectiveness.

Two previous economic evaluation determined the cost-effectiveness of AEP or DEP versus EP in the first-line setting of ES-SCLC in the United States, and found that the ICER of AEP was $528,810/QALY (0.10 QALY gained at an incremental cost of $52,881) and the ICER of DEP was $355,448 (0.22 QALY gained at an incremental cost of $78,199) over EP, respectively (15, 16). The inconsistency of the ICERs between our study and the previous studies might result from the different long-term survival projections. In the present analysis, the OS data beyond the 2-year follow-up period were derived from Surveillance, Epidemiology, and End Results data from 2000 to 2017, rather than extrapolated directly from the selected survival distribution. In addition, previous studies mainly considered the acquisition and administration costs for first-line drugs, as well as the AE management costs of first-line treatments, while our study also considered the acquisition and administration costs for second-line drug, the AE management costs of second-line treatment, routine follow-up costs, supportive care costs and death-associated costs. Nevertheless, they came to a conclusion similar with our current analysis, that is, neither first-line AEP nor DEP was an optimal strategy from an American perspective.

To our knowledge, this study was the first to compare the cost-effectiveness of two newly approved first-line chemo-immunotherapies for patients with ES-SCLC in the United states. The results of our analysis supported the use of first-line AEP as a cost-effective treatment option for patients with ES-SCLC when compared with DEP. In addition, when compared the current preferred options (AEP and DEP) with the previous preferred option (EP chemotherapy) in the first-line setting for patients with ES-SCLC, the present study pointed out that new combination therapies with remarkable effect allow patients to remain on the costly treatment for relatively long periods, and as a result, their health care costs inevitably soared. Results from the present study had a theoretical value and practical significance for value-based cancer treatments which gives priority to the quality rather than quantity of health care services (27).

This study has several strengths. First, we estimated the 10-year time horizon cost-effectiveness of three first-line treatments for ES-SCLC through economic modeling. In our model, clinical

efficacy and safety data were derived from well-conducted phase III clinical trials evidence (the IMpower 133 trial and the CASPIAN trial), and costs were collected from the US payer perspective. As a result, our model can provide a long-term cost and effectiveness projection that can readily translate into clinical practice. Second, the OS data beyond the 2-year follow-up period were derived from Surveillance, Epidemiology, and End Results data from 2000 to 2017 for patients with ES-SCLC (26), which supplement the deficiency that directly extrapolating survival data from the survival distribution used to fit each treatment strategy that may lead to biased long-term OS estimates. Third, to take into account patients' discontinuation of first-line chemo-immunotherapies that was not solely caused by disease progression (10, 12), but also by other reasons, our model used the median number of cycles that better reflect the time spent on first-line therapy. Furthermore, the result of our scenario analysis suggested that our conclusions had not changed regardless of the increase in treatment cycles. Fourth, our study was comprehensive in that it assessed the only two preferred chemo-immunotherapies recommended by the latest NCCN guidelines for ES-SCLC and the clinical commonly used EP chemotherapy.

This study also has several limitations. First, the comparison between first-line AEP and DEP was indirect because there were no clinical data in one trial to evaluate the two alternatives. There is potential uncertainty here, despite a network meta-analysis was employed in the current study. Second, to simplify the calculation, we assumed that the cost of platinum used across three groups was the cost of carboplatin. On this basis, this analysis likely overestimated the cost of EP chemotherapy because carboplatin is slightly expensive than cisplatin. However, sensitivity analyses showed that varying the cost of carboplatin had almost no influence on the model results. Third, the health state utilities in the model were obtained from the published literature because of the quality-of-life information were not available in both the IMpower 133 trial and CASPIAN trials. Although our findings remained robust over a broad range of health state utilities, the model should be validated against more actual health state utilities.

In conclusion, the economic evaluation between the two first-line chemo-immunotherapies for ES-SCLC suggests that AEP was the dominant treatment strategy compared with AEP. When compared the two first-line chemo-immunotherapies with EP chemotherapy, first-line AEP and DEP are not cost-effective for patients with ES-SCLC, but AEP was able to provide a more-efficient balance between increment cost and QALYs than AEP. When new combination therapies with remarkable effect become pivotal in the first-line treatment, the price reduction of these drugs may be essential for achieving cost-effectiveness.

DATA AVAILABILITY STATEMENT

The original contributions presented in the study are included in the article/**Supplementary Material**. Further inquiries can be directed to the corresponding authors.

AUTHOR CONTRIBUTIONS

XZ and QL had full access to all the data in the study take responsibility for the integrity of the data and the accuracy of the data analysis. Concept and design: QL, XZ, and CT. Acquisition, analysis, or interpretation of data: All authors. Drafting of the manuscript: QL, XZ, and CT. Critical revision of the manuscript for important intellectual content: All authors. Statistical analysis: QL. Obtained funding: QL. Supervision: XZ and CT. All authors contributed to the article and approved the submitted version.

FUNDING

This work was supported by the Hunan Provincial Natural Science Foundation [grant 2019JJ50864]; Scientific research project of Hunan Health Commission in 2019 [grant B2019156].

ACKNOWLEDGMENTS

The authors thank Fang Ma for her help in the study design and guiding the manuscript revision.

SUPPLEMENTARY MATERIAL

The Supplementary Material for this article can be found online at: https://www.frontiersin.org/articles/10.3389/fonc.2021.699781/full#supplementary-material

Supplementary Figure 1 | Parametric survival distributions fitted for three first-line treatments. AEP indicated atezolizumab combined with etoposide and platinum; DEP, durvalumab combined with etoposide and platinum; EP, etoposide plus platinum.

Supplementary Figure 2 | Deterministic Sensitivity Analysis for AEP vs EP. The red solid line represents the willingness-to-pay threshold of $100,000 used this analysis. The black dotted line represents the incremental cost-effectiveness ratio (ICER) between alternatives under comparison. The top 10 most influential parameters of the ICERs are displayed. AEP indicated atezolizumab combined with etoposide and platinum; EP, etoposide plus platinum; QALY, quality adjusted life year; ICER, incremental cost-effectiveness ratio; AE, adverse event; PFS, progression-free survival; PS, progressed survival.

Supplementary Figure 3 | Deterministic Sensitivity Analysis for DEP vs EP. The red solid line represents the willingness-to-pay threshold of $100,000 used this analysis. The black dotted line represents the incremental cost-effectiveness ratio (ICER) between alternatives under comparison. The top 10 most influential parameters of the ICERs are displayed. AEP indicated atezolizumab combined with etoposide and platinum; DEP, durvalumab combined with etoposide and platinum; EP, etoposide plus platinum; QALY, quality adjusted life year; ICER, incremental cost-effectiveness ratio; AE, adverse event; OS, overall survival; PFS, progression-free survival; PS, progressed survival.

Supplementary Figure 4 | Acceptability curve for the probabilistic sensitivity analysis. AEP indicated atezolizumab combined with etoposide and platinum; DEP, durvalumab combined with etoposide and platinum; EP, etoposide plus platinum; QALY, quality adjusted life year; ICER, incremental cost-effectiveness ratio.

REFERENCES

1. Bray F, Ferlay J, Soerjomataram I, Siegel RL, Torre LA, Jemal A. Global Cancer Statistics 2018: GLOBOCAN Estimates of Incidence and Mortality Worldwide for 36 Cancers in 185 Countries. *CA Cancer J Clin* (2018) 68(6):394–424. doi: 10.3322/caac.21492
2. Govindan R, Page N, Morgensztern D, Read W, Tierney R, Vlahiotis A, et al. Changing Epidemiology of Small-Cell Lung Cancer in the United States Over the Last 30 Years: Analysis of the Surveillance, Epidemiologic, and End Results Database. *J Clin Oncol* (2006) 24(28):4539–44. doi: 10.1200/JCO.2005.04.4859
3. Oronsky B, Reid TR, Oronsky A, Carter CA. What's New in SCLC? A Review. *Neoplasia* (2017) 19(10):842–7. doi: 10.1016/j.neo.2017.07.007
4. Früh M, De Ruysscher D, Popat S, Crinò L, Peters S, Felip E. Small-Cell Lung Cancer (SCLC): ESMO Clinical Practice Guidelines for Diagnosis, Treatment and Follow-Up. *Ann Oncol* (2013) 24(Suppl 6):vi99–105. doi: 10.1093/annonc/mdt178
5. Rudin CM, Ismaila N, Hann CL, Malhotra N, Movsas B, Norris K, et al. Treatment of Small-Cell Lung Cancer: American Society of Clinical Oncology Endorsement of the American College of Chest Physicians Guideline. *J Clin Oncol* (2015) 33 (34):4106–11. doi: 10.1200/JCO.2015.63.7918
6. National Comprehensive Cancer Network. *NCCN Clinical Practice Guidelines in Oncology: Small Cell Lung Cancer, Version 2* (2018). Available at: https://www.nccn.org/about/news/ebulletin/ebulletindetail.aspx?ebulletinid=1318 (Accessed 12 November 2020).
7. Rossi A, Di Maio M, Chiodini P, Rudd RM, Okamoto H, Skarlos DV, et al. Carboplatin- or Cisplatin-Based Chemotherapy in First-Line Treatment of Small-Cell Lung Cancer: The COCIS Meta-Analysis of Individual Patient Data. *J Clin Oncol* (2012) 30(14):1692–8. doi: 10.1200/JCO.2011.40.4905
8. National Cancer Institute Surveillance. *Epidemiology, and End Results Program* (2020). Available at: https://seer.cancer.gov/archive/csr/1975_2012/browse_csr.php?sectionSEL=15&pageSEL=sect_15_table.13 (Accessed 22 November 2020).
9. US Food and Drug Administration. *FDA Approves Atezolizumab for Extensive-Stage Small Cell Lung Cancer* (2020). Available at: https://www.fda.gov/drugs/drug-approvals-and-databases/fda-approves-atezolizumab-extensive-stage-small-cell-lung-cancer (Accessed 12 September 2020).
10. Horn L, Mansfield AS, Szczęsna A, Havel L, Krzakowski M, Hochmair MJ, et al. First-Line Atezolizumab Plus Chemotherapy in Extensive-Stage Small-Cell Lung Cancer. *N Engl J Med* (2018) 379(23):2220–9. doi: 10.1056/NEJMoa1809064
11. US Food and Drug Administration. *FDA Approves Durvalumab for Extensive-Stage Small Cell Lung Cancer* (2020). Available at: https://www.fda.gov/drugs/resources-information-approved-drugs/fda-approves-durvalumab-extensive-stage-small-cell-lung-cancer (Accessed 12 September 2020).
12. Paz-Ares L, Dvorkin M, Chen Y, Reinmuth N, Hotta K, Trukhin D, et al. Durvalumab Plus Platinum-Etoposide Versus Platinum-Etoposide in First-Line Treatment of Extensive-Stage Small-Cell Lung Cancer (CASPIAN): A Randomised, Controlled, Open-Label, Phase 3 Trial. *Lancet* (2019) 394 (10212):1929–39. doi: 10.1016/S0140-6736(19)32222-6
13. Siegel RL, Miller KD, Fuchs HE, Jemal A. Cancer Statistics, 2021. *CA Cancer J Clin* (2021) 71(1):7–33. doi: 10.3322/caac.21654
14. Mariotto AB, Yabroff KR, Shao Y, Feuer EJ, Brown ML. Projections of the Cost of Cancer Care in the United States: 2010-2020. *J Natl Cancer Inst* (2011) 103(2):117–28. doi: 10.1093/jnci/djq495
15. Zhou K, Zhou J, Huang J, Zhang N, Bai L, Yang Y, et al. Cost-Effectiveness Analysis of Atezolizumab Plus Chemotherapy in the First-Line Treatment of Extensive-Stage Small-Cell Lung Cancer. *Lung Cancer* (2019) 130:1–4. doi: 10.1016/j.lungcan.2019.01.019
16. Zhang L, Hang Y, Liu M, Li N, Cai H. First-Line Durvalumab Plus Platinum-Etoposide Versus Platinum-Etoposide for Extensive-Stage Small-Cell Lung Cancer: A Cost-Effectiveness Analysis. *Front Oncol* (2020) 10:602185. doi: 10.3389/fonc.2020.602185
17. National Comprehensive Cancer Network. *NCCN Clinical Practice Guidelines in Oncology: Small Cell Lung Cancer, Version 3* (2021). Available at: https://www.nccn.org/professionals/physician_gls/default.aspx (Accessed 4 November 2020).
18. Goto K, Ohe Y, Shibata T, Seto T, Takahashi T, Nakagawa K, et al. Combined Chemotherapy With Cisplatin, Etoposide, and Irinotecan Versus Topotecan Alone as Second-Line Treatment for Patients With Sensitive Relapsed Small-Cell Lung Cancer (JCOG0605): A Multicentre, Open-Label, Randomised Phase 3 Trial. *Lancet Onco* (2016) 17(8):1147–57. doi: 10.1016/S1470-2045(16)30104-8
19. Neumann PJ, Cohen JT, Weinstein MC. Updating Cost-Effectiveness–the Curious Resilience of the $50,000-per-QALY Threshold. *N Engl J Med* (2014) 371(9):796–7. doi: 10.1056/NEJMp1405158
20. Hoyle MW, Henley W. Improved Curve Fits to Summary Survival Data: Application to Economic Evaluation of Health Technologies. *BMC Med Res Methodol* (2011) 11:139. doi: 10.1186/1471-2288-11-139
21. Centers for Medicare and Medicaid Services. *October 2020 ASP Drug Pricing Files* (2020). Available at: https://www.cms.gov/license/ama?file=/files/zip/october-2020-asp-pricing-file.zip (Accessed 1September 2020).
22. Agency for Healthcare Research and Quality, U.S. Department of Health & Human Services. *Healthcare Cost and Utilization Project* (2021). Available at: https://hcupnet.ahrq.gov (Accessed 2 January 2021).
23. Centers for Medicare and Medicaid Services. *Medicare Physician Fee Schedule Look-Up Tool* (2021). Available at: https://www.cms.gov/medicare/physician-fee-schedule/search (Accessed 11January 2021).
24. Criss SD, Mooradian MJ, Watson TR, Gainor JF, Reynolds KL, Kong CY. Cost-Effectiveness of Atezolizumab Combination Therapy for First-Line Treatment of Metastatic Nonsquamous Non-Small Cell Lung Cancer in the United States. *JAMA Netw Open* (2019) 2(9):e1911952. doi: 10.1001/jamanetworkopen.2019.11952
25. Nafees B, Lloyd AJ, Dewilde S, Rajan N, Lorenzo M. Health State Utilities In non-Small Cell Lung Cancer: An International Study. *Asia Pac J Clin Oncol* (2017) 13 (5):e195–203. doi: 10.1111/ajco.12477
26. National Cancer Institute Surveillance. *Epidemiology, and End Results Program. SEER*Stat Software Version 8.3.9* (2020). Available at: https://seer.cancer.gov/seerstat/software/ (Accessed 16 September 2020).
27. Services CFMM. *What are the Value-Based Programs?* Available at: https://www.cms.gov/Medicare/Quality-Initiatives-Patient-Assessment-Instruments/Value-Base (Accessed 20 January 2021).

Conflict of Interest: The authors declare that the research was conducted in the absence of any commercial or financial relationships that could be construed as a potential conflict of interest.

Copyright © 2021 Liu, Luo, Yi, Zeng and Tan. This is an open-access article distributed under the terms of the Creative Commons Attribution License (CC BY). The use, distribution or reproduction in other forums is permitted, provided the original author(s) and the copyright owner(s) are credited and that the original publication in this journal is cited, in accordance with accepted academic practice. No use, distribution or reproduction is permitted which does not comply with these terms.

frontiers in Oncology

ORIGINAL RESEARCH
published: 29 June 2021
doi: 10.3389/fonc.2021.703893

Therapeutic and Prognostic Implications of Immune-Related Adverse Events in Advanced Non-Small-Cell Lung Cancer

*Lea Daniello[1,2], Mariam Elshiaty[1,2], Farastuk Bozorgmehr[1,2], Jonas Kuon[1,2], Daniel Kazdal[2,3], Hannah Schindler[1,2], Rajiv Shah[1,2], Anna-Lena Volckmar[3], Fabienne Lusky[1,2], Leonore Diekmann[4], Stephan Liersch[5], Martin Faehling[6], Thomas Muley[2,7], Mark Kriegsmann[2,3], Karolina Benesova[4], Albrecht Stenzinger[2,3], Michael Thomas[1,2] and Petros Christopoulos[1,2]**

[1] Department of Thoracic Oncology, Thoraxklinik and National Center for Tumor Diseases (NCT) at Heidelberg University Hospital, Heidelberg, Germany, [2] Translational Lung Research Center Heidelberg (TLRC-H), Member of the German Center of Lung Research (DZL), Heidelberg, Germany, [3] Institute of Pathology Heidelberg, Heidelberg, Germany, [4] Department of Internal Medicine V, Hematology, Oncology und Rheumatology, Heidelberg University Hospital, Heidelberg, Germany, [5] Department of Pharmacy, Thoraxklinik at Heidelberg University Hospital, Heidelberg, Germany, [6] Department of Cardiology, Angiology and Pneumology, Esslingen Hospital, Esslingen, Germany, [7] Translational Research Unit, Thoraxklinik at Heidelberg University Hospital, Heidelberg, Germany

OPEN ACCESS

Edited by:
Junji Uchino,
Kyoto Prefectural University of Medicine, Japan

Reviewed by:
Joanna Julia Domagala-Kulawik,
Medical University of Warsaw, Poland
Yusuke Okuma,
National Cancer Center Hospital, Japan

***Correspondence:**
Petros Christopoulos
petros.christopoulos@med.uni-heidelberg.de
orcid.org/0000-0002-7966-8980

Specialty section:
This article was submitted to Thoracic Oncology, a section of the journal Frontiers in Oncology

Received: 30 April 2021
Accepted: 09 June 2021
Published: 29 June 2021

Citation:
Daniello L, Elshiaty M, Bozorgmehr F, Kuon J, Kazdal D, Schindler H, Shah R, Volckmar A-L, Lusky F, Diekmann L, Liersch S, Faehling M, Muley T, Kriegsmann M, Benesova K, Stenzinger A, Thomas M and Christopoulos P (2021) Therapeutic and Prognostic Implications of Immune-Related Adverse Events in Advanced Non-Small-Cell Lung Cancer. Front. Oncol. 11:703893. doi: 10.3389/fonc.2021.703893

Introduction: PD-(L)1 inhibitors have improved prognosis of non-small-cell lung cancer (NSCLC), but can also cause immune-related adverse events (irAEs) that complicate management.

Methods: We analyzed NSCLC patients receiving PD-(L)1 inhibitors from 2012 to 2020 in a German academic center.

Results: IrAE showed comparable frequencies in stage IV (198/894 or 22%) *vs.* III (14/45 or 31%, p = 0.15), after anti-PD-(L)1 monotherapy *vs.* chemoimmunotherapy (139/483 *vs.* 58/213, p = 0.75), and across treatment lines. In stage IV, irAE occurred after 3.1 months in median, affected multiple organs (median 2) in 27/894 patients and were associated with PD-L1 positivity (25 *vs.* 14%, p = 0.003), lower neutrophil-to-lymphocyte ratios (29 *vs.* 17%, p < 0.001 for NLR dichotomized at 5), better ECOG status (26 *vs.* 18% for 0 *vs.* 1, p = 0.004), but not related to age, sex, smoking and palliative radiotherapy. Two hundred thirty two irAEs occurred mostly in endocrine glands (4.9%), lungs (4.4%), the musculoskeletal system (4.2%), colon (4.1%), liver (3.7%), and skin (2.6%), while pneumonitis was most frequent with durvalumab following definitive chemoradiation (16% or 7/45, p < 0.01). IrAE severity was grade 1 in 11%, 2 in 41%, 3 in 36%, and 4 in 11% events, while two were lethal (<1%, myocarditis and pneumonitis). Therapy was suspended in 72%, while steroids were initiated in 66% and complemented by other immunosuppressants in 6%, with longest treatment duration for rheumatic events (mean >3 months), and average cumulative prednisone doses >700 mg for all organs, except for skin. Patients developing irAE had longer progression-free (PFS) and overall survival (OS)

in multivariable 12/14-week landmark analyses including ECOG status, treatment line, treatment type, PD-L1 TPS, and NLR (median PFS 17 *vs.* 10 months, HR = 0.68, p = 0.009; median OS 37 *vs.* 15 months, HR = 0.40, p < 0.001), regardless of grade. OS was longest with skin (95% at 2 years) and shortest with pneumonitis, hepatitis, neurologic, and cardiologic irAE (38, 37, 28, and 0% at 2 years, p < 0.001).

Conclusions: Approximately one-fourth of immunotherapy-treated NSCLC patients develop irAEs, most of which necessitate treatment suspension and steroids. Despite more frequent occurrence with PD-L1 positive tumors, lower NLR, and better ECOG PS, irAEs are independently associated with longer survival, especially when affecting the skin. Lethality is below 1%.

Keywords: immune-related adverse events, immunotherapy, immune-checkpoint inhibitors, treatment interruption, prognosis, lethality

INTRODUCTION

Inhibitors of immune checkpoints (ICIs), such as the cytotoxic T-lymphocyte-associated protein 4 (CTLA-4), programmed cell death protein-1 (PD-1), and its ligand programmed death-ligand 1 (PD-L1), are increasingly used for the treatment of metastatic cancers (1). These drugs block inhibitory effects of neoplastic on immune cells, to potentiate immunologic tumor control (2). Nivolumab, pembrolizumab, ipilimumab, and atezolizumab have improved progression-free (PFS) and overall survival (OS) of patients with metastatic non-small-cell lung cancer (NSCLC) in randomized phase 3 trials and currently represent the standard first-line treatment alone or in combination with chemotherapy for most cases (3, 4).

Besides the high antitumor efficacy of ICIs, as exemplified by an unprecedented 5-year survival rate of 32% for stage IV patients with PD-L1 high-expressing NSCLC receiving first-line pembrolizumab monotherapy (5), these drugs can also alter the physiology of immune responses, leading to toxicity collectively described as "immune-related adverse events" (irAEs), which can affect diverse organs and complicate patient management (6). The severity grading for irAEs relies on the National Cancer Institute common toxicity criteria for adverse events (NCI CTCAE) version 5 (7). Grade ≥3 toxicities, especially, can be even life threatening and require special monitoring and therapeutic maneuvers, including dose reductions, treatment interruption, and/or high-dose steroids (8).

With increasing use of ICIs as treatment for NSCLC, precise characterization of predisposing factors, manifestations, management, outcome, and impact on overall prognosis becomes more important for irAEs, because this knowledge could become a valuable aid for decision-making in daily clinical practice. This retrospective study utilizes a large, single-institution cohort to address these issues under real-world conditions.

PATIENTS AND METHODS

Study Population and Data Collection

This study was approved by the ethics committee of Heidelberg University (S-296/2016) and included all advanced NSCLC patients treated with PD-(L)1 inhibitors in the Thoraxklinik Heidelberg between October 2012 and June 2020. Patients that received other immunotherapies, in particular CTLA-4 inhibitors, were excluded from this analysis.

Diagnosis of NSCLC was performed in the Institute of Pathology Heidelberg using tissue specimens according to the criteria of the current WHO classification (2015) for lung cancer, as described previously (9, 10). Clinical data and laboratory results were collected by a systematic review of patient records. The following clinical data were extracted: demographic, baseline clinical and tumor characteristics, including ECOG performance status (PS), smoking status, PD-L1 tumor proportion score (TPS), laboratory results, systemic and local anticancer treatments, date of progression, date of the last follow-up, and date of death. The neutrophile-to-lymphocyte ratio (NLR) was dichotomized at the bibliographical cut-off of 5, which corresponds to the median value for untreated patients (11, 12). PD-L1 TPS was assessed using the clone SP263 (Ventana/Roche, Mannheim, Germany) and trichotomized for analysis as <1, 1–49, and ≥50%. For calculation of PFS, the progression date under immunotherapy was verified by the investigators with review of radiologic images, *i.e.* chest/abdomen CT and brain MRI-based restaging every 6–12 weeks, without formal RECIST reevaluation, as several studies have demonstrated very good agreement between real-world and RECIST-based assessments (13, 14). Patients with irAEs were diagnosed based on clinicolaboratory criteria and treated according to the current guidelines (7, 15). Diagnosis of pneumonitis was based on high-resolution CT (HRCT), considering that bioptic confirmation is generally not required for subsequent patient management (15). For patients with irAE additional data were collected about severity, management, outcome, and impact of irAEs on anticancer treatment. The subset of stage III patients who received durvalumab as consolidation after chemoradiation was analyzed separately (**Figure 1**).

Detailed Characterization of irAEs

Patients who developed irAEs were analyzed further in more detail regarding affected organs and severity grade, time of onset, treatment with steroids—including start date, dose, duration, whether anticancer therapy had to be interrupted or terminated

—or other immunosupressants, and if radiotherapy had been given in the past. Rheumatic irAEs were diagnosed in consultation with an experienced rheumatologist (KB) in order to differentiate them from non-autoimmune joint disease (*e.g.* osteoarthritis) (16, 17).

Statistical Methods

Categorical data were analyzed using the chi-square test, including "goodness-of-fit" tests for the observed frequencies against the even distribution, when applicable. Numerical data were compared across two groups using an unpaired t-test and across three or more groups using one-way ANOVA with the Dunnett's *post-hoc* test with correction for multiple testing. Survival data were analyzed according to Kaplan–Meier and compared between groups with the logrank test. The association of irAE and other variables with survival was analyzed using Cox regression. Immortal time bias was controlled through two landmark analyses, at 12 and 14 weeks, which included only cases surviving beyond the respective landmark, as well as by a time-dependent Cox regression, in which the occurrence of irAEs was considered as time-dependent covariate. Statistical calculations were performed with SPSS version 27 (IBM Corp., Armonk, NY, USA), and plots were generated with SPSS and Microsoft Excel 365 (Redmond, WA, USA). P-values <0.05 were considered as statistically significant.

RESULTS

Study Population and Overview of irAEs

Overall, 939 consecutive patients were included in the study, of which 894 were treated with ICI monotherapy (70%) or chemoimmunotherapy (30%) for metastatic disease as shown in **Table 1**, while 45 patients received durvalumab after chemoradiotherapy of locally advanced tumors (**Figure 1** and **Supplementary Table 1**). Mean age was 65 years, with a predominance of male (60%) and smokers (92%) showing mostly an ECOG PS of 0–1 (98%). IrAEs showed comparable overall frequencies in stage IV *vs.* III (22 *vs.* 31%, p = 0.15), after ICI monotherapy *vs.* chemoimmunotherapy (22 *vs.* 21%, p = 0.75), across treatment lines (21–26% in the first *vs.* 20–33% in subsequent lines, p = 0.08–0.68), and across different ICIs (p = 0.16–0.74), with a trend for lower frequency for PD-L1 compared to PD-1 inhibitor monotherapy (13 *vs.* 23%, p = 0.053, **Table 1**). Among stage IV patients, 232 irAEs were documented, with involvement of multiple organs (two in median) in 14% (27/198) of patients. Most frequently affected were the endocrine glands (in 4.9% of patients, or 44/894), lungs (4.4%), musculoskeletal system (4.2%), colon (4.1%), and liver (3.7%), followed by the skin (2.6%), nervous system (0.7%), heart (0.4%), kidney (0.3%), pancreas (0.3%), and blood (0.1%, p < 0.001 across organs, **Figure 2A** and **Table 2**). CTCAE severity was grade 1 in 11% (25/232), grade 2 in 41%, grade 3 in 36%, and grade 4 in 11% (p < 0.001 across grades, **Figure 2B**), while two events were lethal (2/939 = 0.2%, one instance of myocarditis, and one instance of pneumonitis). The percentages of patients with at least one grade 3–4 irAE was comparable between stage IV (11% or 97/894) and stage III (18% or 8/45, p = 0.14, **Supplementary Table 2**) patients. In stage IV, the severity distribution was skewed for several organs, with predominance of grade 2 irAE for the skin (p = 0.0075), endocrine (p < 0.001), and musculoskeletal systems (p < 0.001), while grade 3 was more frequent for pneumonitis (p < 0.001), colitis (p = 0.02), and hepatitis (p < 0.001, **Figure 2C**). Besides, in stage III

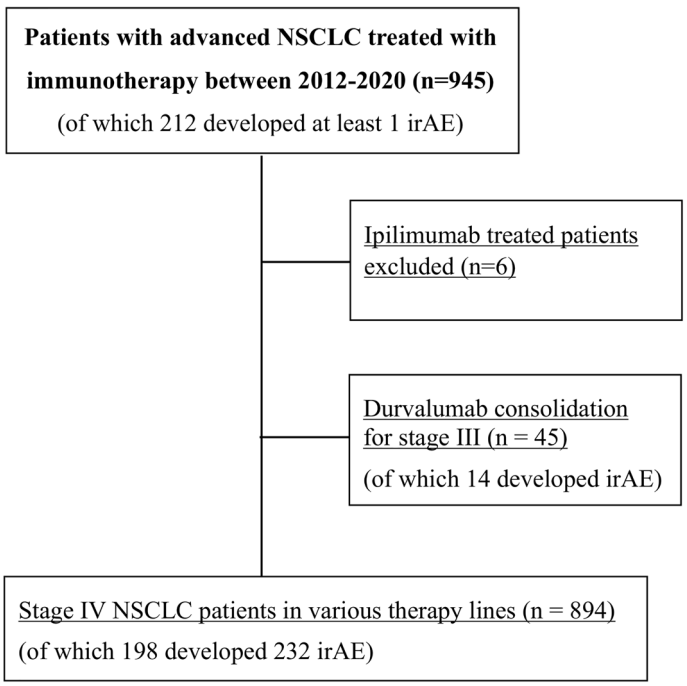

FIGURE 1 | Flowchart of study patients. NSCLC, non-small-cell lung cancer; irAE, immune-related adverse events.

TABLE 1 | Characteristics of stage IV NSCLC patients.

All study patients (N = 894)		No irAE (N = 696)	With irAE (N = 198)	p-value
Age, median; IQR		65;12	65;12	0.57
Sex, male/female		419/272	117/81	0.67
Never/light-smokers (<10 py)		70/650	20/186	0.60
Pack–years, mean (SE)		38 (1.0)	40 (2.0)	0.34
ECOG PS, median (IQR)		**1 (1)**	**0 (1)**	**0.016**
PD-L1 TPS ≥1/<1%, n (%)		**489/140**	**159 (24)/22 (14)**	**0.003**
PD-L1 TPS, mean (SE)		**34.3 (1.5)**	**42.6 (2.8)**	**0.008**
NLR ≥5/<5, n (%)		**444/233**	**93 (17)/98 (29)**	**<0.001**
NLR, mean (SE)		**9.0 (0.3)**	**7.0 (0.7)**	**0.005**
ICI-monotherapy, n (% of ICI-monotherapy)		483	139 (22)	0.75
Chemo-IO, n (% of Chemo-IO)		213	58 (21)	
ICI-monotherapy, 1L, n (% of first line)		159	56 (26)	0.08
ICI-monotherapy, lines 2–8, (% of later lines)		324	83 (20)	
CHT-IO, 1L, n (% of first line)		198	53 (21)	0.68
CHT-IO, lines 2–8, (% of later lines)		15	5 (25)	
ICI drug, 1L, n (% of drug)	Pembrolizumab	118	48 (29)	0.17
	Nivolumab	35	9 (20)	
	Atezolizumab	6	0 (0)	
ICI drug, lines 2–8, n (% of drug)	Nivolumab	213	54 (20)	0.16
	Pembrolizumab	62	20 (24)	
	Atezolizumab	46	8 (15)	
	Durvalumab	3	0 (0)	
ICI type, across lines, n (%)	PD-1 inhibitor	428	131 (23)	0.053
	PD-L1 inhibitor	55	8 (13)	
CHT-IO, 1L, n (% of drug)	CHT + pembrolizumab	189	49 (21)	0.67
	CHT + atezolizumab	4	2 (33)	
	CHT + durvalumab	5	2 (29)	
CHT-IO, lines 2–8, n (% of drug)	CHT + pembrolizumab	4	2 (33)	0.74
	CHT + atezolizumab	9	2 (18)	
	CHT + durvalumab	2	1 (33)	
CHT-IO, across lines, n (%)	CHT + PD-1 inhibitor	193	51 (21)	0.55
	CHT + PD-1 inhibitor	20	7 (26)	
Any radiotherapy		246/701	63/198	0.37
Thoracic radiotherapy (with respect to pneumonitis)		110/860	6/40	0.68

ECOG PS, ECOG performance status; ICI, immune checkpoint inhibitor; IO, immunotherapy; 1L, first line; NLR, neutrophil-to-lymphocyte ratio. All bold values of the table show a significance of p< 0.05.

patients after definitive chemoradiation, grade ≥3 pneumonitis predominated (6/14, **Supplementary Table 2**).

Clinical Characteristics Associated With Occurrence of irAEs

Most patient characteristics, like age, sex, and smoking status, were balanced between patients with or without irAE (**Table 1**). At the same time, irAE occurrence was significantly associated with PD-L1 positivity, *i.e.* TPS ≥1% (25 *vs.* 14%, p = 0.003; mean PD-L1 TPS 43 *vs.* 34% for patients with *vs.* without irAE, p = 0.008), a lower baseline NLR <5 (29 *vs.* 17% for patients with NLR ≥5, p < 0.001; mean NLR 7.0 *vs.* 9.0, p = 0.005), and a better ECOG PS (26 *vs.* 18% for PS 0 *vs.* 1, p = 0.004). In stage IV patients, there was no significant relationship between administration of palliative radiotherapy to any organ and development of any irAE (p = 0.37), or between prior palliative thoracic radiotherapy and development of pneumonitis p = 0.68, **Table 1**). However, the frequency of pneumonitis was significantly higher in stage III patients receiving durvalumab after curative-intent radiotherapy compared to stage IV patients (7/45 = 16% *vs.* 40/894 = 4%, respectively, p = 0.0009). Similarly, the relative frequency of pneumonitis among the observed irAE was significantly higher for stage III compared to stage IV patients (7/14 = 50% *vs.* 40/232 = 17%, respectively, p = 0.0025, **Table 2** and **Supplementary Table 2**). Median time-to-onset of irAE from ICI start was 3.1 months (92 days), with significantly later onset for musculoskeletal (246 days, p = 0.046) and renal events (669 days, p < 0.001, **Table 2**).

Management of irAEs

The majority of irAE interfered with further administration of ICI therapy, leading to suspension in 72% (168/232), and termination in 55% (128/232) of cases, respectively (**Table 2**). This affected practically all patients with grade 3–4 events (98 and 100%, respectively), but ICI therapy was also permanently discontinued for 21% of patients with grade 1 (n = 4), and 51% of patients with grade 2 events (n = 35). There were considerable differences depending on the affected organ, with significantly more pneumonitis (95%), colitis (84%), and hepatitis (94%) irAEs leading to suspension (p < 0.001, **Table 2**). For irAEs of other vital organs, *i.e.* nervous system, heart, kidneys, and blood, the suspension rate was also very high, approaching 100%, but did not reach statistical significance due to the rarity of these events (**Table 2**).

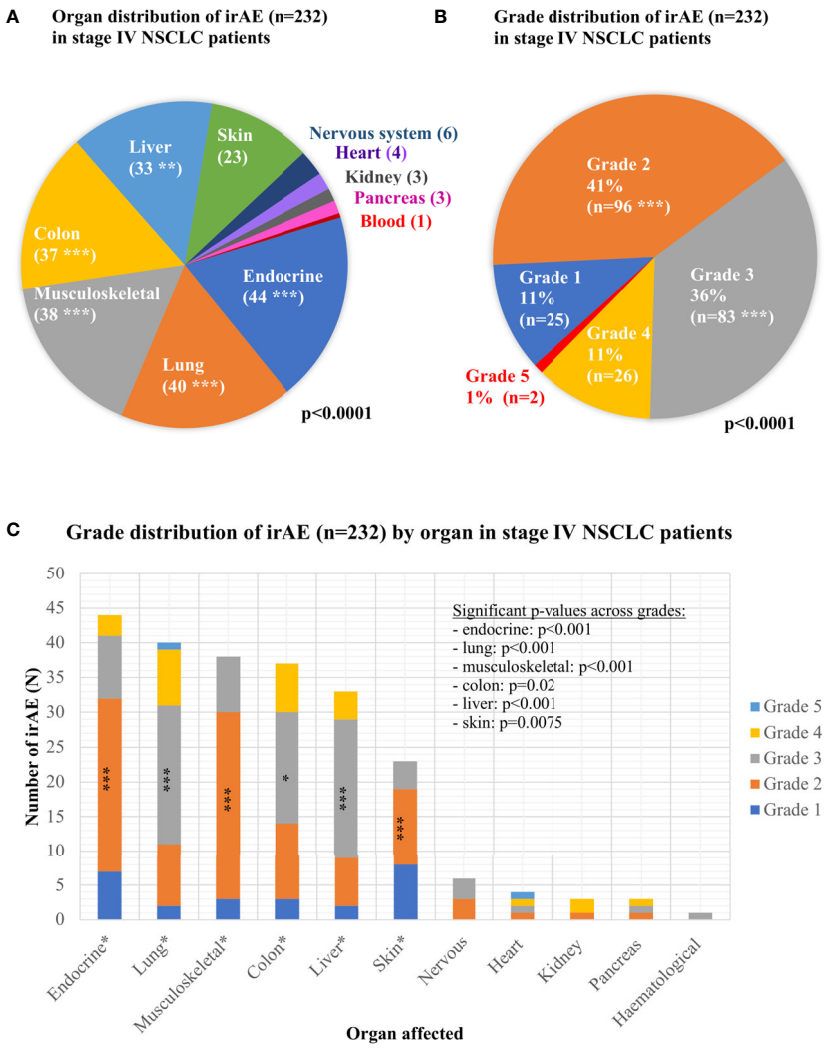

FIGURE 2 | Organ and grade distribution of immune-related adverse events in immunotherapy-treated non-small-cell lung cancer patients. **(A)** Organ distribution of the 232 immune-related adverse events (irAEs) observed in stage IV non-small-cell lung cancer (NSCLC) patients ($p < 0.0001$ with a chi-square test across the various affected organs; detailed results are shown in **Table 2**; ***$p < 0.001$, **$p < 0.01$, *$p < 0.05$). **(B)** Grade distribution of the 232 irAEs observed in stage IV NSCLC patients ($p < 0.0001$ with a chi-square test across grades, grades with significantly increased frequency are marked with asterisks). **(C)** Grade distribution of the irAEs observed in each organ for stage IV NSCLC patients. For each organ, the p-value was calculated with a chi-square test of the observed frequencies for each grade against the even distribution (endocrinological: 44 irAEs overall, grade 1:7, grade 2:25, grade 3:9, grade 4:3, $p < 0.001$; lungs: 40 irAEs overall, grade 1:2, grade 2:9, grade 3:20, grade 4:8, grade 5:1, $p < 0.001$; musculoskeletal system: 38 irAEs overall, grade 1:3, grade 2:27, grade 3:8, grade 4:0, $p < 0.001$; colon: 37 irAE overall, grade 1:3, grade 2:11, grade 3:16, grade 4:7, $p = 0.02$; hepatitis: 33 irAEs overall, grade 1:2, grade 2:7, grade 3:20, grade 4:4, $p < 0.001$; skin: 23 irAEs overall, grade 1:8, grade 2:11, grade 3:4, grade 4:0, $p = 0.0075$; nervous system: six irAEs overall, grade 1:0, grade 2:3, grade 3:3, grade 4:0, $p = 0.06$; heart: four irAEs overall, grade 1:0, grade 2:1, grade 3:1, grade 4:1, grade 5:1, $p = 0.26$; kidneys: three irAEs overall, grade 1:0, grade 2:1, grade 3:0, grade 4:2, $p = 0.30$; pancreas: three irAEs overall, grade 1:0, grade 2:1, grade 3:1, grade 4:0, $p = 0.80$; hematological: one irAE overall, grade 3).

In the majority of cases (66% or 155/232), steroid treatment was required, with increasing frequency and dose for more severe events (**Figure 3A**): no patient with steroid treatment for grade 1 irAE, 51% with grade 2 (mean initial daily dose 20 mg), and >90% with grades 3–4 (mean initial dose 95 mg). The only grade 3–4 cases without steroid therapy were four patients with hypophysitis, who received only hydrocortisone replacement. Overall, hydrocortisone replacement therapy was required for most patients with endocrinologic irAE (24/44 or 55%, namely 22 with hypophysitis, one with thyroiditis, and one with polyendocrinopathy. Utilization of steroid therapy also showed considerable heterogeneity across affected organs and was more frequent for pneumonitis (93%), hepatitis (82%), colitis (81%), and musculoskeletal events (74%, $p < 0.001$, **Table 2**). Steroid therapy was longest for musculoskeletal irAEs, which were the only type of events with average steroid duration exceeding 3 months (128 days, **Table 2** and **Figure 3B**). Several patients received steroids for >1 year, either higher prednisone doses >10 mg (six patients, all with musculoskeletal irAEs), or low-dose maintenance therapy with ≤10 mg prednisone daily, which was

TABLE 2 | Severity, onset, and management of immune-related adverse events in stage IV non-small-cell lung cancer patients.

	IrAE grade and impact on ICI administration					Steroid treatment			
	Any grade, % (n) of all patients	Time to onset (days)	G≥3, % (n) of each organ	ICI suspension, % (n) of each organ	ICI termination, % (n) of each organ	Steroids,% (n) of each organ	Initial daily dose, [1] mean (SD)	Average daily dose, [1] mean (SD)	Duration, days (SD)
Affected organ									
Endocrine	**4.9 (44***)**	132	27 (12)	43 (19)	16 (7)	27 (12)	18 (33)	12 (26)	31 (107)
Lungs	**4.4 (40***)**	105	**73 (29***)**	**95 (38***)**	**80 (32***)**	**93 (37***)**	**75 (41)*****	**53 (60)*****	41 (36)
Musculoskeletal	**4.3 (38***)**	**246***	21 (8)	58 (22)	47 (18)	**74 (28***)**	33 (52)	20 (36)	**128 (202)*****
Colon	**4.1 (37***)**	168	**62 (23*)**	**84 (31***)**	**65 (24***)**	**81 (30***)**	**62 (44)***	**40 (34)***	44 (42)
Liver	**3.7 (33**)**	67	**73 (24**)**	**94 (31***)**	**82 (27***)**	**82 (27***)**	**87 (92)*****	**47 (37)*****	33 (27)
Skin	2.6 (23)	182	17 (5)	52(12)	35 (8)	35 (8)	21 (36)	9 (15)	23 (55)
Nervous system	0.7 (6)	52	67 (4)	100 (6)	67(4)	67 (4)	**111 (196)***	35 (39)	21 (23)
Heart	0.4 (4)	75	100 (4)	100(4)	75 (3)	50 (2)	**135 (244)****	36 (45)	39 (61)
Kidney	0.3 (3)	**669*****	67 (2)	100 (3)	100 (3)	100 (3)	67 (29)	42 (12)	86 (97)
Pancreas	0.3 (3)	311	67 (2)	67 (2)	67 (2)	67 (2)	52 (50)	23 (21)	53 (65)
Blood	0.1 (1)	838	100 (1)	100 (1)	100 (1)	100 (1)	100 (n/a)	57 (na)	20 (na)
p-value	<0.001	<0.001	<0.001	0.003	<0.001	<0.001	<0.001	<0.001	0.002

*IrAEs of various organs are listed in order of decreasing frequency according to **Figure 2C** (n = 894 stage IV patients). Statistical comparisons to detect increased values across organs were performed using either a chi-square test against the even distribution (frequency of irAEs with any grade or grade ≥3, rates of ICI suspension (that is interruption or termination), or termination, rate of steroid treatment, or one-way ANOVA (time to onset, dose and duration of steroids), followed by the Dunnett's post-hoc test with endocrine irAE as reference. Statistically significant results are highlighted in bold.*

*G, grade 3; irAE, immune related adverse events; ICI, immunotherapy; SD, standard deviation; n/a, not applicable; ***p < 0.001; **p < 0.01; *p < 0.05.*

[1]in mg prednisone.

necessary for approximately one-third (14/38 or 37%) of patients with musculoskeletal irAE. On the other hand, the duration of treatment was shortest for skin irAE (average 23 days) and the single case with a hematologic event (20 days, **Table 2**). The cumulative steroid dose was highest for patients with renal (3,330 mg), followed by liver (1,622 mg), and lung irAEs (1,519 mg), but exceeded 700 mg also for all other organs, except for the skin (average 237 mg, **Figure 3B**). A need for additional immunosuppressive therapy was documented in 13/232 events (6%), or 13/198 cases (7%), which corresponded to 13/154 (8.4%) steroid-treated patients: namely 3/28 steroid-treated cases of musculoskeletal events (n = 2 arthritis grade 2, n = 1 arthritis grade 3), 6/30 steroid-treated cases of colitis (n = 1 grade 2, n = 3 grade 3, and n = 2 grade 4), 1/2 steroid-treated cases of myocarditis (grade 4), 2/27 steroid-treated cases of hepatitis (grade 3 and grade 4), and 1/8 steroid-treated cases of dermatitis (grade 3 exacerbated psoriasis). Immunosuppressants administered were mycophenolate mofetil for hepatitis (2×) and myocarditis (1×), mesalamine for colitis (3×), tacrolimus for colitis (1×), infliximab for colitis (2×) and polyarthritis (1×), methotrexate for psoriasis (1×), polyarthritis (1×) and adalimumab as well as leflunomide for arthritis (2× and 1× respectively). Three cases required more than one additional immunosuppressant (n = 2 arthritis, n = 1 colitis). For stage III, steroid therapy was required for most patients with irAEs (79% or 11/14), particularly in case of grade 3–4 events (100% use *vs.* 25% for grade 2, **Supplementary Table 2**).

Prognostic Impact of irAEs

Patients who developed irAEs had a longer PFS [15 *vs.* 9 months, hazard ratio (HR) 0.68 with p = 0.008 in a 12-week landmark analysis, **Supplementary Figure 1A**, **Supplementary Tables 3, 4**; 17 *vs.* 10 months, HR = 0.65 with p = 0.005 in a 14-week landmark analysis, **Figure 4A**, **Tables 3**, **4**], which was significant in multivariable testing along with PD-L1 TPS (p < 0.01), NLR (p > 0.05), treatment line (p > 0.05), type of treatment (chemoimmunotherapy *vs.* IO-monotherapy, p > 0.05), and ECOG PS (p > 0.05, **Table 4** and **Supplementary Table 4**). OS from start of IO treatment was also longer for patients developing irAEs (37 *vs.* 14 months, HR = 0.4 with p < 0.001 in a 12-week landmark analysis, **Supplementary Figure 1B**, **Supplementary Tables 3, 4**; 37 *vs.* 15 months, HR = 0.38 with p < 0.001 in a 14-week landmark analysis, **Figure 4B**, **Tables 3**, **4**), which was significant in multivariable testing along with PD-L1 TPS (p < 0.01), NLR (p < 0.01) treatment line (p > 0.05), type of treatment (p > 0.05), and ECOG PS (p < 0.05, **Table 4**, **Supplementary Table 4**). The independent prognostic value of irAE alongside NLR, PD-L1 TPS, ECOG PS, treatment line, and treatment type was also confirmed in separate multivariable OS analysis using the occurrence of irAE as a time-dependent covariate (**Supplementary Table 5**). OS of patients with irAE varied widely between irAE affecting different organs, being longest for skin (2-year OS 95%), and shortest for pulmonary, hepatic, nervous system, and cardiologic irAE (2-year OS 38, 37, 28, and 0% respectively, p = 0.007, **Figure 5B**) but did not differ significantly by irAE grade (p = 0.71, **Figure 5A**).

DISCUSSION

As survival of NSCLC under immunotherapy is improving, with long-term, 5-year OS rates of 20–30% for stage IV disease

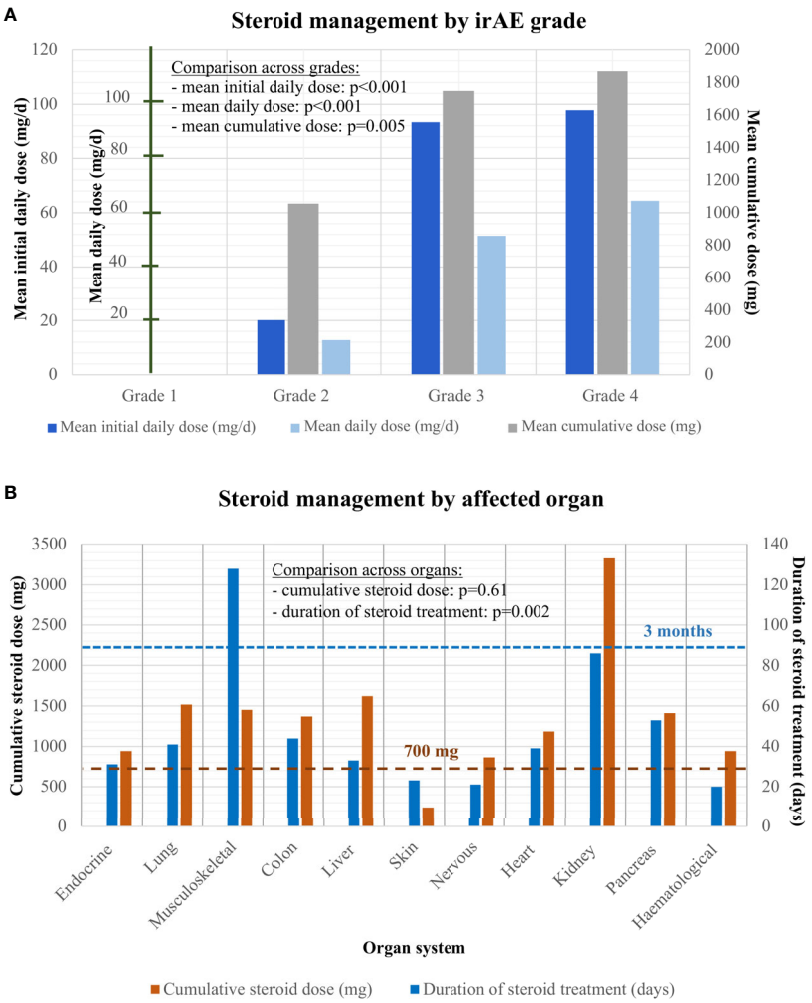

FIGURE 3 | Steroid management of grades 1–4 irAEs. **(A)** Mean initial daily dose, mean average daily dose, and mean cumulative dose for steroid treatment in patients with grade 2–4 irAEs analyzed by one-way ANOVA. While no grade 1 irAE received steroid treatment, mean initial daily, mean average daily and cumulative steroid dose increased steadily from grades 2–4: for grade 2 irAE mean initial dose: 20.2 mg [standard error (SE): 2.9], cumulative dose: 1056.4 mg (SE: 300.3), mean daily dose: 12.9 mg (SE: 2.0); for grade 3 irAE: mean initial dose: 93.4 mg (SE: 9.7), cumulative dose: 1747.5 mg (SE: 186.3), mean daily dose: 51.5 mg (SE: 5.3); for grade 4 irAE mean initial dose: 96.4 mg (SE: 10.9), cumulative dose: 1823.5 mg (SE: 348.4), mean daily dose: 62.8 mg (SE: 8.0). ANOVA with *post-hoc* test for trend across grades: $p < 0.001$ (mean initial daily dose), $p < 0.001$ (mean average daily dose), $p = 0.005$ (cumulative dose). **(B)** Cumulative steroid dose and total duration of steroid treatment by affected organ: endocrine: 942 mg (SE: 536) over 31 days (SE: 16); lungs: 1,519 mg (SE: 248) over 41 days (SE: 6)); musculoskeletal: mean cumulative dose 1455 mg (SE: 442) over 128 days (SE: 33); colon: 1,371 mg (SE: 227) over 44 days (SE: 7); liver: 1,622 mg (SE: 339) over 33 days (SE: 5); skin: 237 mg (SE: 123) over 23 days (SE: 11); nervous system: 863 mg (SE: 427) over 21 days (SE: 9); cardiologic: 1,183 mg (SE: 684) over 39 days (SE: 31); kidney: 3,330 (SE: 2,394) over 86 days (SE: 9); pancreas: 1,413 mg (SE: 1035) over 53 days (SE: 5); blood: 940 mg (SE: na) over 20 days (SE: na). One-way ANOVA $p = 0.002$ for the cumulative dose across affected organs (with statistical significance in *post-hoc* testing for musculoskeletal irAE, please see **Table 2**), and $p = 0.61$ for the treatment duration. Abbreviations: irAEs, immune related adverse events; SE, standard error of the mean; n/a, not applicable.

currently (18, 19), and the use of PD-(L)1 inhibitors is expanding in locally-advanced and early stages (20), the interest for thorough analysis of irAEs is growing, because they pose important practical challenges for oncologists and a major limitation for patient outcome.

The irAE frequency in our study was 22% (189/894) overall, 10.7% (96/894) for grade 3–4 events, and similar between ICI-monotherapy and chemoimmunotherapy, which agrees well with the overall frequency of 20–30% for any grade, and 9–10% for grade 3–4 irAEs reported in the Keynote-24 and Keynote-189 clinical trials (21, 22). The spectrum of involved organs, mainly endocrine glands, lungs, musculoskeletal system, colon, and liver (**Figure 2A**), and median time to onset of 3.1 months were typical and also very similar to that reported by clinical trials and retrospective NSCLC series (21–24). Patient characteristics associated with development of irAEs were PD-L1 positivity ($p = 0.003$), a lower NLR ($p < 0.001$), and a better ECOG PS ($p = 0.004$, **Table 1**). Of note, each of these three parameters is also a predictor of better antitumor efficacy for immunotherapy in NSCLC, both in our patients (**Table 3**) and

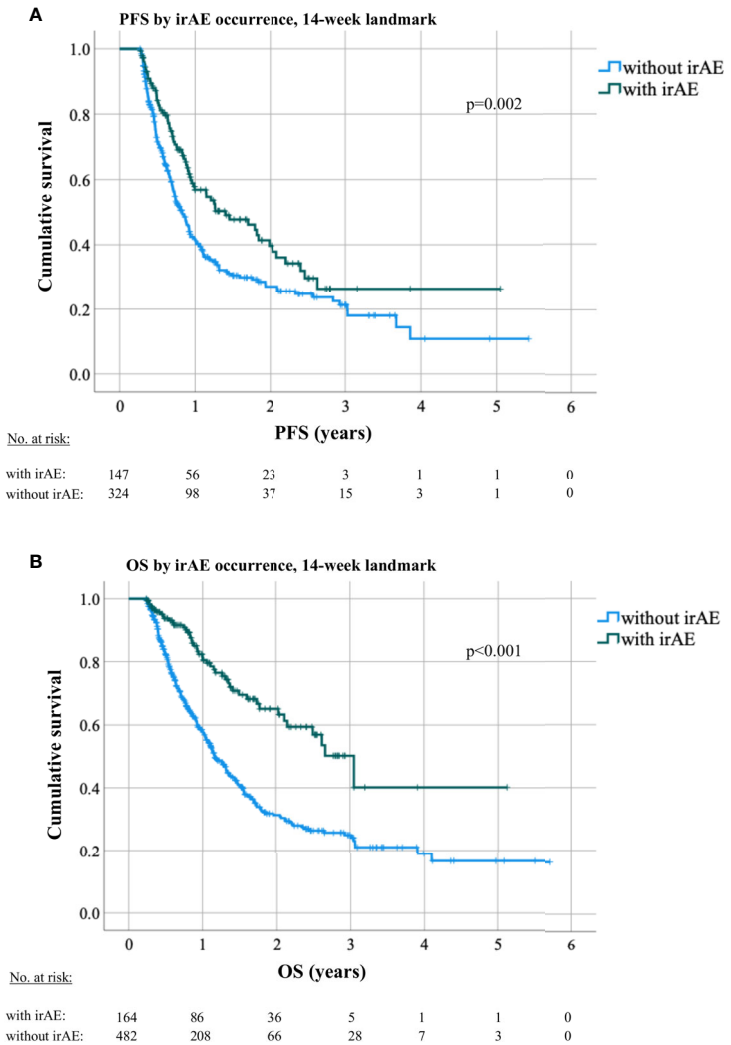

FIGURE 4 | Progression-free and overall survival by occurrence of irAEs in a 14-week landmark analysis. **(A)** The median PFS under immunotherapy was 10 months (8.7–11.4) for patients without irAE *vs.* 17 months (10.3–23.6, logrank p = 0.003) for patients with irAEs in a 14-week landmark analysis. **(B)** The median OS was 15 months (13.5–16.6) for patients without irAE *vs.* 37 months (28.7–44.6, logrank p < 0.001) for patients with irAE in a 14-week landmark analysis.

according to several previous studies (25–29). Therefore, it appears that the efficacy and potential for toxicity are interconnected in case of ICIs. Along the same lines, other studies have linked increase of cytokines, like CXCL9, CXCL10, CXCL11, and CXCL19, under ICIs as a sign of enhanced general immune reactivity with both subsequent tumor responses and development of irAE in NSCLC (30–32). A similar close relationship between efficacy and toxicity is also known to exist in another form of immunotherapy, namely between the graft-*versus*-host and graft-*versus* leukemia effects of allogeneic hematopoietic cell transplantation (33, 34). Besides systemic immunologic parameters, organ-specific factors probably also play a role in the development of specific irAE; for example the frequency of ICI pneumonitis was higher in cases of stage III NSCLC with invariable administration of full-dose thoracic radiotherapy compared to stage IV in our cohort. At the same time, however, it should be noted that palliative radiotherapy was not associated with detectable increase in risk (**Table 1**), which echoes the findings of other investigators and is an important consideration for everyday practice (35, 36). Other examples of organ-related factors that modulate the risk of specific irAE are preexisting interstitial lung disease, which is a strict ICI contraindication due to the very high risk of pneumonitis (37, 38), as well as an increased baseline TSH, which is associated with subsequent development of thyroiditis (39, 40). However, no reliable predictive scheme has been devised yet.

Another clinically important and controversial issue is the relationship between irAE and patient survival (41). Earlier studies in melanoma and NSCLC had shown conflicting results, namely favorable (41–45) or indifferent outcome for patients developing irAEs (46–48), which was in part due to different handling of the "immortal-time bias" (ITB, aka

TABLE 3 | Univariable analysis of progression-free and overall survival according to occurrence of irAE in NSCLC.

PFS with 14-week landmark	HR	P-value	95%-CI
IrAE occurrence	**0.67**	**0.003**	0.51–0.87
PD-L1 TPS (<1, 1–49, 50+)	**0.69**	**<0.001**	0.59–0.82
NLR (≥5, <5)	1.19	0.16	0.93–1.51
Treatment line	1.11	0.14	0.97–1.26
Treatment type[1]	1.30	0.06	1.00–1.70
ECOG PS	1.13	0.31	0.90–1.41
OS with 14-week landmark	**HR**	**P-value**	**95%-CI**
IrAE occurrence	**0.40**	**<0.001**	0.29–0.55
PD-L1 TPS (<1, 1–49, 50+)	**0.77**	**0.002**	0.66–0.91
NLR (≥5, <5)	**1.45**	**0.002**	1.15–1.82
Treatment line	1.18	0.003	1.06–1.32
Treatment type[1]	0.15	0.80	0.59–1.09
ECOG PS	1.22	0.06	0.99–1.52

The association of irAE and other variables with progression-free (PFS) and overall survival (OS) was analyzed using a univariable Cox regression 14-week landmark analysis. Statistically significant results have been highlighted in bold.
PFS, progression-free survival; OS, overall survival; HR, hazard ratio; 95% CI, 95% confidence interval; irAE, immune related adverse events; ECOG PS, Eastern Cooperative Oncology Group Performance Status; IO, immunotherapy; PD-L1 TPS, Programmed Death Ligand 1 Tumor Proportion Score (%); NLR, neutrophil-to-lymphocyte ratio.
[1]chemoimmunotherapy vs. IO-monotherapy.

"guaranteed-time bias") by the various investigators (49). In a recent meta-analysis, both the confounding effect of the ITB and the real, positive association between irAE and patient survival that remains significant after control for ITB could be shown (50). Nevertheless, the relationship between irAE and other predictors for longer PFS and OS, such as PD-L1, NLR, and ECOG PS, evident in our patients (**Table 1**), demonstrates an additional dimension of the question about the potential prognostic utility of irAE, namely whether irAEs have any independent value beyond that of already validated parameters. To our knowledge, the present study is the first to demonstrate this by combining rigorous ITB control using landmark (**Tables 3**, **4**) and time-dependent analyses (**Supplementary Table 5**), with multivariable testing that includes all currently established survival predictors, both laboratory (PD-L1 TPS, NLR) and clinical (treatment type, treatment line, ECOG PS, **Table 4** and **Supplementary Table 5**). Furthermore, particularly relevant for the contemporary practice is the inclusion of a large chemoimmunotherapy subcohort (n > 250, **Table 1**) in this analysis, which is the predominant therapeutic strategy for most NSCLC patients currently (3, 4), in contrast to previous studies who have analyzed IO-monotherapy (41, 50) or small chemoimmunotherapy series with less than 100 patients (51). Our results show that the relationship between occurrence of irAEs and ICI efficacy is very strong (HR = 0.4, **Table 4**), stronger than that of PD-L1 TPS or NLR, and that it persists regardless of concurrent or previous chemotherapy. An additional indication for the potency of this interaction is the lack of negative association between irAE grade and patient survival (**Figure 5A**), which has also been noted by others (52), as well as the recent finding that NSCLC patients with multiple irAEs have an even longer survival (53).

TABLE 4 | Multivariable analysis of progression-free and overall survival according to occurrence of irAE in NSCLC.

PFS with 14-week landmark	HR	P-value	95%-CI
IrAE occurrence	**0.65**	**0.005**	0.48–0.88
PD-L1 TPS (<1, 1–49, 50+)	**0.74**	**0.002**	0.61–0.90
NLR (≥5, <5)	0.99	0.95	0.75–1.29
Treatment line	1.18	0.06	1.00–1.39
Treatment type[1]	1.20	0.36	0.83–1.72
ECOG PS	1.14	0.30	0.89–1.46
OS with 14-week landmark	**HR**	**P-value**	**95%-CI**
IrAE occurrence	**0.38**	**<0.001**	0.27–0.56
PD-L1 TPS (<1, 1–49, 50+)	**0.78**	**0.008**	0.66–0.94
NLR (>5, <5)	**1.37**	**0.01**	1.07–1.76
Treatment line	1.15	0.06	0.99–1.32
Treatment type[1]	0.78	0.20	0.54–1.14
ECOG PS	**1.30**	**0.03**	1.02–1.65

The association of irAE and other variables with progression-free (PFS) and overall survival (OS) was analyzed using a multivariable Cox regression 14-week landmark analysis. Statistically significant results have been highlighted in bold.
PFS, progression-free survival; OS, overall survival; HR, hazard ratio; 95% CI, 95% confidence interval; irAE, immune related adverse events; ECOG PS, Eastern Cooperative Oncology Group Performance Status; IO, immunotherapy; PD-L1 TPS, Programmed Death Ligand 1 Tumor Proportion Score (%); NLR, neutrophil-to-lymphocyte ratio.
[1]chemoimmunotherapy vs. IO-monotherapy.

On the other hand, irAEs are increasingly also recognized as a considerable source of patient morbidity and financial burden for the health system (54), with important differences between the real-world and clinical trial setting (55); however systematic studies about routine irAE management are scarce. Of particular interest in this regard are details about the utilization of corticosteroids, which are used much more frequently than other immunosuppressants and have considerable toxicity potential (56). Our results show that the majority or irAEs (67%) will necessitate treatment with steroids, the average cumulative dose of which will exceed 1 g even for grade 2 events (**Figure 3A**). This is important, because cumulative corticosteroid doses >700 mg are known to result in clinically overt impairment of immune function, *i.e.* increased infections (57), which is well in line with the compromised antitumor efficacy of ICIs reported for patients suffering irAEs (58–60). In

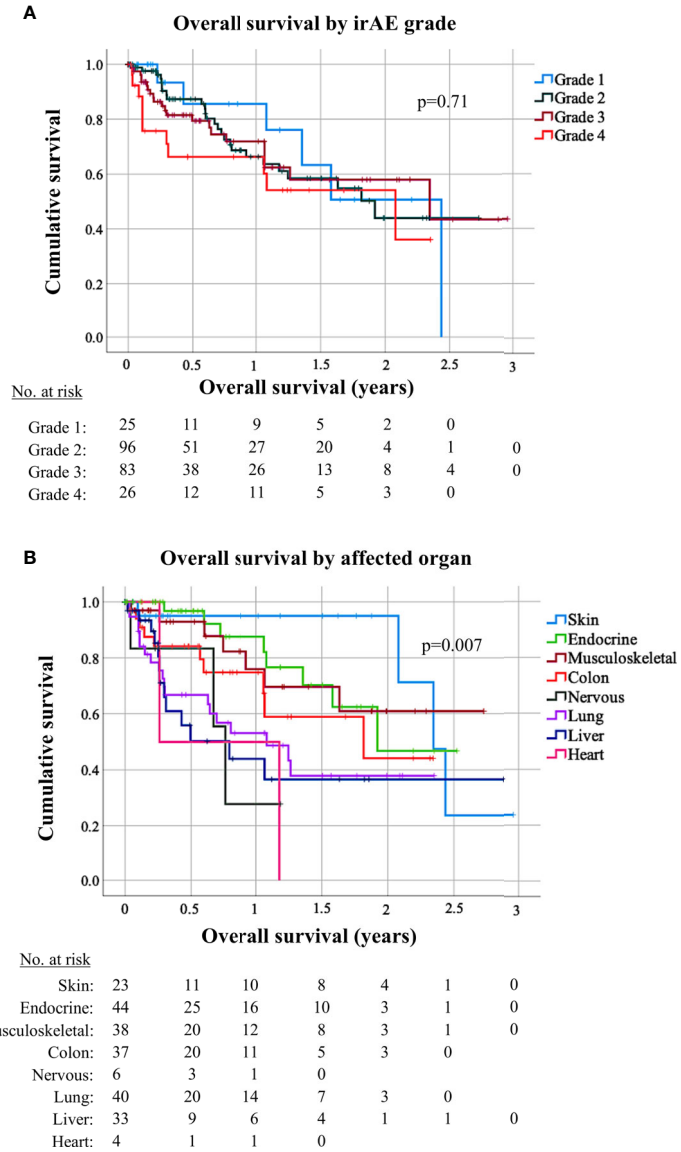

FIGURE 5 | Survival of patients with grade 1–4 immune-related adverse events by affected organ. **(A)** Overall survival (OS) from start of immunotherapy for non-small-cell lung cancer (NSCLC) patients developing immune-related adverse events (irAEs) did not differ significantly by irAE grade (logrank p = 0.71). Median OS was 29 months [95% confidence interval (CI) n/a] in case of grade 1 irAE, 23 months (13.0–31.2) in case of grade 1 irAE, 28 months (3.7–52.6) in case of grade 3 irAE, and 25 months (8.5–41.4) in case of grade 4 irAE. **(B)** OS for NSCLC patients developing irAE showed significant differences according to the irAE type (logrank p = 0.007). Median OS was 28.1 months (CI 23.9–32.3) for patients with dermatologic irAE, with 2-year OS rate 95% (CI 85–100); 23 months (CI n/a) for patients with endocrinologic irAE, with 2-year OS rate 47% (CI 15–79); not reached for patients with musculoskeletal irAE, with a 2-year OS rate 61% (36–85); 22 months (3.1–40.6) for patients with colitis, with a 2-year OS rate 44% (14–75); 13 months (4.2–21.8) for patients with pneumonitis, with a 2-year OS rate 38% (19–57); and 9.5 months (1.4–17.6) for patients with hepatitis, with a 2-year OS rate 37% (14–59); 9.1 months (7.3–10.9) with a 2-year OS rate of 27.8% (CI 0–73) for patients with neurological irAE; and 3.1 months (CI na) for patients with cardiologic irAE with a 2-year OS rate 0%. Only irAE with >3 occurrences in our patients were included in this analysis.

addition, several other adverse effects, like myopathy, lipodystrophy, memory and mood changes, already commence within the first 1–2 months if the daily dose exceeds 10 mg (61–64), which is the case in the majority of irAEs occurring in NSCLC patients (**Figure 2A**). In contrast, chronic side-effects, like bone density loss, which commences at 3 months (65), and cataracts, the risk of which becomes relevant after 1 year (66), are mainly relevant for patients with musculoskeletal irAEs, of which the average duration of steroid treatment uniquely exceeded 3 months (**Figure 3B**), and about one-third required long-term steroid therapy exceeding 12 months in our study. Indeed, immune checkpoint inhibitor-induced inflammatory arthritis has been described to persist after immunotherapy cessation and necessitates long-term therapy to prevent late relapses, for example with lower-dosed (≤10 mg/day) steroids in combination with disease modifying antirheumatic drugs (67). The multifaceted toxicity of corticosteroids is presumably one main reason, why irAEs that usually present with grade ≥3 and require higher steroid doses, like pneumonitis, colitis and hepatitis (**Table 2**), are associated with shorter OS than irAE affecting other organs (**Figure 5B**). In keeping with this, patients with skin irAEs, who require steroids least frequently (**Table 2**) and have the lowest cumulative dose, uniquely below 700 mg on average (**Figure 3B**), showed the longest OS relative to other irAE types (**Figure 5B**). An association between higher steroid doses and shorter OS in NSCLC patients with irAEs has also been noted by other investigators (68). IrAE fatality in our study was approximately 0.2%, similar to the 0.36–0.38% reported by a global meta-analysis for PD-(L)1 inhibitors across cancer types (69).

The main limitations of our study stem from its retrospective nature, which cannot exclude potential confounders, and is also not as accurate regarding estimation of PFS and other parameters as prospective clinical trials. In order to control this, we annotated our cases extensively and performed multivariable analysis including all factors known to be associated with patient survival. In addition, we accounted for ITB by 12- and 14-week landmark, as well as time-dependent analyses. It should also be noted that our study only enrolled patients with NSCLC from Germany, which limits generalizability of the results to other cancer types and/or other countries with potentially different patterns of clinical practice. Also, for some less frequently affected organs, like the nervous system, heart, and blood, the number of available cases was small and precluded in-depth study.

In conclusion, our study demonstrates that irAEs affect approximately 20–25% of ICI-treated NSCLC patients regardless of additional previous chemotherapy, most necessitating treatment suspension and initiation of steroids. Despite more frequent occurrence with PD-L1 positive tumors, lower NLR, and better ECOG PS, irAEs, particularly those affecting the skin, are independently associated with longer survival. Lethality is below 1%.

DATA AVAILABILITY STATEMENT

The raw data supporting the conclusions of this article will be made available by the authors without undue reservation.

ETHICS STATEMENT

The studies involving human participants were reviewed and approved by the ethics committee of Heidelberg University (S-296/2016). Written informed consent for participation was not required for this study in accordance with the national legislation and the institutional requirements.

AUTHOR CONTRIBUTIONS

LDa: conceptualization, methodology, investigation; data curation, formal analysis, visualization, writing—original draft. ME: investigation, data curation, validation, writing—review & editing. FB: investigation, data curation, validation, writing—review & editing. JK: investigation, data curation, validation, writing—review & editing. DK: investigation; data curation, validation, writing—original draft. HS: investigation, data curation, validation, writing—review & editing. RS: investigation, data curation, validation, writing—review & editing. A-LV: investigation; data curation, validation, writing—review & editing. FL: investigation, data curation, validation, writing—review & editing. LDi: investigation, data curation, validation, writing—review & editing. SL: investigation, data curation, validation, writing—review & editing. MF: investigation, data curation, validation, writing—review & editing. TM: investigation, data curation, validation, writing—review & editing. MK: investigation; data curation, writing—review & editing. BK: validation, supervision, project administration, writing—review & editing. AS: validation, supervision, project administration, writing—review & editing. MT: conceptualization, methodology, validation, supervision, funding acquisition, writing—review & editing. PC: conceptualization, methodology, investigation; data curation, formal analysis, visualization, supervision, project administration; writing—original draft, writing—review & editing. All authors contributed to the article and approved the submitted version.

FUNDING

This work was supported by the German Center for Lung Research (DZL).

ACKNOWLEDGMENTS

We would like to thank Simone Kuder for help with the data collection.

SUPPLEMENTARY MATERIAL

The Supplementary Material for this article can be found online at: https://www.frontiersin.org/articles/10.3389/fonc.2021.703893/full#supplementary-material

REFERENCES

1. Robert C. A Decade of Immune-Checkpoint Inhibitors in Cancer Therapy. *Nat Commun* (2020) 11:3801. doi: 10.1038/s41467-020-17670-y
2. Gaissmaier L, Christopoulos P. Immune Modulation in Lung Cancer: Current Concepts and Future Strategies. *Respiration* (2020) 99:903–29. doi: 10.1159/000510385
3. Planchard D, Popat S, Kerr K, Novello S, Smit EF, Faivre-Finn C, et al. Metastatic non-Small Cell Lung Cancer: ESMO Clinical Practice Guidelines for Diagnosis, Treatment and Follow-Up. *Ann Oncol* (2018) 29:iv192–237. doi: 10.1093/annonc/mdy275
4. Planchard D, Popat S, Kerr K, Novello S, Smit EF, Faivre-Finn C, et al. *Esmo Clinical Practice Living Guidelines - Metastatic non-Small-Cell Lung Cancer* (2021). Available at: https://www.esmo.org/guidelines/lung-and-chest-tumours/clinical-practice-living-guidelines-metastatic-non-small-cell-lung-cancer.
5. Reck M, Rodríguez-Abreu D, Robinson AG, Hui R, Csőszi T, Fülöp A, et al. Five-Year Outcomes With Pembrolizumab Versus Chemotherapy for Metastatic non–Small-Cell Lung Cancer With PD-L1 Tumor Proportion Score ≥ 50%. *J Clin Oncol* (2021), JCO.21.00174. doi: 10.1200/JCO.21.00174
6. Grangeon M, Tomasini P, Chaleat S, Jeanson A, Souquet-Bressand M, Khobta N, et al. Association Between Immune-Related Adverse Events and Efficacy of Immune Checkpoint Inhibitors in Non–small-cell Lung Cancer. *Clin Lung Cancer* (2019) 20:201–7. doi: 10.1016/j.cllc.2018.10.002
7. U.S. Department of Health and Human Services, National Institutes of Health and National Cancer institute. *Common Terminology Criteria for Adverse Events (Ctcae) Version 5.0*. (2017).
8. Postow MA, Sidlow R, Hellmann MD. Immune-Related Adverse Events Associated With Immune Checkpoint Blockade. *N Engl J Med* (2018) 378:158–68. doi: 10.1056/NEJMra1703481
9. Travis WD, Brambilla E, Nicholson AG, Yatabe Y, Austin JH, Beasley MB, et al. The 2015 World Health Organization Classification of Lung Tumors: Impact of Genetic, Clinical and Radiologic Advances Since the 2004 Classification. *J Thor Oncol* (2015) 10:1243–60. doi: 10.1097/JTO.0000000000000630
10. Volckmar A-L, Leichsenring J, Kirchner M, Christopoulos P, Neumann O, Budczies J, et al. Combined Targeted DNA and RNA Sequencing of Advanced NSCLC in Routine Molecular Diagnostics: Analysis of the First 3,000 Heidelberg Cases. *Int J Cancer* (2019) 145:649–61. doi: 10.1002/ijc.32133
11. Valero C, Lee M, Hoen D, Weiss K, Kelly DW, Adusumilli PS, et al. Pretreatment Neutrophil-to-Lymphocyte Ratio and Mutational Burden as Biomarkers of Tumor Response to Immune Checkpoint Inhibitors. *Nat Commun* (2021) 12:729. doi: 10.1038/s41467-021-20935-9
12. Suh KJ, Kim SH, Kim YJ, Kim M, Keam B, Kim TM, et al. Post-Treatment Neutrophil-to-Lymphocyte Ratio at Week 6 Is Prognostic in Patients With Advanced Non-Small Cell Lung Cancers Treated With anti-PD-1 Antibody. *Cancer Immunol Immunother* (2018) 67:459–70. doi: 10.1007/s00262-017-2092-x
13. Bartlett CH, Mardekian J, Cotter M, Huang X, Zhang Z, Parrinello CM, et al. Concordance of Real World Progression Free Survival (PFS) on Endocrine Therapy as First Line Treatment for Metastatic Breast Cancer Using Electronic Health Record With Proper Quality Control Versus Conventional PFS From a Phase 3 Trial. *Cancer Res* (2018) 78:P3–17-03. doi: 10.1158/1538-7445.Sabcs17-p3-17-03
14. Ma X, Nussbaum NC, Magee K, Bourla AB, Tucker M, Bellomo L, et al. Comparison of Real-World Response Rate (rwRR) to RECIST-based Response Rate in Patients With Advanced Non-Small Cell Lung Cancer (Ansclc). *Ann Oncol* (2019) 30:1581P. doi: 10.1093/annonc/mdz260.103
15. Haanen JB, Carbonnel F, Robert C, Kerr KM, Peters S, Larkin J, et al. Management of Toxicities From Immunotherapy: ESMO Clinical Practice Guidelines for Diagnosis, Treatment and Follow-Up. *Ann Oncol* (2017) 28: iv119–42. doi: 10.1093/annonc/mdx225
16. Benesova K, Lorenz H-M, Leipe J, Jordan K. How I Treat Cancer: Treatment of Rheumatological Side Effects of Immunotherapy. *ESMO Open* (2019) 4: e000529. doi: 10.1136/esmoopen-2019-000529
17. Buder-Bakhaya K, Benesova K, Schulz C, Anwar H, Dimitrakopoulou-Strauss A, Weber TF, et al. Characterization of Arthralgia Induced by PD-1 Antibody Treatment in Patients With Metastasized Cutaneous Malignancies. *Cancer Immunol Immunother* (2018) 67:175–82. doi: 10.1007/s00262-017-2069-9
18. Brahmer JR, Rodriguez-Abreu D, Robinson AG, Hui R, Csőszi T, Fülöp A, et al. Lba51 KEYNOTE-024 5-Year OS Update: First-Line (1L) Pembrolizumab (Pembro) vs Platinum-Based Chemotherapy (Chemo) in Patients (Pts) With Metastatic NSCLC and PD-L1 Tumour Proportion Score (TPS) ≥50%. *Ann Oncol* (2020) 31:S1181–2. doi: 10.1016/j.annonc.2020.08.2284
19. Gettinger S, Borghaei H, Brahmer J, Chow L, Burgio M, de Castro Carpeno J, et al. Oa14.04 Five-Year Outcomes From the Randomized, Phase 3 Trials CheckMate 017/057: Nivolumab vs Docetaxel in Previously Treated Nsclc. *J Thor Oncol* (2019) 14:S244–5. doi: 10.1016/j.jtho.2019.08.486
20. Heigener DF, Reck M. Immune Checkpoint Inhibition in Non-metastatic non-Small Cell Lung Cancer: Chance for Cure? *Drugs* (2019) 79:1937–45. doi: 10.1007/s40265-019-01222-w
21. Gandhi L, Rodríguez-Abreu D, Gadgeel S, Esteban E, Felip E, de Angelis F, et al. Pembrolizumab Plus Chemotherapy in Metastatic Non-Small-Cell Lung Cancer. *N Engl J Med* (2018) 378:2078–92. doi: 10.1056/NEJMoa1801005
22. Reck M, Rodríguez-Abreu D, Robinson AG, Hui R, Csőszi T, Fülöp A, et al. Pembrolizumab Versus Chemotherapy for PD-L1-Positive Non-Small-Cell Lung Cancer. *N Engl J Med* (2016) 375:1823–33. doi: 10.1056/NEJMoa1606774
23. Remon J, Mezquita L, Corral J, Vilariño N, Reguart N. Immune-Related Adverse Events With Immune Checkpoint Inhibitors in Thoracic Malignancies: Focusing on Non-Small Cell Lung Cancer Patients. *J Thor Dis* (2018) 10:S1516–33. doi: 10.21037/jtd.2017.12.52
24. Naidoo J, Page DB, Li BT, Connell LC, Schindler K, Lacouture ME, et al. Toxicities of the Anti-PD-1 and Anti-PD-L1 Immune Checkpoint Antibodies. *Ann Oncol* (2015) 26:2375–91. doi: 10.1093/annonc/mdv383
25. Xu Y, Wan B, Chen X, Zhan P, Zhao Y, Zhang T, et al. The Association of PD-L1 Expression With the Efficacy of Anti- PD-1/PD-L1 Immunotherapy and Survival of Non-Small Cell Lung Cancer Patients: A Meta-Analysis of Randomized Controlled Trials. *Transl Lung Canc Res* (2019) 8:413–28. doi: 10.21037/tlcr.2019.08.09
26. Li Y, Zhang Z, Hu Y, Yan X, Song Q, Wang G, et al. Pretreatment Neutrophil-to-Lymphocyte Ratio (Nlr) May Predict the Outcomes of Advanced Non-Small-Cell Lung Cancer (Nsclc) Patients Treated With Immune Checkpoint Inhibitors (Icis). *Front Oncol* (2020) 10:654. doi: 10.3389/fonc.2020.00654
27. Dall'Olio FG, Maggio I, Massucci M, Mollica V, Fragomeno B, Ardizzoni A. ECOG Performance Status ≥2 as a Prognostic Factor in Patients With Advanced Non Small Cell Lung Cancer Treated With Immune Checkpoint Inhibitors-a Systematic Review and Meta-Analysis of Real World Data. *Lung Cancer* (2020) 145:95–104. doi: 10.1016/j.lungcan.2020.04.027
28. Addeo A, Metro G, Signorelli D, Economopoulou P, Roila F, Banna GL, et al. Poor Performance Status and Front-Line Pembrolizumab in Advanced Non-Small-Cell Lung Cancer (NSCLC) Patients With PD-L1>50%. *J Clin Oncol* (2020) 38:e21651–1. doi: 10.1200/JCO.2020.38.15_suppl.e21651
29. Rheinheimer S, Heussel C-P, Mayer P, Gaissmaier L, Bozorgmehr F, Winter H, et al. Oligoprogressive Non-Small-Cell Lung Cancer Under Treatment With PD-(L)1 Inhibitors. *Cancers (Basel)* (2020) 12:1046. doi: 10.3390/cancers12041046
30. Wang Y, Chen H, Zhang T, Yang X, Zhong J, Wang Y, et al. Plasma Cytokines interleukin-18 and C-X-C Motif Chemokine Ligand 10 Are Indicative of the Anti-Programmed Cell Death Protein-1 Treatment Response in Lung Cancer Patients. *Annal Transl Med* (2021) 9:33. doi: 10.21037/atm-20-1513
31. Khan S, Khan SA, Luo X, Fattah FJ, Saltarski J, Gloria-McCutchen Y, et al. Immune Dysregulation in Cancer Patients Developing Immune-Related Adverse Events. *Br J Cancer* (2019) 120:63–8. doi: 10.1038/s41416-018-0155-1
32. Hommes JW, Verheijden RJ, Suijkerbuijk KP, Hamann D. Biomarkers of Checkpoint Inhibitor Induced Immune-Related Adverse Events-a Comprehensive Review. *Front Oncol* (2020) 10:585311. doi: 10.3389/fonc.2020.585311
33. Negrin RS. Graft-Versus-Host Disease Versus Graft-Versus-Leukemia. *Hematol Am Soc Hematol Educ Program* (2015) 2015:225–30. doi: 10.1182/asheducation-2015.1.225
34. Pasquini MC. Impact of Graft-Versus-Host Disease on Survival. *Best Pract Res Clin Haematol* (2008) 21:193–204. doi: 10.1016/j.beha.2008.02.011
35. Lesueur P, Escande A, Thariat J, Vauléon E, Monnet I, Cortot A, et al. Safety of Combined PD-1 Pathway Inhibition and Radiation Therapy for Non-Small-Cell Lung Cancer: A Multicentric Retrospective Study From the GFPC. *Cancer Med* (2018) 7:5505–13. doi: 10.1002/cam4.1825
36. Voong KR, Hazell SZ, Fu W, Hu C, Lin CT, Ding K, et al. Relationship Between Prior Radiotherapy and Checkpoint-Inhibitor Pneumonitis in Patients With Advanced Non-Small-Cell Lung Cancer. *Clin Lung Cancer* (2019) 20:e470–9. doi: 10.1016/j.cllc.2019.02.018

37. Gemmill JA L, Sher A. Anti-Pd-1-Related Exacerbation of Interstitial Lung Disease in a Patient With Non-Small Cell Lung Cancer: A Case Presentation and Review of the Literature. *Cancer Invest* (2020) 38:365–71. doi: 10.1080/07357907.2020.1783677
38. Shimoji K, Masuda T, Nakanishi Y, Yamaguchi K, Sakamoto S, Horimasu Y, et al. Pre-Existing Interstitial Lung Abnormalities Are Risk Factors for Immune Checkpoint Inhibitor-Induced Interstitial Lung Disease in Non-NSCLC Cancers. *J Clin Oncol* (2020) 38:e15171–1. doi: 10.1200/JCO.2020.38.15_suppl.e15171
39. Brilli L, Danielli R, Campanile M, Secchi C, Ciuoli C, Calabrò L, et al. Baseline Serum TSH Levels Predict the Absence of Thyroid Dysfunction in Cancer Patients Treated With Immunotherapy. *J Endocrinol Invest* (2020). doi: 10.1007/s40618-020-01480-6. [Epub ahead of print].
40. Kimbara S, Fujiwara Y, Iwama S, Ohashi K, Kuchiba A, Arima H, et al. Association of Antithyroglobulin Antibodies With the Development of Thyroid Dysfunction Induced by Nivolumab. *Cancer Sci* (2018) 109:3583–90. doi: 10.1111/cas.13800
41. Zhou X, Yao Z, Yang H, Liang N, Zhang X, Zhang F. Are Immune-Related Adverse Events Associated With the Efficacy of Immune Checkpoint Inhibitors in Patients With Cancer? A Systematic Review and Meta-Analysis. *BMC Med* (2020) 18:87. doi: 10.1186/s12916-020-01549-2
42. Indini A, Di Guardo L, Cimminiello C, Prisciandaro M, Randon G, de Braud F, et al. Immune-Related Adverse Events Correlate With Improved Survival in Patients Undergoing Anti-PD1 Immunotherapy for Metastatic Melanoma. *J Cancer Res Clin Oncol* (2019) 145:511–21. doi: 10.1007/s00432-018-2819-x
43. Haratani K, Hayashi H, Chiba Y, Kudo K, Yonesaka K, Kato R, et al. Association of Immune-Related Adverse Events With Nivolumab Efficacy in Non-Small-Cell Lung Cancer. *JAMA Oncol* (2018) 4:374–8. doi: 10.1001/jamaoncol.2017.2925
44. Kim H, Kim M, Lee S-H, Park SY, Kim YN, Kim H, et al. Development of Thyroid Dysfunction Is Associated With Clinical Response to PD-1 Blockade Treatment in Patients With Advanced Non-Small Cell Lung Cancer. *Oncoimmunology* (2017) 7:e1375642. doi: 10.1080/2162402X.2017.1375642
45. Judd J, Zibelman M, Handorf E, O'Neill J, Ramamurthy C, Bentota S, et al. Immune-Related Adverse Events as a Biomarker in Non-Melanoma Patients Treated With Programmed Cell Death 1 Inhibitors. *Onoclogist* (2017) 22:1232–7. doi: 10.1634/theoncologist.2017-0133
46. Horvat TZ, Adel NG, Dang T-O, Momtaz P, Postow MA, Callahan MK, et al. Immune-Related Adverse Events, Need for Systemic Immunosuppression, and Effects on Survival and Time to Treatment Failure in Patients With Melanoma Treated With Ipilimumab at Memorial Sloan Kettering Cancer Center. *J Clin Oncol* (2015) 33:3193–8. doi: 10.1200/JCO.2015.60.8448
47. Bjørnhart B, Hansen KH, Jørgensen TL, Herrstedt J, Schytte T. Efficacy and Safety of Immune Checkpoint Inhibitors in a Danish Real Life non-Small Cell Lung Cancer Population: A Retrospective Cohort Study. *Acta Oncol* (2019) 58:953–61. doi: 10.1080/0284186X.2019.1615636
48. Chen X, Nie J, Dai L, Hu W, Zhang J, Han J, et al. Immune-Related Adverse Events and Their Association With the Effectiveness of PD-1/PD-L1 Inhibitors in Non-Small Cell Lung Cancer: A Real-World Study From China. *Front Oncol* (2021) 11:607531. doi: 10.3389/fonc.2021.607531
49. Dall'Olio FG, Di Nunno V, Massari F. Immortal Time Bias Question in the Association Between Toxicity and Outcome of Immune Checkpoint Inhibitors. *J Clin Oncol* (2019) 38:105–6. doi: 10.1200/JCO.19.01728
50. Dall'Olio FG, Rizzo A, Mollica V, Massucci M, Maggio I, Massari F. Immortal Time Bias in the Association Between Toxicity and Response for Immune Checkpoint Inhibitors: A Meta-Analysis. *Immunotherapy* (2021) 13:257–70. doi: 10.2217/imt-2020-0179
51. Morimoto K, Yamada T, Takumi C, Ogura Y, Takeda T, Onoi K, et al. Immune-Related Adverse Events Are Associated With Clinical Benefit in Patients With Non-Small-Cell Lung Cancer Treated With Immunotherapy Plus Chemotherapy: A Retrospective Study. *Front Oncol* (2021) 11:630136. doi: 10.3389/fonc.2021.630136
52. Cortellini A, Chiari R, Ricciuti B, Metro G, Perrone F, Tiseo M, et al. Correlations Between the Immune-Related Adverse Events Spectrum and Efficacy of Anti-PD1 Immunotherapy in NSCLC Patients. *Clin Lung Cancer* (2019) 20:237–247.e1. doi: 10.1016/j.cllc.2019.02.006
53. Shankar B, Zhang J, Naqash AR, Forde PM, Feliciano JL, Marrone KA, et al. Multisystem Immune-Related Adverse Events Associated With Immune Checkpoint Inhibitors for Treatment of Non–Small Cell Lung Cancer. *JAMA Oncol* (2020) 6:1952. doi: 10.1001/jamaoncol.2020.5012
54. Olsson-Brown AC, Baxter M, Dobeson C, Feeney L, Lee R, Maynard A, et al. Real-World Outcomes of Immune-Related Adverse Events in 2,125 Patients Managed With Immunotherapy: A United Kingdom Multicenter Series. *J Clin Oncol* (2020) 38:7065. doi: 10.1200/JCO.2020.38.15_suppl.7065
55. Raschi E, Gatti M, Gelsomino F, Ardizzoni A, Poluzzi E, De Ponti F. Lessons to be Learnt From Real-World Studies on Immune-Related Adverse Events With Checkpoint Inhibitors: A Clinical Perspective From Pharmacovigilance. *Targeted Oncol* (2020) 15:449–66. doi: 10.1007/s11523-020-00738-6
56. Aulakh R, Singh S. Strategies for Minimizing Corticosteroid Toxicity: A Review. *Indian J Pediatr* (2008) 75:1067–73. doi: 10.1007/s12098-008-0211-6
57. Stuck AE, Minder CE, Frey FJ. Risk of Infectious Complications in Patients Taking Glucocorticosteroids. *Rev Infect Dis* (1989) 11:954–63. doi: 10.1093/clinids/11.6.954
58. Ricciuti B, Dahlberg SE, Adeni A, Sholl LM, Nishino M, Awad MM. Immune Checkpoint Inhibitor Outcomes for Patients With Non-Small-Cell Lung Cancer Receiving Baseline Corticosteroids for Palliative Versus Nonpalliative Indications. *J Clin Oncol* (2019) 37:1927–34. doi: 10.1200/JCO.19.00189
59. Drakaki A, Luhn P, Wakelee H, Dhillon PK, Kent M, Shim J, et al. Association of Systemic Corticosteroids With Overall Survival in Patients Receiving Cancer Immunotherapy for Advanced Melanoma, non-Small Cell Lung Cancer or Urothelial Cancer in Routine Clinical Practice. *Ann Oncol* (2019) 30:xi16–7. doi: 10.1093/annonc/mdz449.001
60. de Giglio A, Mezquita L, Auclin E, Blanc-Durand F, El-Amarti L, Caramella C, et al. Impact of Early Introduction of Steroid on Immune-Checkpoint Inhibitors (ICI) in Patients With Advanced non-Small Cell Lung Cancer Treated. *Ann Oncol* (2019) 30:xi16. doi: 10.1093/annonc/mdz449
61. Moghadam-Kia S, Werth VP. Prevention and Treatment of Systemic Glucocorticoid Side Effects. *Int J Dermatol* (2010) 49:239–48. doi: 10.1111/j.1365-4632.2009.04322.x
62. Fardet L, Cabane J, Lebbé C, Morel P, Flahault A. Incidence and Risk Factors for Corticosteroid-Induced Lipodystrophy: A Prospective Study. *J Am Acad Dermatol* (2007) 57:604–9. doi: 10.1016/j.jaad.2007.04.018
63. Brown ES. Effects of Glucocorticoids on Mood, Memory, and the Hippocampus. Treatment and Preventive Therapy. *Ann N Y Acad Sci* (2009) 1179:41–55. doi: 10.1111/j.1749-6632.2009.04981.x
64. Warrington TP, Bostwick JM. Psychiatric Adverse Effects of Corticosteroids. *Mayo Clin Proc* (2006) 81:1361–7. doi: 10.4065/81.10.1361
65. van Staa TP, Leufkens HG, Cooper C. The Epidemiology of Corticosteroid-Induced Osteoporosis: A Meta-Analysis. *Osteoporosis Int* (2002) 13:777–87. doi: 10.1007/s001980200108
66. Urban RC, Cotlier E. Corticosteroid-Induced Cataracts. *Surv Ophthalmol* (1986) 31:102–10. doi: 10.1016/0039-6257(86)90077-9
67. Braaten TJ, Brahmer JR, Forde PM, Le D, Lipson EJ, Naidoo J, et al. Immune Checkpoint Inhibitor-Induced Inflammatory Arthritis Persists After Immunotherapy Cessation. *Ann Rheum Dis* (2020) 79:332–8. doi: 10.1136/annrheumdis-2019-216109
68. Riudavets M, Mosquera J, Garcia-Campelo R, Serra J, Anguera G, Gallardo P, et al. Immune-Related Adverse Events and Corticosteroid Use for Cancer-Related Symptoms Are Associated With Efficacy in Patients With Non-small Cell Lung Cancer Receiving Anti-Pd-(L)1 Blockade Agents. *Front Oncol* (2020) 10:1677. doi: 10.3389/fonc.2020.01677
69. Wang DY, Salem J-E, Cohen JV, Chandra S, Menzer C, Ye F, et al. Fatal Toxic Effects Associated With Immune Checkpoint Inhibitors. *JAMA Oncol* (2018) 4:1721. doi: 10.1001/jamaoncol.2018.3923

Conflict of Interest: FB: research funding from BMS and travel grants from BMS and MSD. JK: research funding from AstraZeneca and Celgene. DK: advisory board and speaker's honoraria from AstraZeneca, BMS, Pfizer. RS: research funding from BMS. KB: research funding from Novartis and Abbvie, speaker's honoraria/advisory board/travel grants from Abbvie, BMS, Gilead/Galapagos, Janssen, Lilly, Medac, MSD, Mundipharma, Novartis, Pfizer, Roche, UCB. AS: advisory board honoraria from BMS, AstraZeneca, ThermoFisher, Novartis, speaker's honoraria from BMS, Illumina, AstraZeneca, Novartis, ThermoFisher, MSD, Roche, and research funding from Chugai. MT: advisory board honoraria from Novartis, Lilly, BMS, MSD, Roche, Celgene, Takeda, AbbVie, Boehringer, speaker's honoraria from Lilly, MSD, Takeda, research funding from AstraZeneca,

BMS, Celgene, Novartis, Roche and travel grants from BMS, MSD, Novartis, Boehringer. PC: research funding from AstraZeneca, Novartis, Roche, Takeda, and advisory board/lecture fees from AstraZeneca, Boehringer Ingelheim, Chugai, Novartis, Pfizer, Roche, Takeda.

The remaining authors declare that the research was conducted in the absence of any commercial or financial relationships that could be construed as a potential conflict of interest.

Copyright © 2021 Daniello, Elshiaty, Bozorgmehr, Kuon, Kazdal, Schindler, Shah, Volckmar, Lusky, Diekmann, Liersch, Faehling, Muley, Kriegsmann, Benesova, Stenzinger, Thomas and Christopoulos. This is an open-access article distributed under the terms of the Creative Commons Attribution License (CC BY). The use, distribution or reproduction in other forums is permitted, provided the original author(s) and the copyright owner(s) are credited and that the original publication in this journal is cited, in accordance with accepted academic practice. No use, distribution or reproduction is permitted which does not comply with these terms.

frontiers in Oncology

SYSTEMATIC REVIEW
published: 15 July 2021
doi: 10.3389/fonc.2021.680615

Postoperative Radiotherapy for Patients With Resectable Stage III-N2 Non-Small Cell Lung Cancer: A Systematic Review and Meta-Analysis

Tianyu Lei†, Jing Li†, Hao Zhong, Huibo Zhang, Yan Jin, Jie Wu, Lan Li, Bin Xu, Qibin Song and Qinyong Hu**

Cancer Center, Renmin Hospital of Wuhan University, Wuhan, China

OPEN ACCESS

Edited by:
Junji Uchino, Kyoto Prefectural University of Medicine, Japan

Reviewed by:
Arya Amini, City of Hope National Medical Center, United States
Lawek Berzenji, University of Antwerp, Belgium

***Correspondence:**
Qibin Song
qibinsong@whu.edu.cn
Qinyong Hu
rm001223@whu.edu.cn

†These authors have contributed equally to this work and share first authorship

Specialty section:
This article was submitted to Thoracic Oncology, a section of the journal Frontiers in Oncology

Received: *15 March 2021*
Accepted: *24 June 2021*
Published: *15 July 2021*

Citation:
Lei T, Li J, Zhong H, Zhang H, Jin Y, Wu J, Li L, Xu B, Song Q and Hu Q (2021) Postoperative Radiotherapy for Patients With Resectable Stage III-N2 Non-Small Cell Lung Cancer: A Systematic Review and Meta-Analysis. Front. Oncol. 11:680615. doi: 10.3389/fonc.2021.680615

Purpose: For resectable cases of stage III-N2 non-small cell lung cancer (NSCLC), the best treatment after surgery is still uncertain. The effect of postoperative radiotherapy (PORT) is controversial. Thus, we performed this updated meta-analysis to reassess the data of PORT in stage III-N2 NSCLC patients, to figure out whether these patients can benefit from PORT.

Methods: We conducted searches of the published literature in EMBASE, PubMed, and the Cochrane Library for relevant randomized control trials (RCTs) comparing PORT group with the non-PORT group in NSCLC patients at stage III-N2. These studies allowed the prior chemotherapy in the treatment. We extracted the data from these articles and used the hazard ratios (HRs) and their 95% confidence intervals (CIs) as summary statistics for estimating the effect of PORT on overall survival (OS), disease-free survival (DFS), local-regional recurrence-free survival (LRFS).

Result: The analyses of seven randomized controlled trials (1,318 participants) show no benefit of PORT on survival (HR, 0.87; 95% CI, 0.71 to 1.07; p = 0.18) but a significantly different effect of PORT on DFS (HR, 0.83; 95% CI, 0.71 to 0.97; p = 0.02) and LRFS (HR, 0.64; 95% CI, 0.50 to 0.81; p = 0.0003). There is not enough evidence of a difference in the effect on survival by the utility of chemotherapy along with PORT though subgroup analysis of no chemotherapy group, concurrent chemoradiotherapy and sequential chemoradiotherapy group. Even in trials with 3D-CRT radiation technique, the pooled analysis shows no benefit of PORT on survival in patients with stage III-N2 NSCLC (data is not shown).

Conclusion: Our findings illustrate that in the postoperative treatment for patients with stage III-N2 NSCLC, PORT contributes to a significantly increased DFS and LR and may not associate with an improved OS, indicating a cautious selection.

Keywords: non-small cell lung cancer, postoperative radiotherapy, surgery, chemotherapy, stage III-N2

INTRODUCTION

Lung cancer is the leading cause of cancer death (18.0% of the total cancer deaths) (1). There are two main forms of lung cancer: NSCLC (85% of patients) and small cell lung cancer (SCLC) (15%) (2). The standard treatment for patients with early stage non-small cell lung cancer (NSCLC) is surgical resection (3), but for patients with apparently completely resected disease, survival is only 40% at five years (4), which may be due to the local-regional recurrent. Especially in patients who are identified as having N2 lymph node involvement, have a worse survival and local-regional recurrence compared with N0 or N1 patients (5). To improve local-regional control of the disease and prolong the survival time, investigators have explored the effect of adjuvant postoperative radiotherapy (PORT) and postoperative chemotherapy (POCT). Burdett et al. (4) initiated an individual participant data meta-analysis for the effect of PORT in NSCLC patients. The pooled analyses showed a significant adverse effect of PORT using cobalt therapy or/and linear accelerators on survival (P = 0.001), with HR 1.18 (95%CI 1.07–1.31). Likewise, data on local-regional recurrence-free survival (HR, 1.12; 95%CI 1.01–1.24) was also significantly in favor of surgery alone without PORT. Many detailed information was included in this trial, while its conclusion could not represent the effect of modern radiotherapy technique. Hence, the role of PORT in NSCLC at stage III-N2 is still unclear. Some previous meta-analyses demonstrated that PORT was associated with improved OS (6, 7), but these meta-analyses included both prospective trials and retrospective studies, which might cause selective bias or other potential bias. Recently, the Lung ART trial in Europe and another trial in China (NCT00880971) have demonstrated different results. Whether patients at stage III-N2 need postoperative radiotherapy or not remains controversial.

Therefore, we include recent high-quality RCTs (evaluated by the ROB2.0 tool provided by the Cochrane website) to perform a meta-analysis to reassess the effect of PORT for resected stage III-N2 NSCLC patients, in an effort to figure out whether patients at stage III-N2 can benefit from PORT. For these patients, chemotherapy is valuable for survival (8, 9), and thus these RCTs allow the prior chemotherapy (pre-operative or post-operative adjuvant chemotherapy, or both) if the research group and the control group both accept the same chemotherapy.

MATERIALS AND METHODS

This meta-analysis is based on the Preferred Reporting Items for Systematic Reviews and Meta-analysis (PRISMA) criteria for systematic review and meta-analysis of preferred reporting projects (10) (see **Supplementary Materials**).

Literature Sources

To identify potentially suitable studies, we searched the Medline, Embase, Cochrane Library, ClinicalTrials.gov for the available published studies before November 6, 2020. We retrieved RCTs from these databases for patients with resectable stage III-N2 NSCLC treated with PORT. The details of the search strategy are presented in **Supplementary Materials**. All published papers with available full texts were retrieved.

Inclusion and Exclusion Criteria

Studies were included if they met the following criteria: 1) types of participants: completely resected III-N2 NSCLC patients; 2) types of interventions: postoperative radiotherapy ((neo-) adjuvant chemotherapy was allowed); 3) types of outcomes: reported overall survival (OS) or disease-free survival (DFS) or local-regional recurrence survival (LRFS); and 4) types of studies: RCTs only.

If multiple articles covered the same study population, the study with the most recent and complete survival data was utilized. Studies were excluded if any of the following criteria is met: 1) letters, editorials, case reports, reviews and retrospective studies; and 2) survival data could not be extracted from the literature.

Two investigators checked all the titles and abstracts respectively, and obtained all the full publications for those thought to be potentially relevant. The flowchart is shown in **Figure 1**.

Data Extractions

The data were extracted by two investigators independently, and the consensus was reached in the case of any discrepancy in all the data. We extracted the following information: first author, years of publication, duration, country of origin, the intervention of each arm, adverse effect, numbers of patient and time-to-event data (OS, DFS or LRFS, especially the value of HR and the 95% confidence interval).

Quality Assessments

The methodological quality of RCT was assessed by a Cochrane risk of bias tool (11), which was consistent with the following seven domains: 1) random sequence generation; 2) allocation concealment 3) blinding of participants and personnel; 4) blinding of outcome assessment; 5) incomplete outcome data; 6) selective reporting; 7) other bias. The result is shown in the graph of bias risk (**Figure 2**).

Statistical Analyses

Data were statically analyzed using the software Review Manager 5.3 (Cochrane Collaboration, Oxford, UK). The hazard ratios (HRs) and their 95% confidence intervals (CIs) were used as summary statistics for OS, DFS, and LRFS in the present meta-analysis.

Crude HRs with 95% CIs were extracted directly from the original reports or calculated by the Kaplan–Meier curves or other estimation methods based on the methods supported by Tierney et al. (12). They developed spreadsheet in Microsoft Excel that carries out the calculations for all of the methods described. We used the Engauge-Digitizer (ver11.1) to extract the data from Kaplan–Meier curves. Then the extracted data and estimate censoring using the minimum and maximum follow-up were inputted to the spreadsheet, to obtain similar summary statistics. We made use of the *Chi*-square and *I*-square tests to evaluate the heterogeneity with the significance set at P <0.05 and/or *I*-square >50%. If there is no significant heterogeneity,

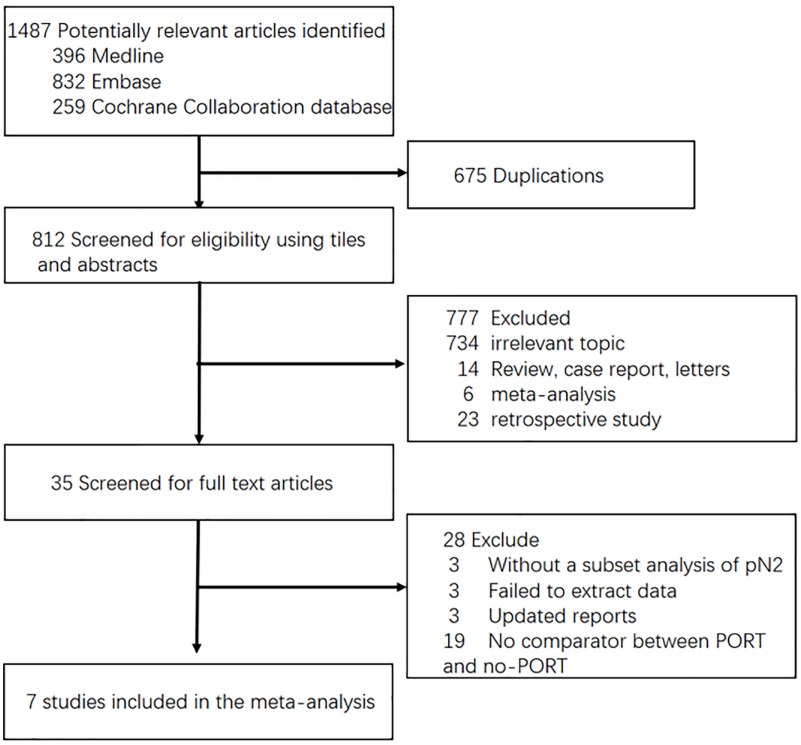

FIGURE 1 | Flow-chart of selecting RCTs for analysis. PORT, Post-operative radiotherapy.

the fixed effects model will be used, otherwise, the randomized effects model is utilized. The results of the summary HRs are presented in the forest plots. The funnel plot is used to measure the publication bias.

RESULTS

Description of Studies

We identified eligible trials and finally included seven trials in this review (see Characteristics of included studies, **Table 1**). We could not include three trials: Smolle-Juettner et al. (20), Mayer et al. (21) and Feng et al. (22). Data for these three trials were unavailable due to the lack of accurate P-value or HR. Thus, this review is based on the results of seven RCTs [Debevec et al. (13); Stephens et al. (14); Perry et al. (15); Shen et al. (16); Sun et al. (17); Hui et al. (18); Pechoux et al. (19)] and 1,318 individuals. Baseline participant characteristics from published literatures show that most participants were male with stage IIIA pN2 squamous cell carcinoma (although histology was unknown for a relatively large number of participants) with good performance status. Among these trials, PORT doses ranged from 30 to 54 Gy, given between 10 and 30 fractions, and considerable diversity was evident in other aspects of radiotherapy planning (**Table 2**). All trials included participants with completely resected tumours for which the disease stage was no greater than IIIB(N2) according to the 8th edition of the AJCC/TNM staging system. Most trials did not provide updated follow-up. In most trials, patients were treated with adjuvant chemotherapy prior or post operation and there were two trials conducting concurrent chemoradiotherapy after resection, two receiving sequential chemoradiotherapy and one having unclear chemotherapy sequence. The other two trials had no chemotherapy.

Effects of Interventions

Results were finally based on information from seven RCTs (1,318 participants, 659 with PORT, 659 without PORT), representing 99% of individuals from all eligible randomized trials. Overall survival data were available for all trials except Pechoux et al. (19) due to its incompletely published data. Recurrence and disease-free survival data were only available for four trials, respectively. We were not able to get most of the additional information on patients' characteristics requested from trialists, and thus, some data were not available. Information on age, sex, stage, number of pN2 and histology was not provided for all trials. Performance status data were available for six trials except the trial of Hui et al. (18) and all scored less than 2 expect one patient in surgery group of Debevec et al.'s (13) trials (performance status (Kamofsky) more than 90 = PS (ECOG) 1, 70–90 = 2, less than 70 = more than 2). Therefore, there were insufficient information for the assessment of treatment by covariate interactions.

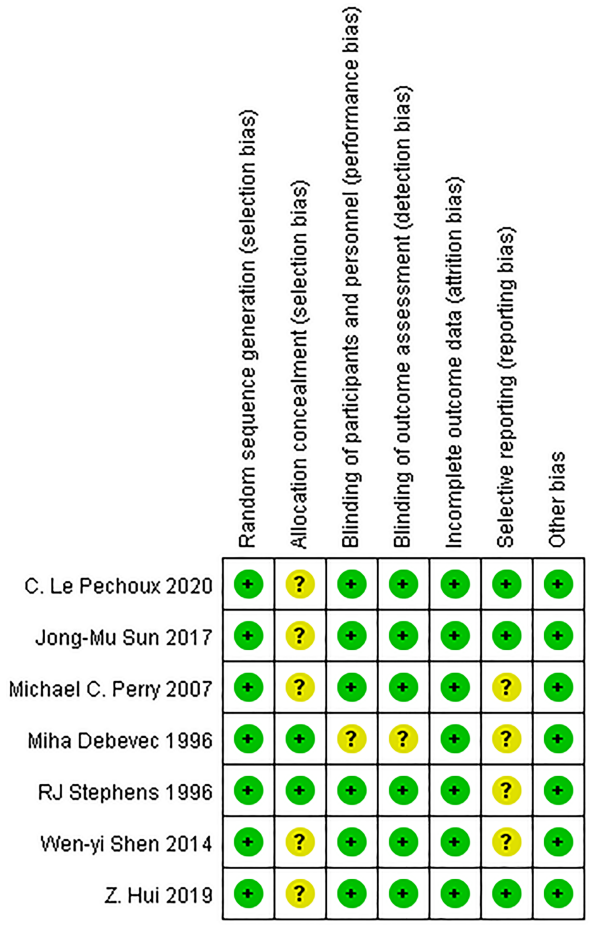

FIGURE 2 | Risk of bias assessment of included studies.

Overall Survival

Overall survival data were available for six trials except the trial of Pechoux et al. (19) with incompletely published data and included information from 817 participants (407 with PORT, 410 without PORT). Although the confidence intervals (CIs) for individual trial results were wide, combined results showed a similar effect of PORT on survival (P = 0.18), with a hazard ratio (HR) of 0.87 (95% CI 0.71 to 1.07) (**Figure 3**). There was no good evidence of increased statistical heterogeneity between trials (I^2 = 0%, P = 0.53).

Disease-Free Survival

Data on disease-free survival were available from four trials. Analysis of disease-free survival based on 1,201 patients, gave an HR of 0.83 (95% CI 0.71 to 0.97) in favor of PORT arm (P = 0.02) (**Figure 4**). There was no evidence of gross statistical heterogeneity between trials (I^2 = 0%, P = 0.70). Results may indicate a significant decrease in disease-free survival on the PORT arm.

Local Recurrence-Free Survival

Four trials provided data on local-regional recurrence. Analysis of local-regional recurrence-free survival based on 706 patients, gave an HR of 0.64 (95% CI 0.50 to 0.81), significantly in favor of PORT arm (P = 0.0003) (**Figure 5**). There was no good evidence of statistical heterogeneity between trials (I^2 = 0%, P = 0.60), which was consistent with the 1,998 analysis (23) (I^2 = 29%, P = 0.19). Results may indicate a significant decrease in local-regional recurrence on the PORT arm.

Subgroup Analyses

We undertook analyses to assess whether there was any evidence that postoperative radiotherapy had a differential effect in subgroups with or without the order of radiotherapy and chemotherapy. For survival (**Figure 1**), there was no evidence that postoperative radiotherapy was differentially effective in any group of patients defined by without chemotherapy (interaction p = 0.19), concurrent chemoradiotherapy (interaction p = 0.32), or sequential chemoradiotherapy (interaction p = 1.00).

Sensitivity Analysis and Investigation of Publication Bias

Sensitivity analysis was performed by removing each study sequentially. According to the results, no significant change was observed for pooled HRs, suggesting that all the pooled results were stable and the overall tendency was consistency, indicating no benefit of PORT, which was consistent with previous studies. Publication bias as assessed by Funnel figure (**Figure 6**) indicated no publication bias.

Toxicity and Side Effect

In the Lung ART trial (19), the PORT group had a higher incidence of grades 3–4 toxicity. According to the cause of death, participants in the PORT group were at a larger risk of dying from the cardio-pulmonary toxicity compared with the control group (16% *vs* 2%), which may partly offset the benefit of local control brought by PORT. In the trial initiated by Sun et al. (17), oral or chest pain was more common in the concurrent chemoradiotherapy arm, while the incidence of myalgia and peripheral neuropathy was higher in the chemotherapy group. The incidence of grades 3–4 toxicity was 36 and 18% in the CCRT arm and chemotherapy, respectively. Another trial (2014) (16) reported that the postoperative concurrent chemoradiotherapy group had a significantly higher incidence of grades 3–4 anemia and esophagitis. Two trials (13, 14) published in 1996 reported that only mild or moderate after effects were observed mainly due to their lower radiation dose compared with the other trials. These evidences suggest that PORT may contribute to a higher incidence of severe toxicity. The improved LRFS and DFS can't be translated into improved OS may partly attribute to the toxicity.

DISCUSSION

Due to the question of whether postoperative radiotherapy is effective in the treatment of NSCLC remained unanswered, the

TABLE 1 | Details and results of certain included studies.

Author	Recruitment	Phase of trials	Median age	N	RT technique	Chemotherapy Regimen	Primary end-point	DFS	OS	LRFS
				Patients				HR	HR	HR
Debevec et al. (13)	1988 to 1992	NA	59 (35–80)	35	Linac	without chemotherapy	NA	NA	0.91 (0.44–1.87), NA	NA
				39	–			–	–	–
Stephens et al. (14)	July 1986 to October 1993	NA	62	52	megavoltage x-ray /Cobalt	without chemotherapy	NA	NA	0.74 (0.48–1.15), P = 0.18	0.55 (0.29–1.05), P = 0.07
				54	–			–	–	–
Perry et al. (15)	May 1998 to June 2000	Phase III	NA	19	NA	sequential chemoradiotherapy	NA	NA	0.95 (0.40–2.28), P = 0.91	NA
				18	–			–	–	–
Shen et al. (16)	April 2004 to March 2009	Phase III	NA	66	3DCRT with linac	concurrent chemoradiotherapy	OS and DFS	0.67 (0.45–0.98), P = 0.041	0.69 (0.457–1.044), P = 0.073	HR = 0.48(0.28–0.83), P = 0.009
				69	–			–	–	–
Sun et al. (17)	June 2009 to September 2014	Phase II	60 (38–78)	51	3DCRT with linac	concurrent chemoradiotherapy	DFS	0.94 (0.58–1.52), P = 0.400	1.33 (0.71–2.49), P = 0.38	0.75 (0.36–1.58), NA
				50	–			–	–	–
Hui et al. (18)	January 2009 to December 2017	Phase III	NA	184	3D-CRT/sIMRT	sequential chemoradiotherapy	DFS	0.85 (0.65–1.10), 1-sided P = 0.10	1.01 (0.68–1.51), P = 0.94	0.71 (0.51–0.97), P = 0.03
				180	–			–	–	–
Le Pechoux et al. (19)	August 2007 to July 2018	phase III	61 (36–85)	252	3D-CRT	prior (neo)-adjuvant CT	DFS	0.85 (0.67–1.07), P = 0.16	NA	NA
				249	–			–	–	–

NA, not available.

TABLE 2 | The detail of radiotherapy and chemotherapy of included studies.

Trial	Radiotherapy dose				Prescription Technique	Clinical target volume	Chemotherapy
	Total dose (Gy)	Fractions	Durations (weeks)	Gy/day			
Debevec et al. (13)	30	10 or 12	2	2.5 or 3.0	Linac	isolateral hilum and mediastinum	No chemotherapy
Stephens et al. (14)	40	15	3	2.7	megavoltage X-ray and Cobalt	NA	No chemotherapy
Perry et al. (15)	50	25	5	2.0	NA	the mediastinum, supraclavicular fossae, and ipsilateral hilum	Paclitaxel and carboplatin
Shen et al. (16)	50.4	28	6	1.8	3DCRT with linac	ipsilateral mediastinum, hilum and subcarinal lymph node area	paclitaxel and cisplatin
JongMu Sun et al. (17)	50	25	5	2.0	3DCRT with linac	mediastinal lymphatic stations and the immediately adjacent lymph node stations	Adjuvant paclitaxel and carboplatin
Hui et al. (18)	50	25	6	2.0	3D-CRT/sIMRT	Ipsilateral hilum, subcarinal region and ipsilateral mediastinum	platinum based chemotherapy
Le Pechoux et al. (19)	54	27–30	6	1.8–2.0	3D-CRT	NA	prior (neo)-adjuvant CT was allowed

NA, not available.

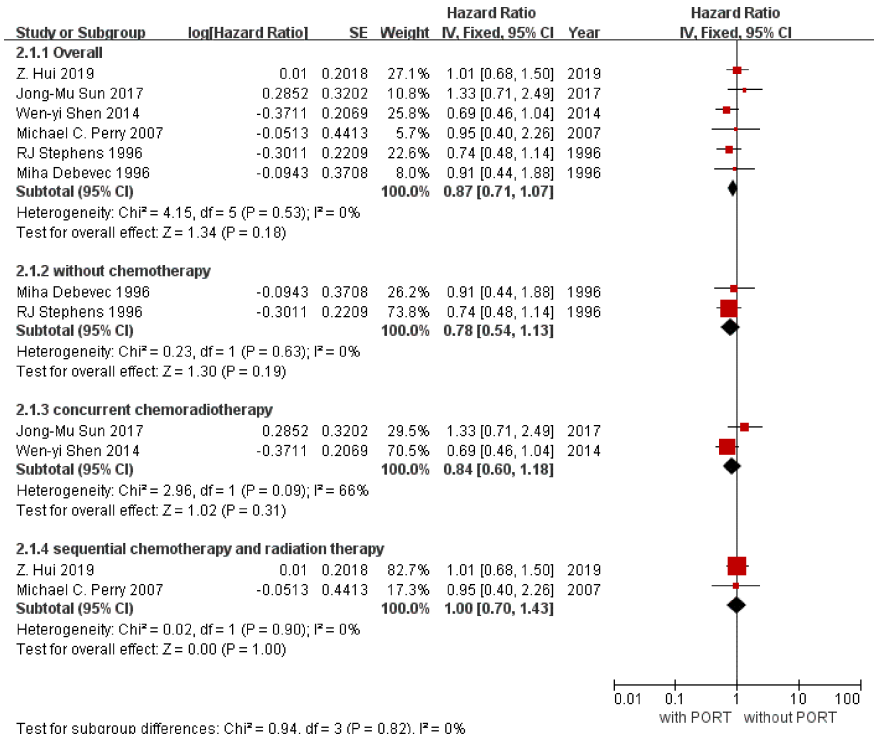

FIGURE 3 | Overall survival. PORT, post-operative radiotherapy; HR, Hazard Ratio.

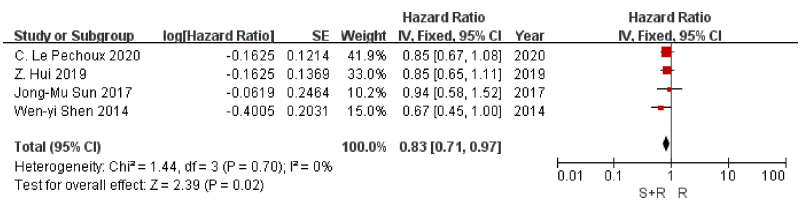

FIGURE 4 | Disease Free Survival. PORT, post-operative radiotherapy; HR, Hazard Ratio.

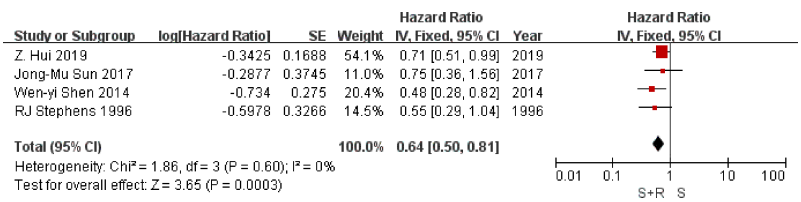

FIGURE 5 | Local-regional recurrence-free survival. PORT, post-operative radiotherapy; HR, Hazard Ratio.

clinical trials from different countries and regions are ongoing in spite of varied clinical practice nationally and internationally. The aim of this systematic review and meta-analysis is to provide an updated, reliable and comprehensive summary of favorable effect of postoperative radiotherapy in NSCLC patients, to provide reliable guidance for clinical practice and future research.

For the primary endpoint of survival, there is ambiguity of evidence in the protective role of PORT in NSCLC patients.

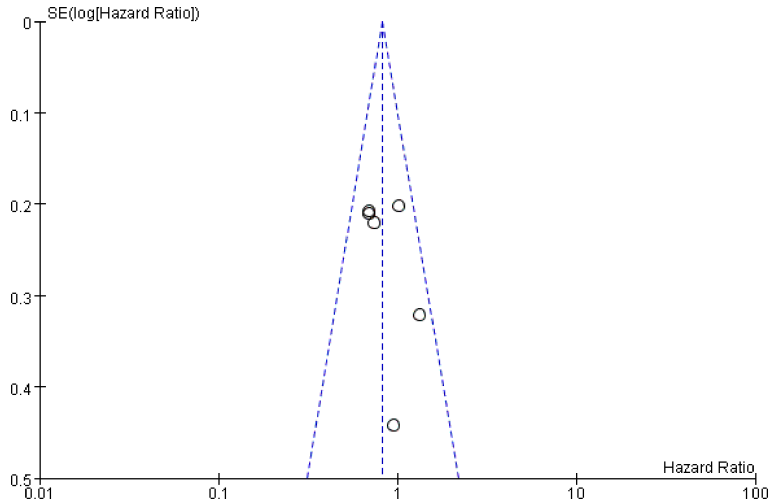

FIGURE 6 | The funnel plot was used to measure the publication bias.

However, although there is slight tendency that PORT plays a less detrimental role in NSCLC patients compared to 1998 meta-analysis (23) (HR, 1.21, 95% CI 1.08 to 1.34) or 2016 meta-analysis (HR, 1.18, 95% CI 1.07 to 1.31), PORT has no benefit in two recent trials (2017 and 2019). Retrospective studies demonstrated that modern PORT seemed to associate with improved OS compared with no PORT for patients with N2 NSCLC after complete resection and adjuvant chemotherapy (4, 24, 25). Likewise, the difference between concurrent chemoradiotherapy after resection and sequential chemotherapy followed by postoperative radiotherapy was not significant for locally advanced or incompletely resected NSCLC (26), which was consistent with our results. Nevertheless, another clinical trial indicated conducting adjuvant sequential CRT was associated with improved survival over concurrent CRT after completely resection in pN2 NSCLC patients (27). Also, a time to radiation of ≥8 weeks with sequential chemotherapy in the setting of PORT was associated with improved OS (P = 0.0045) in patients with NSCLC with pN2 nodes (28). While another analysis of the National Cancer Data Base reported that for completely resected pN2 NSCLC, adjuvant sequential chemoradiation therapy was associated with improved survival over concurrent chemoradiation therapy (Median OS, 53 months versus 37 months; p <0.001) (27), which might result from the toxicity-related factors. In addition, patients with NSCLC who underwent R0 resection and were found to have pN2 disease had improved outcomes when chemotherapy was administered before radiotherapy compared to concurrent chemotherapy, after propensity score matching (26). In conclusion, adjuvant CT has already been regarded as a standard treatment for patients with pathological diagnosed N2 NSCLC (24). Whereas, it's a huge question that whether the addition of radiotherapy to PORT with adjuvant chemotherapy in patients with III N2 NSCLC is necessary and rational and the time to use adjuvant PORT is uncertain due to heterogeneity of different studies.

Through reviewing previous researches, we find an analysis based on the SEER Database has reported that PORT was a favorable prognostic factor for patients with stage IIIA N2 disease with ≥6 positive lymph nodes (HR, 0.742; 95% CI, 0.587–0.938; P = 0.012) (29). Likewise, a meta-analysis consisting of 1 randomized controlled trial and 12 retrospective studies suggested that PORT improved both OS [HR, 0.85; 95% CI: 0.79–0.92] and DFS (HR, 0.57; 95% CI: 0.38–0.85) compared with non-PORT treatment in patients with multiple N2 metastases or multiple N2 station involvement, but there was no significant difference in either OS or DFS between PORT and non-PORT groups for patients with single N2 station involvement (30). These evidences suggest that we can screen patients who may potentially benefit from PORT based on the status of the lymph node involvement. Otherwise, two retrospective studies (31, 32) have reported that among patients with stage N2-IIIA NSCLC after surgery, the role of PORT might be related to the pathological type. Patients with lung squamous carcinoma (LUSC) had a poor prognosis than patients with lung adenocarcinoma (LUAD), on the basis of the 5-year OS rates (LUSC 36.3% *vs*. LUAD 41.5%; P = 0.018). However, LUSC patients with limited N2 lymph node metastasis might benefit from PORT compared to postoperative chemotherapy alone (P = 0.010). These two retrospective studies used the propensity score matching analysis to compensate for differences in baseline characteristics, which might improve the reliability of their conclusion.

All analyses of local-regional recurrence-free survival (P = 0.0003), disease-free survival (P = 0.001) have suggested a local protective role of PORT in patient with N2 NSCLC. This conclusion is consistent to the prior studies (33). As for tolerable toxicity, a retrospective research demonstrated that PORT could improve OS, DFS, LRFS and DMFS with tolerable toxicity after pneumonectomy and adjuvant chemotherapy in pIIIA-N2 NSCLC patients (34). In the Lung ART trial (19), the

adjuvant PORT brought more adverse events mainly about cardio-pulmonary toxicity with modern 3D-CRT technology. However, the distance metastasis in several trials didn't show apparent difference between the PORT arm and the control arm. In Lung ART trials, two groups had similar and relatively high system metastasis rates (PORT 72.9% *vs* Control 64.5%), indicating that adjuvant PORT couldn't improve distant metastasis rates (19). The studies may focus on optimizing treatment regimens to control the metastasis disease. Therefore, whether the utility of immunotherapy or target therapy as emerging systemic treatment agents in patients with pIII-N2 NSCLC will improve their prognosis, it remains to be studied.

Immune checkpoint inhibitors (ICIs), as systematic therapy regent, have been identified to improve survival in patients with advanced NSCLC (35). But for resectable NSCLC, the study is scarce (36). A previous study has largely focused on neoadjuvant immune checkpoint inhibitors. Forde and coworkers showed that single neoadjuvant nivolumab in resectable lung cancer was well-tolerated with few side effects and no delays in surgery (37). Such is the case with sintilimab, another ICI. Likely, neoadjuvant ICIs plus chemotherapy or ICIs regiment was reported to amplify systemic antitumor immunity for achieving a major pathological response, and such that effects could persist after therapeutic surgery (38–41). The WJOG 12119L trial explored the novel treatment strategy of neoadjuvant concurrent chemo-immuno-radiation therapy followed by surgical resection and adjuvant immunotherapy for resectable stage IIIA-B (discrete N2) NSCLC, which might further inhibit distant metastasis during the perioperative period and enhance the prognosis for patients receiving this therapy (42). Notably, atezolizumab is the only effective adjuvant immunotherapy agent following surgery and chemotherapy in people with Stage II-IIIA non-small cell lung cancer (NSCLC) and PD-L1 ≥1%, showing decreasing the risk of disease recurrence or death (disease-free survival; DFS) by 34% (HR, 0.66, 95% CI: 0.50–0.88), compared with best supportive care (BSC) (43). All the trials need to be further validated in large randomized clinical trials.

Additionally, target therapy is recommended to resected pIIIA N2 NSCLC patients with EGFR mutation-positive and receiving prior adjuvant chemotherapy or ineligible to receive platinum-based chemotherapy by the National Comprehensive Cancer Network (NCCN) guidelines. As for resected pIIIA N2 NSCLC patients with EGFR mutation-negative and margin negative (R0), sequential chemotherapy combined with radiotherapy is recommended. Whereas, given that the results of both recent randomized clinic trial Lung ART and this meta-analysis verify that PORT cannot bring benefit for overall survival of these patients, the role of adjuvant PORT is controversial for patients with pIIIA N2 NSCLC. Indeed, currently, although the results of the Lung ART trial (19) were negative, we cannot deny and ignore the value of PORT due to the limitations of this trial. Firstly, the time span of this trial was long, ranging from 2007 to 2018 and in this period, the TNM stage has been revised. Then, the radiotherapy techniques have also been changed to more precise over the times, such as stereotactic body radiation therapy (SBRT) and intensity-modulated radiation therapy (IMRT) while the trial only evaluated the three-dimensional conformal radiation therapy (3D-CRT) with more cardiopulmonary toxicity. In the clinical trial of locally advanced non-small-cell lung cancer, IMRT was considered to correlate with lower rates of severe pneumonitis and cardiac doses compared with 3D-CRT (44). Likewise, a phase II trial has explored that NSCLC patients treated with SBRT had better Health-Related Quality of Life (HRQL) and less toxicity than 3D-CRT (45). With the advancement of radiotherapy technology, from Cobalt-60 to 3D-CRT and then to IMRT or SBRT, radiotherapy technology is gradually getting more precise and reduces the damage to normal tissues. Proton beam therapy (PBT) and carbon ion therapy (CIT) (46, 47), which have emerged in the past decades, can minimize the radiation damage to the human body and have the largest killer effect on tumors due to the Bragg peak effect. In a prospective study (46), the effects of proton radiotherapy and intensity-modulated radiation therapy (IMRT) on postoperative NSCLC were compared, indicating that postoperative PBT in NSCLC is well-tolerated and has similar excellent short-term outcomes when compared with IMRT. However, the study of carbon ion therapy in resectable NSCLC is scarce. In addition to the shift of radiotherapy modality and facilities, the interval between surgery and the onset of radiotherapy and the overall treatment time (OTT) have been reported to be associated with significantly worse local control and overall survival rates (48). Due to the heterogeneity in radiation dose, OTT, fractionation schedules, and the difference between irradiation techniques, the effects of adjuvant PORT are of great difference and heterogeneity.

Furthermore, although trials have been conducted over decades, with changes in diagnosis and assessment of tumour staging, recurrence, and radiotherapy, we still find some consistent conclusion through integrated information including the comparison between different TNM stage versions. This meta-analysis show that no clear evidence indicates the protective effect of PORT on overall survival, but it has a great influence on DFS and LRFS for patients with III-N2 NSCLC. Through the analyses of toxicities and side effects of these randomized clinical trials, we find PORT group may have a higher incidence of severe toxicity compared with no PORT group, which are acceptable and need an early intervention. The improved LRFS and DFS can't be translated into improved OS may partly attribute to the toxicities. Currently, radiotherapy to the mediastinum after surgery cannot be the standard of care to be recommended for all patients with stage III NSCLC with mediastinal nodal involvement. When adjuvant PORT is recommended to a patient with pIIIA-N2 NSCLC, a comprehensive assessment of the patient's status is required. Whereas, with the addition of chemotherapy, immune checkpoint inhibitors, and modern and precise radiotherapy techniques and means, this situation may be improved in the future.

Strengths and Limitations

This meta-analysis analyzed the differential time of added chemotherapy although there was no change of the results which the small sample size might account for. In addition, we

added two new published clinical trials specially the Lung ART trial. All the included studies were assessed as having low risk of bias. The inter-study heterogeneity was very low.

The limitations of this analysis are reflected by the fundamental weaknesses of the included trials. Firstly, due to the lack of dada, subgroup analyses could not be performed by patients' age, sex, histology, and the number of lymph nodes involved, which might influence the extrapolation of the results. Secondly, data are also sparse for survival analysis and cannot draw a Kaplan–Meier curve. Lastly, part of previous trials which may differ from recent studies due to staging, radiotherapy techniques, and chemotherapy influence the reliability of this meta-analysis.

Implications for Practice and Research

This meta-analysis has shown an ambiguous effect of postoperative radiotherapy on survival in patients with pIII-N2 NSCLC. Although PORT tends to be detrimental in early-stage disease, Researchers must re-evaluate the effect of PORT using modern radiotherapy techniques and adjuvant chemotherapy. A recent systematic review (49) has indicated a benefit effect in OS when PORT is given only with linear accelerators rather than cobalt, cobalt and linear accelerators. Likewise, with the development of modern radiotherapy, including image-guided radiotherapy (IGRT) and intensity modulated radiotherapy (IMRT), contemporary techniques could further decrease PORT-related toxicity, such as the reduced risk of death from heart disease (50).

Meanwhile, adjuvant chemotherapy also plays an important role in the treatment of an N2 NSCLC patient (51) which may change the effect of PORT. In further trials, accurate and detailed information on the cause of death will be important, as will data regarding surgical resection, radiotherapy technique and chemotherapy regimen and sequence. Collection of such data may help to explain whether a combination of adjuvant chemotherapy with surgery contributes to improving benefit effect of postoperative radiotherapy or bring more detrimental effects. At the same time, it helps determine the timing of chemotherapy.

Although, currently, radiotherapy to the mediastinum after surgery cannot be the standard of care to be recommended for all patients with stage III NSCLC with mediastinal nodal involvement, we believe that PORT deserves an in-depth investigation in terms of LR, OS and overall toxicity in patients with resectable stage III-N2 disease especially in patients having received adjuvant systematic therapy such as immune checkpoint inhibitors and target therapy or modern radiation technique to explore novel combined strategies.

DATA AVAILABILITY STATEMENT

The original contributions presented in the study are included in the article/**Supplementary Material**. Further inquiries can be directed to the corresponding authors.

AUTHOR CONTRIBUTIONS

BX and HuZ conceived and designed the study. TL and JL performed the search, study selection, and data extraction and enter. HaZ and LL analyzed the results and the statistical analysis. TL, JL, and YJ drafted the manuscript. Critical review the manuscript and polish the language: HuZ and JW. All authors contributed to the article and approved the submitted version.

FUNDING

This work was supported by National Natural Science Foundation of China 81670123 and 81670144. The funders had no role in study design, data collection and analysis, decision to publish, or preparation of the manuscript.

SUPPLEMENTARY MATERIAL

The Supplementary Material for this article can be found online at: https://www.frontiersin.org/articles/10.3389/fonc.2021.680615/full#supplementary-material

REFERENCES

1. Sung H, Ferlay J, Siegel RL, Laversanne M, Soerjomataram I, Jemal A, et al. Global Cancer Statistics 2020: GLOBOCAN Estimates of Incidence and Mortality Worldwide for 36 Cancers in 185 Countries. *CA: Cancer J Clin* (2021) 71(3):209–49. doi: 10.3322/caac.21660
2. Duma N, Santana-Davila R, Molina JR. Non-Small Cell Lung Cancer: Epidemiology, Screening, Diagnosis, and Treatment. *Mayo Clin Proc* (2019) 94(8):1623–40. doi: 10.1016/j.mayocp.2019.01.013
3. Manser R, Wright G, Hart D, Byrnes G, Campbell DA. Surgery for Early Stage Non-Small Cell Lung Cancer. *Cochrane Database Syst Rev* (2005) 1(1). doi: 10.1002/14651858.pub2
4. Burdett S, Rydzewska L, Tierney J, Fisher D, Parmar MK, Arriagada R, et al. Postoperative Radiotherapy for Non-Small Cell Lung Cancer. *Cochrane Database Syst Rev* (2016) 9(9):CD002142. doi: 10.1002/14651858.CD002142.pub4
5. Koike T, Tsuchiya R, Goya T, Sohara Y, Miyaoka E. Prognostic Factors in 3315 Completely Resected Cases of Clinical Stage I Non-Small Cell Lung Cancer in Japan. *J Thorac Oncol* (2007) 2(5):408–13. doi: 10.1097/01.JTO.0000268674.02744.f9
6. Billiet C, Decaluwe H, Peeters S, Vansteenkiste J, Dooms C, Haustermans K, et al. Modern Post-Operative Radiotherapy for Stage III Non-Small Cell Lung Cancer May Improve Local Control and Survival: A Meta-Analysis. *Radiother Oncol* (2014) 110(1):3–8. doi: 10.1016/j.radonc.2013.08.011
7. Patel SH, Ma Y, Wernicke AG, Nori D, Chao KS, Parashar B. Evidence Supporting Contemporary Post-Operative Radiation Therapy (PORT) Using Linear Accelerators in N2 Lung Cancer. *Lung Cancer* (2014) 84(2):156–60. doi: 10.1016/j.lungcan.2014.02.016
8. Douillard J-Y, Rosell R, De Lena M, Carpagnano F, Ramlau R, Gonzáles-Larriba JL, et al. Adjuvant Vinorelbine Plus Cisplatin Versus Observation in Patients With Completely Resected Stage IB–IIIA Non-Small-Cell Lung Cancer (Adjuvant Navelbine International Trialist Association [ANITA]):

A Randomised Controlled Trial. *Lancet Oncol* (2006) 7(9):719–27. doi: 10.1016/s1470-2045(06)70804-x
9. Arriagada R, Bergman B, Dunant A, Le Chevalier T, Pignon JP, Vansteenkiste J. Cisplatin-Based Adjuvant Chemotherapy in Patients With Completely Resected Non-Small-Cell Lung Cancer. *N Engl J Med* (2004) 350(4):351–60. doi: 10.1056/NEJMoa031644
10. Moher D, Liberati A, Tetzlaff J, Altman DG, Group P. Preferred Reporting Items for Systematic Reviews and Meta-Analyses: The PRISMA Statement. *Int J Surg* (2010) 8(5):336–41. doi: 10.1016/j.ijsu.2010.02.007
11. Higgins JP, Altman DG, Gøtzsche PC, Jüni P, Moher D, Oxman AD, et al. The Cochrane Collaboration's Tool for Assessing Risk of Bias in Randomised Trials. *BMJ (Clin Res ed)* (2011) 343:d5928. doi: 10.1136/bmj.d5928 d5928.
12. Tierney JF, Stewart LA, Ghersi D, Burdett S, Sydes MR. Practical Methods for Incorporating Summary Time-to-Event Data Into Meta-Analysis. *Trials* (2007) 8:16. doi: 10.1186/1745-6215-8-16
13. Debevec M, Bitenc M, Vidmar S, Rott T, Orel J, Strojan P, et al. Postoperative Radiotherapy for Radically Resected N2 Non-Small-Cell Lung Cancer (NSCLC): Randomised Clinical Study 1988-1992. *Lung Cancer* (1996) 14 (1):99–107. doi: 10.1016/0169-5002(95)00515-3
14. Stephens RJ, Girling DJ, Bleehen NM, Moghissi K, Yosef HM, Machin D. The Role of Post-Operative Radiotherapy in Non-Small-Cell Lung Cancer: A Multicentre Randomised Trial in Patients With Pathologically Staged T1-2, N1-2, M0 Disease. Medical Research Council Lung Cancer Working Part. *Br J Cancer* (1996) 74(4):632–9. doi: 10.1038/bjc.1996.413
15. Perry MC, Kohman LJ, Bonner JA, Gu L, Wang X, Vokes EE, et al. A Phase III Study of Surgical Resection and Paclitaxel/Carboplatin Chemotherapy With or Without Adjuvant Radiation Therapy for Resected Stage III Non-Small-Cell Lung Cancer: Cancer and Leukemia Group B 9734. *Clin Lung Cancer* (2007) 8(4):268–72. doi: 10.3816/CLC.2007.n.005
16. Shen WY, Ji J, Zuo YS, Pu J, Xu YM, Zong CD, et al. Comparison of Efficacy for Postoperative Chemotherapy and Concurrent Radiochemotherapy in Patients With IIIA-Pn2 Non-Small Cell Lung Cancer: An Early Closed Randomized Controlled Trial. *Radiother Oncol* (2014) 110(1):120–5. doi: 10.1016/j.radonc.2013.10.008
17. Sun JM, Noh JM, Oh D, Kim HK, Lee SH, Choi YS, et al. Randomized Phase II Trial Comparing Chemoradiotherapy With Chemotherapy for Completely Resected Unsuspected N2-Positive Non–Small Cell Lung Cance. *J Thoracic Oncol* (2017) 12(12):1806–13. doi: 10.1016/j.jtho.2017.09.1954
18. Hui Z, Men Y, Hu C, Zhou Z, Liang J, Feng Q, et al. OA12.06 A Prospective Randomized Phase III Study of Precise PORT for Patients With pIIIA-N2 NSCLC After Complete Resection and Adjuvant Chemotherapy. *J Thoracic Oncol* (2019) 14(10):S238–9. doi: 10.1016/j.jtho.2019.08.475
19. Le Pechoux C, Pourel N, Barlesi F, Faivre-Finn C, Lerouge D, Zalcman G, et al. LBA3_PR An International Randomized Trial, Comparing Post-Operative Conformal Radiotherapy (PORT) to No PORT, in Patients With Completely Resected Non-Small Cell Lung Cancer (NSCLC) and Mediastinal N2 Involvement: Primary End-Point Analysis of LungART (IFCT-0503, UK NCRI, SAKK) NCT00410683. *Ann Oncol* (2020) 31(S4):S1178. doi: 10.1016/j.annonc.2020.08.2280
20. Smolle-Juettner FM, Mayer R, Pinter H, Stuecklschweiger G, Kapp KS, Gabor S, et al. "Adjuvan" External Radiation of the Mediastinum in Radically Resected Non-Small Cell Lung Cancer. *Eur J Cardio-Thoracic Surg: Off J Eur Assoc Cardio-Thoracic Surg* (1996) 10(11):947–50. doi: 10.1016/s1010-7940(96)80395-2
21. Mayer R, Smolle-Juettner FM, Szolar D, Stuecklschweiger GF, Quehenberger F, Friehs G, et al. Postoperative Radiotherapy in Radically Resected non-Small Cell Lung Cancer. *Chest* (1997) 112(4):954–9. doi: 10.1378/chest.112.4.954
22. Feng QF, Wang M, Wang LJ, Yang ZY, Zhang YG, Zhang DW, et al. A Study of Postoperative Radiotherapy in Patients With Non-Small-Cell Lung Cancer: A Randomized Trial. *Int J Radiat Oncol Biol Phys* (2000) 47(4):925–9. doi: 10.1016/s0360-3016(00)00509-5
23. Group PM-aT. Postoperative Radiotherapy in Non-Small-Cell Lung Cancer: Systematic Review and Meta-Analysis of Individual Patient Data From Nine Randomised Controlled Trials. PORT Meta-Analysis Trialists Group. *Lancet (London England)* (1998) 352(9124):257–63. doi: 10.1016/S0140-6736(98)06341-7
24. Robinson CG, Patel AP, Bradley JD, DeWees T, Waqar SN, Morgensztern D, et al. Postoperative Radiotherapy for Pathologic N2 Non-Small-Cell Lung Cancer Treated With Adjuvant Chemotherapy: A Review of the National Cancer Data Base. *J Clin Oncol* (2015) 33(8):870–6. doi: 10.1200/jco.2014.58.5380
25. Billiet C, De Ruysscher D, Peeters S, Decaluwé H, Vansteenkiste J, Dooms C, et al. Patterns of Locoregional Relapses in Patients With Contemporarily Staged Stage III-N2 NSCLC Treated With Induction Chemotherapy and Resection: Implications for Postoperative Radiotherapy Target Volume. *J Thorac Oncol* (2016) 11(9):1538–49. doi: 10.1016/j.jtho.2016.05.037
26. Francis S, Orton A, Stoddard G, Tao R, Hitchcock YJ, Akerley W, et al. Sequencing of Postoperative Radiotherapy and Chemotherapy for Locally Advanced or Incompletely Resected Non-Small-Cell Lung Cancer. *J Clin Oncol* (2018) 36(4):333–41. doi: 10.1200/jco.2017.74.4771
27. Moreno AC, Haque W, Verma V, Fang P, Lin SH. Concurrent Versus Sequential Chemoradiation Therapy in Completely Resected Pathologic N2 Non-Small Cell Lung Cancer: Propensity-Matched Analysis of the National Cancer Data Base. *Ann Surg Oncol* (2018) 25(5):1245–53. doi: 10.1245/s10434-018-6399-4
28. Sura K, Grills IS, Vu CC, Stevens CW, Ye H, Guerrero TM. Improved Survival With Increased Time-To-Radiation and Sequential Chemotherapy After Surgery for Pn2 Non-Small-Cell Lung Cancer. *Clin Lung Cancer* (2018) 19 (2):e185–94. doi: 10.1016/j.cllc.2017.10.011
29. Gao F, Li N, Xu Y, Yang G. Effects of Postoperative Radiotherapy on Survival of Patients With Stage IIIA Resected Non-Small Cell Lung Cancer: Analysis of the SEER Database. *J Natl Compr Cancer Netw: JNCCN* (2020) 18(6):718–27. doi: 10.6004/jnccn.2020.7537
30. Liu T, Mu Y, Dang J, Li G. The Role of Postoperative Radiotherapy for Completely Resected pIIIA-N2 Non-Small Cell Lung Cancer Patients With Different Clinicopathological Features: A Systemic Review and Meta-Analysis. *J Cancer* (2019) 10(17):3941–9. doi: 10.7150/jca.28680
31. Su L, Chen M, Su H, Dai Y, Chen S, Li J. Postoperative Chemoradiotherapy is Superior to Postoperative Chemotherapy Alone in Squamous Cell Lung Cancer Patients With Limited N2 Lymph Node Metastasis. *BMC Cancer* (2019) 19(1):1023. doi: 10.1186/s12885-019-6141-z
32. Jin G, Wang X, Xu C, Sun J, Yuan Z, Wang J, et al. Disparities in Survival Following Surgery Among Patients With Different Histological Types of N2-III Non-Small Cell Lung Cancer: A Surveillance, Epidemiology and End Results (SEER) Database Analysis. *Ann Trans Med* (2020) 8(20):1288. doi: 10.21037/atm-20-4357
33. Zhang H, Zhang DX, Ju T, Zhou J. The Effect of Postoperative Radiotherapy on the Survival of Patients With Resectable Stage III-N2 Non-Small-Cell Lung Cancer: A Systematic Review and Meta-Analysis. *Neoplasma* (2019) 66 (5):717–26. doi: 10.4149/neo_2018_181213N965
34. Wang W, Men Y, Wang J, Zhou Z, Chen D, Xiao Z, et al. Postoperative Radiotherapy Is Effective in Improving Survival of Patients With Stage pIII-N2 Non-Small-Cell Lung Cancer After Pneumonectomy. *BMC Cancer* (2019) 19(1):478. doi: 10.1186/s12885-019-5692-3
35. Gray JE, Villegas A, Daniel D, Vicente D, Murakami S, Hui R, et al. Three-Year Overall Survival With Durvalumab After Chemoradiotherapy in Stage III NSCLC-Update From PACIFIC. *J Thorac Oncol* (2020) 15(2):288–93. doi: 10.1016/j.jtho.2019.10.002
36. Jia XH, Xu H, Geng LY, Jiao M, Wang WJ, Jiang LL, et al. Efficacy and Safety of Neoadjuvant Immunotherapy in Resectable Nonsmall Cell Lung Cancer: A Meta-Analysis. *Lung Cancer* (2020) 147:143–53. doi: 10.1016/j.lungcan.2020.07.001
37. Forde PM, Chaft JE, Smith KN, Anagnostou V, Cottrell TR, Hellmann MD, et al. Neoadjuvant PD-1 Blockade in Resectable Lung Cancer. *N Engl J Med* (2018) 378(21):1976–86. doi: 10.1056/NEJMoa1716078
38. Rosell R, Ito M. Neoadjuvant Atezolizumab Plus Chemotherapy in Resectable Non-Small-Cell Lung Cancer. *Lancet Oncol* (2020) 21(6):736–8. doi: 10.1016/s1470-2045(20)30146-7
39. Shu CA, Gainor JF, Awad MM, Chiuzan C, Grigg CM, Pabani A, et al. Neoadjuvant Atezolizumab and Chemotherapy in Patients With Resectable Non-Small-Cell Lung Cancer: An Open-Label, Multicentre, Single-Arm, Phase 2 Trial. *Lancet Oncol* (2020) 21(6):786–95. doi: 10.1016/s1470-2045(20)30140-6
40. Forde PM, Chaft JE, Felip E, Broderick S, Girard N, Awad MM, et al. Checkmate 816: A Phase 3, Randomized, Open-Label Trial of Nivolumab Plus Ipilimumab *vs* Platinum-Doublet Chemotherapy as Neoadjuvant

Treatment for Early-Stage NSCLC. *J Clin Oncol* (2017) 35(15_suppl). doi: 10.1200/JCO.2017.35.15_suppl.TPS8577
41. Cascone T, William WN Jr, Weissferdt A, Leung CH, Lin HY, Pataer A, et al. Neoadjuvant Nivolumab or Nivolumab Plus Ipilimumab in Operable Non-Small Cell Lung Cancer: The Phase 2 Randomized NEOSTAR Trial. *Nat Med* (2021) 27(3):504–14. doi: 10.1038/s41591-020-01224-2
42. Hamada A, Soh J, Hata A, Nakamatsu K, Shimokawa M, Yatabe Y, et al. Phase II Study of Neoadjuvant Concurrent Chemo-Immuno-Radiation Therapy Followed by Surgery and Adjuvant Immunotherapy for Resectable Stage IIIA-B (Discrete N2) Non-Small-Cell Lung Cancer: SQUAT Trial (WJOG 12119l). *Clin Lung Cancer* (2021) 18(35):in press. doi: 10.1016/j.cllc.2021.04.006
43. Vallieres E, Felip E, Altorki N, Zhou C, Zuo Y, Howland M, et al. PS01.55: IMpower010: Phase III Study of Atezolizumab *vs* BSC After Adjuvant Chemotherapy in Patients With Completely Resected NSCLC. *J Thoracic Oncol* (2016) 11(11):S304–S304. doi: 10.1016/j.jtho.2016.09.090
44. Chun SG, Hu C, Choy H, Komaki RU, Timmerman RD, Schild SE, et al. Impact of Intensity-Modulated Radiation Therapy Technique for Locally Advanced Non-Small-Cell Lung Cancer: A Secondary Analysis of the NRG Oncology RTOG 0617 Randomized Clinical Trial. *J Clin Oncol* (2017) 35 (1):56–62. doi: 10.1200/JCO.2016.69.1378
45. Nyman J, Hallqvist A, Lund JA, Brustugun OT, Bergman B, Bergstrom P, et al. SPACE - A Randomized Study of SBRT *vs* Conventional Fractionated Radiotherapy in Medically Inoperable Stage I NSCLC. *Radiother Oncol* (2016) 121(1):1–8. doi: 10.1016/j.radonc.2016.08.015
46. Remick JS, Schonewolf C, Gabriel P, Doucette A, Levin WP, Kucharczuk JC, et al. First Clinical Report of Proton Beam Therapy for Postoperative Radiotherapy for Non–Small-Cell Lung Cancer. *Clin Lung Cancer* (2017) 18 (4):364–71. doi: 10.1016/j.cllc.2016.12.009
47. Ohtaki Y, Shimizu K, Saitoh JI, Kamiyoshihara M, Mogi A, Nakazawa S, et al. Is Salvage Surgery for Patients With Lung Cancer After Carbon Ion Radiotherapy Easy or Difficult? *Interact Cardiovasc Thorac Surg* (2019) 28 (6):953–6. doi: 10.1093/icvts/ivy350
48. Butof R, Simon M, Lock S, Troost EGC, Appold S, Krause M, et al. PORTAF - Postoperative Radiotherapy of Non-Small Cell Lung Cancer: Accelerated Versus Conventional Fractionation - Study Protocol for a Randomized Controlled Trial. *Trials* (2017) 18(1):608. doi: 10.1186/s13063-017-2346-0
49. Billiet C, Decaluwé H, Peeters S, Vansteenkiste J, Dooms C, Haustermans K, et al. Modern Post-Operative Radiotherapy for Stage III Non-Small Cell Lung Cancer may Improve Local Control and Survival: A Meta-Analysis. *Radiother Oncol* (2014) 110(1):3–8. doi: 10.1016/j.radonc.2013.08.011
50. Paumier A, Le Pechoux C. Post-Operative Radiation Therapy. *Transl Lung Cancer Res* (2013) 2(5):423–32. doi: 10.3978/j.issn.2218-6751.2013.10.03
51. Robinson LA, Ruckdeschel JC, Wagner HJr., Stevens CW. Treatment of Non-Small Cell Lung Cancer-Stage IIIA: ACCP Evidence-Based Clinical Practice Guidelines (2nd Edition). *Chest* (2007) 132(3 Suppl):243s–65s. doi: 10.1378/chest.07-1379

Conflict of Interest: The authors declare that the research was conducted in the absence of any commercial or financial relationships that could be construed as a potential conflict of interest.

Copyright © 2021 Lei, Li, Zhong, Zhang, Jin, Wu, Li, Xu, Song and Hu. This is an open-access article distributed under the terms of the Creative Commons Attribution License (CC BY). The use, distribution or reproduction in other forums is permitted, provided the original author(s) and the copyright owner(s) are credited and that the original publication in this journal is cited, in accordance with accepted academic practice. No use, distribution or reproduction is permitted which does not comply with these terms.

frontiers in Oncology

ORIGINAL RESEARCH
published: 19 July 2021
doi: 10.3389/fonc.2021.645486

Development and External Validation of a Nomogram for Predicting Cancer-Specific Survival of Non-Small Cell Lung Cancer Patients With Ipsilateral Pleural Dissemination

Zhenfan Wang[†], *Hao Li*[†], *Taorui Liu*, *Zewen Sun*, *Fan Yang and Guanchao Jiang*[*]

Department of Thoracic Surgery, Centre of Thoracic Minimally Invasive Surgery, Peking University People's Hospital, Beijing, China

OPEN ACCESS

Edited by:
Hideharu Kimura, Kanazawa University, Japan

Reviewed by:
Angelo Carretta, Vita-Salute San Raffaele University, Italy
Yijiu Ren, Tongji University, China

***Correspondence:**
Guanchao Jiang
jiangguanchao@263.net

[†]*These authors have contributed equally to this work*

Specialty section:
This article was submitted to Thoracic Oncology, a section of the journal Frontiers in Oncology

Received: *23 December 2020*
Accepted: *28 June 2021*
Published: *19 July 2021*

Citation:
Wang Z, Li H, Liu T, Sun Z, Yang F and Jiang G (2021) Development and External Validation of a Nomogram for Predicting Cancer-Specific Survival of Non-Small Cell Lung Cancer Patients With Ipsilateral Pleural Dissemination. Front. Oncol. 11:645486. doi: 10.3389/fonc.2021.645486

Background: Non-small-cell lung cancer (NSCLC) patients with ipsilateral pleural dissemination are defined as M1a in the eighth of American Joint Committee on Cancer (AJCC) TNM staging. We aimed to build a nomogram to predict lung cancer specific survival (LCSS) of NSCLC patients with ipsilateral pleural dissemination and to compare the impact of primary tumor resection (PTR) on LCSS among patients with different features.

Methods: A total of 3,918 NSCLC patients with ipsilateral pleural dissemination were identified from the Surveillance, Epidemiology, and End Results (SEER) database. We selected and integrated significant prognostic factors based on competing risk regression to build a nomogram. The model was subjected to internal validation within SEER cohort and external validation with the cohort of 97 patients from Peking University People's Hospital.

Results: Age ($P < 0.001$), gender ($P = 0.037$), T stage ($P = 0.002$), N stage ($P < 0.001$), metastasis pattern ($P = 0.005$), chemotherapy ($P < 0.001$), and PTR ($P < 0.001$) were independent prognostic factors. The calibration curves presented a good consistency and the Harrell's C-index of nomogram were 0.682 (95%CI: 0.673–0.691), 0.687 (95%CI: 0.670–0.704) and 0.667 (95%CI: 0.584–0.750) in training, internal, and external validation cohort, respectively. Interaction tests suggested a greater LCSS difference caused by PTR in patients without chemotherapy (P < 0.001).

Conclusions: We developed a nomogram based on competing risk regression to reliably predict prognosis of NSCLC patients with ipsilateral pleural dissemination and validated this nomogram in an external Chinese cohort. This novel nomogram might be a practical tool for clinicians to anticipate the 1-, 3- and 5-year LCSS for NSCLC patients with pleural dissemination. Subgroup analysis indicated that patients without chemotherapy could get

more benefit from PTR. In order to assess the role of PTR in the management of M1a patients more accurately, further prospective study would be urgently required.

Keywords: nomogram, cancer-specific survival, non-small cell lung cancer, ipsilateral pleural dissemination, surgery

INTRODUCTION

Lung cancer has the highest mortality rate worldwide despite advances in diagnostic and therapeutic techniques. More than one-third of non-small-cell lung cancers (NSCLCs) are diagnosed at stage IV of the disease (1). In the 7th edition of tumor, node and metastasis (TNM) lung cancer staging system, stage IV patients were subdivided and a new M descriptors of M1a were proposed, which was defined as patients with metastasis in the chest cavity, including malignant pleural effusion/nodules, pericardial effusion and contralateral pulmonary nodules (2). According to the International Association for the Study of Lung Cancer (IASLC) staging project, the median survival time (MST) and 5-year survival rate of these M1a patients were 8–11.5 months and 2–10% (2, 3), respectively. In 2017, M1a patients were subdivided as stage IVA in the 8th edition of TNM staging system (3).

Currently, research on the diagnosis and management of NSCLC patients with malignant contralateral pulmonary nodules has generally come to a fundamental consensus (4); however, it is more complicated and controversial for the treatment of patients with ipsilateral pleural dissemination, including malignant pleural effusion/nodules, pericardial effusion. Several studies have focused on the survival of these patients. Dai et al. (5) reported that lymph node involvement was an independent prognostic factor for lung cancer specific survival (LCSS) among all M1a patients, and Wang et al. (6) showed a similar result in patients with unexpected pleural spread at thoracotomy. Our previous study has demonstrated that primary tumor resection (PTR) brought favorable impact on both overall survival (OS) and LCSS for patients with ipsilateral pleural dissemination (7), especially for non-targeted therapy patients (8). Nevertheless, a predictive model specifically describing the LCSS of patients with ipsilateral pleural dissemination is not yet available, and the question about which type of patients are more suitable for PTR remains unclear.

Therefore, we aimed to develop and validate a novel nomogram based on competing risk regression predict the LCSS of NSCLC patients with ipsilateral pleural dissemination and to compare the impact of PTR on LCSS among patients with different feature.

METHOD

Study Population and Selection Criteria

The SEER program, managed by the National Cancer Institute, is one of the largest public databases that collect cancer incidence data from population-based cancer registries covering approximately 30% of the U.S. population. We used the SEER*Stat software (version 8.3.6 https://seer.cancer.gov/data-software/ Surveillance Research Program, National Cancer Institute, Maryland, USA) to derive information of patients from the Incidence-SEER 18 Regs Custom Data (with additional treatment fields), Nov 2019 Submission. The inclusion criteria for patient selection in this study were (a) patients diagnosed with pathologically confirmed NSCLC between 2010 and 2015, (b) stage IV and M1a disease according to the 7th edition of the American Joint Committee on Cancer (AJCC) TNM classification, (c) the SEER variable 'CS Mets at DX' with codes 15, 20, and 24 for ipsilateral pleural effusion, pericardial effusion, and pleural nodules on the ipsilateral lung separated from direct invasion, (d) only one malignant primary lesion. The exclusion criteria included (a) patients younger than 18 years old at the time of diagnosis, (b) metastases in the contralateral lung, (c) data on the survival time, cause of death, surgery information, and tumor size were unavailable, (d) survival time was recorded as zero month.

The independent external validation cohort was derived from NSCLC patients treated in the Peking University People's Hospital, Beijing, China between January 1, 2006 and December 31, 2016. The study time of the validation cohort was quite long to enroll more M1a patients as possible. The inclusion criteria included pathologically confirmed ipsilateral pleural dissemination, age of 18 years or older and complete follow-up information. Patients with malignant contralateral pulmonary nodules, distant organs metastases or history of other malignancies were excluded. Informed consent was waived for this retrospective study by the Research Ethics Committee of the Peking University People's Hospital. Patients treated in our center were followed up every 3 months in the first year and every 6 months thereafter until death. Physical examination, chest computed tomographic (CT) scans and tests of blood tumor markers were conducted routinely at follow-up, and magnetic resonance imaging (MRI) of the brain or 18F-FDG PET–CT was performed if necessary.

Study Variables

The following information for each patient was extracted: baseline sociodemographic information (age, race, gender, vital status, cause of death, and survival months), tumor characteristics (tumor size, anatomic site, histological subtype, T stage, N stage, differentiation grade, and metastasis pattern: pleural effusion, pericardial effusion or pleural nodules) and treatment information (surgery, chemotherapy and radiation). Pleural decortication, pleurodesis, intraoperative intrapleural hyperthermic perfusion or other intrapleural operations were not included because those procedures were not performed in our center and also not documented in the SEER database. In this study, the histological subtypes were classified as

adenocarcinoma, squamous cell carcinoma, large cell carcinoma, and adenosquamous carcinoma. We adjusted the TNM stage of each patient according to the 8th AJCC TNM classification system. In the subgroup analysis, the cut-off value of age at diagnosis was set at median (<70 and ≥70) with reference to the cut-off points used in previous studies (9). Lung cancer-specific survival (LCSS) was the study endpoint, which was defined as the time from the diagnosis to death attributed to lung cancer-specific mortality (LCSM).

Construction of the Nomogram

In this study, all eligible patients from the SEER database (n = 3,918) were randomly assigned into training (70%, n = 2,745) and validation cohort (30%, n = 1,173) to establish and validate the nomogram. This ratio (7:3) ensured the maximal utilization of the data for constructing predictive model with a considerable number of sample size for validation (10–15).

The baseline clinicopathological characteristics and treatment information were analyzed using descriptive methods, with standard summary statistics including median, interquartile range (IQR), and proportions. Differences for continuous, non-normally distributed data were processed by the Mann–Whitney test. Categorical variables were compared by chi-square or Fisher's exact tests, as appropriate.

Fine–Gray competing risk regression was performed to estimate the subhazard ratio (SHR) and evaluate the ability of the parameter in predicting the risk of LCSM, with non-cancer deaths as the competing risk (16). Variables with *P*-value <0.10 identified in univariable analyses were enrolled into multivariable regression. A nomogram was developed based on the prognostic factors with *P*-value < 0.05 in the multivariable analyses.

Validation of the Nomogram

The model was subjected to internal validation in the SEER training cohort, independent validation in the SEER validation cohort, and external validation with the cohort from Peking University People's Hospital. The performance of our nomogram was evaluated by calibration curves (500 bootstrap resamples), Harrell's concordance index (C-index) (17), and the time-dependent receiver operating characteristic curve (the time-dependent ROC curve) (18). The calibration curves were depicted on the basis of predicted and observed probabilities of LCSM, which represented the calibration of our model. Discrimination ability was reflected by C-index and the area under the curves (AUCs) of ROC curves for 1-, 3- and 5-year LCSS, with values closer to 1.0 denoting better discrimination ability.

Modified Nomogram and Subgroup Analysis

To perform an exploratory analysis about the impact of PTR on the LCSS among patients with different risks, we built a modified nomogram including the independent prognostic factors except for surgery status using training cohort. All cases were divided into low-risk and high-risk groups using the cut-off set at the highest third of the risk score calculated from the modified nomogram among training cohort, and the cumulative incidence of LCSM curves in different groups was delineated. Subgroup analysis stratified by clinicopathologic feature based on Fine–Gray test was conducted to compare the influence of PTR on LCSS within each subgroup.

Data analysis were performed using Stata/SE 15.0 for Windows (StataCorp, College Station, TX) and R software version 3.6.0. We used the "mstate" and "rms" package in R software to construct the nomogram, "pec" package to evaluate our model, and "nomogramEx" package to calculate the total score based on nomogram. All statistical tests were two-tailed, and a *P*-value less than 0.05 was considered statistically significant.

RESULT

Patient Characteristics

A total of 3,918 NSCLC patients with ipsilateral pleural dissemination from the SEER database and 97 eligible patients from Peking University People's Hospital were included in this study. The baseline clinicopathological characteristics and treatment information are shown in **Table 1**. All eligible cases from the SEER database (n = 3,918) were randomly divided into training (70%, n = 2,745) and internal validation cohorts (30%, n = 1,173) to develop and validate the nomogram. The patient characteristics were comparable between these two cohorts (all parameters *P*-value >0.05). During a median follow-up times of 8 months (IQR: 3–18), 9 months (IQR: 3–18), and 32 months (IQR: 22–47), 2,145 (78.1%), 941 (80.2%), and 53 (54.6%) LCSMs were recorded in the training cohort, internal validation cohort, and external validation cohort, respectively. The difference of follow-up time between the two cohorts was mainly because near half of the SEER cohort (n = 1,922, 49.1%) died within the 8 months of follow-up, shortening the overall follow-up time of the SEER cohort.

The proportion of patient who underwent PTR in the external validation cohort was relatively higher than that in the training cohort, since our department is a high-volume surgical center, and most of our patients underwent surgical intervention. We depicted two cumulative incidence curves to compare the LCSS between patients with PTR in the SEER and our external cohort. We found that the patients who received PTR in the external validation cohort showed a significant better LCSS than patients in the SEER cohort (**Supplementary Figure 1**). The main reason might be that the patients treated in our department were highly selected. The different baseline features between training and external validation cohorts ensured an effective test for the generalization ability of our model.

In the external validation cohort, 52 patients received adjuvant chemotherapy only, one patient underwent neoadjuvant chemotherapy only and one patient received both adjuvant chemotherapy and neoadjuvant chemotherapy. Our external validation cohort documented the information of target therapy, which was lacking in the SEER database. Fifty-two patients received targeted therapy in the external validation cohort, and they showed better survival than patients without targeted therapy (MST: 57 *vs* 26 months, $P < 0.001$).

TABLE 1 | Baseline clinicopathological characteristics and treatment information of all, training, and validation cohorts.

	Training cohort	Internal validation cohort	External validation cohort
Number of cases	2745	1173	97
Age, years, median (IQR)	70 (61–78)	69 (61–77)	58 (50–67)
Race, n (%)			
White	2069 (75.4)	860 (73.3)	—
Black	399 (14.5)	179 (15.3)	—
Other	277 (10.1)	134 (11.4)	—
Gender, n (%)			
Male	1483 (54.0)	635 (54.1)	45 (46.4)
Female	1262 (46.0)	538 (45.9)	52 (53.6)
Anatomic sites, n (%)			
Bronchus	178 (6.5)	76 (6.5)	0 (0.0)
Lobe	2338 (85.2)	995 (84.9)	97 (100.0)
Unknown	229 (8.3)	102 (8.7)	0 (0)
Histological subtype, n (%)			
Adenocarcinoma	1831 (66.7)	794 (67.7)	91 (93.8)
Squamous cell carcinoma	827 (30.1)	343 (29.2)	5 (5.2)
Large cell carcinoma	42 (1.5)	14 (1.2)	0
Adenosquamous carcinoma	45 (1.6)	22 (1.9)	1 (1.0)
Tumor size, mm, median (IQR)	45 (28–67)	43 (28–66)	27 (20–42)
T stage, n (%)			
T1	251 (9.1)	120 (10.2)	35 (36.1)
T2	627 (22.8)	273 (23.3)	28 (28.9)
T3	640 (23.3)	260 (22.2)	9 (9.3)
T4	1227 (44.7)	520 (44.3)	25 (25.8)
N stage, n (%)			
N0	877 (32.0)	365 (31.1)	78 (80.4)
N1	217 (7.9)	94 (8.0)	3 (3.1)
N2	1291 (47.0)	567 (48.3)	16 (16.5)
N3	360 (13.1)	147 (12.6)	0 (0)
Metastasis pattern, n (%)			
Pleural nodules	443 (16.1)	202 (17.2)	53 (54.6)
Pleural effusion	1999 (72.8)	858 (73.2)	42 (43.3)
Pericardial effusion	303 (11.1)	113 (9.6)	2 (2.1)
Chemotherapy [a], n (%)			
Yes	1704 (62.1)	733 (62.5)	53 (54.6)
No	1041 (37.9)	440 (37.5)	44 (45.4)
Radiotherapy [a], n (%)			
Yes	173 (6.3)	85 (7.3)	7 (7.2)
No	2572 (93.7)	1088 (92.7)	90 (92.8)
Primary tumor resection, n (%)			
Yes	167 (6.1)	87 (7.4)	51 (52.6)
No	2578 (93.9)	1086 (92.6)	46 (47.4)
Extent of surgery, n (%)			
Local tumor destruction	8 (4.8)	3 (3.4)	0 (0)
Sublobar resection	70 (41.9)	37 (42.5)	39 (76.5)
(Bi)lobectomy [b]	66 (39.5)	40 (46.0)	11 (21.5)
Pneumonectomy	23 (13.8)	7 (8.1)	1 (2.0)

IQR, interquartile range.
[a]*These factors do not distinguish between before and after surgery.*
[b]*Includes lobectomy and bilobectomy.*

Independent Prognostic Factors in the Training Cohort

The results of univariable and multivariable analyses were described in **Table 2**. Considering the lack of direct link between race and LCSS and the fact that variable T stage contains the information of tumor size, we did not include race and tumor size in the regression analysis. The univariable analysis indicated that age ($P < 0.001$), gender ($P = 0.009$), histological subtype ($P = 0.033$), T stage ($P = 0.001$), N stage ($P = 0.003$), metastasis pattern ($P < 0.001$), chemotherapy ($P < 0.001$), and PTR ($P < 0.001$) were significant prognostic factors. All significant prognostic factors were entered into the multivariable analysis based on competing risk regression, which revealed age ($P < 0.001$), gender ($P = 0.037$), T stage ($P = 0.002$), N stage ($P < 0.001$), metastasis pattern ($P = 0.005$), chemotherapy ($P < 0.001$), and PTR ($P < 0.001$) were independent prognostic factors to predict LCSS.

Constructing and Validating the Prognostic Nomogram

All independent prognostic factors mentioned above were incorporated to build the predictive model, which was

TABLE 2 | Univariable and multivariable analyses of the ability of each factor in predicting LCSS in the training cohort.

	Univariable analysis		Multivariable predictors	
	SHR (95% CI)	***P*-value**	**SHR (95% CI)**	***P*-value**
Age	1.014 (1.011–1.018)	**<0.001**	1.008 (1.004–1.012)	**<0.001**
Gender		**0.009**		
Male	Reference		Reference	
Female	0.896 (0.825–0.973)		0.911 (0.835–0.994)	**0.037**
Anatomic sites		0.554		
Bronchus	Reference			
Lobe	0.912 90.763–1.091)			
Unknown	0.946 (0.756–1.185)			
Histological		**0.033**		
Adenocarcinoma	Reference			
Squamous cell carcinoma	1.143 (1.043–1.253)		0.986 (0.891–1.090)	0.780
Large cell carcinoma	0.927 (0.658–1.305)		0.814 (0.580–1.142)	0.234
Adenosquamous carcinoma	0.973 (0.689–1.374)		0.935 (0.672–1.300)	0.691
T stage		**0.001**		
T1	Reference		Reference	
T2	1.159 (0.980–1.371)		1.154 (0.971–1.372)	0.104
T3	1.186 (1.003–1.402)		1.166 (0.980–1.387)	0.084
T4	1.329 (1.134–1.558)		1.332 (1.127–1.575)	**0.001**
N stage		**0.003**		
N0	Reference		Reference	
N1	1.003 (0.850–1.183)		1.134 (0.956–1.344)	0.149
N2	1.153 (1.049–1.268)		1.246 (1.124–1.383)	<0.001
N3	1.214 (1.067–1.382)		1.371 (1.191–1.579)	<0.001
Metastasis pattern		**<0.001**		
Pleural nodules	Reference		Reference	
Pleural effusion	1.324 (1.184–1.479)		1.120 (1.072–1.354)	**0.002**
Pericardial effusion	1.380 (1.168–1.630)		1.242 (1.042–1.481)	**0.016**
Chemotherapy		**<0.001**		
No	Reference		Reference	
Yes	0.558 (0.510–0.611)		0.565 (0.512–0.624)	**<0.001**
Radiotherapy		0.137		
No	Reference			
Yes	0.877 (0.737–1.043)			
Primary tumor resection		**<0.001**		
No	Reference		Reference	
Yes	0.527 (0.434–0.637)		0.580 (0.476–0.708)	**<0.001**

The significant P value is in bold font.

visualized in the form of a nomogram (**Figure 1**). The nomogram illustrated that age was the most predominant contributor to the LCSS followed by surgical treatment and chemotherapy. T stage and N stage merely showed a moderate impact on LCSS. Each subtype of the predictors was assigned a score, ranging from 0 (lowest risk) to 100 (highest risk). The estimated probability of LCSS can be easily obtained by drawing a vertical line through the location of total score at the bottom scale.

The validation of the nomogram was shown in **Figure 2**. The calibration curves presented a good consistency between the nomogram predicted and actually observed 1-, 3-, and 5-year LCSS in the training, internal, and external validation cohorts (**Figures 2A–C**). The Harrell's C-indices of nomogram were 0.682 (95%CI: 0.673–0.691), 0.687 (95%CI: 0.670–0.704), and 0.667 (95%CI: 0.584–0.750) in the training, internal, and external validation cohorts, respectively. The AUCs of 1-, 3-, and 5-year ROC also suggested a great predictive power for LCSS at these three timepoints (**Figures 2D–F**).

Impact of PTR on Patients With Different Risk and Subgroup Analysis

To elucidate the impact of PTR on LCSS among patients with different risks, we established a modified nomogram including age, gender, T stage, N stage, metastasis pattern, and chemotherapy (**Supplementary Figure 1**) using the training cohort and calculated the risk score for LCSM of each case based on this modified nomogram. All the patients were classified into low-risk (n = 2,706, 67.4%, score <176.8) and high-risk group (n = 1,309, 32.6%, score≥176.8) with the cut-off point set at the highest third of the score in training cohort. Specifically, 260 (9.6%) low risk patients and 45 (3.4%) high risk patients underwent PTR. These two risk groups showed distinct cumulative incidence curves of LCSM in both SEER and external validation cohorts (**Figures 3A, B**), and surgery experience made significant favorable impact on LCSM within each risk group (**Figure 3C**). Moreover, there was no significant interaction effect between PTR and risk group, indicating similar benefit of PTR can be reaped by patients in different risk groups.

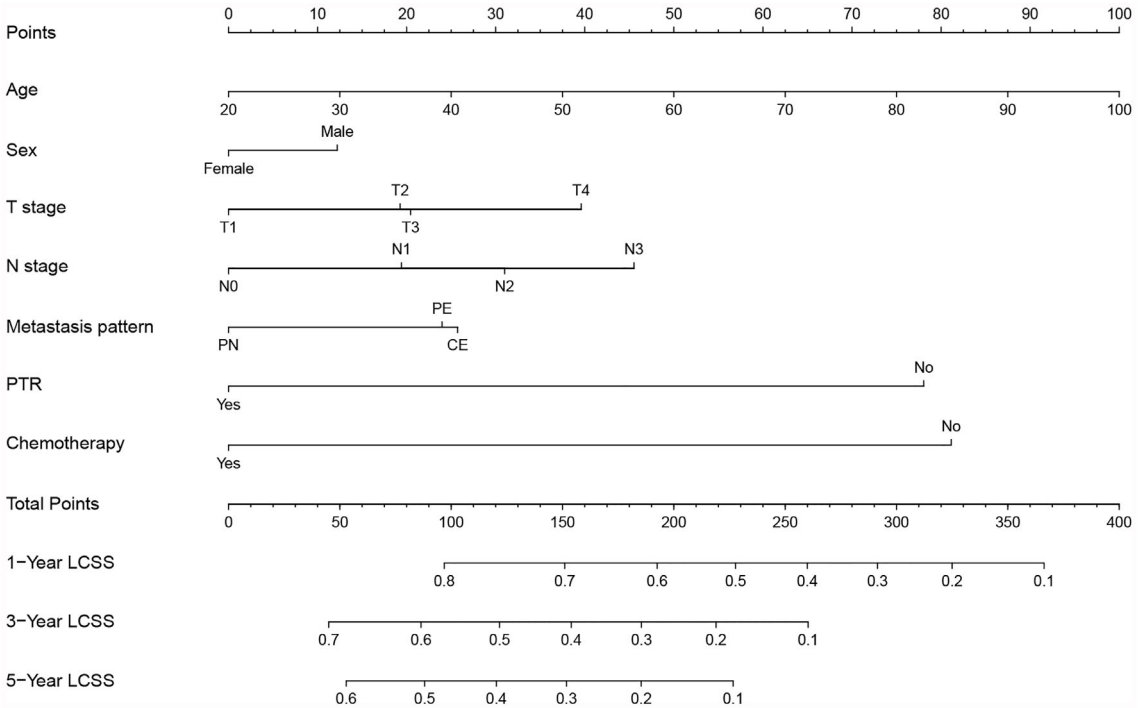

FIGURE 1 | Prognostic nomogram predicting probability of 1-, 3- and 5-year lung cancer-specific survival (LCSS) in NSCLC patients with ipsilateral pleural dissemination. PN, pleural nodules; PE, pleural effusion; CE, pericardial effusion; PTR, primary tumor resection.

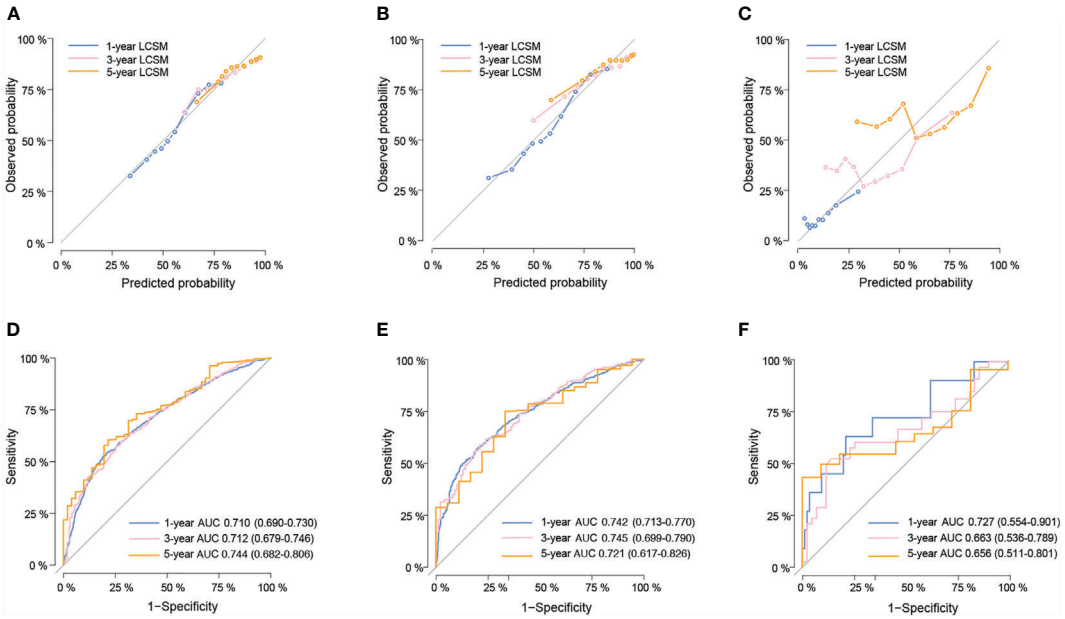

FIGURE 2 | The calibration curves for predicting lung cancer-specific survival (LCSS) in the training **(A)**, internal validation **(B)** and external validation cohort **(C)** respectively. Nomogram-predicted probability is plotted on the x-axis; actual probability is plotted on the y-axis. A curve along the 45-degree line indicates perfect calibration models. Time-dependent ROC curves for the 1-, 3-, and 5-year LCSS probability in the training **(D)**, internal validation **(E)** and external validation cohorts **(F)** respectively.

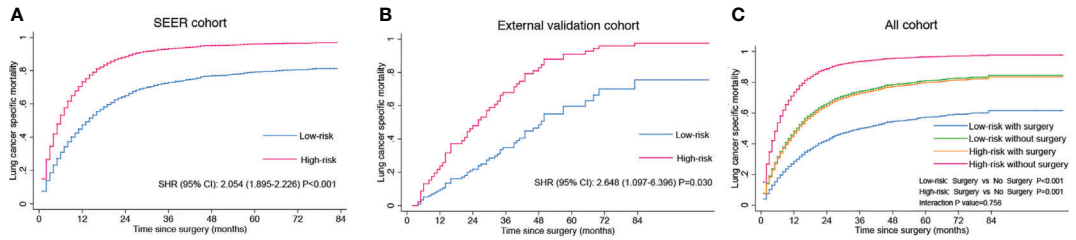

FIGURE 3 | Risk group stratification according to the modified nomogram in the SEER cohort **(A)**, external validation cohort **(B)** and all cohorts **(C)**.

Subgroup analysis and interaction tests were performed among all cases to identified patients who might get more benefit from PTR. We found that PTR was the favorable predictor of LCSS in almost all subgroups. Interestingly, interaction tests suggested a greater LCSS difference caused by PTR in patients without chemotherapy than in patients who received chemotherapy (**Figure 4**).

DISCUSSION

NSCLC with ipsilateral pleural dissemination, which was previously classified as T4 stage (19), is considered as M1a disease in the current 8th TNM staging system due to the extremely poor survival outcomes (3). Currently, prognostic prediction model for these cases is unavailable, and which type

Subgroup	No. of patients with PTR (%)	SHR (95% CI)	Interaction P–value
Overall	**305 (7.6)**	**0.458 (0.396–0.530)**	
Age, years			**0.659**
<70	207 (10.3)	0.451 (0.372–0.546)	
≥70	98 (4.9)	0.511 (0.409–0.641)	
Gender			**0.700**
Male	160 (7.4)	0.445 (0.367–0.540)	
Female	145 (7.8)	0.473 (0.379–0.590)	
Differentiation			**0.456**
Grade I/II	124 (16.6)	0.432 (0.333–0.560)	
Grade III/IV	126(11.9)	0.513 (0.416–0.632)	
Histological subtype			**0.938**
Adenocarcinoma	218 (8.0)	0.450 (0.378–0.537)	
Squamous cell carcinoma	76 (6.5)	0.501 (0.376–0.666)	
T stage			**0.143**
T1	43 (10.6)	0.311 (0.198–0.487)	
T2	82 (8.8)	0.493 (0.374–0.650)	
T3	73 (8.0)	0.567 (0.425–0.757)	
T4	107 (6.0)	0.453 (0.355–0.579)	
N stage			**0.225**
N0	150 (11.4)	0.412 (0.328–0.517)	
N1	40 (12.7)	0.504 (0.333–0.762)	
N2	106 (5.7)	0.570 (0.459–0.708)	
N3	9 (1.8)	0.445 (0.184–1.074)	
Metastasis pattern			**0.337**
Pleural nodules	109 (15.6)	0.404 (0.312–0.524)	
Pleural effusion	176 (6.1)	0.533 (0.441–0.646)	
Pericardial effusion	20 (4.8)	0.417 (0.239–0.727)	
Chemotherapy			**<0.001**
Yes	196 (7.8)	0.525 (0.439–0.628)	
No	109 (7.1)	0.371 (0.289–0.476)	
Radiotherapy			**0.090**
Yes	73 (27.5)	0.588 (0.422–0.819)	
No	232 (6.2)	0.432 (0.365–0.511)	

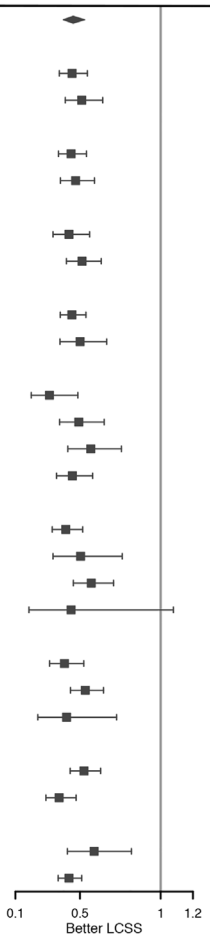

FIGURE 4 | Subgroup analysis of the impact of primary tumor resection (PTR) on lung cancer-specific survival (LCSS) stratified by clinicopathologic feature.

of patients could benefit more from PTR is still unclear. Here, we used a large cohort from the SEER database to establish a nomogram predicting the LCSS of NSCLC patients with ipsilateral pleural dissemination. The external validation favored the satisfactory performance of the nomogram in prognostic prediction. We identified age, gender, TN stage, metastasis pattern, PTR, and chemotherapy as the independent factors for LCSS. We confirmed that surgery intervention was a significant favorable predictor of LCSS in almost all subgroups, except for patients with N3 disease, may be due to the small sample size of N3 patients who underwent surgery (n = 9). Furthermore, interaction tests indicated that patients without chemotherapy could get more benefit from PTR.

NSCLC with ipsilateral pleural dissemination was traditionally regarded as a contraindication for surgical intervention, and system chemotherapy was considered as standard treatment (20). However, more and more evidence has revealed the positive role of surgery in prolonging the survival of M1a patients. In 2001, Ichinose et al. (21) first reported an unexpectedly good survival outcome in patients with carcinomatous pleuritis of minimal disease who underwent resection of the primary tumor, with 5-year survival of 22.8%. Similarly, promising prognoses were observed among patients with pleural dissemination who underwent primary lesion resection in subsequent years of research (6, 22–28). However, most of these studies were single-center focused on the patients with pleural dissemination first detected during operation, which were a highly selected population. Thus, to reflect the real-world situation more precisely, we used large cohort from the SEER database in our previous study (7) that also indicated PTR was associated with better OS and LCSS in patients with ipsilateral pleural dissemination. In this study, we further explored impact of PTR on different subgroups. The survival benefit of PTR tended to be greater in lower T stage and N stage population, similar to the published literature (5, 6, 9, 26, 29, 30), although the interaction test fell short of statistical significance. It was firstly observed in our study that patients without chemotherapy could get more survival benefit from PTR, providing valuable thought for surgical decision making.

In clinical practice, lymph node metastasis is an essential demarcation criterion for the staging of M0 patients, whereas M1a patients are categorized as stage IV regardless of any N status (3), which means the impact of lymph node metastasis on M1a patients deserves more comprehensive studies. Iida et al. (9) used a Japanese multicenter prospective cohort to conduct a retrospective study including 329 patients with pleural carcinomatosis and reported that the best stage N status (N0/N1) was associated with significantly longer survival when compared with N2/N3. Dai et al. performed a retrospective study using a SEER cohort and found that lymph node metastasis was a significant prognostic factor for NSCLC patients with pleural dissemination, and they proposed a speculative explanation that patients with N0 disease might have minor malignant pleural effusion or localized pleural nodules, which could be effectively controlled by comprehensive treatment (5). Hu et al. (31) investigated the SEER database and found that lymph node metastasis was the independent factor with poor prognosis for NSCLC patients with malignant pericardial effusion. It was also confirmed that higher T stage was related with worse prognosis (6, 26).

Systemic chemotherapy was considered as the standard therapy for patients with ipsilateral pleural dissemination (20). Kimura et al. (32) reported that platinum-based chemotherapy may improve the clinical outcomes of patients with pleural dissemination. Here, we confirmed the favorable role of chemotherapy in M1a patients, and we further found PTR brought more survival benefit in non-chemotherapy patients. Our previous study found targeted therapy could significantly improve the OS of M1a patients, and PTR brought more benefit to patients without targeted therapy (8). We speculated that systematic treatment, such as chemotherapy and targeted therapy, could effectively reduce the tumor burden, which solely depended on surgical intervention in patients without systematic treatment. These results indicated PTR was a more valuable treatment for M1a patients who cannot undergo chemotherapy and targeted therapy. Notably, PTR had significant favorable impact on both patients receiving chemotherapy and patients without chemotherapy; therefore, when adjuvant chemotherapy was uncertain, PTR was still preferred for M1a patients. In fact, it is hard to guide surgical decision on the basis of chemotherapy strategy due to the fact that chemotherapy strategy is usually defined only once a thorough pathological analysis has been completed, usually several days after surgery.

Recently, several predictive models for patients with malignant pleural effusion or malignant pleural pericardial effusion had been published. Most of them focused on the concentration of biomarkers in the pleural effusion or serum (33–35); however, the higher cost and the variation of result owing to the different techniques (36), as well as the difficulty in collecting extra tissues in patients with poor physical condition, limited the application of these predictive models (37). Tian et al. used the data of NSCLC patients with malignant pleural effusion or pericardial effusion from SEER database between 2010 and 2015 to developed a nomogram, which included age, gender, race, primary site, histology type, TN status, and effusion patterns with a C-index of 0.736 (38). However, the authors did not excluded patients with contralateral pulmonary nodules or distant organ metastasis, and they did not ensure the patients they enrolled had only one malignant primary tumor. Our nomogram developed in this study had some advantages compared with previous nomogram. We only included patients with ipsilateral pleural dissemination, who were more controversial population in clinical practice. The use of competing risk model could effectively eliminate the influence of death competition on cancer-specific survival. The external validation in a Chinese cohort showed the reliability of the nomogram in predicting LCSS of patients with ipsilateral pleural dissemination. This novel nomogram might be a practical tool for clinicians to optimize the individual treatment strategy for patients with different risks.

This study also has some limitations. First, the SEER-based study was limited by its retrospective nature with inherent biases.

Although we used multivariable competing risk regression analysis to control the impact of confounding covariates, the unavailable confounding factors could not be well ruled out, such as performance status, detailed histological and mutational features, surgical approach (open or VAST), and systematic therapy regimen (neoadjuvant or adjuvant chemotherapy) which were lacking in the SEER database. Second, we were not able to distinguish between clinical and pathological M1a staging due to the lack of information in the SEER database, which hindered further prognostic analysis. Third, our external validation cohort was relatively small compared with the SEER cohort due to the small proportion of M1a NSCLC patients in a surgical center. Further, multi-center cohort might be necessary for the external validation. Finally, we excluded patients whose survival time was recorded as zero month in the SEER cohort to exclude potential confounding factors, because these patients accounted for a large proportion of SEER cohort during the data process (approximately 14.2%). But it would also eliminate the influence of perioperative mortality on the survival analysis.

CONCLUSION

We developed a nomogram based on competing risk regression to reliably predict prognosis of NSCLC patients with ipsilateral pleural dissemination and validated this nomogram in an external Chinese cohort. This novel nomogram might be a practical tool for clinicians to anticipate the 1-, 3- and 5-year LCSS for NSCLC patients with pleural dissemination. Subgroup analysis indicated that patients without chemotherapy could get more benefit from PTR. In order to assess the role of PTR in the management of M1a patients more accurately, further prospective study would be urgently required.

DATA AVAILABILITY STATEMENT

The raw data supporting the conclusions of this article will be made available by the authors, without undue reservation.

ETHICS STATEMENT

Ethical review and approval was not required for the study on human participants in accordance with the local legislation and institutional requirements. The ethics committee waived the requirement of written informed consent for participation.

AUTHOR CONTRIBUTIONS

ZW and HL: data collection, data analysis, and drafting the article. TL and ZS: data collection. FY and GJ: conception of the work and critical revision of the article. GJ: approved the final version of the manuscript on behalf of all authors. All authors contributed to the article and approved the submitted version.

FUNDING

This work was supported by Beijing Municipal Science and Technology Commission (Z181100001718190); the Major Research plan of National Natural Science of China (grant 92059203); the National Natural Science Foundation of China (grant 82002410 and 61877001); Peking University People's Hospital Scientific Research Development Funds (grant RDY2020-02).

ACKNOWLEDGMENTS

We would like to thank all the staff members of the National Cancer Institute who work with the SEER program.

SUPPLEMENTARY MATERIAL

The Supplementary Material for this article can be found online at: https://www.frontiersin.org/articles/10.3389/fonc.2021.645486/full#supplementary-material

REFERENCES

1. Morgensztern D, Ng SH, Gao F, Govindan R. Trends in Stage Distribution for Patients With non-Small Cell Lung Cancer: A National Cancer Database Survey. *J Thorac Oncol* (2010) 5(1):29–33. doi: 10.1097/JTO.0b013e3181c5920c
2. Postmus PE, Brambilla E, Chansky K, Crowley J, Goldstraw P, Patz EFJr., et al. The IASLC Lung Cancer Staging Project: Proposals for Revision of the M Descriptors in the Forthcoming (Seventh) Edition of the TNM Classification of Lung Cancer. *J Thorac Oncol* (2007) 2(8):686–93. doi: 10.1097/JTO.0b013e31811f4703
3. Goldstraw P, Chansky K, Crowley J, Rami-Porta R, Asamura H, Eberhardt WE, et al. The IASLC Lung Cancer Staging Project: Proposals for Revision of the TNM Stage Groupings in the Forthcoming (Eighth) Edition of the TNM Classification for Lung Cancer. *J Thorac Oncol* (2016) 11(1):39–51. doi: 10.1016/j.jtho.2015.09.009
4. Ettinger DS, Aisner DL, Wood DE, Akerley W, Bauman J, Chang JY, et al. Nccn Guidelines Insights: Non-Small Cell Lung Cancer, Version 5.2018. *J Natl Compr Canc Netw* (2018) 16(7):807–21. doi: 10.6004/jnccn.2018.0062
5. Dai C, Ren Y, Xie D, Zheng H, She Y, Fei K, et al. Does Lymph Node Metastasis Have a Negative Prognostic Impact in Patients With NSCLC and M1a Disease? *J Thorac Oncol* (2016) 11(10):1745–54. doi: 10.1016/j.jtho.2016.06.030
6. Wang BY, Wu YC, Hung JJ, Hsu PK, Hsieh CC, Huang CS, et al. Prognosis of non-Small-Cell Lung Cancer With Unexpected Pleural Spread at Thoracotomy. *J Surg Res* (2011) 169(1):e1–5. doi: 10.1016/j.jss.2011.02.028
7. Li H, Sun Z, Yang F, Sui X, Liu T, Wang J. Primary Tumour Resection in non-Small-Cell Lung Cancer Patients With Ipsilateral Pleural Dissemination (M1a): A Population-Based Study. *Eur J Cardiothorac Surg* (2019) 55 (6):1121–9. doi: 10.1093/ejcts/ezy439
8. Li H, Liu T, Sun Z, Yang F. Primary Tumor Resection of non-Small Cell Lung Cancer Patients With Ipsilateral Pleural Dissemination (M1a) in the Era of Targeted Therapy. *Thorac Cancer* (2020) 11(11):3213–22. doi: 10.1111/1759-7714.13649
9. Iida T, Shiba M, Yoshino I, Miyaoka E, Asamura H, Date H, et al. Surgical Intervention for Non-Small-Cell Lung Cancer Patients With Pleural Carcinomatosis: Results From the Japanese Lung Cancer Registry in 2004. *J Thorac Oncol* (2015) 10(7):1076–82. doi: 10.1097/jto.0000000000000554

10. Zeng Y, Mayne N, Yang CJ, D'Amico TA, Ng CSH, Liu CC, et al. A Nomogram for Predicting Cancer-Specific Survival of TNM 8th Edition Stage I non-Small-Cell Lung Cancer. *Ann Surg Oncol* (2019) 26(7):2053–62. doi: 10.1245/s10434-019-07318-7
11. Tang X, Zhou X, Li Y, Tian X, Wang Y, Huang M, et al. A Novel Nomogram and Risk Classification System Predicting the Cancer-Specific Survival of Patients With Initially Diagnosed Metastatic Esophageal Cancer: A Seer-Based Study. *Ann Surg Oncol* (2019) 26(2):321–8. doi: 10.1245/s10434-018-6929-0
12. Lang BH, Wong CK, Yu HW, Lee KE. Postoperative Nomogram for Predicting Disease-Specific Death and Recurrence in Papillary Thyroid Carcinoma. *Head Neck* (2016) 38(Suppl 1):E1256–63. doi: 10.1002/hed.24201
13. Kim SK, Chai YJ, Park I, Woo JW, Lee JH, Lee KE, et al. Nomogram for Predicting Central Node Metastasis in Papillary Thyroid Carcinoma. *J Surg Oncol* (2017) 115(3):266–72. doi: 10.1002/jso.24512
14. Karakiewicz PI, Briganti A, Chun FK, Trinh QD, Perrotte P, Ficarra V, et al. Multi-Institutional Validation of a New Renal Cancer-Specific Survival Nomogram. *J Clin Oncol* (2007) 25(11):1316–22. doi: 10.1200/jco.2006.06.1218
15. Han DS, Suh YS, Kong SH, Lee HJ, Choi Y, Aikou S, et al. Nomogram Predicting Long-Term Survival After D2 Gastrectomy for Gastric Cancer. *J Clin Oncol* (2012) 30(31):3834–40. doi: 10.1200/jco.2012.41.8343
16. Fine JP. Regression Modeling of Competing Crude Failure Probabilities. *Biostatistics* (2001) 2(1):85–97. doi: 10.1093/biostatistics/2.1.85
17. Iasonos A, Schrag D, Raj GV, Panageas KS. How to Build and Interpret a Nomogram for Cancer Prognosis. *J Clin Oncol* (2008) 26(8):1364–70. doi: 10.1200/jco.2007.12.9791
18. Kamarudin AN, Cox T, Kolamunnage-Dona R. Time-Dependent ROC Curve Analysis in Medical Research: Current Methods and Applications. *BMC Med Res Methodol* (2017) 17(1):53. doi: 10.1186/s12874-017-0332-6
19. Mountain CF. Revisions in the International System for Staging Lung Cancer. *Chest* (1997) 111(6):1710–7. doi: 10.1378/chest.111.6.1710
20. Hanna N, Johnson D, Temin S, Baker SJr., Brahmer J, Ellis PM, et al. Systemic Therapy for Stage Iv Non-Small-Cell Lung Cancer: American Society of Clinical Oncology Clinical Practice Guideline Update. *J Clin Oncol* (2017) 35(30):3484–515. doi: 10.1200/jco.2017.74.6065
21. Ichinose Y, Tsuchiya R, Koike T, Kuwahara O, Nakagawa K, Yamato Y, et al. Prognosis of Resected non-Small Cell Lung Cancer Patients With Carcinomatous Pleuritis of Minimal Disease. *Lung Cancer* (2001) 32(1):55–60. doi: 10.1016/s0169-5002(00)00206-3
22. Li C, Kuo SW, Hsu HH, Lin MW, Chen JS. Lung Adenocarcinoma With Intraoperatively Diagnosed Pleural Seeding: Is Main Tumor Resection Beneficial for Prognosis? *J Thorac Cardiovasc Surg* (2018) 155(3):1238–49.e1. doi: 10.1016/j.jtcvs.2017.09.162
23. Ren YJ, She YL, Dai CY, Jiang GN, Fei K, Chen C. Primary Tumour Resection Showed Survival Benefits for non-Small-Cell Lung Cancers With Unexpected Malignant Pleural Dissemination. *Interact Cardiovasc Thorac Surg* (2016) 22 (3):321–6. doi: 10.1093/icvts/ivv353
24. Yun JK, Kim MA, Choi CM, Choi SH, Kim YH, Kim DK, et al. Surgical Outcomes After Pulmonary Resection for Non-Small Cell Lung Cancer With Localized Pleural Seeding First Detected During Surgery. *Thorac Cardiovasc Surg* (2018) 66(2):142–9. doi: 10.1055/s-0035-1564928
25. Mordant P, Arame A, Foucault C, Dujon A, Le Pimpec Barthes F, Riquet M. Surgery for Metastatic Pleural Extension of non-Small-Cell Lung Cancer. *Eur J Cardiothorac Surg* (2011) 40(6):1444–9. doi: 10.1016/j.ejcts.2011.02.076
26. Okamoto T, Iwata T, Mizobuchi T, Hoshino H, Moriya Y, Yoshida S, et al. Pulmonary Resection for Lung Cancer With Malignant Pleural Disease First Detected at Thoracotomy. *Eur J Cardiothorac Surg* (2012) 41(1):25–30. doi: 10.1016/j.ejcts.2011.04.010
27. Li S, Zhang S, Huang M, Ma Y, Yang Y. Management of Occult Malignant Pleural Disease Firstly Detected at Thoracotomy for non-Small Cell Lung Cancer Patients. *J Thorac Dis* (2017) 9(10):3851–8. doi: 10.21037/jtd.2017.09.112
28. Go T, Misaki N, Matsuura N, Chang SS, Tarumi S, Yokomise H. Role of Surgery in Multi-Modality Treatment for Carcinomatous Pleuritis in Patients With non-Small Cell Lung Cancer. *Surg Today* (2015) 45(2):197–202. doi: 10.1007/s00595-014-0987-0
29. Xu Y, Chen N, Wang Z, Zhang Y, Mei J, Liu C, et al. Should Primary Tumor be Resected for non-Small Cell Lung Cancer With Malignant Pleural Disease Unexpectedly Found During Operation?-a Systemic Review and Meta-Analysis. *J Thorac Dis* (2016) 8(10):2843–52. doi: 10.21037/jtd.2016.10.19
30. Ren Y, Dai C, Shen J, Liu Y, Xie D, Zheng H, et al. The Prognosis After Contraindicated Surgery of NSCLC Patients With Malignant Pleural Effusion (M1a) may be Better Than Expected. *Oncotarget* (2016) 7(18):26856–65. doi: 10.18632/oncotarget.8566
31. Hu ZG, Hu K, Li WX, Zeng FJ. Prognostic Factors and Nomogram for Cancer-Specific Death in non Small Cell Lung Cancer With Malignant Pericardial Effusion. *PloS One* (2019) 14(5):e0217007. doi: 10.1371/journal.pone.0217007
32. Kimura M, Murakami H, Naito T, Kenmotsu H, Taira T, Akamatsu H, et al. Outcome of Platinum-Based Chemotherapy for non-Small-Cell Lung Cancer Patients With Pleural Dissemination Detected During Surgery. *Mol Clin Oncol* (2013) 1(6):949–52. doi: 10.3892/mco.2013.164
33. Psallidas I, Kanellakis NI, Gerry S, Thézénas ML, Charles PD, Samsonova A, et al. Development and Validation of Response Markers to Predict Survival and Pleurodesis Success in Patients With Malignant Pleural Effusion (PROMISE): A Multicohort Analysis. *Lancet Oncol* (2018) 19(7):930–9. doi: 10.1016/s1470-2045(18)30294-8
34. Clive AO, Kahan BC, Hooper CE, Bhatnagar R, Morley AJ, Zahan-Evans N, et al. Predicting Survival in Malignant Pleural Effusion: Development and Validation of the LENT Prognostic Score. *Thorax* (2014) 69(12):1098–104. doi: 10.1136/thoraxjnl-2014-205285
35. Tian T, Li J, Hu W, Sun C, Zhou J. Thymidine Kinase 1 Concentration in Pleural Effusion is a Diagnostic Marker and Survival Predictor for Malignant Pleural Effusion. *J Clin Lab Anal* (2019) 33(6):e22901. doi: 10.1002/jcla.22901
36. Psallidas I, Kalomenidis I, Porcel JM, Robinson BW, Stathopoulos GT. Malignant Pleural Effusion: From Bench to Bedside. *Eur Respir Rev* (2016) 25(140):189–98. doi: 10.1183/16000617.0019-2016
37. Patel JN, Ersek JL, Kim ES. Lung Cancer Biomarkers, Targeted Therapies and Clinical Assays. *Transl Lung Cancer Res* (2015) 4(5):503–14. doi: 10.3978/j.issn.2218-6751.2015.06.02
38. Tian T, Zhang P, Zhong F, Sun C, Zhou J, Hu W. Nomogram Construction for Predicting Survival of Patients With non-Small Cell Lung Cancer With Malignant Pleural or Pericardial Effusion Based on SEER Analysis of 10,268 Patients. *Oncol Lett* (2020) 19(1):449–59. doi: 10.3892/ol.2019.11112

Conflict of Interest: The authors declare that the research was conducted in the absence of any commercial or financial relationships that could be construed as a potential conflict of interest.

Copyright © 2021 Wang, Li, Liu, Sun, Yang and Jiang. This is an open-access article distributed under the terms of the Creative Commons Attribution License (CC BY). The use, distribution or reproduction in other forums is permitted, provided the original author(s) and the copyright owner(s) are credited and that the original publication in this journal is cited, in accordance with accepted academic practice. No use, distribution or reproduction is permitted which does not comply with these terms.

frontiers in Pharmacology

ORIGINAL RESEARCH
published: 28 July 2021
doi: 10.3389/fphar.2021.660313

AI-Based Drug Discovery of TKIs Targeting L858R/T790M/C797S-Mutant EGFR in Non-small Cell Lung Cancer

Geunho Choi†, Daegeun Kim† and Junehwan Oh*

AI LAB, AllLive Healthcare Co.,Ltd., Seongnam, Korea

Lung cancer has a high mortality rate, and non-small cell lung cancer (NSCLC) is the most common type of lung cancer. Patients have been observed to acquire resistance against various anticancer agents used for NSCLC due to L858R (or Exon del19)/T790M/C797S-EGFR mutations. Therefore, next-generation drugs are being developed to overcome this problem of acquired resistance. The goal of this study was to use artificial intelligence (AI) to discover drug candidates that can overcome acquired resistance and reduce the limitations of the current drug discovery process, such as high costs and long durations of drug design and production. To generate ligands using AI, we collected data related to tyrosine kinase inhibitors (TKIs) from accessible libraries and used LSTM (Long short term memory) based transfer learning (TL) model. Through the simplified molecular-input line-entry system (SMILES) datasets of the generated ligands, we obtained drug-like ligands via parameter-filtering, cyclic skeleton (CSK) analysis, and virtual screening utilizing deep-learning method. Based on the results of this study, we are developing prospective EGFR TKIs for NSCLC that have overcome the limitations of existing third-generation drugs.

Keywords: NSCLC, EGFR, tyrosine kinase inhibitors (TKIs), transfer learning, LSTM, virtual screening

OPEN ACCESS

Edited by:
Hideharu Kimura,
Kanazawa University, Japan

Reviewed by:
Muthupandian Saravanan,
Saveetha Dental College And Hospitals, India
Prashant S Kharkar,
Institute of Chemical Technology, India

****Correspondence:***
Geunho Choi
cgh2797@naver.com

†These authors have contributed equally to this work

Specialty section:
This article was submitted to Pharmacology of Anti-Cancer Drugs, a section of the journal Frontiers in Pharmacology

Received: *29 January 2021*
Accepted: *19 July 2021*
Published: *28 July 2021*

Citation:
Choi G, Kim D and Oh J (2021) AI-Based Drug Discovery of TKIs Targeting L858R/T790M/C797S-Mutant EGFR in Non-small Cell Lung Cancer. Front. Pharmacol. 12:660313. doi: 10.3389/fphar.2021.660313

INTRODUCTION

Cancer is one of the leading causes of death worldwide (Sung et al., 2021). In the United States, cancer is the second leading cause of death as of 2017–2018, accounting for 21% of the deaths. The mortality rates according to the cancer type from 2014 to 2018 in the United States are as follows (rates are per 100,000 population). Lung and bronchus cancer was 38.5, breast cancer (female) was 20.1, prostate cancer was 19.0, colon and rectum cancer was 13.7, liver and intrahepatic bile duct cancer was 6.6, and Kidney and renal pelvis cancer was 3.6 (Siegel et al., 2021). Among many cancers, lung cancer has a high mortality rate. Approximately 1.7 million people died from lung cancer in 2018, with non-small cell lung cancer (NSCLC) being the cause of death in over 80% of these cases (Yuan et al., 2019). Platinum-based doublet chemotherapy (e.g., cisplatin), which directly induces cancer cell apoptosis, has been used to treat lung cancer since 2005. However, this treatment has drawbacks such as inducement of normal cell apoptosis and achievement of only a short survival period of 10 months. Since the discovery of genetic mutations related to epidermal growth factor receptor (EGFR) in 2004, numerous targeted anticancer agents with fewer side effects compared to chemotherapy have been developed. These agents have extended the survival period of patients with lung cancer to over 24 months (Li et al., 2019) (Jiao et al., 2018) (Yuan et al., 2019).

Ongoing research on targeted anticancer agents has revealed the mechanisms of various targetable pathways associated with lung cancer (e.g., EGFR, PI3K/AKT/mTOR, RAS-MAPK, and JAK/STAT). EGFR, a member of the HER family, is a transmembrane glycoprotein that regulates cell regulatory pathways involved in cell proliferation, differentiation, and apoptosis. Since the discovery of EGFR overexpression in patients with lung cancer, which revealed a correlation between EGFR tyrosine kinase expression and tumor formation, numerous agents with significant therapeutic targets in NSCLC have been developed (Le and Gerber, 2019) (Leonetti et al., 2019).

Gefitinib from AstraZeneca and Erlotinib from Roche, which are first-generation reversible inhibitors of EGFR tyrosine kinase, were approved in 2003–2013, respectively. Afatinib, a second-generation irreversible inhibitor of EGFR tyrosine kinase from Boehringer Ingelheim, was approved in 2013. These first- and second-generation drugs are used as targeted agents for NSCLC and have shown high efficacy for common activating EGFR mutations such as the L858R point mutation and exon 19 deletion. However, after a treatment period of 1–2 years, the second mutation called the "gatekeeper", referring to the T790M-mutation in EGFR exon 20, occurs in 50–60% of patients treated with these agents, in addition to other mutations such as MET amplification and RAS mutations. The "gatekeeper" mutation reduces the effectiveness of the first- and second-generation anticancer agents by inducing drug resistance. Thus, numerous third-generation EGFR tyrosine kinase inhibitors (TKIs) sensitive to TK domain mutations (T790M) have been developed.(Jett and Carr, 2013) (Yuan et al., 2019) (Liu et al., 2018) (Grabe et al., 2018).

Osimertinib (Tagrisso) is a major third-generation EGFR TKI developed by AstraZeneca and approved by the Food and Drug Administration (FDA) in 2015. Osimertinib covalently binds (Ghosh et al., 2019) to the Cys797 residue of EGFR tyrosine kinase and is thus highly selective (Zhai et al., 2020) (Klaeger et al., 2017) and potent for the EGFR T790M mutation and other activating EGFR mutations. In 2015, however, the use of osimertinib as a third-generation EGFR TKI was shown to lead to acquired resistance, resulting from the tertiary point mutation C797S. Substitution of the Cys797 residue with serine 797 led to the loss of covalent interactions and significantly reduced drug efficacy. Consequently, fourth-generation drugs with therapeutic effects against the EGFR C797S-mutation are currently under development. (Jett and Carr, 2013) (Leonetti et al., 2019) (Grabe et al., 2018).

Drug discovery costs are increasing and research and development efficiency is decreasing (Mak and Pichika, 2019) (Scannell et al., 2012) (Schuhmacher et al., 2016). Therefore, increasing efforts have been undertaken to use artificial intelligence (AI) in drug discovery (Chen et al., 2018) (Chan et al., 2019). Unlike conventional drug discovery procedures, AI based drug discovery does not incur high experimental costs and requires only a small number of personnel.

Deep learning (Lecun et al., 2015) is artificial neural networks that mimic the brain, a complex system. Deep learning has been successfully applied to areas such as computer vision (Voulodimos et al., 2018), speech recognition (Nassif et al., 2019), and natural language processing (Young et al., 2018). Recently, studies applying AI such as deep learning to drug discovery are increasing. Researchers have developed a drug generation model using variational autoencoder (Gómez-Bombarelli et al., 2018), generative adversarial autoencoder models (Kadurin et al., 2017). A drug generation model using a recurrent neural network (RNN) architecture and reinforcement learning (Popova et al., 2018) has also been developed. Deep learning is highly sensitive to data quality and quantity. A small dataset is a bottleneck in AI-aided novel drug discovery and can be overcome by transfer learning (TL) (Segler et al., 2018) (Gupta et al., 2018) (Moret et al., 2020) (Cai et al., 2020). TL enables efficient learning even with a small amount of data.

We adopted model (Li et al., 2020) using RNN(LSTM) and TL, and conducted research with the aim of discovering 4th generation new drug candidates as L858R (or Exon del19)/T790M/C797S-mutation EGFR tyrosine kinase inhibitors related to NSCLC.

MATERIALS AND METHODS

Data Curation and Analysis

We downloaded data for 1,961,462 compounds from ChEMBL (Gaulton et al., 2012), a curated compound database, and selected compounds whose names ended with '-tinib' and additionally selected Lazertinib, creating a list of 139 compounds (**Figure 1**). The reason why we specifically chose '–tinib' structures as our base dataset molecules from ChEMBL database is that '-tinib' is an already known tyrosine kinase inhibitor that exhibits certain pharmacological effects in relation to various tyrosine kinases including our targeted protein, EGFR TK and We aim to discover promising

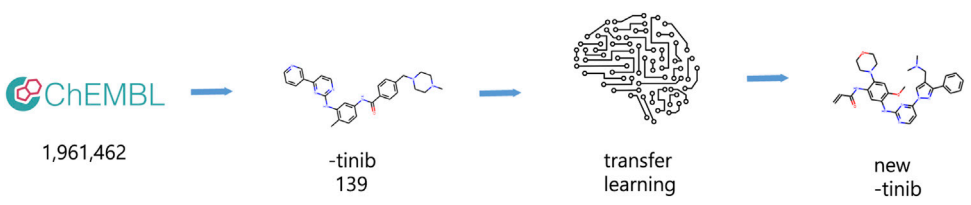

FIGURE 1 | Overall process. Data preparation and generative model process.

candidates as EGFR TKIs reflecting the structural, physicochemical and biochemical features of these '-tinib'. The data used in the paper are available at https://github.com/cgh2797/AI_drug_discovery_EGFR. Data was input in SMILES format using the open-source cheminformatics Rdkit 2020.03.1.0. We performed a 10-fold augmentation on the '-tinib' dataset as it was not large enough to train a model (Bjerrum, 2017). Additionally, we analyzed the structural similarity between compounds by examining their cyclic skeletons (CSKs) (Xu and Johnson, 2002).

LSTM TL

Since the dataset is small and SMILES is a string format, an RNN (LSTM) TL model (Li et al., 2020) was selected. A training dataset (Li et al., 2020) was used as a base dataset, and the dataset of 139 '-tinib' compounds was used as a second dataset for TL after 10-fold augmentation. The data preprocessing method was selected from the previous study (Li et al., 2020). The BasicLSTMCell function in TensorFlow was used for the two LSTM layers of the deep learning model. A dropout was applied to each LSTM layer. The keep probability was 0.8, and the number of hidden layers was 512. For the loss function, TensorFlow's seq2seq.sequence_loss function optimized with the Adam optimizer was used. The learning rate was set to 0.003. Model training was performed using TensorFlow-gpu 1.15.0. NVIDIA GeForce RTX 2080 SUPER was used for computation.

Filtering

Of the generated molecules, invalid molecules whose parameters could not be calculated by Rdkit were filtered out. Next, parameters including molecular weight, LogP, HBA, HBD, TPSA, and rotatable bonds were calculated using Rdkit. The weighted mean of the quantitative estimates of drug-likeness (QED) (Bickerton et al., 2012) was calculated using Rdkit. The desirability functions (d) can be described as asymmetric double sigmoidal (ADS) functions and are expressed as shown in **Eq. 1**. a, b, c, d, e, and f in **Eq. 1** denote the parameters of the ADS function. QED is calculated by taking the geometric mean of the desirability functions multiplied by their weights w and can be expressed as shown in **Eq. 2**. Expanding the equation results in **Eq. 3**: This material is from our original study (Bickerton et al., 2012).

$$D(x) = a + \frac{b}{\left[1 + \exp\left(-\frac{x-c+\frac{d}{2}}{e}\right)\right]}\left[1 - \frac{1}{\left[1 + \exp\left(-\frac{x-c-\frac{d}{2}}{f}\right)\right]}\right] \quad (1)$$

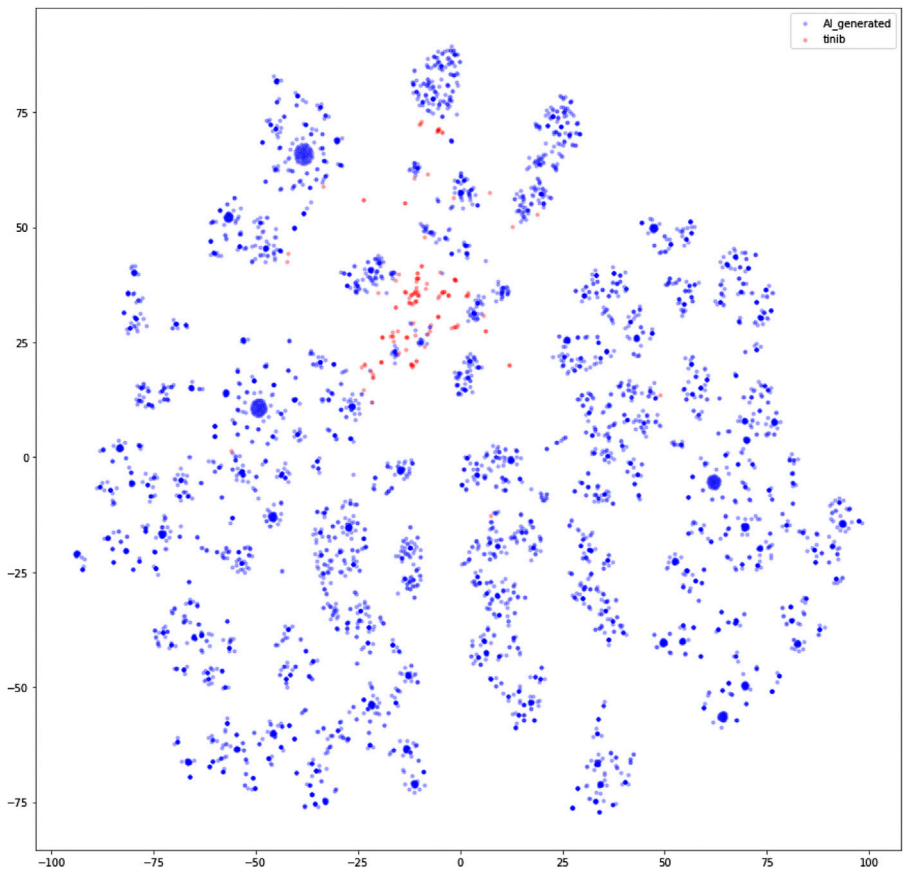

FIGURE 2 | Two-dimensional representation of '–tinib' and AI-generated ligands using t-SNE.

$$\mathrm{QED_W} = exp\left(\frac{\sum_{i=1}^{n} w_i \ln d_i}{\sum_{i=1}^{n} w_i}\right) \quad (2)$$

$$\mathrm{QED_W} = exp\left[\frac{\begin{array}{c} W_{MW}\ln d_{MW} + W_{ALOGP}\ln d_{ALOGP} + W_{HBA}\ln d_{HBA} + W_{HBD}\ln d_{HBD} \\ +W_{PSA}\ln d_{PSA} + W_{ROTB}\ln d_{ROTB} + W_{AROM}\ln d_{AROM} + W_{ALERTS}\ln d_{ALERTS} \end{array}}{W_{MW} + W_{ALOGP} + W_{HBA} + W_{HBD} + W_{PSA} + W_{ROTB} + W_{AROM} + W_{ALERTS}}\right] \quad (3)$$

The synthetic accessibility (SA) (Ertl and Schuffenhauer, 2009) score was calculated as a combination of two components using the Rdkit.

$$Sascore = fragmentScore - complexityPenalty \quad (4)$$

The following screening filters were used for the parameters: $300 \leq MW \leq 700$, $2.0 \leq LogP \leq 6.0$, $2.0 \leq HBD \leq 6.0$, $0 \leq HBA \leq 12.0$, $HBA + HBD \leq 14.0$, $60.0 \leq TPSA \leq 140.0$, and rotational bond$\leq 12.0$. All filters were applied to obtain the desirable ligands.

AI Virtual Screening

In virtual screening, DeepDTA (Öztürk et al., 2018), a convolutional neural network-based drug target affinity prediction model, was used to predict the affinity of the candidate compounds for L858R/T790M/C797S mutant EGFR (PDB code: 6LUD). The output of the model is pK_d (5), which denotes the affinity between a protein and a drug.

$$PK_d = -\log 10\left(\frac{K_d}{1e^9}\right) \quad (5)$$

pK_d was predicted using Tensorflow 2.2.0, keras 2.4.3, and NVIDIA GeForce RTX 2080 SUPER.

RESULTS

AI-Aided Drug Discovery

TL was used to compensate for the small quantity of '–tinib' data obtained from ChEMBL. The compounds generated via TL had unique structures that were similar to the '–tinib', but also exhibited the characteristics of the compounds in the training dataset. The compounds were vectorized using the Morgan Fingerprint (Cereto-Massagué et al., 2015) in Rdkit and visualized after dimensionality reduction into a two-dimensional (2D) space using t-SNE (Maaten and Hinton, 2008) in scikit-learn (**Figure 2**). In the 2D space, compounds with similar structures were clustered closer together, while structurally dissimilar compounds were farther from one another. The AI-generated compounds surrounded the '–tinib' compounds in a ring shape. While the AI-generated compounds were similar to the '–tinib' compounds based on their small distance between one another in the 2D space, they were still far enough to be considered unique, and thereby avoided patent infringement.

Parameter Filtering

Approximately 20% of 10,316 AI-generated ligand SMILES were invalid SMILES that did not meet the encoding rules and were thus removed. Following the removal, the remaining ligands were screened by filtering based on MW, LogP, TPSA, HBA, HBD,

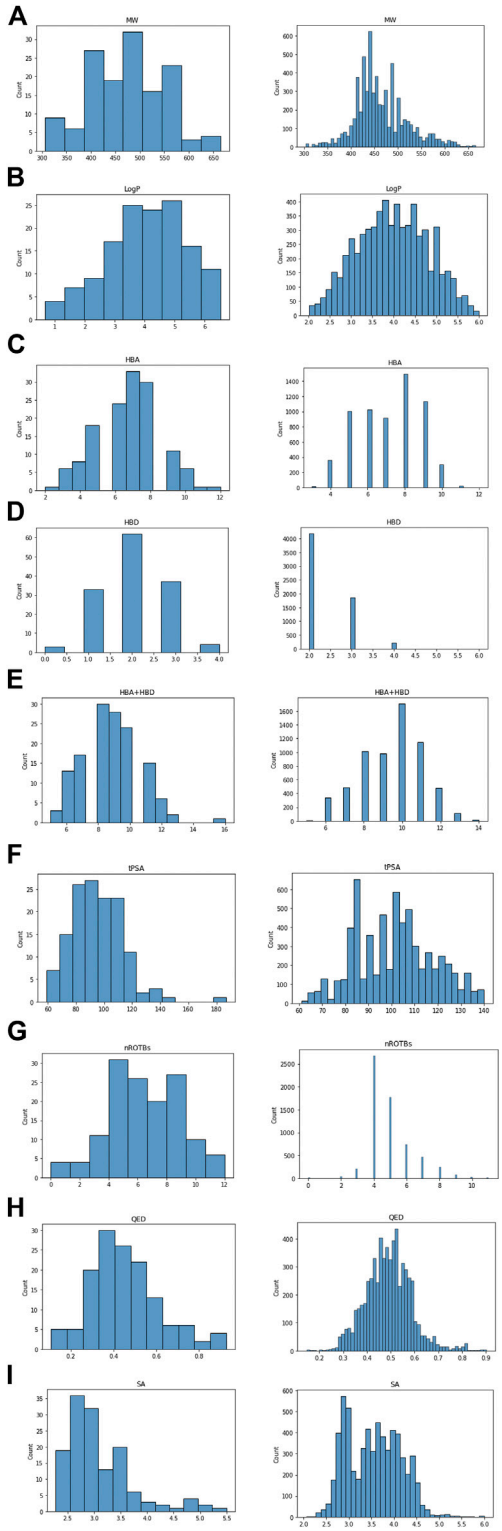

FIGURE 3 | Comparison parameter distribution of '–tinib' and 6,283 ligands made by AI. The figure shows the parameter distribution, the '–tinib' on the left and the AI generated ligands on the right. **(A)** Molecular Weight, **(B)** LogP, **(C)** HBA, **(D)** HBD, **(E)** HBA + HBD, **(F)** tPSA, **(G)** Rotatable bond, **(H)** QED, and **(I)** SA (Synthetic Accessibility) score.

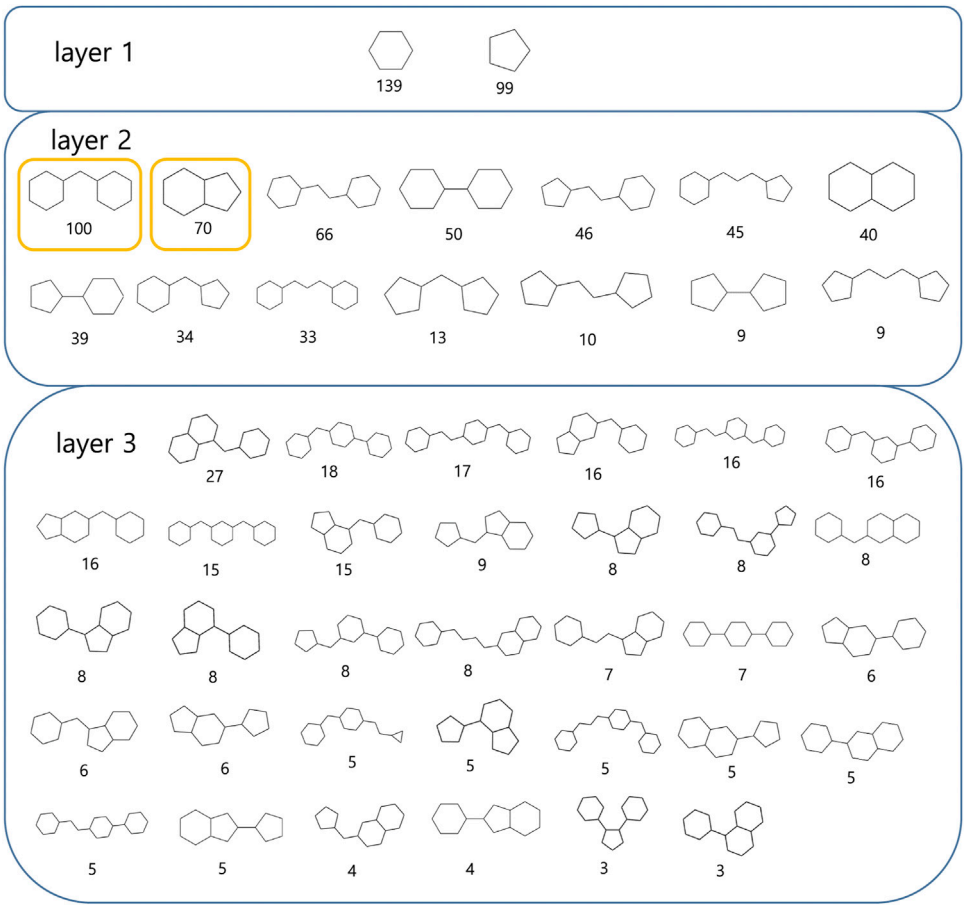

FIGURE 4 | Most frequent CSK from '-tinib'.

HBA + HBD, and rotatable bonds to ultimately remove undruggable molecules. As a result of screening using parameter filtering, we obtain 6,283 ligands out of 10,316. After that, the distributions of parameters such as MW, LogP, TPSA, HBA, HBD, HBA + HBD, rotatable bond, QED, and SA were compared between the AI-generated and '–tinib' compounds (**Figure 3**). The parameters showed highly similar distributions between the two groups of compounds. The physicochemical characteristics of the existing drugs were well-reproduced by the AI-generated compounds.

Structural Similarity Based on CSK

A scaffold is the core structure of a compound. CSK is an abstract version of a scaffold. We examined pharmaceutically meaningful structural similarities between '-tinib' by computing CSKs to select drug-like compounds. We created a hierarchical figure by placing structures with a single ring in layer 1, those with two rings in layer 2, and those with three rings in layer 3 (**Figure 4**).

Bridged-bicyclic rings and fused-bicyclic rings were the two most commonly observed types of CSK, each, with a count of 100 and 70 (marked with yellow). To assess the reproducibility of these results, we analyzed the CSKs of 6,283 molecules generated from the training dataset of 139 '–tinib' compounds using a machine learning model. The 3,308 and 2,254 ligands had bridged-bicyclic rings and fused-bicyclic rings, respectively, and thus, the results were deemed reproducible. We confirmed the structural similarities between the original and AI-generated ligand groups based on CSKs.

AI Virtual Screening

We used DeepDTA, a machine learning-based model, for fast virtual screening of druggable ligands based on their target binding affinity for L858R/T790M/C797S mutant EGFR (PDB code: 6LUD). **Figure 5** shows the affinity distribution predicted by DeepDTA. Ligands with high pK_d score were predicted to have high affinity for the L858R/T790M/C797S mutant EGFR.

Screening Ligands Based on Stringent Criterion

To extract ligands for docking simulation and non-clinical experiments, we screened ligands using stringent criterion. As a result, 360 ligands that we can calculate by docking program

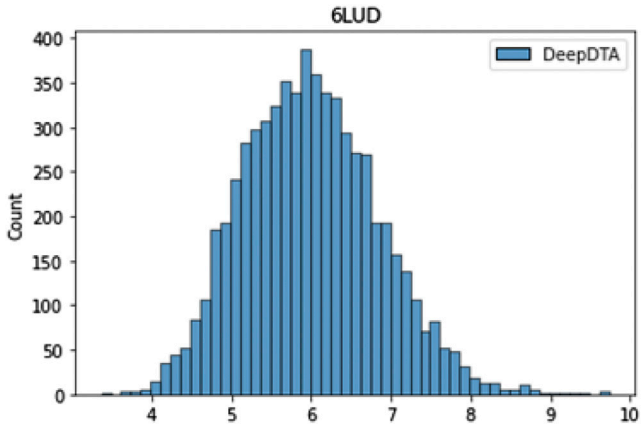

FIGURE 5 | Drug target affinity score distribution predicted by DeepDTA.

were selected. More information on 360 ligands is available at https://github.com/cgh2797/AI_drug_discovery_EGFR.

DISCUSSION

In this study, we used AI-based drug discovery to overcome the issues of high cost and low efficiency of drug research and development at present. We used AI to discover drug-like ligands resembling TKIs associated with EGFR in NSCLC and screened the candidates through the following process.

We extracted 139 ligands associated with TKIs from approximately 1.96 million compounds in ChEMBL. Next, we performed deep learning using an RNN (LSTM) to generate 10,316 SMILES associated with TKI molecules. Through parameter-filtering using in-house methods, we narrowed down the SMILES to 6,283 drug-like ligands with affinity for L858R/T790M/C797S mutant EGFR in NSCLC. To gain additional understanding of the selected ligands, we analyzed their CSKs to examine the structural similarity between the AI-generated molecules and the existing '−tinib' from ChEMBL. We used a deep learning model such as DeepDTA to predict the binding affinities of these compounds for L858R/T790M/C797S mutant EGFR. Finally, by applying stringent criterion, 360 ligands were obtained.

However, there are several limitations to this study. First, it is difficult to create only covalent ligands or determine if the ligands are covalent, when generating various ligands through AI methods. Since we based our results on Osimertinib, which is a representative covalent TKI, obtaining covalently binding ligands is also an ideal aim in this study. Thus, in a follow-up study, we will select promising compounds by determining directly based on scientific rationale whether the 360 ligands are "covalent" or "noncovalent" ligands using an in silico docking prediction method. Second, there are selectivity issues, which should be addressed even within the tyrosine kinase family. Since our research is in its early stage, our primary goal of the research is to preferentially discovery candidates as EGFR TKIs with notable efficacy (i.e., binding affinity). After identifying promising candidates, a more detailed research would be conducted to resolve the selectivity issues. Finally, another limitation of this study is that although new druggable ligands were found, experiments such as in silico docking, synthesis in the laboratory, and preclinical trials were not conducted. Hence, further studies on improving the therapeutic potential of our selected ligands, such as in silico docking prediction, synthesis in the laboratory, and preclinical trials (e.g., efficacy and safety trials), would be undertaken. Accordingly, a more detailed research would also be conducted to resolve the aforementioned tyrosine kinase selectivity issues (e.g., SAR by structural modification).

We don't put meaning to simply discover new druggable ligands similar to existing '−tinib' using AI. Since AI has infinite potential for applications in drug discovery, our goal is not only limited to drug discovery, but also includes the successful development of drugs that can receive FDA approval.

Therefore, our next task is to discover new candidates with good drug-like profiles (efficacy, toxicity, pharmacodynamics, pharmacokinetics, etc.) and identify those eligible for drug approval. We must also explore the possibility of using these compounds in combination therapy. By presenting examples of successful new drug development through these series of processes, new drug development technology using AI will become a new drug discovery paradigm.

DATA AVAILABILITY STATEMENT

The original contributions presented in the study are included in the article/Supplementary Material, further inquiries can be directed to the corresponding author.

AUTHOR CONTRIBUTIONS

GC and JO designed the study. All experiments were performed by GC. Pharmaceutical analyzes were performed by DK. GC and DK contributed to the writing of the manuscript.

REFERENCES

Bickerton, G. R., Paolini, G. V., Besnard, J., Muresan, S., and Hopkins, A. L. (2012). Quantifying the Chemical beauty of Drugs. *Nat. Chem.* 4, 90–98. doi:10.1038/nchem.1243

Bjerrum, E. J. (2017). *Smiles Enumeration as Data Augmentation for Neural Network Modeling of Molecules*. arXiv.

Cai, C., Wang, S., Xu, Y., Zhang, W., Tang, K., Ouyang, Q., et al. (2020). Transfer Learning for Drug Discovery. *J. Med. Chem.* 63, 8683–8694. doi:10.1021/acs.jmedchem.9b02147

Cereto-Massagué, A., Ojeda, M. J., Valls, C., Mulero, M., Garcia-Vallvé, S., and Pujadas, G. (2015). Molecular Fingerprint Similarity Search in Virtual Screening. *Methods* 71, 58–63. doi:10.1016/j.ymeth.2014.08.005

Chan, H. C. S., Shan, H., Dahoun, T., Vogel, H., and Yuan, S. (2019). Advancing Drug Discovery via Artificial Intelligence. *Trends Pharmacol. Sci.* 40, 592–604. doi:10.1016/j.tips.2019.06.004

Chen, H., Engkvist, O., Wang, Y., Olivecrona, M., and Blaschke, T. (2018). The Rise of Deep Learning in Drug Discovery. *Drug Discov. Today* 23, 1241–1250. doi:10.1016/j.drudis.2018.01.039

Ertl, P., and Schuffenhauer, A. (2009). Estimation of Synthetic Accessibility Score of Drug-like Molecules Based on Molecular Complexity and Fragment Contributions. *J. Cheminform.* 1, 1–11. doi:doi:10.1186/1758-2946-1-8

Gaulton, A., Bellis, L. J., Bento, A. P., Chambers, J., Davies, M., Hersey, A., et al. (2012). ChEMBL: A Large-Scale Bioactivity Database for Drug Discovery. *Nucleic Acids Res.* 40, D1100–D1107. doi:10.1093/nar/gkr777

Ghosh, A. K., Samanta, I., Mondal, A., and Liu, W. R. (2019). Covalent Inhibition in Drug Discovery. *ChemMedChem* 14, 889–906. doi:10.1002/cmdc.201900107

Gómez-Bombarelli, R., Wei, J. N., Duvenaud, D., Hernández-Lobato, J. M., Sánchez-Lengeling, B., Sheberla, D., et al. (2018). Automatic Chemical Design Using a Data-Driven Continuous Representation of Molecules. *ACS Cent. Sci.* 4, 268–276. doi:10.1021/acscentsci.7b00572

Grabe, T., Lategahn, J., and Rauh, D. (2018). C797S Resistance: The Undruggable EGFR Mutation in Non-small Cell Lung Cancer?. *ACS Med. Chem. Lett.* 9, 779–782. doi:10.1021/acsmedchemlett.8b00314

Gupta, A., Müller, A. T., Huisman, B. J. H., Fuchs, J. A., Schneider, P., and Schneider, G. (2018). Generative Recurrent Networks for De Novo Drug Design. *Mol. Inf.* 37, 1700111. doi:10.1002/minf.201700111

Jett, J. R., and Carr, L. L. (2013). Targeted Therapy for Non-small Cell Lung Cancer. *Am. J. Respir. Crit. Care Med.* 188, 907–912. doi:10.1164/rccm.201301-0189PP

Jiao, Q., Bi, L., Ren, Y., Song, S., Wang, Q., and Wangshan, Y.-s. (2018). Advances in Studies of Tyrosine Kinase Inhibitors and Their Acquired Resistance. *Mol. Cancer* 17, 1–12. doi:10.1186/s12943-018-0801-5

Kadurin, A., Nikolenko, S., Khrabrov, K., Aliper, A., and Zhavoronkov, A. (2017). DruGAN: An Advanced Generative Adversarial Autoencoder Model for De Novo Generation of New Molecules with Desired Molecular Properties In Silico. *Mol. Pharmaceutics* 14, 3098–3104. doi:10.1021/acs.molpharmaceut.7b00346

Klaeger, S., Heinzlmeir, S., Wilhelm, M., Polzer, H., Vick, B., Koenig, P.-A., et al. (2017). The Target Landscape of Clinical Kinase Drugs. *Science* 358, eaan4368. doi:10.1126/science.aan4368

Le, T., and Gerber, D. (2019). Newer-generation EGFR Inhibitors in Lung Cancer: How Are They Best Used? *Cancers* 11(3), 366. doi:10.3390/cancers11030366

Lecun, Y., Bengio, Y., and Hinton, G. (2015). Deep Learning. *Nature* 521, 436–444. doi:10.1038/nature14539

Leonetti, A., Sharma, S., Minari, R., Perego, P., Giovannetti, E., and Tiseo, M. (2019). Resistance Mechanisms to Osimertinib in EGFR-Mutated Non-small Cell Lung Cancer. *Br. J. Cancer* 121, 725–737. doi:10.1038/s41416-019-0573-8

Li, Q., Zhang, T., Li, S., Tong, L., Li, J., Su, Z., et al. (2019). Discovery of Potent and Noncovalent Reversible EGFR Kinase Inhibitors of EGFRL858R/T790M/C797S. *ACS Med. Chem. Lett.* 10, 869–873. doi:10.1021/acsmedchemlett.8b00564

Li, X., Xu, Y., Yao, H., and Lin, K. (2020). Chemical Space Exploration Based on Recurrent Neural Networks: Applications in Discovering Kinase Inhibitors. *J. Cheminform.* 12, 1–13. doi:10.1186/s13321-020-00446-3

Liu, Q., Yu, S., Zhao, W., Qin, S., Chu, Q., and Wu, K. (2018). EGFR-TKIs Resistance via EGFR-independent Signaling Pathways. *Mol. Cancer* 17, 1–9. doi:10.1186/s12943-018-0793-1

Maaten, L., and Hinton, G. (2008). Visualizing Data Using T-SNE. *J. Mach. Learn. Res.* 9, 2579–2605.

Mak, K.-K., and Pichika, M. R. (2019). Artificial Intelligence in Drug Development: Present Status and Future Prospects. *Drug Discov. Today* 24, 773–780. doi:10.1016/j.drudis.2018.11.014

Moret, M., Friedrich, L., Grisoni, F., Merk, D., and Schneider, G. (2020). Generative Molecular Design in Low Data Regimes. *Nat. Mach. Intell.* 2, 171–180. doi:10.1038/s42256-020-0160-y

Nassif, A. B., Shahin, I., Attili, I., Azzeh, M., and Shaalan, K. (2019). Speech Recognition Using Deep Neural Networks: A Systematic Review. *IEEE Access* 7, 19143–19165. doi:10.1109/ACCESS.2019.2896880

Öztürk, H., Özgür, A., and Ozkirimli, E. (2018). DeepDTA: Deep Drug-Target Binding Affinity Prediction. *Bioinformatics* 34, i821–i829. doi:10.1093/bioinformatics/bty593

Popova, M., Isayev, O., and Tropsha, A. (2018). Deep Reinforcement Learning for De Novo Drug Design. *Sci. Adv.* 4, eaap7885–15. doi:10.1126/sciadv.aap7885

Scannell, J. W., Blanckley, A., Boldon, H., and Warrington, B. (2012). Diagnosing the Decline in Pharmaceutical R&D Efficiency. *Nat. Rev. Drug Discov.* 11, 191–200. doi:10.1038/nrd3681

Schuhmacher, A., Gassmann, O., and Hinder, M. (2016). Changing R&D Models in Research-Based Pharmaceutical Companies. *J. Transl. Med.* 14, 1–11. doi:10.1186/s12967-016-0838-4

Segler, M. H. S., Kogej, T., Tyrchan, C., and Waller, M. P. (2018). Generating Focused Molecule Libraries for Drug Discovery with Recurrent Neural Networks. *ACS Cent. Sci.* 4, 120–131. doi:10.1021/acscentsci.7b00512

Siegel, R. L., Miller, K. D., Fuchs, H. E., and Jemal, A. (2021). Cancer Statistics, 2021. *CA A. Cancer J. Clin.* 71, 7–33. doi:10.3322/caac.21654

Sung, H., Ferlay, J., Siegel, R. L., Laversanne, M., Soerjomataram, I., Jemal, A., et al. (2021). Global Cancer Statistics 2020: GLOBOCAN Estimates of Incidence and Mortality Worldwide for 36 Cancers in 185 Countries. *CA A. Cancer J. Clin.* 71, 209–249. doi:10.3322/caac.21660

Voulodimos, A., Doulamis, N., Doulamis, A., and Protopapadakis, E. (2018). Deep Learning for Computer Vision: A Brief Review. *Comput. Intelligence Neurosci.* 2018, 1–13. doi:10.1155/2018/7068349

Xu, Y.-J., and Johnson, M. (2002). Using Molecular Equivalence Numbers to Visually Explore Structural Features that Distinguish Chemical Libraries. *J. Chem. Inf. Comput. Sci.* 42, 912–926. doi:10.1021/ci025535l

Young, T., Hazarika, D., Poria, S., and Cambria, E. (2018). Recent Trends in Deep Learning Based Natural Language Processing [Review Article]. *IEEE Comput. Intell. Mag.* 13, 55–75. doi:10.1109/MCI.2018.2840738

Yuan, M., Huang, L.-L., Chen, J.-H., Wu, J., and Xu, Q. (2019). The Emerging Treatment Landscape of Targeted Therapy in Non-small-cell Lung Cancer. *Sig Transduct Target. Ther.* 4. doi:10.1038/s41392-019-0099-9

Zhai, X., Ward, R. A., Doig, P., and Argyrou, A. (2020). Insight into the Therapeutic Selectivity of the Irreversible EGFR Tyrosine Kinase Inhibitor Osimertinib through Enzyme Kinetic Studies. *Biochemistry* 59, 1428–1441. doi:10.1021/acs.biochem.0c00104

Conflict of Interest: Authors GC, DK and JO were employed by AllLive Healthcare Co., Ltd.

Publisher's Note: All claims expressed in this article are solely those of the authors and do not necessarily represent those of their affiliated organizations, or those of the publisher, the editors and the reviewers. Any product that may be evaluated in this article, or claim that may be made by its manufacturer, is not guaranteed or endorsed by the publisher.

Copyright © 2021 Choi, Kim and Oh. This is an open-access article distributed under the terms of the Creative Commons Attribution License (CC BY). The use, distribution or reproduction in other forums is permitted, provided the original author(s) and the copyright owner(s) are credited and that the original publication in this journal is cited, in accordance with accepted academic practice. No use, distribution or reproduction is permitted which does not comply with these terms.

frontiers in Oncology

SYSTEMATIC REVIEW
published: 06 August 2021
doi: 10.3389/fonc.2021.702216

Hepatoid Adenocarcinoma of the Lung: A Systematic Review of the Literature From 1981 to 2020

Zan Hou[1,2†], Jiaqing Xie[3†], Li Zhang[4], Gangyi Dai[1], Yuanhang Chen[1] and Lang He[1]*

[1] Department of Oncology, The Affiliated Fifth People's Hospital of Chengdu University of TCM, Chengdu Fifth People's Hospital, Chengdu, China, [2] Department of Radiation Oncology, State Key Laboratory of Oncology in South China, Collaborative Innovation Center for Cancer Medicine, Sun Yat-Sen University Cancer Center, Guangzhou, China, [3] Department of Clinical Laboratory, The Affiliated Fifth People's Hospital of Chengdu University of TCM, Chengdu Fifth People's Hospital, Chengdu, China, [4] Department of Pathology, The Affiliated Fifth People's Hospital of Chengdu University of TCM, Chengdu Fifth People's Hospital, Chengdu, China

OPEN ACCESS

Edited by:
Junji Uchino,
Kyoto Prefectural University of Medicine, Japan

Reviewed by:
Federica Pezzuto,
University of Padua, Italy
Janaki Deepak,
University of Maryland, Baltimore, United States

***Correspondence:**
Lang He
helang126@outlook.com

[†]These authors have contributed equally to this work

Specialty section:
This article was submitted to Thoracic Oncology, a section of the journal Frontiers in Oncology

Received: 29 April 2021
Accepted: 20 July 2021
Published: 06 August 2021

Citation:
Hou Z, Xie J, Zhang L, Dai G, Chen Y and He L (2021) Hepatoid Adenocarcinoma of the Lung: A Systematic Review of the Literature From 1981 to 2020. Front. Oncol. 11:702216. doi: 10.3389/fonc.2021.702216

Objectives: We report the first case of hepatoid adenocarcinoma of the lung (HAL) with PIK3CA mutation. In addition, we analyzed data from HAL cases over the past 40 years to study its main treatment methods, prognosis, and the relationship between prognosis and the serum alpha-fetoprotein (AFP) level before treatment.

Methods: We report a 66-year-old male case who was diagnosed with locally advanced HAL with PIK3CA mutation and carried out a systematic literature search for HAL cases documented between 1981 and 2020. General patient information including case characteristics was extracted and summarized. The median OS (mOS) of HAL patients was determined using the KM survival curve. The Cox proportional hazards regression model was used to evaluate the effect of tumor size, location, and serum AFP value before treatment and radical surgery (RS) on the prognosis of patients.

Results: A total of 46 studies including 51 HAL patients was included in our review. Our study revealed that 52.9% of tumors were located in the upper lobe of the right lung. The proportion of serum AFP-positive patients before treatment, early-stage patients (TNM stage I and II), and patients who had received surgery were 69.2%, 34.1%, and 40%, respectively. The mOS of HAL patients was 16.0 months. The 2-year and 5-year survival rates of the patients were 35.3% and 8.0%, respectively. In the subgroup analysis, the 2-year survival rate for patients who received RS was 62.5%, while for patients who were unable to undergo RS, it was only 12.5% (p = 0.009). The Cox proportional hazards regression model indicated that RS can significantly improve the prognosis of HAL patients (p = 0.011), although the location and size of tumor as well as the serum AFP value before treatment had no significant effect on their prognosis (p = 0.82, p = 0.96, p = 0.25).

Conclusions: HAL patients have a poor prognosis, and the survival benefits for patients receiving chemoradiotherapy or chemotherapy alone appear to be limited. We demonstrate

statistically for the first time that pretreatment serum AFP values are not related to the prognosis of HAL patients and RS can significantly improve patient prognosis.

Keywords: hepatoid adenocarcinoma of the lung, clinical features, treatment, prognosis, case report, systematic review

INTRODUCTION

Hepatoid adenocarcinoma of the lung (HAL) is an extremely rare type of primary lung adenocarcinoma that shares similarities with hepatocellular carcinoma (1). HAL has been shown to produce some products of normal hepatocytes or hepatocellular carcinoma, such as ferritin and alpha-fetoprotein (AFP) (2). However, with the exception of its low incidence and poor prognosis, very little about is known about HAL. The first case of HAL was reported in 1981 by Yasunami et al. (3), while Grossman et al. (4) comprehensively summarized the clinical characteristics of HAL patients documented before 2016. Although this study described the clinical characteristics of 28 HAL patients, the overall survival (OS) data and factors affecting patient prognosis were not examined. More recently, Tonyali et al. (5) carried out a literature review of HAL in 2020, but this study only reviewed the clinical characteristics of 21 patients with HAL and therefore did not include all the documented cases.

By December 2020, although an increasing number of HAL cases had been reported, a summary analysis of all cases reported over the past 40 years had not been carried out. To date, the epidemiology, molecular pathology, effective treatment methods, and factors affecting the prognosis of HAL patients remain unclear. Therefore, in addition to reporting a HAL case with PIK3CA mutation, we have summarized and analyzed all the HAL cases reported in the literature between 1981 and 2020.

MATERIALS AND METHODS

Study Design

The relationship between serum AFP value and prognosis of HAL patients remains unclear. Previous studies have suggested that the serum AFP value before treatment is related to the prognosis of HAL patients, with an initial high AFP level associated with a shorter OS time (6, 7). Since these findings are consistent with our case study, we conducted a systematic review of the literature in order to clarify the relationship between these two factors. We searched multiple databases for papers containing HAL patients that had been published in English between 1981 and 2020. Appropriate papers were screened out through strict inclusion and exclusion criteria. Finally, we were able to determine whether the serum AFP level before treatment significantly affected the prognosis of HAL patients by extracting useful data and conducting appropriate statistical analyses. We also briefly describe the epidemiology and overall prognosis of these patients. The study design is outlined below.

Search Strategy

This study was conducted on the basis of the preferred reporting items for systematic reviews and meta-analysis (PRISMA) statement (8). A comprehensive literature search was conducted on papers published between 1981 and December 31, 2020. The Ovid MEDLINE, Ovid Embase, and Science Citation Index (Web of Science) were searched by two independent reviewers (Zan Hou and Jiaqing Xie) for eligible studies. The overall search strategy was (1) hepatoid (All Fields), (2) adenocarcinoma (All Fields), and (3) lung (All Fields). Searches in electronic databases combined the terms 1, 2, and 3.

Study Selection Criteria

The eligibility of the studies was assessed by two independent reviewers (Zan Hou and Jiaqing Xie) who read titles, abstracts, and full texts. After a systematic screening, the following cases were excluded: (i) the case was not pathologically confirmed as HAL, (ii) the case was not diagnosed as primary HAL, and (iii) the literature did not contain the full text.

Data Extraction

The following data were independently extracted from the included cases by two reviewers (Zan Hou and Jiaqing Xie): (1) Basic information such as year of publication, author's name, patient's gender, and age. (2) Case features including the location and size of the tumor, the serum AFP value before treatment, TNM staging, and gene status. (3) Treatment and prognosis data including the treatment method, whether adequate treatment was conducted, and prognosis. Inadequate treatment referred to patients who refused any or part of the treatment mentioned in the paper. OS was defined from the baseline to death from any cause or last follow-up.

Statistical Analysis

General characteristics of all patients, including the average age, proportion of serum AFP-positive cases, and proportion of surgical treatment were summarized. The average value of continuous variables was expressed by mean ± standard deviation. KM survival curves were generated for all patients with survival data to evaluate the median OS (mOS) of all HAL patients with OS data. Survival rates were compared using the chi-square test. The size and location of tumor, serum AFP value before treatment, whether or not surgery was performed, and OS data of the patients were analyzed using the Cox proportional hazards regression model to determine whether these four indicators had a significant impact on the prognosis of the patients.

The OS data of patients who received inadequate treatment were excluded in any statistical analyses that included OS data. The size of tumor was expressed by its longest diameter. The serum AFP value of all patients with normal serum AFP before treatment was quantified as 7 ng/ml for statistical analysis. Radical surgery (RS) referred to lobectomy of primary lesion plus lymph node dissection. Cases were excluded for RS analysis that did not specify the surgical method, or when the patient underwent lobectomy alone or palliative surgical treatments.

RESULTS

After the selection procedure (**Figure 1**), 46 papers were considered eligible for our systematic review. The data of these cases are listed in **Table 1**. The total number of patients included in this study was 51.

Case Presentation

A 66-year-old Chinese male was admitted to hospital in April 2019 for cough and expectoration that had been accompanied by one incidence of hemoptysis. The enhanced CT scan (**Figures 2A, B**) identified a soft-tissue mass (3.3 × 2.5 × 4.0 cm) in the upper lobe of the right lung. The mass was considered to be lung cancer with subcarinal lymph node metastasis. However, no obvious abnormalities were found in the liver, stomach, and testes, and no tumor metastases were found on the enhanced MRI of the brain and centrum. A puncture biopsy of the lung tissue indicated non-small cell carcinoma and its morphology supported adenocarcinoma. Endobronchial ultrasound (E-BUS) lymph node examination was carried out in a different hospital and showed poorly differentiated carcinoma. Immunohistochemical analysis revealed that the mass was AFP (+) and hepatocyte (–). The patient's liver function, viral hepatitis index, and immunological examination were normal, while the serum AFP value before treatment was 22,323 ng/ml (normal value: 0.0–8.0 ng/ml).

Next-generation sequencing (NGS) and programmed cell death-1 (PD-L1) testing in lung cancer tissues revealed that the EGFR, ALK, ROS-1, BRAF, MET, KRAS, HER2, AKT1, c-KIT, and RET genes were wild type, while the NRAS and PIK3CA genes were mutated. PD-L1 testing was negative.

The patient's personal history indicated that the patient had a smoking index of 800, and denied any history of drinking. There was nothing special about his past medical history or family history. Combined with the above examinations, the patient's diagnosis was adenocarcinoma of the right upper lobe cT2N2MO IIIA and he had no surgical indication. In May 2019, the patient received concurrent chemoradiotherapy (chemotherapy regimen: pemetrexed plus cisplatin), and the efficacy of the patient was evaluated as stable disease (SD). After two cycles of the original chemotherapy regimen, the patient's efficacy was evaluated as progressive disease (PD). The patient later received two cycles of treatment with arotinib and his efficacy was also evaluated as PD. In April 2020, full-body enhanced CT examination revealed enlarged lung masses and increased mediastinal lymph nodes (**Figures 2C, D**), with intracranial and pyramidal metastases, and no obvious abnormalities in other sites. The serum AFP value

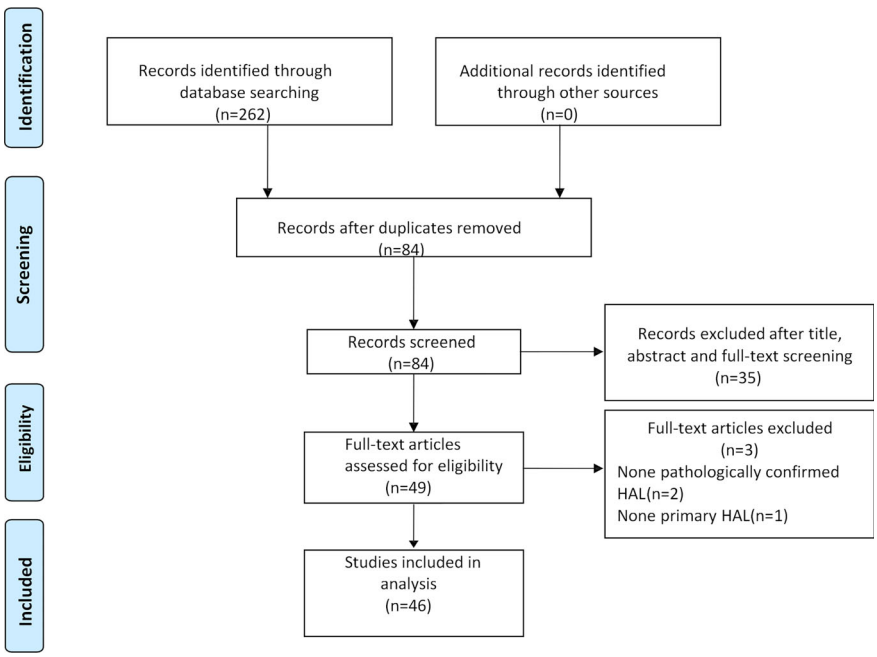

FIGURE 1 | Paper selection flowchart.

TABLE 1 | The clinical data of 51 cases.

Year	Author	Gender-Age (years)	Smoke	Location	Size (cm)	Serum AFP value before treatment (ng/ml)	TNM Stage	KI-67 and Gene mutation detection: Yes/No, Specific mutant gene	Treatment method	Complete treatment: Yes/No	Prognosis
1981	Yasunami (3)	Male-67	NM	Left upper lobe	8	19000	cT3N2Mx	NM	RT	Yes	16 months (dead)
1987	Miyake (9)	Male-73	NM	Left upper lobe	5×6×5	1039	NM	NM	RS+RT	Yes	18 months (dead)
1988	Saka (10)	Male-73	NM	Right upper lobe	3.9×3×3	289	pT2N0M0	NM	RS	Yes	28 months (alive)
1992	Okunaka (11)	Male-49	NM	Right upper lobe	6×5×5	9300	cT3NxMx	NM	RS	Yes	11 months (alive)
1997	Nasu (12)	Male-63	NM	Right upper lobe	14×13 ×12	14,000	cT4N2	NM	Chemo	Yes	11 months (dead)
1997	Arnould (13)	Male-36	Yes	Left upper lobe	11	6090	pT4N2	NM	Chemo	Yes	7 months (dead)
2000	Carlinfante (14)	Male-82	Yes	Left lower lobe	3.5	NM	cT2aN0M0	NM	Surgery (specific unknown)	Yes	84 months (alive)
2002	Hayashi (15)	Male-55	Yes	Right upper lobe	5×4.8×6.5	NM	pT2bN0M0	NM	RS	Yes	32 months (alive)
2002	Hiroshima (16)	Male-71	Yse	Right lower lobe	10.5×8.5×7	7417	pT3N1M0	NM	RS	Yes	12 months (dead)
2003	Iino (17)	Male-63	NM	Right upper lobe	2.8×2.5	NM	pT1N0M0	NM	RS	Yes	5 months (alive)
2003	Terracciano (18)	Male-49	NM	Left lower lobe	5	203,320	pT2bNxM1	NM	Pulmonary lobectomy	Yes	2 months (dead)
2007	Ivan (19)	Male-54	Yes	Left upper lobe	13×11	14540	cT4N3M1	NM	Chemo+brain RT	Yes	NM
2007	Wu (20)	Male-50	Yes	Right upper lobe	6×5×5	Normal	cT2N1M0	NM	RS	Yes	45 months (alive)
2008	Kishimoto (21)	Male-64	NM	Left lower lobe	7.5×7×4	673	cT3N0M0	NM	Surgery (Specific unknown)	Yes	NM
2010	Fornasa (22)	Female-68	No	Left upper lobe	4.5×4×4	Normal	pT2b	NM	Chemo	Yes	15 months (alive)
2012	Khozin (23)	Female-56	Yes	Right anterior cardiophrenic angel; Right middle lobe	5.5; 1.8	Normal	cT4	YES,ALK +	Crizotinib	Yes	6months (dead)
2012	Valentino (24)	Male-71	No	Right lower lobe	1.8×1.5×1.5	1201	pT1N0M1	NM	①RS; ②Chemo+RT	Yes	8months (dead)
2012	Mokrim (25)	Male-52	Yes	Left upper lobe	11.8×12×8	5000	cT4N0M1	NM	Chemo	Yes	5months (dead)
2012	Papatsimpas (6)	Male-48	NM	Right upper lobe	20×11×8	39000	cT4	NM	①Chemo +bevacizumab; ②Erlotinib and palliative RT	Yes	6months (dead)
2013	Cavalcante (26)	Male-66	Yes	Right upper lobe	NM	Normal	cT4NxM1	NM	No treatment	NO	0.5month (dead)
2013	Lin (27)	Male-66	Yes	Right upper lobe	7.3×5.6× 3.3	8686	pT3N0M0	NM	RS	Yes	48 months (alive)
2014	Che (28)	Male-48	Yes	Left upper lobe	7.9×10	6283	pT4N1M0	NM	Chemoradiation	Yes	21 months (dead)
2014	Haninger (29)	Male-51	Yes	Right upper lobe	4.2×3.7	NM	cT2aN3M0	Ki-67 30%NM	Chemoradiation	Yes	14 months (dead)
		Male-52	Yes	Right upper lobe	2.5	NM	cT1bN0M1	Ki-67 10% NM	RS+ Chemoradiation	Yes	37 months (alive)
		Male-64	Yes	Left upper lobe	3.2×2.2	NM	cT2aN0M1	Ki-67 50%; Yes, None	Palliative surgery+ chemoradiation	Yes	10 months (dead)
		Female-54	Yes	Left upper lobe	1	NM	cT1aN0M1	Ki-67 10%	Chemoradiation	Yes	108 months (alive)
		Male-60	Yes	Right upper lobe	11.2×10.1×8.5	4410	cT3N2M1	Ki-67 10%	Chemoradiation	Yes	1 month (alive)
2014	Shaib (30)	Female-53	Yes	Right upper lobe	9.5×9.0×8.0	37,810	pT3N0M0	NM	RS+ Chemo	Yes	48 months (alive)
2015	Gavrancic (31)	Male-64		Right upper lobe	3.8×2.9	181	cT2N2M1	Yes, None	Chemo, Sorafenib, RT	Yes	11 months (dead)
2016	Motooka (32)	Male-69	Yes	Left segments 1 + 2	4.3	4497	cT2aN0M0	Yes, None	RS+ Chemo	Yes	51 months (alive)
2016	Qian (33)	Male-79	Yes	Right parahilar	2.7×2.6	NM	cT1cN0M0	NM	Erlotinib	Yes	NM
2016	Sun (34)	Male-59	Yes	Right upper lobe	4.5×3.8×3.5	Normal	pT2aN0M0	KI-67 20%	RS	Yes	23 months (alive)
2016	Wang (35)	Malr-56	Yes	Right upper lobe	4.0×4.1× 4.8	NM	cT2N1M0	NM	NM	NM	NM
2016	Grossman (4)	Male-54	Yes	Right upper lobe	5×4	Normal	M1 IV	Yes, None	Chemo	Yes	3 months (dead)

(Continued)

TABLE 1 | Continued

Year	Author	Gender-Age (years)	Smoke	Location	Size (cm)	Serum AFP value before treatment (ng/ml)	TNM Stage	KI-67 and Gene mutation detection: Yes/No, Specific mutant gene	Treatment method	Complete treatment: Yes/No	Prognosis
2017	Valle (36)	Male-61	NM	Left lung	NM	Normal	M1 IV	NM	①Chemo; ②RT	Yes	55months (dead)
2018	Li (37)	Male-52	Yes	Right upper lobe	NM	Normal	IVb	KI-67 60%; Yes, None;	Chemo	Yes	2 months (dead)
2018	Basse (38)	Male-43	Yes	Right lung		NM	IV	Yes, None; PD-L1-,dMMR;	①Chemo; ②Chemo; ③Durvalumab	Yes	NM
2019	Ayub (39)	Male-61	Yes	Right upper lobe	2.3	Normal	pT1bN0M0	NM	RS+RT	Yes	6 months (dead)
2019	Chen (40)	Male-53	No	Right upper lobe	5.3×3.5	3296	CT3N0M0	KI 67 20% Yes, EGFR T790M +	①RS+chemo; ②icotinib; ③osimertinib	Yes	29 months (alive)
2019	Kuan (41)	Male-47	Yes	Right upper lobe	14	Normal	cT4NxM0	Yes, None; PD-L1high-level staining.	Pulmonary lobectomy	Yes	4 months (dead)
2019	Li (7)	Male-71	No	Right lower lobe	7×4.5	79480	cT4N3M1	KI-67 80%; Yes, FAT +; *PD-L1*-, MSS;	Radio-Frequency Ablation+Anlotinib	Yes	4 months (dead)
2019	Shi (42)	Male-60	Yes	Right upper lobe	7.5×7.2	1210	pT3N0M0	KI-67 50%	RS+chemo	Yes	15 months (dead)
2019	Wang (43)	Male-70	Yes	Right upper lobe	6.0×4.6	Normal	IV	*Yes*, TP53 +	①Erlotinib; ②Chemo +bevacizumab	Yes	9 months (dead)
2019	Yang (44)	Male-70	Yes	Left lower lobe	6.4×5.5	Normal	pT3N1M0	Ki67 30%; Yes, None;	RS refused further chemotherapy	NO	18 months (dead)
2020	Chen (45)	Female-65	No	Bilateral lung	NM	6818	IV	Yes, K-RAS+; PD-L1≥1%, MSS;	①Chemo; ②Anlotinib; ③Sintilimab	Yes	53 months (dead)
2020	Chen (46)	Male-63	Yes	Left lung	NM	NM	IV	NM	Palliative surgery	Yes	4 months (dead)
2020	Tonyali (5)	Female-62	Yes	Left upper lobe	6	NM	cT4N1M0	Yes, None;	①Chemoradiation; ②Nivolumab	Yes	14 months (dead)
2020	Nargund (47)	Male-66	Yes	Left lower lobe	7.6×7.5×7.5	394	cT3N2M0	NM	Chemo	Yes	NM
		Male-65	Yes	Right upper lobe	6.5×4.5×6.6	993	cT2bN2M0	NM	Chemo	Yes	NM
2020	Wang (48)	Male-41	NM	Right upper lobe	5.2×5.8	Normal	cT3N3M0, IIIC	KI 67 60%; Yes, None;	RT	No	12 months (dead)
Current Case	Hou	Male-66	Yes	Right upper lobe	3.3×2.5×4.0	22323	cT2N2MO, IIIA	KI 67 60%; Yes, NRAS+, PIK3CA+; PD-L1-	①Chemoradiation; ②Anlotinib; ③Sorafenib +Sintilimab	Yes	13 months (dead)

RT, radiotherapy; Chemo, chemotherapy; RS, radical surgery; NM, not mentioned; ①, first-line therapy; ②, second-line therapy; ③, third-line therapy; None, the driver genes detected in the literature were wild-type.

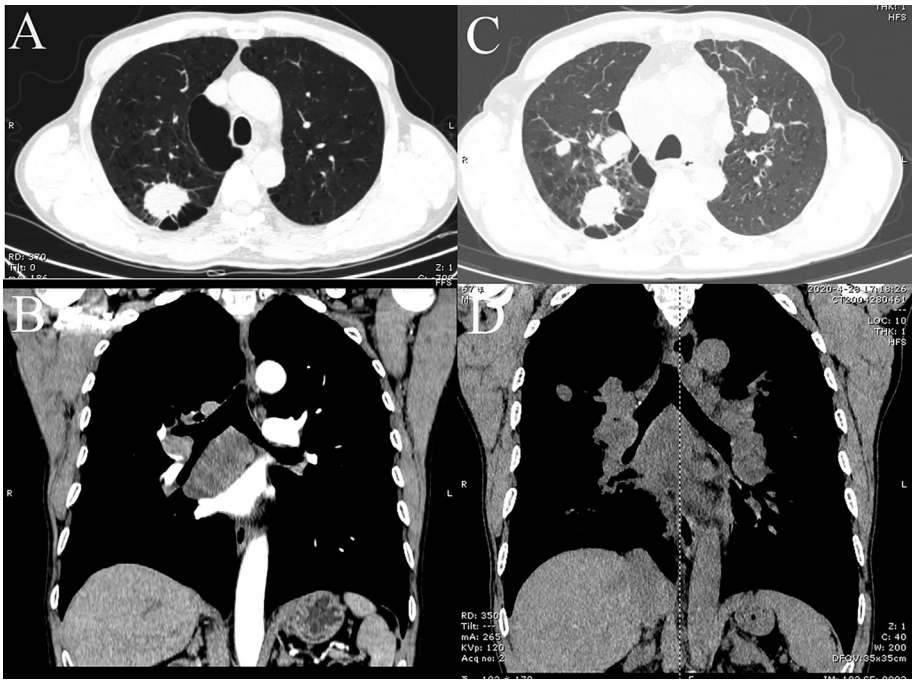

FIGURE 2 | CT images of lung tumor and mediastinal lymph nodes of patient. **(A, B)** Baseline inspection on April 18, 2019, showed right upper lobe tumor and subcarinal lymph node metastasis, respectively. **(C, D)** Images on April 6, 2020, suggested multiple pulmonary metastases and multiple mediastinal lymph node metastases, respectively.

was re-examined and found to be 10,075.99 ng/ml. A puncture biopsy of the cervical lymph node was performed and histological examination revealed an adenocarcinoma with hepatoid differentiation (**Figures 3A, B**). Immunohistochemical stains were positive for CK7, CK8/18, GPC-3, and ki67 (60%), and negative for arg-1, TTF-1, NapsinA, CD20, CDX2, P40, and PSA (**Figures 3C–F**). Thus, the diagnosis of stage cT4N3M1 HAL was made. The patient refused to undergo further genetic and PD-L1 tests. From April 10, 2020, the patient was treated with one cycle of sorafenib and sindilimab, and palliative radiotherapy was given to metastatic bone tumors. On April 28, 2020, the patient was admitted to hospital and his therapeutic effect was evaluated as PD by systemic re-examination. The patient's condition worsened and he died in May 2020. The patient's OS was 13 months after initial diagnosis.

Case Features

The clinical characteristics of 51 cases are listed in **Table 2**. The average age of the patients was 59.9 ± 17.0 years old. There were 45 male cases, accounting for 88.2% of patients, and the percentage of smokers accounted for 87.2%. The average size of the primary tumor was 6.7 ± 1.5 cm. The tumors were located in the upper lobe of the right lung in 52.9% of cases. The proportion of serum AFP-positive patients before treatment, early-stage patients (TNM stage I and II), and patients who had received RS treatment were 69.2%, 34.1%, and 40%, respectively. Only a few HAL patients were reported as having a driver gene mutation and positive PD-L1.

Survival Curve

A total of 42 patients were included in the OS analysis (**Figure 4**). The mOS of these patients was 16.0 months. The 2-year and 5-year survival rates of the patients were 35.3% and 8.0%, respectively. In the subgroup analysis, the 2-year survival rate for patients who received RS was 62.5%, while patients who did not undergo RS had a 2-year survival rate of only 12.5% (p = 0.009).

Cox Proportional Hazards Regression Analysis

The Cox proportional hazards regression analysis was composed of 30 patients who had tumor size, location of tumor, serum AFP level before treatment, specific treatment methods, and survival data (**Table 3**). RS was shown to significantly improve the prognosis of HAL patients (HR 0.23; 95% CI: 0.075–0.71; p = 0.011). Compared with the right upper lobe group, there were no significant differences in the prognosis of the non-right upper lobe group (HR 0.89; 95% CI: 0.33–2.41; p = 0.82). The tumor size and serum AFP value before treatment also had no significant effect on the prognosis (HR 1.00, 95% CI: 0.86–1.20, p = 0.96; HR 1.00, 95% CI: 1.00–1.00, p = 0.25).

DISCUSSION

Extrahepatic hepatoid adenocarcinoma can occur in gastric (63%), ovarian (10%), lung (5%), and uterine (4%) cancers (1).

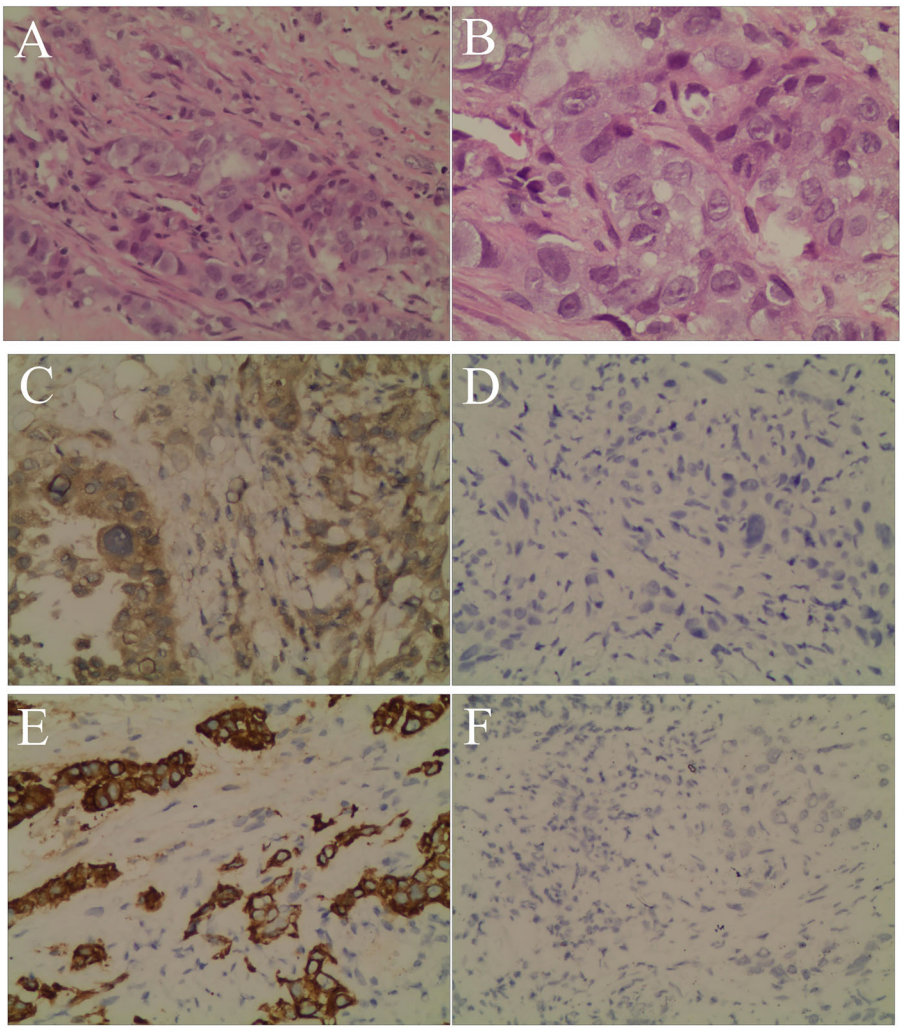

FIGURE 3 | Hematoxylin and eosin staining and immunohistochemistry. **(A)** Neoplastic cells arranged in an alveolar pattern and the glandular lumen can be seen in the lesion area (magnification, ×200). **(B)** Neoplastic cells with prominent and hyperchromatic nucleoli, nuclear pleomorphism, and abundant eosinophilic cytoplasm, consistent with an adenocarcinoma with hepatoid differentiation (magnification, ×400). **(C)** The tumor cells were positive for GPC-3 (magnification, ×200). **(D)** The tumor cells were negative for hepatocyte (magnification, ×200). **(E)** The tumor cells were positive for CK7 (magnification, ×200). **(F)** The tumor cells were negative for TTF-1 (magnification, ×200).

Okunaka et al. (11) defined HAL as lung adenocarcinoma with hepatoid differentiation or features of hepatocellular carcinoma and a positive serum AFP value. However, some studies have found that serum AFP levels can also be normal in HAL patients. Thus, the most recent definition of HAL is lung adenocarcinoma with hepatoid differentiation or features of hepatocellular carcinoma, with or without positive serum AFP values (34). The pathological H&E staining of our case shows large tumor cells, prominent and hyperchromatic nucleoli, nuclear pleomorphism, and abundant eosinophilic cytoplasm, consistent with adenocarcinomas with hepatoid differentiation. The cancer cells may be arranged in solid sheet nests or an alveolar pattern, and glandular lumen structures may be observed in the lesion area. Immunohistochemical analysis of HAL includes AFP, CK7, hepatocyte, GPC-3, and arg-1 staining, which may be partially or wholly positive. Primary HAL is mainly differentiated from primary pulmonary adenocarcinoma, lung metastases of hepatocellular carcinoma, lung metastases of hepatoid adenocarcinoma from other sites (such as the stomach, ovary, and uterus), and germ cell tumors, which can also cause an increase in AFP. Although the diagnosis of HAL relies on morphology, we hold that imagological examination and immunohistochemical analysis, including AFP, CK7, hepatocyte, GPC-3, TTF-1, arg-1, and CDX2 staining, are still important for the diagnosis and differential diagnosis of HAL based on our case study and other studies (48). The mechanism of AFP expression in this type of adenocarcinoma may be related to the homology of the lung and liver. Indeed, the lung and liver belong to primitive fore-gut derivatives during embryonic development, and abnormal

TABLE 2 | The clinical characteristics of 51 cases.

Characteristic	Result
Age (years)	59.9 ± 17.0
Gender	
Male	45
Female	6
Tumor location	
Right upper lobe	27
Not the right upper lobe	24
Tumor size(cm)	6.7 ± 1.5
Smoke	
Yes	34
No	5
Not mentioned	12
AFP	
Positive	27
Negative	12
Not mentioned	12
Stage at diagnosis	
I	6
II	8
III	11
IV	16
Not mentioned	10
Radical surgery	
Yes	20
No	30
Not mentioned	1
EGFR mutation	
Yes	1
No	14
Not mentioned	36
ALK mutation	
Yes	1
No	9
Not mentioned	41

TABLE 3 | Cox proportional hazard regression model.

	P	HR	95% CI	
Tumor location	0.82	0.89	0.33	2.41
Tumor size	0.96	1.00	0.86	1.16
Serum AFP	0.25	1.00	1.00	1.00
Radical surgery	0.011	0.23	0.08	0.71

differentiation of lung cancer cells tends to transform into hepatic cells, thus producing AFP (49).

This study highlights the fact that HAL is more common in middle-aged and elderly male smokers, and generally occurs in the right upper lobe of the lung. Among the patients, approximately 2/3 were serum AFP-positive before treatment. Once confirmed, approximately 2/3 of the patients were classified as middle and advanced stage (stage III and IV) according to the TNM staging system. The probability of EGFR mutation and ALK mutation in non-small cell lung cancer (NSCLC) patients is about 30% and 5%, respectively (50). In this systematic review, we found that the mutation rate of EGFR and ALK in all HAL patients who underwent genetic screening was 6.7% and 10.0%, respectively. Thus, we recommend that all confirmed HAL patients should undergo lung cancer-driven genetic screening, preferably NGS detection,

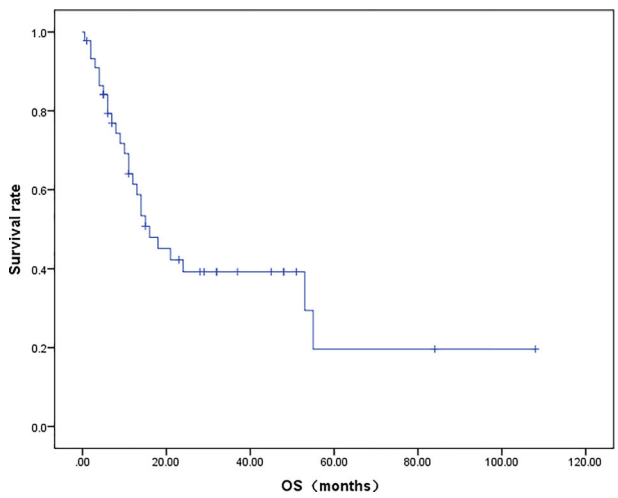

FIGURE 4 | Survival curve of HAL patients.

PD-L1 testing, and microsatellite instability detection, to guide the gene and immunotherapy of HAL patients.

In our systematic review, we found that HAL patients had a poor prognosis, with a 5-year survival rate of only 8.0% and a 2-year survival rate of 35.3%. Due to the small number of HAL cases, there is no relevant guideline or expert consensus on the standard treatment method for this disease. We mainly refer to the National Comprehensive Cancer Network (NCCN) guidelines for lung adenocarcinoma for the treatment of HAL patients. In the current study, we found that HAL patients were mainly treated with RS, followed by chemotherapy with platinum-containing dual drugs and radiotherapy. Only a few patients underwent targeted therapy and immunotherapy.

We demonstrate for the first time that RS significantly prolongs the survival time of HAL patients. HAL patients undergoing chemoradiotherapy or chemotherapy had a 2-year survival rate of only 12.5%, indicating that patients who received this treatment were unable to achieve a long-term survival rate. In our case study, for example, the patient was not sensitive to both radiotherapy and chemotherapy, and achieved an OS of only 13 months. With respect to targeted therapy, Chen et al. (40) reported that a patient with EGFR T790M mutation receiving third-line therapy with osimertinib achieved progression-free survival (PFS) for 8 months. Khozin et al. (23) reported that the disease progression of a female patient with an ALK gene rearrangement was 6 months after treatment with crizotinib. Gavrancic et al. (31) reported a stage IV HAL case, who was treated with sorafenib combined with platinum-containing dual drugs, and achieved an OS of 11 months. In terms of immunotherapy, Basse et al. (38) reported a stage IV HAL patient with negative PD-L1 and mismatch genes repair defect (dMMR), who achieved partial response (PR) after third-line therapy with durvalumab. Here, we report disease progression in a patient with negative PD-L1 after third-line therapy with sorafenib and sintilimab. In contrast, another study described a patient with PD-L1 ≥1% who achieved PR after

third-line therapy with docetaxel plus sintilimab (45). Taken together, these studies indicate that, even with combination therapy, HAL patients with PD-L 1 ≥1% or dMMR are likely to benefit from immunotherapy.

PIK3CA is a proto-oncogene, which can promote cell growth and induce the expression of anti-apoptotic genes after activation. The mutation rate of PIK3CA in NSCLC is about 2% (51). A PIK3CA inhibitor, alpelisib, is currently available and has been approved by the FDA for the treatment of advanced metastatic breast cancer with hormone receptor-positive, human EGFR2-negative, and PIK3CA mutation in men and postmenopausal women (52). Furthermore, its clinical phase II study in lung cancer is underway. In our case study, the efficacy of the three treatment schemes was poor, and thus, the use of a PIK3CA inhibitor may prove to be an effective treatment method.

Our study demonstrates for the first time that the serum AFP value before treatment is not related to the prognosis of HAL patients (HR 1.00, 95% CI: 1.00–1.00, p = 0.246). More studies are required to determine whether the change in serum AFP value before and after treatment has a significant impact on the prognosis of HAL patients. Some studies (53) have suggested that the pretreatment serum AFP heteroplasmon (AFP-L3) is an independent prognostic indicator of hepatic carcinoma. Serum AFP-L3 levels before treatment are negatively correlated with the prognosis of patients with hepatocellular carcinoma. Therefore, future studies could determine whether serum AFP-L3 can be used as an independent prognostic indicator for HAL patients by detecting pretreatment serum AFP-L3 levels.

In summary, HAL is a rare and special type of cancer that contains some features of both hepatocellular carcinoma and lung adenocarcinoma. HAL has similar cell morphology and intracellular antigens to hepatocellular carcinoma, while simultaneously containing some genetic mutations of pulmonary adenocarcinoma. The 5-year survival rate of HAL patients is low, and the 2-year survival rate of patients who do not receive RS is even lower. Thus, more research on gene-targeted and immunotherapy is required. The incidence of HAL is extremely low and less than 60 cases have been reported in the literature in the past 40 years. Therefore, the results of our study have certain limitations due to the small number of cases, and the epidemiology, molecular pathology, effective treatment regimens, and prognosis of HAL patients need to be further investigated.

DATA AVAILABILITY STATEMENT

The original contributions presented in the study are included in the article/supplementary material. Further inquiries can be directed to the corresponding author.

AUTHOR CONTRIBUTIONS

All authors listed have made a substantial, direct, and intellectual contribution to the work, and approved it for publication.

REFERENCES

1. Metzgeroth G, Ströbel P, Baumbusch T, Reiter A, Hastka J. Hepatoid Adenocarcinoma - Review of the Literature Illustrated by a Rare Case Originating in the Peritoneal Cavity. *Onkologie* (2010) 33(5):263–9. doi: 10.1159/000305717
2. Augustin G, Jelincic Z, Tentor D, Majerovic M, Matosevic P. Hepatoid Adenocarcinoma of the Stomach: Case Report and Short Notes on Immunohistochemical Markers. *Acta Gastroenterol Belg* (2009) 72(2):253–6.
3. Yasunami R, Hashimoto Z, Ogura T, Hirao F, Yamamura Y. Primary Lung Cancer Producing Alpha-Fetoprotein: A Case Report. *Cancer* (1981) 47(5):926–9. doi: 10.1002/1097-0142(19810301)47:5<926::aid-cncr2820470518>3.0.co;2-o
4. Grossman K, Beasley MB, Braman SS. Hepatoid Adenocarcinoma of the Lung: Review of a Rare Form of Lung Cancer. *Respir Med* (2016) 119:175–9. doi: 10.1016/j.rmed.2016.09.003
5. Tonyali O, Gonullu O, Ozturk MA, Kosif A, Civi OG. Hepatoid Adenocarcinoma of the Lung and the Review of the Literature. *J Oncol Pharm Pract* (2020) 26(6):1505–10. doi: 10.1177/1078155220903360
6. Papatsimpas G, Kamposioras K, Goula K, Papaparaskeva K, Loukides S, Kotoulas C, et al. Hepatoid Pancoast Tumor. A Case Report and Review of the Literature. *Lung Cancer* (2012) 77(2):239–45. doi: 10.1016/j.lungcan.2012.05.102
7. Li J, Qi H, Xu B, Zhao J, Gao H, Ma X, et al. Genomic Profiles of a Patient of Pulmonary Hepatoid Adenocarcinoma With High AFP Level: A Case Report. *Front Oncol* (2019) 9:1360. doi: 10.3389/fonc.2019.01360
8. Liberati A, Altman DG, Tetzlaff J, Mulrow C, Gøtzsche PC, Ioannidis JP, et al. The Prisma Statement for Reporting Systematic Reviews and Meta-Analyses of Studies That Evaluate Healthcare Interventions: Explanation and Elaboration. *BMJ* (2009) 339:b2700. doi: 10.1136/bmj.b2700
9. Miyake M, Ito M, Mitsuoka A, Taki T, Wada H, Hitomi S, et al. Alpha-Fetoprotein and Human Chorionic Gonadotropin-Producing Lung Cancer. *Cancer* (1987) 59(2):227–32. doi: 10.1002/1097-0142(19870115)59:2<227::aid-cncr2820590209>3.0.co;2-x
10. Saka H, Sakai S, Kondo N, Ito M, Shimokata K. Successful Resection of Alpha-Fetoprotein-Producing Lung Cancer. *Chest* (1988) 94(4):879–80. doi: 10.1378/chest.94.4.879
11. Okunaka T, Kato H, Konaka C, Yamamoto H, Furukawa K. Primary Lung Cancer Producing Alpha-Fetoprotein. *Ann Thorac Surg* (1992) 53(1):151–2. doi: 10.1016/0003-4975(92)90778-3
12. Nasu M, Soma T, Fukushima H, Kudo K, Matsubara O. Hepatoid Carcinoma of the Lung With Production of Alpha-Fetoprotein and Abnormal Prothrombin: An Autopsy Case Report. *Mod Pathol* (1997) 10(10):1054–8.
13. Arnould L, Drouot F, Fargeot P, Bernard A, Foucher P, Collin F, et al. Hepatoid Adenocarcinoma of the Lung: Report of a Case of an Unusual Alpha-Fetoprotein-Producing Lung Tumor. *Am J Surg Pathol* (1997) 21(9):1113–8. doi: 10.1097/00000478-199709000-00018
14. Carlinfante G, Foschini MP, Pasquinelli G, Scotti R, Cavazza A. Hepatoid Carcinoma of the Lung: A Case Report With Immunohistochemical, Ultrastructural and In-Situ Hybridization Findings. *Histopathology* (2000) 37(1):88–9. doi: 10.1046/j.1365-2559.2000.00955-5.x
15. Hayashi Y, Takanashi Y, Ohsawa H, Ishii H, Nakatani Y. Hepatoid Adenocarcinoma in the Lung. *Lung Cancer* (2002) 38(2):211–4. doi: 10.1016/s0169-5002(02)00214-3
16. Hiroshima K, Iyoda A, Toyozaki T, Haga Y, Baba M, Fujisawa T, et al. Alpha-Fetoprotein-Producing Lung Carcinoma: Report of Three Cases. *Pathol Int* (2002) 52(1):46–53. doi: 10.1046/j.1440-1827.2002.01311.x
17. Lino K, Ohta Y, Tamura M, Sato H, Kurumaya H. A Resected Case of Alpha-Fetoproteinproducing Hepatoid Adenocarcinoma of the Lung. *Jpn J Lung Cancer* (2003) 43:29–34. doi: 10.2482/haigan.43.29
18. Terracciano LM, Glatz K, Mhawech P, Vasei M, Lehmann FS, Vecchione R, et al. Hepatoid Adenocarcinoma With Liver Metastasis Mimicking Hepatocellular Carcinoma: An Immunohistochemical and Molecular Study of Eight Cases. *Am J Surg Pathol* (2003) 27(10):1302–12. doi: 10.1097/00000478-200310000-00002

19. Ivan M, Koss M, Chang CF. Hepatoid Adenocarcinoma of the Lung Abstract. *Chest* (2007) 132:Abstract 690. doi: 10.1378/chest.132.4_MeetingAbstracts.690
20. Wu Z, Upadhyaya M, Zhu H, Qiao Z, Chen K, Miao F. Hepatoid Adenocarcinoma: Computed Tomographic Imaging Findings With Histopathologic Correlation in 6 Cases. *J Comput Assist Tomogr* (2007) 31 (6):846–52. doi: 10.1097/RCT.0b013e318038f6dd
21. Kishimoto T, Yano T, Hiroshima K, Inayama Y, Kawachi K, Nakatani Y. A Case of *-Fetoprotein-Producing Pulmonary Carcinoma With Restricted Expression of Hepatocyte Nuclear Factor-4* in Hepatoid Foci: A Case Report With Studies of Previous Cases. *Hum Pathol* (2008) 39(7):1115–20. doi: 10.1016/j.humpath.2007.12.013
22. Fornasa F. Soft-Tissue Localization of Hepatoid Adenocarcinoma: First Case Report. *Case Rep Oncol* (2010) 3(2):212–7. doi: 10.1159/000317419
23. Khozin S, Roth MJ, Rajan A, Smith K, Thomas A, Berman A, et al. Hepatoid Carcinoma of the Lung With Anaplastic Lymphoma Kinase Gene Rearrangement. *J Thorac Oncol* (2012) 7(11):e29–31. doi: 10.1097/JTO.0b013e3182697a23
24. Valentino F, Torchio M, Morbini P, Danova M. Synchronous Presentation of Hepatoid Alpha-Fetoprotein-Producing Lung Cancer and Colorectal Adenocarcinoma. *Tumori* (2012) 98(5):130e–4e. doi: 10.1700/1190.13214
25. Mokrim M, Belbaraka R, Allaoui M, Kairaouani M, Mahassini N, Tahri A, et al. Hepatoid Adenocarcinoma of the Lung: A Case Report and Literature Review. *J Gastrointest Cancer* (2012) 43 Suppl 1:S125–7. doi: 10.1007/s12029-011-9318-5
26. Cavalcante LB, Felipe-Silva A, de Campos FPF, Martines JADS. Hepatoid Adenocarcinoma of the Lung. *Autops Case Rep* (2013) 3(1):5–14. doi: 10.4322/acr.2013.002
27. Lin SF, Hsu WH, Chou TY. Primary Pulmonary Hepatoid Carcinoma: Report of a Case and Review of the Literature. *Kaohsiung J Med Sci* (2013) 29(9):512–6. doi: 10.1016/j.kjms.2013.01.007
28. Che YQ, Wang S, Luo Y, Wang JB, Wang LH. Hepatoid Adenocarcinoma of the Lung: Presenting Mediastinal Metastasis Without Transfer to the Liver. *Oncol Lett* (2014) 8(1):105–10. doi: 10.3892/ol.2014.2064
29. Haninger DM, Kloecker GH, Bousamra Ii M, Nowacki MR, Slone SP. Hepatoid Adenocarcinoma of the Lung: Report of Five Cases and Review of the Literature. *Mod Pathol* (2014) 27(4):535–42. doi: 10.1038/modpathol.2013.170
30. Shaib W, Sharma R, Mosunjac M, Farris AB 3rd, El Rayes B. Hepatoid Adenocarcinoma of the Lung: A Case Report and Review of the Literature. *J Gastrointest Cancer* (2014) 45 Suppl 1:99–102. doi: 10.1007/s12029-013-9558-7
31. Gavrancic T, Park YH. A Novel Approach Using Sorafenib in Alpha Fetoprotein-Producing Hepatoid Adenocarcinoma of the Lung. *J Natl Compr Canc Netw* (2015) 13(4):387–91; quiz 391. doi: 10.6004/jnccn.2015.0054
32. Motooka Y, Yoshimoto K, Semba T, Ikeda K, Mori T, Honda Y, et al. Pulmonary Hepatoid Adenocarcinoma: Report of a Case. *Surg Case Rep* (2016) 2(1):1. doi: 10.1186/s40792-016-0129-6
33. Qian GQ, Yin FY, Li GX, Chu JG. Hepatoid Adenocarcinoma of the Lung. *QJM* (2016) 109(9):619–20. doi: 10.1093/qjmed/hcw107
34. Sun JN, Zhang BL, Li LK, Yu HY, Wang B. Hepatoid Adenocarcinoma of the Lung Without Production of α-Fetoprotein: A Case Report and Review of the Literature. *Oncol Lett* (2016) 12(1):189–94. doi: 10.3892/ol.2016.4559
35. Wang S, Li M, Chen H, Li J, Zeng Q. FDG PET/CT in Hepatoid Adenocarcinoma of the Lung. *Clin Nucl Med* (2016) 41(7):e340–1. doi: 10.1097/RLU.0000000000001231
36. Valle L, Thomas J, Kim C, Szabo E, Brown GT, Citrin D, et al. Hepatoid Adenocarcinoma of the Lung Metastasizing to the Tonsil. *Mol Clin Oncol* (2017) 6(5):705–7. doi: 10.3892/mco.2017.1215
37. Li Q, Zhou DM. Hepatoid Adenocarcinoma of the Lung With Negative Alpha-Fetoprotein: A Case Report. *Zhonghua Zhong Liu Za Zhi* (2018) 40 (12):910–1. doi: 10.3760/cma.j.issn.0253-3766.2018.12.007
38. Basse V, Schick U, Guéguen P, Le Maréchal C, Quintin-Roué I, Descourt R, et al. A Mismatch Repair-Deficient Hepatoid Adenocarcinoma of the Lung Responding to Anti-PD-L1 Durvalumab Therapy Despite No PD-L1 Expression. *J Thorac Oncol* (2018) 13(7):e120–2. doi: 10.1016/j.jtho.2018.03.004
39. Ayub A, Nunez Lopez O, Booth A, Okereke I. Pulmonary Hepatoid Adenocarcinoma. *J Thorac Cardiovasc Surg* (2019) 158(4):e139–40. doi: 10.1016/j.jtcvs.2019.06.023
40. Chen HF, Wang WX, Li XL, Xu CW, Du KQ, Zhu YC, et al. Hepatoid Adenocarcinoma of the Lung With EGFR Mutation and the Response to Tyrosine Kinase Inhibitors. *J Thorac Oncol* (2019) 14(10):e217–9. doi: 10.1016/j.jtho.2019.04.032
41. Kuan K, Khader SN, El Hussein S. Hepatoid Adenocarcinoma of the Lung. *Diagn Cytopathol* (2019) 47(8):831–3. doi: 10.1002/dc.24195
42. Shi YF, Lu JG, Yang QM, Duan J, Lei YM, Zhao W, et al. Primary Hepatoid Adenocarcinoma of the Lung in Yungui Plateau, China: A Case Report. *World J Clin Cases* (2019) 7(13):1711–6. doi: 10.12998/wjcc.v7.i13.1711
43. Wang C, Xu G, Wu G, Chen Z, Sun Z, Zheng P, et al. Hepatoid Adenocarcinoma Of The Lung Metastasizing To The Gingiva. *Onco Targets Ther* (2019) 12:8765–8. doi: 10.2147/OTT.S222974
44. Yang K, Jiang H, Li Q. Primary Pulmonary Hepatoid Adenocarcinoma: A Case Report and Review of the Literature. *Med (Baltimore)* (2019) 98(14): e15053. doi: 10.1097/MD.0000000000015053
45. Chen L, Han X, Gao Y, Zhao Q, Wang Y, Jiang Y, et al. Anti-PD-1 Therapy Achieved Disease Control After Multiline Chemotherapy in Unresectable KRAS-Positive Hepatoid Lung Adenocarcinoma: A Case Report and Literature Review. *Onco Targets Ther* (2020) 13:4359–64. doi: 10.2147/OTT.S248226
46. Chen JX, Lyu LL, Zhu WH, Chen XY, Zheng L. Hepatoid Adenocarcinoma of the Lung Accompanied With Multiple Systemic Metastases. *Chin Med J (Engl)* (2020) 134(2):237–8. doi: 10.1097/CM9.0000000000000963
47. Nargund A, Agrawal M, Dharmalingam P, Amirtham U, MukundaPai M. Primary Hepatoid Adenocarcinoma of the Lung: A Study of Two Cases With Review of Literature. *Indian J Med Paediatr Oncol* (2020) 41:591–5. doi: 10.4103/ijmpo.ijmpo_245_19
48. Wang W, Li G. Radiotherapy of Pulmonary Hepatoid Adenocarcinoma With Intrahepatic Hemangioma: A Case Report. *Onco Targets Ther* (2020) 13:11947–55. doi: 10.2147/OTT.S275340
49. Kitada M, Ozawa K, Sato K, Matsuda Y, Hayashi S, Tokusashi Y, et al. Alpha-Fetoprotein-Producing Primary Lung Carcinoma: A Case Report. *World J Surg Oncol* (2011) 9:47. doi: 10.1186/1477-7819-9-47
50. Chapman AM, Sun KY, Ruestow P, Cowan DM, Madl AK. Lung Cancer Mutation Profile of EGFR, ALK, and KRAS: Meta-Analysis and Comparison of Never and Ever Smokers. *Lung Cancer* (2016) 102:122–34. doi: 10.1016/j.lungcan.2016.10.010
51. The U.S. Food and drug administration. *FDA Approves Alpelisib for Metastatic Breast Cancer [EB/OL]*. Available at: https://www.fda.gov/drugs/resources-information-approved-drugs/fda-approves-alpelisib-metastatic-breast-cancer.
52. Cheng J, Wang W, Zhang Y, Liu X, Li M, Wu Z, et al. Prognostic Role of Pre-Treatment Serum AFP-L3% in Hepatocellular Carcinoma: Systematic Review and Meta-Analysis. *PloS One* (2014) 9(1):e87011. doi: 10.1371/journal.pone.0087011
53. Wu SG, Chang YL, Yu CJ, Yang PC, Shih JY. The Role of PIK3CA Mutations Among Lung Adenocarcinoma Patients With Primary and Acquired Resistance to EGFR Tyrosine Kinase Inhibition. *Sci Rep* (2016) 6:35249. doi: 10.1038/srep35249

Conflict of Interest: The authors declare that the research was conducted in the absence of any commercial or financial relationships that could be construed as a potential conflict of interest.

Publisher's Note: All claims expressed in this article are solely those of the authors and do not necessarily represent those of their affiliated organizations, or those of the publisher, the editors and the reviewers. Any product that may be evaluated in this article, or claim that may be made by its manufacturer, is not guaranteed or endorsed by the publisher.

Copyright © 2021 Hou, Xie, Zhang, Dai, Chen and He. This is an open-access article distributed under the terms of the Creative Commons Attribution License (CC BY). The use, distribution or reproduction in other forums is permitted, provided the original author(s) and the copyright owner(s) are credited and that the original publication in this journal is cited, in accordance with accepted academic practice. No use, distribution or reproduction is permitted which does not comply with these terms.

frontiers in Oncology

ORIGINAL RESEARCH
published: 16 August 2021
doi: 10.3389/fonc.2021.681429

Efficacy of EGFR-TKI Plus Chemotherapy or Monotherapy as First-Line Treatment for Advanced EGFR-Mutant Lung Adenocarcinoma Patients With Co-Mutations

Zhengyu Yang†, Ya Chen†, Yanan Wang†, Shuyuan Wang, Minjuan Hu, Bo Zhang and Baohui Han**

Department of Pulmonary, Shanghai Chest Hospital, Shanghai Jiao Tong University, Shanghai, China

OPEN ACCESS

Edited by:
Hideharu Kimura, Kanazawa University, Japan

Reviewed by:
Sagun Parakh, University of Melbourne, Australia
Shuhang Wang, Chinese Academy of Medical Sciences and Peking Union Medical College, China

***Correspondence:**
Baohui Han
18930858216@163.com
Bo Zhang
zb1063253078@163.com

†These authors have contributed equally to this work

Specialty section:
This article was submitted to Thoracic Oncology, a section of the journal Frontiers in Oncology

Received: *16 March 2021*
Accepted: *27 July 2021*
Published: *16 August 2021*

Citation:
Yang Z, Chen Y, Wang Y, Wang S, Hu M, Zhang B and Han B (2021) Efficacy of EGFR-TKI Plus Chemotherapy or Monotherapy as First-Line Treatment for Advanced EGFR–Mutant Lung Adenocarcinoma Patients With Co-Mutations. Front. Oncol. 11:681429. doi: 10.3389/fonc.2021.681429

Background: Co-mutations was associated with poor response to EGFR-TKIs. First-generation EGFR-TKIs combined with chemotherapy was reported to be more effective than TKIs alone in advanced lung adenocarcinoma patients.

Objective: This retrospective study aimed to explore whether *EGFR*-mutant patients with co-mutations can benefit from EGFR-TKIs plus chemotherapy.

Patients and Methods: We retrospectively collected data of 137 *EGFR*-mutant patients with advanced lung adenocarcinoma who underwent next-generation sequencing in our hospital in 2018. Among them, 96 were treated with EGFR–TKIs alone and 41 received EGFR–TKIs plus chemotherapy. We analyzed the progression-free survival (PFS) of patients with co-mutations using different treatments.

Results: Concurrent *TP53* mutations, especially exon 4 and 6, were associated with a markedly shorter time to progression on EGFR-TKI monotherapy (11.4 months *vs*. 16.6 months, *P*=0.003), while EGFR–TKIs plus chemotherapy would benefit those patients more (with *TP53:* 11.4 months *vs*. 19.1 months, *P*=0.001, HR=0.407; without *TP53*: 16.6 months *vs*. 18.9 months, *P*=0.379, HR=0.706). The incidence of T790M after resistance was equal in patients treated with different treatments (53% *vs*. 53%, *P*=0.985).

Conclusions: In our study, concurrent *TP53* mutations were found to be risk factors for EGFR-TKI monotherapy, but TKI combined with chemotherapy could eliminate this heterogeneity.

Keywords: epidermal growth factor receptor, tyrosine kinase inhibitors, next-generation sequencing, *TP53*, co-mutations

INTRODUCTION

In lung adenocarcinoma (LAC), *Epidermal growth factor receptor* (*EGFR*) is one of the most common driver genes and can be detected in 40%-50% of Asian patients (1, 2). With the development of targeted therapy, most patients with *EGFR* mutations can benefit from first-generation EGFR tyrosine kinase inhibitors (EGFR-TKIs) (such as gefitinib, erlotinib, and icotinib,

etc.) (3, 4). Several recent prospective studies have shown that *EGFR*-mutant patients using EGFR-TKIs combined with chemotherapy can have a better prognosis than TKI alone (5–7).

However, there is significant heterogeneity in patients' objective responses to EGFR-TKI monotherapy, with about 20%-30% of patients failing to respond well or developing drug resistance in the early stage. Previous reports indicated that co-mutations may be associated with poor response to EGFR-TKIs (8–10). Therefore, we tried to explore whether patients with co-mutations can benefit from EGFR-TKIs plus chemotherapy.

In our research, we collected information on patients who used EGFR-TKIs plus chemotherapy and TKIs alone in our hospital. We used the data of next-generation sequencing (NGS) to analyze the most frequent co-mutations, and tried to provide some references for precise treatment.

MATERIALS AND METHODS

Patients

We collected LAC patients who underwent NGS in our hospital in 2018. The specific flow chart for screening patients is shown in **Figure 1**. We also collected the baseline characteristics of the enrolled patients, including age, gender, smoking status, TNM stage, ECOG-PS score, metastases status, and *EGFR* subtype.

At last, 137 patients were enrolled in our study and they met all the following screening criteria. First, they were diagnosed with advanced lung cancer (TNM stage IIIB or IV) and detected *EGFR* sensitive mutations (ex19 deletion or ex21 L858R mutation). Second, they underwent NGS before their first-line treatment and had complete follow-up data in our hospital. All patients gave informed consent before performing operation and treatment.

Next-Generation Sequencing

All surgically removed or biopsy tissues were fixed with formalin and embedded in paraffin. Tumor genomic DNA was extracted with the QIAamp DNA FFPE Tissue Kit (Qiagen, Hilden, Germany). As described previously (11), samples were sequenced by Nextseq500 sequencer (Illumina, Inc, San Diego, CA) and evaluated by a panel covering hotspot regions of 68 key cancer-related genes (**Supplementary Table 1**). The coverage depth of each sample could reach more than 1000×. The genetic profile of samples was shown in **Figure 2**.

According to previous reports (12), TP53 mutations were divided into 2 groups according to different exon mutation sites.

Treatment and Follow-Up

The monotherapy group was administered first-generation EGFR-TKIs, and the specific dose was gefitinib 250 mg once a day, erlotinib 150 mg once a day, or icotinib 125 mg three times a day. The combination therapy group was given EGFR-TKIs combined with chemotherapy (mainly pemetrexed plus platinum) until the condition worsened or unacceptable toxicity occurred. The mean interval between consecutive chemotherapies was 4 weeks. Bases on the Response Evaluation Criteria in Solid Tumors (RECIST v1.1), patients were clinically evaluated every 4 to 6 weeks. Progression-free survival (PFS) is defined as the time from the initiating EGFR-TKIs to the occurrence of disease progression or the last follow-

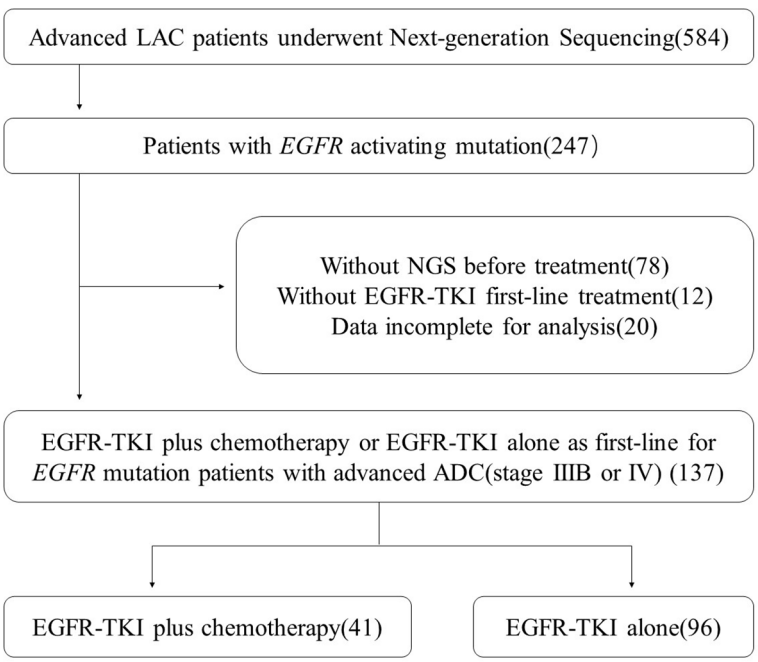

FIGURE 1 | Patient selection flow-chart.

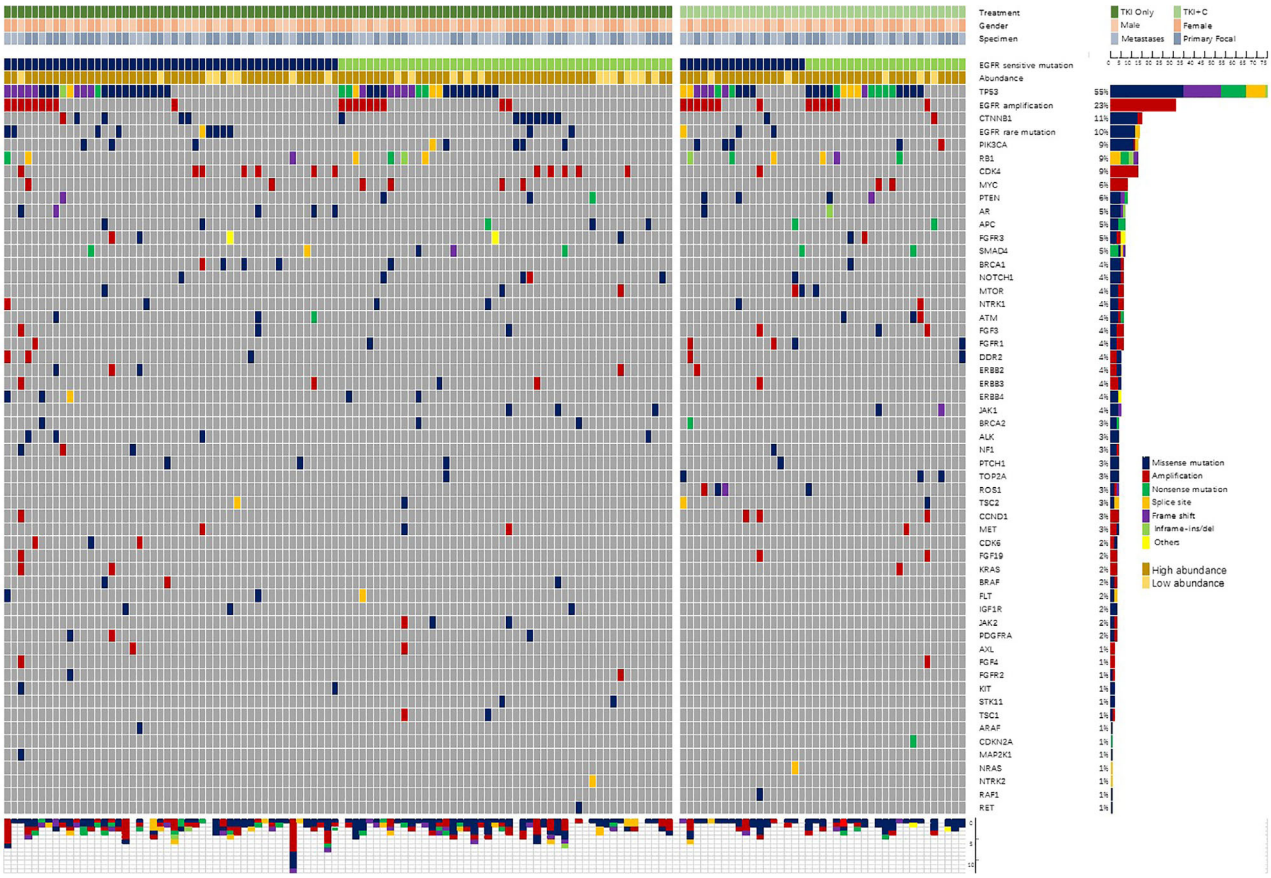

FIGURE 2 | Oncoprint of genomic alterations identified in baseline tumor tissue (n = 137).

up (October 10, 2020). The median follow-up time was 24 months.

Statistical Analysis

Chi-square test, Fisher's exact test and Rank sum test were used to compare categorical variables and continuous variables between groups as appropriate. The Kaplan-Meier method and Log-rank tests were used for PFS analysis to compare the PFS of different groups. A *P* value of less than 0.05 was considered statistically significant. All analyses were performed on the Statistical Package for Social Science (SPSS, Chicago, IL version 22.0).

RESULTS

Characteristics of Patients

A total of 584 advanced LAC patients underwent next-generation sequencing were included in the preliminary screening. The specific flow chart for screening patients is shown in **Figure 1**. Finally, 137 patients with advanced LAC (stage IIIB or IV) receiving EGFR-TKI plus chemotherapy or EGFR-TKI alone as first-line were included in our analysis.

Among the 137 patients, 96 (70%) were treated with EGFR–TKIs alone and 41 (30%) received EGFR–TKIs plus chemotherapy. In the combination therapy group, 39 patients were received pemetrexed plus platinum, and the other 2 patients with gemcitabine plus platinum. The average age in the monotherapy and combination therapy group was 61 years (42 to 80 years) and 62 years (35 to 87 years), respectively. There was no significant difference between the two groups in age, gender, smoking history, ECOG-PS, *EGFR* subtype, and metastasis status (**Table 1**). Among the specimens analyzed by NGS, 52% (71/137) were obtained from primary lung sites, while the others were from metastatic lymph node biopsy or pleural effusion embedding.

Baseline Genomic Characteristics

In addition to *EGFR* sensitive mutations, a total of 364 individual cell mutations and functional mutations were found. At average, a single patient had 2.66 accompanying mutations. Patients with 21L858R mutation tended to have more concomitant mutations than patients with 19del mutation (2.89 *vs.* 2.44, *P*=0.183). The majority were missense mutations (47%, 171/364) and amplification (29%, 106/364). **Figure 2** showed the frequency and composition of the somatic mutations. *TP53* (55%, 75/137)

TABLE 1 | Patients baseline characteristics.

	EGFR-TKI +chemotherapy (n = 41) (%)	EGFR-TKI (n = 96) (%)	*P* Value
Age, y, (range)	60.6 (42,80)	62.0 (35,87)	0.461
Sex			0.613
Female	22 (53.7)	56 (58.3)	
Male	19 (46.3)	40 (41.7)	
Smoking history			0.354
Yes	12 (29.3)	21 (21.9)	
No	29 (70.7)	75 (78.1)	
TNM stage			0.376
IIIB	2 (4.9)	11 (11.5)	
IV	39 (95.1)	85 (88.5)	
ECOG-PS			1.000
0-1	40 (97.6)	93 (96.9)	
2-3	1 (2.4)	3 (3.1)	
EGFR mutation			0.513
Exon 19	23 (56.1)	48 (50.0)	
Exon 21	18 (43.9)	48 (50.0)	
Brain metastasis	9 (22.0)	19 (19.8)	0.774
Bone metastasis	24 (58.5)	41 (42.7)	0.089

was the most frequent concurrent mutation, followed by *EGFR* amplification (23%), *CTNNB1* (11%), *EGFR* rare mutations (10%), *PIK3CA* (9%), *RB1* (9%), *CDK4* (9%), *etc.* Twenty-five patients (18%) were identified with low-abundance *EGFR* mutations, which were detected in samples with a mutation frequency of less than 10%. What's more, *EGFR* amplification (84%, 26/31), *RB1* (85%, 11/13) and *PTEN* (75%, 6/8) were often accompanied by *TP53* mutations.

In our cohort, TP53 mutation sites were distributed in exons 3-10. Of the 75 patients with TP53 mutations, 1, 6, 24, 14, 15, 9, 5, 1 were located in each exon, respectively.

Outcomes in Monotherapy Group and Combination Therapy Group

After monotherapy or combination therapy, the ORR (the proportion of patients with a confirmed complete or partial response) were 53.1% and 73.2%, respectively(P=0.029). The disease control rate (the proportion of patients with a confirmed complete or partial response or stable disease) were 90.6% and 97.6%, respectively(P=0.284). Of the 28 patients with brain metastases at baseline, excluding 8 patients who received local therapy, the intracranial ORR were 72.7% and 77.7%, respectively (P=1.000).

The patients who received combination therapy had significantly longer PFS than those who received monotherapy (**Figure 3A**; 19.1 months *vs.* 14.2 months, P=0.018, HR=0.598 95%Cl, 0.391-0.914). Compared with patients with *EGFR* 19del, patients with *EGFR* 21L858R tended to have shorter PFS in monotherapy group (**Figure 3B**; 12.5 months *vs.* 15.7 months, P=0.133), whereas they benefited more from combination therapy (19del: 19.0 months *vs.* 15.7 months, P=0.234, HR=0.709; 21L858R: 19.3 months *vs.* 12.5 months, P=0.046, HR=0.516).

We performed univariate and multivariate analyses of baseline characteristics and high-frequency mutations (including *TP53*, *EGFR* amplification, *CTNNB1*, *EGFR* rare mutations, *PIK3CA*, *RB1* and *CDK4*) in patients treated with monotherapy (**Table 2**). We found that concurrent *TP53* mutations (HR: 2.044, 95%Cl, 1.295 to 3.225, P=0.002) had a significant effect on PFS in both analyses, while *EGFR*

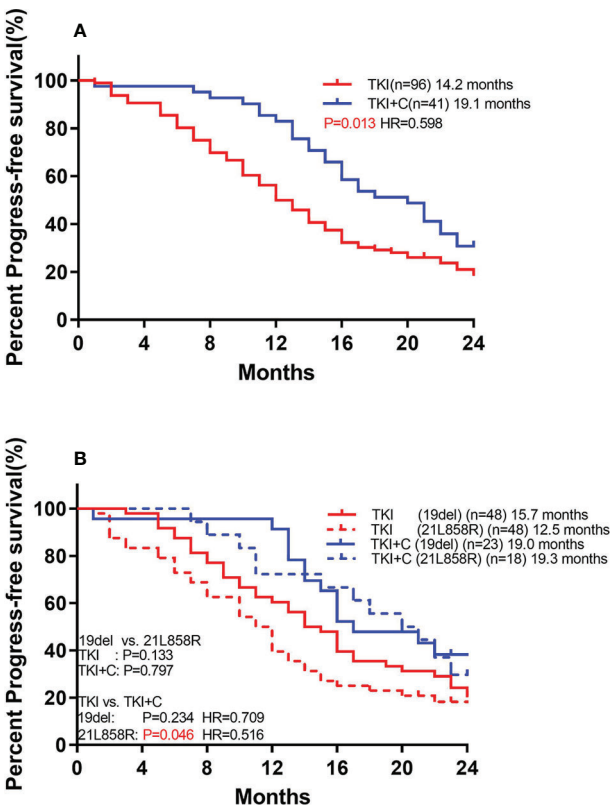

FIGURE 3 | **(A)** Comparison of monotherapy and combination therapy for PFS in patients with *EGFR* mutation. **(B)** Comparison of association of *EGFR* subtype with PFS to monotherapy and combination therapy in patients with *EGFR* mutation.

TABLE 2 | Univariate and multivariate analysis for PFS in monotherapy group.

PFS				
Characteristics	**Univariate analysis HR (95%CI)**	***P***	**Multivariate analysis HR (95%CI)**	***P***
Age				
≤60 Yr *vs*. >60 Yr	0.859 (0.544 – 1.358)	0.515		0.831
Gender				
Male *vs*. female	0.916 (0.583 – 1.439)	0.703		0.498
Smoking Status				
Yes *vs*. no	1.498 (0.880 – 2.550)	0.136		0.144
TNM Stage				
IIIB *vs*. IV	0.877 (0.403 – 1.908)	0.741		0.423
EGFR sensitive mutation				
19DEL *vs*. 21L858R	0.846 (0.675 – 1.060)	0.147		0.072
EGFR mutation abundance				
Low *vs*. high	1.445 (0.807 – 2.584)	0.215		0.226
EGFR amplification				
With *vs*. without	1.852 (1.061 – 3.231)	0.030		0.271
TP53				
With *vs*. without	1.933 (1.226 – 3.048)	0.005	2.044 (1.295 – 3.225)	0.002
CTNNB1				
With *vs*. without	1.013 (0.545 – 1.885)	0.967		0.372
EGFR rare mutations				
With *vs*. without	0.716 (0.342 – 1.499)	0.376		0.434
PIK3CA1				
With *vs*. without	0.894 (0.388 – 2.060)	0.792		0.828
RB1				
With *vs*. without	2.017 (0.918 – 4.429)	0.080		0.273
CDK4				
With *vs*. without	0.942 (0.469 – 1.892)	0.867		0.389

amplification only had a negative effect in univariate analysis (HR: 1.852, 95%Cl, 1.061 to 3.231, *P*=0.030).

We also compared the outcomes of patients with and without *TP53* mutations. Of the 96 patients receiving monotherapy, those with concomitant *TP53* mutation showed a significantly worse response (**Figure 4A**; 11.4 months *vs*. 16.6 months, *P*=0.003). However, patients with or without *TP53* yielded equivalent PFS in combination therapy group (18.9 months *vs*. 19.1 months, *P*=0.552). Patients with *TP53* benefited more from combination therapy (with *TP53*: 11.4 months *vs*. 19.1 months, *P*=0.001, HR=0.407; without *TP53*: 16.6 months *vs*. 18.9 months, *P*=0.379, HR=0.706).

TP53 mutations were further divided into two groups. Group A included exon 4 and 6, and both of these two types of mutations had poor prognosis. Group B included the remaining mutant types which shared a good prognosis. Among monotherapy patients, PFS was significantly lower in group A than in group B (**Figure 4B**; 8.0 months *vs*. 12.7 months, P=0.045). Both groups benefited from the combination therapy, but group A benefited more (Group A: 8.0 months *vs*. 21.0 months, *P*=0.004, HR=0.181; Group B: 12.7 months *vs*. 18.3 months, *P*=0.044, HR=0.555).

Resistance Mechanisms in Monotherapy Group and Combination Therapy Group

Then, we analyzed the baseline and post-resistance samples to explore the resistance mechanisms associated with different treatments. After first-line treatment progression, in patients undergoing *EGFR* T790M testing, 53% (20/38) in monotherapy group and 53% (11/21) in combination therapy group were positive, which was pretty equivalent (*P*=0.985). Mechanisms related to resistance in 26 patients who underwent NGS again after progression were summarized in **Table 3**. Among them, the emergence of *MET* amplification at PD occurred in 3 of monotherapy group and 1 of combination therapy group. One *ERBB2* amplification patient was observed in both groups.

DISCUSSION

In our study, we retrospectively analyzed the concomitant genomic alterations of advanced LAC patients with *EGFR* mutations and accessed the clinical efficacy of EGFR-TKI plus chemotherapy as first-line treatment.

We found that *EGFR* mutations were frequently associated with other mutations, with an average of 2.66 accompanying mutations, consistent with previous reports (13). The most common accompanying mutations were *TP53* (55%), *EGFR* amplification (23%), *CTNNB1* (11%), *EGFR* rare mutations (10%), *PIK3CA* (9%), *RB1* (9%), *CDK4* (9%), and so on. Previous studies have found that co-mutations may activate the alternative signaling pathway or increase tumor heterogeneity, thereby affecting the efficacy of EGFR-TKIs (9, 14).

We found that *TP53* mutations, especially exon 4 and 6, were associated with a markedly shorter time to progression on

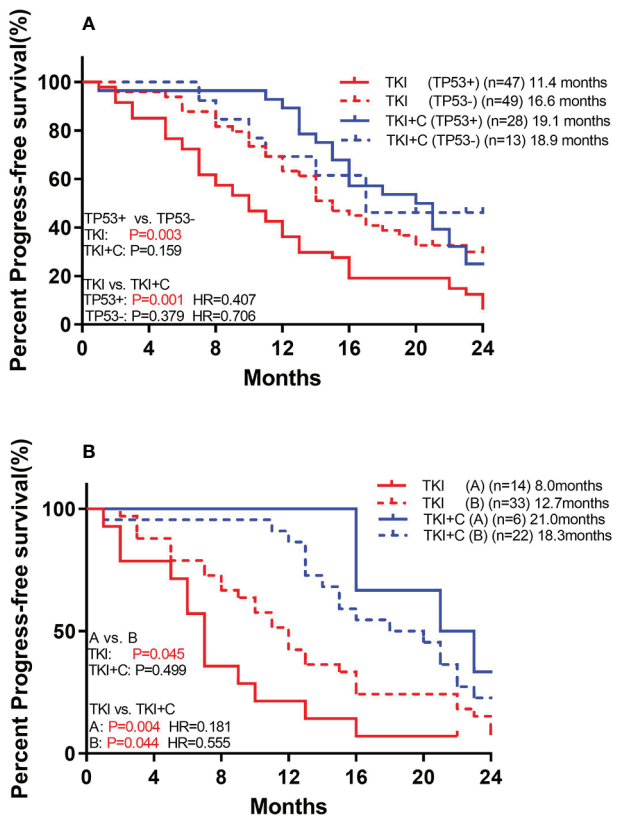

FIGURE 4 | **(A)** Comparison of association of concurrent *TP53* mutation with PFS to monotherapy and combination therapy in patients with *EGFR* mutation **(B)** Comparison of association of *TP53* subtypes with PFS to monotherapy and combination therapy in patients with *EGFR* mutation. [Group **(A)** included exon 4 and 6. Group **(B)** included the remaining mutant types].

EGFR-TKI monotherapy, which was consistent with previous reports (8–10, 12). *TP53* is a key tumor suppressor gene that can enhance sensitivity to EGFR-TKIs and radiotherapy by inducing cell-cycle arrest, apoptosis, and repair of DNA damage (15). The complete loss of *TP53* function, mainly manifested as single-base substitution and loss of alleles, can catalyze the transformation potential of oncogene drivers in lung cancer and inhibit tumor response to chemotherapy, radiotherapy and EGFR-TKIs (15, 16). However, in the combination therapy group, patients with *TP53* also showed a good response, and there was no significant difference in PFS compared with patients without *TP53*. This means that the combination of EGFR-TKI and chemotherapy will benefit patients with concurrent *TP53* mutations more.

Several previous studies reported that *EGFR* amplification in *EGFR*-mutant patients was associated with a longer PFS in TKI treatment (17, 18). In our study, *EGFR* amplification was a risk factor for PFS in univariate analysis but not in multivariate analysis, possibly because it was mainly accompanied by TP53.

In addition, many studies have shown that patients with *EGFR* 21L858R mutation do not respond as well to EGFR-TKI as patients with *EGFR* 19del mutation (19, 20). This may be attributed to the different intrinsic sensitivity of the two mutations to EGFR-TKIs (21). This trend was also observed in our study, in which patients with 21L858R had shorter PFS than those with 19del, but they benefited more from combination therapy.

EGFR-TKI combined with chemotherapy has been reported in a large number of prospective studies to delay resistance (5–7). This combination therapy was found to induce cell apoptosis and inhibit Akt and extracellular signal-regulated kinase phosphorylation (22), and EGFR-TKIs could reduce the level of thymidine synthase to improve the efficacy of pemetrexate (23). What's more, the proportions of patients with T790M positive after progression were similar in the combination therapy and monotherapy group, which meant that the majority of patients with the first-line combination therapy could be successfully treated with the sequential therapy of osimertinib. However, in addition to excellent effect, clinically relevant grade ≥ 3 toxicity in the combination therapy group were doubled (5, 6). There may be more patients over the age of 75 with a high ECOG-PS score in the clinical course, so we need to identify patients who would benefit more from the combination therapy. In our study, we found that patients with 21L858R or coexisting *TP53* mutations did not respond well to monotherapy, but benefited more from combination therapy. In addition, FLAURA (NCT02296125) showed osimertinib as first-line treatment yielded more benefits than first-generation EGFR-TKIs, providing an alternative option for patients with EGFR mutations (24, 25).

Our study has the following limitations. First, as a retrospective study, we failed to compare the adverse effects of

TABLE 3 | Resistance mechanism to monotherapy and combination therapy.

	Monotherapy (n = 13)	Combination therapy (n = 13)
T790M	4 (31%)	6 (46%)
T790M+ *ERBB2* amp	1 (8%)	
***MET* amp**	3 (23%)	1 (8%)
***ERBB2* amp**		1 (8%)
RB1	1 (8%)	
RB1+ TP53		1 (8%)
FGFR2	1 (8%)	
PTEN	1 (8%)	
BRAF		1 (8%)
***MYC* amp**		1 (8%)
Unknown	2 (15%)	2 (15%)

different treatments due to incomplete records. Second, although there was no significant difference in baseline characteristics among patients receiving different treatments, we recognized the existence of selection bias that patients with comorbidities were more likely to be recommended for monotherapy. Third, the mechanism by which combination therapy benefits patients with *TP53* mutations remains unclear and needs further study.

In summary, we retrospectively analyzed genomic changes in patients with advanced lung adenocarcinoma with sensitizing *EGFR* mutations and found that *TP53* was the most frequent concurrent mutations. Grouped by next-generation sequencing results, we compared the efficacy of monotherapy versus combination therapy. We found that patients with 21L858R mutation or concurrent *TP53* mutations did not respond well to EGFR-TKIs alone, but benefited more from EGFR-TKIs plus chemotherapy. In the future clinical treatment process, we should consider to stratify patients according to their *EGFR* subtype and concurrent mutations, and develop more targeted treatment programs.

DATA AVAILABILITY STATEMENT

The original contributions presented in the study are included in the article/**Supplementary Material**, further inquiries can be directed to the corresponding authors.

ETHICS STATEMENT

The studies involving human participants were reviewed and approved by The institutional review board of Shanghai Chest Hospital. The patients/participants provided their written informed consent to participate in this study.

AUTHOR CONTRIBUTIONS

ZY, YC, and YW both have substantial contributions to the conception or design of the work, the collection and analysis of data, the writing and edit of the article. The rest authors have given substantial contributions to the work by providing editing and writing assistance. All authors contributed to the article and approved the submitted version.

FUNDING

This work was supported by the foundation of Shanghai Chest Hospital (Project No. YJXT20190102); the program of system biomedicine innovation center from Shanghai Jiao Tong University (Project No. 15ZH4009); Shanghai Jiao Tong University School of Medicine (Project No. 15ZH1008) and the foundation of Chinese society of clinical oncology (Project No. Y2019AZZD-0355).

ACKNOWLEDGMENTS

The authors thank all of the patients and their families for their contributions to this study. The institutional review board of Shanghai Chest Hospital approved our study, and all patients provided written consent before surgery and clinical treatment.

SUPPLEMENTARY MATERIAL

The Supplementary Material for this article can be found online at: https://www.frontiersin.org/articles/10.3389/fonc.2021.681429/full#supplementary-material

Supplementary Table 1 | Sixty-eight cancer-related Genes sequenced in our panel.

REFERENCES

1. Mitsudomi T, Kosaka T, Endoh H, Horio Y, Hida T, Mori S, et al. Mutations of the Epidermal Growth Factor Receptor Gene Predict Prolonged Survival After Gefitinib Treatment in Patients With Non-Small-Cell Lung Cancer With Postoperative Recurrence. *J Clin Oncol* (2005) 23(11):2513–20. doi: 10.1200/JCO.2005.00.992
2. Rosell R, Moran T, Queralt C, Porta R, Cardenal F, Camps C, et al. Screening for Epidermal Growth Factor Receptor Mutations in Lung Cancer. *N Engl J Med* (2009) 361(10):958–67. doi: 10.1056/NEJMoa0904554
3. Gao G, Ren S, Li A, Xu J, Xu Q, Su C, et al. Epidermal Growth Factor Receptor-Tyrosine Kinase Inhibitor Therapy is Effective as First-Line Treatment of Advanced Non-Small-Cell Lung Cancer With Mutated EGFR: A Meta-Analysis From Six Phase III Randomized Controlled Trials. *Int J Cancer* (2012) 131(5):E822–9. doi: 10.1002/ijc.27396
4. Mitsudomi T, Morita S, Yatabe Y, Negoro S, Okamoto I, Tsurutani J, et al. Gefitinib Versus Cisplatin Plus Docetaxel in Patients With non-Small-Cell Lung Cancer Harbouring Mutations of the Epidermal Growth Factor Receptor (WJTOG3405): An Open Label, Randomised Phase 3 Trial. *Lancet Oncol* (2010) 11(2):121–8. doi: 10.1016/s1470-2045(09)70364-x
5. Hosomi Y, Morita S, Sugawara S, Kato T, Fukuhara T, Gemma A, et al. Gefitinib Alone Versus Gefitinib Plus Chemotherapy for Non-Small-Cell Lung Cancer With Mutated Epidermal Growth Factor Receptor: NEJ009 Study. *J Clin Oncol* (2020) 38(2):115–23. doi: 10.1200/JCO.19.01488
6. Noronha V, Patil VM, Joshi A, Menon N, Chougule A, Mahajan A, et al. Gefitinib Versus Gefitinib Plus Pemetrexed and Carboplatin Chemotherapy in EGFR-Mutated Lung Cancer. *J Clin Oncol* (2020) 38(2):124–36. doi: 10.1200/JCO.19.01154
7. Yang JC, Cheng Y, Murakami H, Yang PC, He J, Nakagawa K, et al. A Randomized Phase 2 Study of Gefitinib With or Without Pemetrexed as First-Line Treatment in Nonsquamous NSCLC With EGFR Mutation: Final Overall Survival and Biomarker Analysis. *J Thorac Oncol* (2020) 15(1):91–100. doi: 10.1016/j.jtho.2019.09.008
8. Labbe C, Cabanero M, Korpanty GJ, Tomasini P, Doherty MK, Mascaux C, et al. Prognostic and Predictive Effects of TP53 Co-Mutation in Patients With EGFR-Mutated Non-Small Cell Lung Cancer (NSCLC). *Lung Cancer* (2017) 111:23–9. doi: 10.1016/j.lungcan.2017.06.014
9. VanderLaan PA, Rangachari D, Mockus SM, Spotlow V, Reddi HV, Malcolm J, et al. Mutations in TP53, PIK3CA, PTEN and Other Genes in EGFR Mutated Lung Cancers: Correlation With Clinical Outcomes. *Lung Cancer* (2017) 106:17–21. doi: 10.1016/j.lungcan.2017.01.011
10. Cheng Y, Ma L, Liu Y, Zhu J, Xin Y, Liu X, et al. Comprehensive Characterization and Clinical Impact of Concomitant Genomic Alterations in EGFR-Mutant NSCLCs Treated With EGFR Kinase

Inhibitors. *Lung Cancer* (2020) 145:63–70. doi: 10.1016/j.lungcan.2020.04.004
11. Zhao Y, Dong Y, Zhao R, Zhang B, Wang S, Zhang L, et al. Expression Profiling of Driver Genes in Female Never-Smokers With Non-Adenocarcinoma Non-Small-Cell Lung Cancer in China. *Clin Lung Cancer* (2020) 21(5):e355–e62. doi: 10.1016/j.cllc.2020.02.005
12. Jiao X-D, Qin B-D, You P, Cai J, Zang Y-S. The Prognostic Value of TP53 and its Correlation With EGFR Mutation in Advanced Non-Small Cell Lung Cancer, an Analysis Based on Cbioportal Data Base. *Lung Cancer* (2018) 123:70–5. doi: 10.1016/j.lungcan.2018.07.003
13. Yu HA, Suzawa K, Jordan E, Zehir A, Ni A, Kim R, et al. Concurrent Alterations in EGFR-Mutant Lung Cancers Associated With Resistance to EGFR Kinase Inhibitors and Characterization of mTOR as a Mediator of Resistance. *Clin Cancer Res* (2018) 24(13):3108–18. doi: 10.1158/1078-0432.CCR-17-2961
14. Chen M, Xu Y, Zhao J, Zhong W, Zhang L, Bi Y, et al. Concurrent Driver Gene Mutations as Negative Predictive Factors in Epidermal Growth Factor Receptor-Positive Non-Small Cell Lung Cancer. *EBioMedicine* (2019) 42:304–10. doi: 10.1016/j.ebiom.2019.03.023
15. Huang S, Benavente S, Armstrong EA, Li C, Wheeler DL, Harari PM. P53 Modulates Acquired Resistance to EGFR Inhibitors and Radiation. *Cancer Res* (2011) 71(22):7071–9. doi: 10.1158/0008-5472.CAN-11-0128
16. Chen Z, Cheng K, Walton Z, Wang Y, Ebi H, Shimamura T, et al. A Murine Lung Cancer Co-Clinical Trial Identifies Genetic Modifiers of Therapeutic Response. *Nature* (2012) 483(7391):613–7. doi: 10.1038/nature10937
17. Shan L, Wang Z, Guo L, Sun H, Qiu T, Ling Y, et al. Concurrence of EGFR Amplification and Sensitizing Mutations Indicate a Better Survival Benefit From EGFR-TKI Therapy in Lung Adenocarcinoma Patients. *Lung Cancer* (2015) 89(3):337–42. doi: 10.1016/j.lungcan.2015.06.008
18. Ruiz-Patino A, Castro CD, Ricaurte LM, Cardona AF, Rojas L, Zatarain-Barron ZL, et al. EGFR Amplification and Sensitizing Mutations Correlate With Survival in Lung Adenocarcinoma Patients Treated With Erlotinib (MutP-CLICaP). *Target Oncol* (2018) 13(5):621–9. doi: 10.1007/s11523-018-0594-x
19. Wang H, Huang J, Yu X, Han S, Yan X, Sun S, et al. Different Efficacy of EGFR Tyrosine Kinase Inhibitors and Prognosis in Patients With Subtypes of EGFR-Mutated Advanced Non-Small Cell Lung Cancer: A Meta-Analysis. *J Cancer Res Clin Oncol* (2014) 140(11):1901–9. doi: 10.1007/s00432-014-1709-0
20. Jackman DM, Yeap BY, Sequist LV, Lindeman N, Holmes AJ, Joshi VA, et al. Exon 19 Deletion Mutations of Epidermal Growth Factor Receptor Are Associated With Prolonged Survival in Non-Small Cell Lung Cancer Patients Treated With Gefitinib or Erlotinib. *Clin Cancer Res* (2006) 12 (13):3908–14. doi: 10.1158/1078-0432.CCR-06-0462
21. Paez JG, Janne PA, Lee JC, Tracy S, Greulich H, Gabriel S, et al. EGFR Mutations in Lung Cancer: Correlation With Clinical Response to Gefitinib Therapy. *Science* (2004) 304(5676):1497–500. doi: 10.1126/science.1099314
22. Yang Z, Tam KY. Combination Strategies Using EGFR-TKi in NSCLC Therapy: Learning From the Gap Between Pre-Clinical Results and Clinical Outcomes. *Int J Biol Sci* (2018) 14(2):204–16. doi: 10.7150/ijbs.22955
23. Galvani E, Peters GJ, Giovannetti E. Thymidylate Synthase Inhibitors for non-Small Cell Lung Cancer. *Expert Opin Investig Drugs* (2011) 20(10):1343–56. doi: 10.1517/13543784.2011.617742
24. Soria JC, Ohe Y, Vansteenkiste J, Reungwetwattana T, Chewaskulyong B, Lee KH, et al. Osimertinib in Untreated EGFR-Mutated Advanced Non-Small-Cell Lung Cancer. *N Engl J Med* (2018) 378(2):113–25. doi: 10.1056/NEJMoa1713137
25. Ramalingam SS, Vansteenkiste J, Planchard D, Cho BC, Gray JE, Ohe Y, et al. Overall Survival With Osimertinib in Untreated, EGFR-Mutated Advanced NSCLC. *N Engl J Med* (2020) 382(1):41–50. doi: 10.1056/NEJMoa1913662

Conflict of Interest: The authors declare that the research was conducted in the absence of any commercial or financial relationships that could be construed as a potential conflict of interest.

Publisher's Note: All claims expressed in this article are solely those of the authors and do not necessarily represent those of their affiliated organizations, or those of the publisher, the editors and the reviewers. Any product that may be evaluated in this article, or claim that may be made by its manufacturer, is not guaranteed or endorsed by the publisher.

Copyright © 2021 Yang, Chen, Wang, Wang, Hu, Zhang and Han. This is an open-access article distributed under the terms of the Creative Commons Attribution License (CC BY). The use, distribution or reproduction in other forums is permitted, provided the original author(s) and the copyright owner(s) are credited and that the original publication in this journal is cited, in accordance with accepted academic practice. No use, distribution or reproduction is permitted which does not comply with these terms.

frontiers in Oncology

MINI REVIEW
published: 23 August 2021
doi: 10.3389/fonc.2021.704084

Targeted Therapy for RET Fusion Lung Cancer: Breakthrough and Unresolved Issue

*Shinkichi Takamori[1], Taichi Matsubara[1], Naoki Haratake[2], Gouji Toyokawa[3], Takatoshi Fujishita[1], Ryo Toyozawa[1], Kensaku Ito[1], Masafumi Yamaguchi[1], Kenichi Taguchi[4], Tatsuro Okamoto[1] and Takashi Seto[1]**

[1] Department of Thoracic Oncology, National Hospital Organization Kyushu Cancer Center, Fukuoka, Japan, [2] Department of Surgery and Science, Graduate School of Medical Sciences, Kyushu University, Fukuoka, Japan, [3] Department of Thoracic Surgery, National Hospital Organization Kyushu Medical Center, Fukuoka, Japan, [4] Cancer Pathology Laboratory, National Hospital Organization Kyushu Cancer Center, Fukuoka, Japan

OPEN ACCESS

Edited by:
Hideharu Kimura,
Kanazawa University, Japan

Reviewed by:
Greg Durm,
Indiana University, United States
Kengo Takeuchi,
Japanese Foundation for Cancer Research, Japan

***Correspondence:**
Takashi Seto
setocruise@gmail.com

Specialty section:
This article was submitted to Thoracic Oncology, a section of the journal Frontiers in Oncology

Received: 01 May 2021
Accepted: 02 August 2021
Published: 23 August 2021

Citation:
Takamori S, Matsubara T, Haratake N, Toyokawa G, Fujishita T, Toyozawa R, Ito K, Yamaguchi M, Taguchi K, Okamoto T and Seto T (2021) Targeted Therapy for RET Fusion Lung Cancer: Breakthrough and Unresolved Issue. Front. Oncol. 11:704084. doi: 10.3389/fonc.2021.704084

Molecular drugs targeting mutated or rearranged oncogene drivers have become one of the standard recognized treatments in patients with advanced and recurrent non-small cell lung cancer. *RET* is located in the long arm of human chromosome 10 and encodes a receptor tyrosine kinase protein, and RET fusion-positive lung adenocarcinoma occurs in 1%–2% of cases. Clinical trials of multikinase inhibitors, including cabozantinib, vandetanib, sorafenib, and lenvatinib, that inhibit RET oncogene activity have shown their antitumor efficacy. Recently, RET inhibitors such as pralsetinib and selpercatinib that are specialized for RET kinase have also been developed, and their efficacy was investigated in previous clinical trials (BLU-667 and LOXO-292). In this review, we summarized the effects and adverse events of multikinase and selective RET inhibitors and the various diagnostic techniques for *RET* gene fusion. In the perspective part, we focused on the unsolved issues on treatment for RET fusion-positive lung cancer and future developments.

Keywords: non-small cell lung cancer, RET, multikinase inhibitor, selective inhibitor, targeted therapy

INTRODUCTION

In recent years, treatment with molecular targeted drugs, focusing on driver genes of advanced and recurrent non-small cell lung cancer, has become one of the standard recognized treatments. In 2012, *RET* fusion gene was identified as a new targetable driver gene (1–3). *RET* is located in the long arm of human chromosome 10 and encodes a receptor tyrosine kinase protein. RET fusion-positive lung adenocarcinoma occurs in 1%–2% of cases, and clinical trials of multikinase inhibitors that inhibit RET oncogene activity such as vandetanib and cabozantinib have indicated their antitumor efficacy. Anticipating the efficacy of precision medicine for RET fusion-positive lung cancer, domestic and international clinical trials of RET inhibitors have been conducted. RET inhibitors such as pralsetinib and selpercatinib that are specialized for RET kinase have been developed, and their efficacy was investigated in several clinical trials.

MULTIKINASE RET INHIBITORS

Cabozantinib

Cabozantinib is a multikinase inhibitor that inhibits specific receptor tyrosine kinase such as RET, vascular endothelial growth factor receptor (VEGFR), mesenchymal–epithelial transition (MET), ROS1, AXL, immunoglobulin-like and epidermal growth factor-like domains 2 (TIE2), and KIT (4). A phase II clinical trial enrolling 26 patients was conducted to determine the efficacy of cabozantinib in metastatic RET fusion-positive lung cancer. The response rate was 28% (95% confidence interval [CI]: 12%–49%), indicating significant efficacy. The report stated that the median progression-free survival was 5.5 months (95% CI: 3.8–8.4 months), and the overall survival was 9.9 months (95% CI: 8.1 months to unreached) (4). Primary adverse events of Grade 3 and higher were elevation in lipase, alanine aminotransferase (AST), and alanine aspartate aminotransferase (ALT) levels, as well as thrombocytopenia and hypophosphatemia, thus necessitating a dosage reduction in 19 patients (73%). The summary of clinical data of RET inhibitors for RET fusion-positive lung cancer is shown in **Table 1**. **Table 2** summarizes clinical trials of RET inhibitors.

Vandetanib

Vandetanib is another multikinase inhibitor that inhibits RET, VEGFR, and epidermal growth factor receptor (EGFR) signaling (5). A phase II investigator-initiated clinical trial (LURET) enrolling 19 patients was conducted in Japan to determine the efficacy of vandetanib in metastatic RET fusion-positive lung cancer. The response rate was 53% (95% CI: 28%–77%), indicating significant efficacy. The median progression-free survival was 4.7 months (95% CI: 2.8–8.5 months) (5). In addition, 11 retrospective studies conducted by the Global Multicenter RET Registry (GLORY) showed the response rate to be 18% and the median progression-free survival to be 2.9 months. In the GLORY study, the median line of systemic therapy of the first RET inhibitors administered was third line, ranging from first to eighth. Primary adverse events included diarrhea, rash, hypertension, and asymptomatic long QT syndrome. Due to these adverse events, dosage reduction was imperative in 20% of the targeted patients, and the treatment was discontinued in 50% of them (6). A similar phase II clinical trial enrolling 17 patients was also conducted in South Korea. The response rate was 18%, and the median progression-free survival was 4.5 months (7). Based on this result, the NCCN Guideline (Version 3; 2020) listed vandetanib under Category 2A as an appropriate treatment for metastatic RET fusion-positive lung cancer (12).

Lenvatinib

Lenvatinib inhibits RET, VEGFR, platelet-derived growth factor receptor (PDGFR), fibroblast growth factor (FGF), and c-KIT (8). Phase II clinical trials enrolling a total of 25 patients were conducted to determine the efficacy of lenvatinib in metastatic RET fusion-positive lung cancer patients in Japan, the United States, Singapore, and Taiwan. The response rate was 16% (95% CI: 12%–49%), and the median progression-free survival was 7.3 months (95% CI: 3.6–10.2 months) (8). Adverse events of Grade 3 and higher were observed in 92% of targeted patients and included hypertension, nausea, vomiting, anorexia, diarrhea, and proteinuria. Dosage reduction was imperative in 64% of targeted patients, and treatment was discontinued in 20% of the targeted patients due to these conditions.

Other Multikinase Inhibitors

Retrospective studies conducted by GLORY revealed therapeutic response in 2/9 sunitinib (inhibitor of RET, VEGFR, PDGFR, c-KIT, and fms-related tyrosine kinase 3 [FLT3]) cases, 1/2 nintedanib (inhibitor of RET, VEGFR, PDGFR, and FGFR) cases, 0/2 ponatinib (inhibitor of RET, VEGFR, PDGFR, FGFR, c-KIT, and Src) cases, 0/2 sorafenib (inhibitor of RET, VEGFR, PDGFR, FLT3, and KIT) cases, and 0/1 regorafenib (inhibitor of RET, VEGFR, FGFR, PDGFR, c-KIT, and TIE2) case (6). A phase II clinical trial enrolling three patients was conducted to determine the efficacy of sorafenib in metastatic RET fusion-positive lung cancer. In this trial, one patient exhibited stable disease, and two patients exhibited progressive disease (9).

SELECTIVE RET INHIBITORS

Pralsetinib

Pralsetinib (BLU-667) is a highly selective RET inhibitor. Pralsetinib inhibits wild-type RET and oncogenic RET fusions (KIF5B-RET, CCDC6-RET, etc.) and mutations (V804L, V804M, and M918T). The ARROW clinical trial (Phase 1/2) reported that the response rate of pralsetinib in treatment-naive RET-altered non-small cell lung cancer patients was 73% (95% CI: 52%–88%), and the response rate in treated patients was 61% (95% CI: 50%–72%) (10). The median follow-up period was 8.8 months, and progression-free survival was not reached. Approximately 50% of the RET-altered non-small cell lung cancer patients were found to have developed brain metastasis, but the intracranial responses of pralsetinib that were tested in the patient group with brain metastasis revealed a satisfactory response rate of 56%. A low occurrence rate of 6.9% for Grade 3 adverse events such as elevation in ALT level, tumor lysis syndrome, and hypertension was reported. No Grade 4 or 5 adverse events were recognized. The U.S. Food and Drug Administration approved pralsetinib in September 2020 and designated it as a breakthrough therapy.

Selpercatinib

Selpercatinib (LOXO-292), similar to pralsetinib, is a highly selective RET inhibitor. Selpercatinib inhibits wild-type RET and oncogenic RET fusions (KIF5B-RET, CCDC6-RET, etc.) and mutations (V804L, V804M, and M918T). The LIBRETTO-001 clinical trial (Phase 1/2) enrolled 39 treatment-naive patients and 105 patients previously treated with platinum-based chemotherapy (11). In this clinical trial, the response rate of selpercatinib in untreated patients was 85% (95% CI: 70%–94%), and progression-free survival was not reached. The response rate of selpercatinib in pretreated and untreated patients was 64% (95% CI: 54%–73%) and 85% (95% CI: 70%–94%), respectively. The median progression-free survival was 17 months (95% CI: 14 months to unreached). These pretreated patients had

TABLE 1 | Summary of clinical data of RET inhibitors for RET fusion-positive lung cancer.

RET inhibitors	Multikinase inhibitors												Selective RET inhibitors	
	Cabozantinib			Vandetanib		Sorafenib		Lenvatinib	Sunitinib	Nintedanib	Ponatinib	Regorafenib	Pralsetinib	Selpercatinib
Countries	USA	Global clinical trial (GLORY)	Japan	South Korea	Global clinical trial (GLORY)	Japan	Global clinical trial (GLORY)	Japan, USA, Singapore, Taiwan	Global clinical trial (GLORY)	Global clinical trial (GLORY)	Global clinical trial (GLORY)	Global clinical trial (GLORY)	Global clinical trial	Global clinical trial
Number of cases	26	19	19	17	11	3	2	25	9	2	2	1	Treated: 92 Treatment-naive: 29	Treated: 105 Treatment-naive: 39
Methods of analysis	NGS, FISH (one must be positive)	NGS, RT-PCR, FISH (one must be positive)	RT-PCR, FISH (both must be positive)	FISH, RT-PCR	NGS, RT-PCR, FISH (one must be positive)	RT-PCR, FISH (one must be positive)	NGS, RT-PCR, FISH (one must be positive)	NGS	NGS, RT-PCR, FISH (one must be positive)	NGS, RT-PCR, FISH (one must be positive)	NGS, RT-PCR, FISH (one must be positive)	NGS, RT-PCR, FISH (one must be positive)	NGS, RT-PCR, FISH (one must be positive)	NGS, RT-PCR, FISH (one must be positive)
Fusion partners	*KIF5B* (16 cases), *CCDC6* (1 case), *TRIM33* (1 case), *CLIP1* (1 case), *ERC1* (1 case), other (6 cases)	NA	*KIF5B* (10 cases), *CCDC6* (6 cases), other (3 cases)	*KIF5B* (5 cases), *CCDC6* (2 cases), *MYO5C* (1 case), unknown (10 cases)	NA	*KIF5B* (1 case), *CCDC6* (1 case), unknown (1 case)	NA	*KIF5B* (13 cases), *CCDC6* (12 cases), unknown (1 case)	NA	NA	NA	NA	*KIF5B* (88 cases), *CCDC6* (19 cases), other/unknown (14 cases)	*KIF5B* (59 cases), *CCDC6* (24 cases), *NCOA4* (2 cases), *RELCH* (2 cases), other/unknown (18 cases)
Response rate	28%	37%	53%	18%	18%	0%	0%	16%	22%	50%	0%	0%	Treated: 55% Untreated: 66%	Treated: 64% Untreated: 85%
Progression-free survival (median)	5.5 months	3.6 months	4.7 months	4.5 months	2.9 months	NA	NA	7.3 months	2.2 months	NA	NA	NA	Unreached	Treated: 17 months Untreated: Unreached
Overall survival (median)	9.9 months	4.9 months	11.1 months	11.6 months	10.2 months	NA	NA	NA	6.8 months	NA	NA	NA	Unreached	Unreached
Grade 3 and higher adverse events	47%	NA	58%	28%	NA	33%	NA	92%	NA	NA	NA	NA	NA	28%

GLORY, Global Multicenter RET Registry; NGS, next-generation sequencing; FISH, fluorescence in situ hybridization; NA, not available.

TABLE 2 | Summary of clinical trials of RET inhibitors for RET fusion-positive lung cancer.

References	Year	Types and phases	Countries	RET inhibitor	Number of cases	Primary endpoint
Drilon et al. (4)	2016	II	USA	Cabozantinib	26	ORR
Yoh et al. (5)	2017	II	Japan	Vandetanib	19	ORR
Gautschi et al. (6)	2017	Retrospective	Global (Europe, Asia, and the USA)	Cabozantinib, vandetanib, sunitinib, sorafenib, alectinib, lenvatinib, nintedanib, ponatinib, regorafenib	165	–
Lee et al. (7)	2017	II	South Korea	Vandetanib	18	ORR
Hida et al. (8)	2019	II	USA, Japan, Singapore, and Taiwan	Lenvatinib	25	ORR
Horiike et al. (9)	2016	II	Japan	Sorafenib	3	–
Gainor et al. (10)	2020	I/II	Global (11 countries)	Pralsetinib	121	ORR
Drilon et al. (11)	2020	I/II	Global (12 countries)	Selpercatinib	144	ORR

ORR, objective response rate.

previously received multiple treatments (the median number of prior treatment lines was 3; 55% had received anti-PD-1/PD-L1 antibodies; and 48% had received at least one multikinase inhibitor); however, the response rate did not significantly differ between untreated and pretreated patients regardless of previous treatments. The intracranial response of selpercatinib showed a satisfactory response rate of 91% (95% CI: 59%–100%). Primary adverse events included diarrhea, general malaise, and xerostomia. Forty-one cases of treatment-related Grade 3 and higher adverse events out of 144 (28%) were reported, including tumor lysis syndrome, elevation in AST/ALT levels, diarrhea, and thrombocytopenia. The U.S. Food and Drug Administration approved selpercatinib in May 2020 and designated it as a breakthrough therapy along with pralsetinib. The response rate of selpercatinib was 60% (95% CI: 43%–75%) in a subgroup of East Asian patients (n = 40), and the results were announced at the 2021 World Conference of Lung Cancer, based on which the therapeutic effects of selpercatinib in East Asians were adjudged to be equal to those in Europeans and Americans.

PERSPECTIVE

Unsolved Issues on Treatment for RET Fusion-Positive Lung Cancer and Future Developments

1) Based on the data above, selective RET inhibitors could be considered for future clinical trials. The progression-free survival of RET fusion-positive lung cancer patients treated with multikinase inhibitors including sunitinib, cabozantinib, and vandetanib was reported as 2.2–4.7 months. Conversely, the progression-free survival for selpercatinib, a selective RET inhibitor, was 17 months, even in pretreated patients. The difference in the progression-free survival could be attributed to the difference in the IC50 values of multikinase inhibitors and selective RET inhibitors (13). For instance, the IC50 value of vandetanib for V804M is 76 nM, but that of selpercatinib is 0.8 nM, which is many folds lower. V804M is a RET inhibitor-resistant gatekeeper mutation, which confers a gain of function on the RET protein. Hypothetically, even if the dose of vandetanib was increased to increase its blood concentration to inhibit V804M, VEGFR2 is forcefully inhibited, thus increasing toxicity. Perhaps in future clinical trials of RET fusion-positive lung cancer, selective RET inhibitors will become mainstream.
2) Recruitment of appropriate patients for determining examination methods in RET fusion-positive lung cancer is crucial. The LURET clinical trial required participation of patients who tested positive by both RT-PCR and fluorescence *in situ* hybridization (FISH) methods (5). In a clinical trial that was performed in South Korea, RET rearrangements were detected by FISH and further confirmed by immunohistochemistry, RT-PCR, or targeted deep sequencing-based panel assay in cases with available study materials (7). A recent study indicated that the diagnostic sensitivity of RET fusion-positive lung cancer using the FISH technique was 100% (85.8%–100%), and the specificity was 85% (62.1–96.8%), although the specificity may be underestimated given that the study set the positivity cutoff to be ≥10% tumor cells, demonstrating a *RET* rearrangement pattern (14). Analysis of lung and thyroid cancer tissues showed a positive rate by RET fusion partners such as *KIF5B* and *CCDC6*, and their sensitivities were 100%. However, the sensitivity for NCOA4 was 66.7% (34.9%–90.1%), although the study investigated small sample size (12 cases) and definitive conclusions cannot be drawn at present (14). The FISH technique may not be accurate for certain fusion partners. Furthermore, the LIBRETTO-001 and ARROW trials accepted patients who tested positive for RET fusion using methods that were utilized at each local facility (next-generation sequencing (NGS), RT-PCR, or FISH). Neither trials required a central confirmatory diagnosis. Thus, definitive methods for detecting RET fusion-positive lung cancer need to be established.
3) In recent years, treatment with immune checkpoint inhibitors, alone or in combination with chemotherapy, has become standard for advanced and recurrent non-small cell lung cancer; therefore, treatment regimens for RET fusion-positive lung cancer patients must be carefully considered. Some RET fusion-positive lung cancer patients reported from their retrospective perspective that targeted treatment is preferable over treatment with immune checkpoint inhibitors for better prognosis (15). Moreover, previous studies indicated that the use of immune checkpoint inhibitors increases the risk of drug-induced pneumonitis if various tyrosine kinase inhibitors such as EGFR-TKIs were

previously administered (16). Therefore, the safety of using immune checkpoint inhibitors after administering RET inhibitors is concerning. Previous studies also showed that RET fusion-positive lung cancer patients may benefit a lot from pemetrexed-based treatments (17); therefore, treatment regimens that include immunotherapy and chemotherapy must be considered. A randomized phase III trial is currently ongoing for RET fusion-positive lung cancer patients to determine the efficacy of combination therapy with selective RET inhibitors and chemotherapy ± pembrolizumab (18, 19). The results of this trial may facilitate development of better treatment regimens.

4) It is crucial to thoroughly comprehend the mechanisms of resistance for RET fusion-positive lung cancer because resistance is inevitable even in cases of initial success after administrating an RET inhibitor. In a previous study, analysis of the biopsy specimens of patients after they received selective RET inhibitors (n = 18) revealed secondary acquired RET mutations in two cases (G810), acquired MET amplification in three cases, and acquired KRAS amplification in one case. It also reported squamous or small-cell histologic transformation (20). Further research on RET inhibitor resistance and development of drugs to overcome the resistance is needed.
5) The LIBRETTO-001 trial involved a subgroup analysis of response rates considering various fusion partners such as *KIF5B*, *CCDC6*, and *NCOA4* and reported that response rates tended to be higher with the *11CCDC6* fusion partner. Because of insufficient examination due to the low frequency of RET fusion gene, further research in a larger sample size considering various treatment strategies based on fusion partners is expected.
6) RET fusion-positive lung cancer is often followed by brain metastasis, but among previously enrolled patients in clinical trials, very few were diagnosed with brain metastasis; thus, there is a lack of sufficient data concerning brain metastasis at this moment. The LIBRETTO-001 and ARROW trials had 11 and nine RET fusion-positive lung cancer patients, respectively, who also had brain metastasis (10, 11). Further examination of the response rates for RET fusion-positive lung cancer and treatment strategies for symptomatic brain metastases is critically needed.
7) Global clinical trials for these rare lung cancers are more beneficial than domestic trials, because global trials allow faster case registration and delivery of faster positive results, thus increasing the number of patients who are benefitted. Furthermore, the bias toward domestic treatment policies can also be diminished.

CONCLUSIONS

Since the discovery of RET fusion gene as a new driver gene for lung cancer in 2012, numerous clinical trials have been conducted, and many highly efficacious selective RET inhibitors have been developed. For RET fusion-positive lung cancer patients, this is good news. Pursuing various methods of RET fusion testing, treatment regimens, response results involving various fusion partners, and overcoming drug resistance will allow development of ideal treatment strategies for RET fusion-positive lung cancer patients.

AUTHOR CONTRIBUTIONS

ST wrote the manuscript. TM and NH collected previous articles. GT and MY significantly contributed to the methodology. TF, RT, and KI significantly contributed to all of the ideas of the current article. KT, TO, and TS supervised the writing of the manuscript. All authors contributed to the article and approved the submitted version.

REFERENCES

1. Kohno T, Ichikawa H, Totoki Y, Yasuda K, Hiramoto M, Nammo T, et al. KIF5B-RET Fusions in Lung Adenocarcinoma. *Nat Med* (2012) 18:375–7. doi: 10.1038/nm.2644
2. Takeuchi K, Soda M, Togashi Y, Suzuki R, Sakata S, Hatano S, et al. RET, ROS1 and ALK Fusions in Lung Cancer. *Nat Med* (2012) 18:378–81. doi: 10.1038/nm.2658
3. Lipson D, Capelletti M, Yelensky R, Otto G, Parker A, Jarosz M, et al. Identification of New ALK and RET Gene Fusions From Colorectal and Lung Cancer Biopsies. *Nat Med* (2012) 18:382–4. doi: 10.1038/nm.2673
4. Drilon A, Rekhtman N, Arcila M, Wang L, Ni A, Albano M, et al. Cabozantinib in Patients With Advanced RET-Rearranged Non-Small-Cell Lung Cancer: An Open-Label, Single-Centre, Phase 2, Single-Arm Trial. *Lancet Oncol* (2016) 17:1653–60. doi: 10.1016/S1470-2045(16)30562-9
5. Yoh K, Seto T, Satouchi M, Nishio M, Yamanoto N, Murakami H, et al. Vandetanib in Patients With Previously Treated RET-Rearranged Advanced non-Small-Cell Lung Cancer (LURET): An Open-Label, Multicentre Phase 2 Trial. *Lancet Respir Med* (2017) 5:42–50. doi: 10.1016/S2213-2600(16)30322-8
6. Gautschi O, Milia J, Filleron T, Wolf J, Carbone DP, Owen D, et al. Targeting RET in Patients With RET-Rearranged Lung Cancers: Results From the Global, Multicenter RET Registry. *J Clin Oncol* (2017) 35:1403–10. doi: 10.1200/JCO.2016.70.9352
7. Lee SH, Lee JK, Ahn MJ, Kim DW, Sun JM, Keam B, et al. Vandetanib in Pretreated Patients With Advanced Non-Small Cell Lung Cancer-Harboring RET Rearrangement: A Phase II Clinical Trial. *Ann Oncol* (2017) 28:292–7. doi: 10.1093/annonc/mdw559
8. Hida T, Velcheti V, Reckamp KL, Nokihara H, Sachdev P, Kubota T, et al. A Phase 2 Study of Lenvatinib in Patients With RET Fusion-Positive Lung Adenocarcinoma. *Lung Cancer* (2019) 138:124–30. doi: 10.1016/j.lungcan.2019.09.011
9. Horiike A, Takeuchi K, Uenami T, Kawano Y, Tanimoto A, Kaburaki K, et al. Sorafenib Treatment for Patients With RET Fusion-Positive Non-Small Cell Lung Cancer. *Lung Cancer* (2016) 93:43–6. doi: 10.1016/j.lungcan.2015.12.011
10. Gainor JF, Curigliano G, Kim D-W, Lee DH, Besse B, Baik CS, et al. Registrational Dataset From the Phase I/II ARROW Trial of Pralsetinib (BLU-667) in Patients (Pts) With Advanced RET Fusion+ Non-Small Cell Lung Cancer (NSCLC). *J Clin Oncol* (2020) 38:9515–5. doi: 10.1200/JCO.2020.38.15_suppl.9515
11. Drilon A, Oxnard GR, Tan DSW, Loong HHF, Johnson M, Gainor J, et al. Efficacy of Selpercatinib in RET Fusion-Positive Non-Small-Cell Lung Cancer. *N Engl J Med* (2020) 383:813–24. doi: 10.1056/NEJMoa2005653
12. National Comprehensive Cancer Network. *Non-Small Cell Lung Cancer (Version 3; 2020-February 11, 2020)*. Available at: https://www2.tri-kobe.org/nccn/guideline/lung/english/non_small.pdf.
13. Subbiah V, Yang D, Velcheti V, Drilon A, Meric-Bernstam F. State-Of-the-Art Strategies for Targeting RET-Dependent Cancers. *J Clin Oncol* (2020) 38:1209–21. doi: 10.1200/JCO.19.02551

14. Yang SR, Aypar U, Rosen EY, Mata DA, Benayed R, Mullaney K, et al. A Performance Comparison of Commonly Used Assays to Detect RET Fusions. *Clin Cancer Res* (2021) 27:1316–28. doi: 10.1158/1078-0432.CCR-20-3208
15. Hegde A, Andreev-Drakhlin AY, Roszik J, Huang L, Liu S, Hess K, et al. Responsiveness to Immune Checkpoint Inhibitors *Versus* Other Systemic Therapies in RET-Aberrant Malignancies. *ESMO Open* (2020) 5:e000799. doi: 10.1136/esmoopen-2020-000799
16. Oshima Y, Tanimoto T, Yuji K, Tojo A. EGFR-TKI-Associated Interstitial Pneumonitis in Nivolumab-Treated Patients With Non-Small Cell Lung Cancer. *JAMA Oncol* (2018) 4:1112–5. doi: 10.1001/jamaoncol.2017.4526
17. Drilon A, Bergagnini I, Delasos L, Sabari J, Woo KM, Plodkowski A, et al. Clinical Outcomes With Pemetrexed-Based Systemic Therapies in RET-Rearranged Lung Cancers. *Ann Oncol* (2016) 27:1286–91. doi: 10.1093/annonc/mdw163
18. Solomon BJ, Zhou CC, Drilon A, Park K, Wolf J, Elamin Y, et al. Phase III Study of Selpercatinib *vs* Chemotherapy +/- Pembrolizumab in Untreated RET Positive Non-Small-Cell Lung Cancer. *Future Oncol* (2021) 17:763–73. doi: 10.2217/fon-2020-0935
19. Besse B, Felip E, Clifford C, Louie-Gao M, Green J, Turner CD, et al. AcceleRET Lung: A Phase III Study of First-Line Pralsetinib in Patients (Pts) With RET-Fusion+ Advanced/Metastatic non-Small Cell Lung Cancer (NSCLC). *J Clin Oncol* (2020) 38:TPS9633–TPS9633. doi: 10.1200/JCO.2020.38.15_suppl.TPS9633
20. Lin JJ, Liu SV, McCoach CE, Zhu VW, Tan AC, Yoda S, et al. Mechanisms of Resistance to Selective RET Tyrosine Kinase Inhibitors in RET Fusion-Positive Non-Small-Cell Lung Cancer. *Ann Oncol* (2020) 31:1725–33. doi: 10.1016/j.annonc.2020.09.015

Conflict of Interest: As a potential personal and financial conflict of interest, RT reports personal fees from Kyowa Hakko Kirin, Nippon Kayaku, and Novartis Pharma; and grants from Abbvie, Daiichi Sankyo, Pfizer Japan, and Takeda Pharmaceutical. MY reports personal fees from AstraZeneca, Nippon Boehringer Ingelheim, Ono Pharmaceutical, and Taiho Pharmaceutical; and grants from Chugai Pharmaceutical and Pfizer Japan. TS reports grants from Bayer Yakuhin, Eisai, Merck Serono, and Novartis Pharma; personal fees from Bristol-Myers Squibb, Kyowa Hakko Kirin, Mochida Pharmaceutical, Ono Pharmaceutical, Roche Singapore, Showa Yakuhin, Taiho Pharmaceutical, and Takeda Pharmaceutical; and grants and personal fees from Astellas Pharma, AstraZeneca, Chugai Pharmaceutical, Daiichi-Sankyo, Eli Lilly Japan, Kissei Pharmaceutical, MSD, Nippon Boehringer Ingelheim, Pfizer Japan, and Yakult Honsha, outside the submitted work.

The remaining authors declare that the research was conducted in the absence of any commercial or financial relationships that could be construed as a potential conflict of interest.

Publisher's Note: All claims expressed in this article are solely those of the authors and do not necessarily represent those of their affiliated organizations, or those of the publisher, the editors and the reviewers. Any product that may be evaluated in this article, or claim that may be made by its manufacturer, is not guaranteed or endorsed by the publisher.

Copyright © 2021 Takamori, Matsubara, Haratake, Toyokawa, Fujishita, Toyozawa, Ito, Yamaguchi, Taguchi, Okamoto and Seto. This is an open-access article distributed under the terms of the Creative Commons Attribution License (CC BY). The use, distribution or reproduction in other forums is permitted, provided the original author(s) and the copyright owner(s) are credited and that the original publication in this journal is cited, in accordance with accepted academic practice. No use, distribution or reproduction is permitted which does not comply with these terms.

frontiers in Oncology

SYSTEMATIC REVIEW
published: 13 September 2021
doi: 10.3389/fonc.2021.698199

An Indirect Comparison Between Nivolumab + Ipilimumab + Two Cycles of Chemotherapy vs. Pembrolizumab + Chemotherapy as First-Line Treatment for Metastatic Non-Small Cell Lung Cancer

Panpan Jiang[1†], Ziyang Mao[1†], Qinyang Wang[1], Xiaohui Jia[1], Luying Geng[1], Hong Xu[1], Lili Jiang[1], Chengcheng Yang[1], Min Jiao[1] and Hui Guo[1,2,3]*

[1] Department of Medical Oncology, The First Affiliated Hospital of Xi'an Jiaotong University, Xi'an, China, [2] Key Laboratory of Environment and Genes Related to Diseases, Xi'an Jiaotong University, Ministry of Education of China, Xi'an, China, [3] Centre for Translational Medicine, The First Affiliated Hospital of Xi'an Jiaotong University, Xi'an, China

OPEN ACCESS

Edited by:
Junji Uchino,
Kyoto Prefectural University of Medicine, Japan

Reviewed by:
Brent McHenry,
Bristol Myers Squibb, United States
Xabier Mielgo Rubio,
Hospital Universitario Fundación Alcorcón, Spain

***Correspondence:**
Hui Guo
guohui@xjtufh.edu.cn

[†]These authors have contributed equally to this work and share first authorship

Specialty section:
This article was submitted to Thoracic Oncology, a section of the journal Frontiers in Oncology

Received: 20 April 2021
Accepted: 19 August 2021
Published: 13 September 2021

Citation:
Jiang P, Mao Z, Wang Q, Jia X, Geng L, Xu H, Jiang L, Yang C, Jiao M and Guo H (2021) An Indirect Comparison Between Nivolumab + Ipilimumab + Two Cycles of Chemotherapy vs. Pembrolizumab + Chemotherapy as First-Line Treatment for Metastatic Non-Small Cell Lung Cancer. Front. Oncol. 11:698199. doi: 10.3389/fonc.2021.698199

Background: Nivolumab + ipilimumab + two cycles chemotherapy (N-I + chemo, intensive immunotherapy but chemo-light) and pembrolizumab + chemotherapy (Pem + chemo) were both recommended as first-line treatment for metastatic non-small cell lung carcinoma (NSCLC) patients. We conducted this indirect comparison to compare the efficacy of and safety between these two treatments for providing reference for decision making.

Methods: Relevant databases were searched for eligible trials. A well-accepted adjusted indirect treatment comparison (ITC) approach was selected to pool efficacy results and safety outcomes. Subgroup analyses were stratified according to PD-L1 expression and clinical characteristics.

Results: Four eligible randomized trials (CheckMate9LA, KEYNOTE-021G, KEYNOTE 189, KEYNOTE 407) involving 2017 patients were available to analyze. The ITC results suggested that N-I + chemo is comparable to Pem + chemo in OS (HR 1.03, 95% CI 0.82-1.30) and ORR (RR 0.81, 95% CI 0.62-1.06), but tended to yield inferior PFS (HR 1.28, 95% CI 1.04-1.59) than did Pem + chemo. As for safety profiles, N-I + chemo showed no significant difference relative to Pem + chemo in any grade adverse events: (RR 1.03, 95% CI 0.99-1.10), but demonstrated reduced toxicity in chemo-related adverse events, such as anemia (RR 0.63, 95% CI 0.49-0.81), neutropenia (RR0.51, 95% CI 0.33-0.79), and thrombocytopenia (RR 0.38, 95% CI 0.21-0.69).

Conclusions: N-I + chemo is a promising treatment option for providing comparable OS related to Pem + chemo. However, for never smoker female patients, Pem + chemo is preferable to choose for demonstrating favorable OS benefit than N-I + chemo.

Keywords: pembrolizumab, nivolumab, ipilimumab, non-small cell lung cancer, efficacy, safety

INTRODUCTION

In the last decade, the treatment landscape of lung cancer has been revolutionized to the era of immunotherapy, and the most prominent representatives are immune checkpoint inhibitors (ICIs), including medications targeting programmed death receptor 1 (PD-1), programmed death-ligand 1 (PD-L1), and cytotoxic T-lymphocyte-associated protein 4 (CTLA-4) (1, 2). Advances in the 1L immunotherapy treatment of driver mutation-negative metastasis non-small cell lung cancer is remarkable (3). Multiple phase III clinical trials have verified the superior efficacy and acceptable toxicity of ICIs in this population, alone or with other regimens (4–7). However, only 20% of patients obtain long-term survival benefit from a single agent of ICIs (8). Accumulated evidence indicated that a synergistic effect of different regimens contributes to the prolonged survival outcomes (9, 10). Therefore, combination therapy was explored to improve the efficacy and expand the beneficiaries. Specifically, chemo-immunotherapy combinations demonstrated particularly encouraging survival outcomes, and among multiple regimens, pembrolizumab + chemotherapy (Pem + chemo) seemed to yield a better survival benefit (11, 12).

Most recently, a new combination approach, nivolumab and ipilimumab in combination with only two cycles of chemotherapy (N-I + chemo), was designed to administrate in CheckMate9LA (NCT 03,215,706) (13) and showed significantly prolonged OS compared with chemotherapy alone (HR=0.66,95% CI: 0.55 to 0.80) after 12.7 months of follow-up. Thus, this chemo-light combination was approved for previously untreated metastatic NSCLC regardless of PD-L1 expression by the United States Food and Drug Administration (FDA) regulatory in May 2020 (14). N-I + chemo is considered as a new promising treatment option which is associated with improved efficacy in the combination of distinct immune checkpoint inhibitors by functioning in complementary mechanisms. Besides, N-I + chemo is well tolerable due to the short cycle chemotherapeutic agents.

N-I + chemo and Pem + chemo, representing two different combination strategies, were both recommended as first-line treatment for metastatic NSCLC patients without EGFR/ALK mutation. However, there is no available direct comparisons between these two regimens to provide a reference for decision making. Indirect comparison methods (ITC) is an established approach to compare interventions from different trials and the reliability and validity of results has been confirmed to be highly consistent with direct comparisons (15, 16). Thus, we use this method to investigate the potential efficacy and safety difference among N-I + chemo and Pem + chemo in patients with NSCLC in order to offer robust evidence for clinicians, patients, and policy makers to make choices based on comprehensive considerations. Subgroup analysis stratification according to the status of PD-L1 expression and patients' characteristics also be conducted to guide clinic individualized treatment.

METHODS

Study Eligibility

We conducted a systematic search on PubMed, Embase, and the Cochrane Central Register of Controlled Trials databases to identify eligible randomized controlled trials performed before January 2021, comparing the efficacy of first-line N-I + chemo or Pem + chemo for metastasis NSCLC patients. Language was restricted to English. Relevant international conferences, such as American Society of Clinical Oncology (ASCO), European Society for Medical Oncology (ESMO), American Association for Cancer Research for Medical Oncology (AACR), and World Conference on Lung Cancer (WCLC) of recent years were also retrieved to avoid missing data. Keywords and relevant variants including "pembrolizumab," "nivolumab," "ipilimumab," "non-small-cell lung cancer," and "randomized controlled trial" were used to build a search strategy. Study screening and evaluation were conducted by two investigators independently, with disagreements solved by discussion.

Data Extraction

Two investigators (P.P.J. and Z.Y.M.) independently examined eligible studies in detail and extracted relevant data. As for conflicts, a superior investigator is involved to adjudicate. The outcomes of this study in which we were most interested included overall survival (OS), progression-free survival (PFS), and objective response rate (ORR). We also extracted the following data: treatment-related adverse events (TRAEs), events leading to discontinuation of treatment, and events leading to death. The hazard ratios (HRs) and their 95% confidence intervals (CIs) were acquired for the analysis of survival (OS and PFS), while the dichotomous data was available for ORR and TRAEs analysis. Subgroup analyses were also conducted in OS and PFS according to different PD-L1 expression, histology, sex, age, smoking status and Eastern Cooperative Oncology Group performance status (ECOG PS).

Statistical Analysis

Traditional meta-analyses were performed to compare the efficacy and safety of Pem + chemo and chemo. The adjusted indirect comparison of N-I + chemo versus Pem + chemo were achieved through an common intervention (chemotherapy), while there is direct comparison between N-I+chemo vs chemo and Pem+chemo vs chemo. The log HR of the indirect comparison was estimated as the following formula:

log HR_{AB} = log HR_{AC}–log HR_{BC}, and its standard error (SE) for the log HR was SE (log HR_{AB}) =√ (SE (log HR_{AC})^2 + SE (log HR_{AB})^2). RR was calculated similarly using this manner (17, 18). TATA 12.0 (Stata Corporation, College Station, TX) is available for all statistical analyses in this study. A two-sided P of <.05 is statistically significant.

RESULTS

Characteristics of the Eligible Studies

Study Selection and Quality Assessment

After rigorous selection, 4 relevant RCTs (5, 6, 13, 19) (involving 2017 patients) were identified for inclusion. A specific selection process is illustrated in **Figure 1**.

Updated outcomes were selected for analysis in our study for concluding reliable results. Among 4 included studies, 3 were related to Pem + chemo, and only 1 trial was on N-I + chemo. All studies but KEYNOTE 021G (NCT 02,039,674) were phase 3, international, multicenter trials. Regarding the risk of bias, the Cochrane Collaboration's risk of bias tool (20) was followed to judge. The main bias was due to insufficient follow-up time and the deficiency of data concerning immune-related adverse events in CheckMate 9LA (NCT 03,215,706). In general, bias assessment results support the high evidence level of our study (**Supplemental Table 1**). Basic characteristics of included studies are presented in **Table 1**. As can be seen from the table, the studies are basically comparable in terms of study design and patient population. Clinical outcomes available for each included RCT are summarized in **Table 2**.

Primary and Exploratory Outcomes

In direct comparison, Pem + chemo appears superior to chemo both in PFS (HR 0.53, 95% CI 0.47-0.61) and OS (HR 0.64, 95% CI 0.56-0.73) (Supplemental Figure 1), while N-I + chemo also showed advantages over chemo in PFS (HR 0.68, 95% CI 0.57-0.82) and OS (HR 0.66, 95% CI 0.55-0.80) (**Figure 2A**). Besides, Pem + chemo demonstrated improved ORR compared with chemo (HR1.90, 95% CI 1.64-2.19). Similar ORR benefit was observed in N-I + chemo vs. chemo (HR 1.54, 95% CI 1.23-1.92). In indirect comparison, N-I + chemo showed no significant difference to Pem + chemo in OS (HR 1.03, 95% CI 0.82-1.30) but is associated with inferior PFS (HR 1.28, 95% CI 1.04-1.59). Regarding ORR, N-I + chemo produced comparable benefits over Pem + chemo (RR 0.81, 95% CI 0.62-1.06) (**Figure 2A**).

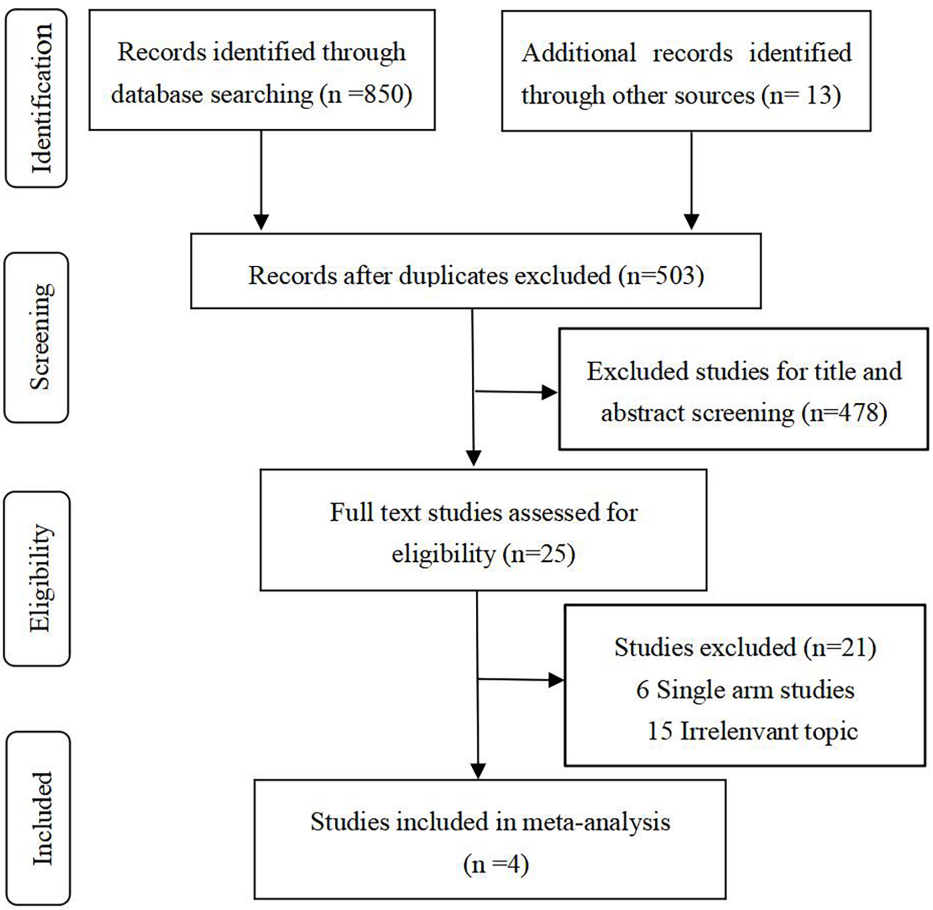

FIGURE 1 | Study flow diagram.

TABLE 1 | Baseline characteristics of included trials.

Items	CheckMate 9LA (NCT03215706)		KEYNOTE-021G (NCT02039674)		KEYNOTE-189 (NCT02578680)		KEYNOTE-407 (NCT02775435)	
Baseline Characteristics	**N-I + chemo**	**chemo**	**Pem + chemo**	**chemo**	**Pem + chemo**	**chemo**	**Pem + chemo**	**chemo**
All eligible patients	361	358	60	63	410	206	278	281
Median age (y)	65.0 (35.0-81.0)	65.0 (26.0-86.0)	62.5 (54.0-70.0)	63.2 (58.0-70.0)	65.0 (34.0-84.0)	63.5 (34.0-84.0)	65.0 (29.0-87.0)	65.0 (36.0-88.0)
Male sex (%)	70.0	70.0	37.0	41.0	62.0	52.9	79.1	83.6
Region (%)								
East-Asia	NA	NA	NA	NA	NA	NA	19.4	18.5
Non-East Asia	NA	NA	NA	NA	NA	NA	80.6	81.5
ECOG score (%)								
0	31.0	31.0	40.0	46.0	45.4	38.8	26.3	32.0
1	68.0	68.0	58.0	54.0	53.7	60.7	73.7	68.0
2	NA	NA	NA	0.0	0.2	0.0	0.0	0.0
Smoking status (%)								
Cunent/fmmer	87.0	86.0	75.0	86.0	88.3	87.9	92.1	93.2
Never	13.0	14.0	25.0	14.0	11.7	12.1	7.9	6.8
Histologic type (%)								
Squamous	31.0	31.0	0.0	0.0	0.0	0.0	97.5	97.5
Non-squamous	69.0	69.0	100.0	100.0	100.0	100.0	2.2	2.5
Brain metastases, n (%)			15.0	10.0	17.8	17.0	7.2	8.2
Liver metastases, n (%)	19.0	64.0	NA	NA	16.1	23.8	NA	NA
PD-LI TPS (%)								
≥1	60.0	61.0	65.0	64.0	63.4	62.2	63.3	63.0
1-49	38.0	32.0	32.0	37.0	31.2	28.2	37.1	37.0
≥50	22.0	29.0	33.0	27.0	32.2	34.0	26.3	26.0
<1	40.0	39.0	35.0	37.0	31.0	30.6	34.2	35.2
Follow-up time (mo)	12.7		31.0		46.3		14.3	

N-1, nivolumab plus ipilimumab; Pem, pembrolizumab; chemo, chemotherapy; y, years; NA, not available; ECOG, Eastem Cooperative Oncology Group; PS, perfmmance status; PD-L1 TPS, PD-L1 tumor proportion score; mo, months.

TABLE 2 | Infmmation on prima1y outcome of the studies included in meta-analysis.

Source	HR for OS (95%CI)					HR for PFS (95%CI)	ORR(%)		Incidence of TRAEs (%)							
	Overall	**PD-LI ≥ 50%**	**1%≤PD-LI <50%**	**PD-L1 ≥ %**	**PD-LI <1%**	**Overall**	**EM**	**CM**	**Grade 1-5 AEs**		**Grade 3-5 AEs**		**leading to discontinuation**		**leading to death**	
									EM	**CM**	**EM**	**CM**	**EM**	**CM**	**EM**	**CM**
CheckMate 9AL	0.66 (0.55-0.80)	0.66 (0.44-0.99)	0.61 (0.44-0.84)	0.64 (0.50-0.82)	0.62 (0.45-0.85)	0.68 (0.57-0.82)	38.0	25.0	92.0	88.0	49.0	40.0	19.0	7.0	2.0	2.0
Keynote021G	0.56 (0.32-0.95)					0.53 (0.33-0.86)	56.7	30.2	93.0	92.0	41.0	27.0	17.0	13.0	2.0	3.0
Keynote189	0.60 (0.50-0.72)	0.71 (0.50-1.00)	0.66 (0.47-0.93)		0.52 (0.37-0.72)	0.50 (0.41-0.59)	48.3	19.9	99.8	99.0	72.1	67.3	33.6	16.3	7.2	6.9
KEYNOTE-407	0.72(0.58-0.88)	0.79 (0.52-1.21)	0.59 (0.42-0.84)	0.67 (0.51-0.87)	0.79 (0.56-1.11)	0.57 (0.47-0.69)	62.6	38.4	98.2	97.9	69.8	68.2	27.3	13.2	4.3	1.8

OS, overall survival; PFS, progression-fi·ee survival; ORR, objective response rate; TRAEs, treatment-related adverse events; AEs, adverse events; PD-LI , programmed cell death-ligand 1; 95% CI, 95% confidence interval (CI); EM, experimental a1m; CM, control aim.

Subgroup Analysis According to PD-L1 Expression

In the PD-L1 TPS <1% population, direct comparison revealed improved OS and PFS whether N-I + chemo vs. chemo or Pem + chemo v.s chemo (**Supplemental Table 2**). Indirect results indicated that OS (HR 0.97, 95% CI 0.65-1.45) and PFS (HR 1.11, 95% CI 0.77-1.61) were comparable between N-I + chemo and Pem + chemo in this population (**Figure 3**).

In the PD-L1TPS ≥1% population, favorable OS and PFS benefit were observed in both the N-I + chemo and the Pem + chemo groups compared to chemo. Indirect comparison showed N-I + chemo was not inferior to Pem + chemo in OS (HR 0.95, 95% CI 0.66-1.39), but showed inferiority in PFS (HR 1.46, 95%

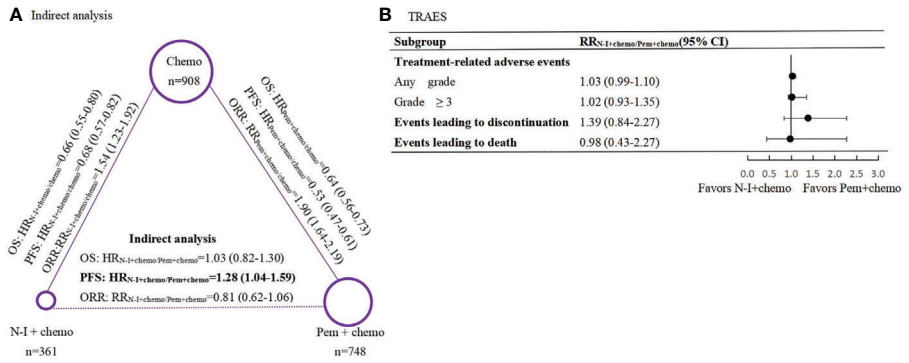

FIGURE 2 | Indirect comparisons of efficacy and safety between N-I + chemo versus Pem + chemo in first-line treatment for patients with advanced NSCLC. **(A)**, Results of indirect analysis for overall survival (OS), progression-free survival (PFS) and objective response rate (ORR) between N-I + chem and Pem + chemo. Each circular represents a treatment. The circle size is associated with the number of enrolled patients. The solid lines represent direct comparisons between the treatments, whereas the dashed line represents the indirect comparison between N-I + chemo versus Pem + chemo. **(B)**, Forest plot of risk ratios (RRs) for treatment-related adverse events (TRAEs) between N-I+chemo and Pem+chemo. N-I, nivolumab plus ipili.mumab; Pem, pembrolizumab; chemo, chemotherapy.

CI 1.11-1.92). Further subgroup analysis was conducted in patients with PD-L1 TPS 1- 49% and 50%. There was no statistical difference between N-I + chemo and Pem + chemo in terms of OS in these two populations, which were generally consistent with results in the overall PD-L1 TPS ≥1% population, indicating the convincing nature of the results. With regard to PFS, N-I + chemo appeared inferior to the PFS benefit compared to Pem + chemo in PD-L1 TPS ≥50% population, with HR of 1.69 (95% CI 1.08-2.66).

Other Subgroup Analysis

Due to the inconsistency of stratification criteria in subgroup analysis among different trials, patients ≧65 years were unavailable for analysis.

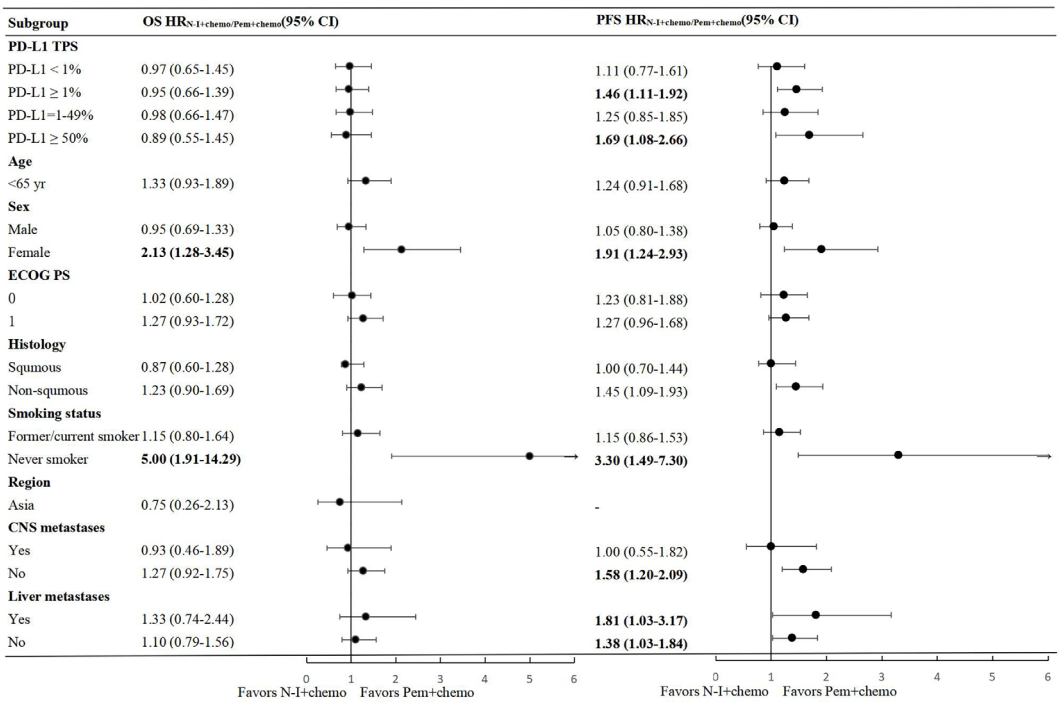

FIGURE 3 | Forest plots of hazard ratios for overall survival and progression free survival in subgroups between N-I + chemo and Pem + chemo. N-I, nivolumab plus ipilimumab; Pem, pembrolizumab; chemo, chemotherapy; CI, confidence interval; ECOG, Eastern Cooperative Oncology Group; PS, performance status.

According to indirect comparison, comparable OS and PFS was observed between N-I + chemo and Pem + chemo in pre-stratified subgroups including ECOG PS, CNS metastasis, and liver metastases (**Figure 3**), which is in accordance with the whole population. Significantly, we found females extended the survival time and postponed the tumor progression from Pem + chemo compared to N-I + chemo, with HR 0.81 (95% CI 0.29-0.78) and 0.52 (95% CI 0.34-0.81) for OS and PFS respectively. The same result appears to never smokers, with improved OS (HR 0.20, 95% CI 0.07-0.52) and PFS (HR 0.30, 95% CI 0.14-0.67) benefit from Pem + chemo than N-I + chemo. Besides, non-squamous NSCLC patients showed significant advantage from Pem + chemo than N-I + chemo in PFS (HR 0.69, 95% CI 0.52-0.92) but this advantage was not apparent in OS (HR 0.81, 95% CI 0.59-1.11).

Safety Analysis

As for safety profiles, our results demonstrated similar risks across multiple safety endpoints between N-I + chemo and Pem + chemo, including any grade AEs (RR1.03, 95% CI 0.99-1.10), grade 3-5 AEs (RR 1.02, 95% CI 0.93-1.35), events leading to drug discontinuation (RR 1.39, 95% CI 0.84-2.27), and events leading to death (RR 0.98, 95% CI 0.43-2.27) (**Figure 2B**). In terms of specific commonly reported TRAEs, N-I + chemo is associated with less hematological toxicity in contrast to Pem + chemo, such as anemia (RR 0.63, 95% CI 0.49-0.81), neutropenia (RR0.51, 95% CI 0.33-0.79), and thrombocytopenia (RR 0.38, 95% CI 0.21-0.69). Nevertheless, the rate of nausea (RR 0.70, 95% CI 0.55-0.90) and colitis (RR 0.38, 95% CI 0.21-0.69) also occurred less frequently in patients who received N-I + chemo (**Table 3**). Direct comparisons of safety between Pem + chemo and chemo are presented in **Supplemental Figure 2**.

DISCUSSION

N-I + chemo and Pem + chemo, representing two different treatment models, were both recommended as first-line treatment options for metastasis NSCLC. It is essential to understand the potential efficacy and safety difference among N-I + chemo and Pem + chemo to provide reference for clinical therapeutic determination. Through comprehensive analysis, our study revealed N-I + chemo (chemo-light) has a comparable OS benefit relative to Pem + chemo, but is associated with a less favorable PFS benefit. Furthermore, any grade AEs as the primary safety endpoint were not observed to be significantly different among N-I + chemo and Pem + chemo. Notably, patients who received N-I + two cycles of chemotherapy experienced less hematologic toxicity.

Current evidence emphasizes the superior survival benefit of Pem + chemo among multiple existing immunotherapies (11, 12, 21)

TABLE 3 | Relative risks for common treatment-related adverse events with N-1 + chemo versus Pem + chemo.

Treatment-related adverse events		$RR_{N\text{-}I+chemo/chemo}$ (95%CI)	$RR_{Pem+chemo/chemo}$ (95%CJ)	$RR_{N\text{-}J+chemo/Pem+chemo}$ (95%CJ)
Rash	Any grade	5.94 (3.19-11.04)	1.68 (1.28-2.19)	3.57 (1.79-7.14)
	Grade ≥ 3	12.67 (0.72-224.13)	1.89 (0.63-5.64)	6.67 (0.31-140.78)
Diarrhea	Any grade	1.76 (1.24-2.50)	1.39 (1.14-1.68)	1.27 (0.85-1.89)
	Grade ≥ 3	7.31 (1.68-31.74)	1.62 (0.87-3.01)	4.54 (0.92-20)
Pruritus	Any grade	1.18 (0.87-1.60)	2.08 (1.36-3.18)	0.57 (0.34-0.95)
	Grade ≥ 3	6.82 (0.35-131.63)	0.34 (0.01-8.21)	2.00 (0.03-210.04)
Fatigue	Any grade	1.56 (1.07-2.28)	1.09 (0.94-1.270	1.43 (0.95-2.13)
	Grade ≥ 3	3.90 (0.83-18.23)	1.58 (0.92-2.70)	2.44 (0.48-12.50)
Decreased appetite	Any grade	1.05 (0.75-1.46)	0.95 (0.79-1.13)	1.11 (0.75-1.61)
	Grade ≥ 3	0.97 (0.25-3.87)	1.08 (0.38-3.10)	0.90 (0.16-5)
Asthenia	Any grade	1.18 (0.87-1.60)	0.95 (0.76-1.17)	1.23 (0.85-1.82)
	Grade ≥ 3	0.27 (0.10-1.37)	1.13 (0.62-2.03)	0.33 (0.09-1.22)
Nausea	Any grade	0.75 (0.60-0.93)	1.07 (0.95-1.21)	0.70 (0.55-0.90)
	Grade ≥ 3	1.62 (0.39-6.75)	1.05 (0.52-2.14)	1.54 (0.32-7.69)
Vomiting	Any grade	0.90 (0.63-1.29)	1.30 (1.04-1.63)	0.69 (0.45-1.06)
	Grade ≥ 3	1.17 (0.36-3.80)	0.91 (0.43-1.93)	1.28 (0.32-5.26)
Constipation	Any grade	0.78 (0.50-1.21)	1.13 (0.94-1.36)	0.69 (0.43-1.11)
	Grade ≥ 3		1.08 (0.28-4.11)	
Anemia	Any grade	0.61 (0.49-0.77)	0.97 (0.87-1.09)	0.63 (0.49-0.81)
	Grade ≥ 3	0.40 (0.25-0.65)	0.93 (0.73-1.20)	0.43 (0.25-0.74)
Neutrophil count decreased	Any grade	0.27 (0.63-2.59)	1.38 (0.58-3.26)	0.92 (0.30-2.78)
	Grade ≥ 3	2.20 (0.42-11.59)	1.05 (0.82-1.34)	0.79 (0.39-1.59)
Neutropenia	Any grade	0.58 (0.39-0.86)	1.13 (0.95-1.35)	0.51 (033-0.79)
	Grade ≥ 3	0.71(0.43-1.17)	1.05 (0.82-1.34)	0.68 (0.39-1.19)
Thrombocytopenia	Any grade	0.49 (0.28-0.86)	1.30 (1.04-1.63)	0.38 (0.21-0.69)
	Grade ≥ 3	1.19 (0.50-2.84)	1.22 (0.80-1.85)	0.97 (0.22-4.35)
Colitis	Any grade	10.72 (1.39-82.62)	3.69 (1.33-10.23)	0.38 (0.21-0.69)
	Grade ≥ 3	10.72 (0.60-193.21)	3.11 (0.92-10.51)	3.45 (0.15-100)
Hypothyroidism	Any grade	55.57 (7.74-399.08)	3.88 (1.83-8.25)	14.29 (1.73-117.83)
	Grade ≥ 3	2.92 (0.01-71.55)	3.58 (0.43-29.63)	0.81 (0.02-33.33)
Adrenal insufficency	Any grade	24.37 (1.45-410.08)	1.73 (0.29-10.20)	14.29 (0.50-403.00)
	Grade ≥ 3	8.77 (0.47-162.36)	1.18 (0.18-7.97)	7.69 (0.24-249.20)

N-I, nivolumab plus ipilimumab; Pem, pembrolizumab; chemo, chemotherapy; RR, relative risk.

in first-line treatment for metastasis NSCLC. Our results showed N-I + chemo as a chemo-light therapy has comparable OS benefit compared with Pem + chemo, which encourages patients to choose N-I + chemo under similar OS benefit while chemotherapy is intolerable. Considerable OS benefit of this chemo-light combination therapy is attributed to several aspects. First, short cycle chemotherapy can increase tumor immunogenicity by eliminating tumor cells and releasing antigen (10, 22), and is also associated with enhanced PD-L1 expression and potentiated T cell-mediated cytotoxicity while treated with nivolumab (23). Moreover, distinct immune checkpoint inhibitors function in complementary mechanisms with improved efficacy (24, 25). As for insufficient PFS benefit of N-I + chemo compared to Pem + chemo revealed in our study, possible explanation may include inadequate follow-up time and unsatisfactory synergy of nivolumab and ipilimumab. Mature data updated in the future will be discussed further.

Given the expression status of PD-L1 is established biomarkers of the efficacy of immunotherapy (26), subgroup analyses according to different level of PD-L1 were conducted to guide more individualized treatment. However, no significant OS benefit difference was observed across different PD-L1 levels, which is generally identical with the results in the whole population.

Unexpectedly, our study suggests Pem + chemo appears to have significantly superior efficacy in deferring tumor progression compared with N-I + chemo in patients with PD-L1 TPS≥50%. This finding overturns our previous hypothesis that patients with high PD-L1 expression can benefit more from dual immune inhibitors. Similarly, in KEYNOTE-598 (NCT 03,302,234) (27), Pem + ipilimumab failed to improve efficacy compared to pembrolizumab monotherapy in the first-line treatment of metastatic NSCLC patients with PD-L1 > 50%, which also suggests the predictive value of PD-L1 expression is unavailable in dual immune inhibitors. Thus, valuable predictive biomarkers for N-I + chemo need further investigation to identify potential beneficiaries. With regard to the other subgroup analyses, comparable OS and PFS benefits were observed between N-I + chemo and Pem + chemo in most groups, but this result is missing females and never smokers. Intriguingly, Pem + chemo appeared more effective than N-I + chemo in females and never smokers, and there are multiple overlaps in these two populations. This result is in conformity to current research evidence. First, studies have reported that female tumors tend to have less cancer-associated antigens than male tumors (28, 29). This indicates that females have less antigenicity which resulted in a less favorable immunotherapy efficacy in female patients (30). Besides this, the disadvantage in drug pharmacokinetics and pharmacodynamics (31, 32) are both considered to be correlated with a compromised efficacy in females. As for efficacy difference observed in smokers and never smokers, potential explanation may be that smokers have different features of gene mutation (33–35) and functions of immunoregulation (36, 37), which is conductive to the response of immunotherapy. Most recent evidence further indicated smoking can promote PD-L1 expression (38) and increase TMB (8). All these factors lead to the conclusion that smokers derive more from intensive immunotherapy than never smokers. As for superior survival benefit observed in non-squamous NSCLC patients who received Pem + chemo treatment, more clinical data are demanded to confirm our findings.

Besides efficacy, the safety profiles are also an essential concern when administrating regiments. Generally, no significant difference was observed in any grade adverse events among N-I + chemo and Pem + chemo in our study. As we expected, short cycle chemotherapy under the model of N-I + chemo was associated with less hematological toxicity, indicating the application superiority for patients unable to suffer long-term standard chemotherapy. With the recent and continuous application of ICIs, increasing attention has been paid to immune-related toxicities. Noteworthy, combined immune blockage with nivolumab and ipilimumab may increase immune-related adverse events (39, 40). However, due to the sparse data, thorough immune-related adverse events are not available to analyze in our study.

As far as we are aware, our study is the first to explore the difference between N-I + chemo and Pem + chemo in NSCLC to provide valuable insight for informing clinical decision making, although of course, more evidence from real-world and direct comparisons is required to support our findings. Another strength of our study was we performed a comprehensive subgroup analysis to explore the potential efficacy difference in patients with different clinical characteristics. Inevitably, several limitations were encountered in our study. First, head-to-head comparison is lacking and there is methodological limitation of indirect comparison for integrating results of trials with heterogeneity. Besides, the immature OS data of N-I + chemo resulting from insufficient follow- up time might lead to a potential bias. Given these limitations, more reliable results based on mature and individual patient's data are required. Additionally, the regimens included in our study represent different combination strategies. However, owing to limited trials included, which treatment strategy is preferable to choose in clinical practice has not been answered. With increasing studies attempting dual checkpoint inhibition combination, future studies evaluating these two treatment models are needed to guide study design and treatment selection.

In conclusion, N-I + chemo is a promising treatment option, especially available to patients who are elderly, weak, or unable to suffer through long-term chemotherapy. However, for never smoker female patients, Pem + chemo is preferable to choose for providing superior OS benefit compared to N-I + chemo. Collectively, efficacy and toxicities should be comprehensively taken into consideration and be balanced, for further formulating individualized treatment.

DATA AVAILABILITY STATEMENT

The original contributions presented in the study are included in the article/**Supplementary Material**. Further inquiries can be directed to the corresponding author.

AUTHOR CONTRIBUTIONS

All authors contributed to the article and approved the submitted version. PJ and ZM: Writing - original draft, writing - review and editing. QW and XJ: conceptualization, methodology. LG and HX: investigation, resources, data curation, extracted data from studies, and matched inclusion and exclusion criteria. LJ and CY: software, formal analysis. MJ: visualization, project

administration. HG: supervision. All authors had full access to all data, critically revised the paper, approved the final analysis, and took responsibility for all aspects of the work to ensure that issues relating to the accuracy or integrity of any part of the work could be appropriately investigated and resolved.

FUNDING

This work was supported by Targeted Therapy Fund of Chinese Society of Clinical Oncology (Y-HR2015-139) and Chinese Society of Clinical Oncology MSD Cancer Research (Y-MSD2020-0247).

ACKNOWLEDGMENTS

We are grateful to Dr. Ke-jun Nan of Xi 'an International Medical Center Hospital for his valuable guidance on manuscript revision.

SUPPLEMENTARY MATERIAL

The Supplementary Material for this article can be found online at: https://www.frontiersin.org/articles/10.3389/fonc.2021.698199/full#supplementary-material

REFERENCES

1. Hanna NH, Robinson AG, Temin S, Baker S Jr, Brahmer JR, Ellis PM, et al. Therapy for Stage IV Non-Small-Cell Lung Cancer With Driver Alterations: ASCO and OH (CCO) Joint Guideline Update. *J Clin Oncol* (2021) 39(9):1040–91. doi: 10.1200/JCO.20.03570
2. Goetze TO. Immunotherapy: A New Era in Small-Cell Lung Cancer. *Lancet* (2019) 394(10212):1884–5. doi: 10.1016/S0140-6736(19)32235-4
3. Ackermann CJ, Adderley H, Ortega-Franco A, Khan A, Reck M, Califano R. First-Line Immune Checkpoint Inhibition for Advanced Non-Small-Cell Lung Cancer: State of the Art and Future Directions. *Drugs* (2020) 80 (17):1783–97. doi: 10.1007/s40265-020-01409-6
4. Reck M, Rodríguez-Abreu D, Robinson AG, Hui R, Csőszi T, Fülöp A, et al. Pembrolizumab Versus Chemotherapy for PD-L1-Positive Non-Small-Cell Lung Cancer. *N Engl J Med* (2016) 375(19):1823–33. doi: 10.1056/NEJMoa1606774
5. Awad MM, Gadgeel SM, Borghaei H, Patnaik A, Yang JC, Powell SF, et al. Long-Term Overall Survival From KEYNOTE-021 Cohort G: Pemetrexed and Carboplatin With or Without Pembrolizumab as First-Line Therapy for Advanced Nonsquamous NSCLC. *J Thorac Oncol* (2021) 16(1):162–8. doi: 10.1016/j.jtho.2020.09.015
6. Gadgeel S, Rodríguez-Abreu D, Speranza G, Esteban E, Felip E, Dómine M, et al. Updated Analysis From KEYNOTE-189: Pembrolizumab or Placebo Plus Pemetrexed and Platinum for Previously Untreated Metastatic Nonsquamous Non-Small-Cell Lung Cancer. *J Clin Oncol* (2020) 38 (14):1505–17. doi: 10.1200/JCO.19.03136
7. Hellmann MD, Paz-Ares L, Bernabe Caro R, Zurawski B, Kim SW, Carcereny Costa E, et al. Nivolumab Plus Ipilimumab in Advanced Non-Small-Cell Lung Cancer. *N Engl J Med* (2019) 381(21):2020–31. doi: 10.1056/NEJMoa1910231
8. Rizvi NA, Hellmann MD, Snyder A, Kvistborg P, Makarov V, Havel JJ, et al. Cancer Immunology. Mutational Landscape Determines Sensitivity to PD-1 Blockade in Non-Small Cell Lung Cancer. *Science* (2015) 348(6230):124–8. doi: 10.1126/science.aaa1348
9. Manegold C, Dingemans AC, Gray JE, Nakagawa K, Nicolson M, Peters S, et al. The Potential of Combined Immunotherapy and Antiangiogenesis for the Synergistic Treatment of Advanced NSCLC. *J Thorac Oncol* (2017) 12 (2):194–207. doi: 10.1016/j.jtho.2016.10.003
10. Emens LA, Middleton G. The Interplay of Immunotherapy and Chemotherapy: Harnessing Potential Synergies. *Cancer Immunol Res* (2015) 3(5):436–43. doi: 10.1158/2326-6066.CIR-15-0064
11. Wang C, Qiao W, Jiang Y, Zhu M, Shao J, Wang T, et al. The Landscape of Immune Checkpoint Inhibitor Plus Chemotherapy Versus Immunotherapy for Advanced non-Small-Cell Lung Cancer: A Systematic Review and Meta-Analysis. *J Cell Physiol* (2020) 235(5):4913–27. doi: 10.1002/jcp.29371
12. Ando K, Kishino Y, Homma T, Kusumoto S, Yamaoka T, Tanaka A, et al. Nivolumab Plus Ipilimumab Versus Existing Immunotherapies in Patients With PD-L1-Positive Advanced Non-Small Cell Lung Cancer: A Systematic Review and Network Meta-Analysis. *Cancers (Basel)* (2020) 12(7):1905. doi: 10.3390/cancers12071905
13. Paz-Ares L, Ciuleanu TE, Cobo M, Schenker M, Zurawski B, Menezes J, et al. First-Line Nivolumab Plus Ipilimumab Combined With Two Cycles of Chemotherapy in Patients With Non-Small-Cell Lung Cancer (CheckMate 9LA): An International, Randomised, Open-Label, Phase 3 Trial. *Lancet Oncol* (2021) 22(2):198–211. doi: 10.1016/S1470-2045(20)30641-0
14. Ettinger DS, Wood DE, Aisner DL, Akerley W, Bauman JR, Bharat A, et al. NCCN Guidelines Insights: Non-Small Cell Lung Cancer, Version 2.2021. *J Natl Compr Canc Netw* (2021) 19(3):254–66. doi: 10.6004/jnccn.2021.0013
15. Song F, Altman DG, Glenny AM, Deeks JJ. Validity of Indirect Comparison for Estimating Efficacy of Competing Interventions: Empirical Evidence From Published Meta-Analyses. *BMJ* (2003) 326(7387):472. doi: 10.1136/bmj.326.7387.472
16. Glenny AM, Altman DG, Song F, Sakarovitch C, Deeks JJ, D'Amico R, et al. Indirect Comparisons of Competing Interventions. *Health Technol Assess* (2005) 9(26):1–iv. doi: 10.3310/hta9260
17. Mauger D, Apter AJ. Indirect Treatment Comparisons and Biologics. *J Allergy Clin Immunol Pract* (2019) 7(1):131–3. doi: 10.1016/j.jaip.2018.11.008
18. Yang Q, Wei Y, Chen YX, Zhou SW, Jiang ZM, Xie DR. Indirect Comparison Showed Survival Benefit From Adjuvant Chemoradiotherapy in Completely Resected Gastric Cancer With D2 Lymphadenectomy. *Gastroenterol Res Pract* (2013) 2013:634929. doi: 10.1155/2013/634929
19. Paz-Ares L, Vicente D, Tafreshi A, Robinson A, Soto Parra H, Mazières J, et al. A Randomized, Placebo-Controlled Trial of Pembrolizumab Plus Chemotherapy in Patients With Metastatic Squamous NSCLC: Protocol-Specified Final Analysis of KEYNOTE-407. *J Thorac Oncol* (2020) 15 (10):1657–69. doi: 10.1016/j.jtho.2020.06.015
20. Higgins JP, Altman DG, Gøtzsche PC, Jüni P, Moher D, Oxman AD, et al. The Cochrane Collaboration's Tool for Assessing Risk of Bias in Randomised Trials. *BMJ* (2011) 343:d5928. doi: 10.1136/bmj.d5928
21. Halmos B, Burke T, Kalyvas C, Insinga R, Vandormael K, Frederickson A, et al. A Matching-Adjusted Indirect Comparison of Pembrolizumab + Chemotherapy vs. Nivolumab + Ipilimumab as First-Line Therapies in Patients With PD-L1 TPS ≥1% Metastatic NSCLC. *Cancers (Basel)* (2020) 12(12):3648. doi: 10.3390/cancers12123648
22. Salas-Benito D, Pérez-Gracia JL, Ponz-Sarvisé M, Rodriguez-Ruiz ME, Martínez-Forero I, Castañón E, et al. Paradigms on Immunotherapy Combinations With Chemotherapy. *Cancer Discovery* (2021). doi: 10.1158/2159-8290
23. Cavazzoni A, Digiacomo G, Alfieri R, La Monica S, Fumarola C, Galetti M, et al. Pemetrexed Enhances Membrane PD-L1 Expression and Potentiates T Cell-Mediated Cytotoxicity by Anti-PD-L1 Antibody Therapy in Non-Small-Cell Lung Cancer. *Cancers (Basel)* (2020) 12(3):666. doi: 10.3390/cancers12030666
24. Sharma P, Allison JP. Dissecting the Mechanisms of Immune Checkpoint Therapy. *Nat Rev Immunol* (2020) 20(2):75–6. doi: 10.1038/s41577-020-0275-8
25. Wei SC, Duffy CR, Allison JP. Fundamental Mechanisms of Immune Checkpoint Blockade Therapy. *Cancer Discovery* (2018) 8(9):1069–86. doi: 10.1158/2159-8290.CD-18-0367
26. Planchard D, Popat S, Kerr K, Novello S, Smit EF, Faivre-Finn C, et al. Correction to: "Metastatic non-Small Cell Lung Cancer: ESMO Clinical Practice Guidelines for Diagnosis, Treatment and Follow-Up". *Ann Oncol* (2019) 30(5):863–70. doi: 10.1093/annonc/mdy474
27. Boyer M, Şendur MAN, Rodríguez-Abreu D, Park K, Lee DH, Çiçin I, et al. Pembrolizumab Plus Ipilimumab or Placebo for Metastatic Non-Small-Cell

Lung Cancer With PD-L1 Tumor Proportion Score ≥ 50%: Randomized, Double-Blind Phase III KEYNOTE-598 Study. *J Clin Oncol* (2021). doi: 10.1200/JCO.20.03579. JCO2003579.
28. Shigematsu Y, Hanagiri T, Shiota H, Kuroda K, Baba T, Mizukami M, et al. Clinical Significance of Cancer/Testis Antigens Expression in Patients With non-Small Cell Lung Cancer. *Lung Cancer* (2010) 68(1):105–10. doi: 10.1016/j.lungcan.2009.05.010
29. Gure AO, Chua R, Williamson B, Gonen M, Ferrera CA, Gnjatic S, et al. Cancer-Testis Genes are Coordinately Expressed and are Markers of Poor Outcome in Non-Small Cell Lung Cancer. *Clin Cancer Res* (2005) 11(22):8055–62. doi: 10.1158/1078-0432.CCR-05-1203
30. Klein SL, Flanagan KL. Sex Differences in Immune Responses. *Nat Rev Immunol* (2016) 16(10):626–38. doi: 10.1038/nri.2016.90
31. Franconi F, Brunelleschi S, Steardo L, Cuomo V. Gender Differences in Drug Responses. *Pharmacol Res* (2007) 55(2):81–95. doi: 10.1016/j.phrs.2006.11.001
32. Kim AM, Tingen CM, Woodruff TK. Sex Bias in Trials and Treatment Must End. *Nature* (2010) 465(7299):688–9. doi: 10.1038/465688a
33. Pope CA 3rd, Burnett RT, Turner MC, Cohen A, Krewski D, Jerrett M, et al. Lung Cancer and Cardiovascular Disease Mortality Associated With Ambient Air Pollution and Cigarette Smoke: Shape of the Exposure-Response Relationships. *Environ Health Perspect* (2011) 119(11):1616–21. doi: 10.1289/ehp.1103639
34. Li Y, Wang Z, Nair A, Song W, Yang P, Zhang X, et al. Comprehensive Profiling of lincRNAs in Lung Adenocarcinoma of Never Smokers Reveals Their Roles in Cancer Development and Prognosis. *Genes (Basel)* (2017) 8 (11):321. doi: 10.3390/genes8110321
35. Condoluci A, Mazzara C, Zoccoli A, Pezzuto A, Tonini G. Impact of Smoking on Lung Cancer Treatment Effectiveness: A Review. *Future Oncol* (2016) 12 (18):2149–61. doi: 10.2217/fon-2015-0055
36. Givi ME, Folkerts G, Wagenaar GT, Redegeld FA, Mortaz E. Cigarette Smoke Differentially Modulates Dendritic Cell Maturation and Function in Time. *Respir Res* (2015) 16:131. doi: 10.1186/s12931-015-0291-6
37. Herberth G, Bauer M, Gasch M, Hinz D, Röder S, Olek S, et al. Maternal and Cord Blood miR-223 Expression Associates With Prenatal Tobacco Smoke Exposure and Low Regulatory T-Cell Numbers. *J Allergy Clin Immunol* (2014) 133(2):543–50. doi: 10.1016/j.jaci.2013.06.036
38. Kerdidani D, Magkouta S, Chouvardas P, Karavana V, Glynos K, Roumelioti F, et al. Cigarette Smoke-Induced Emphysema Exhausts Early Cytotoxic CD8+ T Cell Responses Against Nascent Lung Cancer Cells. *J Immunol* (2018) 201 (5):1558–69. doi: 10.4049/jimmunol.1700700
39. Larkin J, Hodi FS, Wolchok JD. Combined Nivolumab and Ipilimumab or Monotherapy in Untreated Melanoma. *N Engl J Med* (2015) 373(13):1270–1. doi: 10.1056/NEJMc1509660
40. Wei SC, Anang NAS, Sharma R, Andrews MC, Reuben A, Levine JH, et al. Combination Anti-CTLA-4 Plus Anti-PD-1 Checkpoint Blockade Utilizes Cellular Mechanisms Partially Distinct From Monotherapies. *Proc Natl Acad Sci USA* (2019) 116(45):22699–709. doi: 10.1073/pnas.1821218116

Conflict of Interest: The authors declare that the research was conducted in the absence of any commercial or financial relationships that could be construed as a potential conflict of interest.

Publisher's Note: All claims expressed in this article are solely those of the authors and do not necessarily represent those of their affiliated organizations, or those of the publisher, the editors and the reviewers. Any product that may be evaluated in this article, or claim that may be made by its manufacturer, is not guaranteed or endorsed by the publisher.

Copyright © 2021 Jiang, Mao, Wang, Jia, Geng, Xu, Jiang, Yang, Jiao and Guo. This is an open-access article distributed under the terms of the Creative Commons Attribution License (CC BY). The use, distribution or reproduction in other forums is permitted, provided the original author(s) and the copyright owner(s) are credited and that the original publication in this journal is cited, in accordance with accepted academic practice. No use, distribution or reproduction is permitted which does not comply with these terms.

frontiers in Oncology

ORIGINAL RESEARCH
published: 15 September 2021
doi: 10.3389/fonc.2021.706242

Clinical Outcome of CT-Guided Stereotactic Ablative Brachytherapy for Unresectable Early Non-Small Cell Lung Cancer: A Retrospective, Multicenter Study

Zhe Ji[1†], Bin Huo[2†], Shifeng Liu[3†], Qinghua Liang[4], Chao Xing[5], Miaomiao Hu[5], Yanli Ma[6], Zhe Wang[7], Xinxin Zhao[8], Yuqing Song[6], Yufeng Wang[9], Hongmei Han[8], Kaixian Zhang[5], Ruoyu Wang[7], Shude Chai[2], Xuequan Huang[4], Xiaokun Hu[3*] and Junjie Wang[1*] on behalf of China North Radioactive Brachytherapy Group (CNRBG)*

[1] Department of Radiation Oncology, Peking University Third Hospital, Beijing, China, [2] Department of Thoracic Surgery/Department of Oncology, The Second Hospital of Tianjin Medical University, Tianjin, China, [3] Department of Intervention Therapy, The Affiliated Hospital of Qingdao University, Qingdao, China, [4] Center of Minimally Invasive Intervention, Southwest Hospital of Army Medical University (The First Hospital Affiliated to the Army Medical University), Chongqing, China, [5] Department of Oncology, Tengzhou Central People's Hospital, Tengzhou, China, [6] Department of Oncology, Staff Hospital of Chengde Iron and Steel Group Co. Ltd., Chengde, China, [7] Department of Radiation Oncology, Affiliated Zhongshan Hospital of Dalian University, Dalian, China, [8] Department of Oncology Radiotherapy, The First People's Hospital of Kerqin District, Tongliao, China, [9] Department of Nuclear Medicine, Xuzhou Cancer Hospital, Xuzhou, China

OPEN ACCESS

Edited by:
Hideharu Kimura,
Kanazawa University, Japan

Reviewed by:
Angelo Carretta,
Vita-Salute San Raffaele University, Italy
Xuchao Zhang,
Guangdong Provincial People's Hospital, China

***Correspondence:**
Xuequan Huang
hxuequan@163.com
Xiaokun Hu
huxiaokun770@163.com
Junjie Wang
junjiewang_edu@sina.cn

[†]These authors share first authorship

Specialty section:
This article was submitted to Thoracic Oncology, a section of the journal Frontiers in Oncology

Received: 07 May 2021
Accepted: 23 August 2021
Published: 15 September 2021

Citation:
Ji Z, Huo B, Liu S, Liang Q, Xing C, Hu M, Ma Y, Wang Z, Zhao X, Song Y, Wang Y, Han H, Zhang K, Wang R, Chai S, Huang X, Hu X and Wang J (2021) Clinical Outcome of CT-Guided Stereotactic Ablative Brachytherapy for Unresectable Early Non-Small Cell Lung Cancer: A Retrospective, Multicenter Study. Front. Oncol. 11:706242. doi: 10.3389/fonc.2021.706242

Objective: To analyze the efficacy and safety of low dose rate stereotactic ablative brachytherapy (L-SABT) for treatment of unresectable early-stage non-small cell lung cancer (NSCLC).

Methods: Data of patients with early-stage NSCLC who received CT-guided L-SABT (radioactive I-125 seeds implantation) at eight different centers from December 2010 to August 2020 were retrospectively analyzed. Treatment efficacy and complications were evaluated.

Results: A total of 99 patients were included in this study. Median follow-up duration was 46.3 months (6.1-119.3 months). The 1-year, 3-year, and 5-year local control rates were 89.1%, 77.5%, and 75.7%, respectively. The 1-year, 3-year, and 5-year overall survival rates were 96.7%, 70.1%, and 54.4%, respectively. Treatment failure occurred in 38.4% of patients. Local/regional recurrence, distant metastasis, and recurrence combined with metastasis accounted for 15.1%, 12.1%, and 11.1%, respectively. Pneumothorax occurred in 47 patients (47.5%) with 19 cases (19.2%) needing closed drainage. The only radiation-related adverse reaction was two cases of grade 2 radiation pneumonia. KPS 80–100, T1, the lesion was located in the left lobe, GTV D90 ≥150 Gy and the distance between the lesion and chest wall was < 1 cm, were associated with better local control (all $P < 0.05$); on multivariate analysis KPS, GTV D90, and the distance between the lesion and chest wall were independent prognostic factors for local control (all $P < 0.05$). KPS 80–100, T1, GTV D90 ≥150 Gy, and the distance between the lesion and chest wall was < 1 cm were also associated with better survival (all $P < 0.05$); on

multivariate analysis KPS, T stage, and GTV D90 were independent prognostic factors for survival (all $P < 0.05$). The incidence of pneumothorax in patients with lesions <1 cm and ≥1cm from the chest wall was 33.3% and 56.7%, respectively, and the differences were statistically significant ($P = 0.026$).

Conclusion: L-SABT showed acceptable efficacy in the treatment of unresectable early-stage NSCLC. But the incidence of pneumothorax is high. For patients with T1 stage and lesions <1 cm from the chest wall, it may have better efficacy. Prescription dose greater than 150 Gy may bring better results.

Keywords: early non-small cell lung cancer, stereotactic ablative brachytherapy, radioactive seed implantation, efficacy, prognostic factors

INTRODUCTION

Surgery is the main treatment for early non-small cell lung cancer (NSCLC). For unresectable early NSCLC, stereotactic ablative radiotherapy (SABR) is considered the best option (1). However, in the real-world clinical practice, the situation can be more complex. There are also some patients who cannot be operated on who also did not receive external beam radiotherapy (EBRT) because of various reasons. For these patients, the prognosis is poor, with a 5-year survival rate of less than 10% (2). With the development of clinical practice, radioactive I-125 seed implantation (RISI) is more widely used in the local treatment of tumors. This method is to implant the radioactive I-125 seeds into the tumor, and the tumor cells will be killed by continuous gamma ray irradiation generated by the seeds (3). In view of the high dose and low fraction of brachytherapy, we also called RISI as low dose rate stereotactic ablative brachytherapy (L-SABT) (4). L-SABT has been reported to be a safe and effective treatment for various solid tumors (5–8), which provides another treatment option for the clinic. However, L-SABT has rarely been used for the treatment of early-stage tumors (except prostate cancer), and so there is limited data about its efficacy in these cases. This study retrospectively analyzed the data of patients with early NSCLC who received L-SABT, in order to further clarify the clinical efficacy and safety of L-SABT and provide data for the actual clinical practice of the real world.

MATERIAL AND METHODS

Patients

Due to the small number of patients receiving L-SABT for early stage NSCLC, this study combined the data of 8 medical centers between December 2010 and August 2020. Case selection criteria include: (1) they had received pathologically confirmed diagnosis of NSCLC (squamous cell carcinoma or adenocarcinoma, excluding other types of NSCLC) at first visit; (2) they had stage T1–3N0M0 (stage Ia–IIb) based on the UICC TNM classification 8th edition (9) after systemic evaluation (evaluation methods include CT/MRI and/or PET-CT), the re-staging was carried out for cases before 2016; (3) they were not suitable for surgery after being evaluated by an experienced thoracic surgeon or pulmonologist; (4) L-SABT had been used as the initial treatment; (5) D90 (dose that covers 90% of target volume) had been ≥100 Gy on post-treatment evaluation. A total of 99 patients satisfied these criteria and were included in this study.

L-SABT treatment was conducted after obtaining informed consent from patients and their families. This retrospective study has been approved by the ethical committee.

Devices and Instruments

(1) CT: Brilliance Bigbore CT, Philips. (2) I-125 seeds: type 6711_1985, from HTA Co., Ltd, with a half-life of 59.4 days and dose rate constant of 0.965 cGy/(h·U). (3) Radioactive I-125 seed implantation devices: Mick Radio-Nuclear Instruments and Eckert & Ziegler BEBIG. (4) Brachytherapy treatment planning system (BTPS): KLSIRPS-3D, Beijing University of Aeronautics and Astronautics and Beijing Astro Technology LTD, CO., which can calculate and display dose distribution of the target area and generate a dose-volume histogram (DVH). Planning system source data originated from the official, supplementary and reports, and update of the American Association of Physicists in Medicine (AAPM) (10–12).

Preoperative Planning

Enhanced CT scan, with 5-mm slice thickness, was performed within 1 week before seed implantation. The imaging data were transmitted to the treatment planning system for preoperative evaluation and plan design. The treatment planning design involved delineation of gross tumor volume (GTV) and organs at risk (OARs); determination of prescription doses and seed radioactivity; determination of the puncture needle direction, distribution, and depth of insertion; determination of seed quantity; and simulation of the spatial distribution of seeds. The prescription dose was empirically set as ≥100 Gy.

Seeds Implantation

Seeds implantation was performed under 1% lidocaine infiltration anesthesia. The disposable seed implantation needle was inserted into the target lesion under CT guidance. The needle tip was positioned 0.5 cm from the distal tumor margin. The space between each row of needles and between

each seed was 0.5–1.0 cm. CT scan was performed after seeds implantation to make sure that the seeds distribution was as per the treatment plan. When necessary, additional seeds were implanted to avoid dosimetric cold spots.

Postoperative Management and Dose Verification

All patients received anti-infection and hemostasis treatment after implantation. Chest CT scan was performed 24 hours after operation to rule out pneumothorax, hemorrhage, and other complications. Postoperative dose verification was performed (**Figure 1**).

Evaluation Indices

The main evaluation index was the local control rate. The secondary evaluation indices were overall survival, adverse reactions, and failure reasons. CT scan was used to detect tumor size changes during follow-up. The International Response Evaluation Criteria in Solid Tumor (RECIST) were used to evaluate treatment response (13). Complete response was defined as complete disappearance of the target tumor. Partial response was defined as a decrease of target lesion diameter to ≤30% of that at baseline. Progressive disease was defined as target lesion diameter increase by ≥20% or the appearance of new lesions. Stable disease was defined as any change intermediate between partial response and progressive disease. Puncture complications and radiation-related adverse reactions were graded according to Common Terminology Criteria for Adverse Events (CTCAE) version 5.0 (14); there were five grades, as follows: minor/grade 1 (no symptoms and no treatment required), moderate/grade 2 (symptoms present and treatment required), severe/grade 3 (symptoms not controlled by drugs, and instrumentation or invasive procedure required), life-threatening/grade 4 (emergency treatment required), and death/grade 5.

The factors assessed for influence on prognosis included the following: sex, KPS score, stage, pathological type, lesion location, and GTV D90 (dose received by 90% of GTV).

Statistical Analysis

SPSS 25.0 (IBM Corp., Armonk, NY) was used for statistical analysis. Measurement data was expressed in median value (range) or mean value ± standard deviation and numeration data was expressed in absolute value and/or percentage value. The chi-square test was used to compare rates between groups. The Kaplan–Meier method was used to calculate the local control rate and survival rate. Log rank test was used for univariate analysis and Cox regression analysis was used for multivariate analysis. $P \leq 0.05$ was considered statistically significant.

RESULTS

Patients

A total of 99 patients were included in this study. The median age was 69.8 ± 9.06 years old (range, 49–91 years old). The median Karnofsky Performance Status (KPS) score was 80 (range, 60–100). Clinical stages were 47 cases (47.5%) of T1N0M0, 37 cases (37.3%) of T2N0M0, and 15 cases (15.2%) of T3N0M0. Pathological types were 45 cases (45.5%) of squamous cell carcinoma and 54 cases (54.5%) of adenocarcinoma. Because of the differences in patients' economic conditions and medical conditions in local hospitals, 21 patients (21.2%) were staged by CT/MRI and the remaining 78 patients (78.8%) were staged by PET-CT.

Seeds Implantation

Median lesion diameter was 3.2 ± 1.22 cm (range, 1.1-6.4 cm). The median number of seeds implanted was 41.8 ± 20.97 (range, 9-110). Median seeds radioactivity was 0.7 ± 0.07 mCi (range, 0.6–0.8 mCi). Median number of needles was 8 ± 4 (range, 2–25). Median postoperative GTV D90 was 165.8 ± 41.08 Gy (range, 110.4–278.8 Gy).

Treatment Response

At the end of February 2021, the median follow-up duration was 46.3 months (range, 6.1-119.3 months). The 1-year, 3-year, and

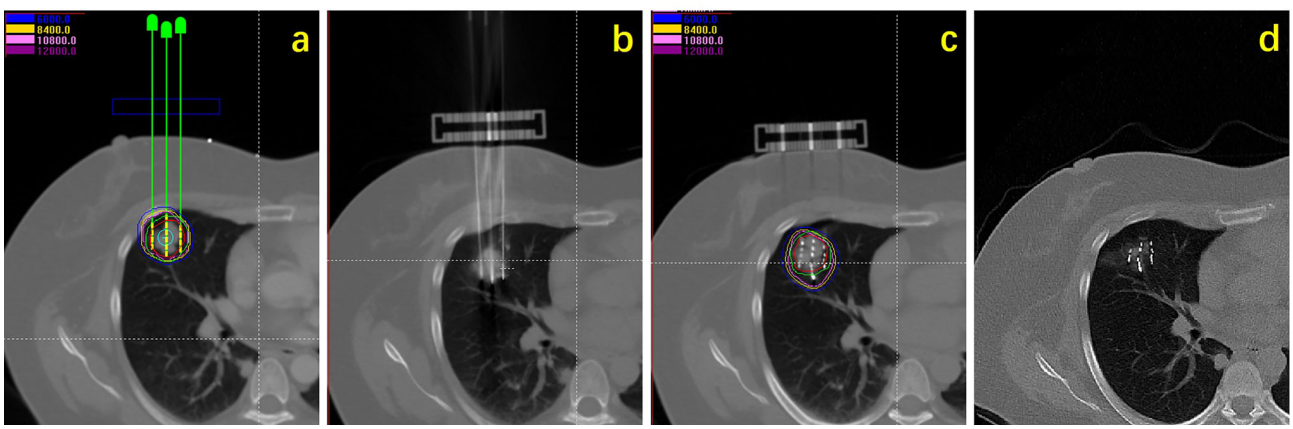

FIGURE 1 | Flow chart showing procedure of seeds implantation: **(A)** Preoperative planning design; **(B)** intraoperative needle insertion; **(C)** seeds implantation and dose verification; **(D)** efficacy observation.

5-year cumulative survival rates for the whole group were 96.7%, 70.1%, and 54.4%, respectively. The 1-year, 3-year, and 5-year progression-free survival rates were 79.5%, 61.10%, and 52.7%, respectively. The 1-year, 3-year, and 5-year local control rates were 89.1%, 77.5%, and 75.7%, respectively. Thirty-five patients (35.4%) died, and 64 patients (64.6%) survived. A total of 38 patients experienced treatment failure, including 10 cases (10.1%) of local recurrence, 4 cases (4.0%) of reginal recurrence, 12 cases (12.1%) of distant metastasis, 1 case (1.0%) of local recurrence with reginal recurrence, 9 cases (9.1%) of local recurrence with distant metastasis, and 2 cases (2.0%) of reginal recurrence with distant metastasis.

Procedure-related complications included pneumothorax, subcutaneous emphysema, hemothorax, hemoptysis, and seeds migration. Pneumothorax was the most common complication, with an incidence of 47.5% (47/99 patients). There were 19 (19.2%) patients with pulmonary compression volume >30%, and they were treated with invasive closed drainage, and all recovered. Most of the complications were grade 1, and only a few were grade 2. There were no grade 3-5 complications (**Table 1**).

Radiation-related adverse reaction was seen in only 2 patients (2.0%) with grade 2 radiation pneumonia. No patient had skin reaction, esophagitis, myelitis, or other visible side effects (**Table 1**).

Factors Affecting Outcomes

On univariate analysis, the factors significantly associated with better overall survival rate were KPS score 80–100, T1 stage, GTV D90 ≥150 Gy, and the distance between the lesion and chest wall was < 1 cm (all $P < 0.05$) (**Table 2**). The 5-year survival rates were 61.3%, 71.4%, 68.1%, and 66.9%, respectively. The factors significantly associated with better local control rate were KPS score 80–100, T1 stage, the lesion was located in the left lobe, GTV D90 ≥150 Gy, and the distance between the lesion and chest wall was < 1 cm (all $P < 0.05$) (**Table 2**). The 5-year local control rates were 81.3%, 86.6%, 90.2%, 87.4%, and 88.7%, respectively. If the dose was further subdivided, the 5-year local control rates of patients with GTV D90 <150 Gy, 150-180 Gy, and >180 Gy were 58.5%, 78.8%, and 96.3% ($P = 0.005$), respectively (**Figure 2G**). Moreover, the 5-year survival rates of patients with GTV D90 <150 Gy, 150-180 Gy, and >180 Gy were 36.1%, 70.7%, and 66.7% ($P = 0.023$), respectively (**Figure 2H**). The 5-year survival rates of male and female patients were 49% and 72.1%, respectively. The difference was close to statistically significant ($P = 0.052$). On multivariate analysis, KPS score, T stage, and GTV D90 were independent factors for survival, and KPS score, GTV D90, and distance between the lesion and chest wall were independent factors for local control ($P < 0.05$) (**Figures 2**, **3**).

In terms of complications, the number of needles and the distance between the lesion and chest wall was significantly correlated with the incidence of pneumothorax. The incidence of pneumothorax in patients with ≤ 6 needles (n=47) and > 6 needles (n=52) was 36.2% and 57.7%, respectively, and the incidence of pneumothorax in patients with lesions <1 cm (n=39) and ≥1cm (n=60) from the chest wall was 33.3% and 56.7%, respectively. The differences were statistically significant (P=0.044 and 0.026, respectively). The postoperative dose (GTV D90) of 2 patients with radiation pneumonitis was 144 Gy and 208.8 Gy, respectively.

TABLE 1 | Complications.

Complications	N	%
Pneumothorax		
No	52	52.5
Yes	47	47.5
Subcutaneous emphysema		
No	96	97.0
Grade 1	3	3.0
Hemothorax		
No	86	86.9
Grade 1	13	13.1
Hemoptysis		
No	67	67.7
Grade 1	30	30.3
Grade 2	2	2.0
Radiation pneumonitis		
Grade 0-1	97	98.0
Grade 2	2	2.0
Seed shifting		
No	97	98.0
Yes	2	2.0

DISCUSSION

The standard treatment for T1–3N0M0 (Ia–IIb) NSCLC is surgery and radical EBRT (including SABR) (1). Currently, few clinicians would choose L-SABT as a treatment for early NSCLC patients, even if surgery is infeasible. However, L-SABT treatment maybe a reasonable choice, with several unique advantages. First, the half-valence layer of I-125 seeds in tissue is 1.7 cm. The dose to the tumor target area is extremely high, while the dose to the surrounding normal tissue is low. The dose rate of γ-ray is low (8–10 cGy/h), which is theoretically less likely to damage normal tissue (15). Second, the distribution of seeds in the lesion can be adjusted during the operation to ensure that the dose distribution in the target area conforms to the actual tumor outline; thus, with L-SABT it is possible to achieve intensity-modulated radiation in a true sense, with better treatment efficacy and less risk of adverse reactions. Third, the γ-rays generated continuously by implanted seeds kill tumor cells over a long period, which could well overcome the errors caused by internal target volume (ITV) and planning target volume (PTV) during treatment. The dose management is more accurate. Fourth, the patient only needs to be hospitalized once, and so the treatment experience is better. Finally, the operation and required facilities (software and hardware) are relatively simple and a linear accelerator is not required, which means the cost of treatment is relatively low and the procedure can even be performed in a primary care hospital. Therefore, in the real-world clinical practice, there are still a few patients with early-stage NSCLC who cannot be operated on who have received L-SABT treatment. This retrospective study focuses on the cases from 8 medical centers over a period of

TABLE 2 | Univariate analysis of factors associated with local control and survival.

Factors	N	Local control rates			p	Overall survival rates			p
		1-year (%)	3-year (%)	5-year (%)		1-year (%)	3-year (%)	5-year (%)	
Gender					0.188				0.052
Male	72	86.7	74.3	71.9		95.7	62.9	49.0	
Female	27	95.8	86.7	86.7		100.0	90.3	72.1	
KPS					0.006				0.016
60-70	15	73.3	59.3	47.4		93.3	51.9	22.2	
80-90	84	92.3	81.3	81.3		96.1	74.0	61.3	
T stage					0.023				0.001
T1	46	95.2	86.6	86.6		97.6	84.3	71.4	
T2-3	53	84.0	70.1	66.0		96.0	58.0	37.2	
Methods of staging					0.320				0.523
PET-CT	78	89.1	81.2	78.9		95.9	71.5	57.9	
CT/MRI	21	89.2	64.7	64.7		100	64.5	43	
Location of lesions					0.011				0.300
Left lobe	41	97.2	90.2	90.2		94.7	71.4	62.6	
Right lobe	58	83.5	68.9	66.1		98.1	69.0	48.7	
Location of lesions					0.572				0.211
Upper lobe	63	87.8	75.9	73.4		98.3	72.9	59.3	
Middle/lower lobe	36	91.3	80.1	80.1		94.1	65.3	46.0	
Pathology					0.242				0.114
SCC*	45	83.3	70.8	70.8		95.2	56.3	52.0	
ADC*	54	94.0	82.7	79.7		98.0	80.8	57.3	
D90					0.004				0.009
≤150 Gy	42	84.8	63.8	59.8		97.4	63.3	36.7	
>150 Gy	57	92.2	87.4	87.4		96.3	74.8	68.1	
Distance from CW*					0.012				0.016
≥1cm	60	82.9	69	64.9		96.2	56.8	46.0	
<1cm	39	97.4	88.7	88.7		97.4	86.3	66.9	

SCC, squamous cell carcinoma; ADC, adenocarcinoma; CW, chest wall.

10 years (2010-2020), which belongs to a relatively large sample study in terms of L-SABT treatment of early NSCLC. We hope that the data of efficacy and toxicity obtained in this study can help clinicians to understand and to evaluate the safety and effectiveness of this treatment for early-stage NSCLC.

In this study, the 3-year and 5-year local control rate was 77.5% and 75.7% (86.6% for T1 patients). In the study of Martinez-Monge et al., they treated 7 T1N0M0 NSCLC patients with L-SABT, a good local control was also found. After median follow-up of 13 months (range, 4.6–41.0+ months) they found no local or regional recurrence (16). Although studies on SABR showed the 3-year local control rate to be ≥90% (17–19), in some studies with long-term follow-up the 5-year local control rate was about 80% (20–22). It could be considered that local control rate of L-SABT may be comparable with SABR. In this study, a large dose span has been observed (100-278.8 Gy), D90 was the independent predictor of local control and overall survival. The local control rate was higher in patients with high D90. For patients with D90 >180 Gy, the local control rate was even as high as 96.3% at 5 years. Moreover, there were no grade 3 or above toxicities. It is suggested that if the dose is further increased, the effect of SABR may be reached or exceeded. In non-prostate tumors, few studies have reported the relationship between the dose of radioactive seeds and local control. In our study, as expected, patients with higher dose had better local control. Although, according to the ABS (American Brachytherapy Society) guidelines, the recommended dose for single application is 100–125 Gy (23), our patients received higher doses on the premise that better efficacy could be achieved without increasing the risk of toxicity. In univariate analysis, T stage and D90 were the influencing factors of local control, but in multivariate analysis, only D90 was the independent influencing factor, suggesting that dose may play a more important role in local control than T stage. In the future, relevant dosimetry studies should be carried out to further clarify the optimal tumor control dose. In addition, in our study, patients with lesions that were close to the chest wall had better local control and survival. Compared with SABR and thermal ablation, for which we need to pay attention to the chest wall toxicity and reaction, L-SABT may be more suitable for this group (lesions <1 from the chest wall). In our sample, the 1-year, 3-year, and 5-year survival rates in this study were 96.7%, 70.1%, and 54.4%, respectively. The 5-year survival rate of T1 patients was 71.4%. Distant metastasis was still the main cause of failure (23.2%), which was similar to that of SABR. Univariate analysis showed that T stage, GTV D90, and distance between the lesion and chest wall were influence factors for survival. However, in multivariate analysis, distance between the lesion and chest wall did not become an independent factor for survival, which may be related to the fact that most of the patients with lesions < 1cm from the chest wall were more likely to be T1 and could reach higher doses. Thermal ablation can also be used as a potentially effective treatment for early NSCLC that is not suitable for surgery (1). The 1-year and 3-year local

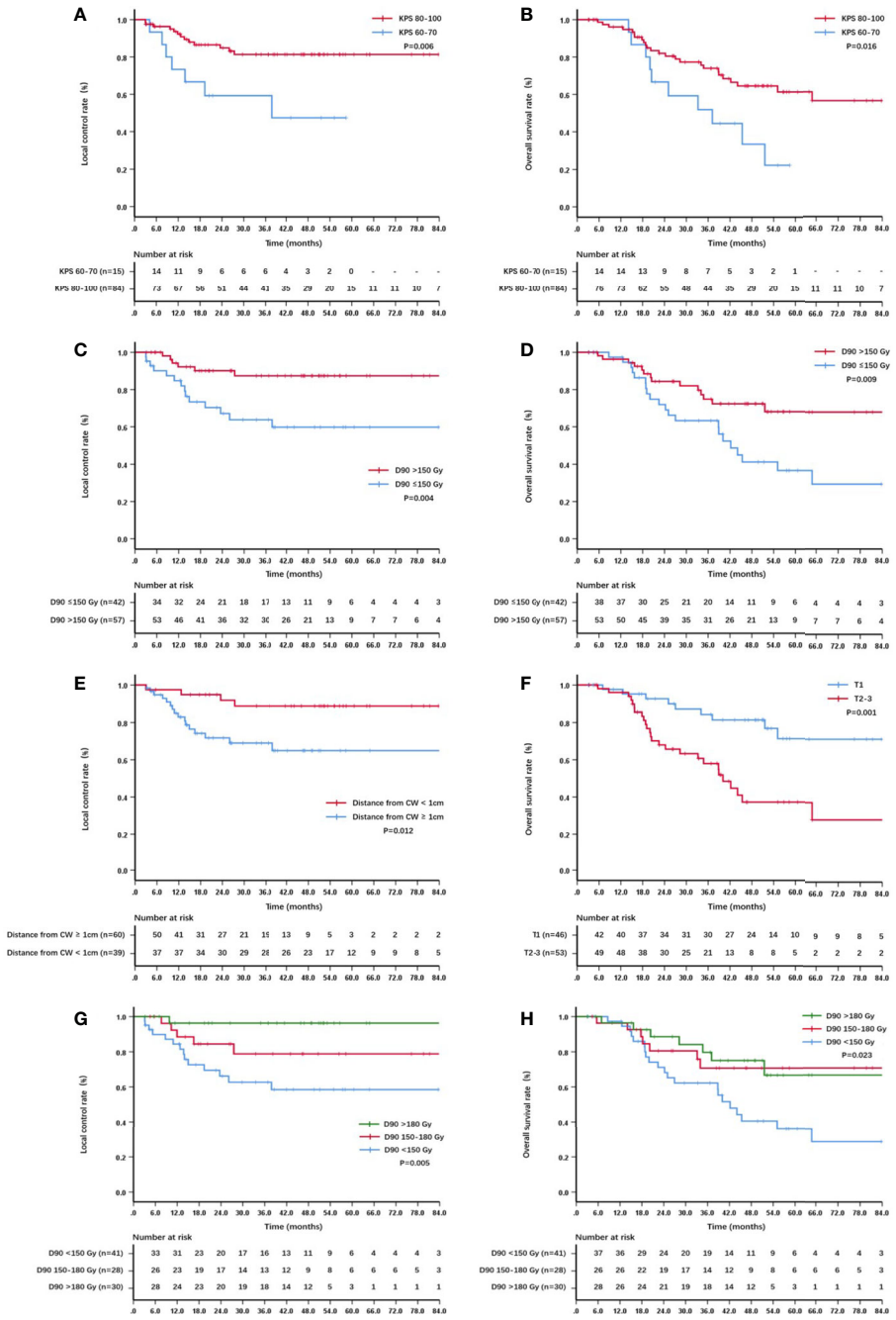

FIGURE 2 | Kaplan–Meier curve about local control and survival: **(A)** The local control of patients with KPS score 60-70 and 80–100; **(B)** the overall survival of patients with KPS score 60-70 and 80–100; **(C)** the local control of patients with GTV D90 <150 Gy and ≥150 Gy; **(D)** the overall survival of patients with GTV D90 <150 Gy and ≥150 Gy; **(E)** the local control of patients with lesions <1 cm and ≥1cm from the chest wall; **(F)** the overall survival of patients with T1 and T2-3; **(G)** the local control of patients with D90 <150 Gy, 150-180 Gy,and >180 Gy; **(H)** the overall survival of patients with D90 <150 Gy, 150-180 Gy and >180 Gy.

control rates can reach 86.0%-96.0%, 64.0% - 77.5%, respectively, and the 1-, 3-, and 5-year survival rates can reach 70.0%-96.0%, 43.0%-67.1%, and 16.0%-36.3%, respectively (24–27). This study has similar local control rates and even better survival rates compared with that.

The main consideration limiting the use of external beam radiation dose is radiation-related adverse reaction. About 5%–10% of patients treated with SABR suffer grade 3 or above toxicities and side effects (pneumonia, chest pain, hemoptysis, and so on) (18, 20, 28). In some studies, the proportion is as high

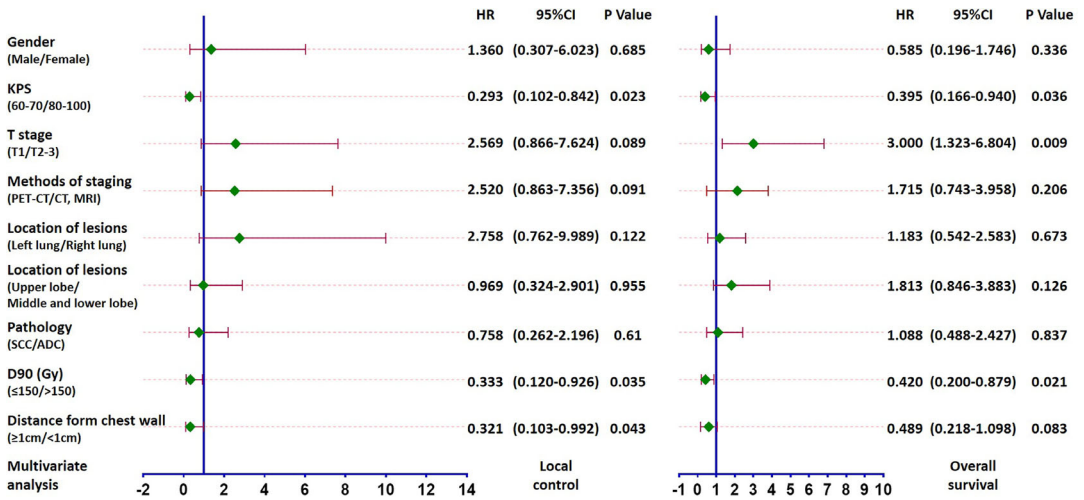

FIGURE 3 | Forest plot based on multivariate analysis of local control and survival: KPS score, GTV D90, and distance between the lesion and chest wall were independent factors for local control and KPS score, T stage and GTV D90 were independent factors for survival (all P < 0.05).

as 15%–30% (21, 22, 29). The incidence of radiation toxicities and side effects is very low with L-SABT. In some studies on head and neck tumors and chest wall tumors, the incidence of grade 1 and 2 skin/mucosa adverse effects was 7%–30%; no grade 3 or 4 toxicities were reported, although most of the patients had received radiotherapy previously (6, 30). One previous study has shown that L-SABT could increase the risk of esophageal fistula and tracheal fistula if the lesion is located in the mediastinum (31). However, the mediastinum is not invaded in early lung cancer. The present study also showed low toxicity with L-SABT. Two patients (with D90 of 144 Gy and 208.8 Gy, respectively) had grade 2 radiation pneumonia which improved with medication. However, it should be noted that there is limited data, and the dose/toxicity relationship of L-SABT needs to be further investigated.

Unlike external radiotherapy, L-SABT treatment is invasive and so there may be puncture-related complications. In the present study, the most common complication was pneumothorax, with an incidence of 47.5%. In previous studies about percutaneous lung biopsy, the incidence of pneumothorax was mostly <30%, with <10% of patients needing drainage (32–34). Pneumothorax is also the most common complication in the ablation therapy of early-stage lung cancer, with an incidence of 12% - 63.8% (24–27). The incidence of pneumothorax was higher in our study, probably because of the longer operation time of L-SABT and the higher number of puncture needles used when compared with the previous studies. The incidence of puncture complications was related to many factors such as operation time, needle adjusting frequency, lesion size, and so on (32–35). In the analysis of influencing factors in this study, the incidence of pneumothorax was lower in patients with ≤ 6 needles and < 1cm from the lesion to the chest wall, which again suggested that patients with smaller lesions and lesions that were closer to the chest wall might be more suitable for L-SABT treatment. Most other complications were mild and had low incidence. In general, the safety of L-SABT treatment is considered acceptable according to the data of this study.

The main shortcoming of previous L-SABT was that the treatment depends too much on personal experience and the quality of implantation was difficult to guarantee. Therefore, the dose range in our study was relatively large (100–278.8 Gy). Recently, we developed a 3D printing template (3DPT) technology. It has been proved that there is favorable consistency between the postoperative dose and preoperative dose through 3DPT combined with CT guidance, which can provide quality assurance for the L-SABT study (36). In addition, seeds strand (37), navigation technology (38), and robotics technology (39), which can be applied to L-SABT, are expected to further improve the accuracy and efficiency of treatment and reduce the incidence of the complications, so that L-SABT in the local treatment of cancer may be more standardized and widely used in the future.

The limitations of the study were as follows: (1) In clinical practice there are very few patients with early NSCLC who do not undergo surgery or SABR and receive L-SABT instead, so the sample size was small (difficult to form big data). (2) Because of the retrospective study, the further details of reasons for not performing surgery or EBRT were not recorded. (3) The toxicities information was not collected in detail enough, and the data obtained are only for reference. (4) Because most of the patients and their families who received L-SABT were not willing to treat their diseases actively enough, the patients' combined treatments (such as chemotherapy, targeted therapy, and so on) was very seldom and difficult to count in detail, which may potentially affect the treatment outcome. It is hoped that there will be an opportunity for future prospective study to further clarify the results of the study.

CONCLUSION

The efficacy of L-SABT was closed to SABR and had low radiotoxicity in the treatment of inoperable early-stage NSCLC. Despite some unique advantages, due to the invasive operation and high incidence of pneumothorax, it is not suitable to be recommended as superior to SABR. If EBRT is not available, it may be used as one of the treatment options under the condition of full multidisciplinary evaluation and informed notification. Especially for patients with T1 lesions and < 1cm from the chest wall, L-SABT may become a more suitable potential candidate, and prescription dose greater than 150 Gy (preferably greater than 180 Gy) may bring better results. With the progress of implantation equipment and technology, if we can further improve the quality of operation and reduce the incidence of complications, L-SABT has the potential to become one of the competitive treatment methods.

DATA AVAILABILITY STATEMENT

The raw data supporting the conclusions of this article will be made available by the authors, without undue reservation.

ETHICS STATEMENT

The studies involving human participants were reviewed and approved by Peking University Third Hospital Medical Science Research Ethics Committee.

AUTHOR CONTRIBUTIONS

1. Guarantor of integrity of the entire study: JW, XQH and XKH. 2. Study concepts and design: JW and SC. 3. Literature research: ZJ and BH. 4. Clinical studies: QL, CX, MH, YM, ZW, XZ, YS, YW and HH. 5. Experimental studies/data analysis: ZJ, BH, SL, QL, CX, ZW. 6. Statistical analysis: ZJ and SL. 7. Manuscript preparation: ZJ, BH and SL. 8. Manuscript editing: KZ, RW and SC. All authors contributed to the article and approved the submitted version.

SUPPLEMENTARY MATERIAL

The Supplementary Material for this article can be found online at: https://www.frontiersin.org/articles/10.3389/fonc.2021.706242/full#supplementary-material

REFERENCES

1. National Comprehensive Cancer Network (NCCN). *Clinical Practice Guidelines in Oncology: non-Small Cell Lung Cancer, Version 2* (2019). Available at: https://www.nccn.org/professionals/physician_gls/default.aspx#nscl.
2. Raz DJ, Zell JA, Ou SH, Gandara DR, Anton-Culver H, Jablons DM. Natural History of Stage I Non-Small Cell Lung Cancer: Implications for Early Detection. *Chest* (2007) 132(1):193–9. doi: 10.1378/chest.06-3096
3. Zhang F, Wang J, Guo J, Li Y, Huang X, Guan Z, et al. Chinese Expert Consensus Workshop Report: Guideline for Permanent Iodine-125 Seed Implantation of Primary and Metastatic Lung Tumors. *Thorac Cancer* (2018) 1(1):1–3. doi: 10.1111/1759-7714.12912
4. Wand J. The Concept of Stereotactic Ablation Brachytherapy and Practice. *Chin J Radiol Med Prot* (2020) 40(3):173–7. doi: 10.3760/cma.j.issn.0254-5098.2020.03.003
5. Ji Z, Jiang Y, Tian S, Guo F, Peng R, Xu F, et al. The Effectiveness and Prognostic Factors of CT-Guided Radioactive I-125 Seed Implantation for the Treatment of Recurrent Head and Neck Cancer After External Beam Radiation Therapy. *Int J Radiat Oncol Biol Phys* (2019) 103(3):638–45. doi: 10.1016/j.ijrobp.2018.10.034
6. Jiang P, Liu C, Wang J, Yang R, Jiang Y, Tian S. Computed Tomography (CT)-Guided Interstitial Permanent Implantation of (125)I Seeds for Refractory Chest Wall Metastasis or Recurrence. *Technol Cancer Res Treat* (2015) 14(1):11–8. doi: 10.7785/tcrt.2012.500402
7. Wang H, Wang J, Jiang Y, Li J, Tian S, Ran W, et al. The Investigation of 125I Seed Implantation as a Salvage Modality for Unresectable Pancreatic Carcinoma. *J Exp Clin Cancer Res* (2013) 32(1):106–13. doi: 10.1186/1756-9966-32-106
8. Wang JJ, Yuan HS, Li JN, Jiang WJ, Jiang YL, Tian SQ. Interstitial Permanent Implantation of 125I Seeds as Salvage Therapy for Re-Recurrent Rectal Carcinoma. *Int J Colorectal Dis* (2009) 24(4):391–9. doi: 10.1007/s00384-008-0628-4
9. Goldstraw P, Chansky K, Crowley J, Rami-Porta R, Asamura H, Eberhardt WEE, et al. The IASLC Lung Cancer Staging Project: Proposals for Revision of the TNM Stage Groupings in the Forthcoming (Eighth) Edition of the TNM Classification for Lung Cancer. *J Thorac Oncol* (2016) 11(1):39–51. doi: 10.1016/j.jtho.2015.09.009
10. Nath R, Anderson LL, Luxton G, Weaver KA, Williamson JF, Meigooni AS. Dosimetry of Interstitial Brachytherapy Sources: Recommendations of the AAPM Radiation Therapy Committee Task Group No. 43. American Association of Physicists in Medicine. *Med Phys* (1995) 22(2):209–34. doi: 10.1118/1.597458
11. Yu Y, Anderson LL, Li Z, Mellenberg DE, Nath R, Schell MC, et al. Permanent Prostate Seed Implant Brachytherapy: Report of the American Association of Physicists in Medicine Task Group No.64. *Med Phys* (1999) 26(10):2054–76. doi: 10.1118/1.598721
12. Rivard MJ, Coursey BM, DeWerd LA, Hanson WF, Huq MS, Ibbott GS, et al. Update of AAPM Task Group No. 43 Report: A Revised AAPM Protocol for Brachytherapy Dose Calculations. *Med Phys* (2004) 31(3):633–74. doi: 10.1118/1.1646040
13. Eisenhauer EA, Therasse P, Bogaerts J, Schwartz LH, Sargent D, Ford R, et al. New Response Evaluation Criteria in Solid Tumours: Revised RECIST Guideline (Version 1.1). *Eur J Cancer* (2009) 45(2):228–47. doi: 10.1016/j.ejca.2008.10.026
14. National Cancer Institute. *Common Terminology Criteria for Adverse Events (CTCAE) Version 5.0* (2017). Available at: https://evs.nci.nih.gov/ftp1/CTCAE/CTCAE_5.0/.
15. Sastry KS. Biological Effects of the Auger Emitter Iodine-125: A Review. Report No. 1 of AAPM Nuclear Medicine Task Group No. 6. *Med Phys* (1992) 19(6):1361–70. doi: 10.1118/1.596926
16. Martinez-Monge R, Pagola M, Vivas I, Lopez-Picazo JM. CT-Guided Permanent Brachytherapy for Patients With Medically Inoperable Early-Stage Non-Small Cell Lung Cancer (NSCLC). *Lung Cancer* (2008) 61 (2):209–13. doi: 10.1016/j.lungcan.2007.12.016
17. Videtic GM, Hu C, Singh AK, Chang JY, Parker W, Olivier KR, et al. A Randomized Phase 2 Study Comparing 2 Stereotactic Body Radiation Therapy Schedules for Medically Inoperable Patients With Stage I Peripheral Non-Small Cell Lung Cancer: NRG Oncology RTOG 0915 (NCCTG N0927). *Int J Radiat Oncol Biol Phys* (2015) 93(4):757–64. doi: 10.1016/j.ijrobp.2015.07.2260
18. Chang JY, Senan S, Paul MA, Mehran RJ, Louie AV, Balter P, et al. Stereotactic Ablative Radiotherapy *Versus* Lobectomy for Operable Stage I Non-Small-Cell Lung Cancer: A Pooled Analysis of Two Randomised Trials. *Lancet Oncol* (2015) 16(6):630–7. doi: 10.1016/S1470-2045(15)70168-3
19. Timmerman R, Paulus R, Galvin J, Michalski J, Straube W, Bradley J, et al. Stereotactic Body Radiation Therapy for Inoperable Early Stage Lung Cancer. *Jama* (2010) 303(11):1070–6. doi: 10.1001/jama.2010.261

20. Shibamoto Y, Hashizume C, Baba F, Ayakawa S, Miyakawa A, Murai T, et al. Stereotactic Body Radiotherapy Using a Radiobiology-Based Regimen for Stage I Non–Small-Cell Lung Cancer: Five-Year Mature Results. *J Thorac Oncol* (2015) 10(6):960–4. doi: 10.1097/JTO.0000000000000525
21. Lindberg K, Nyman J, Riesenfeld Kallskog V, Hoyer M, Lund JA, Lax I, et al. Long-Term Results of a Prospective Phase II Trial of Medically Inoperable Stage I NSCLC Treated With SBRT - the Nordic Experience. *Acta Oncol* (2015) 54(8):1096–104. doi: 10.3109/0284186X.2015.1020966
22. Timmerman R, Hu C, Michalski J, Straube B, Galvin J, Johnstone D, et al. Long-Term Results of RTOG 0236: A Phase II Trial of Stereotactic Body Radiation Therapy (SBRT) in the Treatment of Patients With Medically Inoperable Stage I Non-Small Cell Lung Cancer. *Int J Radiat Oncol Biol Phys* (2014) 90:S30. doi: 10.1016/j.ijrobp.2014.05.135
23. Stewart A, Parashar B, Patel M, O'Farrell D, Biagioli M, Devlin P, et al. American Brachytherapy Society Consensus Guidelines for Thoracic Brachytherapy for Lung Cancer. *Brachytherapy* (2016) 15(1):1–11. doi: 10.1016/j.brachy.2015.09.006
24. Huang BY, Li XM, Song XY, Zhou JJ, Shao Z, Yu ZQ, et al. Long-Term Results of CT-Guided Percutaneous Radiofrequency Ablation of Inoperable Patients With Stage Ia Non-Small Cell Lung Cancer: A Retrospective Cohort Study. *Int J Surg* (2018) 53:143–50. doi: 10.1016/j.ijsu.2018.03.034
25. Yang X, Ye X, Zheng A, Huang G, Ni X, Wang J, et al. Percutaneous Microwave Ablation of Stage I Medically Inoperable Non-Small Cell Lung Cancer: Clinical Evaluation of 47 Cases. *J Surg Oncol* (2014) 110(6):758–63. doi: 10.1002/jso.23701
26. Ambrogi MC, Fanucchi O, Cioni R, Dini P, De Liperi A, Cappelli C, et al. Long-Term Results of Radiofrequency Ablation Treatment of Stage I Non-Small Cell Lung Cancer: A Prospective Intention-to-Treat Study. *J Thorac Oncol* (2011) 6(12):2044–51. doi: 10.1097/JTO.0b013e31822d538d
27. Lencioni R, Crocetti L, Cioni R, Suh R, Glenn D, Regge D, et al. Response to Radiofrequency Ablation of Pulmonary Tumours: A Prospective, Intention-to-Treat, Multicentre Clinical Trial (the RAPTURE Study). *Lancet Oncol* (2008) 9(7):621–8. doi: 10.1016/S1470-2045(08)70155-4
28. Sun B, Brooks ED, Komaki RU, Liao Z, Jeter MD, McAleer MF, et al. 7-Year Follow-Up After Stereotactic Ablative Radiotherapy for Patients With Stage I Non-Small Cell Lung Cancer: Results of a Phase 2 Clinical Trial. *Cancer* (2017) 123(16):3031–9. doi: 10.1002/cncr.30693
29. Bezjak A, Paulus R, Gaspar LE, Timmerman RD, Straube WL, Ryan WF, et al. Efficacy and Toxicity Analysis of NRG Oncology/RTOG 0813 Trial of Stereotactic Body Radiation Therapy (SBRT) for Centrally Located non-Small Cell Lung Cancer (NSCLC). *Int J Radiat Oncol Biol Physics* (2016) 96 (2, Supplement):S8. doi: 10.1016/j.ijrobp.2016.06.035
30. Jiang Y, Ji Z, Guo F, Peng R, Sun H, Fan J, et al. Side Effects of CT-Guided Implantation of (125)I Seeds for Recurrent Malignant Tumors of the Head and Neck Assisted by 3D Printing non Co-Planar Template. *Radiat Oncol* (2018) 13(1):18. doi: 10.1186/s13014-018-0959-4
31. Stewart AJ, O'Farrell DA, Mutyala S, Bueno R, Sugarbaker DJ, Cormack RA, et al. Severe Toxicity After Permanent Radioactive Seed Implantation for Mediastinal Carcinoid Tumors. *Brachytherapy* (2007) 6(1):58–61. doi: 10.1016/j.brachy.2006.08.009
32. Yeow KM, See LC, Lui KW, Lin MC, Tsao TC, Ng KF, et al. Risk Factors for Pneumothorax and Bleeding After CT-Guided Percutaneous Coaxial Cutting Needle Biopsy of Lung Lesions. *J Vasc Interv Radiol* (2001) 12 (11):1305–12. doi: 10.1016/S1051-0443(07)61556-5
33. Yildirim E, Kirbas I, Harman A, Ozyer U, Tore HG, Aytekin C, et al. CT-Guided Cutting Needle Lung Biopsy Using Modified Coaxial Technique: Factors Effecting Risk of Complications. *Eur J Radiol* (2009) 70(1):57–60. doi: 10.1016/j.ejrad.2008.01.006
34. Zheng YF, Jiang LM, Mao WM, Han ZQ. Percutaneous Computed Tomography-Guided Lung Biopsy of Solitary Nodular Ground-Glass Opacity. *J Cancer Res Ther* (2015) 11(1):C231–3. doi: 10.4103/0973-1482.162117
35. Moore EH. Technical Aspects of Needle Aspiration Lung Biopsy: A Personal Perspective. *Radiology* (1998) 208(2):303–18. doi: 10.1148/radiology.208.2.9680552
36. Ji Z, Jiang Y, Guo F, Sun H, Fan J, Zhang L, et al. Dosimetry Verification of Radioactive Seed Implantation for Malignant Tumors Assisted by 3D Printing Individual Templates and CT Guidance. *Appl Radiat Isotopes* (2017) 124:68–74. doi: 10.1016/j.apradiso.2016.12.009
37. Li C, Zhang Y, Chen D, Duan G, Liu Z, Zhang L, et al. Experimental Research on a Novel Iodine-125 Seed Strand Connected Using Magnesium Alloy AZ31. *Recent Pat Anticancer Drug Discov* (2014) 9(2):249–57. doi: 10.2174/1574892809666140130215156
38. Jiang S, Yuan W, Yang Y, Zhang D, Liu N, Wang W. Modelling and Analysis of a Novel CT-Guided Puncture Robot for Lung Brachytherapy. *Advanced Robotics* (2017) 31(11):557–69. doi: 10.1080/01691864.2017.1298465
39. Qin Z, Tai Y, Shi J, Wei L, Chen Z, Li Q, et al. Development of NSCLC Precise Puncture Prototype Based on CT Images Using Augmented Reality Navigation. *ICMIR* (2017) 691(1): 538–544. doi: 10.1007/978-3-319-70990-1_78

Conflict of Interest: Authors YM and YS are employed by Staff Hospital of Chengde Iron and Steel Group Co. Ltd.

The remaining authors declare that the research was conducted in the absence of any commercial or financial relationships that could be construed as a potential conflict of interest.

Publisher's Note: All claims expressed in this article are solely those of the authors and do not necessarily represent those of their affiliated organizations, or those of the publisher, the editors and the reviewers. Any product that may be evaluated in this article, or claim that may be made by its manufacturer, is not guaranteed or endorsed by the publisher.

Copyright © 2021 Ji, Huo, Liu, Liang, Xing, Hu, Ma, Wang, Zhao, Song, Wang, Han, Zhang, Wang, Chai, Huang, Hu and Wang. This is an open-access article distributed under the terms of the Creative Commons Attribution License (CC BY). The use, distribution or reproduction in other forums is permitted, provided the original author(s) and the copyright owner(s) are credited and that the original publication in this journal is cited, in accordance with accepted academic practice. No use, distribution or reproduction is permitted which does not comply with these terms.

frontiers in Oncology

ORIGINAL RESEARCH
published: 22 September 2021
doi: 10.3389/fonc.2021.714549

Comparative Study of Pulmonary Combined Large-Cell Neuroendocrine Carcinoma and Combined Small-Cell Carcinoma in Surgically Resected High-Grade Neuroendocrine Tumors of the Lung

Yanan Wang†, Fangfei Qian†, Ya Chen†, Zhengyu Yang, Minjuan Hu, Jun Lu, Yanwei Zhang, Wei Zhang, Lei Cheng* and Baohui Han**

Department of Pulmonary, Shanghai Chest Hospital, Shanghai Jiao Tong University, Shanghai, China

OPEN ACCESS

Edited by:
Hideharu Kimura, Kanazawa University, Japan

Reviewed by:
Dipesh Uprety, Wayne State University, United States
Ching-Yao Yang, National Taiwan University, Taiwan

***Correspondence:**
Baohui Han
18930858216@163.com
Lei Cheng
leiei_cheng@163.com
Wei Zhang
zhwei2002@hotmail.com

†These authors have contributed equally to this work

Specialty section:
This article was submitted to Thoracic Oncology, a section of the journal Frontiers in Oncology

Received: *25 May 2021*
Accepted: *03 September 2021*
Published: *22 September 2021*

Citation:
Wang Y, Qian F, Chen Y, Yang Z, Hu M, Lu J, Zhang Y, Zhang W, Cheng L and Han B (2021) Comparative Study of Pulmonary Combined Large-Cell Neuroendocrine Carcinoma and Combined Small-Cell Carcinoma in Surgically Resected High-Grade Neuroendocrine Tumors of the Lung. Front. Oncol. 11:714549. doi: 10.3389/fonc.2021.714549

Objectives: Pulmonary large-cell neuroendocrine carcinoma (LCNEC) and small-cell lung cancer (SCLC) are both classified as pure and combined subtypes. Due to the low incidence and difficult diagnosis of combined LCNEC (C-LCNEC) and combined SCLC (C-SCLC), few studies have compared their clinical features and prognosis.

Materials and Methods: We compared the clinical features, mutation status of driver genes (*EGFR, ALK, ROS1, KRAS*, and *BRAF*), and prognosis between C-LCNEC and C-SCLC. Univariate and multivariate Cox regression analyses were applied for survival analysis.

Results: We included a total of 116 patients with C-LCNEC and 76 patients with C-SCLC in the present study. There were significant differences in distribution of smoking history, tumor location, pT stage, pN stage, pTNM stage, visceral pleural invasion (VPI), and combined components between C-LCNEC and C-SCLC ($P<0.05$ for all). C-SCLC was more advanced at diagnosis as compared to C-LCNEC. The incidence of *EGFR* mutations in C-LCNEC patients was higher than C-SCLC patients (25.7 *vs.* 5%, $P=0.004$). We found that tumor size, pN stage, peripheral CEA level, and adjuvant chemotherapy were independently prognostic factors for DFS and OS in C-LCNEC patients, while peripheral NSE level, pT stage, pN stage, VPI and adjuvant chemotherapy were independently associated with DFS and OS for C-SCLC patients ($P<0.05$ for all). Propensity score matching with adjustment for the confounders confirmed a more favorable DFS ($P=0.032$) and OS ($P=0.019$) in patients with C-LCNEC in comparison with C-SCLC patients upon survival analysis.

Conclusions: The mutation landscape of driver genes seemed to act in different way between C-SCLC and C-LCNEC, likely by which result in clinical phenotype difference as well as better outcome in C-LCNEC.

Keywords: pulmonary neuroendocrine carcinoma, pulmonary combined large-cell neuroendocrine carcinoma, combined small-cell lung cancer, prognosis, propensity score matching

INTRODUCTION

Neuroendocrine carcinoma of the lung, which accounts for about 15–20% of primary lung cancer, is divided into four categories: small-cell lung cancer (SCLC), typical carcinoid, atypical carcinoid, and large-cell neuroendocrine carcinoma (LCNEC) (1, 2). Pulmonary large-cell and small-cell neuroendocrine carcinomas are classified as high-grade neuroendocrine carcinomas (HGNEC), characterized by poor histologic differentiation, high aggressiveness, and poor prognosis (3). In 2015, the World Health Organization (WHO) classification divided SCLC into pure SCLC and combined SCLC (C-SCLC). C-SCLC is defined as a SCLC type that is mixed with other components of non-small-cell lung cancer (NSCLC), such as adenocarcinoma (AD), squamous cell carcinoma (SCC), large-cell carcinoma (LCC), LCNEC, and so on. C-SCLC accounts for 2 to 28% of all SCLC (4–6). Like SCLC, LCNEC is also divided into pure LCNEC and combined LCNEC (C-LCNEC), and C-LCNEC is the LCNEC that combined with AD, SCC, and other rare types such as spindle-cell carcinoma and giant-cell carcinoma. The reported incidence of C-LCNEC ranged from 10 to 49% (7–9). Current studies on LCNEC and SCLC generally take all components as a whole instead of specified analysis with focus on pure and combined parts (10–12). Owing to the rarity and the difficulty in diagnosis of C-LCNEC and C-SCLC, it is lack of the statistical description of their clinical features, genomic landscape, prognosis, and the relevant comparisons. The diagnosis of pulmonary neuroendocrine tumors has been advanced in recent years by the development of pathological technology and the wide application of surgery in multimodal treatment of lung cancer (13, 14). Therefore, genomic and clinical analysis on specific subtypes will take the advantage of increased diagnosis to improve the treatment guidance for SCLC and LCNEC. To our knowledge, no large sample studies up to now have compared C-LCNEC with C-SCLC in terms of clinical features and genomic mutation landscape. We conducted this study to fill this gap and wish the results may provide new insights into the treatment of resected C-LCNEC and C-SCLC.

MATERIAL AND METHODS

Patients

We retrospectively analyzed 1,250 patients with high-grade neuroendocrine carcinoma who underwent pulmonary resection in our organization. All surgically resected specimens were independently reviewed by two professional pathologists according to the 2015 WHO criteria for pulmonary neuroendocrine carcinoma (1). The initial diagnosis and classification of the C-LCNEC and C-SCLC were based on the neuroendocrine tumor morphology, which was further confirmed by immunohistochemistry. The tumor staging was based on the 8th edition TNM staging system proposed by the International Association for the Study of Lung Cancer (IASLC) (15). The treatment response was evaluated according to the Response Evaluation Criteria in Solid Tumors (RECIST) version 1.1. Besides NSCLC components, LCNEC might also be mixed with SCLC, but these tumors are classified as C-SCLC and will be excluded from our study. Other exclusion reasons included uncertain diagnosis, palliative surgery, and incomplete medical record and follow-up data.

As presented by the study flow chart (**Figure 1**), we finally included 192 cases of surgically resected combined high-grade neuroendocrine carcinoma in total. Specially, there were 116 patients with C-LCNEC and 76 patients with C-SCLC. The studies involving human participants were reviewed and approved by Shanghai Chest Hospital and affiliation of ethics committee. A written informed consent was signed by included patients before they donated tumor tissues for the purpose of scientific research.

Molecular Analysis

The patient's genomic DNA and RNA were extracted from formalin-fixed, paraffin-embedded tumor tissues and were subjected to the analysis of genetic alterations. We evaluated *EGFR* mutations by amplification refractory mutation system (ARMS) method, *ALK* expression by immunohistochemistry (IHC), ROS1 fusion by *in situ* hybridization (FISH), and *KRAS/BRAF* mutations by polymerase chain reaction (PCR) amplification method.

Follow-Up

Patients were diagnosed between 2008 and 2018, with median follow-up of 76 months and 55.7% deaths at the end of follow-up. Survival information was obtained through inpatient and outpatient records or telephone. Routine examinations such as chest computed tomography (CT) scans, brain magnetic resonance imaging or CT, tumor markers, and the neck and abdominal ultrasound were performed every 3 months for the first 2 years after surgery, followed by every 6 months examinations until 2–5 years. After 5 years, the patients were examined once a year. Patients were censored who were lost to follow-up or did not achieve the endpoint event. Disease-free survival (DFS) was defined as the time from surgery to disease recurrence or last follow-up if censored. Overall survival (OS) was the period between the date of surgery and death, but was extended to the end of follow-up in the presence of censored situation.

Statistical Analysis

We compared the differences in clinicopathological characteristics between C-LCNEC and C-SCLC patients. Chi-square test or Fisher's exact test was used for the comparisons in presence of discrete variables. As a non-parametric analysis method, Mann-Whitney U test was adopted for comparisons of continuous variables that were distributed non-normally. Student t test was used for normal distribution variables. Survival analysis was performed by Cox proportional hazards regression model, and the survival difference was visualized by Kaplan–Meier curve and log-rank test.

To reduce the selection bias as much as possible, propensity score matching (PSM) method was applied to sample C-LCNEC and C-SCLC patients at a 1:1 ratio *via* nearest-neighbor method without replacement (16). Propensity scores for included patients were calculated by a multiple logistic regression with adjustment for clinical features including gender, age, smoking history,

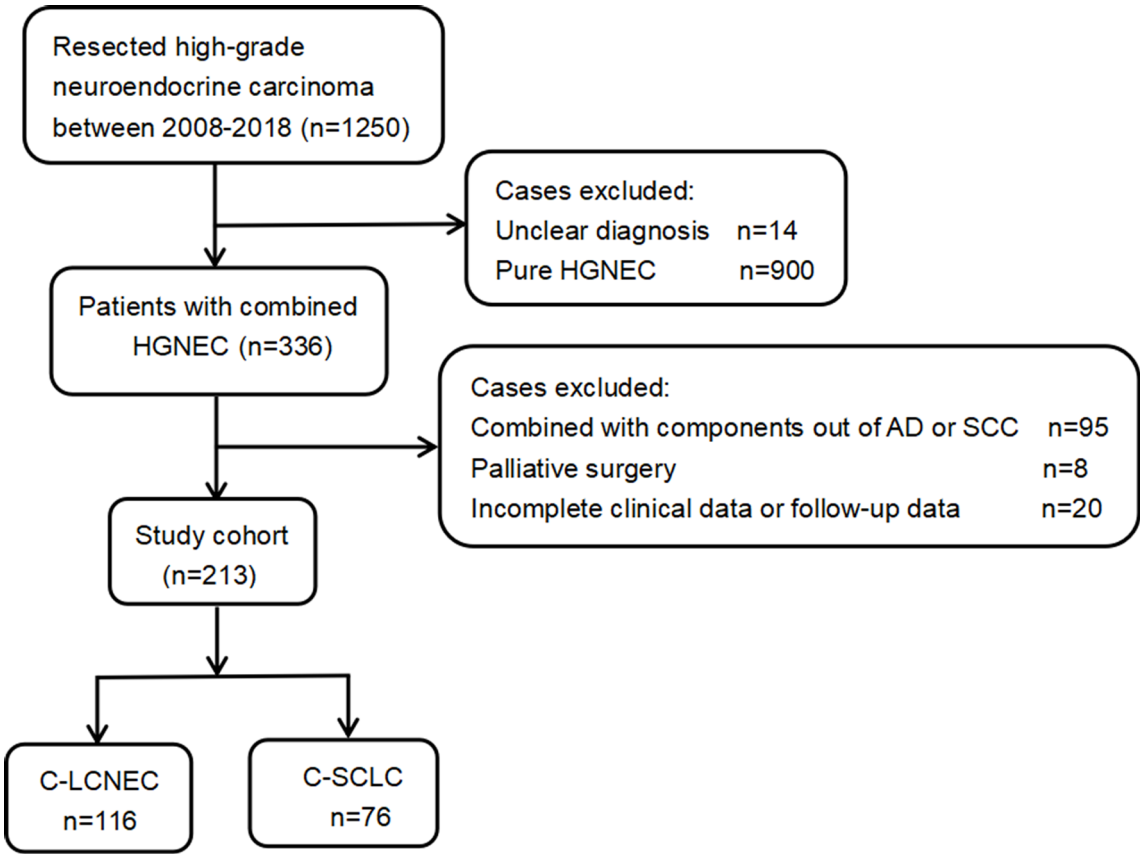

FIGURE 1 | The workflow of patient inclusion for the present study.

primary site, laterality, tumor location, tumor size, pT stage, pN stage, VPI, combined components, CEA, CYFRA21-1, SCCA, NSE, adjuvant chemotherapy, and postoperative adjuvant radiotherapy (PORT). Finally, A total of 75 pairs were successfully matched. We used the SPSS software of version 26.0 (IBM Corporation, Armonk, NY, USA) for statistical analysis, and two-tailed $P<0.05$ was considered statistically significant.

RESULT

Patient Population

The patients' clinicopathologic characteristics are shown in **Table 1**. We included 116 patients pathologically diagnosed as C-LCNEC, and other 76 patients with C-SCLC. C-SCLC patients had a higher proportion of smoking than C-LCNEC patients (P=0.027) and tended to be central-type carcinoma (P=0.015). The pathological staging of C-SCLC was more advanced compared to C-LCNEC, in terms of pT, pN, and pTNM stage (P=0.012, 0.020, and 0.003; respectively). C-LCNEC appeared to have a higher incidence of VPI than C-SCLC (P=0.002). Among 116 C-LCNEC patients, the most common were LCNEC combined with adenocarcinoma (LCNEC/AD, 70.7%, n=82), and then LCNEC combined with squamous cell carcinoma (LCNEC/SCC, 29.3%, n=34). As for C-SCLC, the percentage of SCLC plus adenocarcinoma and squamous cell carcinoma was 50%, respectively. The proportion of combined with AD in C-LCNEC was higher than that in C-SCLC (P=0.013).To adjust the confounding factors between the two groups, we sampled the two patient population with the PSM method. We found similar results upon PSM adjustment by such comparisons mentioned above (**Table 1**).

Genetic Alterations

The mutation data of driver genes such as *EGFR*, *ALK*, *ROS1*, *KRAS*, and *BRAF* were available in 110 patients, including 70 C-LCNEC and 40 C-SCLC patients. As shown in **Figure 2**, we only found the alterations of *ALK* and *EGFR* genes in these patients. The incidence of *EGFR* mutations in C-LCNEC patients was found to be higher than C-SCLC patients (25.7 *vs.* 5%, P=0.004). Specially, there were 18 patients with *EGFR* mutations of C-LCNEC, including 10 patients with 19 exon deletions, 7 patients with 21 exon *L858R* mutation, and 1 patient with exon 20 insertion. For C-SCLC patients, we only identified two patients with *EGFR* 19 exon deletions. The incidence of *ALK* rearrangement were relatively lower, with only four patients

TABLE 1 | Clinical demographics before and after propensity score matching for patients with resected C-LCNEC and C-SCLC.

Characteristic	Before propensity score matching			After propensity score matching		
	C-LCNEC (n = 116) (%)	C-SCLC (n = 76) (%)	*P*	C-LCNEC (n = 75) (%)	C-SCLC (n = 75) (%)	P
Gender			0.117			0.440
Male	96(82.8)	69(90.8)		65 (86.7)	68 (90.7)	
Female	20(17.2)	7(9.2)		10 (13.3)	7 (9.3)	
Age(y)			0.872			0.869
<65	67(57.8)	43(56.6)		42 (56.0)	43 (57.3)	
≥65	49(42.2)	33(43.4)		33 (44.0)	32 (42.7)	
Smoking History			**0.027**			0.299
Yes	64(55.2)	54(71.1)		47 (62.7)	53 (70.7	
No	52(44.8)	22(28.9)		28 (37.3)	43 (29.3)	
Primary Site			0.374			0.227
Upper lobe	69(59.5)	45(59.2)		41 (54.7)	44 (58.7)	
Middle lobe	4(3.4)	6(7.9)		2 (2.7)	6 (8.0)	
Lower lobe	43 (37.1)	25 (32.9)		32 (42.7)	25 (33.3)	
Laterality			0.603			0.511
Left	49 (42.2)	35 (46.1)		31 (41.3)	35 (46.7)	
Right	67 (57.8)	41 (53.9)		44 (58.7)	40 (53.3)	
Tumor location			**0.015**			0.157
Central	22(19.0)	26(34.2)		19 (25.3)	27 (36.0)	
Peripheral	94(81.0)	49(64.5)		56 (74.7)	48 (64.0)	
Tumor size, cm (Mean ± SD)	3.55 ± 1.62	3.73 ± 1.96	0.186	4.30 ± 2.3	4.26 ± 2.2	0.221
pT stage			**0.012**			0.265
T1	25(21.6)	28(36.8)		22 (29.3)	28 (37.3)	
T2	71(61.2)	28(36.8)		39 (52.0)	27 (36.0)	
T3	16(13.8)	16(21.1)		11 (14.7)	16 (4.0)	
T4	4(3.4)	4(5.3)		3 (4.0)	4 (5.3)	
pN stage			**0.020**			0.495
N0	68(58.6)	29(38.2)		24 (44.0)	29 (38.7)	
N1	17(14.7)	15(19.7)		17 (22.7)	14 (18.7)	
N2	31(26.7)	32(42.1)		25 (33.3)	32 (42.7)	
pTNM stage			**0.003**			0.138
I	51 (44.0)	19 (25.0)		24 (32.0)	19 (25.3)	
II	31 (26.7)	17 (22.4)		23 (30.7)	16 (21.3)	
III	34 (29.3)	40 (52.6)		28 (37.3)	40 (53.3)	
VPI			**0.002**			0.611
With	64(55.2)	25(32.9)		46 (61.3)	49 (65.3)	
Without	52(44.8)	51(67.1)		29 (38.7)	26 (34.7)	
Combined components			**0.013**			0.189
AD	82 (70.7)	38 (50.0)		45 (60.0)	37 (49.3)	
SCC	34 (29.3)	38 (50.0)		30 (40.0)	38 (50.7)	
CEA, ng/ml			0.231			0.244
≤5	65(56.0)	42(55.3)		43 (57.3)	42 (56.0)	
>5	40 (34.5)	17(22.4)		27 (36.0)	17 (22.7)	
Unknown	11(9.5)	17 (22.4)		0	0	
CYFRA21-1, ng/ml			0.739			0.810
≤5	85 (73.3)	49 (64.5)		57 (76.0)	49 (65.3)	
>5	20 (17.2)	10 (13.2)		13 (17.3)	10 (13.3)	
Unknown	11(9.5)	17(22.4)		5 (6.7)	16 (21.3)	
SCCA, ng/ml			0.190			0.346
≤1.5	82(70.7)	51 (67.1)		52 (69.3)	51 (68.0)	
>1.5	23 (19.8)	8 (10.5)		18 (24.0)	8 (10.7)	
Unknown	11(9.5)	17 (22.4)		5 (6.7)	16 (21.3)	
NSE, ng/ml			0.552			0.975
≤16	91 (78.4)	53 (69.7)		63 (84.0)	53 (70.7)	
>16	14 (12.1)	6 (7.9)		7 (9.3)	6 (8.0)	
Unknown	11 (9.5)	17 (22.4)		5 (6.7)	16 (21.3)	
CA125, kU/L			0.546			0.365
≤35	95 (81.9)	55 (72.4)		62 (82.7)	55 (73.3)	
>35	10 (8.6)	4 (5.3)		8 (10.7)	4 (5.3)	
Unknown	11 (9.5)	17 (22.4)		5 (6.7)	16 (21.3)	
Adjuvant chemotherapy			0.546			0.852
Yes	88 (75.9)	55 (72.4)		60 (80.0)	55 (73.3)	

(Continued)

TABLE 1 | Continued

Characteristic	Before propensity score matching			After propensity score matching		
	C-LCNEC (n = 116) (%)	C-SCLC (n = 76) (%)	*P*	C-LCNEC (n = 75) (%)	C-SCLC (n = 75) (%)	P
NSCLC-regimen	51 (58.0)	17 (30.9)		26 (43.4)	17 (30.9)	
SCLC-regimen	37 (42.0)	38 (69.1)		34 (56.3)	38 (69.1)	
No	28 (24.1)	21 (27.6)		15 (20.0)	20 (26.7)	
PORT			0.599			0.334
Yes	18 (15.5)	20 (26.3)		56 (74.7)	55 (73.3)	
No	98 (84.5)	56 (73.7)		19 (25.3)	20 (26.7)	

C-LCNEC, combined large-cell neuroendocrine carcinoma; C-SCLC, combined small-cell lung cancer; pTNM stage, pathological tumor node metastasis staging; VPI, Visceral pleural invasion; AD, adenocarcinoma; SCC, squamous cell carcinoma; CEA, carcinoembryonic antigen; CYFRA21-1, Cytokeratin-19-fragment; SCCA, squamous cell carcinoma antigen; NSE, neuron-specific enolase; PORT, postoperative adjuvant radiotherapy.
In bold: P < 0.05.

detected in C-LCNEC, but none were detected in C-SCLC patients, with insignificant statistical differences (5% *vs.* 0, *P*=0.102) likely due to limited sample size.

Postoperative Treatment Modalities

A total of 143 patients received adjuvant chemotherapy, including 88 patients with C-LCNEC and 55 patients with C-SCLC. Adjuvant chemotherapy regimens were divided into two types: SCLC regimens (etoposide plus cisplatin or carboplatin, EP/EC) and NSCLC regimens (platinum-based combined pemetrexed, gemcitabine, docetaxel, paclitaxel, or vinorelbine). Of the 88 C-LCNEC patients, 51 patients received NSCLC regimens, of which pemetrexed/cisplatin or carboplatin contained 32 (62.7%), gemcitabine/docetaxel/paclitaxel/vinorelbine–platinum contained 19 (37.3%), and the remaining 37 patients received SCLC regimens, including 24 patients with EC regimen and 13 patients with EP regimen. Among the 55 C-SCLC patients, 17 patients received NSCLC regimens, including 10 patients receiving pemetrexed/cisplatin or carboplatin regimen and 7 patients receiving gemcitabine/docetaxel/paclitaxel/vinorelbine–platinum regimen, and 38 patients received the SCLC regimens, of which 22 were EC regimen

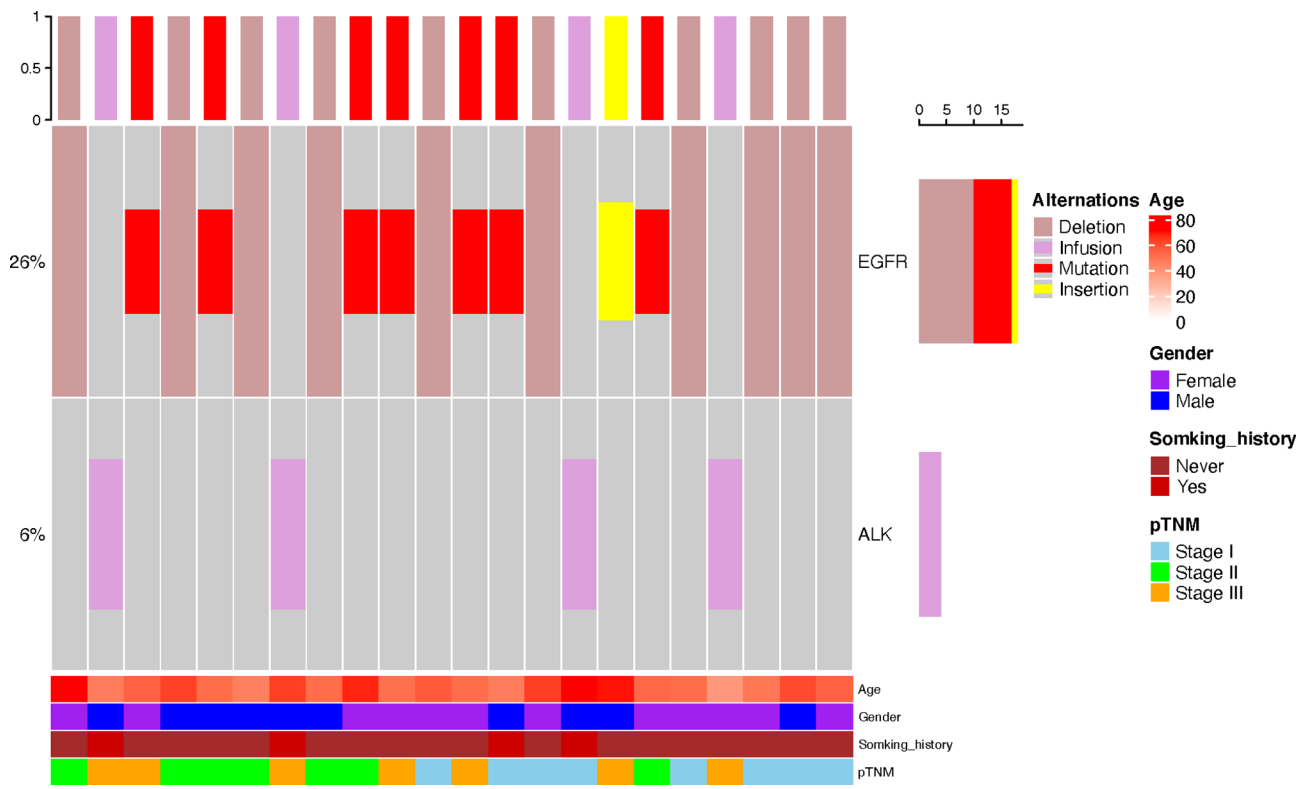

FIGURE 2 | Genetic alternations of patients with resected C-LCNEC and C-SCLC.

and 16 were EP regimen. As shown in **Supplemental Table 1**, a total of nine patients with C-LCNEC who developed distant metastases after surgery were treated with tyrosine Kinase Inhibitor (TKI). Among them, four patients harboring EML4-ALK received crizotinib, and five patients with EGFR 19del/L858R mutations received either first-generation TKI (gefitinib, icotinib, or erlotinib) or second-generation TKI (afatinib). Only one patient with C-SCLC harboring EGFR 19del received icotinib treatment. The overall ORR (the proportion of patients with a confirmed complete or partial response) rate was 60%.

Survival Comparison Between C-LCNEC and C-SCLC

We enrolled the factors that might affect DFS and OS in C-LCNEC and C-SCLC patients into Cox regression models for survival analysis (**Tables 2**, **3**). We initially made univariate Cox analysis and found tumor size, pN stage, CEA, and adjuvant chemotherapy were the main DFS modulator for C-LCNEC with statistical significance ($P<0.05$ for all, **Table 2**). On the other hand, tumor size, pT stage, pN stage, tumor location, peripheral VPI and NSE levels, and adjuvant chemotherapy were significantly associated with DFS in C-SCLC by univariate survival analysis ($P<0.05$ for all, **Table 2**). For OS, univariate analysis indicated that age, tumor size, pT stage, pN stage, CEA, and adjuvant chemotherapy were main predictors for C-LCNEC patients' survival ($P<0.05$ for all; respectively, **Table 3**). On the other hand, pT stage, pN stage, peripheral VPI and NSE levels, and adjuvant chemotherapy were survival predictors in C-SCLC patients as indicated by univariate modeling ($P<0.05$ for all, **Table 3**). These main survival effectors in univariate Cox regression models were further included in multivariate analysis. As results, we found that tumor size, pN stage, peripheral CEA level, and adjuvant chemotherapy were independently associated with DFS and OS in C-LCNEC patients (**Figure 3**). For C-SCLC patients, NSE, pT stage, pN stage, VPI, and adjuvant chemotherapy were independently predictors for DFS and OS (**Figure 3**). We next compared the outcomes of patients between C-LCNEC and C-SCLC and found that there was a longer OS in patients with C-LCNEC ($P=0.006$, **Figure 4B**). But we only observed an insignificant trend towards favorable DFS in patients with C-LCNEC ($P=0.059$, **Figure 4A**). PSM method adopted to reduce the confounders between the groups resulted in better DFS and OS of C-LCNEC patients than C-SCLC patients, highlighting the indeed difference in prognosis between the two lung cancer subtypes (for DFS, $P=0.032$, and for OS, $P=0.019$; **Figures 4C, D**).

DISCUSSION

Pulmonary neuroendocrine carcinoma is relatively aggressive and its diagnosis linked to worse survival in comparison with other lung cancer subtypes. Because the role of surgery has not been fully recognized before, chemotherapy combined with radiotherapy has been the major treatment for pulmonary

TABLE 2 | Impact of clinical characteristics on disease-free survival in patients with resected C-LCNEC and C-SCLC by univariate Cox analysis.

Characteristic	C-LCNEC			C-SCLC		
	HR	95% CI	P	HR	95% CI	P
Age ≥65 (***vs.***<65)	1.018	0.618–1.675	0.944	0.652	0.363–1.173	0.154
Gender male (***vs.*** Female)	1.134	0.592–2.172	0.705	0.921	0.330–2.569	0.875
Smoking history (***vs.*** No)	1.019	0.623–1.667	0.946	0.834	0.433–1.605	0.587
Tumor Size	1.186	1.007–1.396	**0.041**	1.216	1.057–1.397	**0.006**
pT stage (***vs.*** T1)						
T2	0.97	0.517–1.823	0.926	1.415	0.686–2.917	0.347
T3	1.95	0.887–4.283	0.096	3.053	1.42–6.562	**0.004**
T4	2.656	0.582–12.129	0.207	4.151	1.341–12.849	**0.014**
pN stage (***vs.*** N2)						
N0	0.266	0.154–0.459	**<0.001**	0.265	0.126–0.557	**<0.001**
N1	0.604	0.305–1.195	0.148	0.962	0.490–1.886	0.909
Tumor location Central (***vs.*** Peripheral)	1.340	0.683–2.630	0.395	1.959	1.081–3.551	**0.027**
Combined components AD (***vs.*** SCC)	0.830	0.472–1.459	0.517	0.743	0.420–1.318	0.309
VPI (***vs.*** Without)	1.014	0.621–1.655	0.955	2.742	1.506–4.995	**0.001**
Primary Site (***vs.*** upper lobe)						
Middle lobe	0.657	0.396–1.091	0.105	0.901	0.485–1.673	0.742
Lower lobe	1.805	0.629–5.179	0.272	1.546	0.564–4.238	0.398
CEA normal (***vs.*** Abnormal)	0.454	0.268–0.771	**0.003**	1.798	0.900–3.592	0.096
CYFRA21-1 normal (***vs.*** Abnormal)	1.245	0.659–2.353	0.499	1.482	0.644–3.408	0.354
SCCA normal (***vs.*** Abnormal)	1.000	0.542–1.934	0.941	0.687	0.242–1.951	0.481
NSE normal (***vs.*** Abnormal)	1.087	0.514–2.297	0.828	0.150	0.056–0.397	**0.013**
CA125 normal (***vs.*** Abnormal)	1.214	0.550–2.678	0.631	1.393	0.424–4.579	0.585
PORT (***vs.*** No)	1.234	0.671–2.269	0.498	1.460	0.785–2.712	0.232
Adjuvant chemotherapy (***vs.*** No)	0.433	0.251–0.747	**0.003**	0.459	0.244–0.862	**0.016**

C-LCNEC, combined large-cell neuroendocrine carcinoma; C-SCLC, combined small-cell lung cancer; HR, hazard ratio; CI, confidence interval; VPI, Visceral pleural invasion; CEA, carcinoembryonic antigen; CYFRA21-1, Cytokeratin-19-fragment; SCCA, squamous cell carcinoma antigen; NSE, neuron-specific enolase; PORT, postoperative adjuvant radiotherapy
In bold: P < 0.05.

TABLE 3 | Impact of clinical characteristics on overall survival in patients with resected C-LCNEC and C-SCLC by univariate analysis.

Characteristic	C-LCNEC			C-SCLC		
	HR	95% CI	P	HR	95% CI	P
Age ≥65 (***vs.***<65)	1.933	1.038–3.600	**0.038**	0.684	0.374–1.249	0.217
Gender male (***vs.*** Female)	1.68	1.794–3.560	0.175	1.346	0.479–3.784	0.573
Smoking history (***vs.*** No)	0.989	0.716–1.366	0.948	0.864	0.446–1.605	0.666
Tumor Size	1.287	1.046–1.583	**0.017**	1.154	1.00–1.331	**0.050**
pT stage (***vs.*** T1)						
T2	0.991	0.420–2.336	0.983	1.228	0.591–2.551	0.581
T3	3.160	1.197–8.340	0.020	2.691	1.273–5.691	**0.010**
T4	5.226	1.064–25.667	0.042	1.522	0.343–6.745	0.580
pN stage (***vs.*** N2)						
N0	0.199	0.098–0.404	**<0.001**	0.339	0.161–0.714	**0.004**
N1	0.405	0.162–1.012	0.053	1.339	0.653–2.742	0.425
Tumor location Central (***vs.*** Peripheral)	1.284	0.537–3.070	0.574	0.666	0.362–1.223	0.190
Combined components AD (***vs.*** SCC)	0.805	0.583–1.111	0.187	2.144	1.165–3.947	**0.014**
VPI (***vs.*** Without)	0.959	0.467–1.972	0.910	0.736	0.406–1.332	0.311
Primary Site (***vs.*** upper lobe)	1.327	0.967–1.823	0.080	1.126	0.827–1.534	0.449
Middle lobe	0.567	0.299–1.075	0.082	0.792	0.425–1.477	0.464
Lower lobe	1.065	0.247–4.584	0.933	1.082	0.363–3.225	0.888
Laterality	1.445	0.754–2.772	0.268	1.247	0.691–2.248	0.464
CEA normal (***vs.*** Abnormal)	0.272	0.134–0.554	**<0.001**	1.837	0.893–3.779	0.098
CYFRA21-1 normal (***vs.*** Abnormal)	1.630	0.752–3.532	0.215	1.271	0.480–3.359	0.629
SCCA normal (***vs.*** Abnormal)	1.204	0.544–2.663	0.647	1.036	0.398–2.697	0.943
NSE normal (***vs.*** Abnormal)	1.416	0.583–3.442	0.443	0.366	0.138–0.968	0.043
CA125 normal (***vs.*** Abnormal)	0.758	0.230–2.500	0.649	1.655	0.550–0.479	0.410
PORT (***vs.*** No)	1.104	0.485–2.513	0.813	1.331	0.697–2.541	0.386
Adjuvant chemotherapy (***vs.*** No)	0.382	0.198–0.737	**0.004**	0.385	0.207–0.715	**0.003**

C-LCNEC, combined large-cell neuroendocrine carcinoma; C-SCLC, combined small-cell lung cancer; HR, hazard ratio; CI, confidence interval; VPI, Visceral pleural invasion; CEA, carcinoembryonic antigen; CYFRA21-1, Cytokeratin-19-fragment; SCCA, squamous cell carcinoma antigen; NSE, neuron-specific enolase; PORT, postoperative adjuvant radiotherapy
In bold: P < 0.05.

neuroendocrine carcinoma for a long time. Pathological diagnosis through small biopsies and cytological specimens is often inaccurate and may mislead the diagnosis of C-LCNEC and C-SCLC. Based on more recent large retrospective studies, it was found that stage I SCLC could benefit from surgery with a 5-year OS of about 52% (17–19). Thus, the National Comprehensive Cancer Network (NCCN) guidelines recommend surgical treatment for patients with very limited disease (clinical T1–2, N0, M0) (20). As a subtype of NSCLC, surgery was the primary treatment for localized (I–IIIA) LCNEC. Survival benefits from

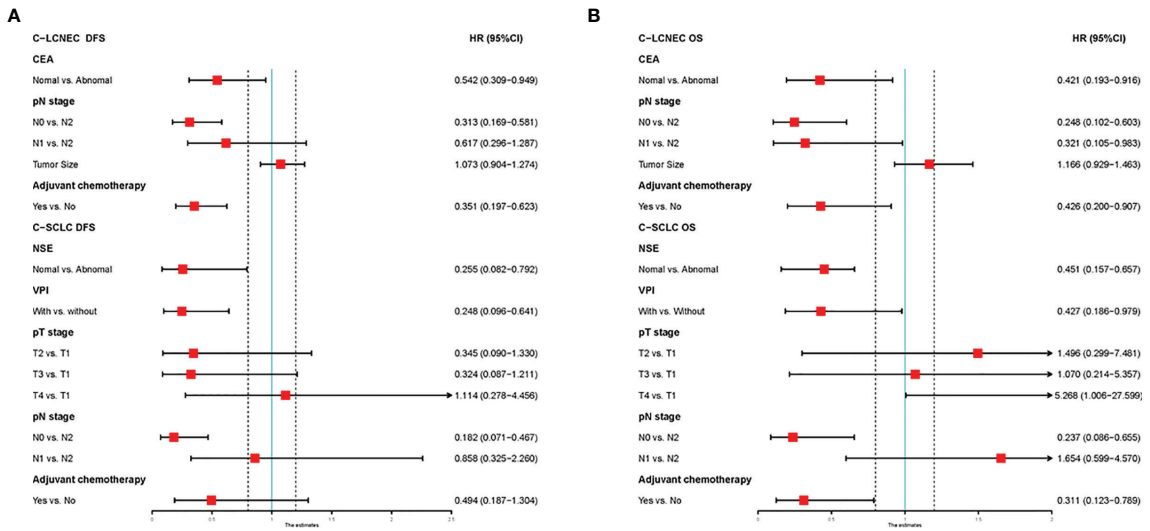

FIGURE 3 | Multivariate Cox regression analysis on clinical characteristics for DFS **(A)** and OS **(B)**.

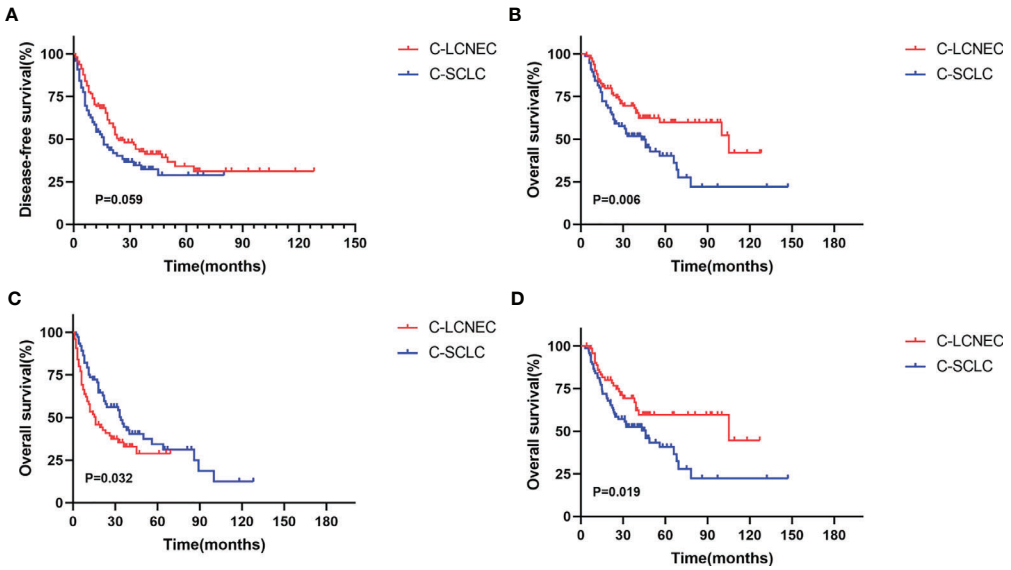

FIGURE 4 | Kaplan-Meier curves for Disease-free survival **(A, C)** and overall survival **(B, D)** before matching and after matching between C-LCNEC and C-SCLC.

surgery for patients with resectable LCNEC have also been demonstrated in several studies (21–23). Because patients could benefit more from surgery than first-line chemoradiotherapy in early-stage patients (24, 25), the number of patients received surgery has gradually increased, which may provide more available tissue for pathologists to accurately identify the combined components. To our knowledge, this study is the first, with relatively large sample size, to describe the clinicopathological features and prognosis of C-LCNEC and C-SCLC patients who had undergone surgery, and make relevant comparison between them.

According to a series of previous studies, it was reportedly to be comparable regarding clinicopathological characteristics and prognosis between LCNEC and SCLC (26, 27). However, Varlotto JM et al. analyzed the data from Surveillance, Epidemiology, and End Results Program (SEER) database and found that there were significant differences between LCNEC and SCLC in tumor size, lymph node metastasis, and differentiation degree (10). However, there was lack of evidence for clinical feature comparisons between C-LCNEC and C-SCLC. In our study we found that C-SCLC patients tended to have a history of smoking than C-LCNEC patients. C-LCNEC were mainly located at periphery lung, while C-SCLC were the tumors mainly in central location. In addition, the pathological staging of C-SCLC was more advanced compared to C-LCNEC, but C-LCNEC was characterized with VPI phenotype and combined AD components with manifestation of higher proportion than C-SCLC. These differences revealed may provide a potential tool for us to distinguish C-LCNEC from C-SCLC.

As expected, the clinical factors that influence the prognosis of C-SCLC and C-LCNEC were also revealed to be not identical. We found that tumor size, pN stage, peripheral CEA level, and adjuvant chemotherapy were independently prognostic factors for DFS and OS of C-LCNEC patients. Our study was first to analyze the prognostic factors of C-LCNEC in the presence of relatively large sample size and may make better understanding of prognosis of such a low-incidence carcinoma type. In line with previous studies, for C-SCLC patients, peripheral NSE level, pT stage, pN stage, VPI, and adjuvant chemotherapy were independently survival predictors for DFS and OS (4, 28).

Because of low incidence, survival comparison has not been previously reported between C-SCLC and C-LCNEC cancers. The previous focus was mainly on generalized SCLC and LCNEC, and demonstrated a better prognosis of LCNEC than SCLC (11, 12, 29). But other studies found no difference in prognosis between the two groups (26, 30, 31). In our study, we compared the outcomes of C-LCNEC with C-SCLC and revealed a prolonged OS of patients with C-LCNEC than those with C-SCLC, but the DFS was comparable. After PSM sampling, the prolonged OS and DFS were both statistically significant for the comparison of C-LCNEC *versus* C-SCLC, likely due to the higher neuroendocrine component of C-SCLC in nature.

It has been reported that the presence of driver mutations was very rare in LCNEC and SCLC but usually occurred in combined subtypes (32–34). Yokomizo et al. found *EGFR* mutations in three of 15 (20%) patients with C-SCLC (35). In another study, NGS was performed in 10 C-LCNEC patients, and five of them had driver gene alteration (32). Natasha et al. performed targeted next-generation sequencing testing on 45 LCNEC patients and classified LCNEC into two major types: SCLC-like (n=18; 40%), characterized byTP53+RB1 co-mutation/loss; NSCLC-like (n=25; 68%), characterized by the lack of coaltered TP53+RB1 (36). This study demonstrated the biological heterogeneity of LCNEC and provided reference for the classification and management of LCNEC patients.

In our study, *EGFR* mutations were presented in 18 patients (25.7%) and 4 patients (5.7%), for C-LCNEC and C-SCLC, respectively. *ALK* rearrangement was only observed in patients with C-LCNEC, and we did not detect alterations in other driver genes for both carcinoma types. A total of 10 patients received TKI treatment after distant metastasis and obtained good survival benefits, with an ORR rate of 60%, which suggests that genetic testing for patients with combined HGNEC is feasible and beneficial, especially for C-LCNEC patients.

Collectively, these results suggest that patients with C-LCNEC and C-SCLC may have different genetic background, which is a potential reason for the different clinical features and prognosis between them.

This article has several limitations. First of all, although we adopted the PSM method to reduce the confounders, the retrospective design of the present study may inevitably introduce bias. Second, although our sample size was relatively larger compared with previous studies, the limited sample size when grouped into C-LCNEC and C-SCLC may reduce the statistical power. Lastly, only a small number of patients in this study underwent driver gene testing, and lack of comprehensive genetic testing made it unable to capture a full spectrum of genomic profiles of HGNEC. Therefore, larger and more comprehensive studies were needed to validate and refine our findings.

In conclusion, the driver mutation landscape between C-LCNEC and C-SCLC acted in a different way, which is a potential cause for different distribution of clinicopathological features and prolonged outcome of C-LCNEC patients. Comparisons of the genetic and clinical dimensions between the two low-incidence carcinoma types may provide potential tools for clinical treatment decision.

DATA AVAILABILITY STATEMENT

The raw data supporting the conclusions of this article will be made available by the authors, without undue reservation.

ETHICS STATEMENT

The studies involving human participants were reviewed and approved by Shanghai Chest Hospital and affiliation of ethics committee. A written informed consent was signed by included patients before they donated tumor tissues for the purpose of scientific research.

AUTHOR CONTRIBUTIONS

YW, FQ, and YC both have substantial contributions to the conception or design of the work, the collection and analysis of data, and the writing and editing of the article. The rest authors have given substantial contributions to the work by providing editing and writing assistance. All authors contributed to the article and approved the submitted version.

FUNDING

This research was supported by the foundation of Shanghai Shenkang Hospital Development Center Emerging Frontier Technology Joint Research Project (Project No. SHDC12015115); the program of system biomedicine innovation center from Shanghai Jiao Tong University (Project No. 15ZH4009); Shanghai Jiao Tong University School of Medicine (Project No. 15ZH1008), and the foundation of Chinese Society of Clinical Oncology (Project No. Y2019AZZD-0355).

ACKNOWLEDGMENTS

The authors thank the study participants for their contribution to the research.

SUPPLEMENTARY MATERIAL

The Supplementary Material for this article can be found online at: https://www.frontiersin.org/articles/10.3389/fonc.2021.714549/full#supplementary-material

REFERENCES

1. Travis WD, Brambilla E, Nicholson AG, Yatabe Y, Austin JHM, Beasley MB, et al. The 2015 World Health Organization Classification of Lung Tumors: Impact of Genetic, Clinical and Radiologic Advances Since the 2004 Classification. *J Thorac Oncol* (2015) 10:1243–60. doi: 10.1097/JTO.0000000000000630
2. Gustafsson BI, Kidd M, Chan A, Malfertheiner MV, Modlin IM. Bronchopulmonary Neuroendocrine Tumors. *Cancer* (2008) 113:5–21. doi: 10.1002/cncr.23542
3. Travis WD. Pathology and Diagnosis of Neuroendocrine Tumors: Lung Neuroendocrine. *Thorac Surg Clin* (2014) 24:257–66. doi: 10.1016/j.thorsurg.2014.04.001
4. Zhang C, Yang H, Zhao H, Lang B, Yu X, Xiao P, et al. Clinical Outcomes of Surgically Resected Combined Small Cell Lung Cancer: A Two-Institutional Experience. *J Thorac Dis* (2017) 9:151–8. doi: 10.21037/jtd.2017.01.07
5. Babakoohi S, Fu P, Yang M, Linden PA, Dowlati A. Combined SCLC Clinical and Pathologic Characteristics. *Clin Lung Cancer* (2013) 14:113–9. doi: 10.1016/j.cllc.2012.07.002
6. Mangum MD, Greco FA, Hainsworth JD, Hande KR, Johnson DH. Combined Small-Cell and Non-Small-Cell Lung Cancer. *J Clin Oncol* (1989) 7:607–12. doi: 10.1200/JCO.1989.7.5.607
7. Zhang JT, Li Y, Yan LX, Zhu ZF, Dong XR, Chu Q, et al. Disparity in Clinical Outcomes Between Pure and Combined Pulmonary Large-Cell Neuroendocrine Carcinoma: A Multi-Center Retrospective Study. *Lung Cancer* (2020) 139:118–23. doi: 10.1016/j.lungcan.2019.11.004
8. Battafarano RJ, Fernandez FG, Ritter J, Meyers BF, Guthrie TJ, Cooper JD, et al. Large Cell Neuroendocrine Carcinoma: An Aggressive Form of Non-Small Cell Lung Cancer. *J Thorac Cardiovasc Surg* (2005) 130:166–72. doi: 10.1016/j.jtcvs.2005.02.064
9. Grand B, Cazes A, Mordant P, Foucault C, Dujon A, Guillevin EF, et al. High Grade Neuroendocrine Lung Tumors: Pathological Characteristics, Surgical Management and Prognostic Implications. *Lung Cancer* (2013) 81:404–9. doi: 10.1016/j.lungcan.2013.05.008
10. Varlotto JM, Medford-Davis LN, Recht A, Flickinger JC, Schaefer E, Zander DS, et al. Should Large Cell Neuroendocrine Lung Carcinoma Be Classified and Treated as a Small Cell Lung Cancer or With Other Large Cell Carcinomas? *J Thorac Oncol* (2011) 6:1050–8. doi: 10.1097/JTO.0b013e318217b6f8

11. Isaka M, Nakagawa K, Ohde Y, Okumura T, Watanabe R, Ito I, et al. A Clinicopathological Study of Peripheral, Small-Sized High-Grade Neuroendocrine Tumours of the Lung: Differences Between Small-Cell Lung Carcinoma and Large-Cell Neuroendocrine Carcinoma. *Eur J Cardiothorac Surg* (2012) 41:841–6. doi: 10.1093/ejcts/ezr132
12. Wang J, Ye L, Cai H, Jin M. Comparative Study of Large Cell Neuroendocrine Carcinoma and Small Cell Lung Carcinoma in High-Grade Neuroendocrine Tumors of the Lung: A Large Population-Based Study. *J Cancer* (2019) 10:4226–36. doi: 10.7150/jca.33367
13. Derks JL, Hendriks LE, Buikhuisen WA, Groen HJ, Thunnissen E, van Suylen RJ, et al. Clinical Features of Large Cell Neuroendocrine Carcinoma: A Population-Based Overview. *Eur Respir J* (2016) 47:615–24. doi: 10.1183/13993003.00618-2015
14. Hallet J, Law CH, Cukier M, Saskin R, Liu N, Singh S. Exploring the Rising Incidence of Neuroendocrine Tumors: A Population-Based Analysis of Epidemiology, Metastatic Presentation, and Outcomes. *Cancer* (2015) 121:589–97. doi: 10.1002/cncr.29099
15. Goldstraw P, Chansky K, Crowley J, Rami-Porta R, Asamura H, Eberhardt WE, et al. The IASLC Lung Cancer Staging Project: Proposals for Revision of the TNM Stage Groupings in the Forthcoming (Eighth) Edition of the TNM Classification for Lung Cancer. *J Thorac Oncol* (2016) 11:39–51. doi: 10.1016/j.jtho.2015.09.009
16. Austin PC. An Introduction to Propensity Score Methods for Reducing the Effects of Confounding in Observational Studies. *Multivariate Behav Res* (2011) 46:399–424. doi: 10.1080/00273171.2011.568786
17. Vallieres E, Shepherd FA, Crowley J, Van Houtte P, Postmus PE, Carney D, et al. The IASLC Lung Cancer Staging Project: Proposals Regarding the Relevance of TNM in the Pathologic Staging of Small Cell Lung Cancer in the Forthcoming (Seventh) Edition of the TNM Classification for Lung Cancer. *J Thorac Oncol* (2009) 4:1049–59. doi: 10.1097/JTO.0b013e3181b27799
18. Yu JB, Decker RH, Detterbeck FC, Wilson LD. Surveillance Epidemiology and End Results Evaluation of the Role of Surgery for Stage I Small Cell Lung Cancer. *J Thorac Oncol* (2010) 5:215–9. doi: 10.1097/JTO.0b013e3181cd3208
19. Badzio A, Kurowski K, Karnicka-Mlodkowska H, Jassem J. A Retrospective Comparative Study of Surgery Followed by Chemotherapy *vs*. Non-Surgical Management in Limited-Disease Small Cell Lung Cancer. *Eur J Cardiothorac Surg* (2004) 26:183–8. doi: 10.1016/j.ejcts.2004.04.012
20. Kalemkerian GP, Loo BW, Akerley W, Attia A, Bassetti M, Boumber Y, et al. NCCN Guidelines Insights: Small Cell Lung Cancer, Version 2.2018. *J Natl Compr Canc Netw* (2018) 16:1171–82. doi: 10.6004/jnccn.2018.0079
21. Naidoo J, Santos-Zabala ML, Iyriboz T, Woo KM, Sima CS, Fiore JJ, et al. Large Cell Neuroendocrine Carcinoma of the Lung: Clinico-Pathologic Features, Treatment, and Outcomes. *Clin Lung Cancer* (2016) 17:e121–9. doi: 10.1016/j.cllc.2016.01.003
22. Fournel L, Falcoz PE, Alifano M, Charpentier MC, Boudaya MS, Magdeleinat P, et al. Surgical Management of Pulmonary Large Cell Neuroendocrine Carcinomas: A 10-Year Experience. *Eur J Cardiothorac Surg* (2013) 43:111–4. doi: 10.1093/ejcts/ezs174
23. Sakurai H, Asamura H. Large-Cell Neuroendocrine Carcinoma of the Lung: Surgical Management. *Thorac Surg Clin* (2014) 24:305–11. doi: 10.1016/j.thorsurg.2014.05.001
24. Combs SE, Hancock JG, Boffa DJ, Decker RH, Detterbeck FC, Kim AW. Bolstering the Case for Lobectomy in Stages I, II, and IIIA Small-Cell Lung Cancer Using the National Cancer Data Base. *J Thorac Oncol* (2015) 10:316–23. doi: 10.1097/JTO.0000000000000402
25. Gaspar LE, McNamara EJ, Gay EG, Putnam JB, Crawford J, Herbst RS, et al. Small-Cell Lung Cancer: Prognostic Factors and Changing Treatment Over 15 Years. *Clin Lung Cancer* (2012) 13:115–22. doi: 10.1016/j.cllc.2011.05.008
26. Asamura H, Kameya T, Matsuno Y, Noguchi M, Tada H, Ishikawa Y, et al. Neuroendocrine Neoplasms of the Lung: A Prognostic Spectrum. *J Clin Oncol* (2006) 24:70–6. doi: 10.1200/JCO.2005.04.1202
27. Iyoda A, Hiroshima K, Baba M, Saitoh Y, Ohwada H, Fujisawa T. Pulmonary Large Cell Carcinomas With Neuroendocrine Features Are High-Grade Neuroendocrine Tumors. *Ann Thorac Surg* (2002) 73:1049–54. doi: 10.1016/S0003-4975(01)03616-5
28. Lei Y, Feng H, Qiang H, Shang Z, Chang Q, Qian J, et al. Clinical Characteristics and Prognostic Factors of Surgically Resected Combined Small Cell Lung Cancer: A Retrospective Study. *Lung Cancer* (2020) 146:244–51. doi: 10.1016/j.lungcan.2020.06.021
29. Kinslow CJ, May MS, Saqi A, Shu CA, Chaudhary KR, Wang TJC, et al. Large-Cell Neuroendocrine Carcinoma of the Lung: A Population-Based Study. *Clin Lung Cancer* (2020) 21:e99–113. doi: 10.1016/j.cllc.2019.07.011
30. Mochizuki E, Matsuura S, Oishi K, Miyashita K, Ichijyo K, Furukawa S, et al. Surgical Resection for Clinical Stage I High-Grade Neuroendocrine Carcinoma of the Lung. *World J Surg Oncol* (2018) 16:33. doi: 10.1186/s12957-018-1337-2
31. Kinoshita T, Yoshida J, Ishii G, Aokage K, Hishida T, Nagai K. The Differences of Biological Behavior Based on the Clinicopathological Data Between Resectable Large-Cell Neuroendocrine Carcinoma and Small-Cell Lung Carcinoma. *Clin Lung Cancer* (2013) 14:535–40. doi: 10.1016/j.cllc.2013.04.003
32. Miyoshi T, Umemura S, Matsumura Y, Mimaki S, Tada S, Makinoshima H, et al. Genomic Profiling of Large-Cell Neuroendocrine Carcinoma of the Lung. *Clin Cancer Res* (2017) 23:757–65. doi: 10.1158/1078-0432.CCR-16-0355
33. Lou G, Yu X, Song Z. Molecular Profiling and Survival of Completely Resected Primary Pulmonary Neuroendocrine Carcinoma. *Clin Lung Cancer* (2017) 18:e197–201. doi: 10.1016/j.cllc.2016.11.014
34. Gugger M, Burckhardt E, Kappeler A, Hirsiger H, Laissue JA, Mazzucchelli L. Quantitative Expansion of Structural Genomic Alterations in the Spectrum of Neuroendocrine Lung Carcinomas. *J Pathol* (2002) 196:408–15. doi: 10.1002/path.1065
35. Yokomizo A, Tindall DJ, Drabkin H, Gemmill R, Franklin W, Yang P, et al. PTEN/MMAC1 Mutations Identified in Small Cell, But Not in Non-Small Cell Lung Cancers. *Oncogene* (1998) 17:475–9. doi: 10.1038/sj.onc.1201956
36. Rekhtman N, Pietanza MC, Hellmann MD, Naidoo J, Arora A, Won H, et al. Next-Generation Sequencing of Pulmonary Large Cell Neuroendocrine Carcinoma Reveals Small Cell Carcinoma-Like and Non-Small Cell Carcinoma-Like Subsets. *Clin Cancer Res* (2016) 22:3618–29. doi: 10.1158/1078-0432.CCR-15-2946

Conflict of Interest: The authors declare that the research was conducted in the absence of any commercial or financial relationships that could be construed as a potential conflict of interest.

Publisher's Note: All claims expressed in this article are solely those of the authors and do not necessarily represent those of their affiliated organizations, or those of the publisher, the editors and the reviewers. Any product that may be evaluated in this article, or claim that may be made by its manufacturer, is not guaranteed or endorsed by the publisher.

Copyright © 2021 Wang, Qian, Chen, Yang, Hu, Lu, Zhang, Zhang, Cheng and Han. This is an open-access article distributed under the terms of the Creative Commons Attribution License (CC BY). The use, distribution or reproduction in other forums is permitted, provided the original author(s) and the copyright owner(s) are credited and that the original publication in this journal is cited, in accordance with accepted academic practice. No use, distribution or reproduction is permitted which does not comply with these terms.

frontiers in Oncology

ORIGINAL RESEARCH
published: 30 November 2021
doi: 10.3389/fonc.2021.707041

The Prognostic Role of Blood Inflammatory Biomarkers and EGFR Mutation Status in Stage IIIA/N2 Non-Small Cell Lung Cancer Patients Treated With Trimodality Therapy

*Hui Yang[1], Kunlun Wang[1], Bingxu Li[1,2], Shenglei Li[1], Yan Li[1] and Ling Yuan[1]**

[1] Department of Radiation Oncology, The Affiliated Cancer Hospital of Zhengzhou University, Zhengzhou, China,
[2] Department of Radiation Oncology, Anyang Cancer Hospital, The Forth Affiliated Hospital of Henan University of Science and Technology, Anyang, China

OPEN ACCESS

Edited by:
Junji Uchino,
Kyoto Prefectural University of Medicine, Japan

Reviewed by:
Dipesh Uprety,
Wayne State University, United States
Shejuan An,
Northwestern University, United States
Jiayuan Sun,
Shanghai Jiaotong University, China

***Correspondence:**
Ling Yuan
HNHNYL@126.com

Specialty section:
This article was submitted to Thoracic Oncology, a section of the journal Frontiers in Oncology

Received: 08 May 2021
Accepted: 15 November 2021
Published: 30 November 2021

Citation:
Yang H, Wang K, Li B, Li S, Li Y and Yuan L (2021) The Prognostic Role of Blood Inflammatory Biomarkers and EGFR Mutation Status in Stage IIIA/N2 Non-Small Cell Lung Cancer Patients Treated With Trimodality Therapy. Front. Oncol. 11:707041. doi: 10.3389/fonc.2021.707041

Objectives: Various blood inflammatory biomarkers were associated with treatment response and prognosis of non-small cell lung cancer (NSCLC) in previous studies. In this study, we retrospectively evaluated the prognostic role of pretreatment blood inflammatory biomarkers and epidermal growth factor receptor (EGFR) mutation status in stage IIIA/N2 NSCLC patients with trimodality therapy.

Methods: Completely resected stage IIIA/N2 NSCLC patients with adjuvant chemotherapy and postoperative radiotherapy (PORT) were assessed in this study. Cutoff values of blood inflammatory factors were calculated by the R package SurvivalROC of R software. SPSS Statistics software was used for survival analyses. Kaplan-Meier survival curve and log-rank test were used to compare the survival difference between every two groups. Univariate and multivariate analyses of predictive factors were performed by Cox proportional hazards regression model.

Results: The univariate analysis showed that T stage (p=0.007), EGFR mutation status (p=0.043), lymphocyte-to-monocyte ratio (LMR) (p=0.067), and systemic immune-inflammation index (SII) (p=0.043) were significant prognostic factors of disease-free survival (DFS). In the multivariate analysis, T2 (HR=0. 885, 95% CI: 0.059-0.583, p=0.004), EGFR mutation-positive (HR=0.108, 95% CI: 0.023-0.498, p=0.004) and elevated pretreatment SII (HR=0.181, 95%CI: 0.046-0.709, p=0.014) were independently related to shorter DFS. High pretreatment neutrophil counts (HR=0.113, p=0.019) and high systemic inflammation response index (SIRI) (HR=0.123, p=0.025) were correlated with worse overall survival (OS) by the univariate analysis. In the multivariate analysis, only high pretreatment SIRI was an independent predictor for poorer OS (HR=0.025, 95% CI: 0.001-0.467, p=0.014).

Conclusions: In conclusion, we identified that high pretreatment SII and SIRI were unfavorable prognostic factors in stage IIIA/N2 NSCLC patients treated with surgery, adjuvant chemotherapy and PORT. Patients with high pretreatment SII, high pretreatment

SIRI, T2, and EGFR mutation-positive may need more forceful adjuvant treatment. Further prospective studies with large-scale are needed to validate our results and identify the proper cut-off values and optimum adjuvant treatment for distinct patient population.

Keywords: stage IIIA/N2, non-small cell lung cancer, blood inflammatory biomarkers, systemic immune-inflammation index, systemic inflammation response index

INTRODUCTION

Among the most common cancers, lung cancer ranks first in cancer-associated death worldwide (1). More than 80% of lung cancer patients are non-small cell lung cancer (NSCLC), and 15% of them were diagnosed as stage IIIA (2). Furthermore, stage IIIA NSCLC patients have heterogeneous clinical features and prognoses. Stage IIIA/N2 NSCLC patients were always the hotspot of study and require multidisciplinary treatment approaches. For unresectable patients, definitive chemoradiotherapy (CRT) followed by maintenance durvalumab was preferred according to the PACIFIC Trial (3). For resectable disease, surgery followed by adjuvant chemotherapy with or without postoperative radiotherapy (PORT) was recommended by the National Comprehensive cancer network (NCCN).

However, at least 30% of stage IIIA/N2 NSCLC patients suffered recurrence or metastasis within five years after complete surgical resection (4). Plenty of randomized controlled trials (RCT) and large-scale retrospective studies revealed the importance of PORT in stage IIIA/N2 NSCLC after complete surgical resection (5–10). PORT not only improved disease-free survival (DFS) but also increased the overall survival time (OS) of patients. The NCT00880971 trial founded that the PORT group had a better 3-years local recurrence-free rate (69.8 *vs* 62.4%, p=0.03) than chemotherapy alone after complete surgery (11). However, the median DFS (26.5 vs 22.7 months, p=0.10), and median OS (not reached vs 90.9 months, p=0.94) had no significant difference between the two groups. The Lung ART study (NCT00410683) also showed that PORT reduced the local recurrence rate (from 46.1 to 25.0%), but could not bring DFS or OS benefit (12). The adjuvant treatments for stage IIIA/N2 patients are still controversial now. Trimodality therapy (surgery, adjuvant chemotherapy and PORT) is one of the suitable treatment modalities so far.

Inflammation response in the tumor environment was closely related to tumor development, growth, and recurrence (13, 14). The peripheral blood cells, including neutrophils, lymphocytes, monocytes, and platelets, play an essential role in the inflammatory response and reflect the anti-tumor immunity in the host (15–17). Based on previous studies, the count of these cells and their ratios are correlated with treatment response and prognosis of cancer patients. Hence, neutrophil counts, lymphocyte counts, monocyte counts, platelet count, neutrophil-to-lymphocyte ratio (NLR), platelet-to-lymphocyte ratio (PLR), lymphocyte-to-monocyte ratio (LMR), systemic immune-inflammation index (SII), and systemic inflammation response index (SIRI) have been identified as blood inflammatory biomarkers and served as prognostic indicators in various cancers (18–22).

Concerning lung cancer, the prognostic role of blood inflammatory biomarkers has been described in previous studies. A meta-analysis reported that higher pretreatment NLR was a significant predicator of poor survival not only in patients treated with chemotherapy but also in patients with immunotherapy or targeted therapy (23). High pretreatment NLR, high PLR, and low LMR were also related to poor outcomes in early stage, locally advanced and advanced NSCLC patients with diverse treatments (24–27). Another study of stage III NSCLC patients treated with concurrent CRT found that high pretreatment SII was independently correlated with chemoradiation resistance and poor prognosis (28). SIRI was also important in unresectable stage III NSCLC patients treated with CRT (29) and advanced NSCLC patients treated with epidermal growth factor receptor (EGFR) tyrosine kinase inhibitors (TKIs) (30).

Since blood inflammatory biomarkers were associated with the prognosis of patients, these factors were crucial to identify high-risk patients and make optimum treatment decision for them. A retrospective study of locally advanced NSCLC patients treated with preoperative CRT and surgery detected that high postoperative NLR was an indicator for poor prognosis (31). Postoperative adjuvant chemotherapy significantly increased the 5-year OS rate in patients with high postoperative NLR (cutoff value: 4.06, p=0.016), and could not improve the prognosis of patients with low NLR (p=0.19) (31). Hence, patients with high postoperative NLR had a poor prognosis, and need postoperative adjuvant chemotherapy to improve the survival time. For patients with low NLR, preoperative CRT and surgery may be enough.

However, the prognostic impact of blood inflammatory biomarkers in stage IIIA/N2 patients treated with trimodality therapy is still unclear. In this study, we retrospectively evaluated the pretreatment blood inflammatory biomarkers and other clinicopathological factors to find potential prognostic biomarkers and identify the high- risk patients who need more forceful adjuvant treatment.

MATERIALS AND METHODS

Patient Selection

This study retrospectively screened patients diagnosed in the Affiliated Cancer Hospital of Zhengzhou University from January 2015 to December 2019. The inclusion criteria were: stage IIIA/N2 according to the 8th edition of the American Joint Committee on Cancer (AJCC) cancer staging system; completely resected; no neoadjuvant therapy; received four cycles of postoperative chemotherapy and radiotherapy after surgery; no history of other malignant tumors. Patients were excluded when

disease progression occurred before the completion of postoperative treatment; postoperative treatment was not completed; or without enough follow-up data.

Data Collection

We collected medical records from the hospital database, including age, gender, pathological type, tumor size, positive lymph nodes, EGFR mutation status, and radiation sequence with chemotherapy (concurrent, sequential). Pretreatment blood inflammatory biomarkers including neutrophil counts, lymphocyte counts, monocyte counts, and platelet count were assumed from routine laboratory results within one week before surgery. NLR=neutrophil count/lymphocyte count; LMR=lymphocyte count/monocyte count; PLR=platelet count/lymphocyte count; SII=platelet count × neutrophil counts/lymphocyte counts; SIRI=neutrophil count × monocyte count/lymphocyte count.

Statistical Analysis

DFS was defined as the duration from surgery to disease progression, or death. OS was established as the time from surgery to cancer-associated death or the date of the last follow-up.

R software (version 4.0.4) and SPSS Statistics software (version 26.0) were used for the analysis in this study. Cutoff values of blood inflammatory factors were calculated by the R package SurvivalROC through receiver operating characteristic (ROC) curves. The SurvivalROC package iteratively tests all cutoff values to find the cut-point that achieves the maximum log-rank statistic. Corresponding two-tailed p values were measured, and a p-value of <0.05 was considered statistically significant. Kaplan-Meier survival curve and log-rank test were used to compare the survival difference between the two groups. Univariate and multivariate analyses of predictive factors were performed by Cox proportional hazards regression model. Proper factors with p<0.1 in univariate analysis were selected into multivariate analysis to validate independent prognostic factors. The results of prognostic factors were expressed as hazard ratio (HR) with a 95% confidence interval (CI).

RESULTS

A total of 34 patients were collected in this study. The median follow-up time was 26.4 months (12.4 to 55.4 months). Median DFS was 38.7 months (95% CI: 28.7-48.7 months) and median OS was 52.7 months (95% CI: 48.3-57.1 months) in all patients. Patients had a median age of 56.5 years (range 38–73 years) at the time of diagnosis. Eleven patients (32.4%) were older than 60 years, while 23 patients (67.6%) were under 60 years. Our patients were predominantly adenocarcinoma (91.2%), only three patients were squamous carcinoma or others. 21 patients were T1 (T1a, 2 patients; T1b, 7 patients; T1c, 12 patients) and 13 patients were T2 (T2a, 11patients; T2b, 2 patients). 41.2% of patients had multistation N2 lymph node, other 20 patients were single-station N2. The EGFR mutation status showed that 61.8% of patients were EGFR mutation-negative. 67.6% of patients underwent sequential chemoradiotherapy, only 11 (32.4%) patients had concurrent chemoradiotherapy (**Table 1**).

Cutoff Values of Blood Inflammatory Biomarkers

ROC curves were generated to determine the cutoff values of blood inflammatory biomarkers. The cutoff values based on DFS for pretreatment neutrophil counts, lymphocyte counts, monocyte counts, platelet counts, NLR, PLR, SII, and SIRI were 3.97, 1.86, 0.35, 253, 2.34, 134.68, 7.46, 708.40, and 0.77, respectively. The cutoff values based on OS were 5.77, 1.86, 0.25, 363, 2.80, 77.06, 7.44, 918.63, and 0.82, respectively. Patients were divided into two groups based on the corresponding cutoff values.

Univariate and Multivariate Analysis of DFS

The univariate analysis and Kaplan-Meier survival curve showed that T stage (HR=0.220, 95% CI: 0.073-0.663, p=0.007), EGFR mutation status (HR=0.278, 95% CI: 0.081-0.959, p=0.043), LMR (HR=0.358, 95% CI: 0.119-1.075, p=0.067), and SII (HR=0.334, 95% CI: 0.116-0.964, p=0.043) were significantly associated with DFS (**Figure 1**). In the multivariate analysis, T2 (HR=0. 885, 95% CI: 0.059-0.583, p=0.004), EGFR mutation-positive (HR=0.108, 95% CI: 0.023-0.498, p=0.004) and elevated pretreatment SII (HR=0.181, 95%CI: 0.046-0.709, p=0.014) were independent predicators for poor DFS. The role of pretreatment neutrophil counts, lymphocyte counts, monocyte counts, platelet counts, NLR, PLR, and SIRI could not be identified in our study (**Table 2**).

Univariate and Multivariate Analysis of OS

High pretreatment neutrophil counts (HR=0.113, 95% CI: 0.018-0.699, p=0.019) and high SIRI (HR=0.123, 95% CI: 0.020-0.722,

TABLE 1 | Baseline characteristics of all patients (n=34).

Characteristics	Number (%)
Gender	
Male	20 (58.8)
Female	14 (41.2)
Age (year)	56.5 (38–73)
≤60	23 (67.6)
>60	11 (32.4)
Histological subtype	
Adenocarcinoma	31 (91.2)
Squamous carcinoma and others	3 (8.8)
Pathological stage	
1	21 (61.8)
1a/1b/1c	2 (5.9)/7 (20.6)/12 (35.3)
2	13 (38.2)
2a/2b	11 (32.4)/2 (5.8)
N2 lymph node	
Multistation	14 (41.2)
Single-station	20 (58.8)
EGFR mutation	
Positive	13 (38.2)
Negative	21 (61.8)
Radiation sequence	
Concurrent	11 (32.4)
Sequential	23 (67.6)

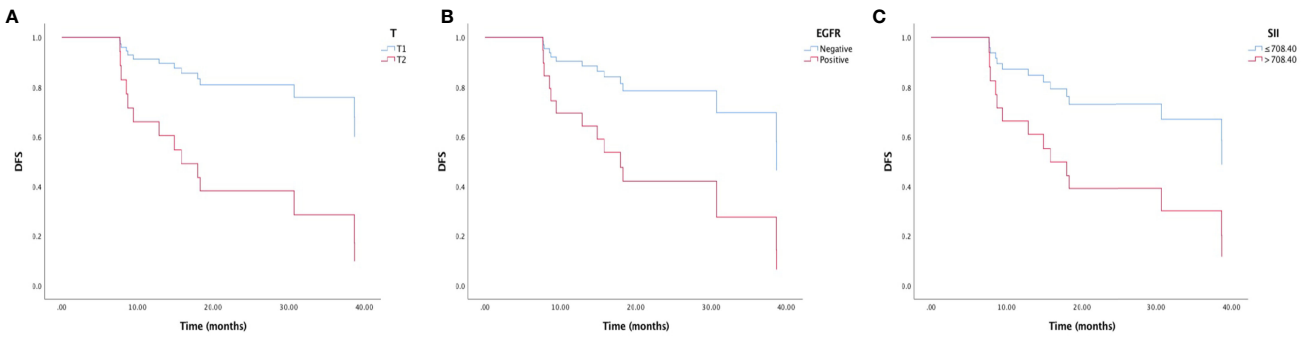

FIGURE 1 | Kaplan-Meier survival curve of disease-free survival (DFS) and **(A)** T stage, **(B)** EGFR mutation status, and **(C)** immune-inflammation index (SII).

p=0.025) were related to worse OS by the univariate analysis and Kaplan-Meier survival curve (**Figure 2**). In the multivariate analysis, only high pretreatment SIRI was an independent predictor for shorter OS (HR=0.025, 95% CI: 0.001-0.467, p=0.014). EGFR mutation and SII were likely to influence OS, but did not reach statistical significance (**Table 3**).

DISCUSSION

Stage IIIA/N2 NSCLC patients have a high risk of local progression and distant metastasis after complete surgical resection. After definitive treatment, some tumor cells still exist in the host microenvironment and cause recurrence and metastasis soon. Previous RCTs have revealed the importance of adjuvant treatment in the distinct patient population. However, not all the patients could bear the toxicity and cost of adjuvant therapies. The multimodal treatment strategies are still controversial now. For patients with a high risk of progression, additional adjuvant therapy should be considered to eliminate residual tumor cells and improve the survival outcomes. It is important to discover accessible indicators for high-risk patients and select appropriate therapeutic modalities.

Since the indices of blood cells are routinely tested at low cost, they may be suitable non-invasive biomarkers for clinicians. Various blood inflammatory biomarkers have been extensively studied in NSCLC. These factors correlated with inflammatory response and reflected the immune status of tumor microenvironment (TME). For example, neutrophils can secrete various inflammatory factors and up-regulate the tumorigenic and angiogenic factors, which creating an inflammatory environment favorable for tumor growth and metastases (13, 16). Platelets are involved in tumor development and progression through promoting angiogenesis (32). Monocytes were reported to promote tumor growth and angiogenesis, and inhibit the antitumor immune response (13, 33). By contrast, lymphocytes, particularly tumor-infiltrating lymphocytes (TILs), may induce cytotoxic cell death and inhibit tumor cell proliferation and migration (13). Thus, neutrophils, platelets and monocytes may have tumor-promoting properties and lymphocytes are essential for tumor defense and immune

TABLE 2 | Univariate and multivariate analyses of DFS.

	Parameter	Univariate HR (95%CI)	p	Multivariate HR (95%CI)	p
Radiation sequence	Concurrent vs. Sequential	0.630 (0.196-2.019)	0.436		
Gender	Male vs. Female	0.509 (0.176-1.473)	0.213		
Age	≤60 vs. >60	3.168 (0.704-14.258)	0.133		
Histological subtype	Adenocarcinoma vs. Squamous carcinoma	1.876 (0.244-14.436)	0.546		
T stage	T1 vs. T2	0.220 (0.073-0.663)	**0.007**	0.885 (0.059-0.583)	**0.004**
N2 station	Single vs. Multistation	1.072 (0.367-3.134)	0.899		
EGFR mutation	Negative vs. Positive	0.278 (0.081-0.959)	**0.043**	0.108 (0.023-0.498)	**0.004**
Neutrophil counts	≤3.97 vs. >3.97	0.550 (0.187-1.613)	0.276		
Lymphocyte counts	≤1.86 vs. >1.86	0.419 (0.131-1.340)	0.142		
Monocyte counts	≤0.35 vs. >0.35	0.339 (0.107-1.076)	0.066		
Platelet counts	≤253 vs. >253	0.313 (0.096-1.024)	0.055		
NLR	≤2.34 vs. >2.34	0.620 (0.214-1.795)	0.378		
PLR	≤134.68 vs. >134.68	0.662 (0.232-1.894)	0.442		
LMR	≤7.46 vs. >7.46	0.358 (0.119-1.075)	**0.067**		
SII	≤708.40 vs. >708.40	0.334 (0.116-0.964)	**0.043**	0.181 (0.046-0.709)	**0.014**
SIRI	≤0.77 vs. >0.77	0.610 (0.182-2.043)	0.423		

Bold values means p values < 0.05.

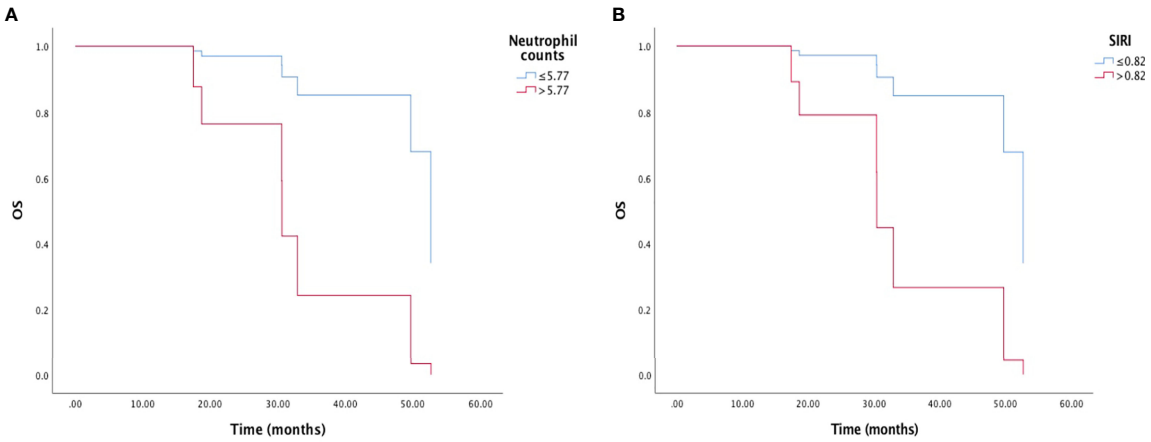

FIGURE 2 | Kaplan-Meier survival curve of overall survival (OS) and **(A)** neutrophil counts, and **(B)** inflammation response index (SIRI).

surveillance. The SII and SIRI are compound inflammatory biomarkers calculated by the counts of neutrophils, monocytes, platelets, and lymphocytes, which could better reflect the tumor immune microenvironment than any single index.

Meanwhile, blood inflammatory biomarkers could predict treatment outcomes and provide valuable information about the possibility of progression and survival time. In our study, we focused on the particular patient population of stage IIIA/N2 NSCLC treated with trimodality therapy and aimed to find potential blood inflammatory biomarkers as prognostic predictors and treatment indicators. We evaluated 34 patients and identified that low pretreatment SII (≤708.40), T2, and EGFR mutation-negative were indicator for longer DFS, and pretreatment SIRI (cutoff value: 0.82) was a prognostic factor for OS. We also analyzed the blood biomarkers of different times (after surgery, before chemotherapy, and before radiotherapy), but did not get any meaningful results. Overall, patients with high SII, high SIRI, T2 or EGFR mutation-negative have a high risk of poor prognosis and may need careful observation and forceful adjuvant treatment.

For oncogenic driver alteration NSCLC patients, the anti-tumor immune response in TME is always uninflamed. EGFR mutation-positive caused lack of TILs, impaired the antigen specific signal, made tumor cells unrecognizable to T cells, reduced programmed death receptor ligand-1 (PD-L1) expression, lower tumor mutation burden (TMB) (34–36). The immunosuppressive TME induced poor prognosis in EGFR mutation-positive NSCLC patients.

As for EGFR mutation-positive stage IIIA/N2 patients, adjuvant TKIs may be more beneficial than chemotherapy. In phase III ADJUVANT/CTONG1104 study (NCT01405079), gefitinib increased the DFS (28.7 months vs. 18.0 months, HR=0.60, 95% CI: 0.42-0.87, p=0.0054) compared with the chemotherapy group (vinorelbine plus cisplatin) in completely resected stage II-IIIA (N1-

TABLE 3 | Univariate and multivariate analyses of OS.

	Parameter	Univariate HR (95%CI)	p	Multivariate HR (95%CI)	p
Radiation sequence	Concurrent vs. Sequential	1.768 (0.290-10.762)	0.536		
Gender	Male vs. Female	0.766 (0.170-3.448)	0.729		
Age	≤60 vs. >60	0.845 (0.155-4.607)	0.846		
Histological subtype	Adenocarcinoma vs. Squamous carcinoma	35.226 (0.008-159235.874)	0.407		
T stage	T1 vs. T2	0.959 (0.192-4.793)	0.959		
N2 station	Single vs. Multistation	2.352 (0.454-12.189)	0.308		
EGFR mutation	Negative vs. Positive	0.190 (0.034-1.058)	0.058		
Neutrophil counts	≤5.77 vs. >5.77	0.113 (0.018-0.699)	**0.019**		
Lymphocyte counts	≤1.86 vs. >1.86	0.900 (0.200-4.049)	0.891		
Monocyte counts	≤0.25 vs. >0.25	0.631 (0.117-3.401)	0.591		
Platelet counts	≤363 vs. >363	0.157 (0.016-1.536)	0.112		
NLR	≤2.80 vs. >2.80	0.474 (0.779-28.57)	0.091		
PLR	≤77.06 vs. >77.06	1.088 (0.126-9.434)	0.939		
LMR	≤7.44 vs. >7.44	0.894 (0.194-4.127)	0.886		
SII	≤918.63 vs. >918.63	0.185 (0.031-1.116)	0.066		
SIRI	≤0.82 vs. >0.82	0.123 (0.020-0.772)	**0.025**	0.025 (0.001-0.467)	0.014

Bold values means p values < 0.05.

N2) EGFR mutation-positive NSCLC (37). The phase 3 ADAURA study (NCT02511106) assessed completely resected early-stage (stage II to IIIA) NSCLC patients with EGFR mutation-positive and reported that DFS was significantly longer in the osimertinib group than placebo group (not reached vs. 19.6 months; HR=0.17, 99.06% CI: 0.11-0.26, p<0.001) (38). There are also studies of adjuvant immunotherapy in the completely resected (stage II-IIIA) EGFR mutation-positive NSCLC patients (39). The best adjuvant treatment and the combination with radiotherapy are unknown in the light of current studies.

Our study has several limitations. First, it was a small, retrospective, single-center study with unavoidable bias. Second, blood inflammatory biomarkers could be influenced by various unidentified factors, such as active infection or concomitant use of nonsteroidal anti-inflammatory drug or autoimmune disease. These factors could bring bias to results. Third, we used the R package SurvivalROC to get the cut-off values of blood inflammatory biomarkers in this study. The optimum method for proper cut-off values is uncertain. The cut-off values also vary in distinct patient population with specific treatment. Fourth, the anaplastic lymphoma kinase (ALK) rearrangement, and reactive oxygen species-1 (ROS-1) rearrangement were not validated because of the small study population. Future prospective studies with larger sample size and proper stratification are needed.

Despite the above limitations, our study was the first to investigate the relationship between blood inflammatory biomarkers and prognosis in stage IIIA/N2 NSCLC patients with trimodality therapy. Further prospective, large-scale studies are needed to further confirm the prognostic role of SII and SIRI. With the rapid development of immunotherapy, target therapy, and anti-vascular therapy, the best adjuvant treatment and corresponding cutoff values for distinct patients is unclear and requires more trials to investigate.

Furthermore, the importance of radiotherapy in enhancing anti-tumor immunity should be noticed in the design of prospective trials. To maximum the synergistic effect of radiotherapy, the radiation technique, target region and dose may be crucial in future prospective trials. T-lymphocytes are very radiosensitive. Larger radiation fields expose more lymphocytes to radiotherapy, which may in turn exhaust the T-cells. The degree of radiotherapy-induced lymphopenia is related to prognosis in NSCLC (40). However, the radiation region for stage III NSCLC patients usually includes draining lymph nodes, which affects the number and distribution of lymphocytes. Reduction in the volume of the radiation target (selective lymph nodal irradiation) and enhanced protection for normal lymph nodes with highly conformal techniques could reduce radiotherapy-induced lymphopenia. Maintaining the lymphocyte count may help to reduce the values of SII and SIRI and enhance anti-tumor immunity and eventually improve the survival of stage III NSCLC. The proper target region and the possibility of reduce the radiation dose to lymph nodes should be tested in future trials for a balance between lymphocytes reservation and local control of the tumor.

In conclusion, we identified that high pretreatment SII and SIRI were unfavorable prognostic factors in stage IIIA/N2 NSCLC patients treated with trimodality therapy. Pretreatment SII and SIRI may be potential indicators for further treatment options. Patients with high pretreatment SII, high pretreatment SIRI, T2, and EGFR mutation-positive may need more forceful adjuvant treatment. However, the proper adjuvant treatment is undecided. Further large-scale, prospective studies are needed to confirm our results, clarify the best cutoff values and most beneficial adjuvant treatment.

DATA AVAILABILITY STATEMENT

The raw data supporting the conclusions of this article will be made available by the authors, without undue reservation.

ETHICS STATEMENT

The studies involving human participants were reviewed and approved by Ethics committee of the Affiliated Cancer Hospital of Zhengzhou University. Written informed consent for participation was not required for this study in accordance with the national legislation and the institutional requirements.

AUTHOR CONTRIBUTIONS

HY and LY designed this study and analyzed the data. HY and KW collected the data and wrote the manuscript. BL, YL, and SL assisted in collecting data and correcting the manuscript. All authors contributed to the article and approved the submitted version.

FUNDING

This study was supported by Science and Technology Department, Henan Province (grant numbers: SB201901113 and 192102310048).

REFERENCES

1. Siegel RL, Miller KD, Jemal A. Cancer Statistics, 2020. *CA Cancer J Clin* (2020) 70(1):7–30. doi: 10.3322/caac.21590
2. Rusch VW, Chansky K, Kindler HL, Nowak AK, Pass HI, Rice DC, et al. The IASLC Mesothelioma Staging Project: Proposals for the M Descriptors and for Revision of the TNM Stage Groupings in the Forthcoming (Eighth) Edition of the TNM Classification for Mesothelioma. *J Thorac Oncol* (2016) 11(12):2112–9. doi: 10.1016/j.jtho.2016.09.124
3. Faivre-Finn C, Vicente D, Kurata T, Planchard D, Paz-Ares L, Vansteenkiste JF, et al. Four-Year Survival With Durvalumab After Chemoradiotherapy in Stage III NSCLC-An Update From the PACIFIC Trial. *J Thorac Oncol* (2021) 16(5):860–7. doi: 10.1016/j.jtho.2020.12.015
4. Lally BE, Zelterman D, Colasanto JM, Haffty BG, Detterbeck FC, Wilson LD. Postoperative Radiotherapy for Stage II or III Non-Small-Cell Lung Cancer

Using the Surveillance, Epidemiology, and End Results Database. *J Clin Oncol* (2006) 24(19):2998–3006. doi: 10.1200/JCO.2005.04.6110
5. Douillard JY, Rosell R, De Lena M, Riggi M, Hurteloup P, Mahe MA. Adjuvant Navelbine International Trialist Association. Impact of Postoperative Radiation Therapy on Survival in Patients With Complete Resection and Stage I, II, or IIIA Non-Small-Cell Lung Cancer Treated With Adjuvant Chemotherapy: The Adjuvant Navelbine International Trialist Association (ANITA) Randomized Trial. *Int J Radiat Oncol Biol Phys* (2008) 72(3):695–701. doi: 10.1016/j.ijrobp.2008.01.044
6. Zou B, Xu Y, Li T, Li W, Tang B, Zhou L, et al. A Multicenter Retrospective Analysis of Survival Outcome Following Postoperative Chemoradiotherapy in Non-Small-Cell Lung Cancer Patients With N2 Nodal Disease. *Int J Radiat Oncol Biol Phys* (2010) 77(2):321–8. doi: 10.1016/j.ijrobp.2009.05.044
7. Shen WY, Ji J, Zuo YS, Pu J, Xu YM, Zong CD, et al. Comparison of Efficacy for Postoperative Chemotherapy and Concurrent Radiochemotherapy in Patients With IIIA-Pn2 Non-Small Cell Lung Cancer: An Early Closed Randomized Controlled Trial. *Radiother Oncol* (2014) 110(1):120–5. doi: 10.1016/j.radonc.2013.10.008
8. Mikell JL, Gillespie TW, Hall WA, Nickleach DC, Liu Y, Lipscomb J, et al. Postoperative Radiotherapy Is Associated With Better Survival in Non-Small Cell Lung Cancer With Involved N2 Lymph Nodes: Results of an Analysis of the National Cancer Data Base. *J Thorac Oncol* (2015) 10(3):462–71. doi: 10.1097/JTO.0000000000000411
9. Corso CD, Rutter CE, Wilson LD, Kim AW, Decker RH, Husain ZA. Re-Evaluation of the Role of Postoperative Radiotherapy and the Impact of Radiation Dose for Non-Small-Cell Lung Cancer Using the National Cancer Database. *J Thorac Oncol* (2015) 10(1):148–55. doi: 10.1097/JTO.0000000000000406
10. Herskovic A, Mauer E, Christos P, Nagar H. Role of Postoperative Radiotherapy in Pathologic Stage IIIA (N2) Non-Small Cell Lung Cancer in a Prospective Nationwide Oncology Outcomes Database. *J Thorac Oncol* (2017) 12(2):302–13. doi: 10.1016/j.jtho.2016.09.135
11. Hui Z, Men Y, Hu C, Zhou Z, Liang J, Feng Q, et al. OA12.06 A Prospective Randomized Phase III Study of Precise PORT for Patients With PIIIA-N2 NSCLC After Complete Resection and Adjuvant Chemotherapy. *J Thorac Oncol* (2019) 14(10):S238–9. doi: 10.1016/j.jtho.2019.08.475
12. Le Pechoux C, Pourel N, Barlesi F, Faivre-Finn C, Lerouge D, Zalcman G, et al. LBA3_PR an International Randomized Trial, Comparing Post-Operative Conformal Radiotherapy (PORT) to No PORT, in Patients With Completely Resected Non-Small Cell Lung Cancer (NSCLC) and Mediastinal N2 Involvement: Primary End-Point Analysis of LungART (IFCT-0503, UK NCRI, SAKK) Nct00410683. *Ann Oncol* (2020) 31(4):S1178. doi: 10.1016/j.anNonc.2020.08.2280
13. Balkwill F, Mantovani A. Inflammation and Cancer: Back to Virchow? *Lancet* (2001) 357(9255):539–45. doi: 10.1016/S0140-6736(00)04046-0
14. Colotta F, Allavena P, Sica A, Garlanda C, Mantovani A. Cancer-Related Inflammation, the Seventh Hallmark of Cancer: Links to Genetic Instability. *Carcinogenesis* (2009) 30(7):1073–81. doi: 10.1093/carcin/bgp127
15. Moses K, Brandau S. Human Neutrophils: Their Role in Cancer and Relation to Myeloid-Derived Suppressor Cells. *Semin Immunol* (2016) 28(2):187–96. doi: 10.1016/j.smim.2016.03.018
16. Brandau S, Dumitru CA, Lang S. Protumor and Antitumor Functions of Neutrophil Granulocytes. *Semin Immunopathol* (2013) 35:163–76. doi: 10.1007/s00281-012-0344-6
17. Jacquelot N, Tellier J, Nutt Sl, Belz Gt. Tertiary Lymphoid Structures and B Lymphocytes in Cancer Prognosis and Response to Immunotherapies. *Oncoimmunology* (2021) 10(1):1900508. doi: 10.1080/2162402X.2021.1900508
18. De Martino M, Pantuck AJ, Hofbauer S, Waldert M, Shariat SF, Belldegrun AS, et al. Prognostic Impact of Preoperative Neutrophil-to-Lymphocyte Ratio in Localized Nonclear Cell Renal Cell Carcinoma. *J Urol* (2013) 190:1999–2004. doi: 10.1016/j.juro.2013.06.082
19. Krenn-Pilko S, Langsenlehner U, Thurner EM, Stojakovic T, Pichler M, Gerger A, et al. The Elevated Preoperative Platelet-to-Lymphocyte Ratio Predicts Poor Prognosis in Breast Cancer Patients. *Br J Cancer* (2014) 110:2524–30. doi: 10.1038/bjc.2014.163
20. Luo G, Guo M, Liu Z, Xiao Z, Jin K, Long J, et al. Blood Neutrophil-Lymphocyte Ratio Predicts Survival in Patients With Advanced Pancreatic Cancer Treated With Chemotherapy. *Ann Surg Oncol* (2015) 22(2):670–6. doi: 10.1245/s10434-014-4021-y
21. Xia LJ, Li W, Zhai JC, Yan CW, Chen JB, Yang H. Significance of Neutrophil-to-Lymphocyte Ratio, Platelet-to-Lymphocyte Ratio, Lymphocyte-to-Monocyte Ratio and Prognostic Nutritional Index for Predicting Clinical Outcomes in T1-2 Rectal Cancer. *BMC Cancer* (2020) 20(1):208. doi: 10.1186/s12885-020-6698-6
22. Li X, Hu P, Liu J, Zhang J, Liu Q. Systemic Immune-Inflammation Index Predicted Overall Survival and Radiosensitivity in Advanced Non-Small-Cell Lung Cancer. *Future Oncol* (2020) 16(5):103–15. doi: 10.2217/fon-2019-0761
23. Wang Z, Zhan P, Lv Y, Shen K, Wei Y, Liu H, et al. Prognostic Role of Pretreatment Neutrophil-to-Lymphocyte Ratio in Non-Small Cell Lung Cancer Patients Treated With Systemic Therapy: A Meta-Analysis. *Transl Lung Cancer Res* (2019) 8(3):214–26. doi: 10.21037/tlcr.2019.06.10
24. Mandaliya H, Jones M, Oldmeadow C, Nordman II. Prognostic Biomarkers in Stage IV Non-Small Cell Lung Cancer (NSCLC): Neutrophil to Lymphocyte Ratio (NLR), Lymphocyte to Monocyte Ratio (LMR), Platelet to Lymphocyte Ratio (PLR) and Advanced Lung Cancer Inflammation Index (ALI). *Transl Lung Cancer Res* (2019) 8(6):886–94. doi: 10.21037/tlcr.2019.11.16
25. Shoji F, Kozuma Y, Toyokawa G, Yamazaki K, Takeo S. Complete Blood Cell Count-Derived Inflammatory Biomarkers in Early-Stage Non-Small-Cell Lung Cancer. *Ann Thorac Cardiovasc Surg* (2020) 26(5):248–55. doi: 10.5761/atcs.oa.19-00315
26. Luo H, Ge H, Cui Y, Zhang J, Fan R, Zheng A, et al. Systemic Inflammation Biomarkers Predict Survival in Patients of Early Stage Non-Small Cell Lung Cancer Treated With Stereotactic Ablative Radiotherapy-A Single Center Experience. *J Cancer* (2018) 9(1):182–8. doi: 10.7150/jca.21703
27. Sebastian NT, Raj R, Prasad R, Barney C, Brownstein J, Grecula J, et al. Association of Pre- and Posttreatment Neutrophil-Lymphocyte Ratio With Recurrence and Mortality in Locally Advanced Non-Small Cell Lung Cancer. *Front Oncol* (2020) 10:598873. doi: 10.3389/fonc.2020.598873
28. Tong YS, Tan J, Zhou XL, Song YQ, Song YJ. Systemic Immune-Inflammation Index Predicting Chemoradiation Resistance and Poor Outcome in Patients With Stage III Non-Small Cell Lung Cancer. *J Transl Med* (2017) 15(1):221. doi: 10.1186/s12967-017-1326-1
29. Hu M, Xu Q, Yang S, Han S, Zhu Y, Lin Q, et al. Pretreatment Systemic Inflammation Response Index (SIRI) Is an Independent Predictor of Survival in Unresectable Stage III Non-Small Cell Lung Cancer Treated With Chemoradiotherapy: A Two-Center Retrospective Study. *Ann Transl Med* (2020) 8(20):1310. doi: 10.21037/atm-20-6484
30. Jiang S, Wang S, Wang Q, Deng C, Feng Y, Ma F, et al. Systemic Inflammation Response Index (SIRI) Independently Predicts Survival in Advanced Lung Adenocarcinoma Patients Treated With First-Generation EGFR-TKIs. *Cancer Manag Res* (2021) 13:1315–22. doi: 10.2147/CMAR.S287897
31. Tsudaka S, Yamamoto H, Sato H, Katsui K, Suzawa K, Shien K, et al. Prognostic Significance of Neutrophil-To-Lymphocyte Ratio in Locally Advanced Non-Small-Cell Lung Cancer Treated With Trimodality Therapy. *Ann Surg Oncol* (2021) 28(9):4880–90. doi: 10.1245/s10434-021-09690-9
32. Wojtukiewicz MZ, Sierko E, Hempel D, Tucker SC, Honn KV. Platelets and Cancer Angiogenesis Nexus. *Cancer Metastasis Rev* (2017) 36(2):249–62. doi: 10.1007/s10555-017-9673-1
33. Singhal S, Stadanlick J, Annunziata MJ, Rao AS, Bhojnagarwala PS, O'Brien S, et al. Human Tumor-Associated Monocytes/Macrophages and Their Regulation of T Cell Responses in Early-Stage Lung Cancer. *Sci Transl Med* (2019) 11(479):eaat1500. doi: 10.1126/scitranslmed.aat1500
34. Dong ZY, Zhang JT, Liu SY, Su J, Zhang C, Xie Z, et al. EGFR Mutation Correlates With Uninflamed Phenotype and Weak Immunogenicity, Causing Impaired Response to PD-1 Blockade in Non-Small Cell Lung Cancer. *Oncoimmunology* (2017) 6(11):e1356145. doi: 10.1080/2162402X.2017.1356145
35. Pitt JM, Vétizou M, Daillère R, Roberti MP, Yamazaki T, Routy B, et al. Resistance Mechanisms to Immune-Checkpoint Blockade in Cancer: Tumor-Intrinsic and -Extrinsic Factors. *Immunity* (2016) 44(6):1255–69. doi: 10.1016/j.immuni.2016.06.001
36. Sharma P, Hu-Lieskovan S, Wargo JA, Ribas A. Primary, Adaptive, and Acquired Resistance to Cancer Immunotherapy. *Cell* (2017) 168(4):707–23. doi: 10.1016/j.cell.2017.01.017
37. Zhong WZ, Wang Q, Mao WM, Xu ST, Wu L, Shen Y, et al. Gefitinib Versus Vinorelbine Plus Cisplatin as Adjuvant Treatment for Stage II-IIIA (N1-N2) EGFR-Mutant NSCLC (ADJUVANT/CTONG1104): A Randomised, Open-Label, Phase 3 Study. *Lancet Oncol* (2018) 19(1):139–48. doi: 10.1016/S1470-2045(17)30729-5
38. Wu YL, Tsuboi M, He J, John T, Grohe C, Majem M, et al. Osimertinib in Resected EGFR-Mutated Non-Small-Cell Lung Cancer. *N Engl J Med* (2020) 383(18):1711–23. doi: 10.1056/NEJMoa2027071

39. Shibaki R, Akamatsu H, Kato T, Nishino K, Okada M, Mitsudomi T, et al. A Phase II Study of Cisplatin Plus Vinorelbine Combined With Atezolizumab as Adjuvant Therapy for Completely Resected Non-Small-Cell Lung Cancer With EGFR Mutation (West Japan Oncology Group 11719l/ADJUST Study). *Ther Adv Med Oncol* (2021) 13:1758835920987647. doi: 10.1177/1758835920987647
40. Venkatesulu BP, Mallick S, Lin SH, Krishnan S. A Systematic Review of the Influence of Radiation-Induced Lymphopenia on Survival Outcomes in Solid Tumors. *Crit Rev Oncol Hematol* (2018) 123:42–51. doi: 10.1016/j.critrevonc.2018.01.003

Conflict of Interest: The authors declare that the research was conducted in the absence of any commercial or financial relationships that could be construed as a potential conflict of interest.

Publisher's Note: All claims expressed in this article are solely those of the authors and do not necessarily represent those of their affiliated organizations, or those of the publisher, the editors and the reviewers. Any product that may be evaluated in this article, or claim that may be made by its manufacturer, is not guaranteed or endorsed by the publisher.

Copyright © 2021 Yang, Wang, Li, Li, Li and Yuan. This is an open-access article distributed under the terms of the Creative Commons Attribution License (CC BY). The use, distribution or reproduction in other forums is permitted, provided the original author(s) and the copyright owner(s) are credited and that the original publication in this journal is cited, in accordance with accepted academic practice. No use, distribution or reproduction is permitted which does not comply with these terms.

Advantages of publishing in Frontiers

OPEN ACCESS
Articles are free to read for greatest visibility and readership

FAST PUBLICATION
Around 90 days from submission to decision

HIGH QUALITY PEER-REVIEW
Rigorous, collaborative, and constructive peer-review

TRANSPARENT PEER-REVIEW
Editors and reviewers acknowledged by name on published articles

Frontiers
Avenue du Tribunal-Fédéral 34
1005 Lausanne | Switzerland

Visit us: www.frontiersin.org
Contact us: frontiersin.org/about/contact

REPRODUCIBILITY OF RESEARCH
Support open data and methods to enhance research reproducibility

DIGITAL PUBLISHING
Articles designed for optimal readership across devices

FOLLOW US
@frontiersin

IMPACT METRICS
Advanced article metrics track visibility across digital media

EXTENSIVE PROMOTION
Marketing and promotion of impactful research

LOOP RESEARCH NETWORK
Our network increases your article's readership